The role of mass movements for slope evolution

—

conceptual approaches and model applications in the Bonn area

Dissertation

zur

Erlangung des Doktorgrades (Dr. rer. nat.)

der

Mathematisch–Naturwissenschaftlichen Fakultät

der

Rheinischen Friedrich–Wilhelms–Universität Bonn

vorgelegt von

Dipl. Geogr. Jochen Schmidt

aus

Grünstadt

Bonn 2001

Angefertigt mit Genehmigung der Mathematisch–Naturwissenschaftlichen Fakultät der Rheinischen Friedrich–Wilhelms–Universität Bonn

1. Referent:	Prof Dr. Richard Dikau
2. Referent:	Prof Dr. Horst J. Neugebauer
Tag der Promotion:	21. September 2001

Abstract

Understanding *slope processes* and *slope systems* in different timescales is focused by a range of approaches from different disciplines. This work is based on a multi–disciplinary research approach within the project SFB350 *'Interactions between and Modelling of Continental Geo-Systems'*. Previous work indicate, that mass movements have a considerable spatial and temporal extent in the Bonn area. Moreover, the spatial pattern of these landslides indicate, that they play an important role in the superordinated system of hillslope evolution. The fundamental research objective of this work is the assessement of mass movement processes as part of hillslope systems of the Bonn area. It is queried how the geomorphological effectiveness of mass movements on hillslopes over longer timescales can be quantified, and more general, how slope development, affected by mass movements can be modelled.

The methodological approach included (1) local observations and analyses of individual landslide objects, (2) analyses of data from two larger field sites, and (3) aggregation techniques of past climate conditions for the Bonn area. The analyses led to simplified models of lithological boundary conditions for the landslides and for the field sites. Three scenarios of climatic variability for the Bonn area were developed for the last 500 years, based on statistical analyses of proxy data. For each scenario, models of typical annual variation of precipitation and temperature were derived. Modelling approaches on different scales were applied. Slope stability models were used to reconstruct failure conditions for the landslide objects under investigation. A simplified model of hillslope hydrology and slope stability was developed to analyse stability of hillslopes for different climatic conditions. This model was used to calculate failure probability in a scenario approach for three sensitive hillslopes in combination with the identified climatic scenarios. Geomorphometric techniques, including hillslope profile analyses, and a simplified model of hillslope development were applied to model hillslope evolution of one field site (catchment 'Melbtal'). A conceptual model for hillslope evolution of the Melbtal was developed on the basis of the results, combining the concept of ergodicity with changing system behaviour.

Movement monitoring and and stability analyses indicated the sensitivity of hillslopes in the Bonn area to groundwater fluctuations caused by intensive precipitation phases. These results suggest the application of scenario models to analyse the sensitivity of the hillslopes to changing climatic conditions. The hillslope evolution model indicated five evolutionary stages for hillslope systems of the Melbtal, according to varying material sensitivity, climatic changes, dominant slope processes, and process coupling. Generally, the model results show a transition from a hillslope systems in the upper valley, which is not affected by landslides to a hillslope system in the lower valley, which is dominated by hillslope instabilities and landslides. The change in hillslope processes can be explained by different lithologic boundary conditions. The valley–side slopes affected by landslides were chosen as boundary conditions for the scenario approach (see above) to investigate the sensitivity of the hillslopes to mass movements. The results from scenario modelling led to different failure probabilities for the modelled hillslopes, which could be related to average

gradient. The failure probabilities, however, showed a complex pattern in relation to the modelled climatic phases, as indicated by frequency spectra of failure probability. The sensitivity of a hillslope to climatic variation is not correlated with average failure probability, i.e. the hillslope with lowest failure probability showed high sensitivity to changing climate patterns. The scenario models, hillslope profile parameters, and field evidence showed, that the reaction of the hillslope system to changing boundary conditions (material sensitivity) is significantly different for the valley side slopes. Hillslope profile parameters indicate, that a critical system state might be reached by interactions of the hillslope (landslide) system with the fluvial system.

The research approach exhibit a series of deficits and error sources. It can be assumed that statistical errors and technical errors are of minor relevance, as the topic of this study is related to relatively large spatio–temporal scales. Certainly, a simplified system of 'real' hillslope evolution was modelled. The question arise, if the used model approach is an oversimplification for the complexity of the considered landform system. Studies on similar catchments in the study area could validate the results derived in this study. Validating the results against field data is certainly necessary, but not carried out in this study, because of missing data (e.g. dating results).

The applied methods and the results indicated several methodological issues and deliveries within the wider framework of the assessment of hillslope systems. *Hillslope profile analysis* gave evidence of spatial structures in hillslope systems, which can be transfered in time using the *conceptual framework* of ergodicity. It could be shown, that combining these results with *simplified hillslope evolution models* deliver **patterns of system behaviour** for the process–response system of hillslopes. The scenario model results indicated **patterns in process behaviour** (in this case landslide processes), which are related to varying boundary conditions and spatial structure of the modelled hillslope. Although no quantification of process rates for varying climatic conditions could be reached, the potentials of this technique for assessing *sensitivity of geomorphic processes to controlling factors* were shown. Certainly, conceptual approaches and scenario models, require field evidence as input data. With respect to the considered scale, this study used **generalised boundary conditions**, here termed as *'Geo–structures'*, as field evidence (e.g. climate scenarios). To accomplish this generalisation task, spatial and temporal aggregation techniques are required, which are only partly available today, e.g. by statistical methods and geomorphometric generalisation techniques.

Based on the applied methodologies, a general framework for assessing geomorphic systems is sketched. It is proposed to model *stages of geomorphic systems*, which are described by higher–scale *patterns in 'Geo–structures'* produced by *changing process interactions* within the related geomorphic evolutionary system (patterns in system behaviour). *Different behaviour of individual processes* for the systems stages can be simulated by model scenarios.

Preface

The idea of this thesis originated from previous studies of the author on aspects of *organisation and interrelationships* in geomorphic systems (e.g. Schmidt *et al.* 1998). Earths landforms and processes exhibit an incredible variability, but also a remarkable amount of organisation, or structure on different scales. Reductionistic attempts in quantifying limited subsets of those structures (as the author presented in Schmidt 1996) are prone to end up in final questions towards the deeper causative factors of these organisations.
Patterns in landforms and processes are clearly related to the interactions and to the internal strucures of the related *earth surface systems*. Earth surface systems, however, are highly complex systems, being created by a vast amount of interacting processes in space and time, but also delivering the boundary conditions for recent process behaviour. The question is how and why these feedbacks lead to organisation and what kind of models are suitable to assess these dynamics.

Understanding geomorphic change of *slope systems* in various timescales is the focus of a wide range of approaches from different disciplines. This work is based on a multi–disciplinary research approach within the research project 'SFB 350, Universität Bonn' (*Collaborative Research Centre 350, University of Bonn*) *"Interactions between and Modelling of Continental Geo-Systems"*. The research foscuses on hillslope systems, dominated by gravitational mass transport processes. It is queried how the geomorphological effect of mass movements on slopes over longer timescales can be quantified, and more general, how slope development, affected by mass movements can be modelled. A methodological approach is presented, which tries to integrate a variety of methods in assessing hillslope systems on different scales. Therefore, this work can be characterised as a multi–method and multi–scale approach. Emphasis lies in comparing and integrating various techniques, with respect to their relevance within the chosen research object *'hillslope'*. Consequently, this thesis involves aspects from several disciplines, including geomorphology for assessing environmental systems, soil mechanics for understanding subsurface structure and material properties, information technologies for managing and exploring environmental data, and physical process understanding for analysis and modelling of mass transport processes on the earth surface.

This document is split into a main document presenting the scientific results, and the Appendix. The Appendix contains basic information, which can be useful as a reference to investigation results, the used software, and equipment. The main document itself is structured in the parts *'Introduction — Concept & Methodology — Theory — Data capture & Management — Data analysis & Interpretation — Model application — Discussion & Conclusions'*.

A few technical notes explain some specific conventions used in this work. The terms 'soil' and 'regolith' are used in this study synonymously as an engineering term, i.e. as "*comparatively soft, loose and uncemented deposits*" (Sutton 1993). The technique used for displaying frequency distributions of measured variables within this thesis is a cumulative frequency–diagram $h(v_c) = h(v_c > v)$, where h is the frequency, where the value of the measured variable v is greater than

v_c. Fractions (e.g., particle size fractions) are used in values relative to 1, the indicated unit is [1]. The German study area led to a lot of German place names, institutions, etc. If translations were possible (or guessed) and used in the text, they are indicated like: 'German name' (*English name*). If coordinates are given (mostly in data tables), the Gauss-Krüger coordinate system was used.
Several investigations contributed directly and indirectly to this study, either by providing data, methods, and/or results. This applies especially to a series of masters theses carried out in close cooperation with the project, and a series of previous studies, predominantly the projects B9 and MABIS as well as the masters thesis of Thomas Heidemann. If information from other work was used, it is indicated in the text.

Acknowledgements

The work presented in this thesis was part of the 'Teilprojekt B13 im SFB 350' (*Subprojekt B13 (SFB 350)*). I gratefully acknowledge the funding of the 'Deutsche Forschungsgemeinschaft' (*German Research Foundation*) for this work.

Various persons have assisted me in the last few years in dealing with an interesting and complex research problem, and the different specific techniques used in this study. I would like to thank all scientists, technical staff, and students of the

- 'Arbeitsgruppe Geomorphologie und Umweltforschung, Bonn' (*Geomorphological and Environmental Research Group, Bonn*),
- 'Geodynamik, Geologisches Institut, Universität Bonn' (*Geodynamics, Department of Geology, University of Bonn*),
- 'Angewandte Geophysik, Geologisches Institut, Universität Bonn' (*Geophysics, Department of Geology, University of Bonn*),
- 'Geographisches Institut, Universität Bonn' (*Department of Geography, University of Bonn*),
- 'Geologisches Institut, Universität Bonn' (*Department of Geology, University of Bonn*),
- 'Meteorologisches Institut, Universität Bonn' (*Department of Meteorology, University of Bonn*),
- 'Insitut für Bodenkunde, Universität Bonn' (*Department of Soil Sciences, University of Bonn*),
- 'SFB 350, Universität Bonn' (*Collaborative Research Centre 350, University of Bonn*), and
- 'Graduiertenkolleg 437' (*Postgraduate School 437*),

who helped me throughout the last years.

Especially, I would like to thank some individuals, who contributed to this work.

Richard Dikau — First I would like to express my graditude to my supervisor Richard Dikau who gave me the opportunity to work on an interesting research topic in an interdisciplinary environment, but who also highly encouraged me to get involved in various aspects of scientific work throughout the last years. He introduced me to the current research questions of geomorphology, and guided me to the most interesting research fields (*Well, at least from my point of view*).
Horst J. Neugebauer — Horst J. Neugebauer was the 'tamer of disciplines and scales' in the project SFB 350. I was (and am still, for sure) inspired by his scientific visions and his way to integrate them within a multi–disciplinary environment.
Hans-Joachim Kümpel — Hans-Joachim Kümpel introduced me to the problems of field geophysics and provided very informally high cost equipment for this work.

Jörg Grunert — Jörg Grunert provided a large amount of information and data through previous work of his group in the study area (projects MABIS and B9, SFB 350). This study would have not been possible without these foundations.
Rüdiger Glaser — Rüdiger Glaser provided his datasets of climate proxy data for middle Europe, which resulted from the project HISKLID. His contribution and assistance in analysing and transferring these data sets to Bonn conditions is highly appreciated.
Jörg Bürkle — Jörg worked as a visiting scientist for the project B13, SFB 350. He assisted in soil mechanical analyses of the sensitive layers of the research area and carried out a series of lab experiments for this study.
Nick Preston — Nick carried out his Phd thesis in the related project B15, SFB 350 (Preston 2001). I gratefully acknowledge his assistance in various field investigations and lab experiments and his valuable comments in various project stages. He was an inspiring discussion partner, available in good and bad project times.
Carsten Alteköster — Carsten is carrying out his PhD thesis on geophysics in the project B13 (Alteköster prep). We spent a lot of time in the field together. It was always good fun to pull the GPR and be surprised by the fancy graphs.
Marcus Fabian — Marcus is carrying out his Phd thesis on subsurface dynamics in the SFB 350 (Fabian prep). I will never forget our back–breaking installation of the AGI-722A Borehole Tiltmeter. Thanks for the tiltmeter and groundwater data!
Ingo Hattendorf — Ingo carried out his PhD thesis in the SFB 350 (Hattendorf 2001). I enjoyed our pleasant time together (in the field, and at the desk) and his patience (and his tea!) dealing with a geomorphologist, always tired from confusing field evidence.
Stefan Hergarten — Stefan work introduced me to the ideas of non–linearity. Thanks for the discussions on complexity and the interdisciplinary work we had throughout these years. Original quotation: *'Well, obviously you've done a lot of work. But have you found out anything useful?'*
Rens van Beek — I am indebted to Rens (now University of Coventry, UK) for his patience in teaching me the usage of PCRASTER and for sharing his ideas and concepts (and code!) in groundwater and stability modelling.
Marc Hannappel — I am indebted to Marc for providing his GIS–system 'Open Landform Geo–Informationsystem' (OreGIS), and for his patience and interdisciplinary spirit in dealing with (not only) mathematical problems of a geoscientist.
Volkhard Schmanke — Volkhard carried out his PhD thesis within the project B9, SFB 350 (Schmanke 1999). I would like to thank him for his assistance and advice to me as a first year Phd student. He supplied very valuable information and data of the research area.
Holger Ingenpaß — Holger carried out his masters thesis within the project B13 on slope stability of the landslide 'si7'. Not only as a student assistant he helped in various field investigations and lab experiments. His work contributed to a fundamental understanding of the landslide 'si7' (Ingenpaß 2000).
Stefan Rasemann — Stefan carried out his masters thesis within the project B13 and provided a detailed understanding of the landform structure of the Melbtal (Rasemann 1999). As a student assistant he helped in various field investigations.
Thorsten May — Thorsten carried out his masters thesis within the project B13 and provided a detailed understanding of the geomorphology and geomorphogenesis of the Melbtal (May 2001). Not only as a student assistant he helped in various field investigations and laboratory experiments.
Jürgen Rogozia — Jürgen carried out his masters thesis within the project B13 on slope stability modelling of the field site Dollendorfer Hardt (Rogozia 2000). He assisted in various field investigations.

Marc–Oliver Loewner — Historic climate variability was one major issue in this work. Marc–Oliver helped as a student assistant in assessing this problem. He will hopefully continue this work for his Phd project. I wish him good luck for that interesting task.
Jan-Christoph Otto — Jan-Christoph worked as a student assistant in various field investigations and laboratory experiments within the project B13.
Thomas Hoffmann — Thomas helped as a student assistant in various field investigations, laboratory work and data compilations within the project B13. I acknowledge his valuable criticism and contribution in several project steps.
Bernd Bichler — Bernd carried out a geological mapping of the Siebengebirge (Bichler 2001). His work delivered a detailed, up–to–date knowledge of the geological situation of the field area Dollendorfer Hardt.
Thomas Parkner — Thomas provided valuable information about the quality of meteorological data sets of the Bonn area (Parkner 2000).
Thomas Glade — I would like to thank Thomas for all his help and advice in (not only) field and lab problems.
Holger Gärtner — Holger contributed in the developing stages of the DBMS of this project as a scientific assistant in the project OPALIS.
Thomas Heidemann — Thomas carried out his masters thesis on landslides of the Melbtal (Heidemann 1996). Many thanks for his help (field guidance!) and the valuable information he provided.
Annette Schäfermeier, Elfriede Mainz — Thanks to the good souls of the Geomorphological Lab of the Department of Geography! They carried out a large amount of nasty particle size analyses.
Günther Heinemann, Bernd Maurer, Thomas Burkhardt — Many thanks for lots of meteorological data of the Bonn area.

Contents

List of Figures

List of Tables

Symbols

β	slope angle
η	dynamic viscosity
γ_w	unit weight of water
γ_b	bulk unit weight
γ_d	dry unit weight
γ_{sat}	saturated unit weight
ϕ'	effective angle of internal friction
ϕ'_r	effective residual friction angle
ϕ	angle of internal friction
ϕ_r	residual friction angle
ψ	total hydrologic potential
ψ_g	gravitational potential
ψ_m	matrix potential
ρ_b	bulk density
ρ_d	dry density
ρ_s	particle density
ρ_{sat}	bulk density (fully saturated)
σ	total stress
σ'_N	normal effective stress
σ_N	normal total stress
τ	shear stress
τ_f	shear strength
τ_r	residual shear strength
ε	strain

A	area
$\vec{a}$	acceleration
c'	effective cohesion
c'_r	effective residual cohesion
c	cohesion
c_r	residual cohesion
c_S	sand content
c_T	clay content
c_U	silt content
CC	chalk content
E	Young's modulus
e	void ratio
f	frequency
$\vec{F}$	force
FOS	Factor of safety
fS	fine sand
fU	fine silt
G	gravel
g	gravitational accelaration
gS	coarse sand
gU	coarse silt
I_A	activity
I_l	liquidity index
I_p	plasticity index
k	hydraulic conductivity
k_s	saturated conductivity
L	length

M	mass
n	porosity
O_c	organic content
p	pressure
POF	Probability of failure
R	gas constant
S	sand
S_r	saturation degree
T	clay
T	temperature
t	time
U	silt
u	porewater pressure
V	volume
$\vec{v}$	velocity
w	moisture content
w_c	saturation moisture content
w_l	liquid limit
w_p	plastic limit
$\vec{x}$	point in space

Acronyms

AML — Arc macro language
Scripting language for developing GIS–tools under Arc/Info

ArcInfo — ArcInfo
A commercial GIS (ESRI) with a huge set of analysis capabilities for various data types

ASCII — American Standard Code for Information Interchange

ASTM — American Society for Testing and Materials

B13 — *Project:* 'Teilprojekt B13 im SFB 350' (*Subprojekt B13 (SFB 350)*) — 'Kinematik und Dynamik gravitativer Prozesse und ihr Beitrag zur Reliefentwicklung' (*Kinematics and dynamics of gravitational processes and their contribution to landform evolution*)

B15 — *Project:* 'Teilprojekt B15 im SFB 350' (*Subprojekt B15 (SFB 350)*) — 'Jungholozäne Reliefentwicklung in lössbedeckten Wassereinzugsgebieten und ihre Modellierung' (*Modelling of Late Holocene Relief Development in Loess-covered Catchments*)

B9 — *Project:* 'Teilprojekt B9 im SFB 350' (*Subprojekt B9 (SFB 350)*) — Bodenabtrag in einem kleinen Wassereinzugsgebiet der Sieg: Erosionsstatus, aktuelle Prozesse und Anwendung von Prognosemodellen

BK 5308 — *Map:* 'Bodenkarte von NRW 1:50000, Blatt Bonn' (*Soil map of Nordrhein–Westfalen, scale 1:50000, map sheet Bonn*)

BK Burghardt — *Map:* 'Bodenkarte des Naturparks Siebengebirge 1:25000' (*soil map 'Siebengebirge', scale 1:25000*)

BK Holler — *Map:* 'Bodenkarte 1:2500, Dollendorfer Hardt' (*soil map 1:2500, 'Dollendorfer Hardt'*)

BK Kottenforst — *Map:* 'Bodenkarte des Staatsforstes Kottenforst 1:10000' (*soil map of the Kottenforst (Bonn, Germany), scale 1:10000*)

BK Schegiewal — *Map:* 'Bodenkundliche Karte der Umgebung von Römlinghoven' (*Soil map of the area of Römlinghoven (Bonn, Germany)*)

BSCS — British Soil Classification System

C1 — *Project:* 'Teilprojekt C1 im SFB 350' (*Subprojekt C1 (SFB 350)*) — Erfassung und Interpretation lokaler Krustendynamik im Zusammenhang mit Fluidbewegungen und rezenter Tektonik

CHASM — Combined Hydrology and Stability Model
Integrated slope hydrology / slope stability software package that assists in the assessment of slope stability

DBMS — Database Management Systems

D–DIVER — pressure transducer D–DIVER (van Essen)

DEM — Digital Elevation Model

DEM 1 — *Map:* Digital elevation model for Bonn area, resolution 1m

DEM 10 — *Map:* Digital elevation model for Bonn area, resolution 10m

DEM 50 — *Map:* Digital elevation model for the Lower Rheinisch Bay area, resolution 50m

DEM SI7 — *Map:* Digital elevation model, landslide si7

DFG — 'Deutsche Forschungsgemeinschaft' (*German Research Foundation*)

DGK5 — *Map:* Deutsche Grundkarte 1:5000

DIN — German Industrial Standard

DTD — document type definition
Formal description in XML declaration Syntax of a particular type of XML document

FOS — Factor of safety

GIS — Geo–Informationsystems

GK 5208 — *Map:* 'Geologische Karte von Preußen und benachbarten Bundesländern' (*Geological map of Nordrhein–Westfalen, scale 1:25000, map sheet Bonn*)

GK 5209 — *Map:* 'Geologische Karte von NRW 1:25000, Blatt Siegburg GK 5209' (*Geological map of Nordrhein–Westfalen 1:25000, map sheet Siegburg*)

GK 5308 — *Map:* 'Geologische Karte von NRW 1:25000, Blatt Bonn–Bad Godesberg GK 5308' (*Geological map of Nordrhein–Westfalen, scale 1:25000, map sheet Bonn–Bad Godesberg*)

GK 5309 — *Map:* 'Geologische Karte von NRW 1:25000, Blatt Königswinter, GK 5309' (*Geological map of Nordrhein–Westfalen, scale 1:25000, map sheet Königswinter*)

GK Bichler — *Map:* 'Geologische Kartierung des Siebengebirges' (*Geological mapping of the Siebengebirge, scale 1:10000*)

GK Schegiewal — *Map:* 'Geologische Karte der Umgebung von Römlinghoven' (*Geological map of the area of Römlinghoven (Bonn, Germany)*)

GLA NRW — 'Geologischer Dienst NRW' (*Geological Survey, NRW*)

GMT — The Generic Mapping Tools
A Collection of UNIX tools to manipulate spatial data sets (including filtering, trend fitting, gridding, projecting, etc.) and to produce Encapsulated PostScript File (EPS) illustrations

GnuPlot — GnuPlot
Command-line driven interactive function and data plotting utility for various platforms and output formats

GPR — Ground Penetrating Radar

GRK 437 — *Project:* 'Graduiertenkolleg 437' (*Postgraduate School 437*) — 'Das Relief — eine strukturierte und veränderliche Grenzfläche' (*Landform — a structured and variable boundary surface*)

HAP — Slope profile analysis package
Software package to delineate and analyse hillslope profiles

HDS — Richard's n-store Hillslope Dynamics Simulator
A Model for evolution of hillslope profiles

HISKLID — *Project:* 'Historische Klimadatenbank Deutschland' (*Historical climate database Germany*) — 'Historische Klimadatenbank Deutschland' (*Historical climate database Germany*)

HKG 5208 — *Map:* 'Hydrologische Karte von Nordrhein–Westfalen, Grundrißkarte, 5208 Bonn' (*Hydrologic map of Nordrhein–Westfalen, plan map, 5208 Bonn*)

HKG 5209 — *Map:* 'Hydrologische Karte von Nordrhein–Westfalen, Grundrißkarte, 5209 Siegburg' (*Hydrologic map of Nordrhein–Westfalen, plan map, 5209 Siegburg*)

MABIS — *Project:* 'Massenbewegungen in Süd- und Westdeutschland' (*mass movements in southwest Germany*)

ODBC — Open DataBase Connectivity

OPALIS — *Project:* 'Offene Paläoökologische Informationsysteme' (*Open Paleoecological Information Systems*) — 'Offene Paläoökologische Informationsysteme' (*Open Paleoecological Information Systems*)

OreGIS — Open Landform Geo–Informationsystem
Software package to represent a Digital Surface Model, its derivatives and some landform classifications on various generalisation levels

Perl — Practical Extraction and Report Language
A high-level programming language with process, file, and text manipulation facilities make it particularly well-suited for tasks involving quick prototyping, system utilities, software tools, system management tasks, database access, graphical programming, networking, and world wide web programming

PostgreSQL — PostgreSQL
A object-relational DBMS, supporting almost all SQL constructs, including subselects, transactions, and user-defined types and functions

R — R statitics package
A language and environment for statistical computing and graphics

SFB 350 — *Project:* 'SFB 350, Universität Bonn' (*Collaborative Research Centre 350, University of Bonn*) — 'Wechselwirkungen kontinentaler Stoffsysteme und ihre Modellierung' (*Interactions between and Modeling of Continental Geo-Systems*)

SOC — Self–organized criticality

SQL — Standard query language

TCL 1800 — Tachymeter TCL1800 (Leica)

USCS — Unified Soil Classification System

VRML — Virtual Reality Markup Language
Markup language to deliver interactive 3D objects and worlds across the internet

XML — extensible markup language
The universal format for structured documents and data on the Web

XSL — extensible stylesheet language
An XSL stylesheet specifies the presentation of a class of XML documents by describing how an instance of the class is transformed into an XML document that uses the formatting vocabulary

Part I.

Introduction

1. Research problem and hypothesis

1.1. Mass movements & hillslope dynamics — a multidisciplinary research problem

It is an open question as to what extent landslide activity contributes to landform evolution (e.g. Dikau 1999, Crozier and Glade 1999). Recent investigations addressing the problem range from local field investigations, detailed or simplified physical process modelling, statistical modelling, to conceptual, and genetic approaches. However, despite promising concepts resulting from these approaches (compare Hansen 1984, Hergarten and Neugebauer 1999a), the research efforts so far have not led to a fundamental understanding and quantification of the role of landslides within the system of hillslope evolution in different environments.
Different research approaches and disciplines are concerned with the problem (Figure 1.1). Hansen (1984) classified approaches in landslide research into *earth science approaches* and *engineering approaches*, respectively (compare Anderson 1987). Earth science approaches dominantly focus on determination of slope instability by assessing the spatio–temporal variability of landslides and their causative factors, while engineering approaches classically deal with site–specific slope stability. Therefore, both approaches work on different scales (compare Chapter 2). However, a basic requirement of both approaches is to define relationships between environmental factors and landslide (process) characteristics. Currently available models have limitations in describing spatio–temporal patterns of slope instability, and especially in combining the above approaches (compare Hansen 1984, and see below). A fundamental problem is, that relationships between landslide occurrence (and other landslide parameters) and the causative factors are inherently *nonlinear*, and vary over space and time. The following notes summarise major concepts contributed from different disciplines.

Fundamental background of **geomorphologic research** (e.g. van Beek and van Asch 1999, Brooks *et al.* 1999, Casale *et al.* 1993, Crozier 1986, Hansen 1984) is the assessment of landslide processes as part of the landform system, i.e. as part of higher order geomorphic system (e.g. Crozier 1999, Palmquist and Bible 1980). Therefore, it is mandatory to *simplify process description* and to focus on landslide occurrence and the relevant factors in space and time (e.g. Crozier and Glade 1999, Preston 1999, compare Chapter 2). Yamada (1999) presented a study in landscape evolution of a zero order basin by assessing recent soil creep and slope stability, and *actualistic transfer* of measurements and model results. However, with respect to the spatio–temporal variability of boundary conditions and the complexity of the considered systems it is questionable, if those simplistic *linear* approaches deliver reliable results.
Temporal descriptors, such as lifetime of landforms, recurrence interval of events, have to be used to assess discontinuous processes like landsliding in the framework of the complexity of hillslope systems (Brunsden and Thornes 1979, Cendrero and Dramis 1996). These descriptors can lead to the determination of *frequency and magnitude of landslide activity* in space and time (e.g. Crozier 1996a). Predicting frequency and magnitude in landslide processes using process descriptions, as

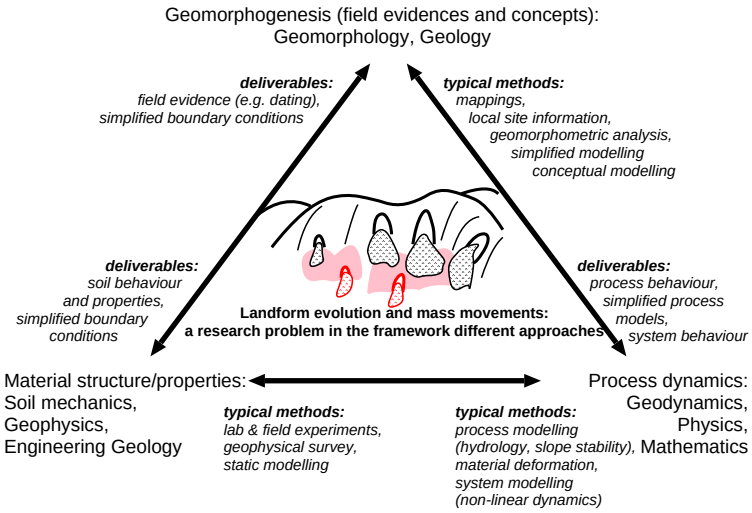

Figure 1.1.: Interdisciplinary geoscientific position of the research problem. Several disciplines are concerned with the phenomena 'landform evolution' using different methodologies and aiming at specific aspects. Each approach, however, has a specific range of deliveries to contribute to fundamental understanding of landform evolution.

applied in recent stability and movement models, is an important agenda in landslide research. However, Crozier (1999) and Richards (1999) are discussing the frequency–magnitude concept critically with respect to its applicability for complex geomorphic systems, including episodic transport processes producing erosion forms and sediment bodies with varying size and age. *Thresholds* have been widely applied as a possiblity to model the relation of causative factors and complex response (Glade 1997). The concept of thresholds is often used in modelling landform evolution, because of its attractive simplicity (Francis 1987). The *variability of thresholds* in space and especially in time (which means under varying boundary conditions) is one crucial problem. This variability appears to be related to internal dispositive factors (Crozier 1996a), reflecting system non–linearity. However, the utilitity of the concept of variable thresholds in modelling landform evolution using slope stability models has been shown in several studies (e.g. van Beek and van Asch 1999, Brooks *et al.* 1999, Casale *et al.* 1993).
A related problem, stressed by Palmquist and Bible (1980), is the identification and differentiation of external and internal dispositive factors as landslide causes and triggering factors leading to slope failure. They propose the identification of important dispositve factors to group landslide occurrence with specific statistical characteristics in space and time. Crozier (1999) proposed to upscale physical properties into geomorphic meaningful *effective parameters*, i.e. 'potency', 'susceptibility', and 'occurrence'. Freeze (1987) and Palmquist and Bible (1980) used effective climate parameters in simplified model approaches to assess *scenarios of system behaviour*.
In addition to the more or less process based approaches various *conceptual approaches* tried to assess hillslope systems influenced by mass movements (e.g. Brunsden 1973, Cendrero and Dramis 1996, Haigh 1988, Palmquist and Bible 1980). These usually involve the definition of a set of simplified environmental variables (see above) and a conceptual, descriptive framework of their relationships.

Engineering geology and soil mechanics usually focus on site–specific stability analysis by modelling local *stress/strength conditions*, or small scale *behaviour of soils* (see Chapter 4).

However, as strength and rheological behaviour of soils are dependent on geomorphic history, a close connection to scales of landform evolution exist. Anderson (1987) indicated a number of joint topics of geomorphology and engineering geology, including *mechanisms of complex failure*, *hillslope geometry* as a complex geomorphic product, and *effects of weathering and pedogenesis* on long–term slope stability. Hence, geotechnical engineering provide a range of methodologies, valuable for assessing the higher scale hillslope system, and vise versa.
Modelling approaches from various disciplines (**physics, mathematics, geodynamics, geomorphology**) are assessing sediment dynamics on hillslopes and within catchments, by developing *physically based models* of sediment transport for individual processes (Chapter 5, compare e.g. Brooks and Anderson 1995, Hattendorf 2001). These approaches contribute to the understanding of dynamics individual process behaviour and their dependencies to relevant boundary conditions. However, the problem is, how to apply these models in the framework of landform evolution (Preston *et al.* rev).
Therefore, approaches in **modelling landform evolution** by process based models have been developed (see section 5.3). These mathematical models usually simulate sediment transfer on a artificial discretisation in space and time, using simple descriptions of processes. Model validation is limited due to missing field evidence. Moreover, most model approaches focus on specific aspects of the total range of geomorphic processes acting in geomorphic systems. Although several authors (Ahnert 1988, and others) showed the potentials of these models to explore landform evolution, it is questionable if they are applicable to simulate complex behaviour of geomorphic systems.

However, a variety of geomorphic processes interacting in space and time lead to complex landform systems (see Chapter 6) which are "*contrasted with the simplicity of the basic laws of physics*" (Goldenfeld and Kadanoff 1999). On the other hand, complex interactions of different processes often lead to structure and order in landforms. Appropriate ways of **approaching complex systems** have to be considered, leading to a series of recent publications, mainly from the field of physics (e.g. Hergarten and Neugebauer 2000, Werner 1999). After the paradigma of *'chaos'* dominated (not only) the scientific world in the last years, discussions on *non–linear dynamics* of complex system leading to new concepts as the 'Self–organized criticality' (SOC) (compare Bak 1996). These approaches show, that complexity may lead to new properties of integral systems, which cannot be predicted either from simple evolution models or from combining process models, and arise from system structure itself. Therefore, new concepts are needed to describe non–linear behaviour of complex geomorphic systems.

1.2. Mass movements & hillslope dynamics — fundamental scale problems

The research topic exhibits fundamental *scaling problems*. Whereas occurrence and rates of landslide processes and subprocesses are dependent on a range of boundary conditions, and partly acting on very small scales (i.e. landslides exhibit multiple scales itself, compare Hattendorf 2001), these processes are part of a landform system acting on a variety of larger scales (these issues will be discussed in section 2.2). This means, scaling methods have to be developed to transfer small scale information through the system (*'bottom–up–regionalisation problem'*, i.e. what does a geomorphic system 'see' from individual processes?) (Figure 1.2). With respect to the discontinuity in mass transport and in formative activity of geomorphic processes, including landslides, this problem cannot be solved by methods of simple averaging and balancing (see above). On the other hand,

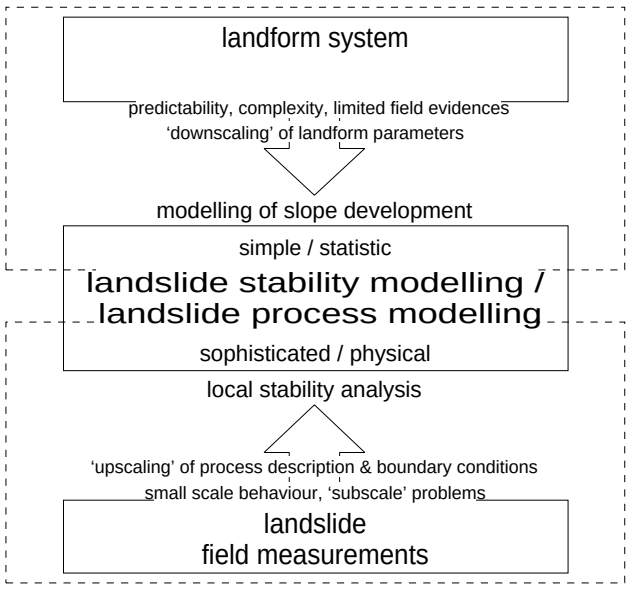

Figure 1.2.: Sktech of the problem of 'process modelling and landform evolution' for landslide processes. Landslide analysis is mostly limited to site–specific situations. Landform evolution models treat the gravitational processes often by simple assumptions. Finding links between these approaches is an important research issue, leading to the problems of 'upscaling' process behaviour and of 'downscaling' landform parameters (see text).

inherent non–linear relationships within the system of landform evolution might *limit predictability* and lead to the question, which features can be modelled at all, and shall be targeted as quantities for modelling (see Chapter 2) (*'top–down–scaling problem'*, Figure 1.2).

The multi–scale character of the research topic is related to the problem of *'process modelling and landform evolution'*. Research approaches in hillslopes studies can be roughly divided into actual process modelling approaches, and conceptual studies looking at the behaviour of slope systems on longer timescales (see section 1.1). Comparatively few studies tried to integrate these views (van Beek and van Asch 1999, Brooks *et al.* 1999, Casale *et al.* 1993, Coulthard *et al.* 1998, Hansen 1984). The workshop *'Process Modelling and Landform Evolution'*, held by the 'SFB 350, Universität Bonn' (*Collaborative Research Centre 350, University of Bonn*) in Bonn (1997), addressed the problem of discrepancy between measurement and modelling of actual geomorphic processes and description and modelling of landform evolution (Hergarten and Neugebauer 1999a). Actual modelling approaches use well known field sites and more or less sophisticated models. Evolution models often use simplified field data (e.g. ideal slope profiles or artificial landform topography) and comparatively simple, statistical or conceptual approaches (Figure 1.2, compare Cendrero and Dramis 1996, Hergarten and Neugebauer 1999b, Kirkby 1987). Appropriate field data for validation of landform evolution models are undefined and/or missing (see section 2.1 and compare Dikau 1999). Therefore, validation of these models often must be done by methods such as the principle of actualism or the ergodic principle (Dikau 1999, van Beek and van Asch 1999, Brooks *et al.* 1999). Especially for mass movements, the problem of filling the gap between actual process description and long term geomorphic evolution is obvious as in no other research field (Dikau 1999), because *"on the geological time span over which slope profiles evolve, landslides and other rapid mass movements occur almost instantaneously"* (Kirkby 1987).

1.3. Research questions and hypothesis

The general study object of this work is the hillslope system. Previous studies indicated the sensitivity of hillslopes in the Bonn area with respect to mass movement processes (Part IV). The aim of this study is to evaluate different modelling approaches in quantifying the role of landslides within hillslope systems of the Bonn area. A specific focus within that framework is to examine the potentials of available models of slope stability to assess slope systems in timescales of approximately hundreds of years (compare Brooks *et al.* 1999). Hence, the key questions of the study can be posed as follows:

> *How can the evolution of hillslope systems, which are affected by mass movements, be assessed? To what extend can physically based stability models contribute to a better understanding of long–term changes of hillslope systems, which are affected by mass movements?*

Stability models are often poor in terms of modelling a single landslide, which is related to poor parameter knowledge, and to simplified process description (Hattendorf 2001). However, if these models use general valid descriptions of the physical relationships and processes, they should be applicable on a higher scale to simulate measures of landslide processes within a slope system relevant to slope development.

> *Therefore, the hypothesis is made, that physically based models of gravitational hillslope processes can be applied to 'typical', regionalised boundary conditions in time and space. These scenario models can be used to understand the role of landslides within the system of hillslope evolution, and, more specifically, simulate net effect of landslides for longer time scales.* (this hypothesis will be further exemplified in Chapter 3)

The hypothesis further imply, that isolated, single–scale approaches (e.g landslide modelling) are not appropriate to solve the research problem. The complex system of hillslope development contains phenomena and processes with different scale characteristics (compare Chapter 2). Consequently, this study combines different approaches on different scales (Chapter 3). It a purpose of this work to show the necessity and the utility of multi–scale and multi–method research approaches.

Several subordinate issues arise from the general aims.

- What are the relevant scales of the system of hillslope processes within higher–scale system of landform evolution (e.g. hillslope evolution, catchment evolution) and what features can be target quantities to model landform change?
- What kind of field evidence can be used to quantify changes of hillslopes and the controlling factors within different time scales?
- How can spatio–temporal boundary conditions of relevant processes be parameterised on the relevant scales, e.g. as effective factors for simplified process models?
- What are relevant process descriptions with respect to the considered scale of hillslope change and how can they derived from small scale process descriptions?

1.4. Thesis structure

The methodological approach is based on the combination of field investigations, local and regional stability analysis, assessment of spatio–temporal variations of relevant boundary conditions and applying models of slope evolution. Details of this approach and the basic assumptions, leading to the conception and methods of this work are discussed in Part II.

Relevant fundamentals for the considered system and its subsystems include (1) soil mechanics, as the science of the mechanical material properties affecting the hillslope system, (2) physical models of hillslope hydrology, slope stability, and landform evolution, and (3) approaches towards geomorphic evolutionary systems. These topics are shortly introduced in Part III.

Previous work indicate the relevance of landslide processes with respect to the slope system in the Bonn area. Part IV introduces the study area and the specific situation of the field sites used in this study. Present knowledge about the relevant boundary conditions, i.e. geologic and geomorphic history and historic variations of climate and landuse conditions are shortly reviewed.

In Part V, the basic procedures of data capture and data management are described. Relevant data sets, e.g. locations of the drillings etc. are presented. Most of the results itself can be found in the Appendix. Specific emphasis is given to the database management system, which was developed and used in this study.

As earlier indicated, the purpose of this work is to show the utility of multi–scale approaches for assessing complex systems. Therefore, methodologies on different scales were applied in data analysis and modelling (Parts VI and VII).

- Landslide field research leads to *knowledge about recent processes and related boundary conditions*. Therefore, data from the field sites were analysed (Part VI). These include kinematics of the investigated landslides and subsurface structure of the field sites. The results lead to aggregated models of the surface and subsurface structure of the field sites. Results from monitoring and slope stability modelling (section 12.1) identified dominant dispositive and triggering factors for landslide occurrence.
- Morphometric analysis and hillslope evolution modelling inferred phases in valley development and lead to a *qualitative model of hillslope evolution* (Chapter 13). Therefore, the results from field analysis (Part VI) can be set into a higher–scale temporal framework of valley development.
- A model of historical climatic variation of the Bonn area, derived from proxy data, delivered *climate regimes*, i.e. parameterisations for different past climatic phases (Chapter 11).
- Scenario models are used to estimate *spatio–temporal variability of slope stability* for the field sites in historic time scales (section 12.2). The model scenarios are derived from the climate analysis and the aggregated hillslope models (see above). The model results indicate different sensitivity of the modelled hillslopes and different patterns of process behaviour with respect to varying boundary conditions. The findings contribute to a better understanding of the behaviour of the higher–scale hillslope evolutionary system and complement the conceptual model approaches (Chapter 13).

Part II.

Conception & methods

Introductory notes

This part discusses major problems and issues within the research problem of understanding and modelling of landform evolution in general, and, more specifically with respect to landslide processes. It is questioned, (1) which appropriate target quantities in modelling landform evolution can be derived, (2) how boundary conditions can be assessed, and (3) which modelling concepts might be appropriate.

On the basis of this discussion, a research strategy is developed as conceptual basis for this work. The corresponding approach consists of a series of interconnected methods, applied on different scales, including landslide field assessment, modelling of subsurface structures, paleo climate series analysis, and hillslope evolution modelling.

2. Landform evolution: What is it and how to model it?

2.1. Landform evolution & geomorphic systems

A fundamental objective of geomorphology is *understanding and modelling of geomorphic systems*. This objective includes assessment of geomorphic processes (process geomorphology), analysis of landforms (geomorphometry), and understanding of change of landform surfaces (geomorphogenesis). Various methodological approaches have been used to assess geomorphic change of landform surfaces, ranging from the classical works of Gilbert (1877), Davis (1899), Penck (1924), King (1953) to more modern conceptual studies (Hack 1960, Haigh 1987, Schumm and Lichty 1965, to name only a few) (see section 6.1 and Part I), and to recent computer modelling approaches, where process geomorphology meets geomorphogenesis (e.g. Ahnert 1976, 1987a, 1988, Kirkby 1987, 1992, Braun and Sambridge 1997, Hergarten and Neugebauer 1999b, Coulthard *et al.* 1998) (see Chapter 5). However, as Dikau (1999) states, these approaches have not led to satisfying answers. Several problems and issues can be identified within the framework of understanding and modelling of landform change.

Limited environmental data in time and space

Detailed description and modelling of development of landforms require a large amount of four dimensional data in space and time, which is normally not available. Considering environmental information typically available for modelling landform evolution, the situation can sketched as follows (see Figure 2.1). Data in comparatively high spatio–temporal resolution is available only for recent times (e.g. DEMs, mapping data, remote sensing, climate time series). In timescales relevant for landform evolution (usually $> 10^3 a$), data is only available for specific sites, e.g. through dating results or stratigraphic interpretation, and with limited resolution and reliability (high error), e.g. climate proxy data (see Chapter 11). Most of the past spatio–temporal space remains empty. This problem has direct implications for validating landform evolution models, i.e. mostly data are missing for validation of sophisticated modelling approaches (Coulthard 2001). Therefore, the related model results remain a hypothesis for 'real' landform development. Additionally considering the system complexity (see below), this implies, that details of landform change can never be resolved, neither by modelling approaches, nor by data sources.

Complexity and multiple scales in Geo–systems

System complexity and *scale issues* play fundamental roles in modelling landform evolution, or, more general, in understanding geomorphic systems. Clearly, environmental systems are complex, i.e. showing a high (unpredictable?) variability of poperties in space and time (Bak 1996). Numerous authors discussed scale and complexity in geomorphology (e.g. Boer 1992, Dikau 1990, Dodds and Rothman 2000, Haigh 1987, Starkel 1999). "*The complicated architechture of the earth's surface is a joint product of various forces, which mobilise different substances. ... This product of various transfer of matter, in the mean time, forms a geometric base for all on going transporta-*

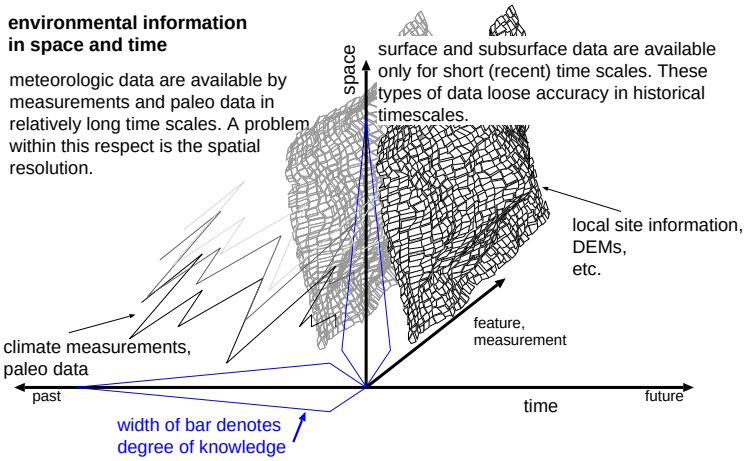

Figure 2.1.: Environmental information in space and time. High resolution data is available for recent times only. On the other hand, in time scales relevant for landform evolution, data is only available for specific sites (e.g. dating results). Missing data is one major problem in modelling landform evolution.

tion of material in the environment" (Starkel 1999). As the involved processes exhibit different frequency magnitude spectra, and are interacting, a complex system is created, which might lead to the conclusion, that "*we should all just go home and have a beer*" (Phillips 1999). Analysing and simplyfing this complexity, however, suggests the formation of subsystems and related landform elements, acting on different scales. A series of propositions have been made towards the definition of spatio–temporal quantifications of different scales in earth surface systems (e.g. Boer 1992, Dikau 1990, Starkel 1999).
However, the usage of the term *'scale'* shows a large diversity in dependency to the specific application and/or the research subject (Zhang *et al.* pres). In geomorphology, *'scale'* is a measure, describing spatio–temporal extent (in various measures), for a specific cut–out of a complex geomorphic system ('operational scale' after Zhang *et al.* pres). Therefore, the environment is modelled as a complex system, consisting of subsystems acting on different scales, which are related to specific landform properties. Each environmental study has to take care about the scale of the considered subsystems, their connectivities, and scale–dependent parameters in an interacting *hierarchy of multiple scales*.
Moreover, new system behaviour might be created due to multi–scale characteristics. The system will behave complex (*chaotic*) and instable (involving many thresholds), at first sight. However, as discussed by various authors (e.g. Bak 1996, Hergarten and Neugebauer 1999b, 2000) behaviour of such complex systems can lead to a self–organizing system resting in a canon of critical states, which show unpredictable perturbations (compare Chapter 6). This implies, that complexity limits predictability of a system, and, on the other hand indicate to predictable system properties.

How to model landform change?

Recent approaches in landform evolution modelling range from (physically based) simplified models of hillslope development (Ahnert 1987a, Kirkby 1987), models of three–dimensional landform evolution (Braun and Sambridge 1997) (section 5.3) to geomorphogenetic interpretation of field data based on simple 'head models' of processes. The latter approach includes high subjectivity and is often based on spatio–temporal singularities, which means, comparability and possibilities for deriving more general quantitative rules in landform evolution are limited. Problems of the

physically based process modelling approaches include the lack of appropriate field data which leads to difficulties in validating the model results, as discussed above. Therefore, often simplified or artificial boundary conditions have to be used in landform evolution modelling. However, it is a question, which possibilities and results can be expected in general from modelling of landform evolution. Modelling of the 'reality' of landform change using high resolution, four dimensional algorithms is not possible and will never be, because of the high uncertainties and the system complexity. Available models of this type can be used to assess possible developments of landform systems ('retrovalidation', see Coulthard 2001). However, the question can be posed if it is justified to apply high resolution algorithms to assess the problem. At least, these model types might be oversised for the problem of landform evolution, i.e. interpreting the corresponding modelling results has to incorporate generalisation techniques, anyway.

Therefore, the hypothesis is made, that new modelling approaches are needed to assess the complexity of geomorphic change in time, which are capable to model a regionalised 'reality' of landform dynamics, i.e. incorporating scaling approaches which are adapted to the considered scales of landscape systems. The following paragraphs try to approach the problem, what type of information and parametrisation these new model types could involve. Therefore, as a first step the scope and the subject of understanding and modelling of landform evolution have to be clearly identified.

What means 'modelling of landform change'?
Three closely coupled subtopics can be identified (see above).

What is temporal *change of geomorphic form*? — Identification of key parameters.
Usually change of a 2/3-dimensional representation in time is modelled (e.g. Coulthard *et al.* 1998). But can these modelling results considered to represent change of geomorphic form in time adequately? A geomorphic system consists of a nested hierarchy of geomorphic forms (i.e. the *morphological system*, see Chapter 6), resulting from geomorphic subsystems acting on different spatial and temporal scales (compare Chorley and Kennedy 1971, Chorley *et al.* 1984). The issue is to understand the interaction of these subsystem in order to model the temporal development of the spatial composition and structure of forms. Therefore, it is necessary to define, which features of landform and landform change are relevant for a certain scale. A directly related question is, how to quantify and parameterise these features and the related scales. Therefore, *key parameters of landforms* have to be defined (Beven 1996), describing geomorphic forms on different spatial scales (with respect to different geomorphic subsystems acting on a specific temporal and spatial scale). Forms are often described statistically (e.g. by geomorphometric parameters, see Table 2.1). However, in recent times measures of fractality and non–linearity have become increasingly popular, they tend to include self–organising characteristics of complex systems (Hergarten and Neugebauer 1999b). Generally, this implies, that for modelling landform change a 'generalised reality' of landform has to be modelled, necessitating adequate *generalisation techniques for landforms*.

How can *geomorphic process behaviour* be described? — Frequency spectra of processes.
Usually rates of sediment transport, i.e. mass/time are used, which can be calculated by mass transport laws applicable to short time frames. In longer timescales process specific rates of long–term denudation, which vary with boundary conditions, are used in modelling approaches for landform evolution (e.g. Kirkby 1992). Geomorphologic work is another proposed measure to model long–term geomorphic effectiveness of processes (Caine 1976). A

Table 2.1.: Descriptors of geomorphic systems with respect to landform evolution. The categories *form*, *process* and *system* are used.

	'ordinary statistics'	**non–linearity**
form	geomorphometric parameters, hillslope profile parameters, subsurface structure, representative soil parameters	self similarity: parameter–size statistics, fractals
process	process rates, denudation rates, geomorphologic work	self organisation: frequency–magnitude statistics
system	system properties (compare Chapter 6)	SOC–behaviour, chaotic behaviour

lack of these measures is, that they do not consider episodic behaviour of geomorphic processes. *Frequency–magnitude relationships* can therefore be helpful in describing effectiveness of geomorphic process. Numerous studies have tried to assess frequency–magnitude characteristics of geomorphic processes under different environmental conditions (e.g. Hovius *et al.* 1997, 2000, Ohmori and Hirano 1988). However, frequency–magnitude characteristics seem to be related to fundamental properties of the considered geomorphic system (compare Chapter 6), e.g. including possible episodic and non–linear behaviour (compare Hergarten and Neugebauer 1999b, Phillips 1999). Therefore, it is proposed to derive new types of long–term sediment transport laws, which relate environmental conditions to system properties and to frequency and magnitude of long–term process activity (Preston *et al.* rev).

How can *geomorphic process systems* be described? — System stages

With respect to the limits of data and models in landform evolution (see above), a major outcome and aim of modelling approaches is the understanding of system behaviour. Landscape systems have been classified by terms describing system stage (e.g. 'cyclic', 'graded', 'steady', 'transient') and (possible) changes in system stages (e.g. 'stable', 'metastable', 'unstable') due to change in controlling variables (compare Phillips 1999, Schumm 1979). These system states depend on system complexity, including external and internal variables. Temporal variation of geomorphic form parameters or geomorphic process rates can be used to identify transient and steady systems (compare Chapter 6). Thresholds of these variables define boundaries of different system states (Schumm 1979). Another range of methods for system analysis is given by non–linear physics, e.g the *Routh–Hurwitz criteria* (Chapter 6, compare Phillips 1999). Although various approaches exist in analysis of geomorphic systems, no standard tools are available, indicating a major research lack within the wider topic of understanding landform change.

Several interconnected questions can be identified as major issues for developing a consistent model of geomorphic systems, and, more general for understanding landform evolution.

- Which are the major temporal and spatial scales existing in a landform system?
- What are fundamental parameters of landform structure (e.g. parameters describing geomorphic structure) and processes (e.g. parameters of frequency–magnitude functions), that describe geomorphic evolution at the different scales?
- How can parameters of landform structure and processes be be used to describe system properties of the related landform system?

Table 2.2.: General subordinate processes of landslides and examples of relevant parameters (compare Terzaghi 1950).

processes	**relevant parameters**
soil creep	slope angle, shear strength, soil moisture
landslide initiation	slope angle, shear strength, soil moisture
rapid landslide event	hillslope geometry
slow remnant movement on pre–existing shear planes	slope angle, shear strength, soil moisture
persistence of landslide debris — process coupling	other processes within the geomorphic system

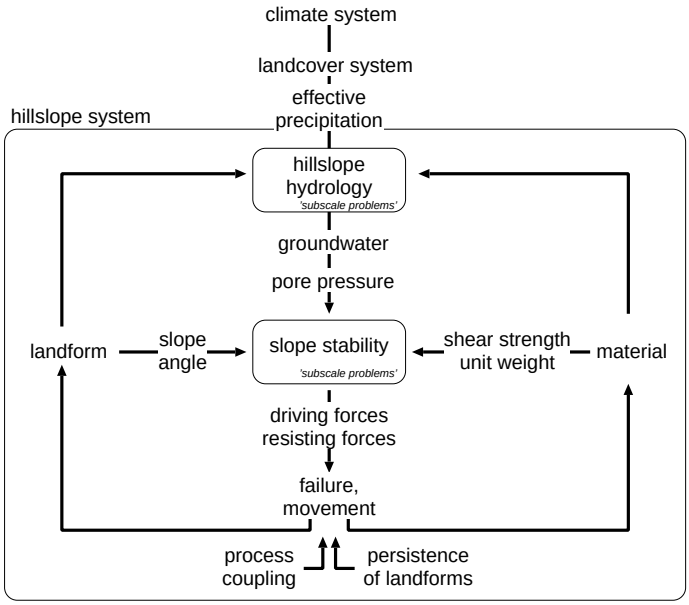

Figure 2.2.: System of gravitational processes and their controlling factors. Occurrence and rate of landsliding is a phenomena, controlled by small scale process behaviour at a shear surface, whereas the feedback with the related hillslope system acts on larger scales. Moreover, higher order systems, as climate and landcover system, are coupled with the hillslope system.

The discussion so far should a major message. It is proposed to assess landform evolution by modelling the considered *geomorphic system*, rather than to apply physically based equations, based on a arbitrary space–time discretisation. Therefore, an budget approach, based on a geomorphic discretisation is proposed to model landform surfaces. This involves modelling of the components of geomorphic systems (in a scale hierarchy) and the frequency–magnitude properties of the related geomorphic processes. Details of the proposed approach are not topic of this work and are discussed in Preston *et al.* (rev). However, this approach implies, that there is a need for (1) identification of landform structure, related to multiple scales in landform systems, and (2) determination of laws describing frequency–magnitude properties of geomorphic processes under varying geomorphic conditions on different scales. These objectives can be seen as 'driving forces' for this study.

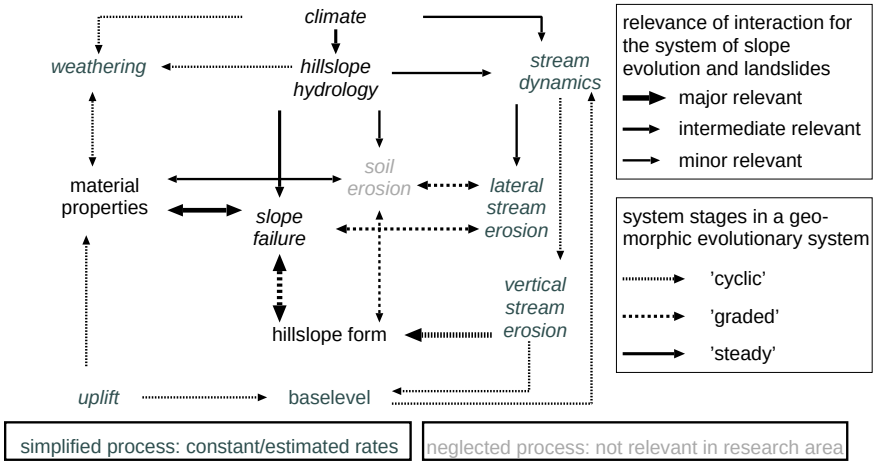

Figure 2.3.: Mass movements as part of the hillslope system. Sketch of the relevant system components for the research area (Part IV). Considering the contribution of mass movements to slope development, system interactions show different relevance (indicated by arrow thickness). Certain subsystems can be identified working in different scales. Soil erosion is considered to be neglectable for the sites of this study (Part IV).

2.2. Landslides and hillslope development: a multi–scale problem

Problems in modelling slope evolution by landslides

Several subprocesses within the wider field of mass movements contribute to change in hillslope form over time can be identified on a general level (Table 2.2). Each process has specific mechanisms and a canon of relevant parameters. The occurrence and rate of these processes is dependent on a series of (either triggering and dispositive factors) factors (Figure 2.2). However, the *internal processes* that operate within a landslide and control this dependency are only poorly understood. Therefore, the small scale system of gravitational movements (Figure 2.2) also exhibit complex behaviour (Hattendorf 2001). Moreover, the *boundary conditions*, which control landslide activity are unknown or only poorly known in a temporal (e.g. paleo surfaces) and spatial (e.g. soil parameters) context (see above).

The discussion so far is related to modelling of landslide processes. A series of additional problems emerge, when considering landslides as part of a higher scale evolving landscape system. In the timescales of slope evolution, landslide activity is a highly *episodic process*. Landslide processes and the correlate sediments are *coupled* with other slope processes (compare Figure 2.3), and often control the occurrence of *subsequent landslides* (leading to several generations of landslides). Therefore, *dating of landslides* in a representative way is difficult (compare Lang *et al.* 1999). This implies that getting field evidence in slope development through mass movement by determination of size and date of all previous landslides is hardly possible or impossible.

Landslides and hillslope development: a multi–scale system

As discussed in the previous section, modelling of landform evolution needs evaluation of the specific process system, of the considered spatial and temporal scales, and the relevant geomorphic parameters describing form and processes. Figure 2.3 shows a simple sketch of the slope system as a geomorphic process responce system indicating the main interactions of geomorphic form and processes for the situation of the research site (Part IV). With respect to the problem of land-

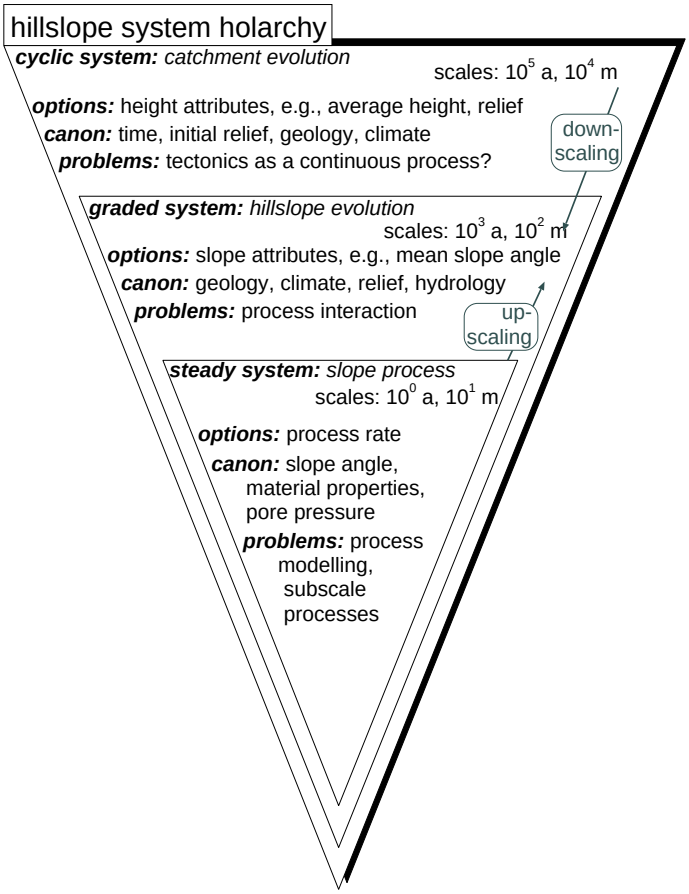

Figure 2.4.: Spatio–temporal hierarchies within the slope system scetched within a holarchy (after Haigh 1987). Some examples, according to the system classification after Schumm and Lichty (1965) are given. The study presented here, focuses on the intermediate, graded hillslope evolution scale. It is an important question how to perform the scale linkages from process description to the hillslope evolution scale and how to downscale the relevant boundary conditions (e.g. relief) from the cyclic scale.

slide occurrence in time, the various interactions have different significance. This means, certain boundary conditions and processes, which are of minor interest for the investigated process scale, can be neclected and/or simplified. Moreover, a specific range of the process–form interactions in Figure 2.3 has to be considered as boundary conditions (independent variables after Schumm and Lichty 1965), because different subsystems act on different scales. As an initial attempt, three subsystems are identified for the research area (according to different timescales defined by Schumm and Lichty 1965) (Figure 2.3, compare Part IV): the 'steady' process scale describing mainly process behaviour in time; the 'graded' hillslope subsystem, incoorporating form–process interactions leading to feedback and equilibrium in slope form; the 'cyclic' system leading to progressive changes of major boundary conditions of the hillslope system (e.g. relief). Figure 2.4 presents a hierarchical structure of different these subsystems and related temporal and spatial scales. Two major question can be identified: (1) How can steady, process–scale relationships be upscaled to fit in the slope evolutionary scale, and (2) how can changes in the cyclic scale be downscaled to boundary conditions of the slope system?

As a summary, the following statements can be made.

- It is not possible to model the geomorphologic development of a specfic site in detail, because of unknown or unprecisely known boundary conditions and inadequate models. Even if it were possible to model a specfic slope, it is not known whether the model results are representative in a regional context or only a spatial singularity. A slope is part of a hierarchical system of landforms and landform processes and cannot be seen isolated in terms of landform evolution (Dikau 1999). Generalisation schemes are required, indicating dominant features or 'effective parameters' which can be modelled for a certain scale ('downscaling').

- Modelling slope development by landsliding has to be done in a 'regionalised' way, as an 'upscaling' of landslide activity (steady system after Schumm and Lichty 1965) to timescales of the 'graded' slope system (Figure 2.4). This temporal upscaling process must consider episodic characteristics of landslide processes. It may be possible to solve this upscaling problem (accepting a statistical uncertainty) by assessing frequency magnitude characteristics of steady process activity (e.g. by applying models) for typical boundary conditions for the specific area. Aggregation of 'typical' boundary conditions has to be related to the properties of the higher scale system (compare Figure 2.4), e.g. tectonic uplift, river incision, geology, climate.

- The reliability of this approach depends on

  - the used downscaling method as decribed in Figure 2.4, i.e. how representatively the spatial slope model describes typical situations in the investigated area with respect to the investigated scale (which means the quantification of 'typical'), and whether it is possible to describe its position and function in the related geomorphic system,
  - the used upscaling method, i.e. the models and parameters used to 'average' slope processes, and
  - the quality of the model used to describe processes on the steady scale (compare Figure 2.4), i.e. how good the model approach solves the subscale complexity sketched in Figure 2.2.

Modelling hillslope evolution in time can therefore not be done by investigating one specific slope, it is also related to a spatial problem. Process models in general, and especially classic stability models, are often poor in terms of modelling a specific landslide (poor representation of parameters, and of internal system complexity, see above) (compare Hattendorf 2001). However, if these models describe of the physical relationships of processes and landform sufficiently, they should be able to deliver results applicable for the higher scale slope system. The required modelling step can be carried out by simulating measures of landslide processes within a slope system relevant to slope development for typical boundary conditions (compare Cendrero and Dramis 1996, Crozier 1973, 1996b,a, Dikau *et al.* 1996b).

3. Conception & methodological approach

3.1. Conception

Based on the above discussion, the research presented in this study is aiming at the assessment of landslide variability in space and time within the system of hillslope evolution of the research area. As argued in the previous section, an understanding of (1) the considered hillslope system, as well as of (2) the relationship of slope stability to the relevant boundary conditions is mandatory. As a *first restriction*, the complexity of possible landslide mechanisms, contributing to hillslope evolution is limited in this study to *first time failure* assessment (compare Table 2.2), as only classic slope stability models were applied for landslide modelling within this study. It is not the aim of this study to develop new (dynamic) landslide modelling approaches. Pre–disposing factors, which vary in space and time, in combination with specific triggering factors lead to slope failure. However, as discussed above, in scales of slope evolution only statistical descriptors (like the frequency–magnitude distribution of landslide events) of the processes can be assessed. Therfore, the system's preparatory and triggering inputs can be regionalised to typical process domains and regimes. With respect to slope failure, this means that the major factors geomorphometry, landcover, geology and climate have to be aggregated (Figure 2.2). Process behaviour for 'typical' situations of these factors can then be used as an estimate for statistical variability of the modelled process, within the system of hillslope evolution (see above). As a *second restriction*, effects of *changing landcover conditions* are not explored due to limited data availability for the research area (see Part IV).

With respect to the relevant system scales as discussed in section 2.2 (Figure 2.4), and the limited data availability in historic and geologic timescales over which landforms evolve (section 2.1), a model conception on three temporal scales (Figure 3.1) was developed.

- In recent time scales (approx. 100a), reliable climate records and knowledge about spatial boundary conditions and process activity (Hardenbicker 1994, Heidemann 1996, Weber 1991) are available to a sufficient degree. Thus, stability models can be parameterised and are applicable *to understand slope stability conditions under recent boundary conditions.*
- In historic to prehistoric times, a series of proxy data series have been elaborated (Glaser 1998, Glaser *et al.* 1999, 2000, Pfister 1992), describing changing climatic conditions to a certain degree. These data can be applied to assess *temporal variability of slope stability* with respect to climatic changes. However, a serious amount of uncertainty remain in that approach due to the unknown changing spatial boundary conditions in time (geomorphometry, landuse, vegetation, etc.). This can only be solved by geomorphic reconstruction (e.g. by space–for–time substituion). Therefore, *variability of slope stability* can be assessed in scenario approaches using simplified reconstructed geomorphic and climatic conditions.
- In geologic timescales neither spatial nor temporal parameters are known to feed into process models. Hence, *simplified modelling approaches*, including qualitative, conceptual modelling approaches are appropriate to assess long–term behaviour of hillslope systems.

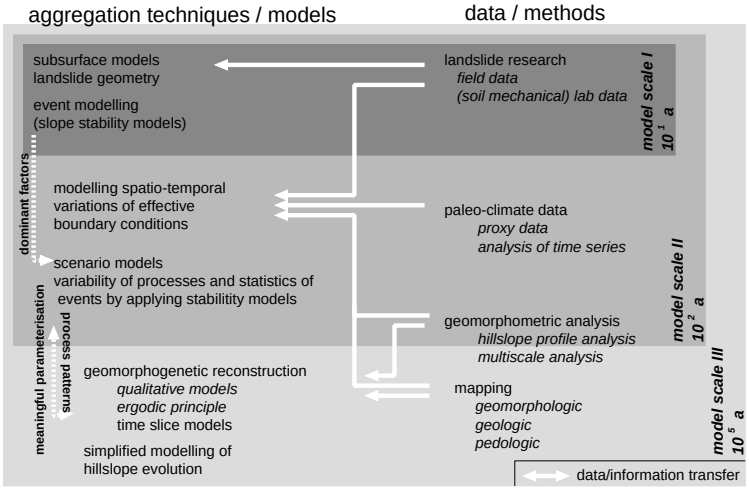

Figure 3.1.: Overview of research concept. With respect to available environmental information and the system complexity and scales, the research approach is based on three different scales. Each scale requires appropriate aggregation techniques and modelling approaches. Scale I describe recent conditions, were process models can be parameterised and vaildated. In scale II, process models can be applied in an 'scenario' approach, by modelling reconstructed boundary conditions. For scale III, data reliability decreases, so only simplified and qualitative evolutionary models can be applied.

3.2. Methodological approach

Based on the the above statements, a research strategy was developed to investigate slope development by mass movement using coupled local and regional approaches and multiple techniques (Figure 3.2). Important in this approach is to gain understanding of typical sites (hillslopes) and to gather as much additional information as possible for the specific site, site environment and the past temporal variability of relevant factors. The key questions are:

- How is a specific slope related to its position in the related assemblage of landforms, and are there possibilities to infer a model of hillslope evolution and landslide occurrence?
- How does a specific slope behave in terms of landslide processes, i.e. which are the dominant triggering and preparatory factors?
- Have there been distinct climatic changes in the past, changing the slope system to another state, in which landslide processes exhibit different behaviour with respect to the hillslope system?

Therefore, the following methodological framework and working programme was developed (Figure 3.2).

- *Local field survey and slope stability assessment* is used to investigate individual landslide objects (Chapter 10). This includes landslide monitoring, lab analysis, and models of failure scenarios for the landslides to assess dependency of failure on triggering factors and geologic and morphologic boundary conditions (section 12.1).
- Geomorphometric, geologic, and morphological data of the field sites are analysed to assess *spatial boundary conditions* (Chapter 10). Geomorphometric slope profile analysis, geologic

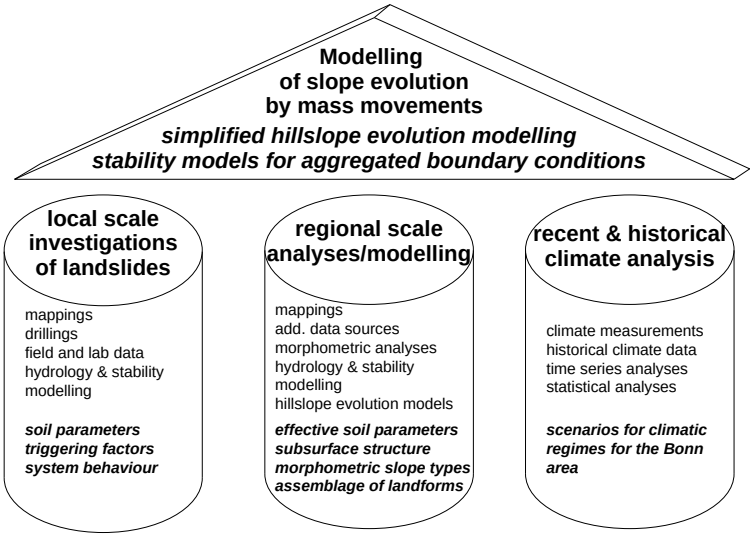

Figure 3.2.: Overview of the methodological parts to assess mass movement as part of slope development (see text). The applied methods are classified in the categories (1) local landslide investigation, (2) regional analysis, and (3) climate analysis. Two major modelling approaches in this study are hillslope evolution modelling and slope stability modelling.

surveying and geomorphologic interpretation is used to understand recent form sequences and to infer spatio–temporal models of landform change (Chapter 10, Chapter 13).

- Climate forcing is assumed to be independent (an external factor) to the hillslope systems under investigation in this study. Therefore, *parameterisation of climatic variability* is carried out as an individual research approach (Chapter 11).

- *Variability of slope stability and failure probability in a space and time* is assessed using results from the previous steps. Climate measurement and climate proxy data are used to model probability of slope failure under different climatic scenarios (section 12.2). Moreover, a hillslope evolution model is applied to complement qualitative geomorphological interpretations (section 13.2) of slope development. The different model approaches are combined to (1) assess their suitability within the framework of understanding hillslope systems, and to (2) develop a model of slope evolution for the research site (Chapter 13).

These modelling efforts are intended to allow an estimation of failure probability under changing morphometric, climatic and geological boundary conditions and relate these results to models of hillslope evolution. It should be noted, that the described assessment of temporal variability of slope stability is solely based on the influence of time and climatic variability on porewater pressure (compare Chapter 12) and changing geomorphometric and geologic hillslope conditions. Other long–term effects, like changing soil parameters (weathering, overconsolidation) or landuse change are not considered in this approach. The methods used in this study are sketched in Figure 3.3 and summarised in Table 3.1. Specific descriptions of individual methods, if necessary, are given the chapters, referenced by Table 3.1.

Table 3.1.: Research aims, methods and techniques with links to the corresponding chapters (columns 'described' and 'applied' inicate chapter numbers).

research aim	**method/technique**	**described**	**applied**
data capture (Chapter 8)			
subsurface structure of landslides	direct/indirect subsurface investigation	8.2	10
recent groundwater dynamics	dipmeter, pressure transducers	8.2	10
recent landslide activity	inclinometer, tiltmeter	8.2	10
soil properties	laboratory experiments	8.3,4	10
data storage (Chapter 9)			
meta information	XML–database	9.2	*
field & lab data	SQL–database (PostgreSQL)	9.2	*
geo data	GIS (ArcInfo)	9.2	*
data query & analysis	developed query tools	9.3	*
data analysis (Part VI)			
subsurface structures	regionalisation (GIS)	10	10
representative soil properties	statistics (R)	10	10
climatic variability	statistics (R)	11	11
modelling approaches (Part VII)			
groundwater modelling	developed groundwater model (PCRASTER)	12.2	12.2
stability modelling	stability models (Slope2d, CHASM)	5.2	12.1
morphometric analysis	profile analysis, multi–scale analysis, (HAP, OreGIS)	13.1	13.1
hillslope evolution modelling	simplified process model (HDS)	5.3	13.2
landform evolution modelling	conceptual modelling	6	13.3

* tools for data management are fundamental for this work and are therefore ubiquitous applied.

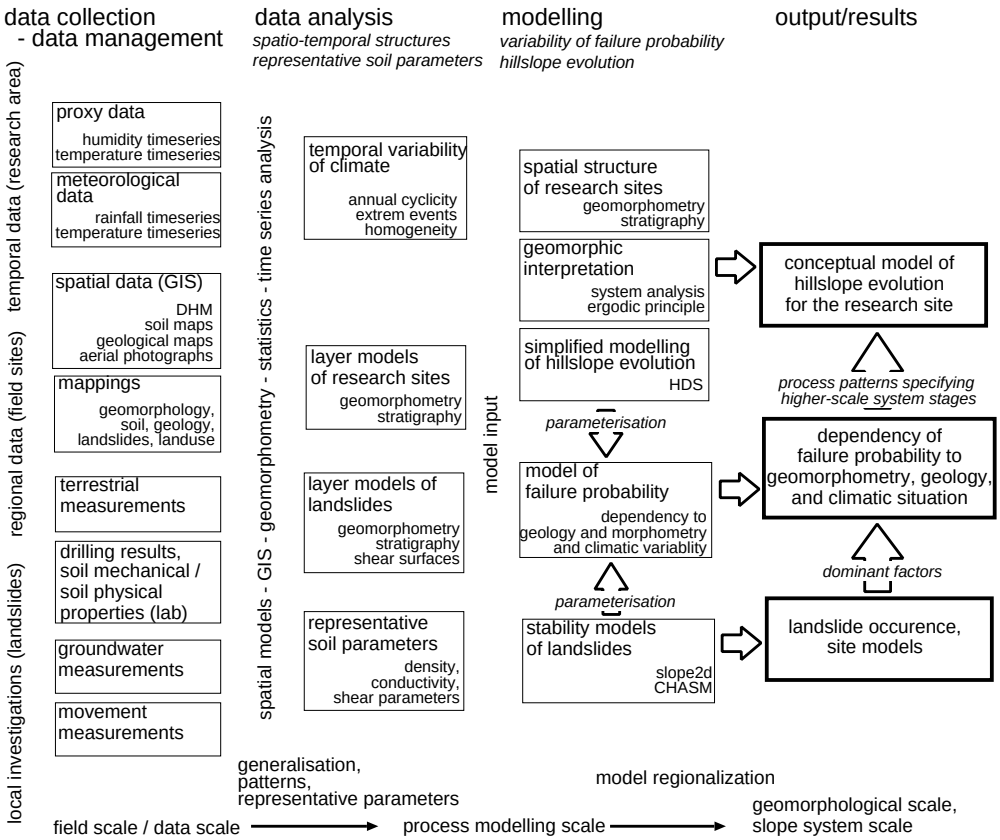

Figure 3.3.: Sketch of the methodologies used in this study, with an indication of their interconnections. The programme is classified into the steps data collection (Part V), data analysis (Part VI), and modelling (Part VII). Major scaling issues are steps from the data scale to the process scale (i.e. parameterisation), and from the process scale to evolutionary scale (i.e. model generalisation).

Summary

With respect to the ever–present uncertainty and the system complexity, it is argued, that detailed four dimensional modelling approaches, delivering sequences of geomorphological surfaces in time, might not be adequate. Target quantities might rather be major changes in the considered geomorphic system, i.e. system stages, response times, etc (compare Preston 2001). Therefore, application of detailed description of individual processes is inexpedient. Longer term process behaviour, e.g. frequency–magnitude characteristics of processes have to be considered. It is proposed to use model scenarios for generalised boundary conditions as an appropriate method in assessing the posed problem of process modelling and landform evolution. However, with respect to the available data sources in space and time and multiple scales in the system, different techniques have to be used (1) to assess field evidence for past geomorphic conditions, and (2) to regionalise scenario boundary conditions.

Therefore, this study is based on a conception combining local process (landslide) investigations with scenario models of boundary conditions and conceptual and modelling approaches in hillslope evolution. A variety of methods are applied, including local landslide investigation and slope stability analysis, geomorphometric analysis, simplified hillslope evolution modelling, and scenario modelling for failure probability. Fundamental objectives are (1) modelling of hillslope development using simplified modelling approaches, (2) modelling of failure probability under varying boundary conditions, and (3) combining these approaches in a model of hillslope evolution for the research area.

Part III.

Theoretical & methodological background

Introductory notes

Concepts and methods used in this study (compare Part II) reach from field investigation of local landslides, local and regional stability analysis, to models of hillslope evolution. Therefore, a variety of science fields and related techniques are involved. These include (1) soil mechanics, (2) process–based modelling of hillslope hydrology, slope stability and hillslope development, and (3) general concepts and theories of geomorphic systems and landform evolution. In the following chapters, short notes on the these topics are given as background information.

First, an introduction into soil mechanical concepts and related experiments, describing (mainly mechanical) characteristics of soils is given (compare Table 8.3, page 80). Secondly, some fundamental concepts in mathematical modelling of hillslope hydrology, slope stability, and hillslope evolution are introduced. The third chapter very shortly discusses fundamental approaches to geomorphic systems and landform evolution, including approaches from system theory and conceptual landform evolution models.

Note. *The landslides investigated in this work are rather shallow slides and flows in regolith. Therefore, only mechanical properties and behaviour of regolith are considered (i.e. rock mechanics is not considered).*

Note. *The laboratory techniques described in the following chapter often refer to the German Industrial Standard (DIN). Standards for the relevant experiments are published in DIN (1993).*

4. Soil mechanics

4.1. Basic properties and classification of regolith

Soils are, from a soil mechanical point of view, assemblages of particles, liquid (usually water) and gas (usually air), i.e. porous media. Important properties of these assemblages include the relationship of the different phases, the distribution of particle sizes, and the degree of plasticity (e.g. Barnes 1995, Kuntsche 2000, Lambe and Whitman 1979, Lang *et al.* 1996, Richwien and Golücke 1997, Sutton 1993).

Phase relationships

Some basic parameters describing the relation of phases in soils are listed in Table 4.1. Densities are usually expressed in units of mass per volume or unit weights (force per volume, i.e. scaled with gravity g). The lab experiments used in this study to derive the parameters indicated in Table 4.1 are (1) determination of bulk density (DIN 18125), (2) determination of moisture content by ovendrying (DIN 18121), and (3) determination of particle density (pycnometer method, DIN 18124). Additionally, maximum water content was derived by saturation experiments. An alternative experiment, designed to derive maximum water content as an index value, is the method after Enslin (DIN 18132).

Particle size distribution

Natural soils are mixtures of particles, particle sizes vary from µm to m. Particle size distributions are usually determined by two processes, sieving — mostly for gravels and sands (> 0.06 µm, DIN and BSCS), and sedimentation — for silts and clays. The sedimentation experiments used in this study to determine particle size distributions are the pipette method (DIN 19683) and the hydrometer method (DIN 18123) (see DIN 1993, Barnes 1995, Kuntsche 2000, for details). A series of modern techniques have been applied to facilitate and accelerate the test procedure (e.g. laser spectra methods). However, no approved cognitions are available for the comparability of the different methods (Beuselin *et al.* 1998, Konert and Vandenberghe 1997). The used techniques deliver fractions of particle sizes for specific particle size intervals (depending on the specific test procedure), which are usually displayed in a cumulative diagram (see Appendix C.1 for test results of this study). The data can be used to estimate grading characteristics (e.g. clay content c_T, silt content c_U, etc.). However, there is no internationally agreed classification for particle sizes. In this study, the German system was used (see AGBODEN 1994) which is similar to the British BSCS. Other classification systems (ASTM, USCS) vary considerably from these (compare e.g. Barnes 1995). A set of parameters is used to describe the shape of the grading curve (Barnes 1995).

$$U = \frac{d_{60}}{d_{10}}, \quad C = \frac{d_{30}^2}{d_{10} d_{60}}$$

U *uniformity coefficient*
C *coefficient of curvature*
d_i *i % of soil has particle size $< d_i$* [m]

Table 4.1.: Phase parameters of soils.

parameter	**symbol**	**calculation**
mass of particles	m_s	
mass of water	m_w	
volume of particles	V_s	
volume of water	V_w	
volume of air	V_a	
moisture content	w	$\frac{m_w}{m_s}$
void ratio	e	$\frac{V_a+V_w}{V_s}$
porosity	n	$\frac{V_a+V_w}{V_a+V_w+V_s}$
degree of saturation	S_r	$\frac{V_w}{V_a+V_w}$
particle density	ρ_s	$\frac{m_w}{V_s}$
bulk density	ρ_b	$\frac{m_s+m_w}{V_a+V_w+V_s}$
dry density	ρ_d	$\frac{m_s}{V_a+V_w+V_s}$

Plasticity — consistency limits

Consistency limits (or Atterberg limits) are used to describe plasticity and cohesiveness of soils (compare Whyte 1982). These properties depend on the amount of fines (silt, clay), on the mineralogy of the fines, and on moisture content. Clayey and silty soils will become softer (plastic) with increasing moisture content, until the mass transforms to a liquid state. If moisture content decreases until there is insufficient moisture to provide cohesiveness, soils become friable and finally solid. The transition between these states are described by the correspondong moisture contents. Although these definitions are somewhat unprecise, a series of test procedures have become common practice in soil mechanical investigations.

- *liquid limit* w_l— moisture content at the transition from plastic to liquid state.
  Two methods are available: the *penetrometer method* and the *Casagrande method* (which was used in this study) (Barnes 1995).

- *plastic limit* w_p— moisture content at the transition from plastic state to stiff (friable) state.
  A thread of soil is dried and repeatedly rolled over a glas plate until it shears at a diameter of 3 mm. The moisture content of this sample defines the plastic limit.

- *shrinkage limit* — moisture content at the transition from stiff (friable) state to soild state.
  The test consists of measuring the volume of an undisturbed sample as moisture content decreases. The shrinkage limit is the moisture content below which the volume ceases to descrease. The test procedure requires relatively high experimental expenditure (Barnes 1995). This test procedure was not carried out in this study.

A series of indices can be derived from these three quantities, which are frequently used in soil mechanics, including the *plasticity index* $I_p = w_l - w_p$, the *liquidity index* $I_l = \frac{w-w_p}{I_p}$, and the *activity* $I_A = \frac{I_p}{c_T}$ (c_T =clay content).

Organic content and chalk content of regolith
Organic content and chalk content of soils can be used to assess soil genesis and age, and, with respect to landslides, are possible indicators of old slip surfaces. The lab experiments used in this study to determine organic content are the method of ignition loss (DIN 18128) and the Lichterfeld method. The chalk content was determined using the Scheibler method (DIN 18129) (compare DIN 1993).

Classification of regolith
Different techniques and systems are used to compare and classify soil samples. Generally, different properties of soils (see above) are classified by qualitative terms.

Particle sizes — Generally, fine (> 0.06 µm, BSCS) and coarse soils are distinguished. More detailed, the ratios of the different particle sizes are used to express the dominant particle size classes of the soil (e.g. 'Silty CLAY'). As abbreviations for these particle size characteristics, the German system was used in this study (e.g. Tu for 'Silty CLAY', see AGBODEN 1994, Barnes 1995).

Plasticity — Qualitative terms (e.g. high plastic) are used to describe plasticity of soils. These are defined by classes of plasticity parameters as described above (see e.g. AGBODEN 1994, Barnes 1995).

Shear strength — Qualitative terms, ranging from 'very soft' to 'stiff' and 'hard' are used to classify strength of soils in the field. These terms are related to undrained shear strength (Barnes 1995).

Soil moisture — Terms ranging from 'dry' to 'moist' and 'wet' are used to classify soil wetness. However, as soil moisture is very much related to other properties, field interpretation may often be missleading, and soil moisture terms should always be used together with terms describing particle size and plasticity (Barnes 1995).

4.2. Mechanical behaviour of regolith

4.2.1. Pressure in regoltith

Stresses are caused by forces acting in a regolith body. These forces are produced by gravity acting as a volume force on the soil body itself, and by additional surface forces, produced by plants, buildings, streets etc. Stress fields in soils are not isotropic, i.e. usually horizontal stress does not equal vertical stress. In basic soil mechanics with respect to slope stability, usually only vertical stresses due to gravitational force are considered, "*but it is important to remember that horizontal stresses also act*" (Barnes 1995), and can be crucial for the failure process (e.g. Hattendorf 2001). For slope stability calculations, stress components of gravity acting in downslope direction τ, and perpendicular to a potential shear surface σ_N have to be considered (Figure 4.1).

$$\tau = \gamma_b z \sin\beta \cos\beta \tag{4.1}$$

$$\sigma_N = \gamma_b z \cos^2\beta \tag{4.2}$$

γ_b *bulk unit weight* [kN/m^3]
z *depth of shear surface* [m]

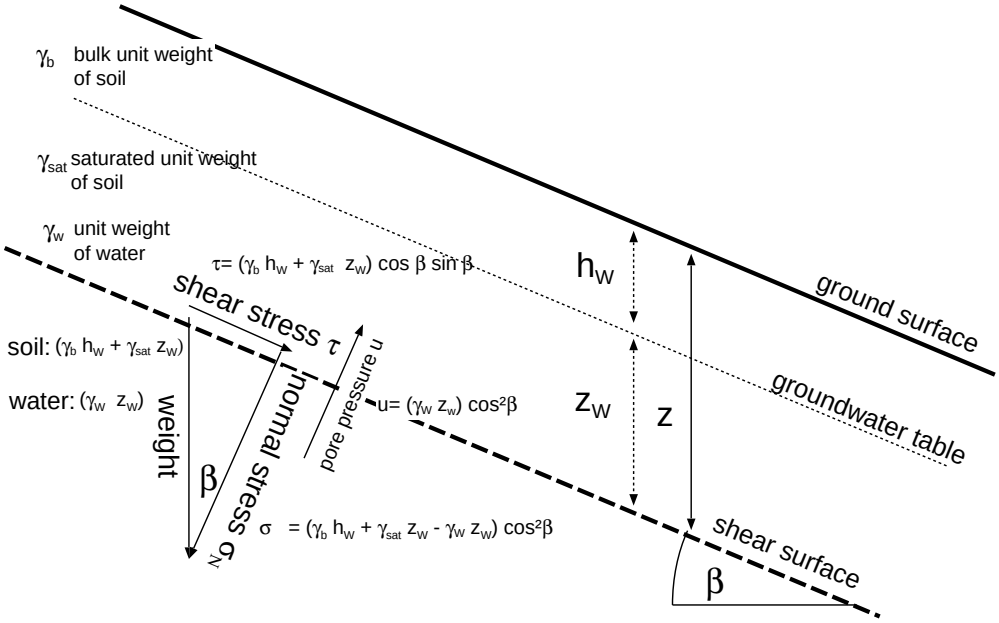

Figure 4.1.: Shear stress conditions on a plane, ground surface parallel shear surface.

β *slope angle* [°]

Equations 4.1 and 4.2 describe stress conditions occurring at a potential shear surface due to gravitational acceleration acting on a soil body under simplified conditions, i.e. a single shear plane at homogeneous depth z is assumed being parallel to ground surface (Figure 4.1), γ_b describes the average bulk unit weight of the entire soil column. σ_N is the normal stress accounting to friction, i.e. the stress between soil particles. Under the influence of groundwater (Figure 4.1), on the one hand, weight of soil water adds to pressure conditions, on the other hand, water pressure u is bearing parts of the applied weight. Therefore, effective normal stress σ'_N is introduced (the assumption is made, that the area of particles contacts is neglectable against the total area of applied stress, see e.g. Kenney 1984).

$$\tau = (\gamma_b(z - z_w) + \gamma_{sat} z_w) \sin\beta \cos\beta \tag{4.3}$$

$$\begin{aligned} \sigma'_N &= \sigma_N - u \\ &= (\gamma_b(z - z_w) + \gamma_{sat} z_w - \gamma_w z_w) \cos^2\beta \end{aligned} \tag{4.4}$$

γ_{sat} *saturated unit weight* [kN/m^3]
γ_w *unit weight of water* [kN/m^3]
z_w *height of groundwater table above shear surface* [m]

It shall be noted, that stress fields and stress propagations in soils, especially under human influence, e.g. through foundations, form complex research topics itself (e.g. Barnes 1995), which are not discussed here.

4.2.2. Deformation of regolith

Strain ε is the deformation of a soil body, measured as a ratio of the change in dimensions of the stressed body to its original dimensions. Type and degree of deformation depend on properties of the material and the applied stresses. Strain may involve changes in volume, length, displacement, or distortion. Rheology is a own research subject leading to a variety of complex models of material behaviour (Selby 1993). However, with respect to the applicability and parameterisation to real world conditions, simple models have been derived as mathematical idealisations for the complex response of soils to stresses.

Elastic behaviour

The spring is the mechanical model for an elastic material. Strain responds linear to stresses and no hysteresis effects are present. This linear relationship is known as *Hooke's law* (here displayed in one dimension), the related coefficient is *Young's modulus* E.

$$\sigma = E\varepsilon$$

σ *total stress* [kN/m^2]
E *Young's modulus* [kN/m^2]
ε *strain*

Hooke's law is an appropriate approximation for many materials and small strains. Real material, however, exhibit a curvilinear stress path, i.e. hysteresis effects occur (Selby 1993). Moreover, for larger strains, in most materials, behaviour changes from elastic to plastic behaviour at the yield point, the corresponding stress is the yield stress (compare Figure 4.3). A sliding block represents the mechanical model for *plastic* material. A stress of a certain magnitude (the yield strength of the material) has to be applied, after which deformation occurs at a constant rate.

Viscosity

A dashpot is the mechanical model for viscous materials. Strain is proportional to the applied stresses and time, i.e. strain change $\dot{\varepsilon}$ is proportional to stress.

$$\dot{\varepsilon} = \frac{\sigma}{\eta}$$

ε *strain*
σ *total stress* [kN/m^2]
η *dynamic viscosity* [Ns/m^2]

"*Viscosity ... is a concept that is applied to all fluids and solids and links the behaviour of the two types of material*" (Selby 1993).

Mixed behaviour

In reality, materials often exhibit a rheological behaviour, which can be described by variety of mixed models, e.g. elastoplastic behaviour, elasticoviscous behaviour, viscoelastic behaviour, or plasticoviscous (Bingham) behaviour (Selby 1993). Determination of idealised material properties, e.g. Young's modulus E, viscosity η, are fundamental issues in soil and rock mechanics.

Stress history: overconsolidation

Regolith is, in geological timescales, subject to changing stresses. Stress increase due to depositional loading, and during erosion phases effective stresses will descrease. A normally consolidated clay

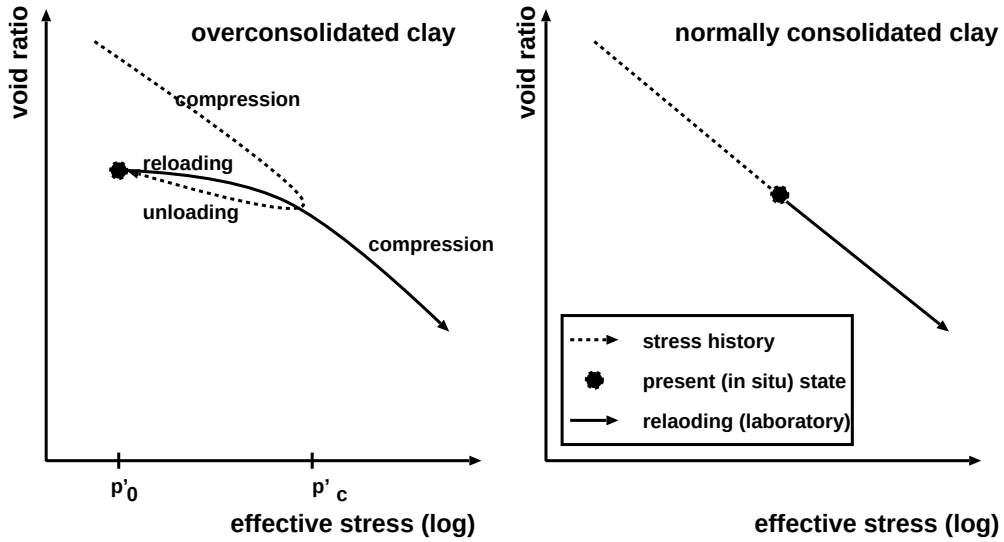

Figure 4.2.: Stress history of normal consolidated and overconsolidated clays, displayed as stress–void ratio diagrams.

has undergone deposition only, leading to a constant decrease of void ratio due to continuous consolidation (Figure 4.2). Overconsolidated clays have been subject to past stresses p'_c larger than present time stresses p'_0. A descrease of stress will result in in an increase of void ratio, but only the reversible components of volume change are recovered (Figure 4.2). The overconsolidation ratio $OCR = p'_c/p'_0$ is a measure for the degree of overconsolidation, which can be derived from logarithmic stress–void ratio diagram (from laboratory experiments) (Figure 4.2). Determination of p'_c is the crucial procedure and various problems have to be considered within that respect (compare e.g. Barnes 1995).

4.2.3. Strength of regolith

Failure conditions in stress–strain relationships

As discussed in the previous section, soil materials exhibit stress–strain relationships as a mixture of 'ideal' stress–strain models. A typical stress–strain curve (Figure 4.3) shows initial *elastic* behaviour, until, after a certain stress level (*yield stress* or *yield strength* τ_y) is reached, the soil structure will deform permanently in a more *plastic* manner. For loose sands and soft, normally consolidated clays (Barnes 1995), stress may increase, even at large strains, so a maximum strain must be defined (*ultimate strength* τ_u). For dense sands and stiff clays, the stress–strain curve shows a maximum, the *peak strength* τ_p. The *critical state strengh* τ_c is reached after a considerable amount of strain, when soils reach a constant volume state without changing void ratio. After a large amount of strain (often many cycles in a direct shear box experiment, see below), the soil particles at the shear surface might rearrange to a parallel orientation, leading to the lowest possible shear strength, the *residual shear strength* τ_r. "*This strength is very important in the reactivation of old landslides and is obviously more significant for platy minerals*" (Barnes 1995).

Therefore, different measures are available from the stress–strain curve to define failure of soils. For experimental reasons (high strains needed), it is often difficult to determine τ_u, τ_c, and τ_r separately, therefore experimental soil mechanics mostly focus on the determination of peak

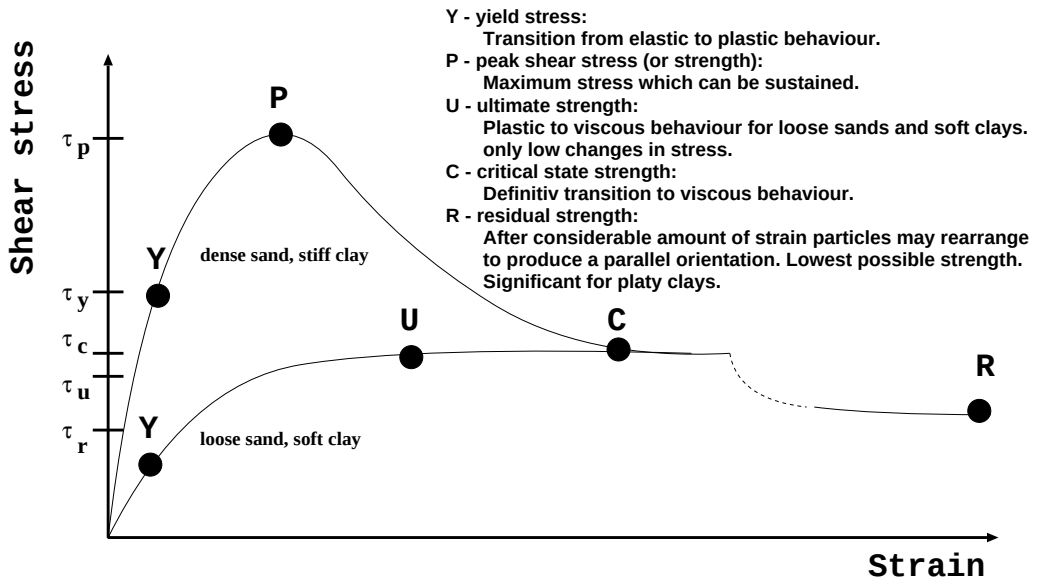

Figure 4.3.: Typical stress–strain curve of soil material (after Barnes 1995). Different points of this graph are of particular interest for understanding soil mechanical behaviour and for defining failure conditions.

shear strength τ_p and an approximation of residual strength τ_r. It has to be noted, that not only definitions of failure vary for regolith types, but also the modes of failure are varying with the involved material properties. Possible failure modes include uniform shear for soft plastic material, shear zones, and well–defined single shear planes in brittle material (Figure 4.4, compare Vickers 1978).

The Mohr–Coulomb relationship for shear strength

Shear strength, in either of the forms as discussed above, depends on many factors (see e.g. Selby 1993). Most important factors are cohesion (bonding of soil particles) and friction (frictional resistance between soil particles). Under the assumption of a linear relationship between friction and normal stress σ_N, the Coulomb–equation (Equation 4.5) is used to calculate shear strength τ_f.

$$\tau_f = c + \sigma_N \tan \phi \tag{4.5}$$

τ_f	*shear strength* [kN/m^2]
σ_N	*normal total stress* [kN/m^2]
ϕ	*angle of internal friction* [°]
c	*cohesion* [kN/m^2]

The linear relationship of Equation 4.5 is an approximation, therefore, in experimental determination (see below), a limited range of σ_N has to be chosen. Cohesion c is a measure of the shear strength, independent of normal stress. In its broadest sense, it is resulting from any force, which binds soil particles together. These forces are influenced by processes of chemical cementation, electrostatic bonding, or capillary tension. Effects like root cohesion (see e.g. Greenway *et al.* 1984, Phillips and Watson 1994) may add to this term. The term tan ϕ, which is used as the factor relating shear strength τ_f and normal stress σ_N, leads to the internal angle of friction ϕ, which can

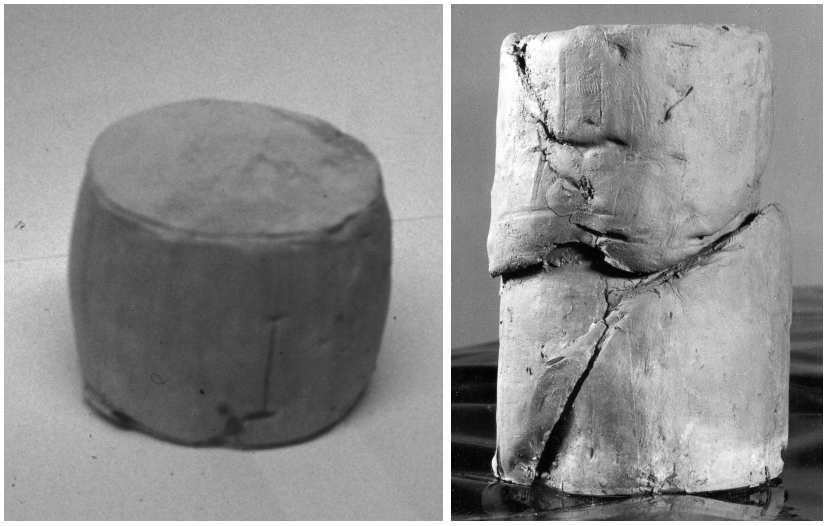

(a) Uniform shear for plastic Tertiary clay from the field site Melbtal.

(b) Distinct shear plane for grey Tertiary clay from the field site Dollendorfer Hardt.

Figure 4.4.: Different failure modes for materials types used in triaxial tests in this study.

be interpreted as the slope angle, under which a rigid block on a cohesionless shearplane will fail. Friction is the resistance to shearing resulting from two surfaces moving at a shear plane past each other. The contact of the mineral particles lead to frictional strength of the soil body. Therefore, friction is dependent on arrangment, size, shape and the internal resistance of the grains (Selby 1993).

Water and shear strength

In a moist, but unsaturated soil, the particles have an apparent cohesion (Selby 1993) caused by tension, and are under suction, so pore water pressure is said to be negative. For saturated soils, there are no tension forces and part of the normal stress is transferred to the water, i.e. pore water pressure is positive (upthrust effect, compare subsection 4.2.1). Cohesion c becomes effective cohesion c' (reduced by surface tension), and normal stress becomes effective normal stress $\sigma'_N = \sigma_N - u$. Therefore, the Mohr–Coulomb–equation reads as Equation 4.6.

$$\tau_f = c' + (\sigma_N - u) \tan \phi' = c' + \sigma'_N \tan \phi' \tag{4.6}$$

c' *effective cohesion* [kN/m^2]
σ'_N *normal effective stress* [kN/m^2]
ϕ' *effective angle of internal friction* [°]
u *porewater pressure* [kN/m^2]

Assuming a mass of soil above a planar shear surface parallel to the ground surface with end and side effects ignored (Figure 4.1), the shear strength can be calculated as follows.

$$\begin{aligned} \tau_f &= c' + (\sigma_N - u) \tan \phi' \\ &= c' + (\gamma_b (z - z_w) + \gamma_{sat} z - \gamma_w z_w) \cos^2 \beta \tan \phi' \end{aligned} \tag{4.7}$$

γ_w *unit weight of water* [kN/m^3]
z *depth of shear plane* [m]
z_w *height of water table above shear plane* [m]

In the more general case of two principal effective stresses σ'_1 (e.g. gravity) and σ'_3 (e.g. pressure due to unit weight of material), whereas the plane, σ'_3 is acting on, is inclined with β to the slip surface, normal stress σ'_N and shear stress τ define the so–called Mohr–circle which has the Mohr–Coulomb equation (Equation 4.5) as an envelope (compare e.g. Sutton 1993, Vickers 1978).

A range of laboratory techniques are available for measuring shear strength (compare Barnes 1995, Kuntsche 2000, Lambe and Whitman 1979, Lang *et al.* 1996, Richwien and Golücke 1997, Sutton 1993), including the widely used methods of direct shear box test and triaxial test, which were also used in this study.

Determination of shear strength by shear box tests
A soil sample is placed in a circular (in this study: 7 cm diameter; 2 cm height) or quadratic steel box (the shear box), which has separated upper and lower sections, defining a shear plane. These two sections can be separately moved against each other using e.g. a geared electric motor. Normal stress σ_N is applied by weights (or hydraulically) on top of the shear box. Vertical and horizontal displacements ε are monitored. Horizontal stresses τ are measured. If the apparatus is controlled by an computer device, the test can be carried out either strain–controlled (constant strain, this method was used in this study) or stress–controlled (constant stress). The direct shear box test delivers a stress–strain curve and a strain–volume (height) change curve for each test procedure (see Appendix C.4). Repeated tests with the same sample type and different normal loads lead to a series of tupels of shear strength τ_f and normal strength σ_N, from which cohesion c and friction angle ϕ can be estimated using the Moore–Coulomb model (Equation 4.5). In this study, an apparatus as shown in Figure 4.5 was used.

Several disadvantages have to be considered.

- A pre–defined, artificial shear surface is used.
- Normal stress is applied only in one direction, the in situ conditions consider a spatial stress field.
- The area of shearing surface changes with the progress of shearing.
- The apparatus permits only small shearing distances (in this study 1.5 cm).
- Pore water pressure cannot be controlled.

To overcome some of these problems, the more complex triaxial test was designed.

Determination of shear strength by triaxial tests
"*This apparatus was developed in the 1930s and has largely replaced the direct shear test in commercial laboratories*" (Barnes 1995). Different than the direct shear test, the cylindrical sample is

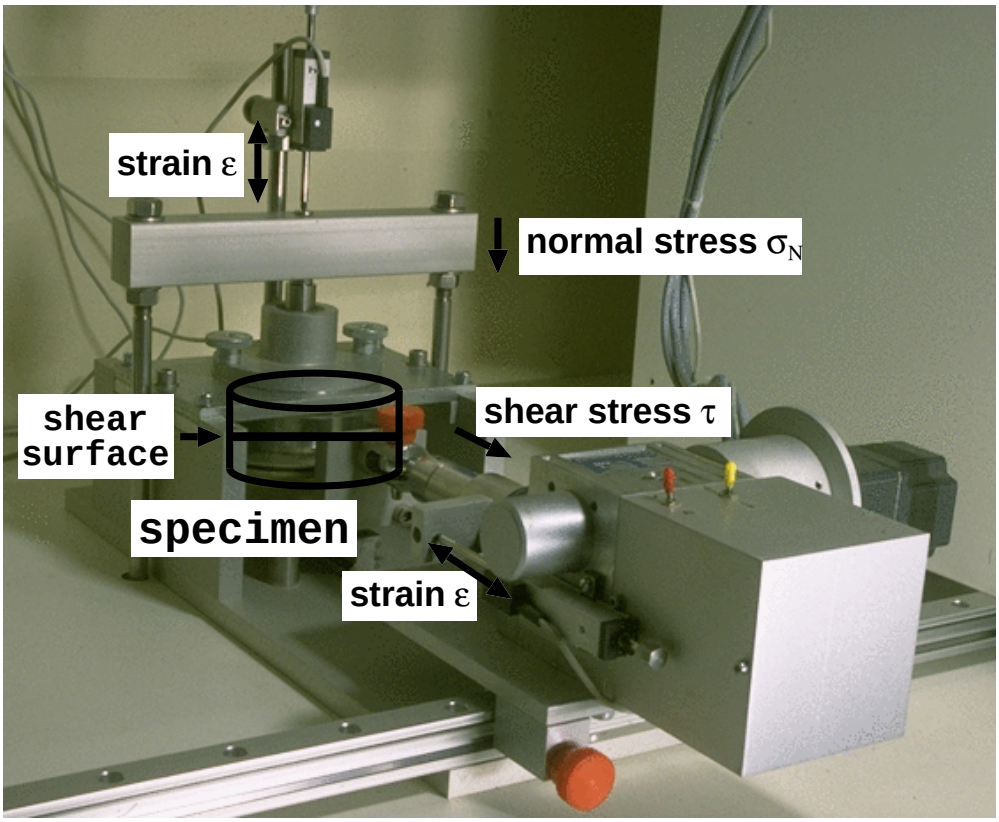

Figure 4.5.: Direct shear box (Dieter Moser GmbH Systemtechnik), used in this study.

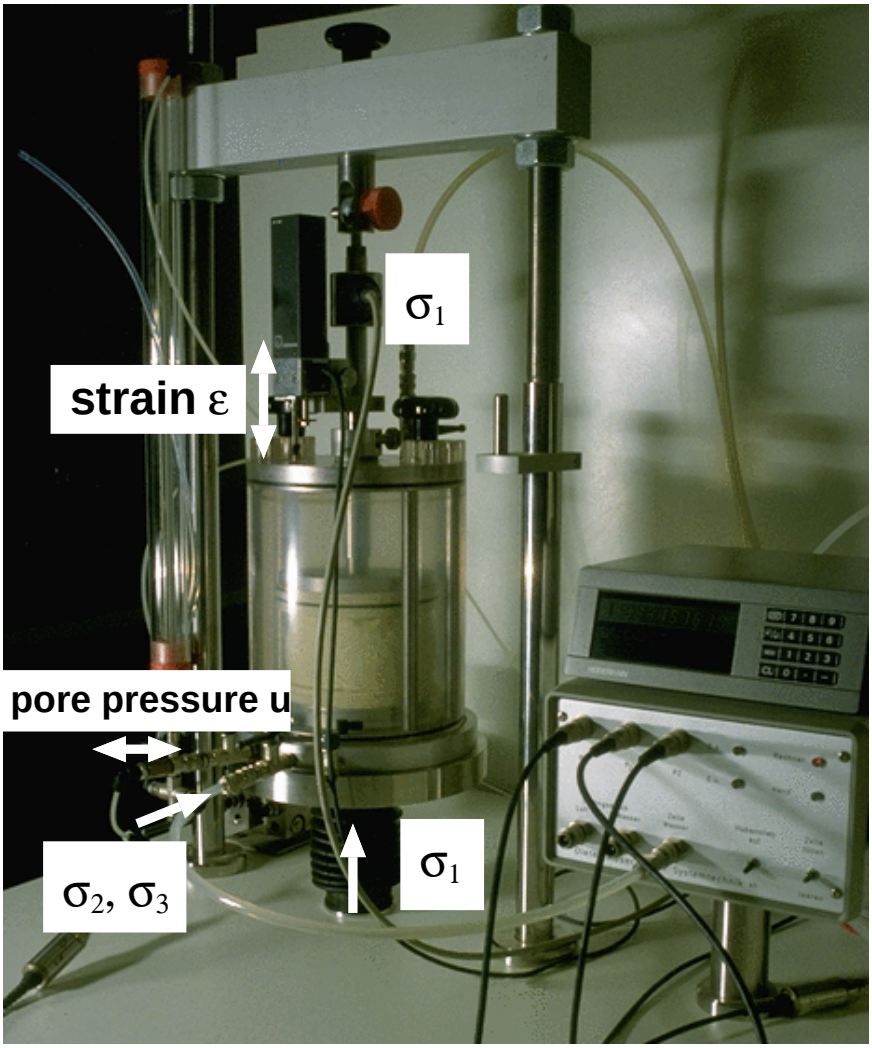

Figure 4.6.: The Triaxial apparatus (Dieter Moser GmbH Systemtechnik) used in this study.

placed in a rubber membrane between caps in a cell (the 'triaxial cell') filled with fluid (typically water, less often oil). An hydraulic load can be applied to the specimen via the upper or the lower cap. The related force and strain can be controlled and measured. Soil water pressure and the cell water surrounding the specimen can be controlled. In this study, an apparatus as shown in Figure 4.6 was used.

Therefore, the major variables can be controlled (compare Vickers 1978), i.e. stresses in vertical (σ_1) and horizontal ($\sigma_2 = \sigma_3$) directions, pore water pressure u and pore water volume change, and strain ε by vertical displacement (more complex constructions allow measurement of volumetric strain).

Different test procedure can be performed, including the following experiments (see e.g. Barnes 1995, Kuntsche 2000, Sutton 1993, for details).

Unconsolidated, undrained test (UU). No consolidation is perfomed, vertical load σ_1 is applied rapidly, and no drainage of soil water is permitted, leading to an increase of pore water pressure u. This test type is used to measure undrained shear strength c_u.

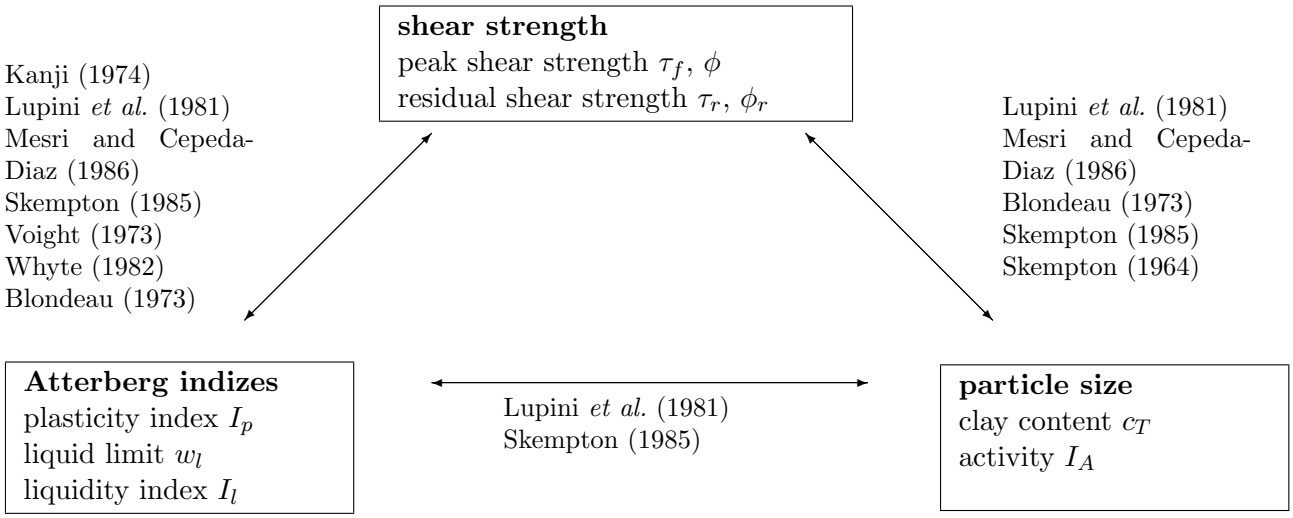

Figure 4.7.: Some relationships of soil mechanical properties. Shown are generalized relationships from literature review.

Consolidated undrained test (CU). Constant cell pressure is applied, which increases pore pressure. Consolidation and saturation of the sample is allowed. Saturation degree can be controlled by slightly increasing cell pressure, and testing reaction of pore pressure ('B–test'). If consolidation is reached (no significant strain), the sample is sheared by increasing σ_1, while no drainage is permitted and pore pressure u is logged. This test type is used to estimate effective strength parameters c' and ϕ'.

Drained test (D). Constant cell pressure is applied, but soil water drainage is allowed. The vertical load σ_1 is then applied at sufficiently rates, that pore pressure u does not increase, and soil water change is logged.

The logged measurements can be plotted as stress–strain curves, whereas stress usually reads as the deviator stress $\sigma_1 - \sigma_3$ or the stress ratio $\frac{\sigma_1 - u}{\sigma_3 - u}$. Stress path can be plotted as $0.5(\sigma_1 - \sigma_3)$ against $0.5(\sigma_1 + \sigma_3)$ to determine the Mohr–envelope (see above) and the shear parameters (see Appendix C.4 for test results of this study). For details of test procedure see e.g. Vickers (1978).

4.3. Variability and interdependencies of soil parameters

A remarkable amount of work have been carried out on the variability of soil parameters and the related effects on modelling and analysis approaches in environmental sciences (e.g. Merz 1996, Merz and Plate 1997, Merz and Bárdossy 1998, Mulder and van Asch 1988, Schmidt *et al.* 1998). These studies have led to (1) quantifications of the order of magnitude of possible variations of soil properties (compare Appendix E), (2) establishment of correlations between soil parameters, and (3) qualitative and quantitative dependencies of soil parameters to spatial Geo–structures (e.g. landform surface characteristics). However, a large uncertainty remains with respect to the quantification of spatial relationships and intercorrelations of soil parameters. Obviously, it is not easy

to find uniform descriptions for these interactions on a physical basis.
Soil parameters, especially soil mechanical parameters, show a high variability (see the examples from Chowdhury 1984), not only in a spatial context, but also for a specified location. A controversy exists with respect to the statistical distribution of soil parameters (compare e.g. Mulder and van Asch 1988). In slope stability studies, commonly used assumptions are a normal, log–normal or beta distributions (Chowdhury 1984).
There is an extensive literature on relationships between different measured soil properties (e.g. Blondeau 1973, Lupini *et al.* 1981, Whyte 1982). In particular, efforts have been made to establish functional relationships between shear strength and other measures, which are more easy to determine (as clay content or consistency). Most of these relationships relate shear strength τ_f (or ϕ) to clay content or consistency limits (Figure 4.7). Both cohesional and frictional components of shear strength are clearly influenced by presence of clay particles. Clay content, on the other hand is related to plasticity and liquidity of regolith (Lupini *et al.* 1981, Skempton 1985). Therefore, these interrelationships can be scetched as Figure 4.7. However, the derived relationships, show considerable variations. Müller (1987) presented an analysis of correlations and statistical distributions of soil parameters of the Siebengebirge near Bonn.
A variety of studies indicated, that, besides a large variability, soil parameters also exhibit a degree of spatial organisation, which can be expressed as relations to other parameters of landforms (Brinkmann *et al.* 2001). Numerous studies indicated the relevance of these *geomorphic structures* for environmental processes (e.g. Merz 1996, Merz and Plate 1997, Merz and Bárdossy 1998, Schmidt *et al.* 1998). Other studies showed that these spatial structures tend to be not universal (e.g. Mulder and van Asch 1988). Hence, universal (or better: physical) laws for these relationships are missing, but, because of their applicable value, are strongly required. This question is clearly related to the fundamental research problem of this study, i.e. the understanding of organisation in long–term landform development (i.e. form–process interaction, see Part II).

5. Hillslope processes

5.1. Groundwater hydrology

Fundamental flow laws

As indicated above, soil water strongly influences stress and strength conditions. To model soil water dynamics, matter transport laws have to be established representing the interactions and flows of the system of hillslope hydrology. A series of flow laws have been developed to describe fluid flow in porous media (either saturated or unsaturated), and surface flow behaviour (compare e.g. Anderson and Burt 1990, Baumgartner and Liebscher 1990, Dingman 1994, Kirkby 1978, Kutilek and Nielsen 1994). Most important for this work are flows in porous media used in modelling groundwater hydrology. For laminar flow (low Reynolds numbers), the fluid movement can be described by *Stokes' equation*. However, solving Stokes' equation for an irregular composition of grains within soils is not feasible. Therefore, macroscopic models have to be found, relating measurable flux properties to aggregated material parameters. The widely used *Darcy's law* describes the average flow velocity $\vec{v}$ of a fluid in saturated or unsaturated porous media (here displayed for isotropic conditions).

$$\vec{v}(\vec{x},t) = -k(\vec{x},w)\nabla\psi(\vec{x},t) \tag{5.1}$$

$\vec{v}$	*average flow velocity of fluid in a porous media* [m/s]
k	*hydraulic conductivity* [m/s]
w	*moisture content* [1]
ψ	*total hydrologic potential* [m]

The hydraulic ψ potential can be calculated as the sum of gravitational potential, matrix potential, osmotic potential, pneumatic potential, and external potential (Kutilek and Nielsen 1994). Potential units are defined here as the equivalent height of a water column. The continuity equation for soil water $\nabla\vec{v} + \partial_t w = 0$ leads to a formulation for soil water dynamics termed as *Richard's equation*.

$$\partial_t w = \partial_x(k\partial_x\psi) + \partial_y(k\partial_y\psi) + \partial_z(k\partial_z\psi) \tag{5.2}$$

The infinitesimal character of these equations applies only in the macroscopic sense given by Darcy's law: The considered volume element has to be macroscopically small and microscopically large to reflect average flow characteristics of the porous medium. Richard's equation is a nonlinear partial differential equation of second order and can be solved analytically under certain conditions.

In the majority of applications, the total potential ψ is defined as the sum gravitational potential and matrix potential $\psi = \psi_g + \psi_m$, where the the matrix potential ψ_m subsumes effects of absorption, capillarity, as well as of the weight of the water column. The total potential is often written as $H = h + z$, where z is defined by a reference level and the pressure head is $h > 0$ for

saturated soils and $h < 0$ for unsaturated soils. For static, saturated conditions, i.e. $\partial_t w = 0$, $\vec{v}(\vec{x}) = \vec{v}$, and $k(\vec{x}) = k_s$, Darcy's law is only variable in space $\vec{v} = -k_s \nabla \psi$. For unsaturated conditions, $k = k(w)$ has to be determined.

Permeability of regolith

Permeability of soils is a key property with respect to the assessment of soil water and groundwater flow problems. Permeability is dependent on the nature of voids of the soil, the saturation degree of the voids, and the properties of the fluid (unit weight and viscosity). Darcy's law (Equation 5.1) states, that flow velocity in porous media is proportional to hydraulic gradient, and the linear factor is the conductivity k. Conductivity k is a convenient measure for permeability of soils, expressing the flow velocity at hydraulic gradients of 1. Some relationships have been proposed to derive k from particle size characteristics (compare e.g. Barnes 1995). However, as conductivity shows a high variability due to local soil variations as macropores, these relationships tend to be low significant. In general, the order of magnitude of the permeability under saturated conditions k_s can be estimated sufficiently from soil type (Appendix E), i.e. from particle size distribution and porosity. Moreover, dependencies of k on moisture content and pressure head have to be derived (known as soil water retention curves) to assess unsaturated flow problems. Therefore, a series of simplified relationships has been proposed. A frequently used model was derived by VAN GENUCHTEN and MUALEM (compare e.g. Kutilek and Nielsen 1994). Although a series of rules and relationships have been developed, laboratory experiments are needed to quantify conductivity for local regolith conditions. Two common experiments were used in this study to determine the saturated conductivity k_s of soils.

constant head permeameter (DIN 18130). Water is flowing at a constant rate q through a saturated sample of cross sectional area A, while a hydraulic head h is applied over an effective sample length L (see e.g. Barnes 1995). The saturated conductivity k_s can be calculated from Equation 5.3.

$$k_s = \frac{qL}{Ah} \tag{5.3}$$

k_s	*saturated conductivity* [m/s]
q	*flow rate* [m^3/s]
L	*effective sample height* [m]
A	*sample cross sectional area* [m^2]
h	*hydraulic head* [m]

falling head permeameter (DIN 18130). Water flows down a standpipe (cross sectional area a) through a saturated sample of cross sectional area A and length L. Water height in standpipe is measured at time intervals (h_0,t_0), (h_1,t_1). The saturated conductivity k_s can be calculated from Equation 5.4.

$$k_s = \ln \frac{h_1}{h_0} \frac{aL}{A\,(t_1 - t_0)} \tag{5.4}$$

k_s *saturated conductivity* [m/s]
L *sample height* [m]
A *sample cross sectional area* [m^2]
a *standpipe cross sectional area* [m^2]
t_i *time steps* [s]
h_i *hydraulic head at time step* t_i [m]

5.2. Slope stability

5.2.1. Types of slope failure

Mass movements, or more colloquially referred to as landslides, exibit many forms. Various classification schemes for mass movements have been proposed (e.g. Dikau *et al.* 1996b, Hutchinson 1988, Varnes 1978, see Table 5.1). These classification schemes are based on a series of landslide parameters describing movement mechanics, geometry, material, velocity, moisture content. However, in 'real–world' conditions often gravitational phenomena show complex behaviour involving different types of failure. For mechanical consideration, i.e. with the background of stability analysis, important factors include movement mechanism and geometry, soil moisture and groundwater conditions, and material properties. Therefore, a *landslide classification* is a first important step in either geomorphological and geotechnical analysis (Barnes 1995).

Table 5.1.: Classification of mass movements (after Dikau *et al.* 1996b).

Type	**Rock**	**Debris**	**Soil**
Fall	rockfall	debris fall	soil fall
Topple	rock topple	debris topple	soil topple
Slide (rotational)	single (slump) multiple successive	single multiple successive	single multiple successive
Slide (translational)	block slide	block slide	slab slide
Planar	rockslide	debris slide	mudslide
Lateral spreading	rock spreading	debris spread	soil (debris)spreading
Flow	rock flow (Sackung)	debris flow	soil flow
Complex	e.g. rock avalanche	e.g. flow slide	e.g. slump–earthflow

5.2.2. Stability of slopes — the model of the Factor of safety (FOS)

Stress and strength conditions at a point on a potential shear surface determine the force balance, i.e. if stress exceeds strength, the potential mass will become unstable. However, in the case of movement, the static assumptions of stress and strength as described in Chapter 4 are not applicable to assess movement dynamics. As soil mechanics mostly considers only prevention of a collapse, limit equilibrium methods are usually applied (Lambe and Whitman 1979), which consider only static (pre–failure) conditions. Therefore, frequently the factor of safety FOS is used.

$$FOS = \frac{\sum resistingforces}{\sum drivingforces}$$

Table 5.2.: Parameters usually applied in analysis of slope stability. The spatial resolution depends on model type and site information.

parameter	**symbol**	**typical unit**
slope angle	β	$^\circ$
depth of shear surface	z	m
height of groundwater table	h	m
effective cohesion	c'	kN/m^2
root cohesion	c_{root}	kN/m^2
effective angle of internal friction	ϕ'	$^\circ$
bulk density	ρ_b	g/cm^3
saturation density	ρ_{sat}	g/cm^3
load (trees, buildings, etc.)	q	kN/m^2

$FOS < 1$ leads to failure, whereas a mass with $FOS > 1$ is stable. Resisting and driving forces can be calculated from strength and stress conditions as descibed in Chapter 4 (see subsection 5.2.3). To parametrise the relevant equations, a series of variables are required (Table 5.2).

5.2.3. Analysis of slope stability

A series of methods have been proposed to calculate stability of slopes under various assumptions, modifying complex real–world conditions to models of more or less simple boundary conditions (Barnes 1995, Bishop and Morgenstern 1960, Kuntsche 2000, Lambe and Whitman 1979, Morgenstern 1965, Sutton 1993). Most of these models have been developed in engineering geology under rigorous practical aspects, therefore they represent a compromise between precision of description of process behaviour and practical applicability.

Planar translational slides

Simplest assumption is a mass of soil above a planar shear surface parallel to the ground surface with end and side effects ignored (the so–called *Infinite Slope Model*, see Figure 4.1). The factor of safety can be calculated as (see Equation 4.7 and Equation 4.1).

$$FOS = \frac{c' + (\gamma_b(z - z_w) + \gamma_{sat} z_w - \gamma_w z_w)\cos^2\beta \tan\phi'}{(\gamma_b(z - z_w) + \gamma_{sat} z_w)\sin\beta\cos\beta} \tag{5.5}$$

FOS *Factor of safety*
c' *effective cohesion* [kN/m^2]
γ_b *bulk unit weight* [kN/m^3]
γ_w *unit weight of water* [kN/m^3]
z_w *water table height above shear surface* [m]
z *depth of shear surface below ground surface* [m]
β *slope angle* [$^\circ$]
ϕ' *effective angle of internal friction* [$^\circ$]

For applying the Infinite Slope Model, a series of parameters are required (compare Table 5.2). Deriving these parameters mainly involves a definition of geometry: (i) ground surface, (ii) shear surface, (iii) groundwater table, and the estimation of material properties at the shear surface (c', ϕ') and of average properties of the material above the shear surface (γ_b). A series of studies showed the capability of this model to estimate potential unstable areas (van Asch *et al.* 1992, Möller 1999, Mulder 1991, Rogozia 2000, Terlien *et al.* 1996).

However, "*this type of analysis is applicable to granular soils, soils with no cohesion (c' =0), soils with bedding or laminations dipping parallel to the slope, soils with weathering profiles producing upper weaker horizons and slopes where there has already been a shallow slab slide such that the shear strength on the slip surface has reduced to its residual value*" (Barnes 1995).

The infinite slope model calculates a local factor for a infinitesimal point assuming that the boundary conditions of the whole slope are like the ones in the point. No internal frictional forces are considered. Hence, it represents a strongly simplfied situation, which has to be considered in applications.

A series of (even more simple) situations can be derived from the general case of a planar slide (Barnes 1995, Lambe and Whitman 1979):

Dry cohesionless slope: $c' = 0, z_w = 0$**.** This situation represent the often used sandpile experiment (or a sliding block). Because of $FOS = \frac{\tan\phi'}{\tan\beta}$, the critical slope angle β ($FOS = 1$) yields $\beta = \phi'$.

Wet cohesionless slope: $c' = 0, z_w = z$**.**

$$FOS = \frac{(\gamma_b - \gamma_w)\tan\phi'}{\gamma_b \tan\beta}$$

Cohesionless slope: $c' = 0, \gamma_b \approx \gamma_{sat}$**.**

$$FOS = \left(1 - \frac{\gamma_b - \frac{z_w}{z}\gamma_w}{\gamma_b}\right)\frac{\tan\phi'}{\tan\beta}$$

Cohesionless, suction controlled slope: $c' = 0$**.** "*The capillary zone above the water table in a fine sand or silt can be significant, and will produce negative pore pressures within this zone given by $u = -\gamma_w h$*" (Barnes 1995).

$$FOS = \frac{\tan\phi'(\gamma_b z\cos^2\beta - \gamma_w h)}{\gamma_b z \sin\beta\cos\beta}$$

Layered soil. Barnes (1995) describes a method analysing the depth dependency of shear stress τ and shear strength τ_f as a method to provide information about potential shear surfaces in a layered soil with different layer properies.

Rotational failure

"*The most common form of failure of a slope in cohesive soil is a rotational slip along a curved surface ...*" (Sutton 1993). Therefore, a series of analysis procedures with varying complexity have been developed. The following list gives an crude overview of the common standard techniques.

Method of slices — Fellenius method. The sliding mass is devided into a number of vertical slices of uniform width. With sufficiently large number of slices, the shear surface for each slice can be approximated by a plane, and individual stress–strength conditions can be calculated accordingly (see above). It is assumed that interslice forces balance each other, therefore the factor of safety can be calculated from the sum of driving forces and the sum of resisting moments. This solution underestimates the factor of safety up to 20% (Sutton 1993).

Method of slices — simplified Bishop method. Different than the Fellenius approach, normal interslice forces are not equal in this model, leading to an equation which has to be solved iteratively (Sutton 1993).

Stability analysis charts — Taylor, Bishop–Morgenstern, Barnes. A series of easy–to–use stability charts have been developed by various authors for rapid field assessment (e.g. Barnes 1995). Usually, diagrams are provided to obtain stability coefficients from variables like slope angle, friction angle and depth of shear surface. These stability coefficients can be used in simple equations to calculate a safety factor.

Non–circular slip surfaces — method of Janbu

For non–circular shear surfaces, the sliding mass can also be seperated into slices. Assuming overall horizontal equilibrium of interslice forces, an average factor of safety along the slip surface can be calculated iteratively using the so–called 'Janbu–Method'. Other methods for non–circular slip surfaces include the Morgenstern–Price method and the method of wedges (Barnes 1995).

It shall be noted, that the presented models represent classic standard techniques in modelling of slope stability (which were utilised in this study, see Chapter 12). They imply considerable simplifications to 'real' world conditions. A variety of more sophisticated approaches exist, by calculating stress fields based on finite element of finite difference methods (e.g. Hattendorf 2001).

5.3. Mathematical models of landform evolution and slope development

Classical approaches: hillslope evolution modelling

A series of approaches have been presented towards modelling of hillslope evolution (e.g., Ahnert 1987a,b, 1988, 1992, Armstrong 1980, 1987, Kirkby 1992). They are mostly based on simple assumptions of individual processes and a sediment routing according to the conservation of mass on a regular spatio–temporal discretisation (Equation 5.6).

$$\begin{aligned} -\frac{\partial z(x)}{\partial t} &= \frac{\partial q}{\partial x} \\ q &= f\left(\frac{\partial z}{\partial x}, x, z, \ldots\right) \end{aligned} \tag{5.6}$$

z *elevation* [m]
q *sediment flux* [m^3/ms]

As an example of these approaches the model HDS by Richard Tran Mills is presented, which is based on work of Kirkby (1992). This model was applied in this study to model hillslope evolution of the field area Melbtal (section 13.2). Richard's n-store Hillslope Dynamics Simulator (HDS) simulates the evolution of hillslope profiles through time using a linear–store model based on the mass balance equation. The effects of landslides, wash, and creep/solifluction/rainsplash are modelled using simplified process laws. HDS is a Windows application that utilises a fully graphical user interface and allows visualisation of evolving hillslopes (section 13.2), as well as output of numerical data to ASCII files. It is written in Microsoft Visual Basic 5, and the source code is freely available (http://stderr.org/ hds/). HDS reads a hillslope profile in ASCII format as input. This is broken down to a user defined number of elements, which are used to route sediment according to the following process models (see Table 5.3 for parameters).

Solution processes. sol_k — **solution rate (Kirkby type)** [µm/a]**.** Kirkby (1992) modelled the sediment flux S out of a cell due to solution as being linearly proportional to the distance x from the divide $S = xsol_k$. In Kirkby's original approach (Kirkby 1992), solution does not operate unless the downslope gradient exceeds g_{sol} [°] ('solution threshold angle').
sol_c — **uniform vertical solution rate** [µm/a]**.** The rate of solution should somehow increase with distance from the divide, but the linear relationship (see above) give poor results, as some sort of solution should occur around the divide as well. Hence, a solution as a rate of uniform vertical lowering is also modelled $S = sol_c$.

Creep, splash & wash processes. The total sediment flux S out of a cell from creep and wash processes is dependent on distance from the divide x and the hillslope gradient g. Therefore, for large x, S increases with x, leading to convex hillslope profiles (Kirkby 1992).

$$S = K(1 + \frac{x}{u})g \tag{5.7}$$

Landslide processes. Landslide occurrence and magnitude is controlled by hillslope gradient g. Landslides can occur above a threshold gradient g_ψ with an average rate a and a travelling distance h_0. Above a second threshold gradient g_t, landslides will never come to rest, i.e. the debris is leaving the modelled system.

$$D = ag(g - g_\psi), \quad g_\psi < g > g_t \tag{5.8}$$
$$h = \frac{h_0}{g_t - g}$$

basal removal. A fixed proportion b of the sediment entering the basal cell is removed with each iteration.

As this model approach indicates, the governing equations rely on relatively simple assumptions about relationships of process rates to geomorphometric properties (mostly slope angle and some parameterisation of the distance to the divide). Nevertheless, as these types of models simulate interaction of several processes, they are useful for assessing coupled system behaviour under varying boundary conditions (see section 13.2, compare e.g. Ahnert 1976, Roering *et al.* 2001).

Four dimensional approaches for modelling landform development

A series of approaches have been presented, modelling the temporal change of a landform surface (Braun and Sambridge 1997, Coulthard *et al.* 1998, 1999, Willgoose *et al.* 1991) (see Coulthard 2001, for a review). As it is the case for the two dimensional approaches, these models are essentially mass balance models, routing sediment through an arbitrary spatio–temporal discretisation of terrain (three dimensional version of Equation 5.6). Most models use comparatively simple process descriptions. Recently, Coulthard *et al.* (1998) presented a four dimensional, high resolution landform evolution model with detailed descriptions of individual processes. However, problems of these modelling approaches remain with regard to their ability to represent sediment flux and related landform change at large spatio–temporal scales (Preston *et al.* rev). First, parameterisation problems increase with higher degree of accuracy in process representation. Moreover, validation is impossible as related field data are missing. As discussed in Chapter 2, those detailed modelling approaches might be not appropriate or 'over–sized' for assessing the problem of landform evolution with high degrees of uncertainties. Considering the complexity of four dimensional landform

Table 5.3.: Model parameters of HDS.

symbol	unit	parameter	description
solution parameters			
sol_k	[µm/a]	Kirkby–solution rate	solution rate, proportional to the distance from the divide
g_{sol}	[degree]	solution threshold angle	solution does not operate unless the downslope gradient exceeds g_{sol}
sol_c	[µm/a]	uniform solution rate	solution rate of spatially uniform lowering
creep, splash & wash parameters			
K	[cm/a]	creep/splash rate	average creep/splash rate, to be scaled with distance from the divide and gradient
u	[m]	wash distance	distance at which wash becomes greater than creep
landslide parameters			
a	[mm/a]	rate of free degradation	average rate of erosion due to landsliding
g_ψ	[°]	landslide threshold angle	landslide threshold angle below which there is no landslide activity
g_t	[°]	talus angle	talus angle above which slides will never come to rest
h_0	[m]	mean travel distance	mean travel distance indicates the average runout distance for landslides, which should be roughly their mid–height
basal removal			
b	[1]	basal removal	proportion of sediment entering the basal cell removed with each iteration

development, it is questionable, if process–based modelling can adequatly represent the system behaviour. Therefore, Beven (1996) argues, that this model type should be used to predict plausible patterns in landform evolution. Roering *et al.* (1999) presented an approach into that direction by modelling general geomorphometric relationships of evolving three dimensional topographic surfaces.

6. Geomorphic systems and theories of landform evolution

6.1. General models of landform evolution

The first approaches in modelling landform evolution were looking at general laws within the evolution of landforms (see Melhorn and Flemal 1981, for an overview). The general principles of long–term evolution of landform surfaces, formulated by Gilbert (1877) have had deep impacts on geomorphology until today. However, Davis (1899) invented the first general theory of landscape development, the famous 'Geographical Cycle', which has been applied to a variety of environments (see Melhorn and Flemal 1981). Latter approaches into that direction, especially by Penck (1924) and King (1953), emphasised dynamic behaviour of landscape systems leading to fundamental concepts as 'parallel retreat' or 'knickpoint migration' (see Melhorn and Flemal 1981). Whereas these theories trying to approach the problem of general, long–term development of landscape systems, field evidence often exhibits a large diversity and lead to contradictions. Therefore, since approximately 1960, process–based approaches have become popular, thereby revisiting the early ideas of Gilbert, and leading to concepts as 'dynamic equilibrium' (Hack 1960), 'complex response', or 'frequency and magnitude' (e.g. Schumm and Lichty 1965), which try to express general geomorphic principles rather than to explain general landform evolution (see below). It has become obvious, that research in landform evolution deals with a highly complex system, i.e. the landscape system. Therefore, reductionistic approaches (as general theories of landform evolution) may not lead to an adequate understanding of this system, necessitating research towards the geomorphic system, its components, and interactions.

6.2. Geomorphic systems

Each study, dealing with aspect of the environment, is operating on simplified parts and isolated structures (sections) of the 'real' world. "*All such studies have, as their central theme, the analysis of the manner in which the components ... of the real world are internally structured ... and, how each section links to other structure. These structures are commonly termed SYSTEMS*" (Chorley and Kennedy 1971). Chorley and Kennedy (1971) presented a scheme for conceptualising environmental systems. Important components within that scheme are system characteristics, system states, system response and system types, delivering general tools for simplifying and describing complex systems.

System characteristics

System size or *system complexity* is a system characteristic, describing its degree of internal structure. It has not necessarily to be connected with the extent of the related 'real' world phenomena, as the same phenomena can be modelled by different structures. Chorley and Kennedy (1971) proposed a number of variables as a measure for system size ('scale'). *System pattern* describes the

pattern, which the connectivities of the subsystems / variables within a system form, e.g. several variables can form a cluster of joint effects on another. The degree of interaction is strongly influenced by the system pattern, which can be expressed using the degree of freedom (Chorley and Kennedy 1971). *Element connectivity* describes how elements of the system elements are connected to each other, either (1) by exchanging energy, mass or information, or (2) in terms of relationships between element properties. Thus, *causality* and *correlation* are used to describe the direction and the degree of interdependencies. Often one or more subsystems / variables of a system are linked to *externalities*, which are not part of the system itself. These linkages strongly influence the systems behaviour. *System output* can be measured by fluxes of energy, mass or information, and by changes in form.

System state

A first necessary distinction is, if the considered system is *open* or *closed*. Generally all 'real' systems are open, often however, for reductionistic reasons, the used model assumes a closed system, i.e. with no connectivities to externalities (see above). *Feedbacks* within the system or subsystems can lead to self–regulation and *static or dynamic equilibriums* (negative feedback, compare Chorley *et al.* 1984), or to unstable conditions in a positive feedback. Positive feedbacks cannot operate unchecked, limits are given by possible variable ranges. Often positive feedbacks, depict *transient* stages until the system runs into a new equilbrium, because system structure changes by variables, which are crossing thresholds. *Metastable systems* show a general equilibrium, which is disturbed by steplike discontinuities from internal or external thresholds (Chorley *et al.* 1984).

Systems types in geomorphology

The structural classification, given by (Chorley and Kennedy 1971), divides geomorphic systems into morphological systems, cascading systems, process-response systems, and control systems. *Morphological systems* comprise physical properties describing morphological characteristics of environmental systems and the relationships between these properties. Important measures for morphological systems are given by geomorphometry. A variety of *geomorphometric parameters* have been used to describe characteristics of geomorphologic systems (see e.g. Schmidt and Dikau 1999, Dikau and Schmidt 1999, Schmidt *et al.* 2000). Other properties include subsurface properties, as particle size distribution etc (compare Chapter 4). The 'net' of relationships between these morphological variables give indications about general morphological behaviour of the system, following pertubations of individual variables (e.g. readjustment, negative feedback, etc., see above). *Cascading systems* are composed of subsystems, which are dynamically linked by transfer of mass or energy. Energy or mass are routed through this cascade of topologically connected components. Examples are catchment hydrology or large basin sediment systems. Complex environmental systems can be resolved in varying detail into cascading systems (often classified by black, grey, and white box approaches). Morphological properties (e.g. porosity) are important regulators for behaviour of energy and matter flows (e.g. soil water redistribution). *Process–response systems* are formed by intersecting morphological and cascading systems. Therefore, "*emphasis is placed on identifying the relationships between a process and the forms resulting from it*" (Chorley and Kennedy 1971). The states of storages are, for example, important system links, controlled and described by both morphological variables and transfer of mass and energy. *Control systems* are defined as as process–response systems with certain key elements (e.g. human impact) exert considerable control over system behaviour.

Input/output and complex response

Predicting the reaction of a system (output) to a change in the relevant boundary conditions or system variables (input, e.g. precipitation event) is an important research task, e.g. obvious in

'climate change' research. The *sensitivity* or *resistivity* of a system to disturbing input has to be quantified, therefore Brunsden and Thornes (1979) developed the concept of landscape sensitivity. The ability to resist or to absorb pertubations can be expressed by the systems *buffering capacity*. An important part of these relationships is expressed by *thresholds* of geomorphic systems (Schumm 1979). System reaction, however, might not follow directly after an event, but after a certain *reaction time*. *Relaxation time* is the time required by the system to reorganise into a new (or the old) steady state, if pertubation caused a change. Reaction and relaxation differs widely in natural systems, and is dependent on system complexity (number of elements) and the magnitude and direction of change (Chorley and Kennedy 1971). It is important to determine *frequency and magnitude* of disturbing pertubations in space and time, especially with respect to reoccurring events and related signal overlays (transient form ratio, compare Brunsden and Thornes 1979). Relationships between frequency and magnitude of an event and the magnitude of the related system response lead to the concept of *geomorphic effectiveness* and the *formative* (i.e. most effective) event. Many environemntal systems, however, do not show convenient convergencies to equilibrium stages. *Chaotic* behaviour leads to increasing growth of minor pertubations and therefore to unpredictability of the considered system. Some techniques from non–linear physics are available to approach these types of systems.

6.3. Complexity and structure — methods from non–linear physics

Despite the complexity, environmental systems exhibit, on the other hand an obvious degree of order and structure exists on various scales. A variety of measures from (non–linear) physics are used to assess system complexity and order. *Entropy* is used as a measure for order; closed systems tend to continuously redistribute energy throughout the system and thereby increase entropy. However, this principle is applicable for simple models only, as the 'Geographic Cycle' (see above). Considering open systems, other measures are required to describe system dynamics. If an earth surface system can be depicted as a box–and–arrow diagram, the *interaction matrix* of elements delivers *Lyapunov exponents* of the system (e.g. Phillips 1999). The *Routh–Hurwitz criteria* can then be used to determine whether or not the system has any positive Lyapunov exponents. Positive Lyapunov exponents indicate, that the system is potentially sensitive to small pertubations and variations in initial conditions and that these minor variations grow over time (deterministic *chaotic* systems). For real environmental systems, however, the Lyapunov spectrum normally cannot be determined. Therefore, a convenient measure are *randomly selected pairs of a single observable* (e.g. relief) of the system (Phillips 1999). For chaotic systems, these these diverge exponentially. Moreover, chaotic behaviour over time directly creates *spatial disorder*, i.e. spatial complexity will increase over time. Environmental systems are often self–organising, i.e. they show chaotic behaviour but form regular patterns in space and time. *Self–organisation* requires increasing total entropy, but at some level entropy must descrease (Phillips 1999). This can occur simultaneously, if the system is unstable, i.e. has a positive Lyapunov exponenent, but the sum of Lyapunov exponenents is negative.

This section could only present some aspects of system analysis, which is a major research topic of some disciplines (e.g. geomorphology, physics) (compare e.g. Bak 1996, Hergarten and Neugebauer 2000, Phillips 1999).

Summary

Stresses and strength of regolith at an inclined potential shear surface can be assessed using site geometry, basic material properties and models about stress fields and friction. Stability conditions of simple and more complex shear surfaces can be calculated by a variety of simplified modelling approaches. However, it is unclear, if limit equilibrium approaches from soil mechanics adequately solve the problem of upscaling small scale stress conditions acting at a shear surface (compare Hattendorf 2001). Soil water is an important factor for both strength and stress fields in soils. Therefore, analysis of slope stability has necessarily to include soil water assessment. Hillslope hydrology is usually modelled by flow laws for saturated and unsaturated conditions, which represent approximations of the *Richards equation*. Critical for each approach in 'actual process modelling' is the parameterisation of relevant material properties, which exhibit a large variability, either statistically (especially from experiment procedure) and spatially. Therefore, *aggregation* techniques for boundary conditions are mandatory in process modelling. These techniques have to consider spatio–temporal structures of relevant boundary conditions. However, as these structures itself are a result of evolving geomorphic systems, this aggregation problem is directly related to the superordinated problem of landform evolution (Brinkmann *et al.* 2001).

Landform changes over longer timescales have been assessed by various methods, ranging from simplified process modelling, to system theory and theories of general landform evolution, operating on large scales. Process modelling approaches suffer from missing data for parameterisation of 'real' world conditions with respect to the used model discretisation (discussed in Chapter 2). Theoretical models often remain vague, therefore their applicability to explain 'real' world geomorphological field evidence often is limited. However, each process model requires a conceptualisation with respect to the considered processes and the related scales. System analysis and system theory deliver a general framework for modelling complex geomorphic systems, e.g. by deriving relevant parameterisations for process modelling approaches. Most earth surface systems are complex and exhibit non–linearities leading to chaotic behaviour and self–organisation, which fundamentally limits its predictability. Therefore, methods from non–linear physics are useful to identify and describe these system stages (compare Phillips 1999).

Part IV.

Study area & field sites

7. The Bonn area — geographic boundary conditions

7.1. Geomorphology and geology

Geologic history & present landforms

The study area is the region around Bonn (Germany), a transitional zone between the 'Rheinische Schiefergebirge' (*rhenish massive*) and the subsidence area of the 'Niederrheinische Bucht' (*Lower Rhine region*). The study region has experienced complicated geologic history with phases of varying tectonic actvity, erosion, and deposition (e.g. Burghardt 1979, Fuchs 1983, Grunert 1988, GLA 1988, Klostermann 1992, Meyer and Stets 1996). Lower Devonian shales, sandstone, and quartzite of Rheinische Schiefergebirge are forming the base layer. Uplift of the Rheinische Schiefergebirge and subsidence of the Niederrheinische Bucht, especially during the late Tertiary and Quarternary (Fuchs 1983), led to phases of erosion and deposition, and marine transgression and regression. Therefore, the Devonian baselayer is overlayed by Tertiary sediments, varying from marine clays to sands and fluvial gravels. Under Pleistocene periglacial conditions, terrace material and loess were deposited (e.g. Klostermann 1992). West of the Rhine, terrace sediments are found above a series of Tertiary layers (clay, sand, and gravel) and the Devonian base layer (compare Figure 7.1). Pleistocene tectonic processes uplifted the plateau of the Kottenforst as a horst with steep slopes to the Low Terrace of the Rhine (Figure 7.2). Pleistocene and Holocene fluvial processes dissected the plateau of the Kottenforst and formed a series of small valleys (e.g., Godesbachtal, Melbtal, Katzenlochbachtal) which are often cut down to the Devonian base layer. Approximately at the transition between the Oligocene and Miocene, volcanic activity led to the formation of the Siebengebirge (compare Figure 7.2). Therefore, east of the present Rhine, layers of vulcanic sediments (trachytic tephras) covering large parts of the area and a series of eroded latitic, basaltic and andesitic intrusions form the peaks of the Siebengebirge. The slopes are covered with Pleistocene sediments above volcanic ashes (trachyte tuff). Trachyte tuff is interfingered with Tertiary sediments. The valley floors of the Siebengebirge often reach the Devonian base layer.

Landslide occurrence

Landslides can be found in varying size and age on the slopes both of the Kottenforst and on the hillslopes in the Siebengebirge (Figure 7.2, compare Grunert and Schmanke 1997). Previous investigations and several problems encountered during the construction of roads and buildings indicated serious slope instability problems in the region.

Archive data and geomorphological evidences indicated a series of old landslides on the hillslopes in the Bonn area (Grunert and Hardenbicker 1993, 1991, Hardenbicker 1993, 1994, Grunert and Schmanke 1997). Landslide susceptibility in the Bonn area is influenced by the specific the geologic situation, i.e. sensitive, clay–rich Devonian, Tertiary and trachytic layers (see above and compare Grunert and Schmanke 1997). Most of the landslides were interpreted as Holocene mass displacements, a series of events occurred in the 20th century (Hardenbicker 1991). Most of the re-

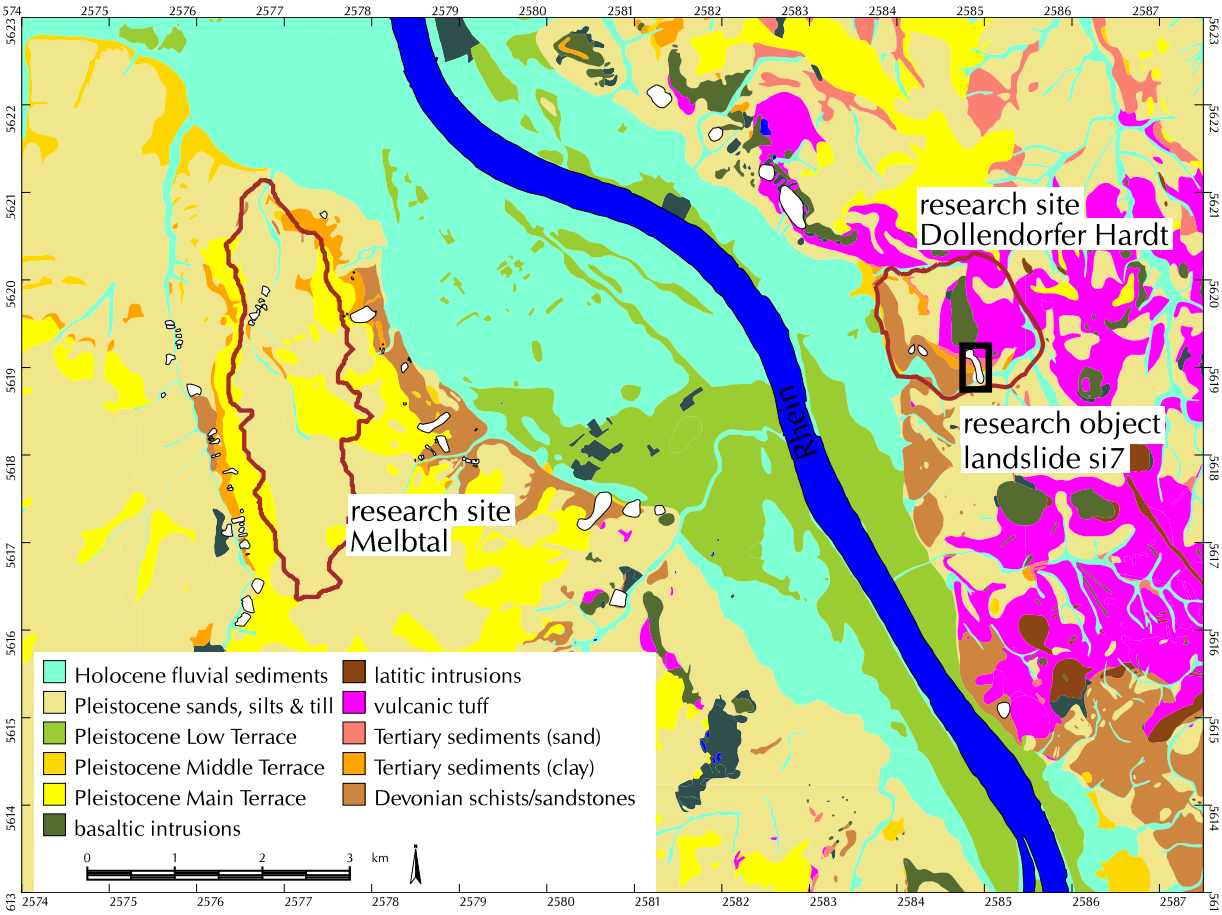

Figure 7.1.: The Bonn area: geological situation. Data source: Geological Map 1:25.000. Digitised by D. Kirschhausen, V. Schmanke and U. Hardenbicker. White polygons denote landslides. Landslide database compiled and digitised by D. Kirschhausen and U. Hardenbicker.

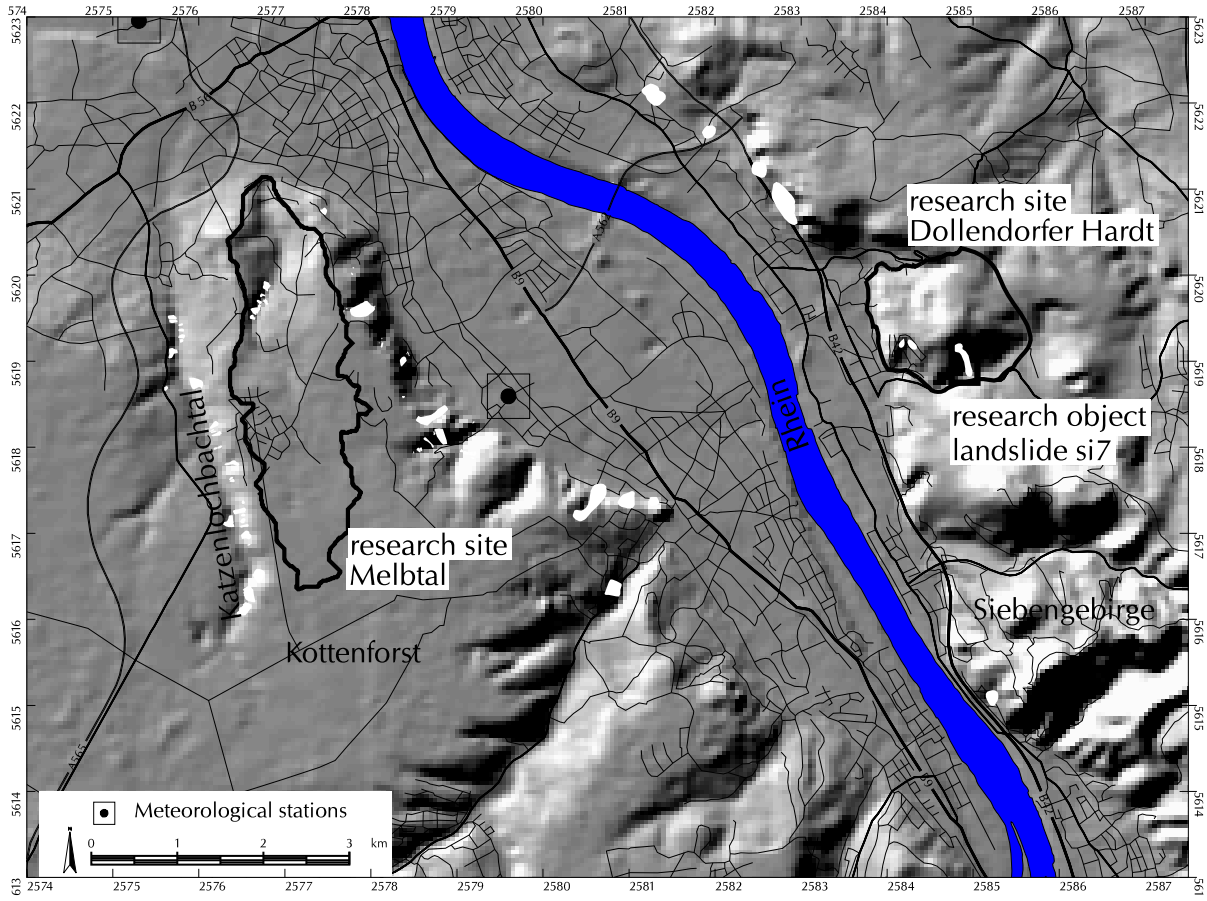

Figure 7.2.: Topography and landslides in the Bonn area. White polygons denote landslides. Locations of two meteorological stations are shown: 'Meteorological department' (north), and 'Friesdorf' (south). Areas of high landslide susceptibility are valleys (e.g., Katzenlochbachtal, Melbtal), incised in the horst structure of the Kottenforst and the mountainous area east of the river Rhine, the Siebengebirge. Two field sites, the Dollendorfer Hardt and the Melbtal were chosen for detailed investigations. Data source: Topographic Map 1:25.000, Digitised by D. Kirschhausen, V. Schmanke and U. Hardenbicker, landslide database compiled and digitised by D. Kirschhausen and U. Hardenbicker.

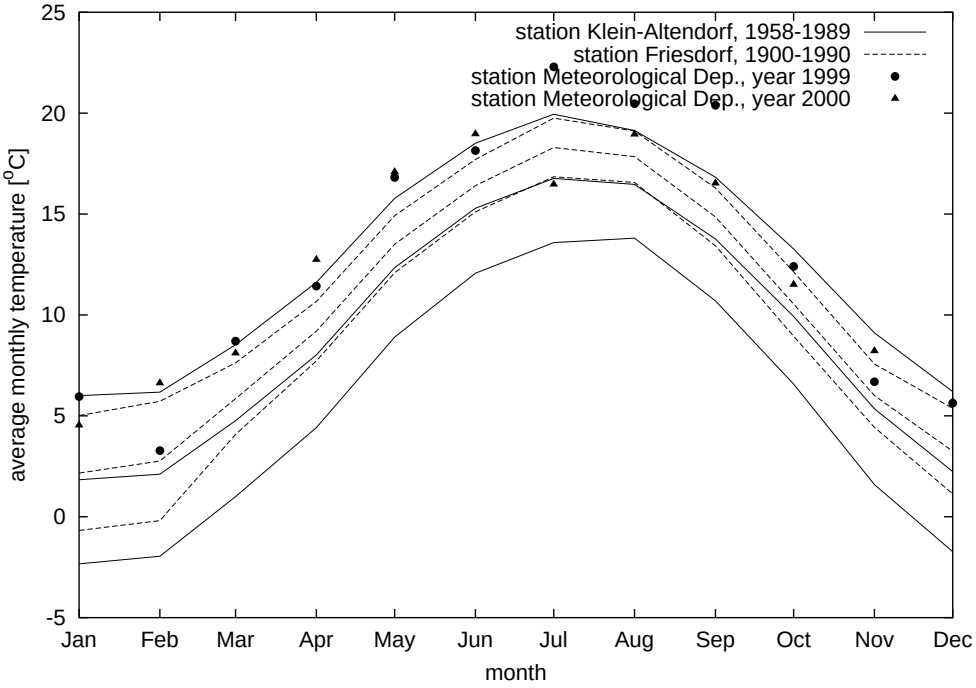

Figure 7.3.: Annual temperature pattern for the Bonn area. Monthly average temperatures from two long–term monitoring meteorological stations (compare section 8.4) are plotted as averages and standard deviations (lower and upper curves). Additionally, data from the measurement years of this study are plotted (points).

cent landslides were influenced by construction activities. Triggering conditions can be dominantly attributed to intensive rainfall phases (Hardenbicker 1994).

7.2. Climatic variability

Bonn has a moderate maritime climate, dominated by oceanic air masses (average annual temperature about 9 °C; average annual rainfall about 600 mm to 750 mm). The thermic conditions (Figure 7.3) denote mild winters (ca. 2 °C monthly average) and moderate warm summers (ca. 18 °C monthly average). However, extreme cold winters can reach down to −10 °C. The long–term monthly precipitation sums (Figure 7.4) show a minimum in winter (february, about 40 mm) and a maximum in summer (july, about 70 mm). Precipitation in summer is mostly concentrated to convective rainfall events (thunderstorms). Temperature and precipitation of the measurement years of this study (years 1999, 2000, compare Figures 7.3,7.4), showed the high variability of temperature and precipitation in comparison to long–term data (especially in summer).
During the pleistocene, the region experienced cold and dry periglacial conditions, with markedly lower temperatures (Siegburg 1987). Holocene climate variability indicates a series of climatic fluctuations (e.g. Thompson *et al.* 1993), including cool and humid periods, which are of particular relevance for landslide occurrence (compare Hardenbicker 1994). Specifically, the *'Little Ice age'* was a period of cooler temperatures, increased storminess and high climatic fluctuations lasting from Middle Ages till approximately 1850 (compare Chapter 11).

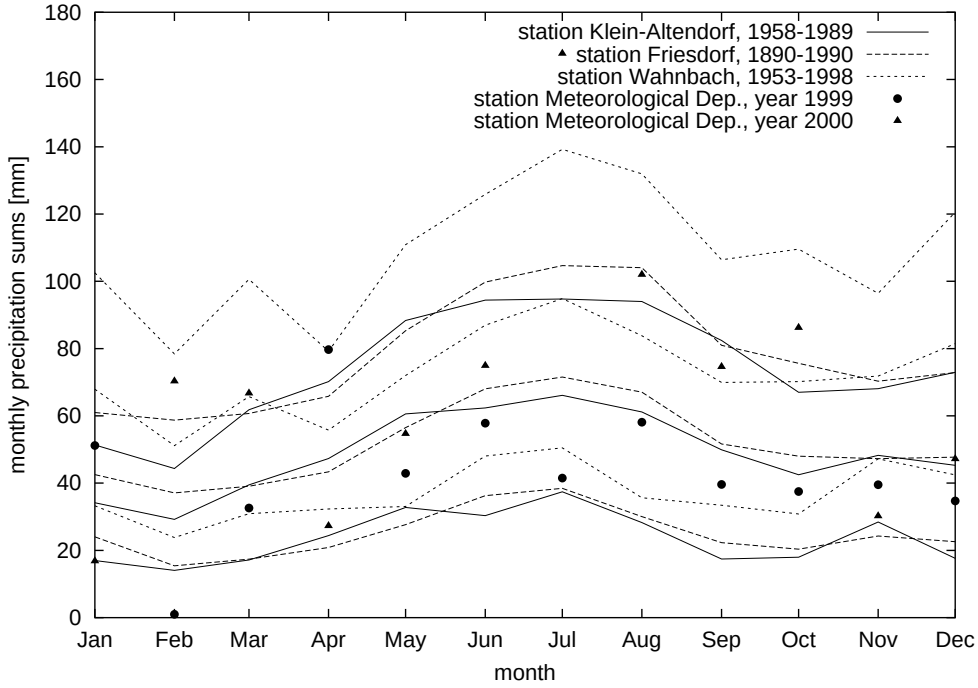

Figure 7.4.: Annual precipitation pattern for the Bonn area. Monthly sums from three long–term monitoring meteorological stations (compare section 8.4) are plotted as averages and standard deviations (lower and upper curve). Additionally, data from the measurement years of this study are plotted (points).

7.3. Field sites

Two field sites, which are representative for the Bonn area in geomorphometric and geologic terms were chosen. The first site is the hill Dollendorfer Hardt in the Siebengebirge (Figure 7.2). The Dollendorfer Hardt serves as a study site, representative for the lithologic and morphometric conditions of the Siebengebirge. The second site is the Melbtal, a small valley west of the Rhine, cut into the Kottenforst plateau (Figure 7.2). The Melbtal serves as a representative for a series of valleys insected in uplifted plateaus west of the Rhine. Both field sites are forested, and therefore considered not currently subject to other hillslope processes than landslides (e.g. soil erosion pocesses). This assumption, however could not be validated by field evidence and implies a significant source of error for this study (compare section 14.1).

7.3.1. Dollendorfer Hardt

Landforms and lithology

The geologic and geomorphologic conditions of the field site Dollendorfer Hardt can be derived from the general discussion of the situation in the research area (see above). The Dollendorfer Hardt is a hill (2.2 km^2, compare Figure 7.2) of the Siebengebirge, formed by Tertiary basaltic intrusion and Tertiary and Quarternary erosion and sedimentation processes (Burghardt 1979). Landforms and lithology (Figures 7.1, 7.5) are dominated by a basaltic dome forming the top of the hill, and trachyt tuff, Tertiary sediments (clays, sands) and Devonian base layer (from top to bottom) exposed on the hillslopes. The north east part is largely covered with terrace material and loess (Hardenbicker 1994, Rogozia 2000, Schegiewal 1972). The south and west facing hillslopes of the

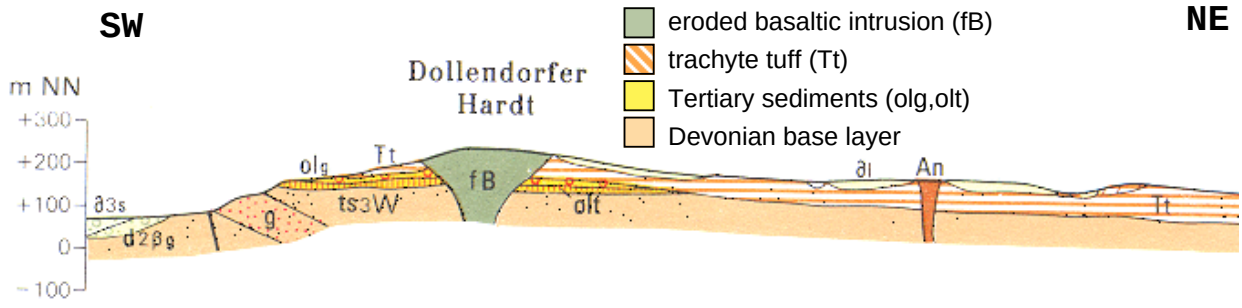

Figure 7.5.: Detail of GK 5209. Geological profile of the field site Dollendorfer Hardt.

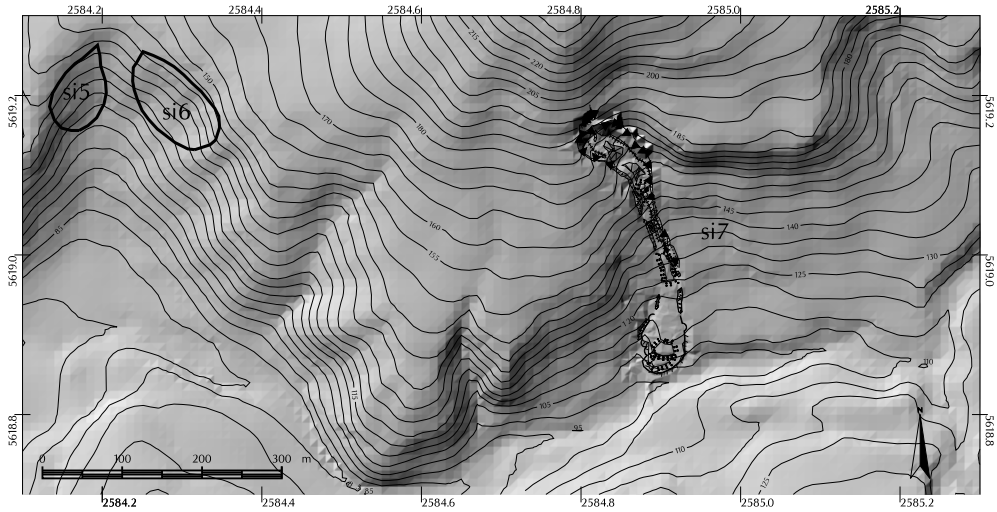

Figure 7.6.: Localities of the landslide 'si7' and two other landslides, Dollendorfer Hardt. The landslide 'si7' is situated at the south facing hillslope of the Dollendorfer Hardt, in an upslope position with high slope angles. Two other landslides ('si5', 'si6') occurred in Devonian sediments, on hillslopes covered by vineyards.

Dollendorfer Hardt show relatively high slope angles (maximum slope angles approximately 35 ° to 40 °), whereas the north and east facing slopes gently connect to the northern Siebengebirge and the Pleiser Hügelland, respectively (Siegburg 1987).

Vegetation & land use

The field site Dollendorfer Hardt is located in a forested area since historic times. Dominatly, deciduous forest (beech trees) can be found, which is the natural landcover for the area. However, historic sources and aerial images of the last 50 years indicate intensive foresting in the area (compare Weber 1991). Parts of the Dollendorfer Hardt are under agricultural use, especially wine growing on the south–west facing hillslopes. Field evidence indicate historic mining activities (basalt and Tertiary clays) leading to a intensive man–made landform change in parts of the field site (see Rogozia 2000).

Landslide occurrence

Three landslides are documented (this century) for the area of the Dollendorfer Hardt. The landslide 'si7' (affected area: $30,000\ m^2$) on the south facing hillslope was investigated by previous studies (Hardenbicker 1994, Weber 1991) and was chosen for detailed investigation in this study

(subsection 10.1.2). The first event at this locality took place in 1958 (Hardenbicker 1994), and subsequent failures have occurred since then, a second major event in 1972 reached the valley bottom (Weber 1991). The landslide morphology implies complex failure with initial multiple rotational slides, turning into a flow in the transport zone, which built up levées (see subsection 10.1.2). The initiating conditions can be attributed to human activity, as the first landslide occurred after a path was build in the scar area (Hardenbicker 1994). Two other landslides (*'si5'* and *'si6'*) occurred on the south–west facing hillslopes of the Dollendorfer Hardt (see Figure 7.6), which caused damage to vineyards and streets. Therefore, intensive investigations and remediation were carried out (Jäger 1991). The landslides are translational slides, the shear surfaces were approximatly at 6 m depth. The material properties for the underlying Devonian sediments were analysed by Jäger (1991) (see Appendix E). The triggering conditions were intensive precipitation phases in winter 1982 and spring 1983. However, as Jäger (1991) states, the area was affected by old Pleistocene landslides, which influenced the occurrence of the recent landslides. In both cases, initial remediation works (including draining) and/or abandonment of the vineyards lead to stabilisation of the hillslopes. Convergencies on a hillslope, approximately 100 m west of the landslide 'si7', were interpreted as an old landslide scar. Pedologic studies (Holler 1998) showed no evidence of a young event, leading to the hypothesis of a Pleistocene landslide.
The three landslides, documented for the Dollendorfer Hardt, have been developed mainly in *Tertiary and Devonian clay–rich sediments*. The landslide 'si7' also involves failure in trachyte tuff. However, as the landslide 'si7' has a history of progressive failure (Weber 1991), the failure in trachyte tuff might be a secondary event, induced by initial failure of underlying Tertiary material (compare subsection 10.1.2). All landslides are influenced by *human activity* (compare Hardenbicker 1994). The triggering factors in all cases can be attributed to *extraordinary wet conditions in spring*. There are evidence of *historic or prehistoric phases of increased landslide activity*.

7.3.2. Melbtal

Landforms and lithology

The field site Melbtal is a small valley (4.6 km^2) insected by the creek *Engelsbach* in the plateau of the Kottenforst. The Engelsbach is supposed to follow a tectonic fault line (Figure 7.7), however, no firm evidence exists detailing course and height of the fault line (compare Heidemann 1996, Kaiser-Kühn 1988). The general lithology (e.g. map GK 5208, Figure 7.1) (from bottom to top) shows a Devonian baselayer ('Siegener Schichten'), Tertiary layers (clay, sand, lignite, 'Kölner Schichten'), and terrace and loess sediments on the top of the surrounding Kottenforst. Tectonic processes lead to tilting of these layers as indicated in Figure 7.7. Loess and terrace sediments can be found on the valley side slopes due to Pleistocene processes (loess formation and periglacial processes). The west facing valley side slopes show more extended loess accumulation (compare Figure 7.7 and section 10.2).
Because of the lithologic situation of the Melbtal and the general tectonic situation in this area, it can be inferred, that main terrace sedimentation was the last sedimentation phase before incision of the valley. Therefore, the maximum age of the Melbtal can be estimated by the age of sedimentation of the main terrace. The age of the main terrace, however, has been dated by various studies in the comparatively large time frame of 900,000 bp to 600,000 bp (compare e.g. GLA 1988, Klostermann 1992, May 2001).

Vegetation & land use

Presently, the Melbtal is mainly forested with some pasture usage on the west facing hillslope in the lower valley part. The valley is surrounded by districts of Bonn, the village 'Ippendorf' is

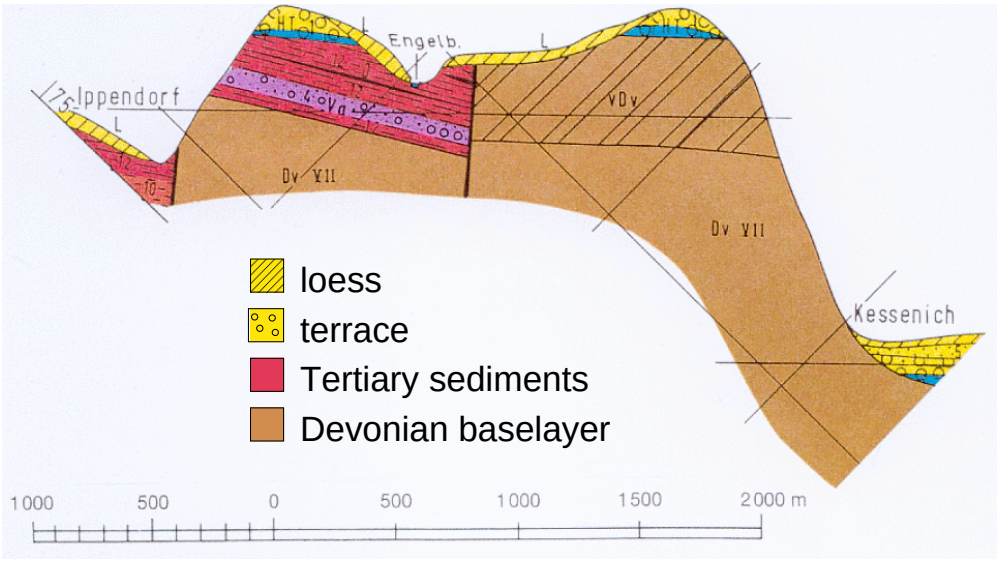

Figure 7.7.: Lithology of the field area Melbtal. This cut–out from the hydrologic map (HKG 5208) indicates a fault line near the valley course and the general lithological situation.

located on the western divide of the Melbtal, the village 'Venusberg' covers the eastern divide, and at the valley outlet directly connects to the village 'Poppelsdorf'. In historic times, more or less intensive usage of the Melbtal also led to phases of total deforestation (May 2001). Evidence of historic mining activities is present in recent landforms as hollows or scarps. Because mining activities were not intensive, these features are limited with respect to their spatial extent, but can be frequently found in the Melbtal. Generally, the Melbtal has not been subject to intensive landuse and mining activities in a systematic way. However, because the area has been directly connected to settlements since approximately 1000 years (May 2001), an extensive usage (wood, pasture, small mining, etc.) took place over the whole period. Most human impacts on the environment are caused by individual activities. Therefore, quantification and dating of the history of human usage and their impacts on the environment is difficult due to few historic evidence (e.g. archive documents, etc.).

Landslide occurrence

Sensitive Tertiary layers of clay, sands and lignite lead to considerable slope instability of the hillslopes. A series of landslides are located in the lower valley part, where these sensitive layers are exposed on the hillslopes (sizes ranging from 300 m^2 to 8000 m^2, compare Hardenbicker 1994, Heidemann 1996). The youngest landslide (1988) damaged a cemetery and required expensive remediation and reconstruction work (Kaiser-Kühn 1988). The occurrence of landslides in the field site Melbtal is related to *heterogeneous Tertiary sediments*, distinct changes of sand, clay and lignite layers with significant different permeabilities imply the existence of perched water tables and potential shear zones. Especially Tertiary lignite layers with higher permeability and low shear strength are sensitive layers, which can be found frequently in the lower valley. Similar to the field site Dollendorfer Hardt, the observed landslides (this century) occurred in *periods of intensive rainfall in spring* (Hardenbicker 1994). *Human activity* is an important disposing factor for landslides occurred in this century (Heidemann 1996). Moreover, sediments and morphology give evidence of *historic or prehistoric phases of increased landslide activity* (Hardenbicker 1994).

Part V.

Data capture & data management

Introductory notes

The multi–scale and multi–method approach (Chapter 3) chosen in this study requires capture and management of a considerable amount of different types of data. This part first gives an overview of the data collected in this study, as well as of the corresponding techniques (Chapter 8). Detailed lists of the results of this work (e.g. maps, field and lab data) and some of the relevant meta information (e.g. techniques, institutions) can be found in the Appendix.

Landslide studies are a typical research field, where databases play an important role with respect to data management and analysis (e.g. Dikau *et al.* 1996a). The variety of captured data types and used analysis tools require a careful data management to ensure effective data storage and retrieval. Database management systems (DBMS) include components for data storage and data query. Both components can be realised by various existing software tools. Developing a consistent and effective scheme within this framework requires (1) an inventory of the project aims (i.e. what kind of data analyses and data queries are planned) as well as of the incoorporated data types, (2) a semantic model of the data types, and (3) a technical realisation within the framework of (Geo) Information–Technologies. These steps are described in Chapter 9. The data management scheme is described, which were developed and used to maintain the data collected in this study.

8. Data capture

8.1. Spatial Geo–Data ('maps')

Maps are fundamental sources of information for geomorphological studies. They deliver a wide range of information, useful in landslides studies (Table 8.1). A series of maps were used in this study, lists of analogue and digital maps can be found in the Appendix F.4 and Appendix F.5. Some of the basic spatial information sources used in this study shall be shortly introduced.

Topographic maps
Topographic maps represent a basic working tool for geographic referencing, orientation and field mapping. The used topographic map sheets include the 'Topographische Karte 1:25000' (*Topographic map, scale 1:25000*), and the 'Deutsche Grundkarte 1:5000' (*German Basemap, scale 1:5000*). A series of analogue and digital map sheets of these series were available, covering most of the study area and the whole area of the field sites.

Geologic maps
'Geologische Karte von Nordrhein–Westfalen 1:25000' (*Geologic map of Nordrhein–Westfalen, scale 1:25000*) (Figure 7.1, page 64). *[analogue, digital]*
The map sheets covering the research area include GK 5209, GK 5308, GK 5309, and the GK 5208. The sheets were digitised by Volkhard Schmanke, Ulrike Hardenbicker and Diana Kirschhausen (projects MABIS, SFB 350) and were converted to an ArcInfo coverage within the GIS database (Chapter 9). The map sheets reveal the fundamental geologic and tectonic situation of the Bonn area and the field sites described in Part IV. As Rogozia (2000) states, all of the geologic map sheets of the Bonn area are comparatively old editions and the newer ones are only partly updated editions. Therefore, the information content should be interpreted with considerable criticism, bearing in mind, that Bonn is a highly dynamic urban area, especially in the last 50 years.

'Geologische Karte der Umgebung von Römlinghoven' (*Geological map of the area of Römlinghoven (Bonn, Germany)*) (GK Schegiewal). *[analogue, digital]*
GK Schegiewal was mapped by Schegiewal (1972). The analogue map was digitised with minor corrections and extentions (Rogozia 2000) and converted to an ArcInfo coverage. The map displays details of the geologic situation of the field site Dollendorfer Hardt, which are not captured by the 'Geologische Karte von Nordrhein–Westfalen 1:25000'.

'Geologische Kartierung des Siebengebirges' (*Geological mapping of the Siebengebirge, scale 1:10000*) (GK Bichler). *[analogue, digital]*
Bichler (2001) carried out a new mapping of the northern Siebengebirge, and thereby revised the results of Schegiewal (1972) (see above), presenting an up–to–date geological mapping for the field site Dollendorfer Hardt.

A series of analogous hydrologic map sheets were available (e.g. HKG 5209, HKG 5208) for the

Table 8.1.: Maps as an information source for landslide research: map types and examples of usage.

map type	**examples of use in landslide research**
topographic maps	basic information for mapping locating features (boreholes) visualisation map production
elevation models	surface information visualisation map production input for landslide hazard analysis
geologic maps & hydrologic maps	subsurface information background for field and lab analysis input for landslide hazard analysis
pedologic maps	subsurface information background for field and lab analysis criteria for landslide activity

research area. These provide additional information about the three–dimensional structure of the subsurface material and its properties (e.g. particle size distribution, permeability). These data are of particular interest for modelling three–dimensional subsurface structure and parameterising regolith properties of the field sites (compare Figure 7.7, page 70 and Part VI).

Pedologic maps

'Bodenkarte von NRW 1:50000, Blatt Bonn' (*Soil map of Nordrhein–Westfalen, scale 1:50000, map sheet Bonn*) (BK 5308). *[analogue]*
Map sheet BK 5308 delivers an overview of the spatial distribution of soil types within the Bonn area. The soil map also indicates important geologic and hydrologic situations for landslide research, as permeable horizons leading to gleyisation.

'Bodenkarte des Staatsforstes Kottenforst 1:10000' (*soil map of the Kottenforst (Bonn, Germany), scale 1:10000*) (BK Kottenforst). *[analogue, digital]*
The map sheets of the BK Kottenforst give detailed information about the soil types in the Kottenforst area near the field site Melbtal.

'Bodenkarte des Naturparks Siebengebirge 1:25000' (*soil map 'Siebengebirge', scale 1:25000*). *[analogue]*
This pedologic map was published by Burghardt (1979), covering the area of the Siebengebirge.

'Bodenkarte zur forstlichen Standorterkundung, 1:5000' (*Forest soil map 1:5000, Siebengebirge*). *[digital]*
This soil map was produced by the 'Geologischer Dienst NRW' (*Geological Survey, NRW*) for the forested area of the Siebengebirge. The map gives detailed information about the soil types in the area of the Siebengebirge and is therefore relevant for the field site Dollendorfer Hardt.

'Bodenkundliche Karte der Umgebung von Römlinghoven' (*Soil map of the area of Römlinghoven (Bonn, Germany)*) (BK Schegiewal). *[analogue, digital]*
BK Schegiewal was produced as part of the Phd project of Schegiewal (1976). The map provides detailed information about the soil types of the field site Dollendorfer Hardt.

'Bodenkarte 1:2500, Dollendorfer Hardt' (*soil map 1:2500, 'Dollendorfer Hardt'*) (BK Holler). *[analogue]*
Holler (1998) mapped soil types of the field site Dollendorfer Hardt based on 144 drillings and additional lab analysis. The results provide a comparatively detailed insight in the variability of soil types and soil properties of the site and give some indications about the dependencies of soil types to occurrence of mass movements.

Digital elevation models (DEMs)

Digital elevation model for the Lower Rheinisch Bay area, resolution 50m (DEM 50). *[digital]*
This map was supplied from the SFB 350. It originates from combining two height datasets of the 'Landesvermessungsamt Nordrhein–Westfalen' (*Land Survey Department Nordrhein–Westfalen*) and 'Landesvermessungsamt Rheinland–Pfalz' (*Land Survey Department Nordrhein–Westfalen*), covering the area of Nordrhein–Westfalen and Rheinland–Pfalz.

Digital elevation model for Bonn area, resolution 10m (DEM 10). *[digital]*
This digital map was derived from a series of map sheets acquired within the project B13 from the 'Landesvermessungsamt Nordrhein–Westfalen' (*Land Survey Department Nordrhein–Westfalen*). The DEM covers large parts of the area of Bonn. The DEM 10 was derived from interpolation of digitized contour lines of the 'Deutsche Grundkarte 1:5000' (*Topographic map, scale 1:5000*) (Föckeler and Kuhn 1990). The analogous map sheets, which served as the basis for the digitised contour lines for the research sites, are from 1968 (Dollendorfer Hardt) and 1952 (Melbtal), respectively. This rather old data basis suggests problems in using the models for present day situations. The map scale and the interpolation process imply, that landform changes in horizontal ranges of several tens of meters have effects on the data quality. Bonn has been a highly dynamic area in the last 50 years with intensive building activities, indicating that this potential source of error, especially for urban areas. However, as this study is looking for major long term changes within relatively 'natural' slope systems, possible errors of the DEM 10 were not studied within this framework (compare Part IV).

Digital elevation model for Bonn area, resolution 1m (DEM 1). *[digital]*
This raster map was supplied from the Kataster- und Vermessungsamt, Stadt Bonn. It is a DEM in raster format with 1 m horizontal resolution, which was generated from airborne laser data. Rasemann (1999) exemplified systematic errors in the data resulting from interpolation processes.

Digital elevation model, landslide si7 (DEM SI7). *[digital]*
This DEM was derived from data from terrestrial measurements of the landslide 'si7' (compare Appendix F.2.1 for details of the procedure). A bilinear interpolation within the GIS ArcInfo (compare subsection 10.1.2) was used. It shows the main features of the landslide landslide 'si7' and serves as a basic information for stability modelling of the landslide (compare Chapter 8 and Chapter 12).

Landslide maps

Active landslides, Bonn area and inactive landslides, Bonn area. *[digital]*
Active and inactive landslides in the Bonn area were mapped by the group of Prof. J. Grunert within the projects MABIS and SFB 350. These landslide database were compiled and digitised as polygon coverages by D. Kirschhausen and U. Hardenbicker. The datasets were provided by V. Schmanke.

Table 8.2.: Field data and field investigation techniques used in this study (DIN refers to the German Industrial Standard, compare DIN 1993).

measurement	**technique**
precipitation, temperature & air pressure	data available from several meteorological stations in the Bonn area (section 8.4)
surface structures	terrestrial surveying (manual and tachymetric)
subsurface structure	drillings, outcrops (DIN 4021)
	penetration tests (DIN 4094), field vane tests (DIN 4096)
	geophysical surveying (not presented in this work): GPR, electromagnetics, geoelectrics, refraction seismics
groundwater height	groundwater gauges (DIN 4022)
	dipmeter
	pressure transducers (D–DIVER)
regolith movement	inclinometer
	tiltmeter (cooperation with project C1)

8.2. Field work

A series of field investigation techniques were used in this study to assess surface and subsurface structure of the field sites. Table 8.2 gives a summary of the used methods. Listings can be found in Appendix B.

Mapping and terrestrial measurements

Capturing landform elements, their position, topology and the related material is one major information source, useful in assessing and understanding geomorphic systems. Geomorphologic mapping is one standard methodology within that framework. Terrestrial measurements were carried out manually (compare May 2001), but also using an automatic tachymeter (TCL 1800, see Appendix F.1). The related postprocessing techniques (e.g. conversion of the data in a georeferenced GIS) are described in the Appendix F.2.1. Tachymeter measurements (more than 1400 points) were used to capture details of the surface morphology of the landslide 'si7'. The measurements were used to produce a high resolution DEM (DEM SI7, compare section 8.1) as well as geomorphic maps indicating type and extent of the geomorphic features of the landslide (see Figure 10.2). These data sets were used in interpretation, analysis and modelling of the landslide 'si7' (see Part VI and Chapter 12).

Drilling and mechanical subsurface exploration

A series of direct subsurface explorations were carried out during the field work of this study, related projects, and previous work. Extended shallow drillings (¡2 m) were performed at the field site Dollendorfer Hardt by Holler (1998) and Bichler (2001). A series of drilling catenas are available (Heidemann 1996, Schmanke 1999) for specific landslides in the Melbtal. Therefore, it was decided, to concentrate the drillings in the field area Dollendorfer Hardt on the landslide 'si7' (Figure 10.3, page 105). On the other hand, the drillings in the field area Melbtal were perfomed in a coarse drilling raster to provide more information about the spatial distribution of sensitive sediments (Figure 10.10, page 111). The techniques include direct outcrops, closed core percussion drilling, open core percussion drilling, and manual auger and percussion drilling ('Pürckhauer') (compare Barnes 1995, Dunnicliff 1993). Occasionally, field penetration tests and field vane tests were used as indirect mechanical exploration techniques. Details of the drilling results, including a series of bore logs can be found in Appendix B.1.

Geophysical subsurface exploration

Direct subsurface exploration techniques suffer the lack of delivering only a discrete, pointwise information of the soil. A variety of studies showed the potentials of geophysical investigation techniques with respect to their applicability in landslide areas (e.g. van Beurden 1997, Caris and Asch 1991, Scheller 1996). Hattendorf (1996) presented a study in shear surface reconstruction for a small landslide near Bonn by electromagnetic surveying. A series of geophysical surveys were carried out during the field work of this study and a related project (Phd project of Carsten Alteköster, 'Angewandte Geophysik, Geologisches Institut, Universität Bonn' (*Geophysics, Department of Geology, University of Bonn*)). One initial aim was to test these exploration techniques for their applicability in the Bonn area and, if possible, to extend the discrete information from the drilling results to two dimensional views of the subsurface structure. Therefore, surveys on landslides and undisturbed hillslopes (detection of shear zones), and extended surveys on the field sites (detection of lithologic changes) were carried out. The applied techniques include electromagnetic, seismic, and geoelectric soundings, and GPR–surveys. Lists of surveys can be found in Appendix B. However, due to the extensive methodological programme, only initial tests for some of these methods were carried out. As the related data and the findings were not used with respect of the fundamental aim of the study (compare Part I and Part II), the data are not presented and analysed within this work. Nevertheless, the data were stored as part of the developed DBMS (Chapter 9). The GPR–surveys will be discussed in the framework of the Phd thesis of Carsten Alteköster (Alteköster prep).

Ground water monitoring

A series of groundwater gauges were installed in the area of the landslide 'si7' and at the field site Melbtal to explore spatio–temporal groundwater dynamics. The installation sites can be found in Part VI (Figure 10.3, page 105, Figure 10.10, page 111) and in Appendix B.4. These installations served to assess the groundwater variability of the hillslopes surrounding the landslide 'si7' in greater detail, whereas the Melbtal was monitored in coarse meshed distances to provide information about lateral extent of the aquifers and changes in lithology (see Part IV). The installation type in each case was a standpipe gauge (see e.g. Barnes 1995). For groundwater monitoring, initially a dipmeter was used. The tubes showing high groundwater variability were equiped with automatic monitoring pressure transducers (D–DIVER, see Appendix F.1). The D–DIVER is a integrated measurement unit, capable of measuring and logging pressure of sourrounding medium. As no pressure difference is measured, air pressure correction has to be performed, which was carried out using available meteorological data (see Appendix F.2.3 for details of the procedure). The processed groundwater data are displayed in Appendix B.4.

Movement monitoring

A series of inclinometer tubes were installed in the landslide 'si7' (field site Dollendorfer Hardt) and in the landslide 'me5' (field site Melbtal). The installation sites can be found in Part VI (Figure 10.3, page 105, Figure 10.10, page 111) and in the Appendix B.3. The installation type and procedure is described in Glötzl (1994). The processed data are displayed in the Appendix B.3. The middle part of the landslide 'si7' was chosen for detailed investigations, including one installed 'quasi–continously' (10 min interval) monitoring tiltmeter (AGI-722A Borehole Tiltmeter), because of high movement rates, detected by inclinometer measurements (compare subsection 10.1.2). This installation was carried out in cooperation with the project C1 (SFB 350) (compare Fabian *et al.* 2000, Fabian prep, Kümpel 1996, for details on installations and monitoring procedures for tiltmeters).

Table 8.3.: Types of laboratory techniques used in this study and related soil sample requirements (DIN refers to the German Industrial Standard, compare DIN 1993).

soil parameter	symbol	technique	DIN	sample	
moisture content	w	oven drying	18121	50 g	wet
organic content	O_c	ignition loss	18128	5050 g	ovendry
particle size distribution	e.g. c_T	sieving	19683	20 g	dry
		pipette method	19683	20 g	dry
		hydrometer method	18123	20 g	dry
bulk density, dry density	ρ_b, ρ_d	oven drying	18125	cylinder	wet
particle density	ρ_s	pycnometer method	18124	30 g	ovendry
maximum moisture content	w_c	method after Enslin	18132	2 g	ovendry
saturated density	ρ_{sat}	saturation test		cylinder	wet
consistency limits	w_p,w_l	Casagrande test	18122	300 g	dry
shear strength	τ_u	lab vane test	18137	cylinder	wet
	ϕ,c,ϕ_r,c_r	shear box test	18137	cylinder	wet
	ϕ',c',ϕ'_r,c'_r	triaxial test	18137	cylinder	wet
saturated conductivity	k_s	constant head permeameter	18130	cylinder	wet
		falling head permeameter	18130	cylinder	wet

'wet' indicates the natural field moisture content,'dry' indicates air dried condition.

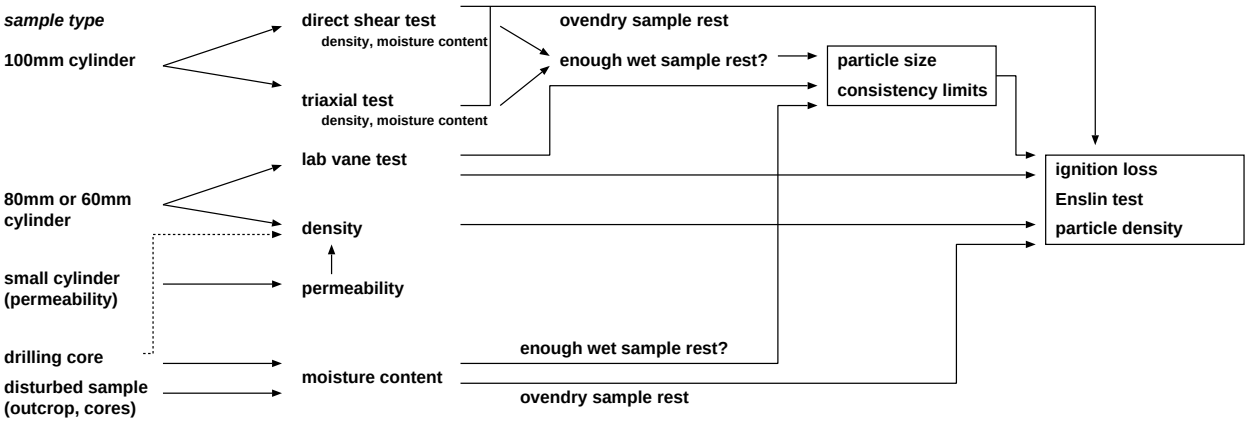

Figure 8.1.: Sketch of lab analysis procedure applied in this study

8.3. Laboratory analyses

Laboratory programme

A series of laboratory experiments are useful for estimating soil properties within the framework of landslide analysis programmes (compare Chapter 4 and see e.g. Lambe and Whitman 1979, Barnes 1995, Kuntsche 2000, Selby 1993). A set of experiments was chosen for this study (compare Table 8.3) to determine basic soil properties, shear strength parameters, and permeability of relevant layers of the research sites (compare study aims described in Part I and Chapter 3). As Table 8.3 indicates, different tests have different sampling requirements. Therefore, it was necessary to design a lab programme in order to use soil samples effectively. This especially applies to undisturbed samples of high sampling quality (compare Barnes 1995). Figure 8.1 sketches how sampling and lab analysis were structured and performed in this study.

Most laboratory experiments where carried out in the Geochemical, Hydrological and Geomorphological Lab and the Soil Mechanics Lab of the 'Geographisches Institut, Universität Bonn'

(*Department of Geography, University of Bonn*). A series of experiments were performed in the 'Geotechnisches Labor, Fachhochschule Wiesbaden, Fachbereich Bauingenieurwesen' (*Geotechnical Laboratory, Fachhochschule Wiesbaden, Fachbereich Bauingenieurwesen*) under the supervision of Jörg Bürkle, who worked as a visiting scientist for the project B13. Field and lab experiments in this study were performed, if possible, according to the guidelines of the German Industrial Standard (DIN 1993) (compare Table 8.3). The following sections give some indications about the spatial extent and procedure of sampling for the different lab experiments.

Basic soil properties

Figure 8.1 indicates, that a choice of basic soil properties can be determined for drilling cores (compare section 8.2), including particle size distribution, moisture content, consistency limits, particle density, and maximum moisture content (Enslin–method). Because of the large amount of samples collected, it was not feasible to carry out all experiment types with all samples, therefore the amount of lab test for minor important properties were reduced to important samples. This especially applies to particle density (high lab efforts, low variability, well known empirical values for typical soils, a series of representative test were carried out for different soil types), ENSLIN experiment (relatively high lab efforts, a series of representative test were carried out for different soil types), and consistency limits (low variability, well known empirical values for typical soils, a series of representative test were carried out for different soil types). Fine grain fractions were determined using two test procedures (pipette method and hydrometer method).

Shear strength & saturated hydraulic conductivity

Determination of shear strength parameters was performed by direct shear tests and triaxial tests (Chapter 4). The tests were perfomed in the Soil Mechanics Lab of the 'Geographisches Institut, Universität Bonn' (*Department of Geography, University of Bonn*). Saturated hydraulic conductivity was determined by the methods of constant head permeameter and falling head permeameter (DIN 18130, compare Chapter 4 and DIN 1993). These experiments where carried out in the laboratories of the 'Insitut für Bodenkunde, Universität Bonn' (*Department of Soil Sciences, University of Bonn*) and 'Geologisches Institut, Universität Bonn' (*Department of Geology, University of Bonn*). Because of the high sampling quality needed for these tests, undisturbed samples were taken solely from outcrops. The field sites have the advantage, that each sensitive layer can be assessed by direct outcrops due to horizontal layers on the hillslopes. Therefore, the lab tests concentrated on identifying parameters for specific lithologic layers by sampling from outcrops of well–known lithology, rather than to assess spatial variability of strength parameters (compare Mulder and van Asch (1988) and section 4.3). It was assumed, and proved, that the inter–layer variability exceeds the inner–layer variability significantly to justify this procedure (compare Part VI).

8.4. Climate time series

Climate data on different scales were applied in this study (Table 8.4). Climate information of recent years are required to understand and to model groundwater conditions of the field sites in combination with the captured groundwater data (see above). Climate data for the last decades and proxy data for the last centuries were used to model past process variability (Chapter 11).

Weather records for the Bonn area

A series of measurements from climate stations were available for the Bonn area. These include high resolution measurements (minutes) for recent years, and low resolution (daily, monthly) long–term measurements. For recent years, precipitation measurements were available for four stations

Table 8.4.: Climate time series used in the study. Coordinates given in Gauss–Krüger System.

begin	end	res.	parameter	station/area	coordinates	height
short–term data						
1998	2000	5min	precipitation	Frankenforst 1	2584907,5621070	181
1998	2000	5min	precipitation	Frankenforst 2	2585513,5621234	147
1998	2000	5min	precipitation	Frankenforst 3	2586341,5621031	148
1998	2000	5min	precipitation	Frankenforst 4	2586010,5620841	156
1994	2001	5min	precipitation	Meteorological dept., Bonn	2575305,5622963	75
1994	2001	5min	temperature	Meteorological dept., Bonn	2575305,5622963	75
1994	2001	5min	air pressure	Meteorological dept., Bonn	2575305,5622963	75
long–term data						
1900	1990	month	temperature	Friesdorf	2579600,5618600	62
1889	1990	month	precipitation	Friesdorf	2579600,5618600	62
1959	1989	day	temperature	Klein–Altendorf	2570410,5610656	185
1958	1989	day	precipitation	Klein–Altendorf	2570410,5610656	185
1959	1997	day	precipitation	Wahnbach (Seligenthal)	2590405,5630600	78
proxies / paleo data						
1500	1995	month	humidity proxy	middle Europe	–	–
1500	1995	month	thermal proxy	middle Europe	–	–
1000	1995	season	humidity proxy	middle Europe	–	–
1000	1995	season	thermal proxy	middle Europe	–	–
1000	1995	season	paleo precipitation	middle Europe	–	–
1000	1995	season	paleo temperature	middle Europe	–	–

within the *Versuchsgut Frankenforst*, an agricultural test area of the 'Universität Bonn' (*University of Bonn*) near the field site Dollendorfer Hardt (Preston 2001). However, because of low data quality of these datasets (compare Parkner 2000) and for consistency reasons, data sets from the 'Meteorologisches Institut, Universität Bonn' (*Department of Meteorology, University of Bonn*) were used in this study. The datasets of the Meteorological department also provide temperature and air pressure information which is necessary for correction of the groundwater data (see above). Long–term records were available for station *'Klein–Altendorf'*, which is approximately 12 km southwest of the field site Melbtal and 17 km southwest of the field site Dollendorfer Hardt. The station *'Wahnbach'* is located 16 km northeast of the field site Melbtal and 12 km northeast of the field site Dollendorfer Hardt. The station *'Friesdorf'* is located directly in Bonn, between the field sites. However, because of inconsistencies and problems with the latter data series (station misplacement and station movements during measurement period), and the low data resolution, this dataset was not used as direct model input.

Climate-Proxy data for middle Europe for the last 1000 years

A series of datasets of climate proxy data for middle Europe were provided by Rüdiger Glaser (project HISKLID, compare Glaser 1998, Glaser *et al.* 1999, 2000). These include humidity and temperature indices since 1500 AD and 1000 AD in monthly and seasonal resolution, respectively. Additionally, paleo datasets of seasonal precipitation and temperature were available, which were calculated from recent weather records, available for middle European meteorological stations (details in Glaser *et al.* 2000). These data were used to assess and parameterise historic climatic variablity of the research area (compare Chapter 11).

9. Data management concept and implementation of a DBMS

9.1. Data types & query requirements

9.1.1. Inventory of used data types

Research in mass movements and more general, each environmental research programme, usually incorporates various data types ranging from field and laboratory data to analysis and modelling results. Moreover, often secondary data, e.g. from previous studies and consultancies, deliver additional information. Therefore, a DBMS not only has to include the data itself, but also relevant meta information, e.g. about data sources, data quality etc (Gärtner *et al.* 2000, 2001). Meta information can potentially include a huge variety of information types (compare FGDC 1998). Therefore, the meta data scheme for this study was reduced to represent basic information about data source, data capture and location (Table 9.1). On a general level, the primary data captured by this study can be categorised as shown in Table 9.2 (compare Chapter 8). The data types captured and used in this study can be divided (with respect to the data dimensions) in three types: (1) *spatial Geo–data (termed as 'Geo–data' in the following)*, representing the 2–dimensional spatial distribution of a phenomena (e.g. drilling sites, height values, soil types), (2) mainly numerical *data from field experiments*, which are mostly 1–dimensional data types (distance–attribute), and (3) mainly numerical *data from laboratory experiments*, which represent information of a 'quasi–point' (sample) within the 4–dimensional space. Each type of information naturally implies additional *meta information*.

9.1.2. The query component

Data captured in this study are used in various exploration, analysis and modelling steps. Typical representation techniques in different dimensions (D) include 2D–maps, '3D'(2.5D)–views, 2D–profiles, 1D–borelogs, and diagrams of data (e.g. lab data). General requirement therefore is an easy and fast access to the data in different data views according to the specific application. Within this respect, three types of data queries with varying complexity can be distinguished (Table 9.3).

Table 9.1.: Overview and examples of relevant meta information used in this study.

meta data type	**examples**
data source	*reference*, e.g. project, consultancy report, literature reference
	contact, e.g. institution, producer, reference person, etc.
data capture/production	experiment
	equipment
data location	*location* (e.g. type, name)
	georeference (coordinates, date)
	origin and quality of georeference

Table 9.2.: Overview of data types used in this study (compare Chapter 8).

data type	**data category**	**dimension**
spatial Geo–data ("maps")	DEMs	2D(horizontal)
	topographic maps	2D(horizontal)
	digital vector data	2D(horizontal)
	(digital) aerial photographs	2D(horizontal)
	analogeous maps	2D(horizontal)
geophysical surveys	electromagnetic soundings	2D(profile)
	GPR surveyss	2D(profile)
	geoelectric soundings	2D(profile)
	seismic soundings	2D(profile)
drillings & outcrops	soil descriptions	1D(profile)
	interpretations of outcrop results	1D(profile)
	field penetration tests	1D(profile)
	field vane tests	1D(profile)
lab data	soil samples	0D(point)
	lab experiments	0D(point)
time series	climate measurements	1D(time)
	historical proxy data	1D(time)
	groundwater measurements	1D(time)
	inclinometer measurements	1D(time)
photographs	photographs of outcrops and other field sites	0D(point)
	photographs of drilling cores	0D(point)
	photographs of fieldwork	0D(point)
	photographs of equipment	–
analogous data	analogous maps	2D(horizontal)
	literature (e.g. for reference of datasets)	–
	consultancy reports	–

Table 9.3.: Categories of query types as used in this study. Query type III indicates typical geographical query types as: *'query all drilling sites within a specified map sheet'*. Generally, the different query types require relations to meta information, especially location (georeference) for each dataset (compare Table 9.1).

Query type I: existence queries (e.g. quality maintainance).	
GIS-datasets	— data source, author, spatial extent, etc.
analogous maps	— data source, author, spatial extent, etc.
literature/consultancy reports	— author/institution, location, etc.
photos	— location/object, author, etc.
field & lab data	— experiment type, resp. person, date, location, sample, depth, etc.
time series	— experiment type, resp. person, location, temporal extend, etc.
Query type II: data values from data sets	
map production (overlay)	— typical GIS–functionality (2D/2.5D–visualisation)
geophyiscs	— diagrams (1D/2D–visualisation: location, length–measurement)
drillings & outcrops	— borelogs (1D/2D–visualisation: location, depth–attribute)
climate & groundwater	— diagrams (2D–visualisation: time–variable)
inclinometer data	— diagrams (2D–visualisation: depth–displacement, time–displacement)
lab data	— diagrams (2D–visualisation, mostly non spatio–temporal)
Query type III: spatio–temporal connectivities of different datasets	
map (DEM) + geophysics	— 2D–profiles, 2.5D–views (spatial relation)
map + outcrops	— 2D–profiles, 2.5D–views (spatial relation)
map + groundwater	— 2D–profiles, 2.5D–views (spatial relation)
outcrops + lab data	— 1D, 2D (semantic relation via soil sample)

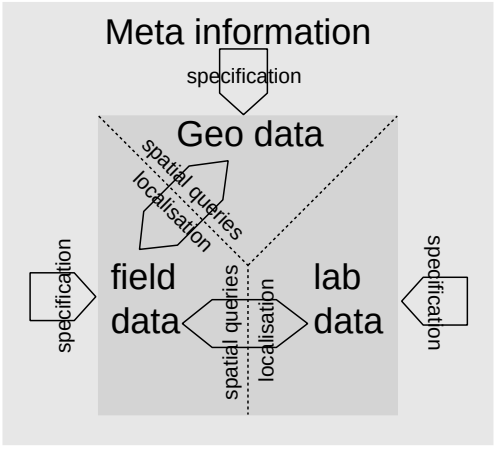

Figure 9.1.: Concept of the developed data structure. For technical considerations (see text), the data model was split into three parts: Geo–data, field & lab data, and meta data. Each part was modelled and realised separately. The communication between the different systems can be easily performed on the client side.

9.2. The conceptual data model

The next step was to develop an adequate data model based on the inventory of data types and query structures. The development went through a series of changes, improvements and simplifications until a final data model was implemented. The development and testing phase took approximately one year, indicating the long development time of a data scheme to be adapted to the required needs. As shown in section 9.1, the captured information can be divided into spatial data (maps), field data, and lab data, and meta information (Figure 9.1). Geo–data are usually stored in GIS for easy reference and spatial query and performance reasons. Meta information contains high amount of text information. Therefore, it was considered to use different DBMS techniques to handle these information types (see below). Hence, the data modelling step was performed separately for the data types with strong emphasis on the interconnections.

Field & lab data (Figure 9.2)
The final structure for field & lab data was chosen for its comparatively simplicity. Three central entity types control the data model: a entity type *'lab'* describing lab work, each lab work is performed on the basis of a soil sample which is represented in the entity type *'soilsample'*. Each sampling procedure has been carried out at a specific field work which defines the third central entity type *'field'*. These three entity types are characterised by a few attributes containing meta information, e.g. the responsible person, the experiment type, the project, the location, and the institution. The attributes are modelled by relations to separate entity types containing the relevant meta information (e.g. name). These entity types, and their internal relations, however, are modelled in detail within the meta–data component (see below). So far, only meta information about field and lab work is available within the described system. The data itself are modelled by a series of entity types, representing the raw data of the field and lab experiments. These datasets show a diverse structure, therefore each experiment type has to be modelled by at least one seperate entity type. In some cases, e.g. lab experiments with time series measurements (shear tests), more entity types have to be provided. Each of these entity types is related either to a *'lab'* entity or to a *'field'* entity. A special procedure was chosen to handle meta information and geometry for locations. The name of an location was represented by a separate entity type *'location'*. Initially,

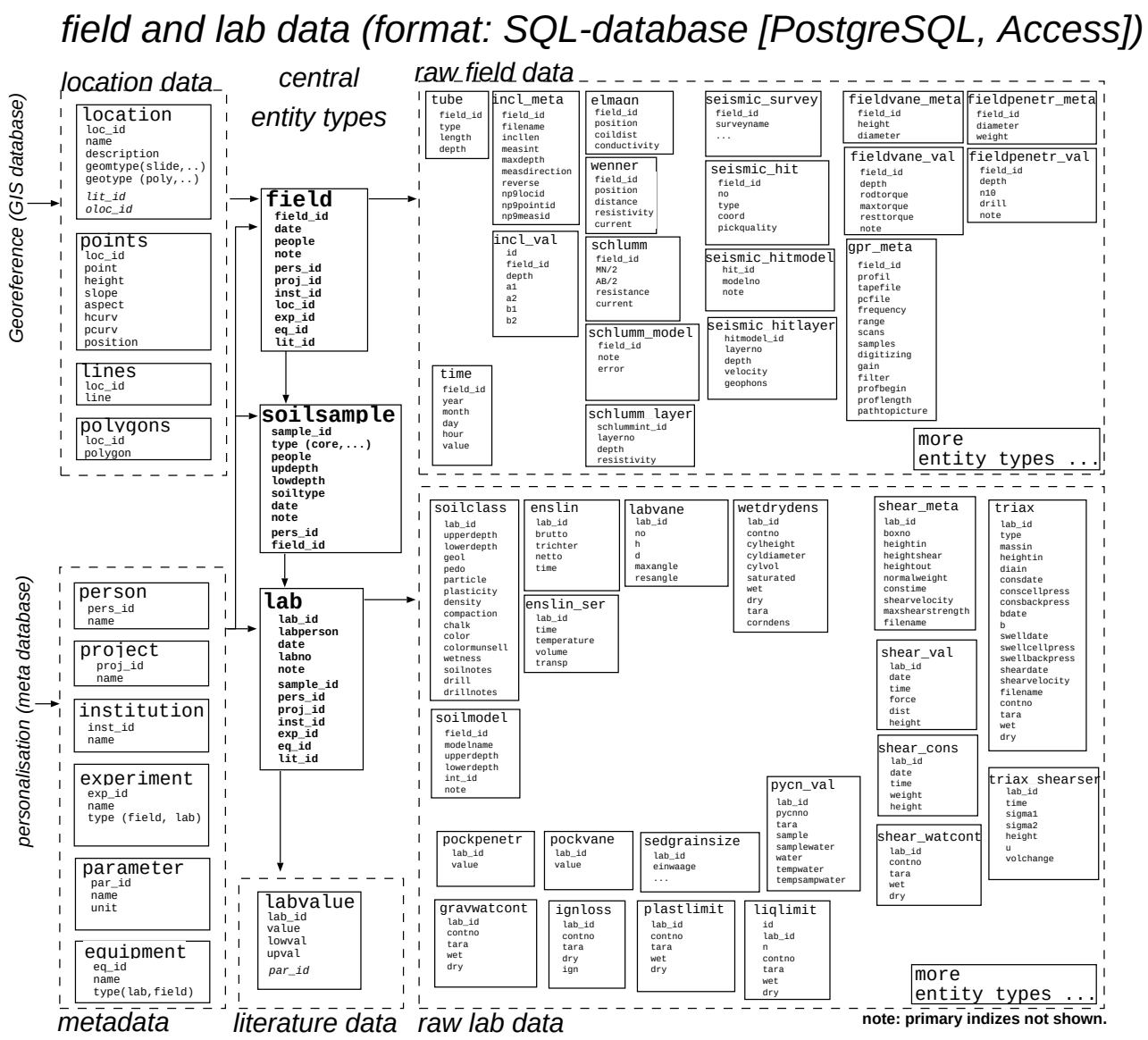

Figure 9.2.: Field & lab data model. Field & lab are divided into raw data and meta data. The relationships are modelled by the connected central entity types *'field'*, *'lab'*, and *'soil sample'*. Meta data are modelled in detail separately in the meta data model (Figure 9.3). Locations were stored as *'points'*, *'lines'*, and *'polygons'*.

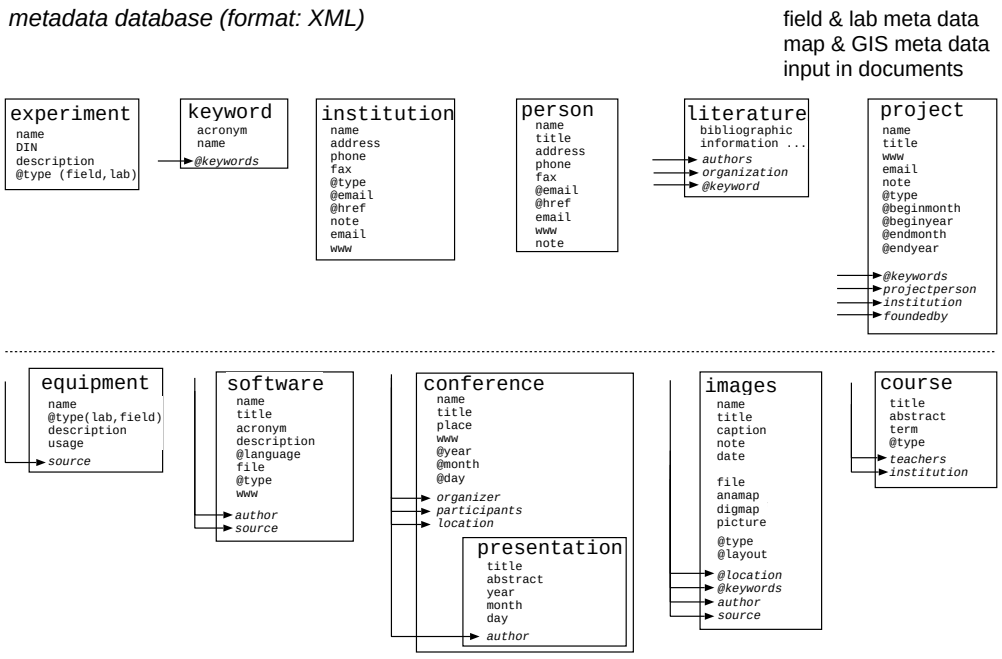

Figure 9.3.: Meta information scheme used in this study. Main purpose is to serve as a reference for field & lab data and Geo–data. One advantage of the implementation in XML is the usage of flexible references to different entity types.

location geometry were stored in the Geo–database (see below). However, the storage of geometries within the field/lab database has the technical advantage of allowing direct queries connecting the basic lab and field data and geometries (e.g. *query all particle size determinations of samples within that landslide object at a certain depth*). Therefore, three separate entity types *'point'*, *'line'* and *'poly'* were designed, storing the geometric information. This separation has been done with respect to the representation of these entity types within a relational database system not allowing the mixture of data types (see below).

Meta–data (Figure 9.3)

A series of common entity types are required to describe meta information about field and lab work as well as meta information contained in Geo–datasets (see Table 9.1, Figure 9.1, compare FGDC 1998). This concerns e.g. data sources (institutions, project, persons), references (literature, presentations at conferences), subjects (keywords), and methods of data capture (experiment, equipment, software). However, these entity types itself are interconnected via a series of relationships. A schematic structure of the entity types and the relations is shown in Figure 9.3. The entity type *'image'* is used to provide meta information both for photographs and Geo–data (maps). The entity types *'experiment', 'equipment', 'insitution', 'person', 'project', 'literature'* were used as metadata references for field & lab data.

Geo–data

Spatial datasets descend from either own work or external sources. External sources can be e.g. official institutions producing official map sheets, or results from projects/consultancies. One method used in this study is terrestrial measurement, producing georeferenced points for measured sites. This data source was used to define locations for various entity types (drillings, surveys, etc), and additionally to produce a high resolution DEM. Moreover, a series of official maps were digitised

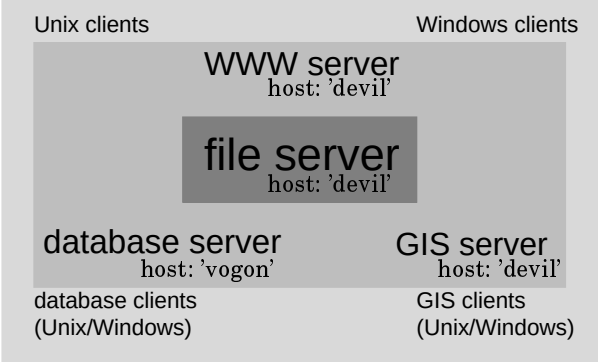

Figure 9.4.: Sketch of the computational environment for the database development.

within the project B13 (see Chapter 8). The meta information for the Geo–data is stored in the meta information scheme.

9.3. Technical realisation of the concept

9.3.1. Overview of the developed DBMS

Technical background

The provided hardware infrastructure within the SFB 350 and the 'Arbeitsgruppe Geomorphologie und Umweltforschung, Bonn' (*Geomorphological and Environmental Research Group, Bonn*) was used to setup an environment for implementing and maintaining the designed data management system (Figure 9.4). A file server provides a file system for data storage. A database server and a GIS server provide connections to the clients. Moreover, a WWW–server provides information for the WWW, based on the available data sources. Clients can connect from either UNIX systems or Windows environments (via a Samba server). This connection was necessary, as the software products used in this study work on different operating systems (see below).

The field & lab data part — PostgreSQL (http://www.postgresql.org)

The DBMS PostgreSQL was used as the back–end database server for the field and lab database. Comparatively low adiministrative efforts, no–cost availablility and availability of a series of tools and clients led to the decision for this database system. PostgreSQL supports standard SQL. Moreover, PostgreSQL supports geometric datatypes (e.g. point, line, path, polygon, compare Lockhart 2000). The storage of geometries within the database has the advantage of direct queries connecting the basic lab and field data and geometries (see above). The listings of SQL–code in the Appendix, which were used to create the data tables of this work, may give some indications of the data base and its usage.

The meta data part — XML (http://www.w3.org/XML/)

The described meta information concept was realised using the extensible markup language (XML). XML is a markup scheme, especially useful in storing data types with high proportion of text. It is very flexible in creating links to entities of different types, e.g. a producer reference for the entity type *'software'* can be directed to institutions, projects or persons. XML is, as the name says, easily extensible. XML can be directly connected to the WWW via a series of techniques. In this study, XSL (extensible stylesheet language) was used.

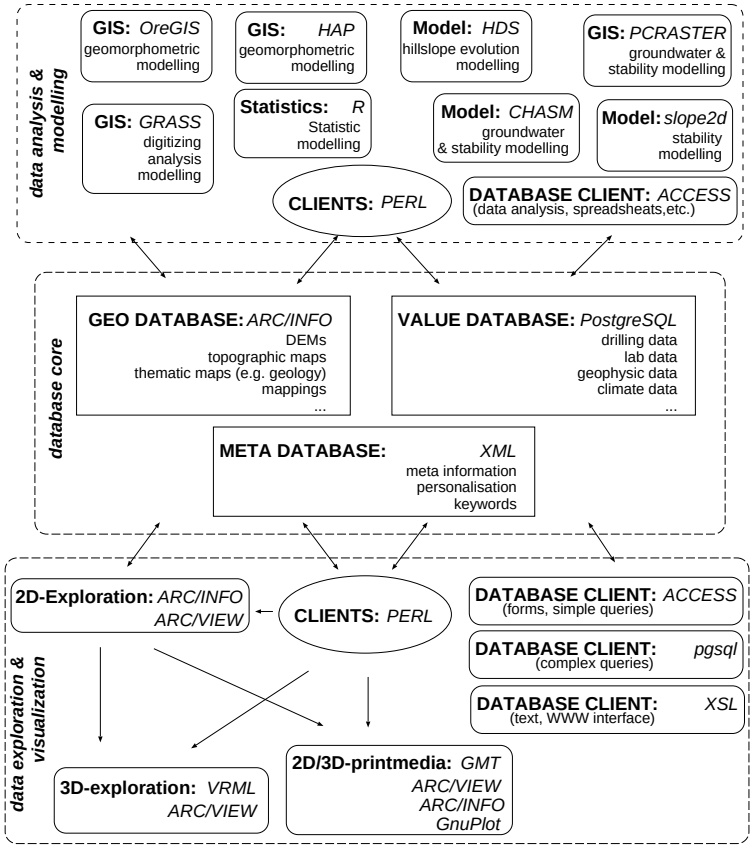

Figure 9.5.: Sketch of data base core and query components used in this study. Query components are subdivided into exploration and analysis tasks. A variety of tools were used to explore, visualise, and analyse the data.

The Geo–data part — ArcInfo (http://www.esri.com/software/arcinfo/index.html)

The GIS ArcInfo provides an powerful Geo–information environment for handling a variety of Geo–data types, and analysing the data with a large set of tools. It was chosen as the central GIS within the SFB 350, and used in this study for storage and query of Geo–data.

9.3.2. Data retrieval components

One advantage of the technical server–side realisation of the DBMS concept is the multi–platform availability of the database (see above). Various tools available on the operating systems UNIX and Windows can be applied to query the database at the same time (Figure 9.4 and Figure 9.5). Therefore, modelling tools working on different platforms can be supplied with data. A lot of figures and tables of this work were created 'on the fly' using different client techniques. The requirements of a query component as defined in subsection 9.1.2 were realised in a series of client tools. A characteristics of the developed database structure is the use of different systems for data storage and management (subsection 9.3.1). The retrieval however, requires the integrated access to these different systems (PostgreSQL, ArcInfo, XML). Moreover, a variety of analysis and visualisation tools were used to parse and to display the data, including GnuPlot, GMT, VRML (Figure 9.5, see Appendix F.3). The programming language Perl offers access to all of these systems and has the advantage of a comparatively easy and powerful programming structure (Wall and Schwartz

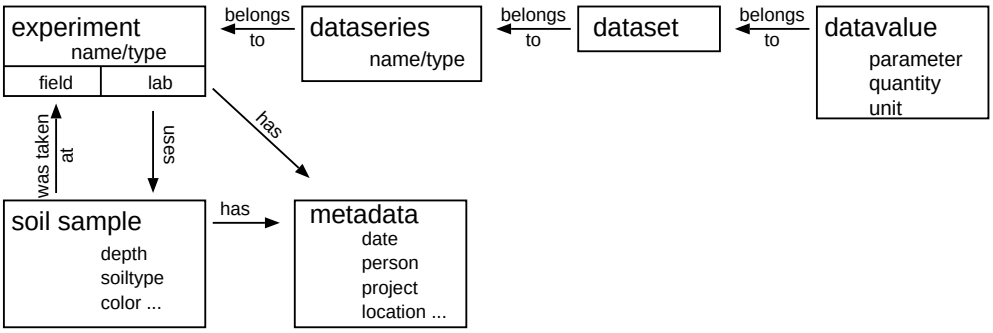

Figure 9.6.: Scheme of a proposed data model. The model offers the possibilty to capture different types of field and lab experiments using a small set of entity types.

1991). Therefore, Perl was preferentially chosen as environment for developing a series of client tools (see Appendix F.3 for details), including the following programs.

mapgen.pl — map generation.
A Perl script producing AML code for direct map generation from the GIS database. Most of the maps of this work were produced using this client.

profgen.pl — profile & 3D–view generation.
A Perl script producing GMT (The Generic Mapping Tools) code or VRML code to display drillings information, provided by the field & lab database, in combination with DEMs, provided by the GIS database. Possible outputs are 2D–profiles or 3D–views (Figure 10.4, page 106).

boregen.pl — A borelog generator.
A Perl script producing GMT code to display borehole logs from information on drillings and lab results, provided by the field & lab database (see Appendix B.1 for program output).

sql2gnuplot–toolbox — A diagram generator for field & lab data.
A series of Perl scripts producing GnuPlot code to analyse and display field and lab information provided by the field & lab database. Most of the diagrams in this work were produced using this client.

fieldlabb13 — A MS–Access client for field and lab data
Data input and data query to the field&lab database can be easily performed using this Windows client, which connects to the PostgreSQL backend via ODBC connectivity. A series of forms and standard queries provide access to the data.

9.4. Discussion

Improvements: A universal model for field & lab data

The final data model (section 9.2) used in this study implies a series of disadvantages. Most important, the fixed data structure (i.e. every experiment has to be represented by a series of entity types) can lead to a huge amount of tables within the database implementation, necessitating high administrative work, and therefore has a limited flexibility. An impoved data structure is proposed which is capable of representing all possible data from field and lab experiments by a series of simple

Listing 9.1: An improved data model for field and lab data: representation as a DTD (simplified version).

```
<!ELEMENT experiment (metadata|dataseries*|soilsample*|experiment*)>
<!ATTLIST experiment type CDATA #IMPLIED>

<!ELEMENT dataseries (dataset*)>
<!ATTLIST dataseries name CDATA #IMPLIED>

<!ELEMENT dataset (datavalue*)>

<!ELEMENT datavalue (#PCDATA)>
<!ATTLIST datavalue
          name ENTITY #REQUIRED
          quantityref IDREF #IMPLIED
          unit ENTITY #IMPLIED
>

<!ELEMENT soilsample (metadata|experiment*)>
<!ATTLIST soilsample
            id ID #REQUIRED
            sample_id ID #REQUIRED
            sampletype CDATA #IMPLIED
            contno CDATA #IMPLIED
            upperdepth CDATA #IMPLIED
             ... and several more
>

<!ELEMENT metadata (date?|responsibleperson*|persons*|project*
                    | institution *|labnumber?|note*|sample?
                    |location ?|georeference ?|experimenttype?
                    |equipment?|literature*)>
             ... here follow the elements for 'metadata'
```

entity types (Figure 9.6). This model was implemented as an XML–document type definition (DTD) (Listing 9.1) and tested by a series of clients. The model represents each experiment (either field or lab) as an entity type *'experiment'*. Each entity of experiment can contain meta information (*'metadata'*) as well as several *'dataseries'* (the measurements). Additionally, *'soil samples'* can be connected to the experiment, if they are taken at a field experiment (drilling, outcrop). A *'dataseries'* consists of *'datasets'* (or simultaneous measurements), each dataset consists of a series of *'datavalues'* (measurement). Each measurement is a quantitative value (either string, boolean, integer or floating) for a certain parameter (may be represented as an external entity type). The proposed data structure not only facilitates the database–management due to limited number of entity types, but can also provide a flexible user–interface leaving the representation of field and lab data at the users side. Although this structure is easy to represent in an DTD as shown in Listing 9.1, a SQL–implementation leads to the problem of integrating different possible data types for the data–values. On the other hand, the realised XML–implementation leads to a large amount of data overhead and inefficient data storage (ASCII) and data query. Therefore, this proposal was not used in this study.

Multi–tool architecture

A obvious degree of data redundancy exists due to the split of the model in different systems. This accounts especially for the connectivity of the SQL–database and the meta information system. Moreover, there is the danger of data loss by changing primary keys, which are not controlled by one database system. This problem can only be handled by a stringent client technique or a server–side technique combining the different systems. Delivering technical realisations for those approaches were out of reach within this study.

Summary

Various data types have been collected in this study. Geo–data (clearly georeferenced data, e.g. maps), field data, lab data and meta–information were considered as information sources which have to be stored and maintained. Therefore, a semantic model was developed and used to set up a DBMS. However, it was not the aim of this study to develop a highly consistent DBMS for all the data captured, but to assess and to prove the capabilities of different techniques for handling different data types. Within that respect it can be stated, that a classical DBMS scheme was developed, combining advantages of different techniques in handling different types of data. The performance of an SQL–server technique in combination with the flexibility of an XML–scheme and GIS technologies for handling Geo–data is to a certain degree an effective data management technique within the framework of classical technologies.

However, improvements could be reached by migrating GIS–data and meta information to a integrated (SQL–) database server, i.e. using the GIS (and other analysis tasks) as a front end technique solely for data analysis and visualisation tasks. Demands towards such systems from a geomorphological point of view were sketched by the author in Schmidt and Gärtner (2000). Another aspect arises from limitations of classical relational DBMS for representing complex entity types and relationships. Gärtner *et al.* (2000, 2001) therefore argues, that object–oriented database modelling techniques deliver a more appropriate technical framework for realizing DBMS in an integrated, interoperative manner for multi–disciplinary data sources. Initial studies in cooperation with the project OPALIS ('Offene Paläoökologische Informationsysteme' (*Open Paleoecological Information Systems*)) indicate the limitations of the classical relational data model and prove the advantages of object–oriented database solutions with respect to integrated data management of diverse geoscientific data. Gärtner *et al.* (2001) presented a study towards an object–oriented datamodel for geoscientific data, based on the data sources of this study.

Part VI.

Data analysis & interpretation — spatio–temporal aggregation

Introductory notes

Investigations of the field sites and the landslide objects involved a range of field and laboratory techniques (compare Chapter 8). Analyses of these primary data aimed at (1) assessment of hillslope hydrology and landslide activity of individual landslide objects, (2) analysis of subsurface structure of the field sites and investigated landslides to derive simplified layer models, and (3) the derivation of representative regolith properties. The aggregated models of surface and subsurface structure, i.e. lithological layers and shear surfaces, are applied in the modelling approches described in Part VII. A large amount of data was collected in this study. For convenience of the reader, only the essential findings are presented in this chapter, which especially contribute to the aims as described above. First, subsurface structures of the field site Dollendorfer Hardt is assessed to derive a generalised model for the lithology of this site (section 10.1). In subsection 10.1.2, results from the landslide 'si7' at the field site Dollendorfer Hardt are presented, including groundwater patterns, landslide kinematics, and subsurface structure. For the field site Melbtal, position and structure of the landslides and the general lithological situation of the valley were analysed (section 10.2). In subsection 10.2.2, a model for the landslide 'me5' at the field site Melbtal is developed, based on previous work and findings of this study. The figures of the following sections are sometimes clustered at the end of the section, to ensure a continuous text. Sorry for the inconveniences!

Note. *For referencing purposes, drilling locations and installation sites are indicated with IDs, e.g. 'dobo1109981'. The numbers aredoll unique IDs, derived from installation date. IDs like 'do...' indicate sites on the Dollendorfer Hardt, whereas 'me...' are sites from the Melbtal. '..bo...' are drillings, '..auf...' are outcrops, and '..inst...' are installation sites, whereas a drilling and installation with the same number indicate the same location (e.g. the borehole 'dobo1109981' was used for installation of gauge 'doinst1109981'). The coordinates of the related locations can be found in Appendix B and in Figures 10.3, 10.10 in this part.*

Another methodological part of this study (Chapter 3) aimed at the development of scenarios for changing climatic boundary conditions for the research area (Chapter 11). Available data include short–term and long–term records from meteorological stations of the Bonn area, and a series of proxy data sets for middle Europe (see section 8.4). A series of statistical techniques were applied, including regression techniques and cluster analysis. These analyses steps aimed at (1) finding relations between Bonn data and proxy data, (2) indicating patterns in the proxy time series, and (3) deriving scenarios of past climate variability in the Bonn area.

10. Subsurface layer models and representative soil parameters

10.1. The field site Dollendorfer Hardt

10.1.1. Lithology

Extensive shallow drilling was carried out at the research site Dollendorfer Hardt by Holler (1998) and Bichler (2001). These data, various available geologic and pedologic maps (compare section 8.1), the results from the subsurface exploration of the landslide 'si7' (subsection 10.1.2), and results from several previous studies were analysed to assess the lithologic structure of the field site Dollendorfer Hardt.
The results from drilling at the landslide 'si7' (subsection 10.1.2) indicate a layering of trachyte tuff above clay–rich Tertiary materials and Tertiary layers which consist of gravels, sands and silts. These findings are contradictory to the situation as sketched in the geological map GK 5209, which shows Tertiary sand above Tertiary clay layers (see above and compare Bichler 2001, Ingenpaß 2000). Generally, Tertiary sediments exhibit a high variability in particle size, and therefore are prone to perched water tables, as indicated by previous studies in the area (compare Nienhaus 1990). A fault line in the course of the landslide 'si7' was found by Schegiewal (1972). The new geological mapping of Bichler (2001) confirmed these results. The Tertiary layers are at a lower hillslope position east of the landslide 'si7', in comparison to the part of the field site west of the landslide. The Devonian baselayer, which is midslope west of the landslide, cannot be found east of the landslide. The geological map GK 5209 depicts no fault line at this locality. Drilling and records from a historic mining and landfill area, which was located on the west facing hillslope of the Dollendorfer Hardt, indicate that the Tertiary and Devonian layers dip towards northwest (Figure 10.1, compare Rogozia 2000).
The available data were used to develop a simplified layer model for the shallow lithologic situation at the field site Dollendorfer Hardt (Figure 10.1), by applying the following modelling steps.

- Comparison of available maps (section 8.1) with respect to consistencies in lithologic boundaries (see above).
- Digitising of layer boundaries from maps and overlay with the DEM (DEM 10) to derive 3D–layer boundaries.
- Including of available height information of layer boundaries from drilling.
- Interpolation of 2D–layer boundaries on the basis of the derived information and simplified geometric assumptions (planar layer boundaries, compare Figure 10.1). For this purpose, the ArcInfo–command `trend` and the GMT–command `trend2d` were used.

Representative soil properties for the modelled subsurface layers can be obtained from the analysis results from the landslide 'si7' and previous studies (compare subsection 10.1.2, Table 10.2).

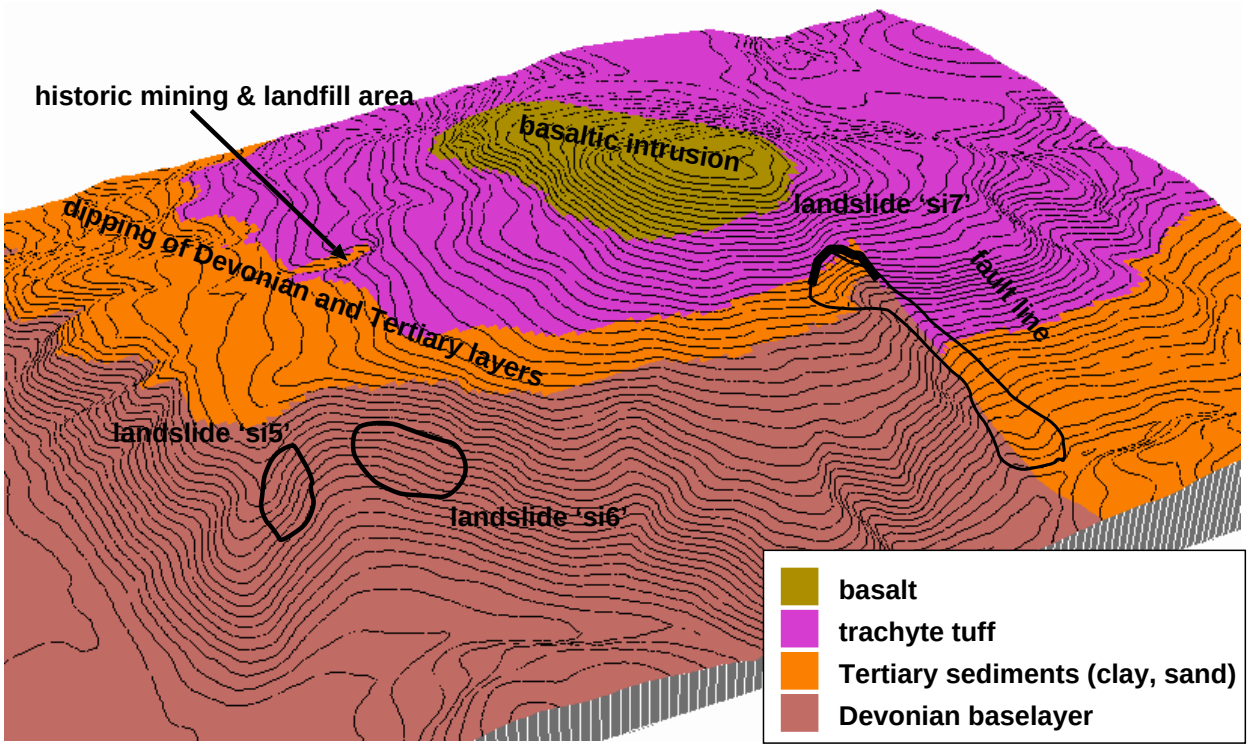

Figure 10.1.: Model of lithological layers for the field site Dollendorfer Hardt. Four major lithological units were derived, based on available drillings and geological maps. The upper and lower layer boundaries were modelled as planes, using GIS functionality. Tertiary sediments showed high heterogeneity, no consistent internal structure of this layer could be derived, therefore only one homogeneous layer were modelled. Pleistocene layers as loess and terrace sediments, which can be found in the northern part of the site, were not considered in the model.

10.1.2. The landslide 'si7': geomorphic structure and kinematics

The landslide 'si7' is located at the south facing hillslope of the Dollendorfer Hardt (Figure 7.6, page 68). The landslide scarp is situated in a steep upslope position. The landslide runout path follows a topographic convergency. The landslide debris reached the valley bottom and formed a series of landslide tongues.

Morphologic structure

The surface structure of the landslide was surveyed using an automatic tachymeter (TCL 1800). The data were used to produce a DEM with a resolution of 0.5 m and a geomorphologic map of the landslide features (Figure 10.2). The landslide can clearly be divided into three parts with respect to process and morphology. The upper part is the scar zone with the scarp and four rotational, back–tilted landslide blocks. The comparatively narrow (¡10 m) and steep middle part is the landslide transport zone characterised by levées and remnant landslide debris blocks (see below). The footslope zone is the landslide accumulation zone with an irregular, hummocky surface of several landslide tongues.

Subsurface structure (compare Appendix B.1)

A series of drillings were carried out on the landslide and the undisturbed side slope (Figure 10.3, compare Appendix B.1). Qualitative interpretation of the drilling logs roughly confirm the lithologic situation, as displayed on the geologic map (GK 5209). Tertiary vulcanic material (trachyte tuff) overlay heterogeneous Tertiary sediments (mainly clay above sand layers) in the landslide scar area. As indicated in the previous section, field evidence of the internal structure of Tertiary layer (clay–rich layers above sand–rich layers) does not agree with the model of the geological map GK 5209. Approximately in midslope position, Devonian material is exposed west of the landslide (*'dobo190398.1'*), whereas an outcrop directly east of the landslide (*'doauf020498.1'*) in the transport zone shows exposed Tertiary clays.
A remnant landslide block in the transport zone was chosen for detailed investigation (Figure 10.4). Morphology and information from local officials give evidence of recent movements in this hillslope position. The drillings provided a detailed insight into this specific part of the landslide. Two types of landslide debris could be distinguished: a lower clay–rich layer dominated by Tertiary clays, and an upper layer, dominated by trachytic and basaltic fragments.
The drillings from the landslide tongue showed high degrees of disturbance of the underlying material, clear changes in stratigraphy (i.e. differences in landslide debris) could not be derived. It was not possible to identify underlying undisturbed material from the drilling cores (maximum drilling depth: 7.5 m).

Representative soil parameters and layer models (compare Appendix C)

Disturbed samples (from core drillings) and undisturbed samples (from outcrops) were used in an intensive lab programme (compare section 8.3) to determine soil properties. Selected lab results are listed in Appendix C. A series of material types were available for undisturbed sampling. These include trachyte tuff, basaltic tuffs and Tertiary clays, sands and silts. Some samples of Devonian material were available from drilling cores, additionally, analysis results from previous studies were available (Jäger 1991). The analysis results for 'ideal' samples from outcrops were used for a preliminary quantification of material properties. Then, the analysis results from the drilling cores were compared to these (particle size distribution, consistency limits, particle density and saturated water content), and used to refine qualitative interpretation of the drilling cores. Finally, lab results from all samples (outcrop and cores) were used to derive representative soil properties for the defined layers. These results for individual (outcrop / drilling) locations were then used in

combination with available mappings to interpolate layer models for the landslide (see below). The complete procedure to derive simplified layer models and to aggregate representative soil properties is sketched in Figure 10.5. The results (compare Figure 10.6 and Table 10.1) show, that a clear distinction for the different material types could be derived. The Tertiary layer consists of (from top to bottom) an upper white clay layer with very low permeability, an upper sand/silt layer, a lower grey Tertiary layer with considerably higher plasticity, and a lower sand layer. Trachyte tuff indicates a significantly higher activity, due to the higher proportion of expansive clay minerals (Figure 10.6, compare Hardenbicker 1994).

Groundwater situation (compare Appendix B.4)

Groundwater tubes (Figure 10.3) on the landslide and on the undisturbed hillslopes were used to monitor spatio–temporal variations of groundwater. Pressure transducers (D–DIVER) were used to obtain quasi–continuous timeseries (sampling interval: 1 h) of groundwater levels for a series of gauges, installed on the hillslope. These timeseries give information about the influence of precipitation, lithology and geomorphometric position on groundwater dynamics. The data indicated a complex hydrologic regime (Figure 10.7). The landslide scar area generally shows high groundwater levels with clear reactions to precipitation events. This can be attributed to topographic convergency effects. The midslope gauges in the transport zone (locations *'dobo190398.1'*, *'dobo180400.2'*) showed comparatively low variations indicating effects of seasonal precipitation variations and direct responses only to extraordinary intensive events (e.g. humid summer 2000). The groundwater gauge in the accumulation area (location *'dobo180698.1'*) indicated low variations and responded only to very wet winter/spring seasons (1998/1999, 2000/2001). From the gauges on the undisturbed hillslope (Figure 10.3), only the uppermost installation (location *'dobo110898.1'*, compare Appendix B.4, page A–33) showed groundwater variations, the four lower gauges (locations *'dobo130898.1'*, *'dobo200898.1'*, *'dobo250898.1'*, *'dobo190398.2'*) were dry during the whole period of measurement.

Landslide acitivity (compare Appendix B.3)

Seasonal occurrence of cracks in the transport zone gave evidence of movements in the middle part of the landslide. Initially, three inclinometer stations were installed on the landslide: in the lower rotational landslide block (location *'dobo120898.1'*), in the transport zone (location *'dobo221098.1'*), and in the accumulation area (location *'dobo030998.1'*, compare Figure 10.3).
The inclinometer installed in the lowermost rotational block of the scar zone (location *'dobo120898.1'*, Appendix B.3, page A–27) showed continuous deformation of the inclinometer tube in downslope direction as a reaction to the intensive precipitation events in spring 1999, which can be interpreted, according to the borehole log (*'dobo120898.1'*, Appendix B.1, page A–12), as mobilisation of younger, trachytic landslide material. Continuous monitoring indicated only a seasonal deformation processes, which turned in a retrograde displacement in dryer seasons. Yamada (1999) gives an explanation of such behaviour, which is related to swelling/shrinking behaviour of saturated soils, and measurement devices, which are installed not normal to the ground surface (tubes were installed approximately vertical in this study).
After the first inclinometer (location *'dobo221098.1'*, compare Appendix B.3, page A–28) broke in the transport zone, two additional devices (locations *'dobo180400.1'*, *'dobo190400.1'*, compare Appendix B.3, pages A–29, A–30) and one continuously monitoring tiltmeter (location *'dobo050400.1'*, Figure 10.8) were installed. The signals detected by the inclinometer measurements and the tiltmeter (Figures 10.4, 10.8) indicated displacement of the younger landslide mass at a shear zone (approximate depth: 3 m) in the middle part of the landslide, which coincide with the drilling results. Approximately 3 cm/m inclination change per month were recorded as reaction to the

intensive rainfall phases in spring 2001.
The inclinometer tube in the accumulation area (location *'dobo030998.1'*, Appendix B.3, page A–31) showed a similar swelling/shrinking behaviour as the station in the lower rotational block (location *'dobo120898.1'*, see above), but of lower magnitude.

Summary

- The drilling and outcrop results suggest a layer sequence on the south facing hillslope of the Dollendorfer Hardt as displayed in Table 10.2 and Figure 10.9. Statistical tests (T–test) revealed, that material types, identified from qualitative assessment, generally show significant differences in soil properties (compare Appendix C.6). Trachyte tuff, Tertiary silt and sand layers, and the Devoian base layer show some similarities in mechanical properties (clay content), the same applies for both (grey/white) Tertiary clay layers (for consistency limits). The weathered Devonian base layer has high clay and silt contents and relatively low sand contents (compare Appendix C.1).

- A permeable layer of trachyte tuff above a series of Tertiary sediments of varying permeability (Table 10.2), indicate a stratigraphy prone to perched water tables. A groundwater table was found directly above the grey Tertiary layer (location *'dobo110898.1'*, Appendix B.4, page A–33). Shear strength, as determined from shear box tests and triaxial tests (see Appendix C.4), show high variabilities. Low values for the peak and residual friction angle, were derived for the grey Tertiary clay layer at the landslide scar (Table 10.2), indicating a potential shear zone of the landslide.

- The landslide is located in the course of a fault line, indicating disturbance of the underlying material as an additional factor, leading to a decrease in shear strength.

- Landslide debris can be divided into two material types, a lower layer is dominated by clay–rich material (similar to grey Tertiary clay), the upper debris is characterised by high fractions of trachytic material. Additionally, the tongue morphology (Figure 10.2) implies the occurrence of two major landslide events. Because of the high degree of disturbance of the underlying material, these findings could not be confirmed from borehole logs in the accumulation zone. Archive studies from Hardenbicker (1994) and (Weber 1991) dated these landslide events to 1958 and 1972. According to the results, two major events occurred at this site: the first event involved mainly Tertiary clays (low shear strength, see above), the second event led to failure of trachyte tuff (compare section 12.1).

- The movement measurements indicated an elastic pattern for the lower rotational landslide block. The landslide transport zone shows permanent displacements of the younger landslide mass (depth approximately 3 m) in the order of magnitude of several cm in wet spring (1999, 2001). These activity patterns show the high relevance of seasonally rising groundwater levels due to intensive precipitation events in spring for landslide activity, as indicated by previous studies (Hardenbicker 1994).

- The available information were used to model a landslide structure as sketched in Figure 10.9. Lithological layers were modelled horizontally. However, the complex stratigraphy of the landslide material in the scar area, led to a considerable amount of uncertainty within the models of shear surfaces, especially for the lowermost landslide block. The high degree of disturbance of the material in the scar area (e.g. 10 m disturbed material in upper rotational block), led to the hypothesis that the site has been affected by older landslides (Hardenbicker 1994).

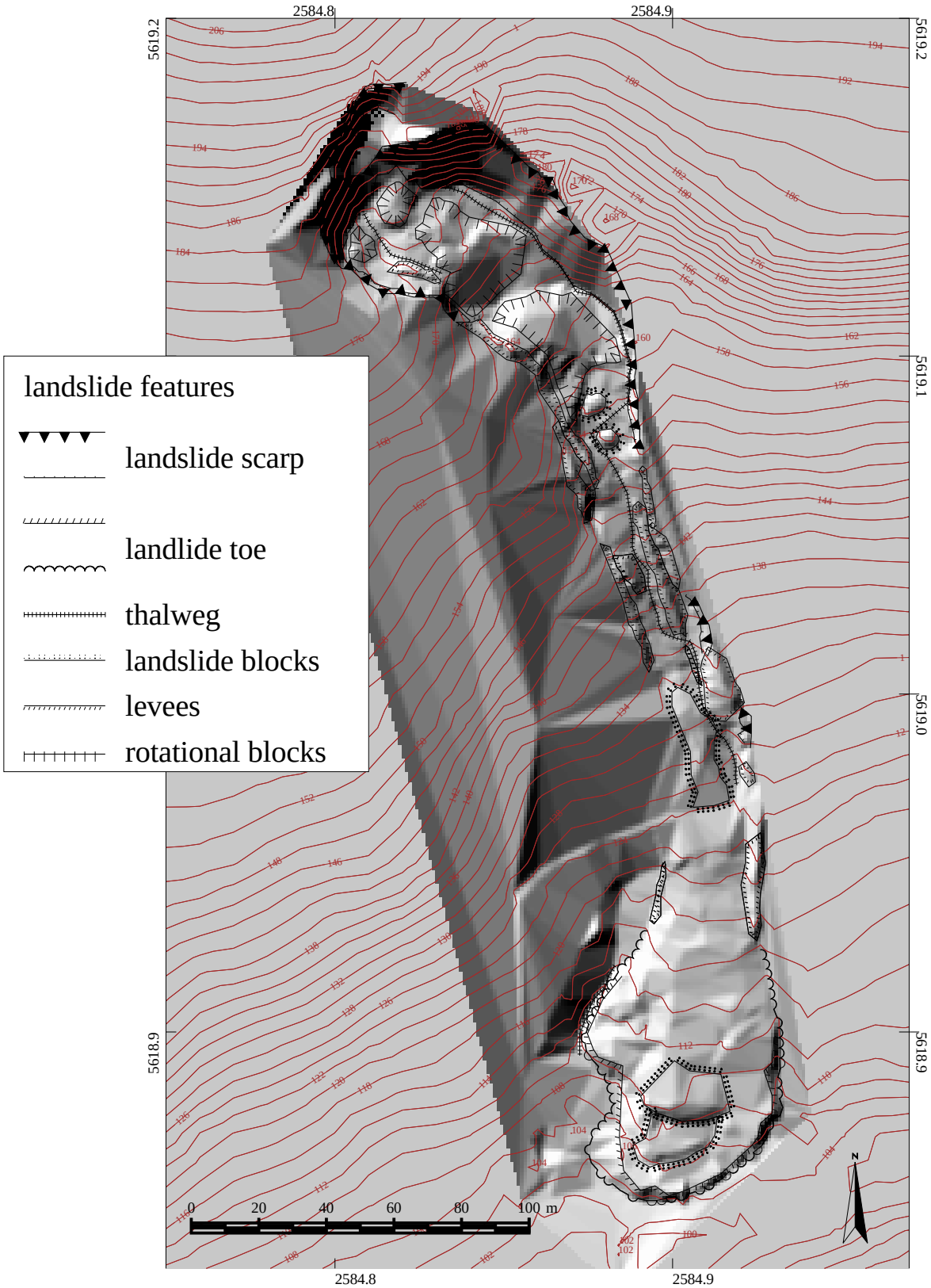

Figure 10.2.: Mapped geomorphological features of the landslide 'si7', superimposed on a shaded relief, generated from a high resolution DEM. Triangular structures are artefacts from bilinear interpolation and low data density. The landslide can be clearly devided into scar area, transport zone, and landslide tongue.

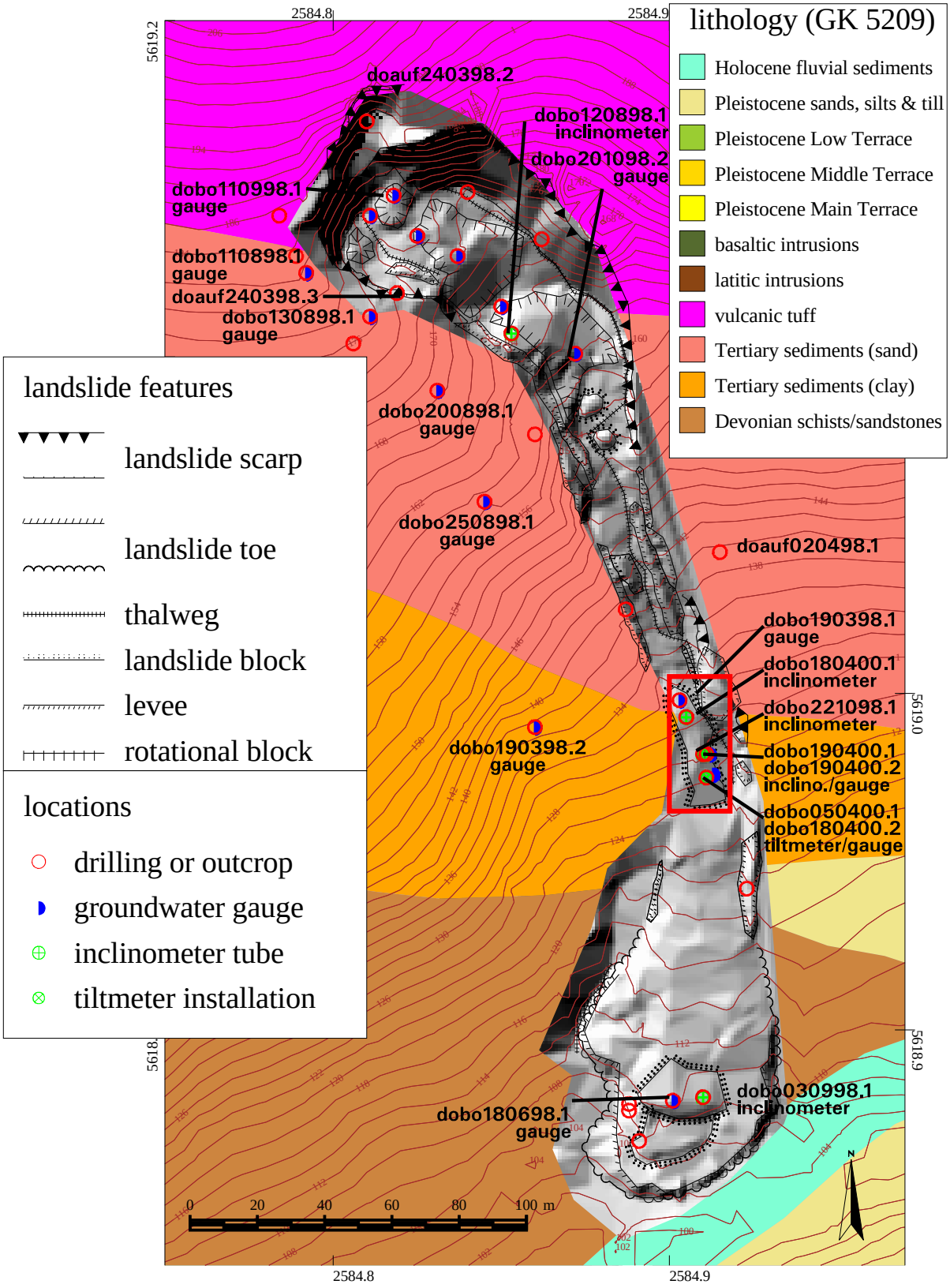

Figure 10.3.: Locations of drillings, outcrops, and measurement equipment on the landslide 'si7'. Additionally, lithological units from the geological map (GK 5209) are displayed. The box indicates a part of the transport zone, which was chosen for detailed investigation (Figure 10.4).

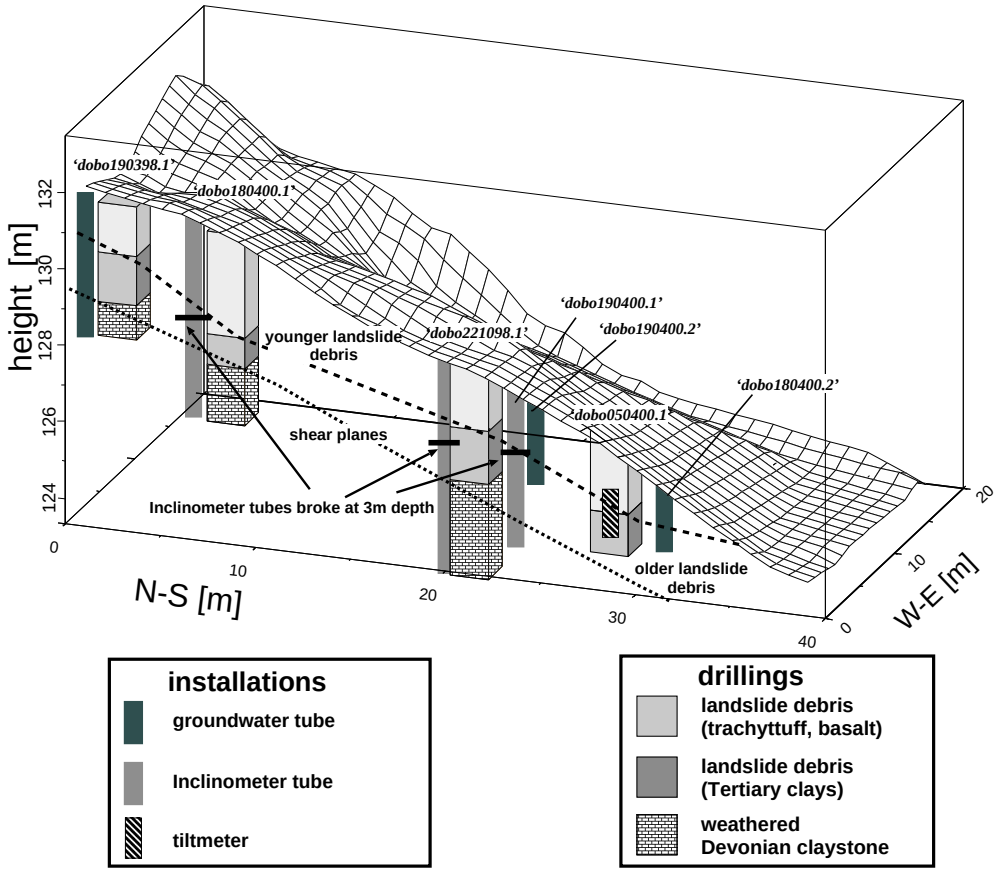

Figure 10.4.: The middle part of the landslide 'si7' (see Figure 10.3 for georeference). The surface is shown as a grid. Drilling locations, and measurement installations are shown as boxes (see legend). The stratigraphy and the measurement results give evidence of landslide debris resulting from two events, and seasonal movements of the younger landslide mass.

Table 10.1.: Statistical properties of values from lab results landslide 'si7'. Shown are densities (ρ_b,ρ_d,ρ_{sat},ρ_s), consistency (w_l,w_p,I_p) and saturated conductivity k_s (see Chapter 'Symbols' in the beginning of this document). Listed values are average and standard deviation ($\mu \pm \sigma$) of soil properties from laboratory experiments for different lithologic units. Saturated conductivity is displayed as negative logarithm.

material	ρ_b [g/cm^3]	ρ_d [g/cm^3]	ρ_{sat} [g/cm^3]	ρ_s [g/cm^3]	w_l [1]	w_p [1]	I_p [1]	k_s [- log m/s]
trachyt tuff	1.91 ± 0.13	1.61 ± 0.11	2 ± 0.16	2.64 ± 0.91	0.34 ± 0.05	0.21 ± 0.04	0.13 ± 0.05	5.8 ± 1.7
Tertiary clay (white)	2.03 ± 0.18	1.73 ± 0.16	2.18 ± 0.15	2.64 ± 0.91	0.31 ± 0.04	0.19 ± 0.03	0.12 ± 0.05	8.4 ± 1.2
Tertiary clay (grey)	1.94 ± 0.1	1.65 ± 0.08	2.04 ± 0.04	$2.49\pm$	0.43 ± 0.12	0.20 ± 0.04	0.23 ± 0.11	7.2 ± 0.9
Loess	–	–	–	0.24	0.23	0.01	2.55	–
Tertiary sand/silt	1.78 ± 0.14	1.42 ± 0.16	1.88 ± 0.1	2.52 ± 0.47	0.26 ± 0.07	0.18 ± 0.04	0.08 ± 0.07	5.3 ± 0.67
Devon	1.77	–	–	–	0.38	0.25 ± 0.01	0.13 ± 0.02	–

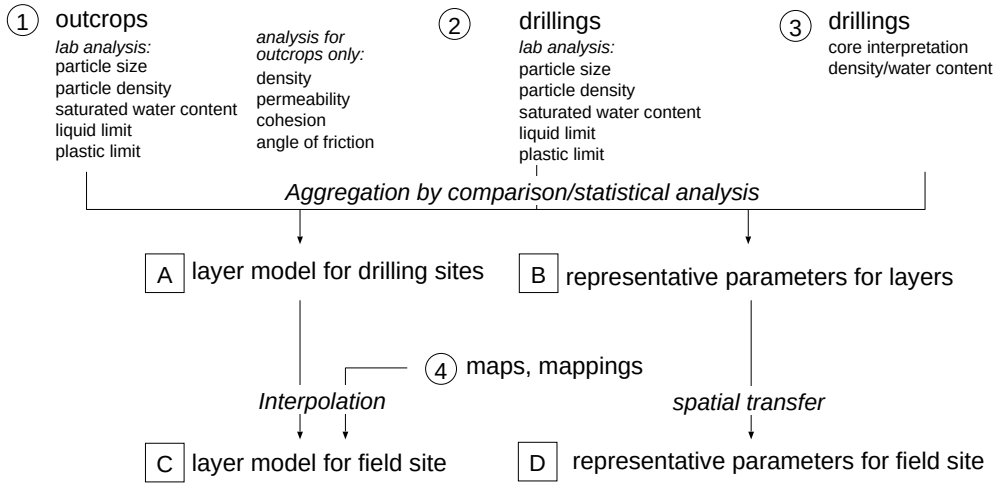

Figure 10.5.: Methodological framework for deriving aggregated layer models and representative soil parameters. First, lab results from outcrops (1) were compared to lab data from drilling cores (2) to refine initial qualitative layer interpretations (3). The resulting layer models for the drillings sites (A) and representative soil parameters (B) were used to interpolate layer models for the field site (C+D), taking external information, as mappings (4) into account.

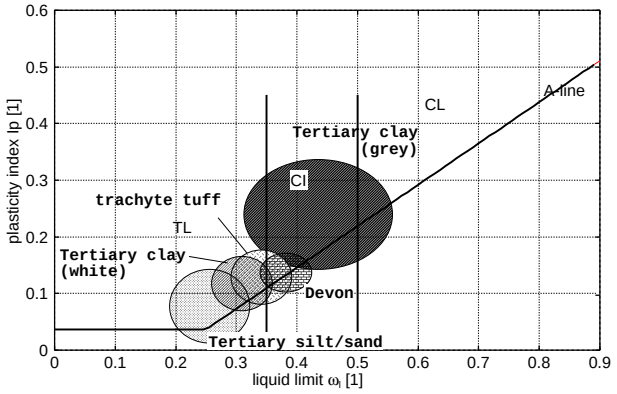

(a) Plasticity chart for material types of the landslide 'si7'

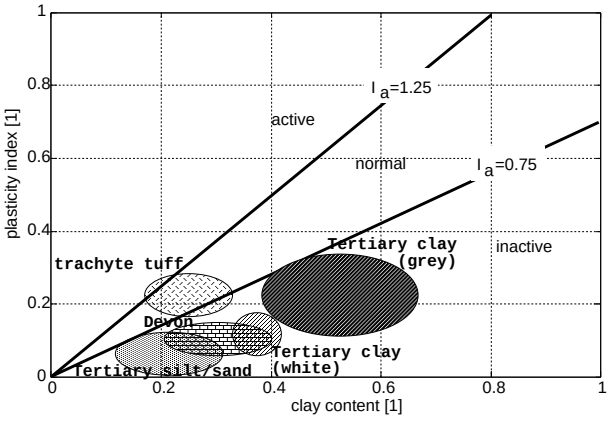

(b) Activity chart for material types of the landslide 'si7'

Figure 10.6.: Plasticity chart (a) and activity chart (b) for material types of the landslide 'si7'. The diagram indicates typical value ranges for different material types from statistics of lab experiments (Table 10.1).

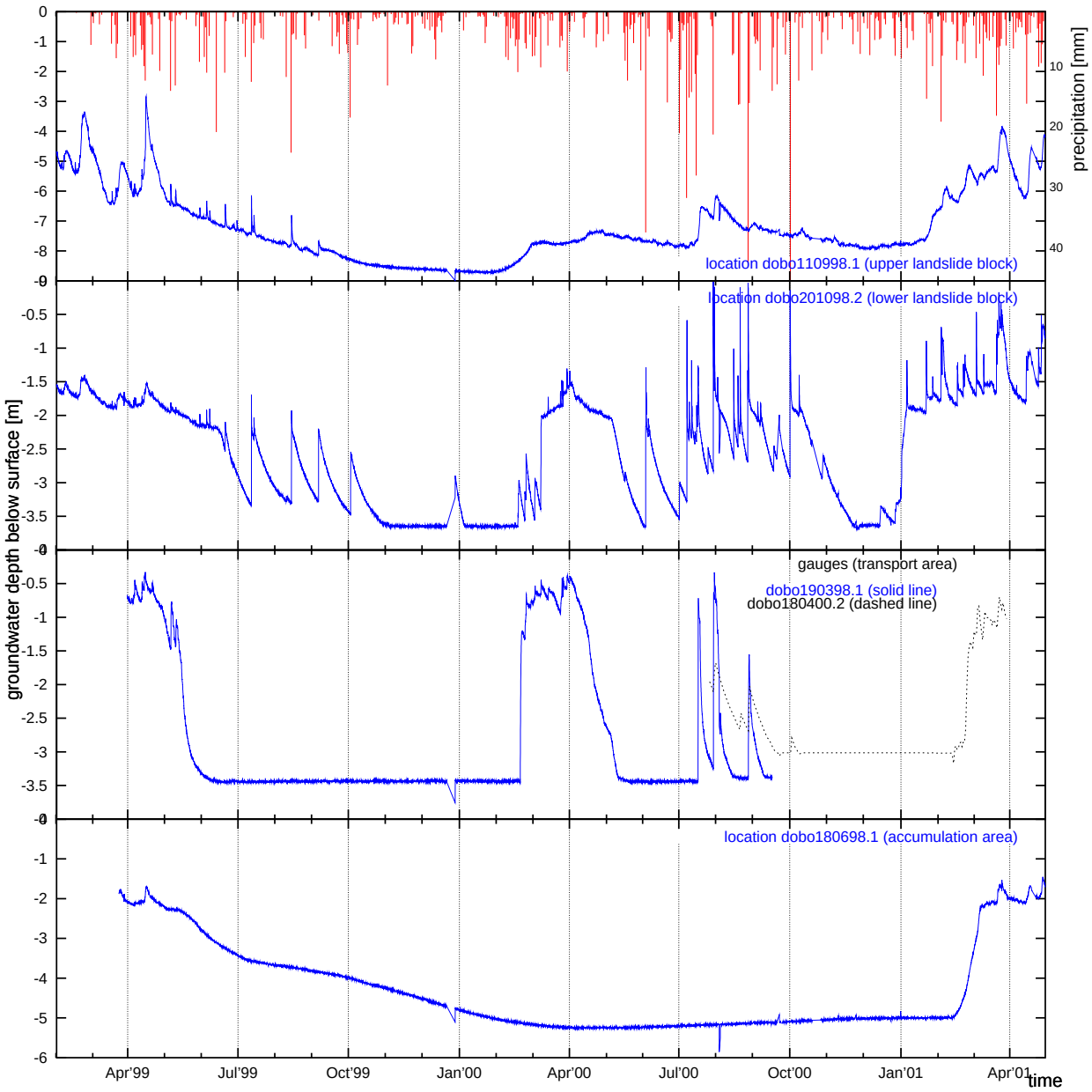

Figure 10.7.: Monitored groundwater levels, landslide 'si7' and precipitation data (station 'Meteorological department'). The data show a complex spatio–temporal pattern of the landslide groundwater situation: The landslide scar area (locations *'dobo110998.1'*, *'dobo201098.1'*) generally showed high groundwater levels with strong reactions to precipitation events. The gauges in the transport and accumulation zone showed comparatively low fluctuations, responding mainly to seasonal precipitation variations.

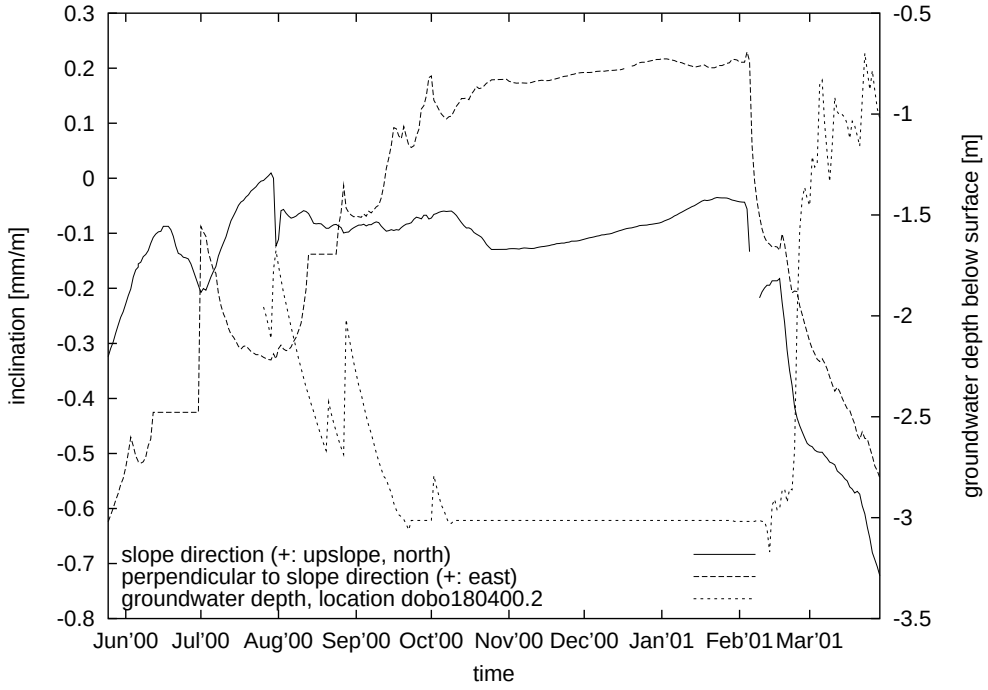

Figure 10.8.: Movement measurements (tiltmeter, location *'dobo050400.1'*) and groundwater data, middle part of landslide 'si7' (project C1, Marcus Fabian, compare Figure 10.4). The signals indicated strong downslope movements (negative inclination change), as a reaction to groundwater rise in spring 2001.

Table 10.2.: Typical stratigraphy and material properties in the landslide scar area of the landslide 'si7' (see 'Symbols' in the beginning of this document). Height is given as the approximate lower layer boundary. Values were derived from analysis results of this study and literature values.

material	height [m]	ρ_b [g/cm^3]	ρ_d [g/cm^3]	ρ_{sat} [g/cm^3]	n [1]	w [1]	w_c [1]	c'/c'_r [kN/m^3]	ϕ'/ϕ'_r [kN/m^3]	k_s [m/s]
trachyte tuff	185 m	1.9	1.6	2.0	0.4	0.2	0.25	20/20	32/27	10^{-6}
Tertiary clay (white)	180 m	2	1.7	2.2	0.35	0.2	0.3	0/0	30/28	$10^{-8} - 10^{-9}$
Tertiary clay (grey)	170 m	2	1.7	2.1	0.35	0.2	0.25	20/10	23/14	10^{-7}
Tertiary silt/sand	145 m	1.8	1.4	1.9	0.45	0.3	0.35	60/40	25/20	$10^{-5} - 10^{-6}$
Devonian clay/silt	–	1.9*	1.6*	2.1*	0.4*	0.2*	0.3*	30/10	20/13	$10^{-6} - 10^{-10}$*

* estimated from literature values (see Appendix E).

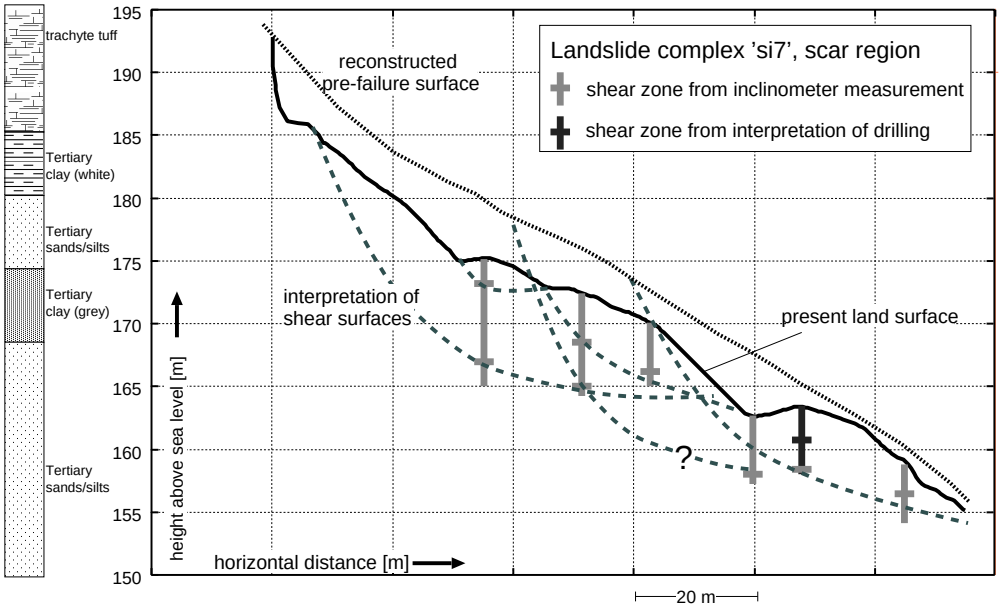

Figure 10.9.: Two dimensional model of the landslide 'si7'. Profile of lithologic layers, interpolated shear surfaces and reconstructed pre–failure surfaces (from profiles of undisturbed slopes) are included.

10.2. The field site Melbtal

10.2.1. Landslides and lithology

Landslides

A series of landslides in the Melbtal were mapped by Hardenbicker (1994) (compare Figure 10.10). A landslide event (*'me6'*) in 1988 caused severe damage and required intensive remediation work (Kaiser-Kühn 1988). Drilling and groundwater investigation results are available from Heidemann (1996) and Schmanke (1999) for two specific landslides (*'me1'* and *'me5'*, see Figure 10.10). In general, all mapped landslides are located within the lower part of the valley, where sensitive Tertiary layers are exposed. Landslide mechanisms and geometry imply translational and rotational failure, coupled with fluvial erosive activity of the *Engelsbach*. The depths of shear surfaces vary from 4 m to 8 m. Figure 10.11 scetches the geomorphologic and lithologic situation of some landslides in the Melbtal, constructed from the mentioned data sources and findings from this work (see below).

Subsurface structure — results from drillings and outcrops (compare Appendix B.1)

A series of drillings were carried out on the valley side slopes to gain a more detailed insight into the lithological conditions of the lower, sensitive valley part (Figure 10.10, Appendix B.1) (compare May 2001). The west facing valley slopes indicated undisturbed regular stratigraphy, whereas the borehole logs from the east facing hillslopes often were characterised by frequent layer changes. The borehole logs from the west facing valley slopes showed a general stratigraphy (from top to bottom) of (1) loess layers (up to 4 m), (2) several m homogeneous Tertiary sand, (3) small lignite layers (tens of cm), and (4) layers of grey Tertiary clay. The borehole logs from the east facing hillslopes often show several lignite layers. For example, geomorphologic evidence suggest that the borehole *'mebo010999.1'* is located on an undisturbed hillslope. The borehole log (Appendix B.1, page A–17), however, showed a complex stratigraphy with frequent changes in soil properties.

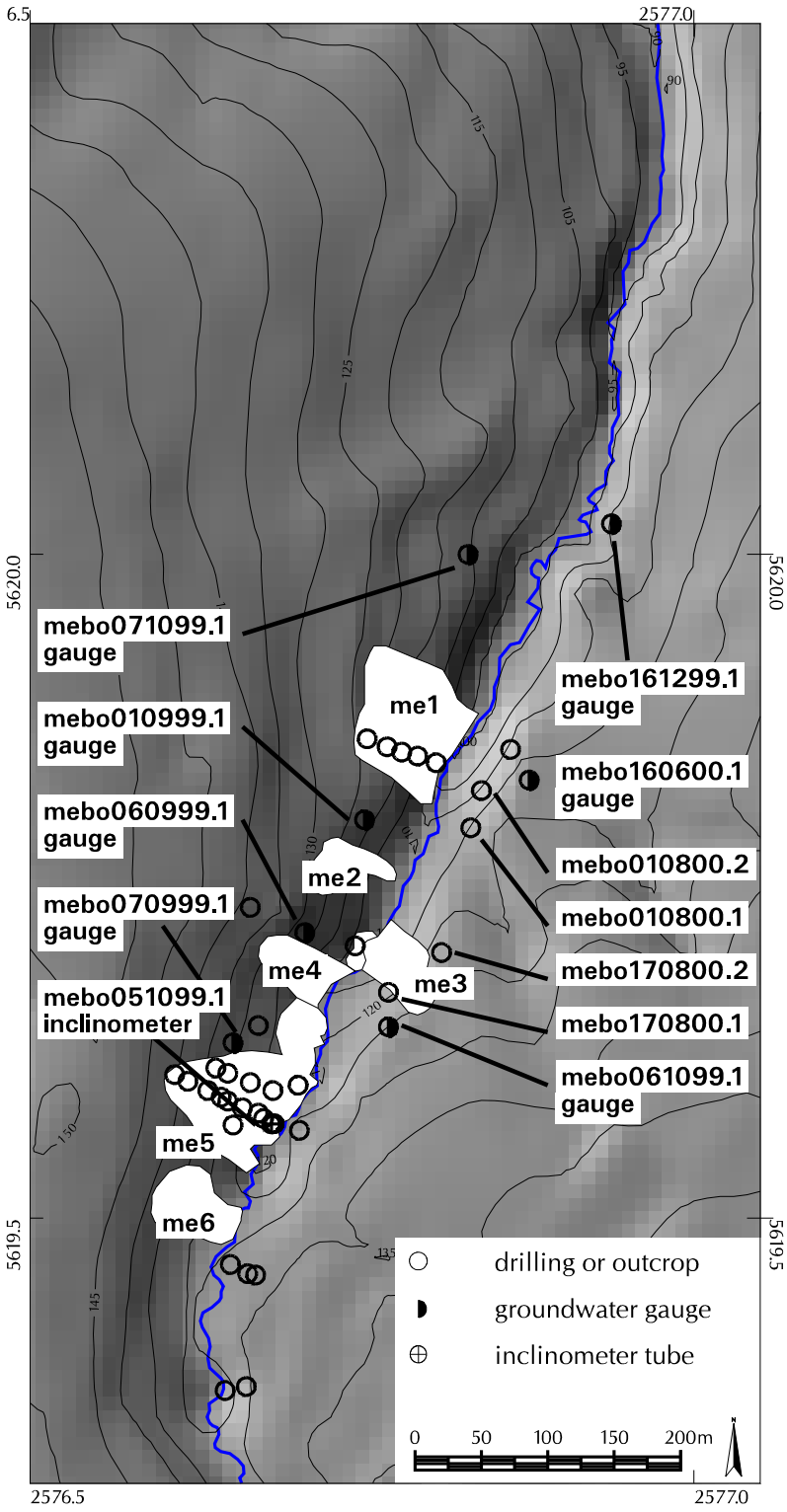

Figure 10.10.: Locations of landslides, drillings (data from this study and Heidemann 1996) and measurement equipment in the lower part of the Melbtal, superimposed on a shaded perspective of a DEM. White polygons denote landslides.

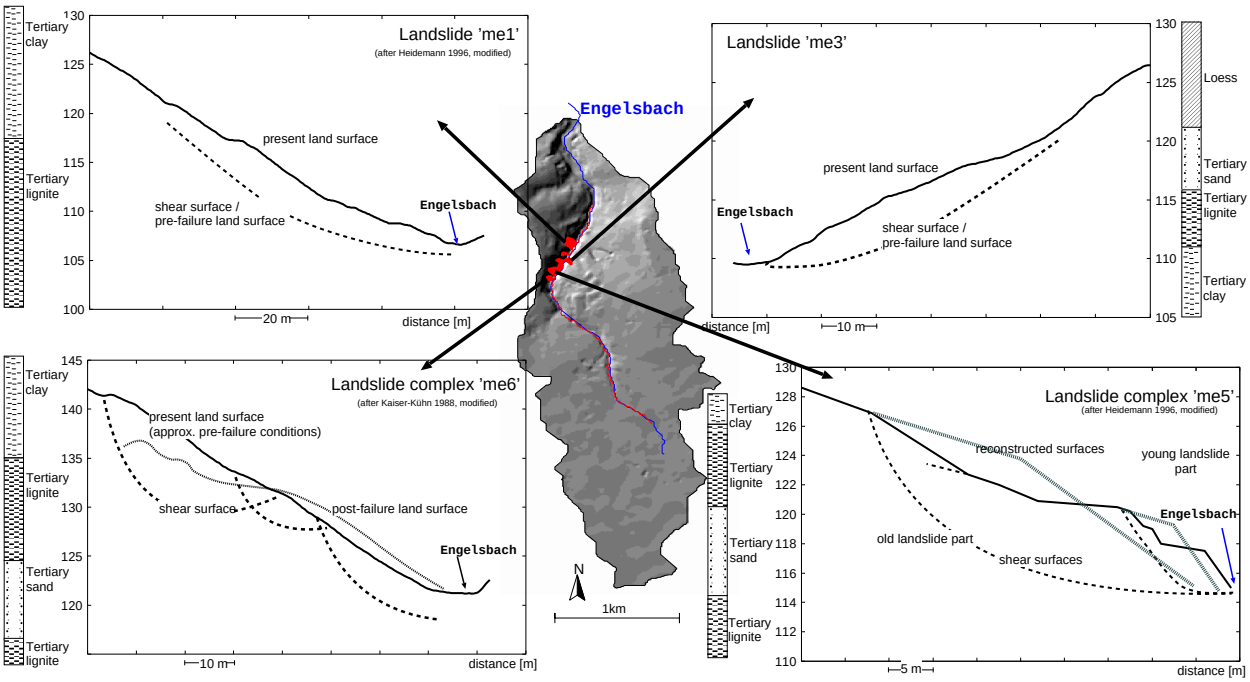

Figure 10.11.: Models of some landslides in the Melbtal according to results from this study and previous investigations. The position of landslides indicate the coupling with the stream and the dependency of landslide occurrence to sensitive layers of Tertiary lignite and clay.

Therefore, only a very crude (high deviations possible!) subsurface layer model could be derived for the east facing hillslopes of the lower valley, including (from top to bottom) (1) an upper clay layer above a (2) upper lignite layer, (3) mixed silt/sand layers, and (4) a lower lignite layer above (5) a lignite–rich clay layer. Two possible hypotheses arise from this field evidence: (1) most of the east facing hillslope is disturbed by recent and old landslides (evidence for only one landslide on the west facing hillslopes) or other (maybe periglacial) hillslope processes, or/and (2) a fault line in the area of the Melbtal led to uplift of the west facing valley side relative to the east facing slopes, leading to different exposed stratigraphies (compare Figure 7.7, page 70 and Heidemann 1996, May 2001). Generally, the landslide occurrence of the lower part of the Melbtal can be related to sensitive situation of Tertiary lignite above clay layers. Most landslide occurrences can be related to lignite layers as shear zones (Figure 10.11).

Representative soil properties (compare Appendix C)

The method for deriving representative parameters is the same as described for the field site Dollendorfer Hardt (subsection 10.1.2, compare Figure 10.5, page 107). Due to the clear distinction of sand, clay, lignite and gravel layers (see above), the classified materials differ significantly in their properties (Table 10.3, compare Appendix C.1, C.6).

Groundwater situation (compare Appendix B.4)

Groundwater height was monitored (autumn 1999 – spring 2001) by a series of gauges in the field area (Figure 10.10, see the diagrams in Appendix B.4). Four gauges were equiped with an hourly sampling D–DIVER. The locations *'mebo060999.1'* and *'mebo061099.1'* (Appendix B.4, pages A–39,A–40) showed relatively homogeneous groundwater levels with low variations, which can be attributed to sand–rich, permeable layers on top of clays leading to fast lateral soil water transport

Table 10.3.: Statistical properties of values from lab results, Melbtal. Listed are average and standard deviation ($\mu \pm \sigma$) of clay and sand fractions (c_T,c_S), densities (ρ_b,ρ_d,ρ_{sat}) and saturated conductivity k_s from laboratory experiments for different lithologic units. See 'Symbols' in the beginning of this document.

material	c_T [1]	c_S [1]	ρ_b [g/cm^3]	ρ_d [g/cm^3]	ρ_{sat} [g/cm^3]	k_s [-log m/s]
loess	0.2 ± 0.08	0.04 ± 0.04	1.42 ± 0.07	1.36 ± 0.06	1.88 ± 0.06	5.8 ± 0.41
terrace	0.11	0.22	1.88 ± 0.05	1.64 ± 0.05	2.03 ± 0.03	3.9 ± 0.68
Tertiary clay	0.61 ± 0.24	0.08 ± 0.1	2.08 ± 0.07	1.94 ± 0.19	2.25 ± 0.21	6.1 ± 0.44
lignite	–	–	1.62 ± 0.36	0.94 ± 0.2	1.65 ± 0.15	6.7 ± 0.98
Tertiary sand/silt	0.08 ± 0.12	0.63 ± 0.36	1.61 ± 0.05	1.51 ± 0.19	2.08 ± 0.16	6.2 ± 0.66

Table 10.4.: Typical stratigraphy and material properties of the Melbtal (see chapter 'Symbols' in the beginning of this document). Values were derived from analysis results of this study and literature values.

material	particle size	ρ_b [g/cm^3]	ρ_d [g/cm^3]	ρ_{sat} [g/cm^3]	n [1]	w [1]	w_c [1]	c'/c'_r [kN/m^3]	ϕ'/ϕ'_r [kN/m^3]	k_s [m/s]
loess	silt	1.5	1.4	1.9	0.45	0.1	0.4	30*/-	30*/-	10^{-6}
terrace	sandy gravel	1.9	1.6	2.0	0.4	0.2	0.3	30*/-	30*/-	10^{-4}
Tertiary clay	clay	2.1	1.9	2.3	0.25	0.1	0.2	50/30	25/20	10^{-6}
Tertiary silt/sand	silt/sand	1.6	1.5	2.1	0.4	0.1	0.4	30*/-	30*/-	10^{-6}
Tertiary lignite	clay	1.7	0.9	1.7	0.6	0.8	0.8	0*/-	20*/-	10^{-6}

* estimated from literature values (compare Appendix E).

and exfiltration in downslope positions, as indicated by wet areas in the whole lower valley course (compare Hardenbicker 1994). For the locations *'mebo070999.1'* and *'mebo071099.1'* (Appendix B.4, pages A–40,A–39), which show higher clay content and higher material heterogeneity, larger variabilties in groundwater levels could be detected. The timeseries generally depict less effects of seasonality, as it was the case for the field site Dollendorfer Hardt.

Summary

- Due to the distinct differences in subsurface material, a model for representative parameter values for different soil layers could be developed for the Melbtal (Table 10.4).
- Shear strength has been determined for the potential shear surfaces, i.e. Tertiary clay below permeable lignite layers (see Appendix C.4) indicating values of $c' = 50$ kN/m^2 and $\phi' = 25\,^\circ$ (Table 10.4).
- Whereas the individual drillings often show certain layer patterns, tracing of layers and development of a general layer model for the field site Melbtal was not feasible. Instead, local models were developed for the individual valley hillslopes to assess effects of lithologic change on slope stability (Chapter 12).

10.2.2. The landslide 'me5'

This landslide has been extensively investigated by previous studies. Mappings (Hardenbicker 1994, Heidemann 1996), a series of drilling logs (Heidemann 1996), as well as initial results about groundwater and soil water situation (Schmanke 1999) are available.

Morphology, subsurface structure, and groundwater situation

Morphologic evidence and drilling results (Heidemann 1996) imply, that the landslide complex is built up of older landslide masses, which extend to the upper hillslope (see Figure 10.10 and

Figure 10.12.: Younger landslide area within the landslide complex 'me5'. Note the tilted trees and the coupling with the stream (in foreground). (photo: Volkhard Schmanke)

compare Schmanke 1999). A younger landslide occurred in the tongue area of the older complex (Figure 10.12) approximately in 1920 (Heidemann 1996). Soil water and pore pressure measurements carried out by Schmanke (1999) indicate high soil water content and lower suction values for the young landslide mass at a depth of 1.5 m. These findings are in accordance with the inclinometer results of this study (see below) and the drilling results of Heidemann (1996) (Figure 10.14), locating the shear surface of the younger landslide. Groundwater measurements from Schmanke (1999) indicate, that high groundwater tables occurred in wet seasons (winter and spring). The groundwater pattern in the landslide area, measured by Schmanke (1999), depicts high variability due to heterogeneity of the Tertiary material and the disturbed subsurface structure in the landslide area. The stratigraphy of the Tertiary material showed a high variability (compare Heidemann 1996). However, outcrops near the landslide (compare Heidemann 1996, May 2001) led to a simplified model of the stratigraphy, starting from the top (1) a clay–rich layer, (2) an upper lignite layer, (3) a sand layer, and (4) a lower lignite layer (Figure 10.14).

Landslide acitivity

Although the fluvial activity of the creek *Engelsbach* leads to recent undercutting of the landslide tongue (Figure 10.12, compare May 2001), surface measurements from Schmanke (1999) gave no evidence about movements of this landslide. Therefore, an inclinometer tube (location *'mebo051099.1'*) was installed in the upper part of the younger landslide area of the landslide 'me5' (Figures 10.14, 10.10). After minor variations in 2000, a strong downslope movement was monitored in spring 2001 (Figure 10.13). This signal indicates two different shear surfaces at 1.5 m to 2 m (younger landslide mass), and at approximately 4.5 m (older landslide mass). The signals showed maximum movements in the order of 1 cm/m inclination change per month. A structure as sketched in Figure 10.14 can be deduced for the landslide *'me5'*, by combining available mapping and drilling results with the recorded movements.

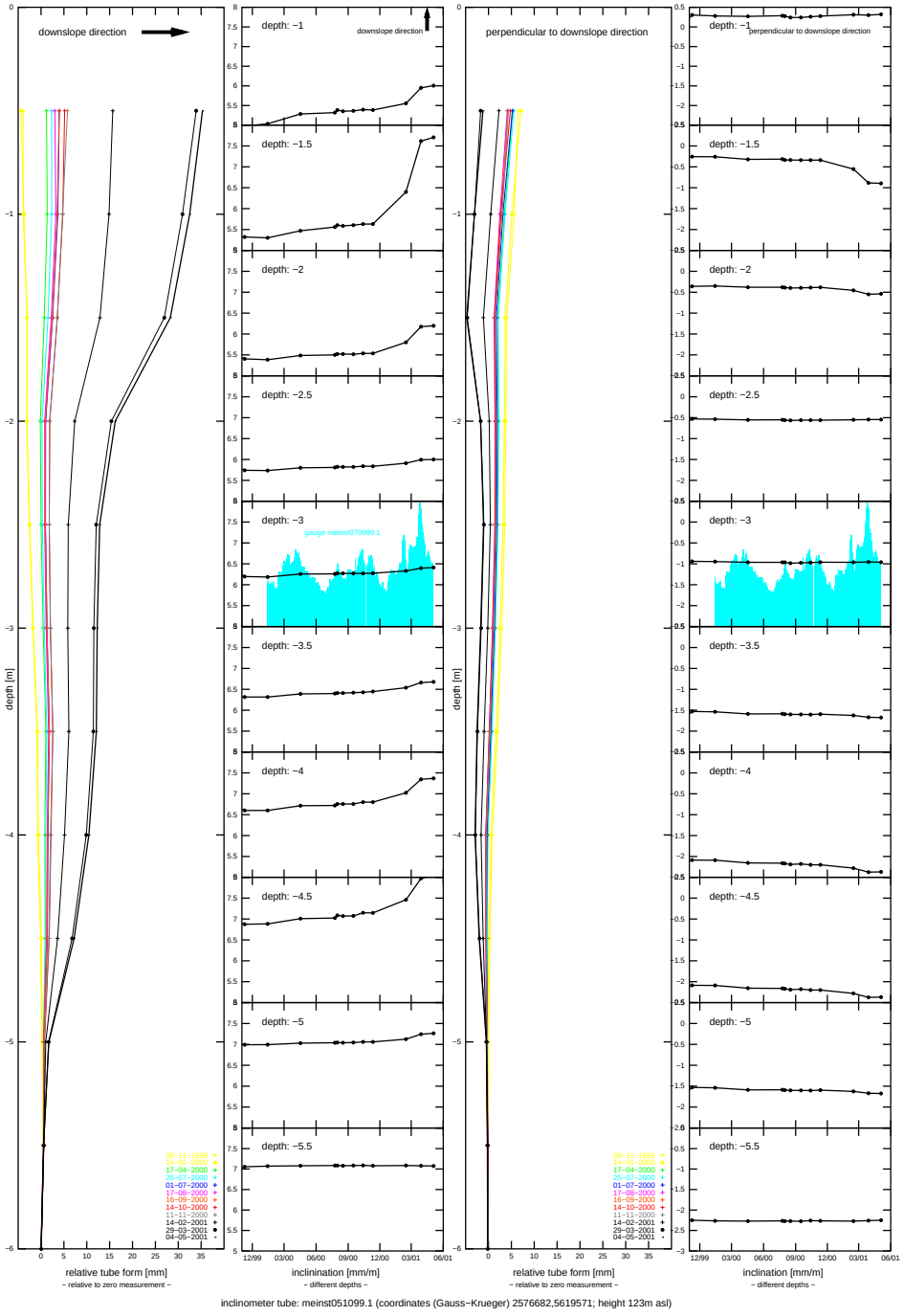

Figure 10.13.: Inclinometer measurements, location *'mebo051099.1'*. After minor variations in 2000, a strong downslope movement were monitored in spring' 01, which is related to increasing groundwater table (groundwater heights from location *'mebo070999.1'* are shown as blue impulses). Moreover, this signal indicates two different shear surfaces, one between 1.5 m and 2 m (younger landslide mass, approximately 3 cm/m displacement), and one at approximately 4.5 m (older landslide mass, approximately 1 cm/m displacement).

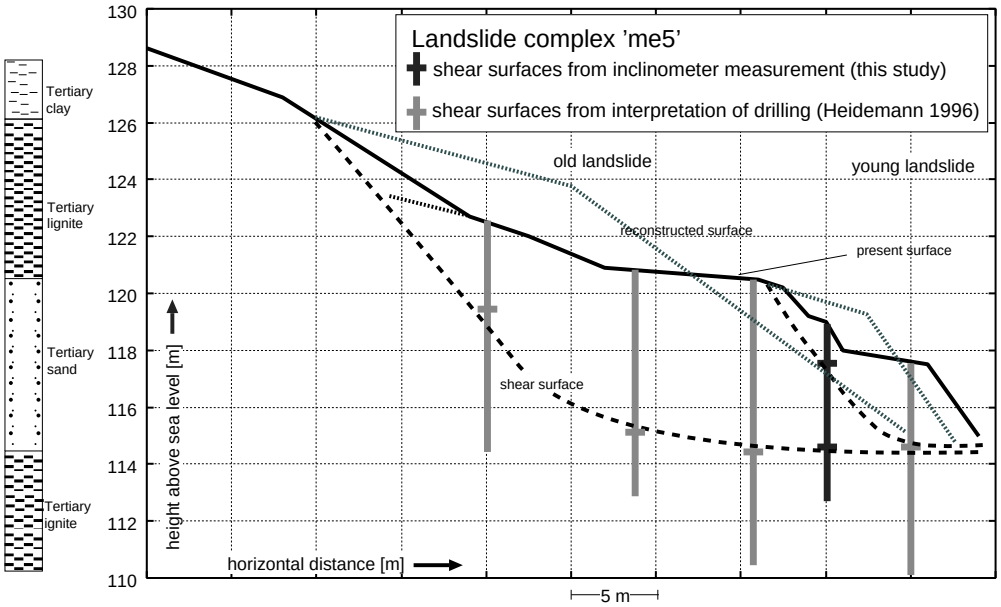

Figure 10.14.: Subsurface model of the landslide 'me5' (after Heidemann 1996, extended). Lithologic layers, interpolated shear zones and reconstructed pre–failure surfaces are included.

11. Assessing historic climatic variations for the research area

This chapter presents an attempt at parameterising historic climatic variability of the Bonn area. Scenarios of historic climatic conditions were derived by delineating typical annual climatic patterns using statistical analyses of available weather records and proxy data. The timeseries used in these analyses were three long–term meteorological dataseries from the Bonn area (stations 'Friesdorf', 'Klein–Altendorf', 'Wahnbach') and recalculated paleo data representing middle European conditions (seasonal resolution) since 1500 AD (Glaser *et al.* 2000) (see section 8.4 for details). First, analysis results of relationships between weather records and paleo data are presented, then an attempt to delineate scenarios of past climate variability is described.

11.1. Correlation of Bonn climate with paleo climate for middle Europe

As a first step, the datasets were plotted as timeseries of annual averages (sums for precipitation, respectively) for the period of data overlap (Figure 11.1). Data from Bonn stations show similar temporal patterns (parallelism) among each other and in comparison to the paleo data. A linear regression analysis was applied to the data sets, based on seasonal values for the complete period of data overlap. High correlation values were derived, especially for the temperature data (Figure 11.2, 11.3, compare Glaser *et al.* 2000, Pfister 1992). Additionally, the plots indicate, that the paleo data series for the measurement period (this century) are in the range of their historical variability ('pre–measurement period'). Seasonal dependencies (Figure 11.4) and long–term temporal changes (Figure 11.5) of the considered relationships were tested in a separate analysis. Regression calculated for the individual seasons reveal only minor variations of the derived relationships (Figure 11.4). Moving window regression indicated relatively high variance of the derived relationships in dependency to time (Figure 11.5). A significant decrease for the correlation coefficient since 1970 was detected (Figure 11.5b).

The results show, that the Bonn data and paleo data exhibit a high linearity. A set of linear equations were established as transfer functions for middle European paleo climate series to the Bonn area. These models are based on the period of data overlap (length of weather records, maximum 1900–1995, compare section 8.4). However, the total variability in paleo data does not differ significantly with the data set used for the regression models, indicating that no extrapolation is necessary for the mentioned transfer function.
Decreasing correlation of the Bonn data and paleo data for the last three decades might be explained by an increasing variability of climate parameters during this period. These very initial results indicate, that the used proxies deliver research potential with respect to indicators and quantifiers of recent climatic change (compare Glaser *et al.* 2000).

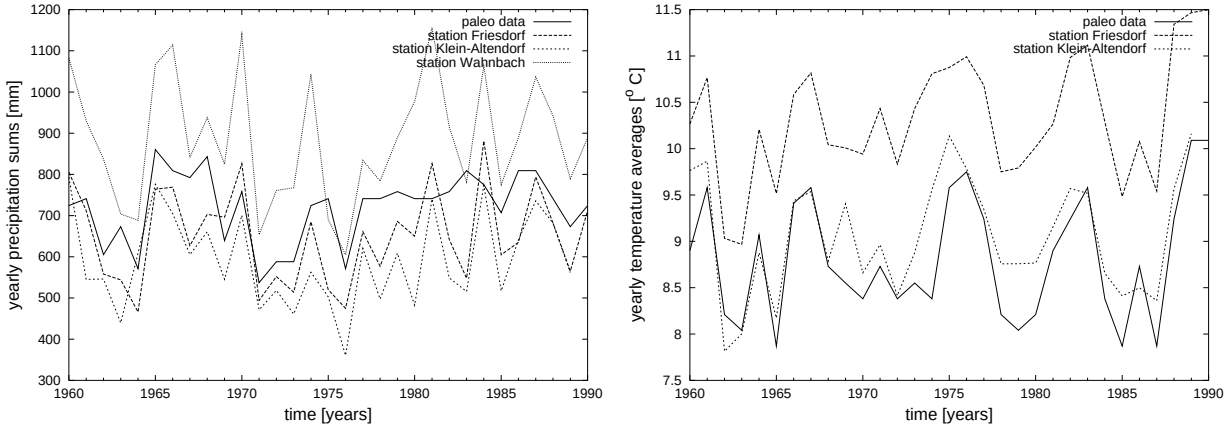

Figure 11.1.: Annual precipitation and temperature plotted versus time for meteorological stations in the Bonn area and paleo data (Glaser *et al.* 2000).

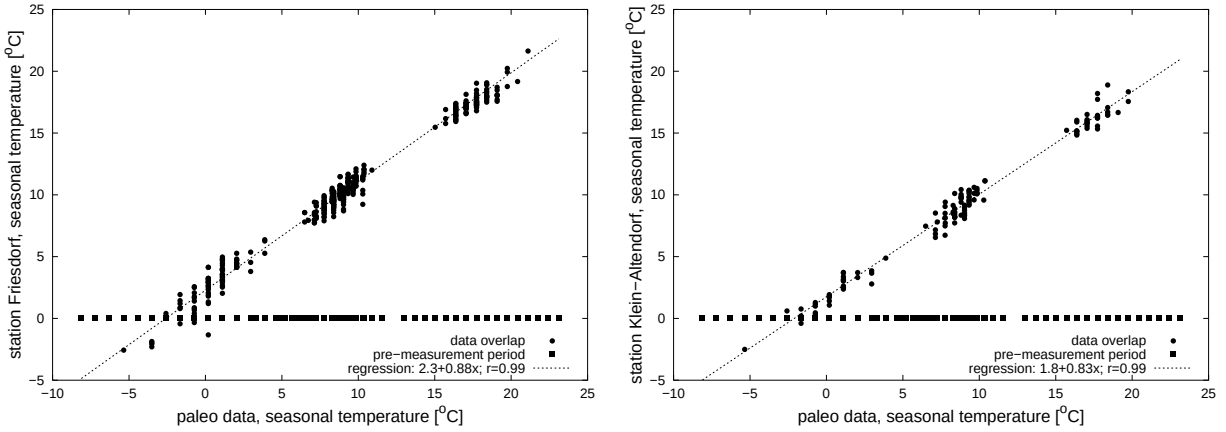

Figure 11.2.: Scatterplots of average seasonal temperature of meteorological stations in Bonn with reconstructed paleo temperature for middle Europe. Additionally, regression lines are given. 'Pre–measurement period' indicates paleo data, which are not in the period of weather records, and therefore are not included in the regression analysis.

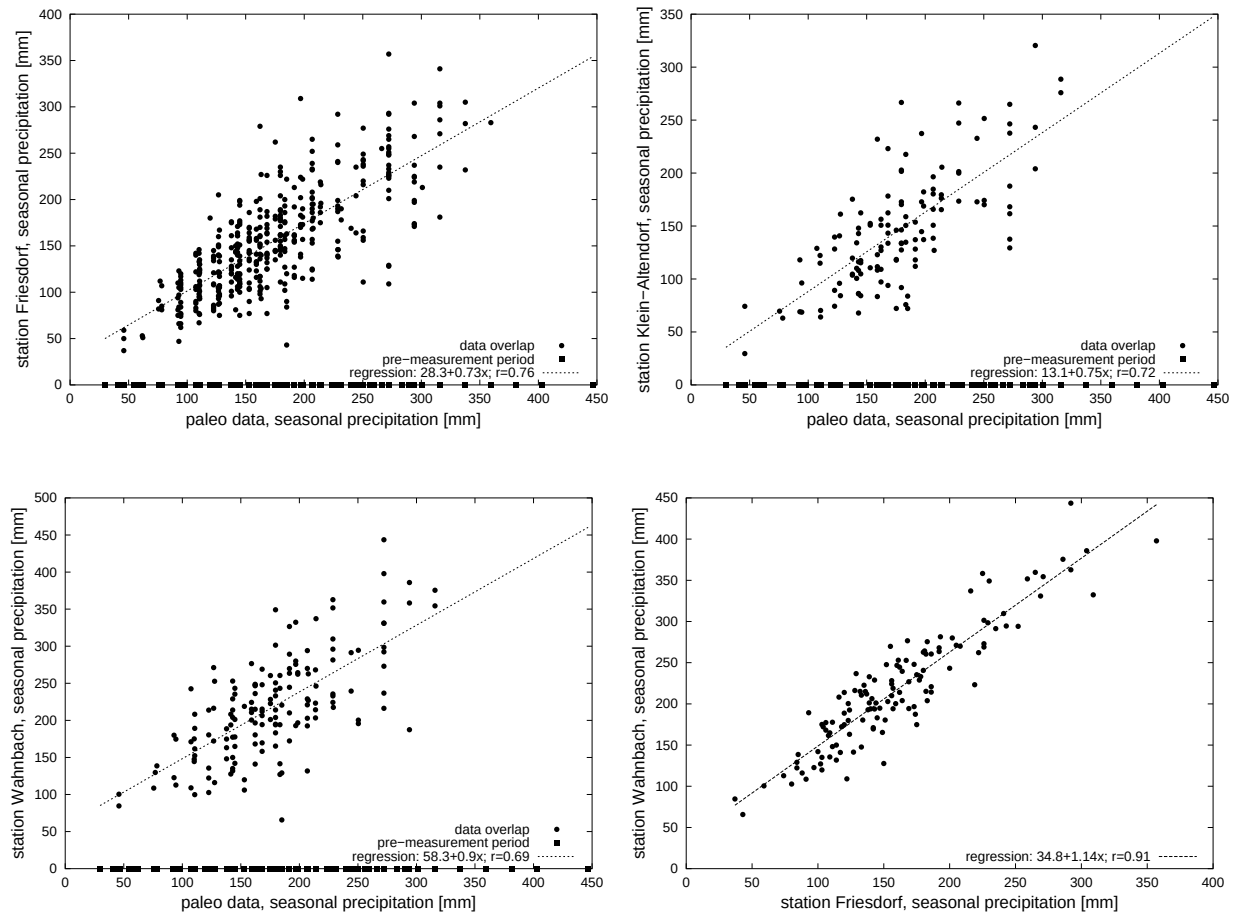

Figure 11.3.: Scatterplots of seasonal precipitation sums of meteorological stations in Bonn with reconstructed paleo precipitation. Additionally, regression lines are given. 'Pre–measurement period' indicates paleo data, which are not in the period of weather records, and therefore are not included in the regression analysis.

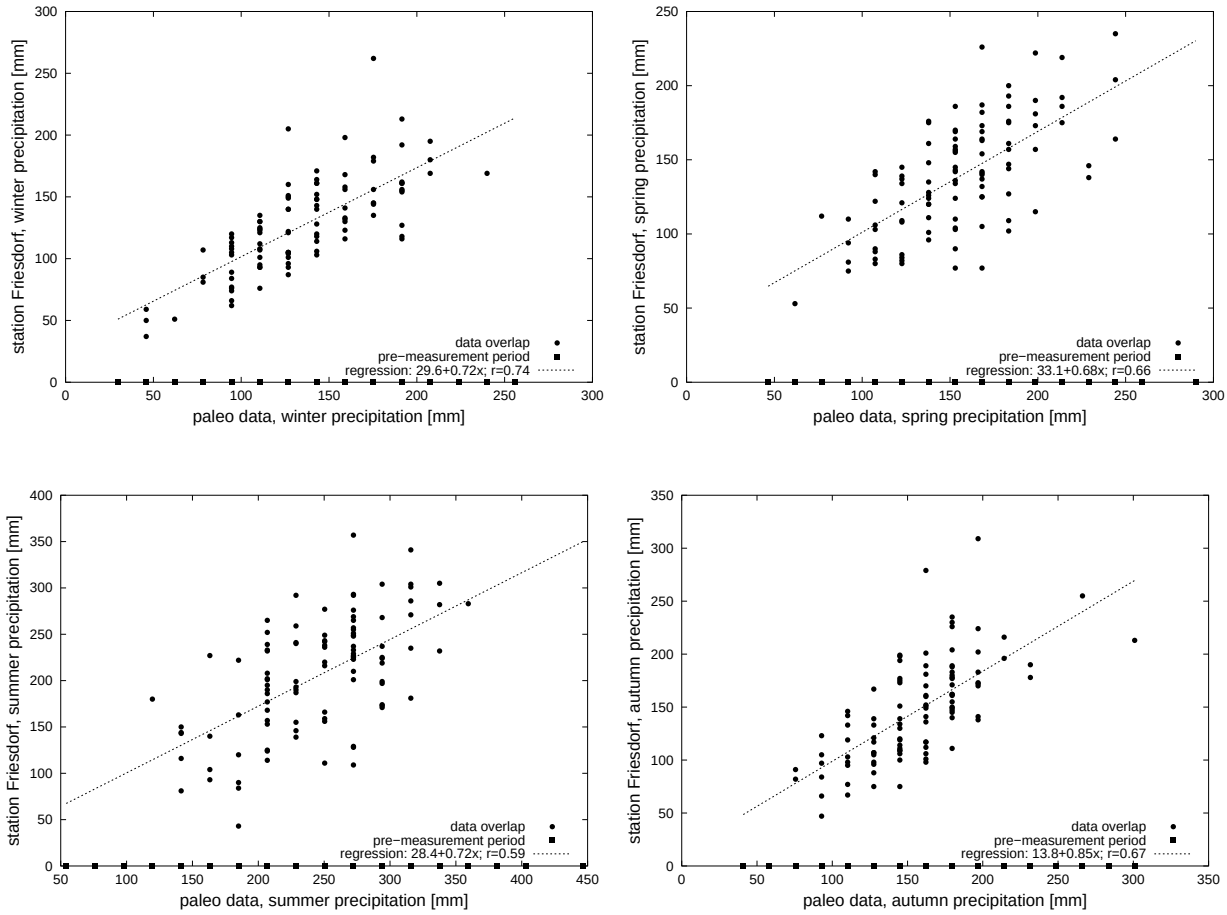

Figure 11.4.: Scatterplots of seasonal precipitation sums of meteorological stations in Bonn with reconstructed paleo precipitation (individual seasons). Results are displayed for station Friesdorf. Additionally, regression lines are given. 'Pre–measurement period' indicates paleo data, which are not in the period of weather records, and therefore are not included in the regression analysis. In comparison with the total regression (all seasons), the models show relatively low deviations.

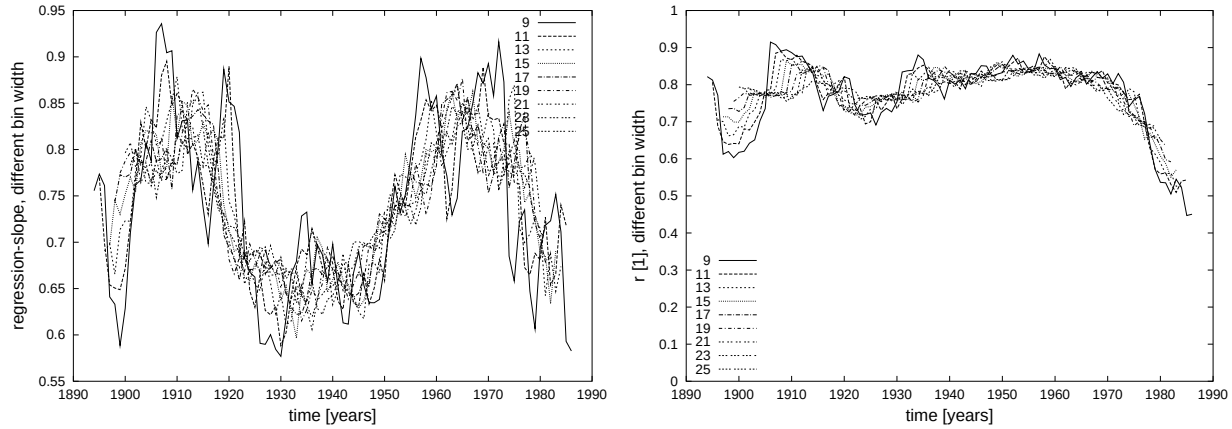

(a) regression coefficient (slope)

(b) correlation coefficient

Figure 11.5.: Moving window regression and correlation for reconstructed precipitation and data from station 'Friesdorf'. The legend indicates window size in years. A significant decrease in correlation could be detected for the last three decades (b).

11.2. Scenarios for past climate variability

A series of analyses were performed to assess temporal patterns of the paleo data. A Gauss filter was applied to the data sets to enhance long–term trends and transitions (Figure 11.6). A trend was detected for long wavelength (ca. 100 years, compare Figure 11.6). The filtered data indicate three major system stages in middle European climate: (1) a phase of decreasing temperature and precipitation before ca 1740 AD, (2) a transition phase with a relatively distinct temperature rise of more than 1 °C from ca 1740 AD to 1800 AD, and (3) the time period since 1800 AD, indicating a higher temperature level, and lower, but increasing, precipitation. Glaser *et al.* (2000) showed that climatic trends of the used data sets since 1500 AD indicate specific seasonal patterns, i.e. past climatic variations are especially related to winter precipitation and winter/spring temperatures.

Intensity plots of relationships between seasonal paleo data are also indicators of patterns, i.e. clusters in the seasonal data (Figure 11.7), which suggest the possibility of deliniating a classification in similar data subsets. Therefore, a cluster analysis was applied to the seasonal data, based on the hypothesis, that significant climatic trends are related to patterns of seasonality. As input data, seasonal values for temperature and precipitation of the paleo data for each year (= one dataset) were used. The cluster algorithm delivers clusters (or classes) of years with similar seasonal patterns. The cluster algorithm `cclust` of the statistical package R was applied, which iteravely moves a user defined number of cluster centers to their Voronoi–sets. The analysis delivered a classification in three data subsets on an annual basis (Figure 11.8). All three classes (year types) scatter over the whole data period. A frequency plot, however, depicts a pattern of different accumulation of the classified years with respect to their temporal distribution (Figure 11.8a). The classified years were used to calculate average curves of seasonal precipitation (Figure 11.8b) and temperature (not shown) from the paleo data sets. These three types ('classes') of years clearly represent the detected climatic trend, as described above.

class 1 is a year type with high precipitation and comparatively low temperatures (especially summer precipitation and temperatures) revealing high frequencies before 1750 AD.

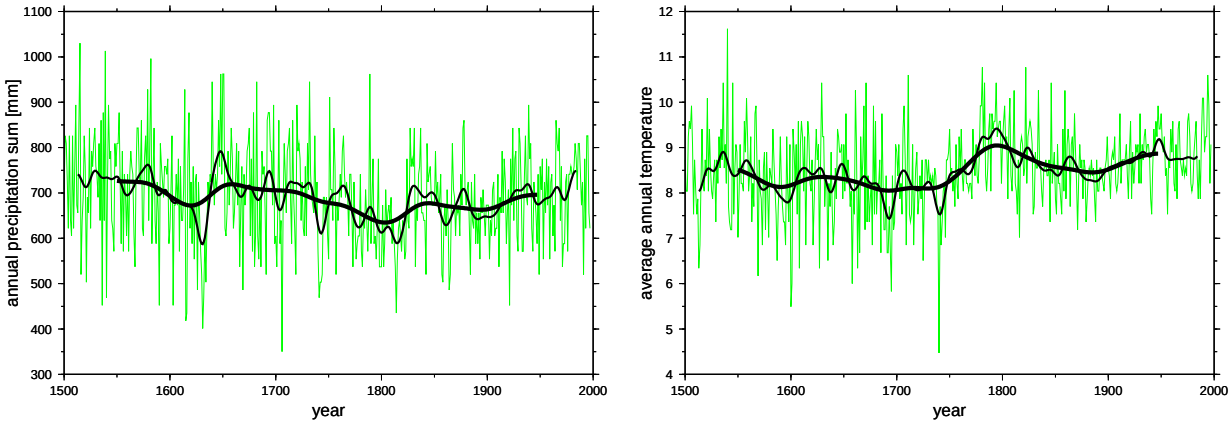

Figure 11.6.: Annual precipitation and temperature (paleo data) since 1500 AD. A Gauss filter was applied (thick lines, σ=25 a and 100 a) to derive general trends in the data (see text).

class 2 shows intermediate temperatures (but low winter temperatures) and lower precipitation (especially in winter) and contributes dominantly to the period between 1750 AD and 1900 AD.

class 3 indicates an annual pattern of high temperatures and relatively low precipitation (especially in summer), frequencies rise for the period since 1850 AD.

These results were used to classify data sets of weather records from the Bonn area according to the derived year types, i.e. the weather records were devided into three subsets. One fundamental prerequisite for this transfer is, that the variability captured by recent data sets is in the order of magnitude of the variability of the historic data sets (no extrapolation!). The correlation analysis presented above (Figure 11.2, Figure 11.3) reveals, that the total variability of seasonal paleo data is in the range of recent seasonal variability of the same data sets. Therefore, the classified years of the period of meteorological records can be used as representatives for past climate conditions.

Mean monthly values of precipitation and temperature for the Bonn data sets (Figure 11.9) of these three sets of typical years show the same seasonal patterns as the paleo data (Figure 11.8). This exemplifies, that the available data sets for the Bonn area can be used as an estimate for historic climate variability. The presented procedure is based on similarity analysis and actualistic transfer, delineating typical past conditions and relating them to similar recent conditions.

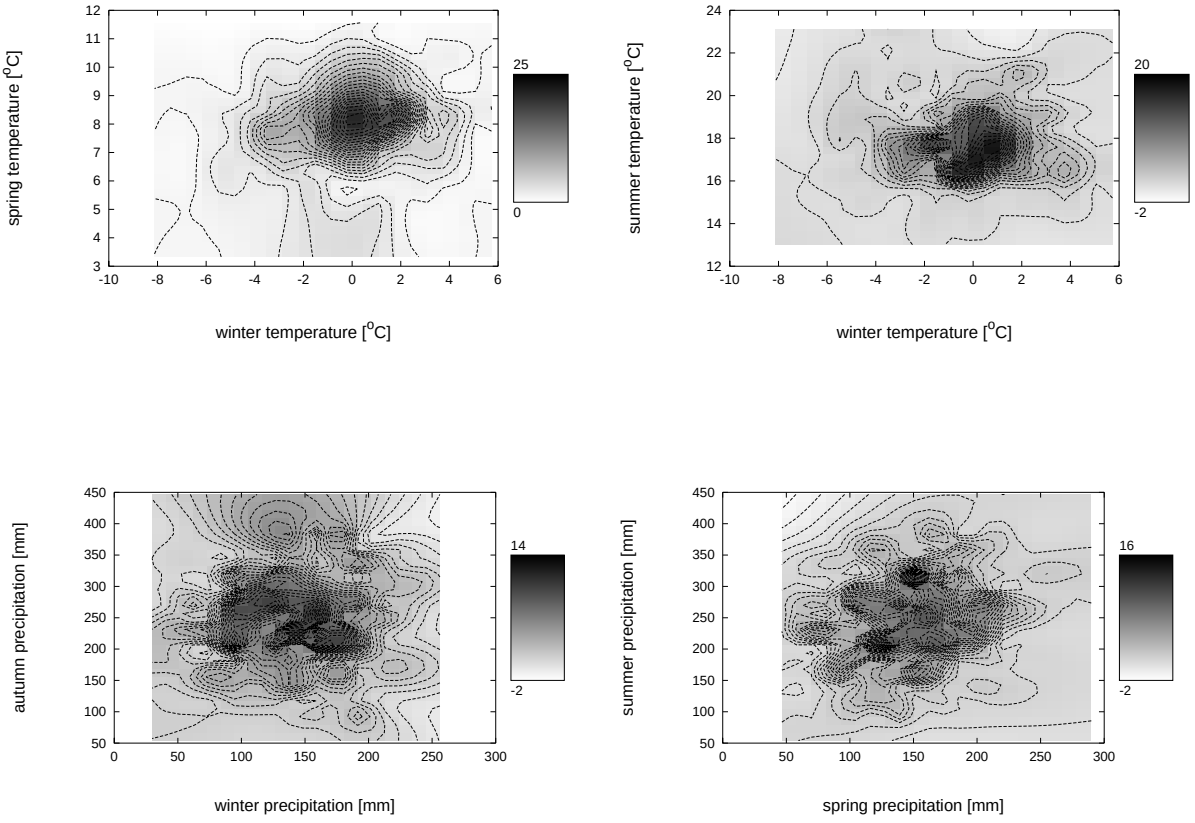

Figure 11.7.: Intensity plots of seasonal paleo data. Intensity indicates data density. The plots show 'data islands', indicating clusters of years with similar seasonal patterns in the data sets.

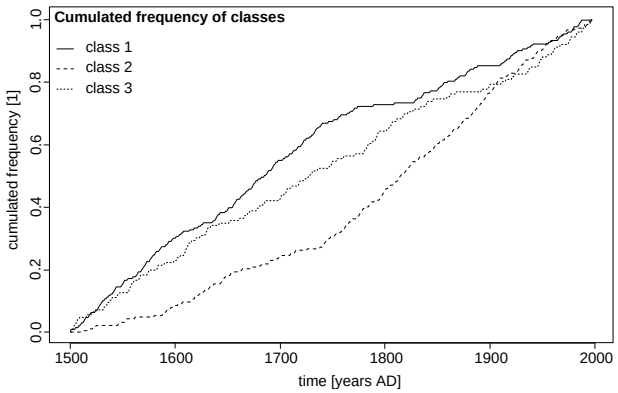

(a) Cumulated frequency distribution of classes.

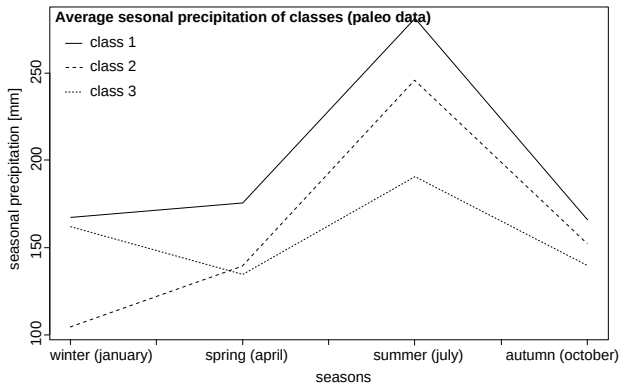

(b) Average sesonal precipation for classes.

Figure 11.8.: Year types and typical annual cycles derived by applying cluster analyses to the paleo data. The temporal frequency distributions (a) indicate, that the classified year classes exhibit different frequency in time. Therefore, the classes can be related to climatic periods (Figure 11.6). Average seasonal precipitation (b) indicates typical characteristics of each class.

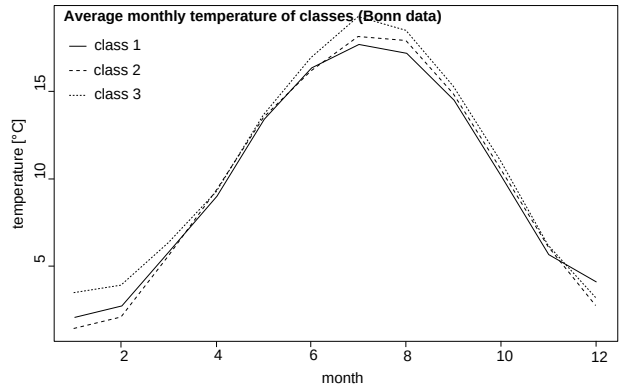

(a) Typical cyclicity in temperature.

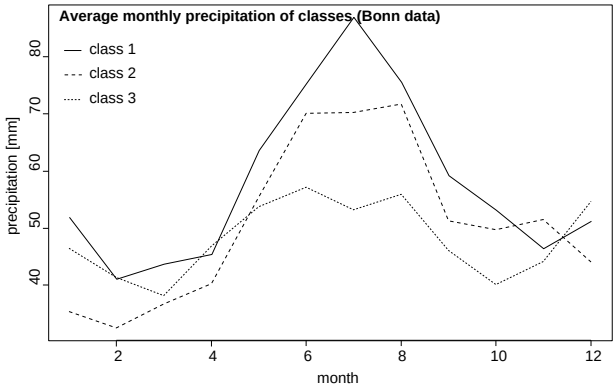

(b) Typical cyclicity in precipitation.

Figure 11.9.: Average monthly temperature and precipitation, derived from Bonn climate records for the classified years. The results indicate, that the three sets of 'typical' years show distinct differences of annual cyclicity of precipitation and temperature on a monthly basis.

Summary

The collected field and lab data show a large variability with respect to subsurface structures and soil properties. A series of simplified layer models for the field sites and the landslides under investigation could be derived. Statistical analyses proved, that the derived soil layers differ significantly in particle size, consistency, densities and permeability. Results from movement monitoring showed activities of two landslides on existing shear surfaces for intensive precipitation phases in spring 1999 and spring 2001. However, long–term monitoring is needed to understand these displacement patterns in detail. These results, in combination with available drilling logs, were used to delineate models of shear surfaces for two landslides.

Statistical anaylsis reveals, that the available reconstructed paleo data for middle Europe and weather records from Bonn stations show linear relationships on a seasonal basis. This relationship shows decreasing correlation for the last three decades, which might be an indicator for increasing climatic variability due to climate change. Trends and the variability of the paleo datasets indicate the existence of clusters, i.e. (1) past climate system changes, and (2) years with similar seasonal patterns. A set of climate scenarios could be derived by cluster analysis. These scenarios are related to three past climatic phases since 1500 AD. Parameterisation for these scenario phases were carried out by actualistic transfer using available long–term weather records of the Bonn area.

Therefore, models and parameterisations of some of the relevant boundary conditions (i.e. soil structures, soil properties and climate forcings) have been derived. These results are used in modelling approaches of slope stability and slope evolution, presented in the next part.

Part VII.

Modelling approaches: slope stability and hillslope evolution

Introductory notes

As discussed in Chapter 3, this study approaches hillslope systems by modelling processes and phenomena on different scales. Physically–based models for groundwater redistribution, (hill)slope stability, and hillslope development were applied.

Slope stability was assessed using data on recent boundary conditions (climate, geometry, soil properties) and conventional modelling approaches. Classical slope stability analysis were applied to models of the landslides 'si7' and 'me5' (derived in Chapter 10).
An attempt in assessing spatio–temporal variability of slope stability is presented by applying climate scenarios derived in Chapter 11 and geomorphologic models about landform and subsurface material, derived from the results of Chapter 10. These scenario models of boundary conditions were applied in a combined four dimensional model of groundwater and slope stability.

Hillslope development of the field site Melbtal was analysed using geomorphometric techniques and a process based model for hillslope evolution. The modelling results were evaluated to achieve a combined assessment of the evolution of hillslope systems of the field site Melbtal. Therefore, a conceptual geomorphological model of different stages in hillslope evolution was developed.

12. Slope stability analysis

12.1. Stability models for landslide objects

The programmes Slope2d and CHASM ('Combined Hydrology and Stability Model') were used in this study for slope stability analysis (see Appendix F.3). They provide conventional methods for deriving safety factors for defined shear surfaces (Janbu method), and for searching potential shear surfaces (Bishop method) for two dimensional hillslope profiles (see section 5.2). CHASM additionally includes a model for hillslope hydrology (hourly resolution, precipitation event model).

12.1.1. Stability scenarios, landslide 'si7'

The slope stability models were applied to reconstructed pre–failure situations of the landslide 'si7', according to the field & lab results described in Chapter 10. Two events were taken into consideration, as identified by results of this work and previous studies. Each event is modelled as successive failure of rotational slides (Figure 12.1). The reconstructed pre–failure surfaces were taken for the first event from the adjacent, undisturbed hillslopes, the following surfaces were sequentially derived from the modelled shear geometry.

First time failure, lower rotational block. Initial modelling results showed, and the shear geometry suggest (Figure 10.9, page 110), that failure of the lower landslide part caused successive destabilisation and failure of the upper part (multiple rotational failure). To model failure conditions (i.e. FOS =1) for the lower landslide part (Figure 12.1a), perched water tables producing high pore water pressure (3 m to 5 m water column) in the Tertiary sediments, and high soil moisture contents reducing cohesion of the involved layers are required, because the involved sandy and silty layers yield high frictional shear strength. In these model runs, no groundwater body was considered. The lithology in this part of the hillslope is built up of permeable Tertiary sands below low permeable Tertiary clays. The measurements of this study (compare subsection 10.1.2) suggest no groundwater body in the Tertiary sand layers. The only groundwater body recognised, results from soil water accumulation above the lower, low permeable (grey) clay layer. However, the complex stratigraphy suggest the occurrence of perched water layers in the heterogeneous lower (grey) Tertiary clay, leading to high pore water pressures as modelled in this scenario.

First time failure, upper rotational block. The secondary failure of the upper landslide part is preliminarily caused by destabilisation (increasing gradient) due to first time failure. Additionally, high pore pressures by perched water tables in Tertiary sediments and a groundwater body above the grey Tertiary clay layer were modelled to reach FOS =1 (Figure 12.1b).

Second time failure, failure of clay. Model results suggest that the secondary failure (1972, compare subsection 10.1.2) also occurred in two sequences, because of high shear strength of trachyte tuff. A first event, involving the upper part of the Tertiary layers (Figure 12.1c)

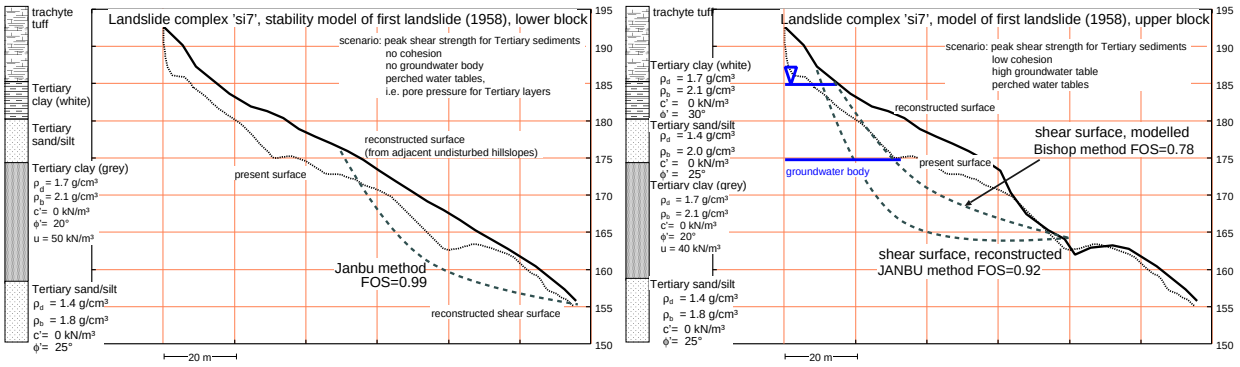

(a) First event, initial failure.

(b) First event, progressive failure.

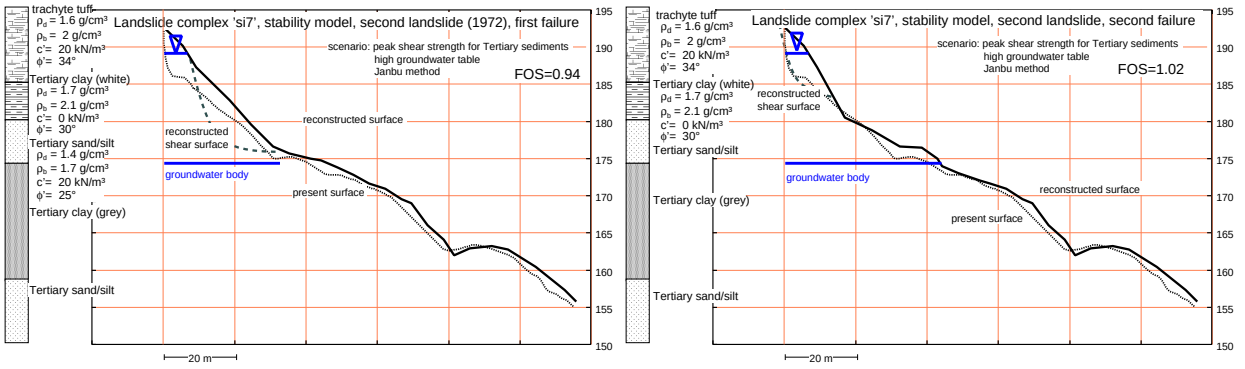

(c) Second event, initial failure.

(d) Second event, progressive failure.

Figure 12.1.: Stability analysis (Slope2d), landslide 'si7'. Different scenarios were applied to model the complex landslide situation. Two events (1958, 1972) were modelled, each in a two–step rotational failure mode.

led to destabilisation of the volcanic material. This initial failure event is modelled by two scenarios. (1) Failure at high pore water pressures (high groundwater table in trachyte tuff) is probable due to high permeability and high macro pore content of the trachyte material, overlying the Tertiary clay with low permeabilities (this scenario is shown in Figure 12.1c). (2) Alternatively, failure under residual conditions for the upper Tertiary (white) clay layer is a second possible scenario (not shown). This scenario requires only low groundwater levels. Residual strength conditions in Teriary clay can be explained by a high degree of disturbance of the material due to the first time failure (Figure 12.1b).

Second time failure, trachyte failure. Due to the high slope angle produced by the first time failure, the layers of trachyte tuff reach failure conditions, as indicated in Figure 12.1d. However, because of the high frictional resistance of trachyte tuff, saturated conditions have to be modelled to obtain FOS =1.

The model results suggest that intensive triggering factors (i.e. high groundwater rise) and resulting perched water tables are needed to bring the hillslope into initial failure conditions. Once initial failure has occurred, secondary failures are induced under less extreme conditions. Therefore, the landslide scar progressively retreats since first time failure. The present scar of trachyte tuff implies future landslide activity as it exhibits higher slope angles (higher instability) as last time failure (Figure 12.1d). The modelling results suggest no 'simple' model for first time failure of the landslide 'si7'. The high degree of heterogeneity in material properties and stratigraphy suggest the presence of perched water tables leading to failure conditions under extreme meteorological conditions. However, modelling these complex groundwater situations in detail were not feasable with the modelling approaches used in this study (see section 12.2). The model results indicate, that failure of trachyte tuff occurred as a secondary failure. The relative high shear strength (subsection 10.1.2) of this lithologic unit suggest significantly lower sensitivity as underlying Tertiary sediments.

12.1.2. Stability scenarios, landslide 'me5'

Analyses of the landslide 'me5' suggest two landslide events (see subsection 10.2.2). For the analysis, stability of shear surfaces as shown in Figure 10.14 were modelled using the Janbu and Bishop methods (see section 5.2). Pre–failure shear surfaces were reconstructed according to shear geometry and adjacent hillslopes. These surface models certainly contains high degrees of subjectivity and uncertainties. The model results (Figure 12.2) show that both scenarios require high groundwater tables to reach to failure conditions (FOS =1). Especially for the old landslide event, this implies existence of perched water tables according to the inhomogeneous lithology. These findings agree with previous stability modelling results for the landslide *'me6'* (Kaiser-Kühn 1988), indicating the influence of groundwater on hillslope stability in this part of the Melbtal. However, high (near surface) groundwater tables for present day (lithological and meteorological) conditions were measured by Schmanke (1999).

Generally, the model results show the potential influence of groundwater as a triggering factor on slope stability. The case of the landslide 'si7' exhibit a more complex situation due to high degrees of heterogeneity of lithology and material properties. However, other possible factors, as seismic activity, have not been considered in this simple modelling approach. Nevertheless, the

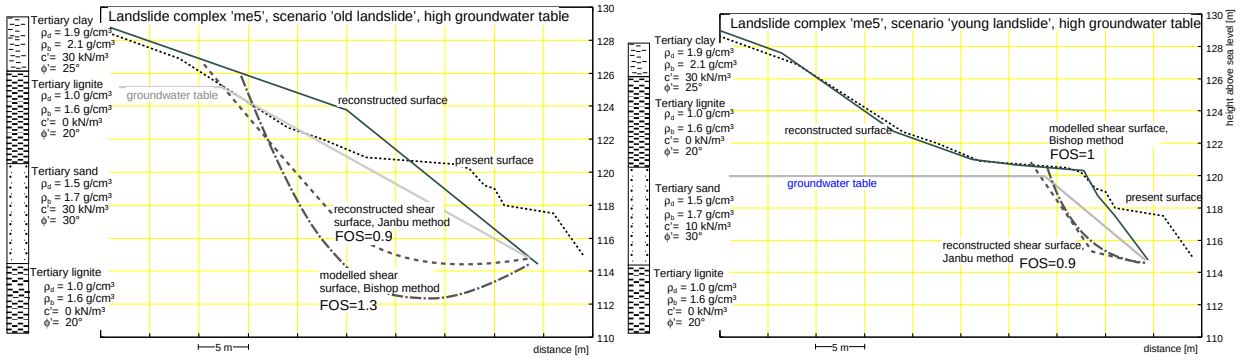

(a) Old (Pleistocene?) landslide event.

(b) Young (1920) landslide event.

Figure 12.2.: Stability analysis (Slope2d), landslide 'me5'. Two events were modelled, using pre–defined shear surfaces. Applying the Bishop method, rotational shear surfaces could be derived, matching the models of shear geometry from the field investigation sufficiently.

results indicate that saturated conditions are of crucial importance for slope stability in the study area. Therefore, an approach was chosen to assess spatio–temporal patterns of slope stability by modelling groundwater variations under changing climatic conditions (section 12.2).

12.2. Scenario models for historical groundwater conditions and failure probability

This section presents an analysis into historical variations of slope stability. Historical thereby means the time period, for which reliable proxy data were available for this study, i.e. 500 a bp (see Chapter 11). In this study, only static stability models were used (i.e. no models for process rates!). Therefore, conventional stability analysis was used to calculate failure probability for different geomorphologic and climatic conditions.

The overall concept for this modelling step (Figure 12.3) is based on applying combined groundwater/stability models to a series of modelled environmental realisations (Part VI). As the variablility of geomorphologic and geological conditions is not known in the considered time frame, related scenarios are modelled by present day realisations. The model input therefore is given by present day DEM and modelled lithological layers (Chapter 10). In combination with conceptual models (e.g. ergodic transfer, compare Chapter 13) these scenarios can be related to past geomorphologic and geologic conditions. The results from Chapter 11 were used to model historic climate conditions, affecting groundwater and pore water pressure as a sensitive variable for slope stability. The long–term timeseries for the Bonn area, necessary for this modelling approach, are available in daily resolution (compare Chapter 11), this gives the minimum temporal resolution for model input.

Two modelling approaches were considered (Figure 12.3): (1) applying analysis of rotational failure (Bishop–method) to assess stability distributions of typical hillslopes (compare Chapter 13), and (2) calculating local stability using the *'infinite slope model'*. The first idea was realised by applying the 'Combined Hydrology and Stability Model' CHASM. However, since CHASM is event based, it was not possible to model long (annual) sequences, which would have been necessary for

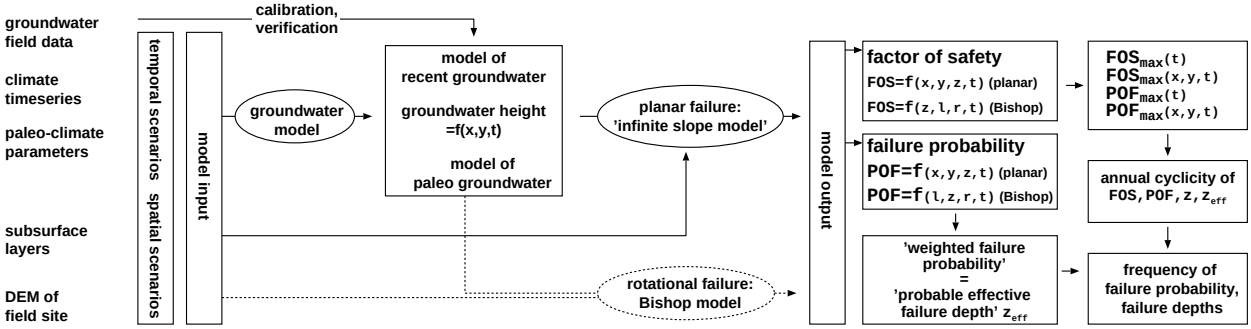

Figure 12.3.: Spatio–temporal modelling approach. Sketch of the modelling approach to calculate slope stability and failure probability under varying environmental conditions in a scenario approach. Scenarios of spatial (morphometric, lithologic) and temporal (precipitation, temperature) boundary conditions are used as model input into combined models of hillslope hydrology and hillslope stability. In this study a model for planar failure was implemented. The model output has to be recalculated to facilitate comparison of model scenarios (see text).

this approach. Therefore, the second approach was realised by setting up a combined groundwater and stability model for planar failure in a GIS framework, which is capable to model safety factors and failure probabilities for longer time scales (subsection 12.2.1).

12.2.1. Development of a GIS–based model of groundwater dynamics and failure probability

Development of a GIS–based groundwater model

Aim of the approach described in this section is the development of a groundwater model for small scale areas (up to several km^2, such as the field sites Dollendorfer Hardt and the Melbtal). The model should be able to simulate typical annual patterns of groundwater variation, based on the scenarios derived in Chapter 11. As technical platform, the GIS PCRASTER was used. This system allows dynamic modelling and visualisation of processes (PCRASTER 1996, Wesseling *et al.* 1996). A macro language is provided to develop dynamic models (van Beek and van Asch 1999, Wesseling *et al.* 1996) within the GIS environment. Therefore, PCRASTER combines GIS concepts with dynamic modelling approaches (compare also Schmidt and Gärtner 2000, for issues in coupling GIS with process models). According to the problem, a relatively simple model approach was chosen. The model can be termed as a 3D–tank model, simulating lateral and vertical saturated flow in daily timesteps.

The model is based on a spatial discretisation as presented in Figure 12.4. The study area is split up into equidistant cells in horizontal direction according to the resolution of the digital elevation model available. Each cell consists of several layers, which are represented by lithological units. These are provided by raster maps, giving heights of lower layer boundaries for each cell. Each specific lithological unit has to be parameterised by specific material properties: saturated hydraulic conductivity k_s, initial moisture content w, maximum water content w_c.

Precipitation, *evaporation* and *interception* are used as spatially uniform daily timeseries for the whole simulated area to calculate *net precipitation*. *Infiltration* is modelled as minimum of net precipitation and maximum infiltration capacity. Maximum infiltration capacity is determined by

soil water storage of the top layer and a permeability term. The soil water transport processes are modelled as *vertical fluxes* between layers, and *lateral fluxes* between the columns of each cell (compare Figure 12.4) using *Darcy's law* (Equation 5.1, page 47) for saturated conditions. *Vertical fluxes* are modelled according to the degree of saturation and hydraulic conductivity of the considered layer (see below). Vertical flux leaving the lowest layer is modelled as flow in an infinite storage and is limited by the hydraulic properties of the lowest layer (conductivity and soil water content) and an additional conductivity term. The groundwater table is derived from saturation degree of the uppermost, not fully saturated layer for each cell. Only one *lateral flux* is modelled for each column (i.e. not layer specific), dependent on the effective height difference in saturated layers (i.e. groundwater table).

Different approaches can be used to parameterise and discretise saturated flow in the used mesh. Saturated flow according to *Darcy's law* is determined by saturated hydraulic condctivity k_s and potential head ψ (section 5.1). Potential head may be expressed as difference of water levels Δh separated by the distance l. In the case of vertical percolation between two layers (compare Figure 12.4), *Darcy's law* can be parameterised in different ways (Figure 12.5). First, saturated contuctivity can be expressed by the upper layer or by the harmonic average of the adjected layers. Second, the distance l can be expressed in different ways as showed in Figure 12.5. Similarly, saturated lateral flow between columns can be derived geometrically in different ways. In the described model approach, lateral flow is parameterised by the harmonic average of the permeability of columns (= mean lateral column permeabilty as arithmetic mean of layers) and the according difference of water tables.

Development of a GIS–based model of failure probability

The groundwater model as described above was extended by a module calculating local safety factors (FOS), based on the *'planar slope' model* (section 5.2, Equation 5.5, page 50) for different soil depth, and for each node of the used grid. Therefore, additional material parameters are required for each lithological unit: dry unit weight γ_d, effective cohesion c', and effective angle of friction ϕ'. Moreover, an approach for calculating probability of failure (POF) was implemented. Probability of failure can be derived using a method described by Lee *et al.* (1983), based on variability of driving and resisting forces. Therefore, variances of shear parameters have to be provided, which are used to calculate variances of driving and resisting forces. The output of this model are values for the factor of safety $FOS(\vec{x}, t)$ and probability of failure $POF(\vec{x}, t)$ for each node in the applied four dimensional mesh, i.e. for each cell, a series of user–defined depth and for each model day.

Analysis of model output

The high resolution model results have to be recalculated, to allow comparisons of different model scenarios (Figure 12.3). Modelled values of failure probability (POF) and factor of safety (FOS) values are missleading, because they relate to different depths (which represent a different geomorphic effectivity). Therefore, the probability of failure is combined with the related depth. This gives a quantity, which is termed as *'probable effective failure depth'* z_{eff} in this study.

$$z_{eff}(x, y, z, t) = POF(x, y, z, t) * z$$

Calculating the maximum of POF (or minimum of FOS) for each cell and each timestep delivers the depth of most probable failure z' and the related failure probability POF' and stability factor FOS'.

$$POF'(x, y, t) = max_z(POF) \quad \rightarrow z'(x, y, t), \quad z'_{eff}(x, y, t) = POF' * z'$$

net precipitation:

$P_{net} = P - INT - EV$
P = precipitation
INT = interception
EV = evapotranspiration
EX = exfiltration (not modelled)

vertical flux:

$Q_v = k_s \frac{\Delta h}{\Delta d}$
Δh effective height of water table
Δd height difference

lateral flux per column:

$Q_h = k_s \frac{\Delta h}{\Delta d}$
Δh water table difference
Δd distance

boundary conditions:

geometry (as sketched)
layer properties: k_s, w_c, w

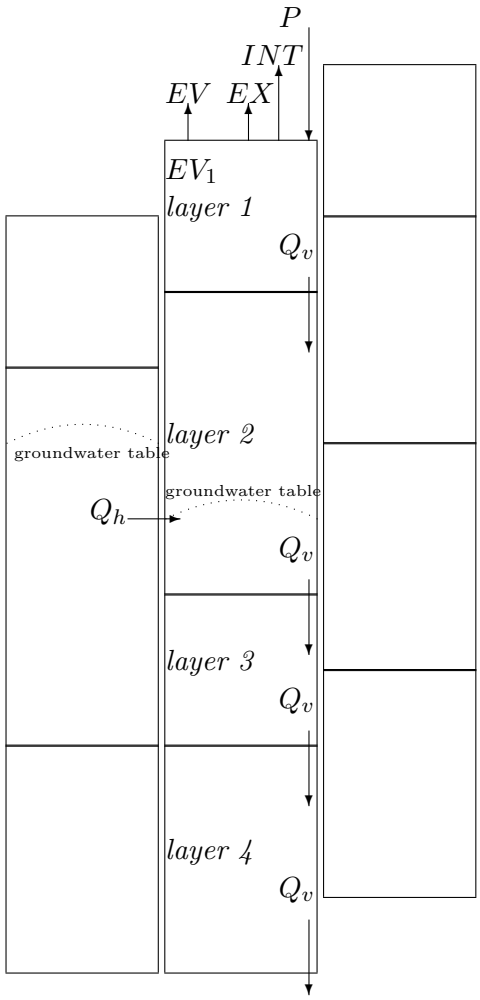

Figure 12.4.: Scheme of processes used in a simple groundwater model based on vertical and lateral saturated fluxes.

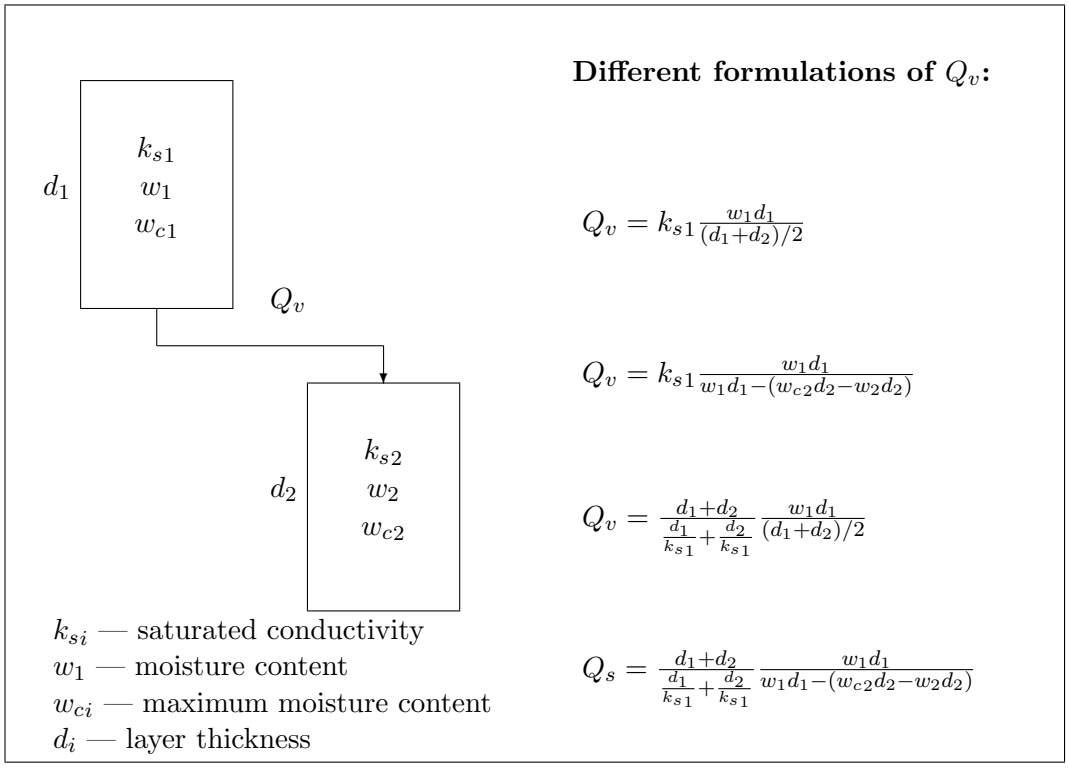

Figure 12.5.: Different formulations of vertical saturated flow in the groundwater model.

Averaging these values over the modelled area yields mean failure probability $\overline{POF}(t)$, mean stability factor $\overline{FOS}(t)$, mean failure depth $\overline{z}(t)$, and mean effective failure depth $\overline{z_{eff}}(t)$ per timestep. These timeseries can be used to interpret temporal development of slope instability.

$$\overline{POF}(t) = avg_{x,y}(POF'(x,y,t)), \quad \overline{z}(t) = avg_{x,y}(z'(x,y,t)), \quad \overline{z_{eff}}(t) = avg_{x,y}(POF' * z')$$

Calculating the maximum of POF (or minimum of FOS) for each cell and all timesteps delivers the depth of most probable failure z'' and the related failure probability POF'' and stability factor FOS'' for the whole period of model run (in this study a year), i.e. one spatially distributed result for the whole model run. These values indicate the depth of most probable failure and the related failure probability.

$$POF''(x,y) = max_{z,t}(POF), \quad \rightarrow z''(x,y), \quad z''_{eff}(x,y) = POF'' * z''$$

These results can be used to derive frequency distributions of failure probabilities, failure depth or volumes for each model run, e.g. $f(z'_{eff} > z_c)$ (f = frequency of nodes satisfying condition).

Therefore, the model output include

- four dimensional fields of $FOS(x,y,z,t)$ and $POF(x,y,z,t)$,
- three dimensional fields of maximum failure probability $FOS(x,y,t)$ ($POF(x,y,t)$)
- timeseries of average maximum failure probability ($\overline{POF}(t)$ and $\overline{FOS}(t)$),
- maps of maximum failure probability ($FOS''(x,y)$ and $POF''(x,y)$), and
- frequencies of failure probability and unstable volume (depth).

12.2.2. Model application — scenario modelling

Model parameterisation

This section presents results of modelling failure probability for different model scenarios. Model parameterisation was carried out using the results from Part VI. A few cut–outs of the research sites were used to parameterise the spatial boundary conditions. The related subsurface structure and regolith properties were chosen according to the results of Chapter 10 (see Tables 10.2 and 10.4). As spatial scenarios, two hillslopes from the field site Melbtal (Figure 12.6), and the south facing hillslope of the field site Dollendorfer Hardt (Figure 10.1, page 100) were used. Aim was to explore the sensitivity of the different lithological and geomorphometric conditions, as identified in Chapter 10.

'Hillslope me3' is the representative model for west facing, lower valley slope positions of the Melbtal, where Tertiary sediments are exposed on the valley sides (Figure 12.6a). The model was taken from hillslopes near the landslide 'me3'. The lithology is modelled as a sequence (from top to bottom) of loess, Tertiary sand, lignite and Tertiary clay, as indicated by the borehole logs on the west facing valley side (Chapter 10).

'Hillslope me5' is the representative hillslope for east facing, lower valley slope positions of the Melbtal, where Tertiary sediments are exposed on the valley sides(Figure 12.6b). The cut–out was taken from hillslopes near the landslide 'me5'. The lithology is modelled as a sequence (from top to bottom) of Tertiary clay, lignite, Tertiary sand, lignite, and Tertiary clay, which is the representative lithology in the area of the landslides 'me5' and 'me6' (Chapter 10).

'Hillslope si7'. The south facing hillslope of the Dollendorfer Hardt was chosen as the third scenario, representing a sensitive lithologic situation of the Siebengebirge. The lithology was modelled according to the subsurface model derived in section 10.1 (Figure 10.1, page 100; Table 10.2, page 109).

Timeseries of daily precipitation and temperature were derived from the station *'Meteorological department'* for recent years, and the station *'Klein–Altendorf'* delivered long–term meteorological conditions (Chapter 8). Scenarios for paleo conditions for precipitation and temperature were derived from the results of Chapter 11 (Figure 12.7). As model input for the results presented in this chapter, three timeseries of precipitation and temperature for the three scenarios derived in Chapter 11 were used. Each timeseries has daily resolution and represent the 'average year' for the scenario classes (i.e. timeseries for all years for one class were averaged). Evaporation was calculated using the method after Thornthwaite (compare Jäger 1997, Schrödter 1985) from monthly temperature, and averaged on a daily basis. No interception was modelled.

Model calibration and qualitative verification

The monitored timeseries of groundwater were used for calibrating and validating of the groundwater model part. Due to the simplicity of the modelling approach, no event–based consistency were derived. A direct comparison of measured groundwater levels (gauges) with modelled groundwater heights was not feasible, because of the rough generalisation of lithologic layers. Therefore, only qualitative validation could be carried out by comparing the general groundwater patterns in their relation to topography, lithology and annual cyclicity. The modelled groundwater levels for the two scenarios of the Melbtal show similar patterns in comparison to the observed data, e.g. locations *'mebo061099.1'* and *'mebo060999.1'* show minor groundwater variations on a lower level in comparison to location *'mebo070999.1'* (Figure 12.8, compare Appendix B.4). For the Dollendorfer

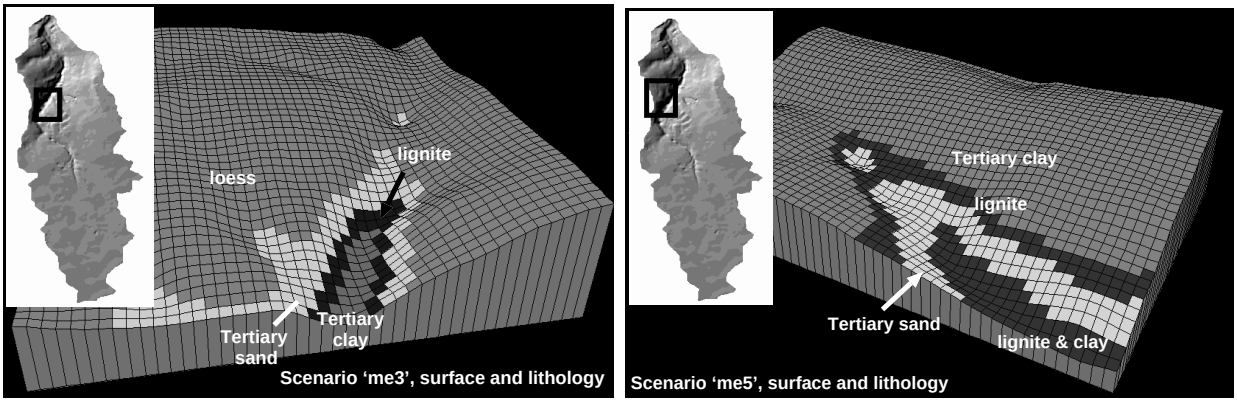

(a) Melbtal, scenario hillslope 'me3'

(b) Melbtal, scenario hillslope 'me5'

Figure 12.6.: Boundary conditions for two scenarios, Melbtal. Two cut–outs of the hillslopes of the Melbtal were used as model input. Lithological layers were modelled horizontally.

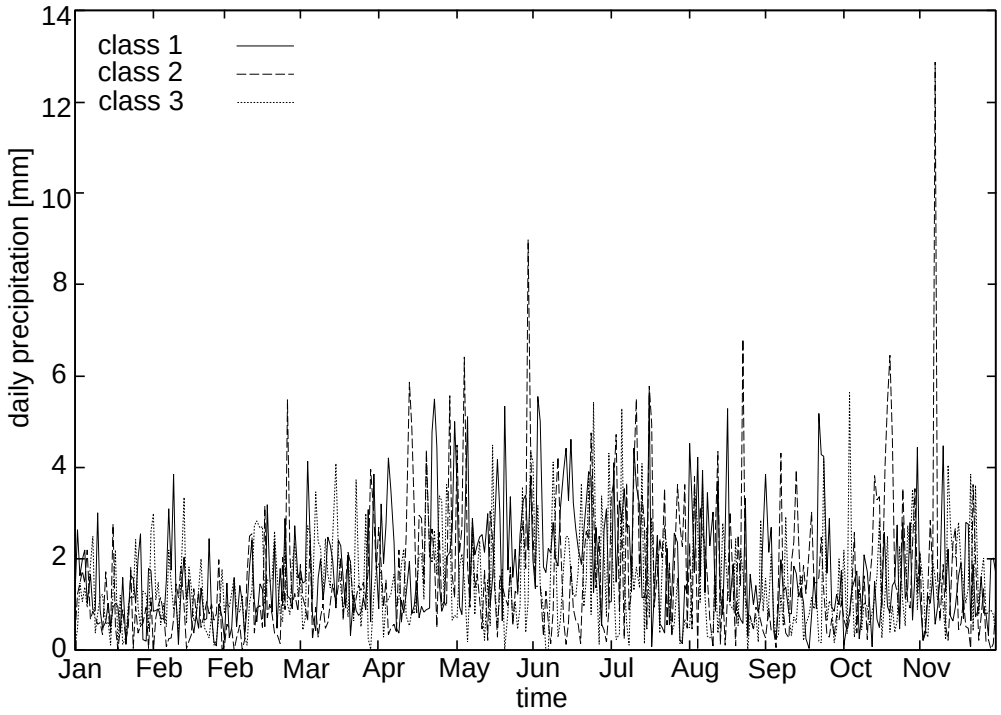

Figure 12.7.: Precipitation input for model scenarios (daily values). Three classes were derived from analyses in Chapter 11, by applying the classified years to data from station 'Klein–Altendorf' (see Figure 11.9, page 124 for a more convenient graph of monthly averages). The modelled precipitation values for 'class 2' indicate a high frequency of intensive precipitation events, especially in winter half year. The annual precipitation sums are shown in Table 12.1

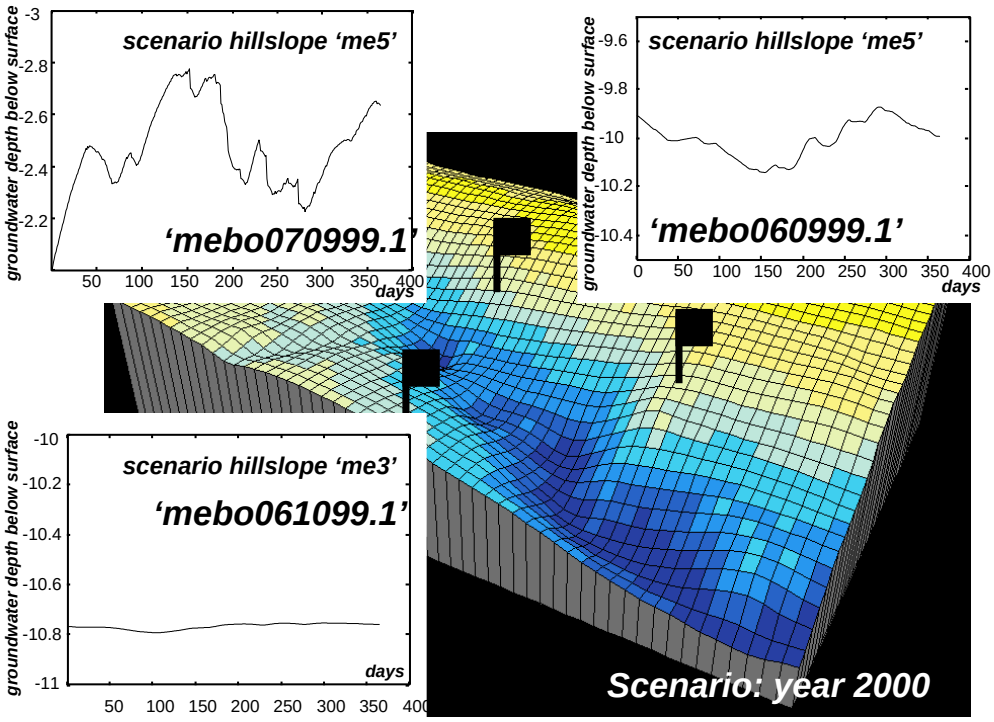

Figure 12.8.: Modelled groundwater patterns, Melbtal. Dark areas indicate saturated conditions, bright areas denote low groundwater tables. As precipitation and temperature, data from the year 2000 were used. The model results match the general measured groundwater pattern: gauges *'mebo061099.1'* and *'mebo060999.1'* indicate only minor variations, whereas *'mebo070999.1'* shows higher fluctuations (compare Appendix B.4).

Hardt, no good agreement of the groundwater model results with observated patterns (compare subsection 10.1.2) could be obtained. This indicates, that either the groundwater model used (see above) was to simple for modelling complex groundwater situation, or the parameterisiation of lithological layers (e.g. only one homogeneous Tertiary layer, compare Figure 10.1, page 100) was not sufficient.

Model results

The model output was recalculated as described in the previous section. The modelled spatial patterns of maximum failure probability for the model runs $POF''(x, y)$ indicate sensitivity of high slope angles and Tertiary layers (Figures 12.9, 12.10). Figure 12.11 displays frequency distributions of average effective failure depth $\overline{z_{eff}}(t)$ and $\overline{POF}(t)$, modelled for each timestep for the different scenario hillslopes and climate scenarios. The modelled scenarios (Figure 12.11 and Table 12.1) lead to the following results.

- Generally, the low values for failure probability and for effective failure depth are resulting from high frequency of nodes of lower sensitivity, which were included in the recalculations. However, the values show differences for the three scenarios (Table 12.1). The scenario 'hillslope me3' (west facing valley side of Melbtal) indicate lower (approximately half) average maximum failure probabilities and effective failure depth as the scenario 'hillsope me5' (east facing valley slope), which agree with the higher degree of disturbance of the east facing valley slopes. The scenario 'hillslope si7' delivered higher average maximum failure probabilities

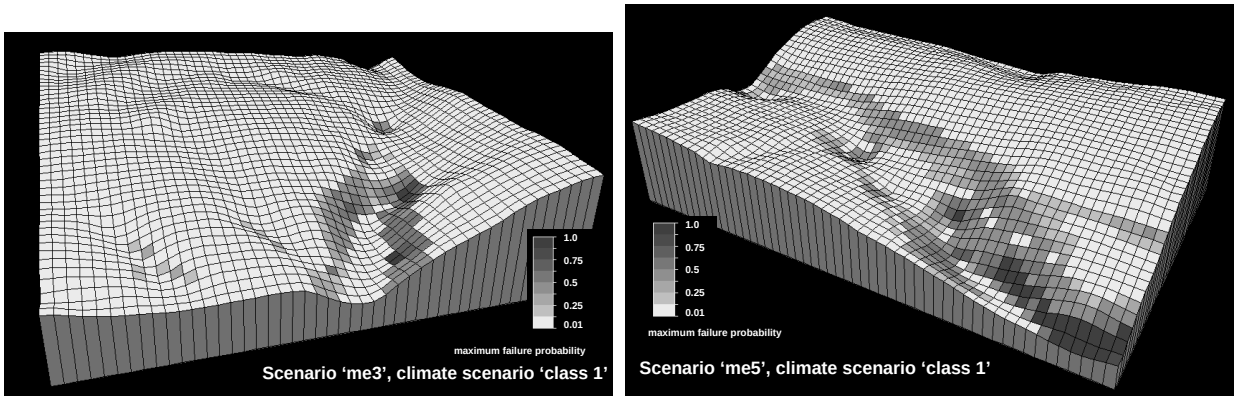

(a) Melbtal, scenario 'hillslope me3'

(b) Melbtal, scenario 'hillslope me5'

Figure 12.9.: Spatial patterns of modelled maximum failure probability $POF''(x, y)$, Melbtal. Displayed are results for scenario 'class 1', representing climate conditions for the scenario 1, as derived in Chapter 11. The results indicate the higher sensitivity of the scenario 'hillslope me5'.

$\overline{POF}$ and higher average effective failure depth $\overline{z_{eff}}$, which can be contributed to the higher gradients at this site (Table 12.1).

- All scenarios reveal the higher geomorphic effectivity of climate sceanrio 'class 2', although 'class 1' has higher annual precipitation sums. This can be attributed to the higher frequency of intensive precipitation events in winter half year in this class (Figure 12.7). 'Class 2' was modelled as the 'climatic transitions phase' from little ice age conditions to recent conditions (compare Chapter 11). As the cluster algorithm considered seasonal data only, 'class 2' was not derived initially from small scale characteristics. The transfer to the Bonn data set, however, produced the pattern of higher frequency of intensive events. It can can be hypothesised that the climatic transition phase is prone to climatic fluctuations and fluctuations in annual weather pattern. However, a deeper understanding in the behaviour of the past climate system is necessary to verify this hypothesis (see section 14.1). Generally, for all three hillslope scenarios, the increasing effective failure depth $\overline{z_{eff}}$ can be contributed to higher failure probability, not to increase in failure depth z (Figure 12.11a,c).

- Figure 12.11 indicates, that the effect of 'class 2' on increasing failure probability has significantly more effect for scenario 'hillslope me3' as for the hillslope 'me5' (shift in the frequency distribution), i.e. 'hillslope me3' is more sensitive to climatic changes (high groundwater tables). More specifically, higher failure probabilities occur for 'hillslope me3' under the effect of climate 'class 2'. The frequency distributions indicate, that for hillslope 'me3', frequencies of high failure probabilities rise, whereas for hillslope 'si7', frequencies of low failure probabilities rise. This means, the spatial configuration of the site (i.e. geomorphometry) leads to higher goundwater tables for less sensitive areas for hillslope 'si7', whereas topography of the 'hillslope me3' leads to higher groundwater tables (and therefore higher failure probabilities) in the sensitive areas. These results show, that sensitivity to failure shows a clear relationship to general measures as gradient. However, the sensitivity to climatic variations is dependend to the internal spatial configuration of each site.

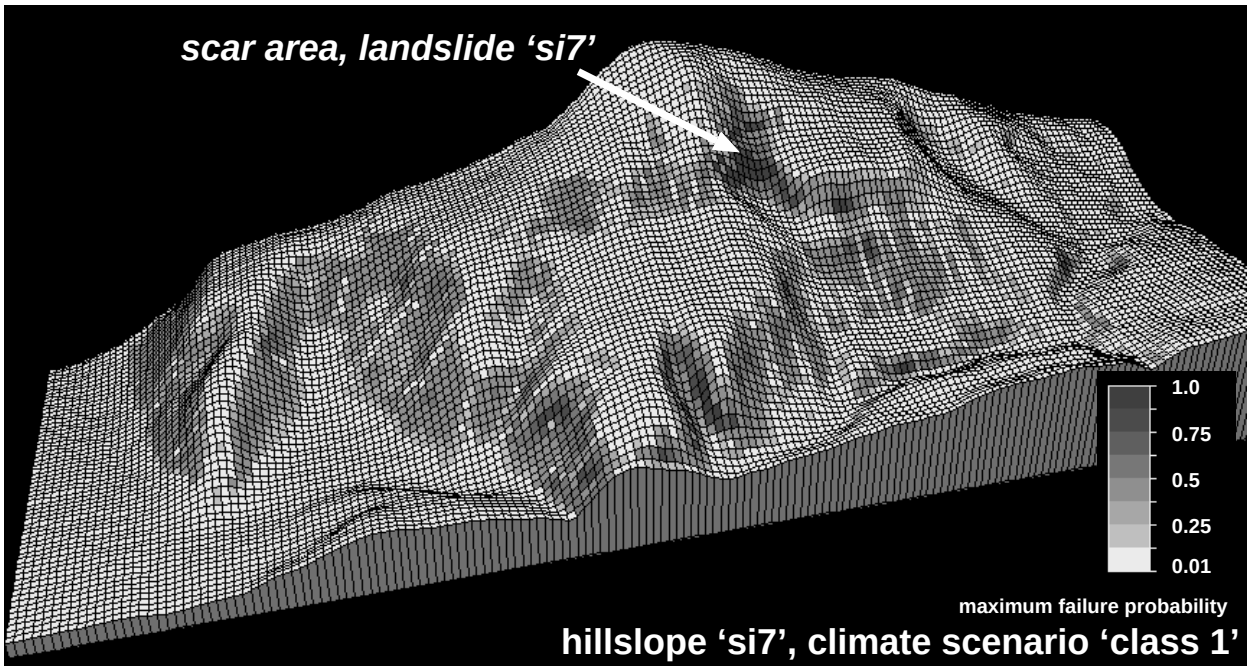

Figure 12.10.: Spatial patterns of modelled failure probability $POF''(x, y)$, Dollendorfer Hardt. Displayed are results for climate scenario 'class 1'. The scar area of landslide 'si7' shows the highest failure probabilities.

Table 12.1.: Summary of scenario modelling results. As integral measures of model output for the different scenarios, average failure probability $\overline{POF}$ and average effective failure depth $\overline{z_{eff}}$ are used.

			climate scenarios		
			class 1	class 2	class 3
spatial scenarios	average gradient	annual precipitation	640mm	570mm	531mm
Melbtal, hillslope 'me3'	7.43°	$\overline{POF}$ [1]	0.0429	0.0431	0.0429
		$\overline{z_{eff}}$ [m]	0.254	0.255	0.254
Melbtal, hillslope 'me5'	8.14°	$\overline{POF}$ [1]	0.0979	0.0981	0.0979
		$\overline{z_{eff}}$ [m]	0.592	0.594	0.590
Dollendorfer Hardt, hillslope 'si7'	12.22°	$\overline{POF}$ [1]	0.113	0.115	0.112
		$\overline{z_{eff}}$ [m]	0.895	0.908	0.886

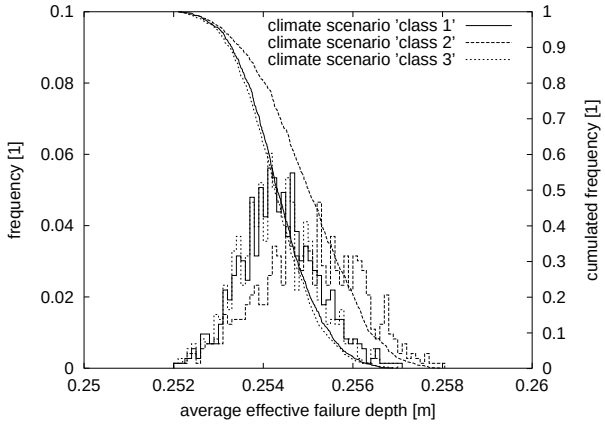

(a) Melbtal, scenario hillslope 'me3', average effective failure depth

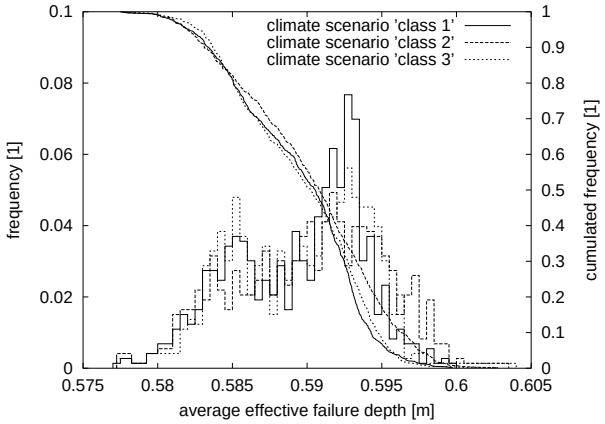

(b) Melbtal, scenario hillslope 'me5', average effective failure depth

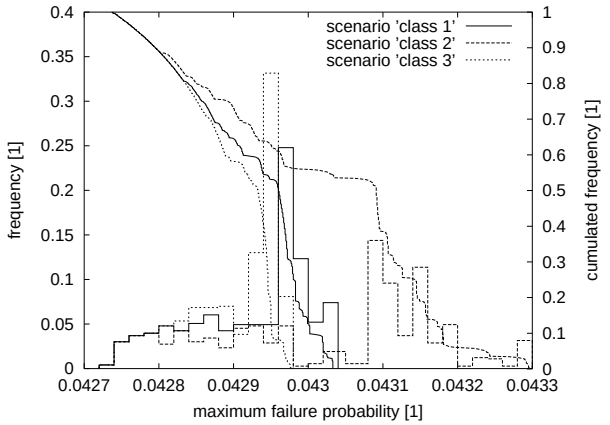

(c) Melbtal, scenario hillslope 'me3', average failure probability

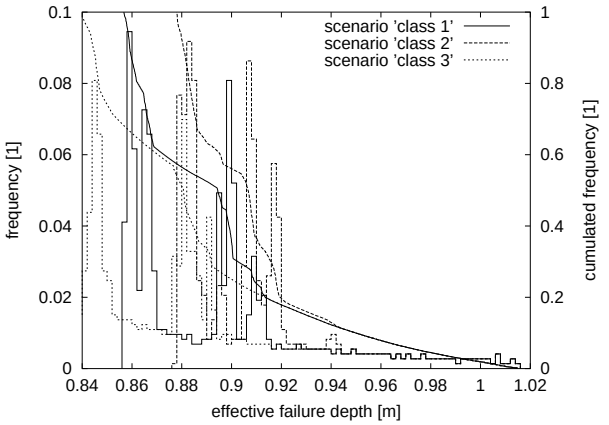

(d) Dollendorfer Hardt, scenario hillslope 'si7', average effective failure depth

Figure 12.11.: Frequency distribution of modelled effective failure depth, Melbtal and Dollendorfer Hardt. Model results for three modelled climate scenarios. Shown are the cumulated (lines, right axes) and non–cumulated (steps, left axes) frequency distributions of average effective failure depth $\overline{z_{eff}}(t)$, and average failure probability $\overline{POF}(t)$, modelled for each timestep. The results show the high geomorphic effectivity of climate 'class 2' (i.e. increasing failure probability), especially for hillslope 'me3' and hillslope 'si7'.

13. Modelling hillslope evolution of the field site Melbtal

This model approach refers to the total timescale of catchment evolution for the Melbtal (compare Chapter 3). As argued in Part IV, the geologic and geomorphologic situation implies a temporal scale of valley formation of approximately 700 ka to 900 ka bp (discussed in detail by May 2001). For the temporal scale of valley evolution, varying geomorphic activity has to be considered, because of changing boundary conditions. These include underlying materials, changing climate (external factors) and different stages of process coupling within the system (internal factors) (compare May 2001).

13.1. Geomorphometric structure — signals of geomorphic history in present form

Understanding hillslope evolution, or more general, geomorphic history of the study site requires field evidence of past geomorphic conditions, i.e. processes and forms (Dikau 1999). This is usually carried out by dating of paleo–surfaces or sediment bodies (compare Preston 2001). However, for the research area no dating results are available. It is highly questionable, if reliable dating results could be obtained for the environment of the Melbtal, because of the complex lithology and the process system (e.g. slope–channel coupling). Therefore, field evidence in this study is build on direct available observations of present geomorphic form. The concept of ergodicity, which has been extensively used in other sudies of catchment evolution (e.g. Ahnert 1988), implies that the system of spatio–temporal hillslope development can be represented by spatial sequences of hillslopes in a catchment. To analyse these relationships, techniques of hillslope profile analysis, and geomorphometric generalisation were used.

13.1.1. Hillslope profile analysis

Note. *The interpretations presented in this chapter are based on the results of Rasemann (1999).*

Delineation of hillslope profiles and hillslope parameters was carried out by the 'Slope profile analysis package' (HAP) developed by Rasemann (1999). As no standard procedure is available for extracting *representative hillslope profiles* (Rasemann 1999), 27 profiles for the Melbtal were delineated in a trial an error procedure (Figures 13.1, 13.2, and 13.3). However, as most of the profiles converge quickly in zero–order tributaries to the Engelsbach, this sequence is supposed to be a good approximation of a representative profile sequence for the Melbtal.

As Figure 13.2 shows, the profile sequence indicates a spatial transition of the valley character from a trough valley in the upper part to V–shaped form in the lower valley. This changing valley character is reflected by a series of profile parameters (Figure 13.4, compare Rasemann 1999). Length/distance ratio and average slope angle show a trend to higher slope angles, until

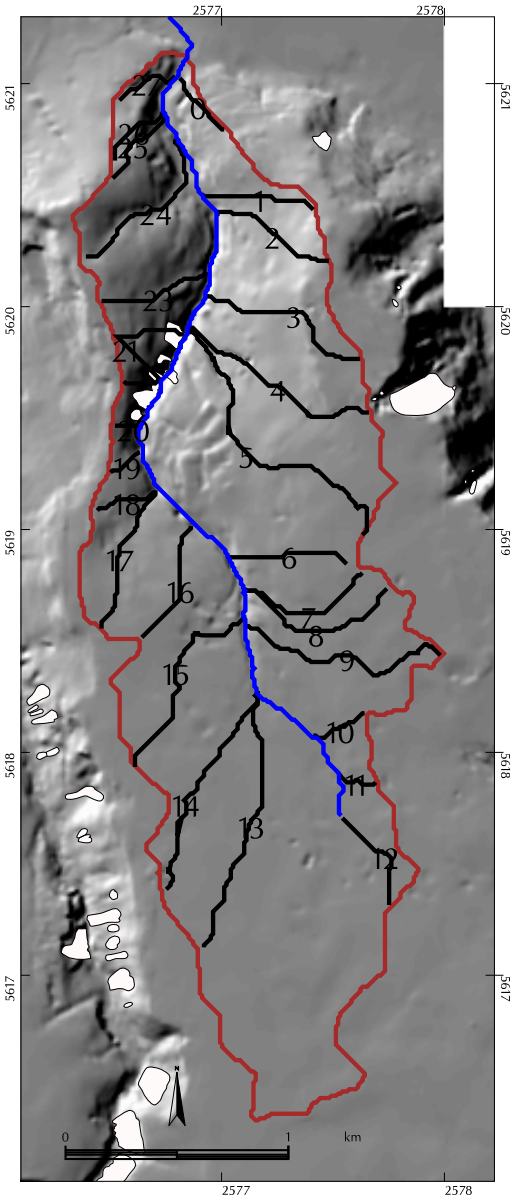

Figure 13.1.: Delineated hillslope profiles in the field site Melbtal. Plan view with landslides. Background is a shaded perspective of 10 m grid size DEM. White polygons denote landslides.

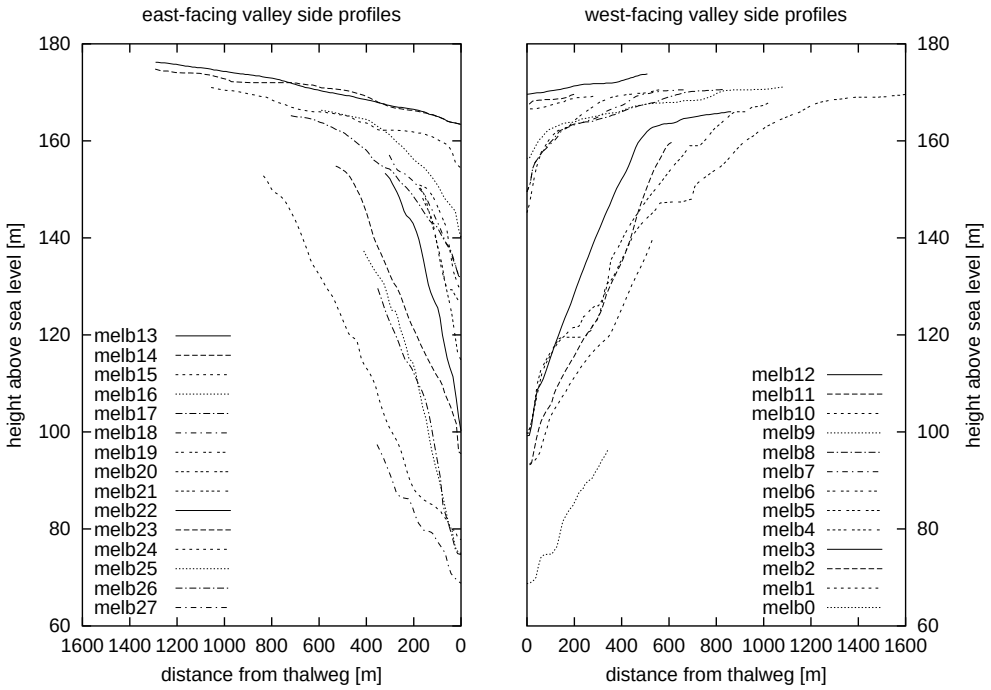

Figure 13.2.: Delineated hillslope profiles in the field site Melbtal, seperated by valley side slopes.

a equilibrium is reached (profiles 3 and 20). High fluctuations for hillslope angle and average difference of hillslope angle at this position indicate, that the slope system might reached a critical state (Hergarten and Neugebauer 1999b, 2000). According to Phillips (1999) diverging observables indicate chaotic or critical systems. Because of the low sampling rate (i.e. number of profiles), the profile parameters only give some hints for a critical state. However, results presented by Rasemann (1999) for the Katzenlochbachtal, a valley directly west of the Melbtal with similar lithology, showed a comparable pattern of profile parameters, which substantiate the thesis of a critical state. Using the principle of ergodicity, it can be hypothesised, that the delineated spatial sequence of profiles should reflect temporal stages of valley development. To analyse these relationships, a series of profiles are distinguished (for east facing valley side only), which potentially (assuming ergodicity) represent distinct steps in the hillslope development of the Melbtal (Figure 13.5).

Profile 13 reveals a convex slope profile with low gradient (¡3°) fully developed in loess and terrace sediments (trough valley).

Profile 15 shows a constant lowering of approximately 5 m height and an additional initial valley incision of approximately 5 m in comparison to *profile 13*. The geologic map GK 5208 reveals Pleistocene sediments (loess, terrace) as subsurface material. The question arises which processes during which time span achieved this sediment removal. The low gradient of the initial profile suggests only solution or solifluction processes. Figure 13.3 indicates increasing upslope drainage area at this valley position. Therefore, the initial valley incision can be attributed to a threshold of drainage area leading to increasing fluvial activity (influence of higher order system of catchment evolution).

Profile 16 shows an increasing incision of the valley floor, whereas the parts near the watershed remain nearly constant in height. This indicates, that increasing fluvial downcutting initiated

Figure 13.3.: Hillslope profiles and thalweg profile at the field site Melbtal. Additionally the upslope drainage area ('flowaccumulation') of the thalweg is shown. Increasing slope angle of the profiles coincides with reinforced thalweg lowering. This can be attributed to increasing upslope drainage area, and Tertiary material in the lower valley, indicating lithologic control of valley evolution (after Rasemann 1999, modified).

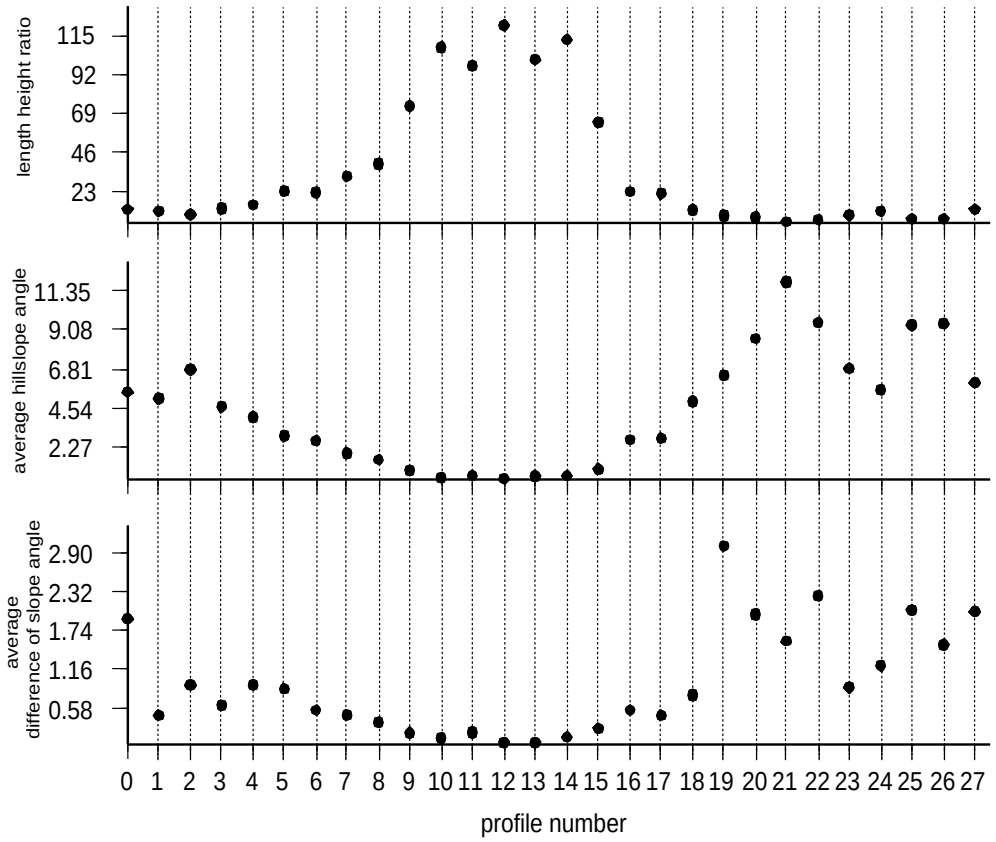

Figure 13.4.: Hillslope profile parameters, Melbtal. See Figure 13.3 and Figure 13.1 for locations and IDs. Generally, the figures depict a gradual increase of relief with down valley position (see text) (after Rasemann 1999, modified).

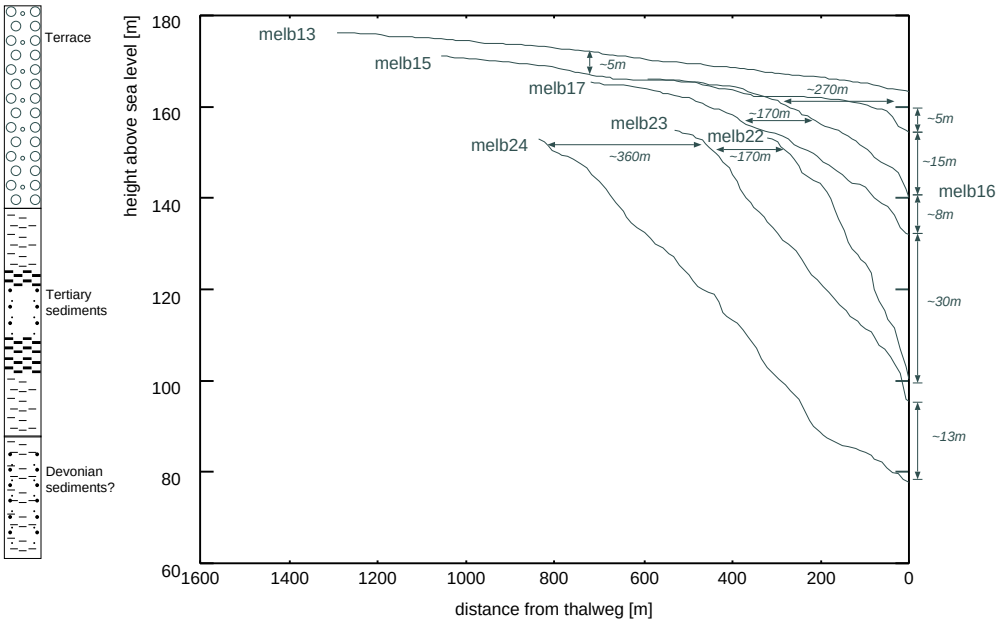

Figure 13.5.: Representative hillslope profiles of the Melbtal marking distinct steps in the catchment evolution, according to the ergodic principle (compare Figure 13.2). Additionally, approximate heights for the lithological layers (from geological maps and literature, compare May 2001) are given.

hillslope processes, which are dependent on hillslope angle (i.e. erosion processes), in comparison to previous homogeneous lowering. At this stage, the valley floor also shows increased lowering leading to a convexity in the thalweg profile (Figure 13.3).

Profile 17 again is mainly developed in Pleistocene terrace material and loess. It shows a convex profile form, which can be attributed to the increasing influence of erosion processes (Ahnert 1976): intensity of process rates by wash processes tend to increase with distance from the watershed (compare section 5.3).

Profile 22 shows a change in form development: increasing incision is evident, whereas hillslope processes could not maintain the slope angle from *profile 17* (no constant retreat any more). As the profiles enter after *profile 17* Tertiary material, this behaviour can be explained by higher erodibility of Tertiary sand and clay.

Profile 23 reveals very low incision rates, but a gradient lowering. Hillslope sediment production might have become so high, that high amounts of stream power are needed to remove the delivered material from footslope. Hillslope profile form changes from a convex form to a straight (slightly concave) form. This indicates different hillslope processes, i.e landslide processes become more dominant as they tend to produce concave forms (Ahnert 1976).

Profile 24 indicates again combined incision and hillslope retreat (similar to *profile 16* and *profile 17*, but at higher gradients). The system might have reached a new equilibrium between hillslope sediment production and fluvial erosion/incision at this stage.

13.1.2. Geomorphometric generalisation

The software OreGIS (Open Landform Geo–Informationsystem) was developed within the project GRK 437 by Marc Hannappel. OreGIS provides a tool for multi–scale geomorphometric analysis, i.e. a DEM, its derivatives, and several landform classifications can be visualised on continuous generalisation levels. The results from hillslope profile analyis (subsection 13.1.1) imply, that there are distinct changes in thalweg and hillslope morphometry within the field site Melbtal, which should be detected on a higher–scale realisation of landform morphometry. OreGIS was applied to the 10 m DEM available for the field site Melbtal (Chapter 8). Figure 13.6 displays profile and contour curvature trends (convex/straight/concave) (1) calculated for all data points and (2) on a generalisation level, involving less than 1% of the information from the original DEM. As Figure 13.6 shows, the generalisation enhances significant geomorhometric structures. Distinct changes in curvature tendencies can be detected along the thalweg profile in the generalised valley structure. The thalweg course in general is characterised by straight and concave curvature tendencies, whereas two transition zones, show high proportions of convex curvature, can be identified qualitatively. Generally, these findings support the results from subsection 13.1.1. Moreover, the conclusion can be drawn, that a multiscale representation of terrain assists for purposes of landform analysis. The approach presented in the last section suffered from the problem of deriving representative hillslope profile sequences for the study site, representing the general morphometric development for the valley side slopes from source to outlet. This was not possible, because terrain (and the DEM) inherits high complexities, i.e. form hierachies (Dikau 1990). Geomorphometric generalisation techniques, as applied in this section can therefore be helpful in generating a higher–order terrain representation, enhancing systematic form relationships, e.g. resulting from valley development. A generalised terrain representation can be useful in delineating representative hillslope sequences (see above), by more objective means.

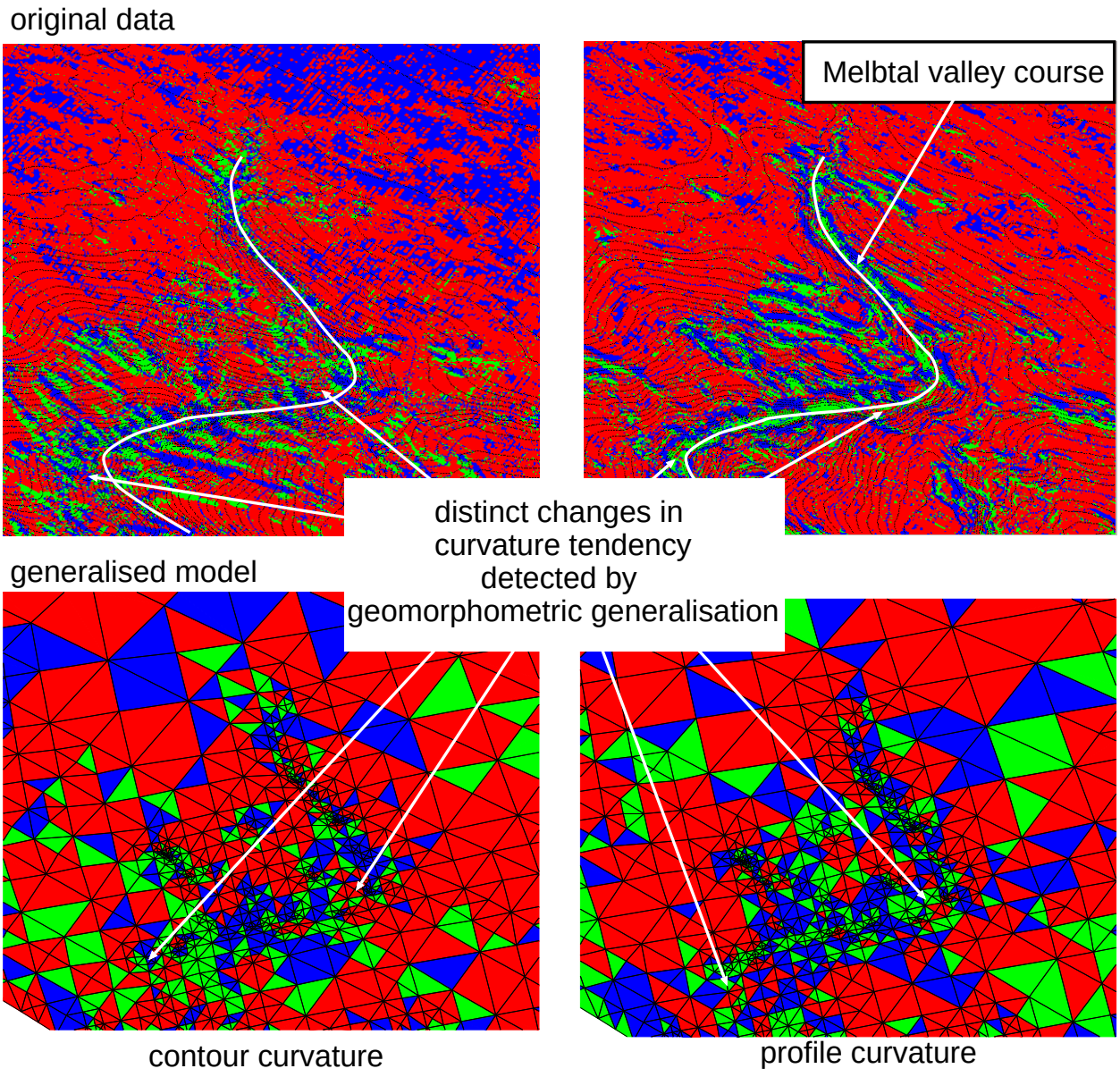

Figure 13.6.: Curvature tendencies for the field site Melbtal (10m DEM) for whole dataset and a generalisation level involving less than 1% of the information (red: convex / blue: straight / green: concave).

13.2. Application of a hillslope evolution model

The model HDS (Richard's n-store Hillslope Dynamics Simulator) simulates the evolution of two dimensional hillslope profiles under varying boundary conditions (see section 5.3). The model was applied to the series of hillslope profiles (Figure 13.5), delineated in subsection 13.1.1. Under the assumption of ergodicity, this sequence represent distinct steps in the hillslope development of the Melbtal. Aim was to provide information about the geomorphic development of the field site Melbtal, i.e. to get an understanding, which processes and system stages have been acted on the Melbtal and have led to its present form.

13.2.1. Modelling results

For technical reasons, the profile data have to be reworked, so that the horizontal profile dimensions of a initial and end profile match. This was carried out homogeneously for the hillslope profile sequence, and two model runs with different adapted hillslope length were performed (profile length 1600 m: Table 13.1, profile length 800 m: Table 13.2).

HDS does not model vertical incision of a stream as the lower process boundary condition of hillslope processes (or tectonic uplift as an upper boundary condition). The findings from the field work and the modelling results described below suggest, that vertical incision of the Engelsbach and related undercutting of the valley side slopes is one major process driving slope evolution of the Melbtal. Therefore, a 'trick' is used to model stream incision with HDS. The variable b (fraction of basal removal) should be kept normally between 0 and 1. b represents a proportion of the sediment entering the basal cell of the profile, which is removed with each iteration (by fluvial processes, compare section 5.3). If b is set ('illegally') to a value greater than 1, more sediment will be removed from the basal cell, i.e. sediment is removed by external processes. As b is a fraction of sediment removal, it produces an increased stream incision with hillslope sediment production, leading to a positive feedback. Therefore, this option should be handled with care, i.e. values should not be much greater than 1. A second possibility is to modify the initial profile at the basal cell to create an initial gradient, which progressively moves backward due to slope processes. This method was not chosen, because it does not reflect the temporal continuous sediment removal by stream incision, and it produces high slope gradients and therefore leads to not normal process behaviour. A series of model runs were perfomed on basis of the chosen hillslope profiles. The sequence of hillslope profiles suggest changing environmental conditions leading to complex variations in hillslope development, i.e. hillslope retreat and valley incision, as discussed in subsection 13.1.1. Therefore, the model was applied stepwise to model each step to the next hillslope profile separately. The according model parameterisations can be found in Table 13.1 and Table 13.2. Some diagrams of the model output are displayed in Figure 13.7, Figure 13.8 shows an overlay of 'real' and modelled best–fit profiles for one model run.

13.2.2. Interpretation

model runs *profile 13* to *profile 15*: constant elevation lowering; initial valley incision.
For initial model runs, low creep/wash rates ($K = 10$ cm/a) and normal solution rates lead to long model times of hillslope evolution ($\rightarrow$ 400 ka to 460 ka!). High creep/wash rates ($K = 100$ cm/a, usually reached by *solifluction* processes) in combination with low valley incision rates, leading to time periods of ca 400 ka before *profile 15* is reached approximately. However, the profile forms of *profile 13* and *profile 15* indicate a constant lowering. Using solifluction processes in combination with high solution rates lead to a fast constant height

Table 13.1.: Parameters for model runs (run 1, homogeneous profile length of 1600 m) using HDS for modelling a hillslope profile sequence (Figure 13.5) of the research site Melbtal. See section 5.3 for explanation of the model and the model parameters.

profile			solution			erosion		landslides				base lowering
initial	end	years	sol_k	g_{sol}	sol_c	K	u	a	g_ψ	g	h_0	b
		[ka]	[µm/a]	[°]	[µm/a]	[cm/a]	[m]	[mm/a]	[°]	[°]	[m]	[1]
13	15	460	0	1	10	10	1000	50	28	35	50	1.5
13	15	360	0	1	10	100	800	50	28	35	50	1.1
13	15	85	0	1	50	100	500	50	28	35	50	1.15
15	16	290	0	1	1	100	500	50	28	35	50	1.05
15	16	20	0	1	0	100	200	50	28	35	50	1.1
16	17	230	0	1	0	30	200	50	28	35	50	1.02
16	17	170	0	1	0	10	100	50	28	35	50	1.02
16	17	60	0	1	0	30	100	50	28	35	50	1.02
17	22	260	0	1	0	20	300	50	28	35	50	1.1
17	22	120	0	1	0	40	300	50	17	35	50	1.1
22	23	120	0	1	0	50	200	50	15	35	150	0.99
23	24	200	0	1	0	100	200	50	23	35	150	1.02
23	24	120	0	1	0	40	100	50	28	35	150	1.02

Table 13.2.: Parameters for model runs (run 2, homogeneous profile length of 800 m) using HDS for modelling a hillslope profile sequence (Figure 13.5) of the research site Melbtal. See section 5.3 for explanation of the model and the model parameters.

profile			solution			erosion		landslides				base lowering
initial	end	years	sol_k	g_{sol}	sol_c	K	u	a	g_ψ	g	h_0	b
		[ka]	[µm/a]	[°]	[µm/a]	[cm/a]	[m]	[mm/a]	[°]	[°]	[m]	[1]
13	15	170	0	0	20	100	200	50	28	35	50	1.05
13	15	400	0	0	10	100	400	50	28	35	50	1.05
13	15	70	0	0	50	100	100	50	28	35	50	1.03
13	15	120	0	0	30	100	200	50	28	35	50	1.06
13	15	80	0	0	50	100	200	50	28	35	50	1.07
15	16	140	0	0	0	100	200	50	28	35	50	1.05
15	16	250	0	0	0	100	200	50	28	35	50	1.03
15	16	40	0	0	0	100	100	50	28	35	50	1.05
15	16	75	0	0	0	50	200	50	28	35	50	1.05
16	17	85	0	0	0	100	100	50	28	35	50	1.01
16	17	170	0	0	0	50	100	50	28	35	50	1.01
17	22	30	0	0	0	100	100	50	17	35	50	1.06
17	22	65	0	0	0	50	100	50	17	35	50	1.06
17	22	160	0	0	0	20	100	50	17	35	50	1.06
22	23	70	0	0	0	0	0	100	6	35	150	1
22	23	160	0	0	0	100	150	50	28	35	50	0.99
22	23	80	0	0	0	100	100	50	28	35	50	0.99
23	24	320	0	0	0	100	100	50	15	35	150	1.01
23	24	320	0	0	0	100	100	50	20	35	150	1.02,.99

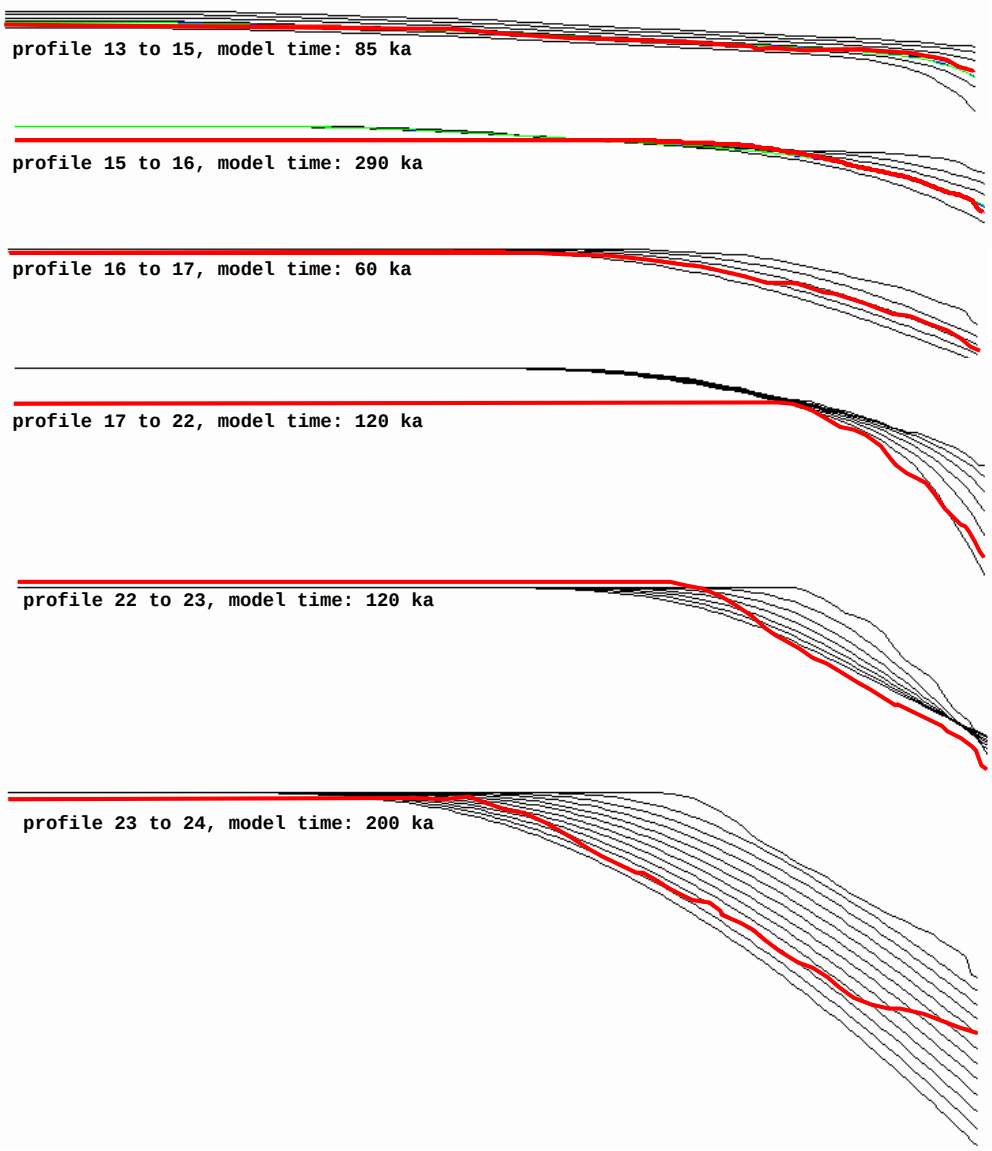

Figure 13.7.: Hillslope evolution modelled by HDS (run 1). Some examples of model sequences. Thin lines are modelled profiles, thick lines indicate 'real world destination' profiles.

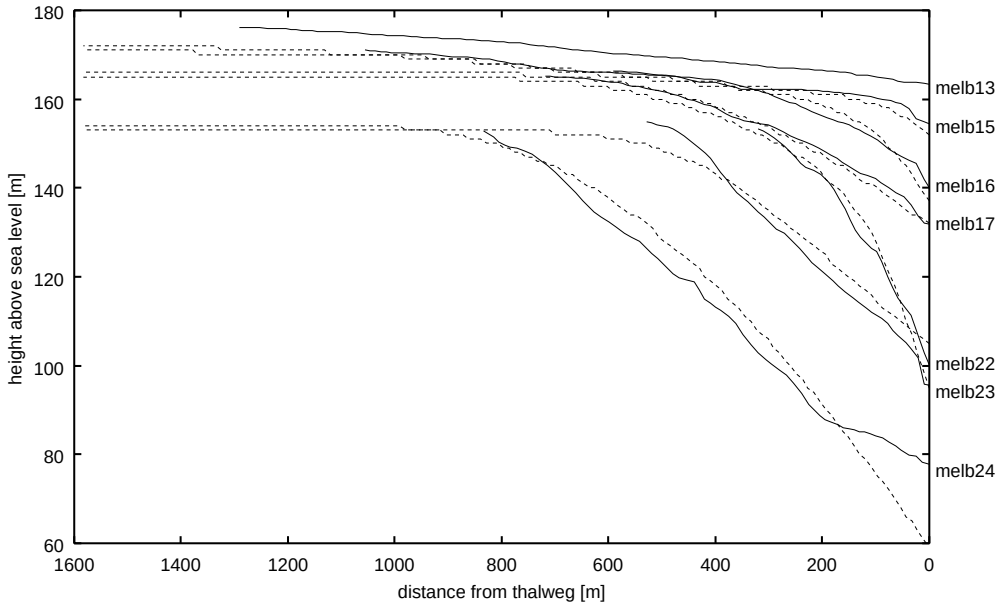

Figure 13.8.: Hillslope evolution modelled by HDS: 'destination' hillslope profiles (solid) and best–fit modelled hillslope profiles (dashed).

lowering and an initial valley incision, as indicated by *profile 15*. The time till *profile 15* is reached in these model runs shows a great variability. Different parameter combinations of solution rates and incision can produce the same final profile within different time periods. The model runs indicate, that (1) uniform continuous lowering of the whole profile by solution, (2) high rates for hillslope erosion processes, and (3) small to medium incision rates are needed to produce *profile 15*. A time frame could not be fixed. However, solution/solifluction rates and incision rates are closely coupled in producing the final profile, which shows a constant lowering of 5 m and an additional valley incision of 5 m. If one of these rates could be fixed, the other is approximately determined by the coupled processes and the final profile form.

model run *profile 15* to *profile 16*: incision, constant hillslope retreat.
The model runs indicate that high sediment transport rates by solifluction and relatively small incision rates are needed to produce increased incision to *profile 16*. Model time vary according to the used incision b and the erosion parameter u (*'wash distance'*).

model run *profile 16* to *profile 17*: constant hillslope retreat.
The constant retreat of *profile 16* to *profile 17* can be reached by lower sediment transport rates (no more solifluction needed, because of the increased hillsope length) in combination with low incision rates. Variations in the times for this evolution step can be modelled by varying rates of wash/creep (K) and the 'wash distance' u.

model run *profile 17* to *profile 22*: increased incision.
High incision rates indicated by the hillslopes of this modelling step require high sediment removal rates (b). As the material changes within this profile sequence to Tertiary material, with considerably lower shear strength (compare Part VI, Appendix E), these changes in rates can be explained by lithologic variance. Moreover, reducing landslide threshold angle g_ψ can reduce the model time significantly.

model run *profile 22* to *profile 23*: no incision, gradient lowering.
Moderate to high erosion processes produce this profile sequence. A model run (Table 13.2) showed that landsliding at very low shear resistance (i.e. low landslide threshold angle) can also explain this sequence. Low resistance can be expected, if extreme meteorological conditions and residual conditions are considered (Heidemann 1996).

model run *profile 23* to *profile 24*: incision, constant hillslope retreat.
For constant hillslope retreat of this sequence, high erosion rates (high K) are needed to reduce the model time to an acceptable period. This indicate acting of high–intensity erosion processes as periglacial solifluction processes.

Generally, the model runs suggest an age of the catchment ranging between approximately 1500 ka and 600 ka, which is consistent with the estimated age by main terrasse sediments, which were deposited before valley incision (900 ka to 600 ka, Part IV, compare Klostermann 1992, May 2001). As most of the model steps could be perfomed by varying parameter combinations leading to different model times, an estimate of relative time periods for the different evolution steps, i.e. a dating of the profiles could not be derived by this modelling approach. However, the results indicate that the different evolution steps require significantly different environmental conditions. The model results suggest that initial valley development required periglacial conditions conditions to produce increased donslope wasting also for low slope angles as indicated by the upper valley profiles. Once a certain hillslope length is reached, lower erosion rates led to constant retreat. A lithologic change and the related system reaction (increased incision, increased erosion by landslide process) could be modelled. The high sediment output in the lower valley part suggest again acting of periglacial processes. Therefore, the findings can contribute in establishing a relation between known environmental phases in the past and temporal hillslope sequences derived by ergodic transfer.

13.3. Summary: a conceptual landform evolution model based on the modelling results

May (2001) developed and tested several hypotheses of the geomorphologic evolution of the Melbtal based on field evidence. In this section, parts of this approach are taken up to develop a conceptual model of hillslope evolution of the Melbtal, based on the results presented earlier in this chapter. Generally, the landform system Melbtal is affected by climatic changes (ice ages), different lithologies and internal system coupling (e.g. slope–channel coupling). Due to this complex situation, May (2001) doubts the applicability of ergodic transfer for the case of the Melbtal. The results from geomorphometric analysis and hillslope evolution modelling, however, imply different stages for the system of hillslope development of the Melbtal (Figure 13.9) as an overlay of general cyclic valley development with varying material sensitivity and climatic transitions. The hillslope evolution model gives some indication about dominant processes for these stages. Therefore, the ergodic principle can be applied in a modified way, i.e. taking changing process activities and a resulting non–linear, but continuous hillslope evolution into account, which can be described by the following stages.

Stage I: initial valley development in Pleistocene terrace material and loess under periglacial conditions.
This phase was characterised by development of an inital trough valley. A threshold in upslope drainage area (ca 100 ha to 150 ha, compare Figure 13.9), led to increased incision of

the creek *Engelsbach*, i.e. in the system of catchment evolution crossed a threshold, relevant for the hillslope system. The modelling results (section 13.2) suggest, that this initial incision coincided with Pleistocene solifluction processes to produce high erosion rates for low hillslope gradients. Convex hillslope forms indicate dominant aquatic or solifluction erosion processes (subsection 13.1.1), which tend to deliver higher rates with increasing distance from divide.

Stage II: constant hillslope retreat under moderate (interglacial) climatic conditions — dynamic equilibrium.
The convex hillslopes formed by *stage I* constantly retreated, preserving a hillslope angle of approximately 5 ° to 8 ° (dependent on the material properties, i.e. shear strength of exposed terrace and loess), and indicating a first *equilibrium* in hillslope evolution. The model results show that, due to the increased hillslope length and slope angle, moderate aquatic erosion processes, maybe under interglacial climatic conditions are sufficient to control that change in form.

Stage III: increasing incision in Tertiary material — *transient state.*
When Tertiary layers are reached (approximate height 140 m), increased incision led to higher gradient of the valley sides near the thalweg. On smaller scales, this phenomena can be observed today (May 2001). An 'oversteepening' of the hillslope profile was produced (subsequent profiles show higher slope angles, see Figure 13.5, page 150). The increasing gradient, and the system reaction indicated in stage IV, lead to the conclusion, that the hillslope system required a sufficient *reaction time* to this change in *external* boundary conditions.

Stage IV: gravitational processes under moderate or periglacial conditions — *system relaxation.*
The increasing incision led to (1) to a knickpoint migration in thalweg profile (Figure 13.9), and (2) increasing slope angles. Therefore, geomorphic activity on the hillslopes increased, especially by the occurrence of landslides (low shear strength of Tertiary material, high groundwater tables layers of different permeability). The hillslope system reacted now to the changes in boundary conditions and relaxed to a new equilibrium in gradient. It is assumed, that hillslope oversteepening, in combination with particular sensitive, interbedded Tertiary layers, and Pleistocene climatic conditions (increased water supply) also led to larger landslides, explaining the disturbed subsurface structure of the east facing hillslopes in the lower valley part. Palmquist and Bible (1980) presented a model of knickpoint migration and related landslide occurrence, with landslides age being related to distance from knickpoint. Although the general situation in the Melbtal suggests similarites to this model, it could not be verified, because of missing field evidence (dated landslides).

Stage V: constant hillslope retreat under periglacial climatic conditions — dynamic equilibrium or critical state?
Once increased valley incision and slope processes are balanced, a new *equilibrium* at a higher hillslope gradient might be reached (indacted by the hillslope profiles, see subsection 13.1.1). However, the sediment delivery by landslides and fluvial removal (or incision) might exhibit a complex behaviour in time due to the occurrence of different event sizes (General–Anzeiger july, 31th 2000). Hillslope profile analysis (subsection 13.1.1) gives some indication, that not just a new equilibrium, but a *self–organizing* state was reached showing high perturbations in processes and related forms (Figure 13.4). Modelling studies showed, that coupling of gravitational hillslope processes with fluvial erosion suggest the development of a critical system (compare Hergarten and Neugebauer 1999b).

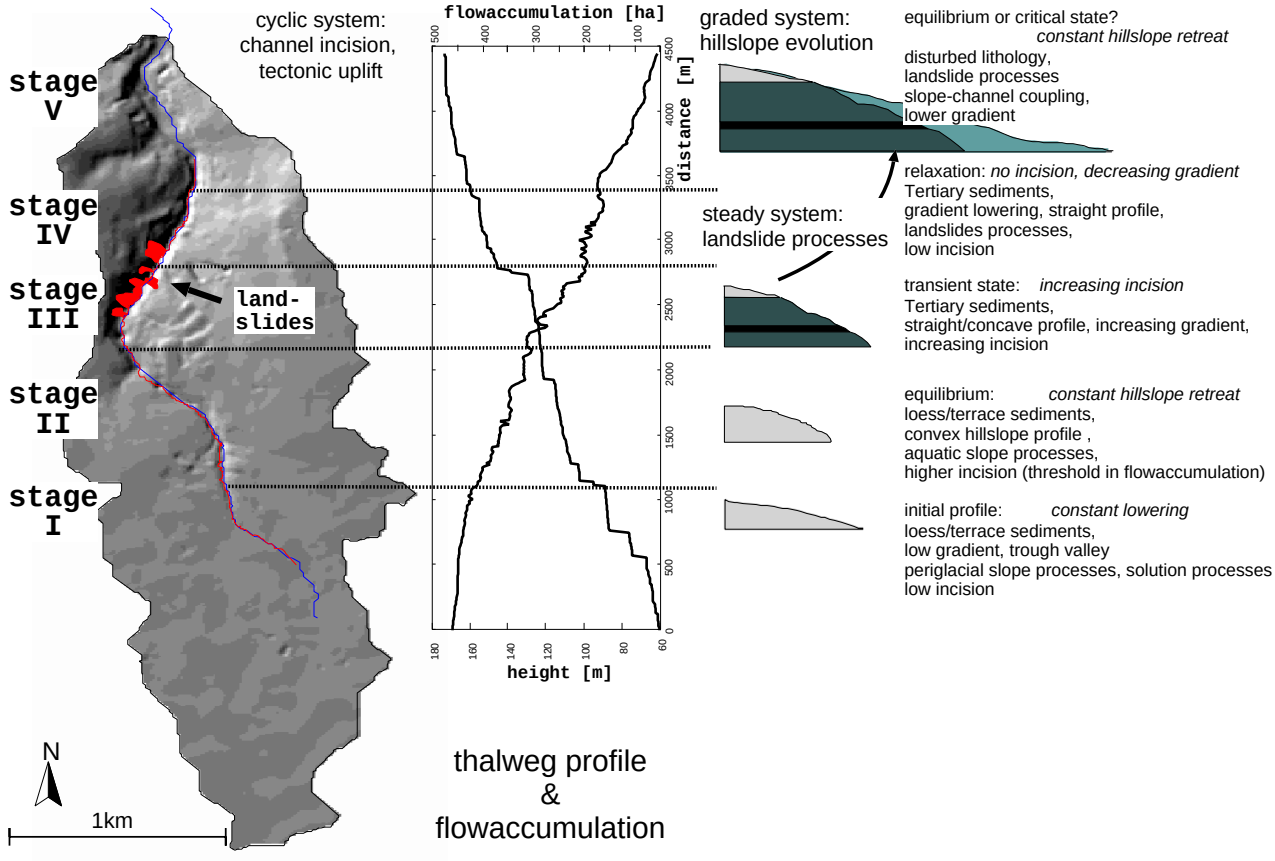

Figure 13.9.: A conceptual model for catchment evolution and hillslope development for the field site Melbtal. Different stages of valley development are inferred from geomorphometric evidence and hillslope evolution model results (see text).

Summary

Modelling slope stability of local landslide objects showed that high water tables, i.e. saturated conditions lead to unstable conditions (FOS ¡1) for both modelled landslides. The landslide 'si7' could be modelled in a successive failure mode by two major failure events, each as a multiple rotational failure. This landslide model agrees with the field evidence, i.e. the detected shear surfaces and structures in landslide debris. Moreover the results indicate, that initial failure occurred in Tertiary material, and that landslide sensitivity of the lithologic unit of trachyte tuff is much lower than for Tertiary sediments. The landslide 'me5' was modelled by two events, both indicating relevance of high groundwater tables for failure conditions. However, in these model results no other triggering factors, e.g. earthquakes or loading, were considered.

A model was presented for four dimensional simluation of groundwater dynamics and failure probability. Model scenarios for the three sensitive hillslopes in the research area with significantly different lithology and landforms, and for three different climate scenarios were perfomed. The results indicate (1) different landslide sensitivity of the hillslope scenarios, and (2) varying sensitivity to climatic changes. Sensitivity to climate boundary conditions, however, indicated no simple pattern, i.e. the hillslope model scenario with the lowest landslide sensitivity showed high sensitivity to climatic changes.

A conceptual landform evolution model for the field site Melbtal was developed on the basis of geomorphometric analysis and long–term hillslope evolution modelling. The results suggest a five stage model of hillslope evolution for the catchment, whereas the stages are defined by changes in material, climate, the related system reaction and external thresholds (catchment evolutionary system) in upslope drainage area. There are some evidences, that the system stages are related to transition in system behaviour, i.e. alternating non–chaotic and self–organising modes in valley development as a reaction to changing boundary conditions.

Part VIII.

Discussion and Conclusions

14. Discussion and Conclusions

14.1. Discussion

This study presented an approach in assessing landslides and hillslope systems using methodologies and techniques at different scales. Due to the intensive field and lab programme, only some initial steps into modelling of slope stability and hillslope evolution could be presented. However, the results demonstrate the utility and the potentials of different techniques within the considered research framework and give some indication about research fields for further work.
One initial research aim considered *relevant scales, model approches and parameterisations for describing the evolution of hillslope systems* (compare section 1.3). This part was approached by developing a conceptual model of hillslope evolution for the field site Melbtal. In this study, geomorphometric analyses in combination with simplified hillslope evolution modelling and conceptual approaches were applied (Chapter 13). Hillslope profile analysis delivered parameterisations for a profile sequence for the research site Melbtal, which indicates different stages in catchment evolution under the assumption of ergodicity. Geomorphometric hillslope profile parameters are descriptors, not only for the geometric development of hillslopes (e.g. increasing hillslope angle, etc.), there are indications that they deliver information of the general system development and system stages of hillslope systems. A hillslope evolution model gave additional information about system stages and dominant processes (i.e. extending the morphological system to a process–response system). A conceptual model of five evolutionary stages of the hillslope system of the Melbtal was developed on the basis of these results. The model combines the general concept of ergodicity with changing system behaviour, according to material sensitivity, climatic changes and process coupling. These results demonstrate the value and necessity of conceptual approaches for assessing stages in hillslope evolutionary systems, related issues will be discussed more in detail in subsection 14.1.1.
Another research issue of this study focused on the question of *how stabilty models can be transfered to scales of hillslope evolution* (compare section 1.3). This problem was approached by scenario models based on aggregated boundary conditions. The results from stability modelling of landslide objects (section 12.1) indicated the high sensitivity of Tertiary layers in the research areas. As triggering factors, high groundwater tables were identified. These findings suggest the application of scenario approaches for modelling the influence of different precipitation conditions on failure probability. Therefore, a series of aggregation techniques were applied, including climate scenarios for the research area. Simplified models for subsurface structure for the research sites (Part VI) were derived from field data and the results of the hillslope evolution model as described above. The results of these aggregation steps imply a series of further general research issues, which are discussed in subsection 14.1.2. A simple model for groundwater and failure probability was applied to climate scenarios and models of sensitive regions of the research sites (section 12.2). The results of this approach depict the variable sensitivity of hillslope systems with different lithologic and morphometric boundary conditions to changing climatic characteristics. Frequency spectra of failure probability are influenced by climatic change in different probability ranges for the different sites. Therefore, stages III and IV of the developed hillslope evolution model (increasing influence

of landslides in the slope system, compare Figure 13.9, page 159) have to be refined with respect to different sensitivities of the valley side slopes of the Melbtal: the west facing valley slopes generally exhibit lower landslide sensitivity (i.e. lower failure probability), but higher sensitivity to climatic change (i.e. higher relative change in failure probability) as shown from the scenario modelling results. Therefore, different system reaction after valley incision in Tertiary sediments is evident from hillslope profile parameters (Figure 13.4, page 149): the west facing valley slopes seemed to require higher reaction times after valley incision in the Tertiary sediments to reach an assumed equilibrium/critical state, because of lower sensitivity. However, various error sources are present in the applied aggregation and modelling steps (subsection 14.1.3).
With respect to the posed hypothesis (section 1.3), it can be stated, that the scenario modelling approach delivered valuable information of sensitivities of slope systems in the Bonn to failure, a quantification of process rates (or unstable material) could not be reached. In the following sections, some specific aspects of this work, related problems, and research issues are discussed.

14.1.1. Modelling hillslope systems — field evidence and conceptual models

Geomorphometric modelling and field evidence in landform evolution

Assessment of geomorphic change certainly requires field evidence. Hillslope profile sequences have been widely used to accomplish this task (e.g. Ahnert 1988). This study showed that, in the case of missing dating results, hillslope profile analysis provide a valuable tool to assess geomorphic history of a hillslope system. However, deriving a set of adequate hillslope sequences for the specified research approach is not a simple task as inherent semantic, geocomputational and scale problems arise (Rasemann 1999). Some of these problems can be approached using scaling approaches in geomorphometric modelling as shown in subsection 13.1.2, however, these are not generally available. Combining classical geomorphometric algorithms, e.g. hillslope delineation with *multi–scale representations of the earth surface* in geocomputational environments therefore is an issue, delivering potential applications for geomorphologic research on larger temporal scales. Moreover, tools for geomorphometrical generalisation are desired to deliver aggregated boundary conditions, applicable in scenario models (see below).

Necessity of conceptual models and simplified modelling approaches

Uncertainty in recent and past enviromental processes and environmental conditons is high. Therefore, process models and conceptual approaches require parameterisation and interpretation of boundary conditions (see below). This study presented an approach in combining scenario–models with conceptual modelling as a link between process models and long–term landform evolution. The utility and necessity of conceptual models in large scale landscape assessment, as indicated in other studies (Haigh 1988, Slaymaker 1992), is emphasised by the results of this study. However, integration of process description is needed to fill vague conceptual approaches with figures and to quantify landform evolution. The results in modelling evolution shows the applicability of comparatively simple models of hillslope development to a relatively complex catchment as the field site Melbtal. These findings encourage the usage of those models for understanding geomorphic change, related to changing environmental conditions in the past and in the future. *Results from similar and different field sites* (i.e. applying models to other valleys nearby the field site Melbtal, compare Part IV) could validate the model results of this study, and maybe justify some of the conclusions, in that way that more distinct relations between environmental boundary conditions and change of hillslope form on a broader empirical basis can be derived.

14.1.2. Spatio–temporal aggregation & scenario modelling for assessing geomorphic change

Surface/subsurface models as geomorphic scenarios

This study presented an approach in scenario modelling, requiring the derivation of meaningful model scenarios for relevant boundary conditions. This included modelling of surface and subsurface structure. With respect to scales of landform evolution, this modelling step is clearly related to regionalisiation (or aggregation) issues. The complexity of real world conditions has to be aggregated to dominant structures. Related tools are geomorphometric modelling, but also aggregation of subsurface structures within the higher–scale framework of landform evolution (see above). Modelling subsurface structure usually involves in many aggregation steps specific site knowledge and also some degree of subjective interpretation (Chapter 10). Therefore, expert systems and new geocomputational environments, which incorporate e.g. basic knowledge about inconsistencies in subsurface structures (compare Siehl 1993), could facilitate this modelling step. For aggregating landforms, geomorphometric generalisation is required, leading to the issues of developing new concepts and tools in geomorphometry (subsection 14.1.1).

Soil properties and representative parameters

Derivation of representative soil properties is one important step in the aggregation procedure, which is directly related to the mentioned problem of subsurface aggregation. In this study, soil parameters for lithological units were derived using statistical tools. An important issue is to consider *spatial structure of soil properties* (*'geomorphic structure'*, compare Schmidt *et al.* 1998, 2000), i.e. relationships of geomorphometric, geologic and pedologic parameters as a result of geomorphic history, which especially applies to Quarternary sediments (compare Preston 2001). As Brinkmann *et al.* (2001) argued, modelling these relationships require a sound understanding of the underlying geomorphic systems, i.e. the problem of geomorphic structures is closely related to the general problem of geomorphic evolution, a solution cannot be found separately. In aggregation of geomorphic structure, therefore the coupled the system of geomorphic evolution has to be considered.

Proxy–data and climate scenarios

Developing models representing historic climatic variablity is an own research framework (compare e.g. Glaser 1998, Glaser *et al.* 1999, Pfister and Lauterburg 1992, Pfister 1992, Schüle and Pfister 1992). Due to the complexity of the overall research aim, this study could only present a very initial statistical approach into this direction, indicating the potential of proxy data in assessing past climate variablility. However, the problem of decreasing temporal resolution and increasing uncertainty in past data remains unsolved. For example, frequency–magnitude distributions of past climate events, which are highly important for geomorphic processes in general, and especially for landslides (as shown by the scenario models in section 12.2), were not modelled in this study. The relation between local climate on a monthly or daily scale, as used in this study, and on a event (e.g. minute) scale is highly non–linear, therefore the presented model results remain speculative. It is proposed to *model past climatic variablity on a stronger physical/meteorological basis* rather than to use statistical methods (Pfister 1992, Thompson *et al.* 1993). Identifying spatio–temporal climate patterns, e.g. sequences of 'Grosswetterlagen', and their relationships with patterns in climate elements could be a possible step into this direction. These sequences can be used in actualistic transfer or in combination with climate models to assess past recurrence intervals and spatial variability of climate events. Brandão and Fragoso (1999) presented an approach in delineating 'synoptic weather types' for assessing frequency and magnitude characteristics of rainfall.

The results of the climate series analysis in this study indicated a signifant de–correlation of paleo–data with recent weather records for the last 30 years. This might partly be explained by increasing climate variability due to *global climate change*, indicating an *application of higher resolution proxy–data*. With that background, applicability of recent conditions to model paleo–process variability is questionable.

Scenario modelling as a tool for long–term behaviour of processes
This study presented an attempt to quantify geomorphic effectiveness of landslide processes in an scenario approach. The model approach based on the application of classical, comparatively simple model concepts for the relevant processes (hillslope hydrology, hillslope stability). It was *not* evaluated, to which degree more *advanced modelling approaches* could influence the modelling results. However, these modelling approaches clearly require more efforts in model parameterisation. Testing different models for the relevant small scale processes would be certainly an issue to detect major shifts in the modelled system and to clearify, which precision of small scale process description is required to deliver reliable output on higher scales. Moreover, *verifying the results against field data* is certainly necessary, but not carried out in this study, because of missing data (e.g. dating of older landslides).

14.1.3. Implications of data and model errors

Statistical and systematic errors resulting from measurement techniques
The used measurement techniques imply a series of error sources due to technical limitations of the measurement devices, and because of problems in experiment execution. Appendix D presents an attempt to assess potential error sources and related errors. The research topic of this study deals with large spatio–temporal scales. The data analyses (Chapter 10) presented in this study aimed at a crude model of material structure and material properties, i.e. identifying major subsurface structures. Therefore, it can be assumed that statistical errors and technical errors are of minor relevance for this study. For example, statistical and systematic errors related to experiment design (i.e. the underlying measurement model, compare Appendix D) are considerable small in comparison to small (within–outcrop) to medium scale (within–layer) variability of soil properties (Appendix C.6, compare Chowdhury 1984), which have to be neglected with respect to the major soil structures, anyway.

Some specific problems
In this study, relevant regolith properties were related to lithological layers. Generally, good agreements of the results from field and lab data, and consistent soil parameterisations were reached. However, a series of specific problems encountered during this work.

- Disagreement of different techniques measuring the same quantities: different techniques for determining particle size distribution (pipette method, hydrometer method), delivered for some soil types different results.
- Problems occurred in determining particle size distribution by pipette method for soils with high fractions of trachyte tuff, leading to high errors and high variability of the results.
- The inclinometer signals partly delivered 'elastic' behaviour of the soils under investigation (subsection 10.1.2). Understanding these small scale dynamics and their dependencies to boundary conditions (especially to groundwater variations) require continuous monitoring and small scale modelling approaches.

These specific problems could not be clarified in this work, they are offering potentials for *detailed methodological studies on the soil properties and small scale soil dynamics* for the research area.

Systematic errors resulting from basic model assumptions
This study focused on capturing data relevant for mass movement processes. Coupled processes as tectonic uplift, baselevel lowering, fluvial processes were not assessed or treated as simplified boundary conditions. More detailed quantification of these process rates would certainly improve the model approach, especially with respect to possible validation of the hillslope evolution modelling part (Chapter 13). Therefore, measurement techniques and model approaches to estimate frequency–magnitude characteristics of the *fluvial sediment dynamics* within the field site Melbtal should be applied. Rates of fluvial sediment transport in scales relevant for hillslope evolution are only accessible by (1) long–term measurements and/or (2) dating the correlate sediments. Both data sources were not available for the study site. It would be certainly an issue to quantify these rates, e.g. by modelling approaches. Tectonic uplift on longer timescales, can only be measured if dateable markers are available, which was not proved and is highly questionable for the study site. Research results from Meyer and Stets (1998), give some indication of the total magnitude of tectonic uplift for the late Pleistocene (approximately 120 m since formation of main terrace, approximately at the Brunhes–Matuyama transition, ca 900,000 bp). However, these figures give only very crude estimations, which are not sufficient to understand landform change at the considered scale. In this study, only mass movement processes were investigated in detail for the study area. However, the geomorphic history implies a series of other processes, i.e. *soil erosion processes, periglacial processes, solution processes*, etc. The model results from long–term modelling (Chapter 13) also showed the relevance of these processes in order to explain hillslope evolutionary system of the field site Melbtal. Vegetation and landuse conditions were not considered as changing variables in the model approach. Historical sources show considerable variations of vegetation cover due to human impact (Part IV). Assessment of *variability of past landcover changes*, e.g. in the same manner as the climatic variations were treated in scenario models in this study, would be a valuable research issue for quantifying spatio–temporal variability of relevant model parameters (interception, evaporation, etc.) and landscape sensitivity.

14.1.4. Implications for landslide hazard assessment

The approach presented in this study shows similarites with approaches of landslide hazard assessment, which especially applies to the estimation of failure probabilities in space and time. Classical approaches in assessement of landslide hazard include (e.g. Aleotti and Chowdhury 1999, Möller 1999, Rogozia 2000) (1) qualitative methods, e.g. by 'expert–overlay' of factorial maps (e.g. Mulder and van Asch 1987, Grunert and Schmanke 1997), (2) statistical models, which relate empirical evidence of landslide occurrence to relevant parameters (Aleotti and Chowdhury 1999, Mulder and van Asch 1987, van Westen *et al.* 1997), and (3) deterministic models, e.g. Factor of safety (FOS). Several drawbacks of these methodologies can be identified, leading to issues with respect to the approach presented in this study. The (mostly) static hazard models do not consider the *dynamics of the related geomorphic system*. However, in areas with high landslide danger, landslides are usually part of an active geomorphic system, and coupled with other geomorphic processes (see e.g. Crozier and Preston 1999, Preston 1996, 1999, and compare Chapter 2). Therefore, it is proposed to include the assessment of the underlying geomorphic system in hazard approaches. In addition to classic mapping and spatial analyses, as frequently used in classic hazard approaches, other geomorphic techniques reaching for temporal variability (geomorphometry, landform evolution modelling, dating) and conceptual geomorphic models should be considered.

Frequently, hazard models are invariant in time, i.e. they do not consider *changing boundary conditions*, e.g. recurrence of climate events and changing climate conditions in the past and in the future. This study showed that it is possible to model process scenarios using proxy–data, which could be a valuable tool, to assess long–term *temporal variability* of hazards, caused by geomorphic processes. This certainly also applies to changing vegetation and landuse conditions.

14.2. Conclusions

Landslides and their role as a component of slope systems incorporate phenomena and processes with different scale characteristics. In this study, a variety of methods were applied to assess hillslope systems and the role of mass movements within hillslope systems. Each of the applied methodologies certainly delivers potential for detailed research (see section 14.1). However, this study tried to emphasise the *integration of different methods*. Therefore, as a conclusion, the different parts of this work are set within the framework of a general research concept for the assessment of geomorphic system on higher scales (Figure 14.1), which shall be shortly outlined.
Landform systems are inherently complex and exhibit non–linear behaviour. They contain a hierarchy of processes and forms. Assessing these systems can therefore not be done by investigating local phenomena, but has to include information about the spatio–temporal hierarchy of landform elements, reflecting its multi–scale character. A fundamental concept of the presented research approach therefore is to simplify complexity to dominant *patterns in form, process, and systems* on different scales. **System analysis** is a necessary step for generalising complex landform reality to major structures and parameters. This study indicated, that combining **conceptual approaches** and **simplified evolution modelling** provide valuable information about major system stages, even if no temporal constraints are available. **Dating results** can certainly contribute to system approaches and validate the related findings, as showed e.g. by Preston (2001). However, adequate **aggregation techniques** are a fundamental requirement delivering field evidence for conceptual and model approaches. **Geomorphometric analysis** has been proved to be a valuable method in analysing scales and patterns in landform systems. Landforms not only reflect information about a process history, but are also major boundary conditions for recent processes, altering landform surface again. Geomorphometry therefore is an important information source for understanding geomorphic systems, as landform contain signals of geomorphic history on various scales. Together with conceptual and simplified modelling approaches, geomorphometric analysis can deliver information about relative ages of landforms, where direct dating is not feasible. As landform surfaces include multiple hierarchical scales, present concepts and tools in geomorphometric analysis have to be refined by generalisation techniques, including 'multi–scale reality' of landform surfaces. Similarily, subsurface information is an archive of past process history and required parameterisation for recent process modelling and past process history. However, as material structure and properties are products of recent and past geomorphic processes and controlling these on the other hand, this dynamic system leads to the existence of distinct spatial patterns and relationships between material and form properties, which were termed as **geomorphic structure** (Schmidt *et al.* 1998). Hence, the question of assessing landform evolution by analysing geomorphic systems is directly coupled with existing geomorphic structures as a result of landform evolution.
Assessing **variability of climatic & landuse conditions** is a major problem for evaluating past environmental conditions of geomorphic systems. Upscaling available archive information like proxy data to aggregate scenarios is a valuable tool, at least to reflect major changes in terrestrial Geo–systems. This study presented an inital statistical analysis approach in the variability and pattern of proxies, indicating the potentials of this data source for assessing past environmental

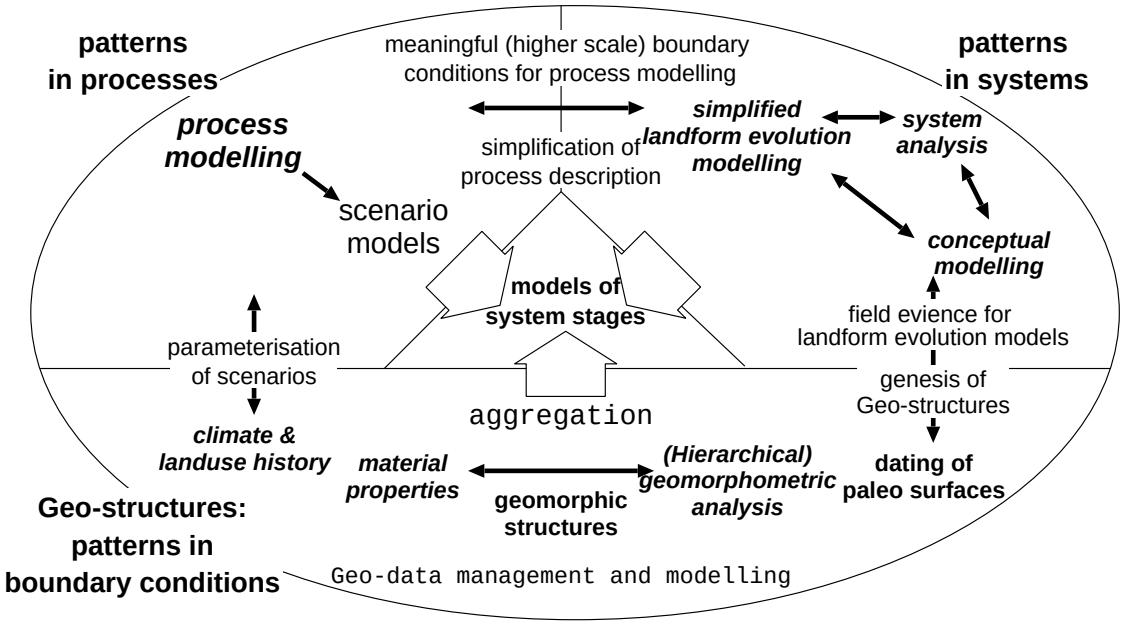

Figure 14.1.: Outline of an integrated assessment in geomorphic systems on various scales, based on the methodologies applied in this study. The interconnected parts are assessment of (1) Geo–structures by aggregation techniques, (2) process patterns by scenario models, and (3) system patterns by conceptual approaches, system approaches and simplified modelling approaches. These parts contribute to general models of geomorphic systems by aggregated system stages (see text).

changes.

Scenario models were used in this study as a technique to *upscale* process description into higher scales of geomorphic systems and landform evolution. These model types can deliver quantifications of sensitivity of different aggregated environmental conditions, and the related findings can contribute to delineate and specify system stages (see above). However, scenario models depend on (1) a meaningful aggregation of boundary conditions (as described above), and (2) a general understanding of the related environmental systems (see above). Therefore, the presented parts are closely interconnected (as shown in Figure 14.1). With respect to complex landform systems, it is argued, that modelling landform evolution, should be carried out by delineating models of system stages. Each of the described parts, i.e. patterns in systems, structures in boundary conditions, and patterns in process behaviour provide deliveries for deriving models of major system stages in geomorphic systems.

Most of the described steps, as aggregation techniques, for example, require sound databasis of the considered environmental system. Advancement in investigation and data collection techniques lead to an increase in acquiring and processing of environmental information, (not only) relevant for landslide studies. Increasing availability of data (especially in a world wide context) leads to the profound need of combined (Geo–) databases. Considering the multi–disciplinary background, the main difficulties are the limited ability in (1) assessing, (2) processing and (3) analysing these data sources. Therefore, new methods have to be devised, and appropriate architectural concepts of **Geo–information management** have to be developed for digital data storage, and for data analysis based on a multi–scale reality of environmental systems.

Parting words

However, in emphasising the integration of different methods on different scales, this approach was reductionistic itself (e.g. with respect to neglected boundary conditions, etc.), as each scientific approach has to be! With respect to system complexity, completely different approaches might also be justified...

> *"...It was not until I was content to forget about Davis and Penck and learn to stop being clever and interpreting landscape, but just to sit silently on the hillsides with my chin in my hands and let the landscape teach me that I really began to understand it. It is very like being in big game country. So long one goes on walking one sees nothing; when one sits and becomes part of the landscape, then the animals come out all about one."*
>
> (L.C. King, cited in Melhorn and Flemal 1981)

Bibliography

AGBODEN (1994). Bodenkundliche Kartieranleitung. Arbeitsgruppe Boden.

Ahnert, F. (1976). Brief description of a comprehensive three–dimensional process–response model of landform development. *Zeitschrift für Geomorphologie, N.F., Supplement Band*, **25**, 29–49.

Ahnert, F. (1987a). Approaches to dynamic equilibrium in theoretical simulations of slope development. *Earth Surface Processes and Landforms*, **12**(1), 3–15.

Ahnert, F. (1987b). Process–response models of denudation at different spatial scales. *Catena Supplement Band*, **10**, 31–50.

Ahnert, F. (1988). Modelling landform change. In M. G. Anderson, editor, *Modelling Geomorphological Systems*, pages 375–400. John Wiley & Sons, Chichester.

Ahnert, F. (1992). Modelling landform evolution: The climatic input. *The second William Vaughan Seminar, Department of Geography, University of Cambridge.*

Aleotti, P. and Chowdhury, R. (1999). Landslide hazard assessment: summary review and new perspectives. *Bulletin of Engineering Geology and the Environment*, **58**, 21–44.

Alteköster, C. (prep). *Untersuchungen zur Reproduzierbarkeit von Bodenradarmessungen.* Ph.D. thesis, Department of Geology, University of Bonn. (in preparation).

Anderson, M. (1987). Modelling slope stability: the complementary nature of geotechnical and geomorphological approaches. In M. Anderson and K. Richards, editors, *Slope Stability*, pages 1–9. John Wiley & Sons, Chichester.

Anderson, M. and Burt, T., editors (1990). *Process Studies in Hillslope Hydrology.* John Wiley & Sons, Chichester.

Armstrong, A. (1980). Soils and slopes in a humid temperate environment: A simulation study. *Catena*, **7**, 327–338.

Armstrong, A. (1987). Slopes, boundary conditions, and the development of convexo–concave forms — some numerical experiments. *Earth Surface Processes and Landforms*, **12**(1), 17–30.

Bak, P. (1996). *How nature works: the science of self–organized criticality.* Springer–Verlag, Berlin Heidelberg New York.

Barnes, G. (1995). *Soil mechanics. Principles and practice.* Macmillan.

Baumgartner, A. and Liebscher, H.-J. (1990). *Allgemeine Hydrologie Quantitative Hydrologie*, pages 503–522. Gebrüder Borntreager.

Beuselin, L., Govers, G., Poesen, J., *et al.* (1998). Grain–size analysis by laser diffractometry: comparison with the sieve–pipette method. *Catena*, **32**, 193–208.

Beven, K. (1996). Equifinality and uncertainty in geomorphological modelling. In B. Rhoads and C. Thorn, editors, *The scientific nature of geomorphology*, pages 289–313. John Wiley & Sons, Chichester.

Bichler, B. (2001). Diplomkartierung im nördlichen Siebengebirge vom Ennert bis zur Dollendorfer Hardt. Department of Geology, University of Bonn.

Bishop, A. and Morgenstern, N. (1960). Stability coefficients for earth slopes. *Geotechnique*, **10**, 129–150.

Blondeau, F. (1973). The residual shear strength of some French clays: measurement and application to a natural slope landslide. *Geologia Applicata e Idrogeologia*, **8**(1), 125–141.

Boer, D. (1992). Hierarchies and spatial scale in process geomorphology: a review. *Geomorphology*, **4**, 303–318.

Brandão, C. and Fragoso, M. (1999). Extreme storms and rainfall erosivity factor in Évora (Portugal). *Zeitschrift für Geomorphologie, N.F., Supplement Band*, **115**, 113–123.

Braun, J. and Sambridge, M. (1997). Modelling landscape evolution on geological time scales: a new method based on irregular spatial discretization. *Basin Research*, **9**(1), 27–52.

Brinkmann, J., Schmidt, J., and Dikau, R. (2001). Terrain modelling and soil distribution: possibilities, problems and future issues. *Transactions in GIS*. in press.

Brooks, S. and Anderson, M. (1995). The determination of suction–controlled slope stability in humid temperate environments. *Geografiska Annaler*, **77A**(1–2), 11–22.

Brooks, S., Anderson, M., Ennion, T., *et al.* (1999). Exploring the potential for physically–based models and contemporary slope processes to examine the causes of holocene mass movement. In S. Hergarten and H. Neugebauer, editors, *Process modelling and landform evolution*, volume 78 of *Lecture Notes in Earth Sciences*, pages 205–230. Springer–Verlag, Berlin Heidelberg New York.

Brunsden, D. (1973). The application of system theory to the study of mass movement. *Geologica Applicata e Idrogeologia, University of Bari*, **8**, 185–207.

Brunsden, D. and Thornes, J. (1979). Landscape sensivity and change. *Transactions, Institute of British Geographers. New Series*, **4**(4), 463–484.

Burghardt, O. (1979). *Siebengebirge — Landschaft im Wandel*. Geologisches Landesamt Nordrhein–Westfalen.

Caine, N. (1976). A uniform measure of subaerial erosion. *Geological Society of America Bulletin*, **87**, 137–140.

Caris, J. and Asch, T. W. (1991). Geophysical, geotechnical and hydrological investigations of a small landslide in the French Alps. *Egineering Geology*, **31**, 249–276.

Casale, R., Fantechi, R., and Flageollet, J., editors (1993). *Temporal occurence and forecasting of landslides in the European Community*. Final report, Vol. I and II of the EC Programme EPOCH, Contract no. 90 0025.

Cendrero, A. and Dramis, F. (1996). The contribution of landslides to landscape evolution in europe. *Geomorphology*, **15**, 191–211.

Chorley, R., Schumm, S., and Sugden, D. (1984). *Geomorphology*. Methuen.

Chorley, R. J. and Kennedy, B. A. (1971). *Physical Geography. A systems approach*. Prentice Hall, London.

Chow, V., Maidment, D., and Mays, L. (1988). *Applied Hydrology*. McGraw–Hill.

Chowdhury, R. (1984). Recent developments in landslide studies: Probalilistic methods. State–of–the–Art–Report — Session VII (a). In *4th International Symposium on Landslides, Toronto*, pages 209–228.

Coulthard, T. J. (2001). Landscape evolution models: a software review. *Hydrological Processes*, **15**, 165–173.

Coulthard, T. J., Kirkby, M. J., and Macklin, M. G. (1998). Non–linearity and spatial resolution in a cellular automaton model of a small upland basin. *Hydrology and Earth Sciences*, **2**(2-3), 257–264.

Coulthard, T. J., Kirkby, M. J., and Macklin, M. G. (1999). Modelling the impacts of Holocene environmental change in an upland river catchment, using a cellular automaton approach. In A. Brown and T. Quine, editors, *Fluvial processes and environmental change*, pages 33–46. John Wiley & Sons, Chichester.

Crozier, M. J. (1973). Techniques for morphometric analysis of landslips. *Zeitschrift für Geomorphologie, N.F.*, **17**(1), 78–101.

Crozier, M. J. (1986). *Landslides: causes, consequences & environment*. Routledge, London, New York.

Crozier, M. J. (1996a). Magnitude/Frequency issues in landslide hazard assessment. *Heidelberger Geographische Arbeiten*, **104**, 221–236.

Crozier, M. J. (1996b). Runout behaviour of shallow, rapid earthflows. *Zeitschrift für Geomorphologie, N.F., Supplement Band*, **105**, 35–48.

Crozier, M. J. (1999). The frequency and magnitude of geomorphic processes and landform behaviour. *Zeitschrift für Geomorphologie, N.F., Supplement Band*, **115**, 35–50.

Crozier, M. J. and Glade, T. (1999). Frequency and magnitude of landsliding: fundamental research issues. *Zeitschrift für Geomorphologie, N.F., Supplement Band*, **115**, 141–155.

Crozier, M. J. and Preston, N. (1999). Modelling changes in terrain resistance as a component of landform evolution in unstable hill country. In S. Hergarten and H. Neugebauer, editors, *Process modelling and landform evolution*, volume 78 of *Lecture Notes in Earth Sciences*, pages 267–284. Springer–Verlag, Berlin Heidelberg New York.

D–Diver Manual (1998). *D–Diver Manual*. Van Essen Instruments bv.

Davis, W. M. (1899). The geographical cycle. *Geographical Journal*, **14**, 481–504.

Dikau, R. (1990). Geomorphic landform modelling based on hierarchy theory. In *Proceedings of the 4th International Symposium on Spatial Data Handling, July 23–27, 1990, Zürich*, volume 1, pages 230–239.

Dikau, R. (1999). The need for field evidence in modelling landform evolution. In S. Hergarten and H. Neugebauer, editors, *Process modelling and landform evolution*, volume 78 of *Lecture Notes in Earth Sciences*, pages 3–12. Springer–Verlag, Berlin Heidelberg New York.

Dikau, R. and Schmidt, J. (1999). Georeliefklassifikation. In R. Schneider-Sliwa, D. Schaub, and G. Gerold, editors, *Angewandte Landschaftsökologie*, pages 217–244. Springer–Verlag, Berlin Heidelberg New York.

Dikau, R., Cavallin, A., and Jäger, S. (1996a). Databases and GIS for landslide research in Europe. *Geomorphology*, **15**, 227–239.

Dikau, R., Brunsden, D., Schrott, L., *et al.*, editors (1996b). *Landslide recognition.* Number 5 in International Association of Geomorphologists Publication. John Wiley & Sons, Chichester.

DIN (1993). *Erkundung und Untersuchung des Baugrundes (DIN–Taschenbuch 113).* DIN, Deutsches Institut für Normung e.V., Berlin Köln.

Dingman, S. (1994). *Physical Hydrology.* Macmillan.

Dodds, P. and Rothman, D. (2000). Scaling, universality, and geomorphology. *Annual Review of Earth Planetary Sciences*, **28**, 571–610.

Dunnicliff, J. (1993). *Geotechnical instrumentation for monitoring field performance.* John Wiley & Sons, New York, Chichester.

Fabian, M. (prep). *Messung und Modellierung des Bodenverformungsfeldes in der Umgebung bepumpter Brunnen.* Ph.D. thesis, Department of Geology, University of Bonn. (in preparation).

Fabian, M., Rebscher, D., and Kümpel, H.-J. (2000). Bohrlochneigungsmessungen, Ergebnisse zum Pumpversuch Bremerhaven–Wulsdorf. *Schriftenreihe des SFB 350*, **94**.

FGDC (1998). *Content standard for digital geospatial metadata.* Federal Geographic Data Committee (FGDC). Federal Geographic Data Committee. FGDC–STD–001–1998.

Föckeler, A. and Kuhn, H. (1990). Aufbau und Anwendung von Digitalen Geländemodellen in Nordrhein–Westfalen. *GIS*, **4**.

Francis, S. (1987). Slope development through the threshold slope concept. In M. Anderson and K. Richards, editors, *Slope stability*, pages 601–624. John Wiley & Sons, Chichester.

Freeze, R. (1987). Modelling interrelationsships between climate, hydrology, and hydrogeology and the development of slopes. In M. Anderson and K. Richards, editors, *Slope stability*, pages 381–403. John Wiley & Sons, Chichester.

Fuchs, K., editor (1983). *Plateau uplift. The renish shield — a case history.* Springer–Verlag, Berlin Heidelberg New York.

Gärtner, H., Bergmann, A., Breunig, M., *et al.* (2000). OPALIS — An Open Paleoecological Information System. *Geoinformationssyteme*, **13**, 6–11.

Gärtner, H., Bergmann, A., and Schmidt, J. (2001). Object–Oriented modeling of data sources as a tool for the integration of heterogeneous geoscientific information. *Computers and Geosciences*, **27**(8), 975–985.

General–Anzeiger july, 31th (2000). 43 Feuerwehr–Einsätze in zweieinhalb Stunden. General–Anzeiger, july 31th, 2000.

Gilbert, G. C. (1877). Report on the geology of the Henry Mountains. Technical report, U.S. Geographical and Geological Survey.

GLA (1988). Geologie am Niederrhein. Geologisches Landesamt Nordrhein–Westfalen, Krefeld.

Glade, T. (1997). *The temporal and spatial occurrence of rainstorm–triggered landslides events in New Zealand*. Ph.D. thesis, School of Earth Sciences, Victoria University of Wellington.

Glaser, R. (1998). Historische Hochwässer im Maingebiet — Möglichkeiten und Perspektiven auf der Basis der Historischen Klimadatenbank Deutschland (HISKLID). *Erfurter Geographische Studien*, **7**, 109–128.

Glaser, R. *et al.* (1999). Seasonal temperature and precipitation fluctuations in selected parts of Europe during the sixteenth century. *Climatic change*, **43**, 169–200.

Glaser, R., Beck, C., and Beyer, U. (2000). Vom mittelalterlichen Wärmeoptimum über die Kleine Eiszeit ins moderne Treibhausklima. *Petermanns Geographische Mitteilungen*, **144**(4), 44–53.

Glötzl, F. (1994). Digital – Inklinometer. Funktion und Anwendung. *Baumesstechnik*, **Bericht 15**. Fachseminar "Messen in der Geotechnik", Institut für Grundbau und Bodenmechanik, Technische Universität Braunschweig.

Goldenfeld, N. and Kadanoff, L. (1999). Simple lessons from complexity. *Science*, **284**, 87–89.

Greenway, D., Anderson, M., and Brian-Boys, K. (1984). Influence of vegetation on slope stability in Hong Kong. In *4th International Symposium on Landslides, Toronto*, pages 394–404.

Grunert, J. (1988). Geomorphologische Entwicklung des Bonner Raumes. *Arbeiten zur Rheinischen Landeskunde*, **58**, 165–180.

Grunert, J. and Hardenbicker, U. (1991). Hangrutschungen im Bonner Raum — ihre Genese und Kartierung für Planungszwecke. *Zeitschrift für Geomorphologie, N.F., Supplement Band*, **89**, 35–48.

Grunert, J. and Hardenbicker, U. (1993). Gravitative Hangabtragung im Bonner Raum während des Holozäns. *Würzburger Geographische Arbeiten*, **87**, 325–338.

Grunert, J. and Schmanke, V. (1997). Hangstabilität im Südwesten Bonns. *Geographische Rundschau*, **49**(10), 584–590.

Hack, J. (1960). Interpretation of erosional topography in humid temperate regions. *American Journal of Science, Bradley Volume*, **258–A**, 80–97.

Haigh, M. (1987). The holon: hierarchy theory and landscape research. *Catena Supplement*, **10**, 181–192.

Haigh, M. (1988). Dynamic systems approaches in landslide hazard research. *Zeitschrift für Geomorphologie, N.F., Supplement Band*, **67**, 79–91.

Hansen, A. (1984). Engineering geomorphology: the application of an evoluionary model of Hong Kong's terrain. *Zeitschrift für Geomorphologie, N.F., Supplement Band*, **51**, 39–50.

Hardenbicker, U. (1991). Verbreitung und Chronologie der Hangrutschungen im Bonner Raum. *Arbeiten zur Rheinischen Landeskunde*, **60**, 9–18.

Hardenbicker, U. (1993). Neue Ergebnisse der Hangrutschungsforschung im Bonner Raum (Südrand der Niederrheinischen Bucht). *Berliner Geographische Abhandlungen*, **78**, 155–174.

Hardenbicker, U. (1994). Hangrutschungen im Bonner Raum — Naturräumliche Einordnung und ihre anthropogenen Ursachen. *Arbeiten zur Rheinischen Landeskunde*, **64**. Ph.D. thesis, Department of Geography, University of Bonn.

Hattendorf, I. (1996). *Untersuchungen von Hangrutschungsgebieten mittels elektromagnetischer Induktion.* Master's thesis, Department of Geology, University of Bonn.

Hattendorf, I. (2001). *Generalized Boussinesq flow and progressive slope failure.* Ph.D. thesis, Department of Geology, University of Bonn.

Heidemann, T. (1996). *Geologische und bodenmechanische Untersuchungen an ausgewählten Hangrutschungen im Bonner Raum.* Master's thesis, Department of Geography, University of Bonn.

Hergarten, S. and Neugebauer, H., editors (1999a). *Process Modelling and Landform Evolution*, volume 78 of *Lecture Notes in Earth Sciences*. Springer–Verlag, Berlin Heidelberg New York.

Hergarten, S. and Neugebauer, H. (1999b). Self–organized criticality in landsliding processes. In S. Hergarten and H. Neugebauer, editors, *Process modelling and landform evolution*, volume 78 of *Lecture Notes in Earth Sciences*, pages 231–249. Springer–Verlag, Berlin Heidelberg New York.

Hergarten, S. and Neugebauer, H. J. (2000). Self–organized criticality in two–variable models. *Physical Review E*, **61**(3), 2382–2385.

Holler, S. (1998). *Bodentypenverbreitung in Beziehung zu gravitativen Prozessen im Bonner Raum.* Master's thesis, Department of Geography, University of Bonn.

Hovius, N., Stark, C. P., and Allen, P. A. (1997). Sediment flux from a mountain belt derived by landslide mapping. *Geology*, **25**(3), 231–234.

Hovius, N., Stark, C. P., Chu, H.-T., *et al.* (2000). Supply and removal of sediment in a landslide–dominated mountain belt: Central Range, Taiwan. *Journal of Geology*, **108**, 73–89.

Hutchinson, J. (1988). General report: Morphological and geotechnical parameters of landslides in relation to geology and hydrogeology. In *5th International Symposium on landslides*, volume 1, pages 3–35.

Ingenpaß, H. (2000). *Geotechnische Untersuchungen an einer Hangrutschung im Siebengebirge bei Bonn.* Master's thesis, Department of Geography, University of Bonn.

Jäger, B. (1991). Hangrutschungen im Flurbereinigungsgebiet Siebengebirge. In *Berichte der 8ten Nationalen Tagung für Ingenieurgeologie*, pages 128–135.

Jäger, S. (1997). Fallstudien zur Bewertung von Massenbewegungen als geomorphologische Naturgefahr. *Heidelberger Gepgraphische Arbeiten*, **108**.

Kaiser-Kühn (1988). Alter Friedhof in Ippendorf, Hangrutschung im April 1988, Baugrundgutachten. Technical report, Ingenieurgeologisches Büro Kaiser–Kühn.

Kanji, M. (1974). The relationship between drained friction angles and Atterberg limits of natural soils. *Geotechnique*, **24**, 671–674.

Kenney, C. (1984). Properties and behaviours of soils relevant to slope instability. In D. Brunsden and D. Prior, editors, *Slope Instability*, pages 27–65. John Wiley & Sons, Chichester.

King, L. (1953). Canons of landscpe evolution. *Geological Society of America Bulletin*, **64**, 721–752.

Kirkby, M., editor (1978). *Hillslope Hydrology*. John Wiley & Sons, Chichester.

Kirkby, M. (1987). General models of long–term slope evolution through mass movement. In M. Anderson and K. Richards, editors, *Slope stability*, pages 359–379. John Wiley & Sons, Chichester.

Kirkby, M. J. (1992). An erosion–limited hillslope evolution model. *Catena Supplement*, **23**, 157–187.

Klostermann, J. (1992). *Das Quartär der Niederrheinischen Bucht*. Geologisches Landesamt Nordrhein–Westfalen, Krefeld.

Konert, M. and Vandenberghe, J. (1997). Comparison of laser grain size analysis with pipette and sieve analysis: a solution for the underestimation of the clay fraction. *Sedimentology*, **44**(3), 523–536.

Kümpel, H.-J. (1996). In–situ Deformationsmessungen zur Bestimmung hydraulischer Bodenkennwerte. *Schriftenreihe des SFB 350*, **37**.

Kuntsche, K. (2000). *Geotechnik*. Fiedr. Vieweg & Sohn Verlagsgesellschaft mbH, Braunschweig/Wiesbaden.

Kutilek, M. and Nielsen, D. (1994). *Soil Hydrology*. Catena Verlag.

Lambe, T. and Whitman, V. (1979). *Soil mechanics, SI Version*. John Wiley & Sons, Chichester.

Lang, A., Moya, J., Corominas, J., *et al.* (1999). Classic and new dating methods for assessing the temporal occurrence of mass movements. *Geomorphology*, **30**(1–2), 33–52.

Lang, H.-J., Huder, J., and Amman, P. (1996). *Bodenmechanik und Grundbau*. Springer–Verlag, Berlin Heidelberg New York.

Lee, I., White, W., and Ingles, O. (1983). *Geotechnical Ingeneering*, pages 57–89. Pitman.

Lockhart, T. (2000). *PostgreSQL User's Guide*.

Lupini, J., Skinner, A., and Vaughan, P. (1981). The drained residual strength of cohesive soils. *Geotechnique*, **31**(2), 181–213.

May, T. (2001). *Systemanalytische Konzeptionen ind geomorphologische Untersuchungen zur Entwicklung des Melbtales bei Bonn*. Master's thesis, Department of Geography, University of Bonn.

Melhorn, W. and Flemal, R., editors (1981). *Theories of landform development*, volume 6 of *The Binghampton symposia in geomorphology: international series*, London. George Allen & Unwin. A Proceedings Volume of the Sixth Annual Geomorphology Symposia Series held at Binghampton, New York, September 26–27, 1975.

Merz, B. (1996). Modellierung des Niederschlag–Abfluss–Vorgangs in kleinen Einzugsgebieten unter Berücksichtigung der natürlichen Variabilität. *Mitteilungen des Instituts für Hydrologie und Wasserwirtschaft Universität Karlsruhe (TH)*, **56**.

Merz, B. and Bárdossy, A. (1998). Effects of spatial variability on the rainfall runoff process in a small loess catchment. *Journal of Hydrology*, **213**(4), 304–317.

Merz, B. and Plate, E. (1997). An analysis of the effects of spatial variability of soil and soil moisture on runoff. *Water Resources Research*, **33**(12), 2909–2922.

Mesri, G. and Cepeda-Diaz, A. (1986). Residual shear strength of clays and shales. *Geotechnique*, **36**(2), 269–274.

Meyer, W. and Stets, J. (1996). *Das Rheintal zwischen Bingen und Bonn*, volume 89 of *Sammlung Geologischer Führer*. Gebrüder Borntraeger, Stuttgart.

Meyer, W. and Stets, J. (1998). Junge Tektonik im Rheinischen Schiefergebirge und ihre Quantifizierung. *Zeitschrift der deutschen geologischen Gesellschaft*, **149**(3), 359–379.

Möller, R. (1999). *Untersuchungen zur räumlichen Bewertung von Naturgefahren durch Hangrutschungen im Nordwestlichen Rheinhessen*. Master's thesis, Department of Geography, University of Bonn.

Morgenstern, N. (1965). The analysis of the stability of general slip surfaces. *Geotechnique*, **15**(1), 79–93.

Mulder, H. (1991). *Assessment of landslide hazard*. Ph.D. thesis, Faculty of Geographical Sciences, University of Utrecht.

Mulder, H. and van Asch, T. (1987). Quantitative approaches in landslide hazard analysis. *Travaux de l'Institut de Geographie de Reims*, **69–72**, 43–53.

Mulder, H. F. H. M. and van Asch, T. W. J. (1988). On the nature and magnitude of variance of important geotechnical parameters. In C. Bonnard, editor, *Proceedings of the 5th International Symposium on Landslides*, pages 239–245, Rotterdam. Balkema.

Müller, L. (1987). Spezielle geologische und geotechnische Untersuchungen bei der Sanierung von Rutschungen im nördlichen Siebengebirge. *Mitteilungen zur Ingenieurgeologie und Hydrogeologie*, **27**.

Nienhaus, U. (1990). Geologische und hydrogeologische Verhältnisse im südlichen Siebengebirgsgraben und deren Bedeutung für die Grundwassernutzung und den Grundwasserschutz. *Mitteilungen zur Ingenieurgeologie und Hydrogeologie*, **38**, 206.

Ohmori, H. and Hirano, M. (1988). Magnitude, frequency and geomorphological significance of rocky mud flows, landcreep and the collapse of steep slopes. *Zeitschrift für Geomorphologie, N.F., Supplement Band*, **67**, 55–65.

Palmquist, R. and Bible, G. (1980). Conceptual modelling of landslide distribution in time and space. *Bulletin of the International Association of Engineering Geology*, **21**, 178–186.

Parkner, T. (2000). *Soil erosion modelling at Gut Frankenforst near Bonn between 1954 and today*. Master's thesis, Department of Geography, University of Bonn.

PCRASTER (1996). *PCRaster Manual*. PCRaster Environmental Software, The Netherlands.

Penck, W. (1924). *Die Morphologische Analyse*, volume 2 of *Geographische Abhandlungen*. J. Engelhorn, Stuttgart.

Pfister, C. (1992). Monthly temperature and precipitation in central Europe 1525-1979: quantifying documentary evidence on weather and its effects. In R. Bradley and P. Jones, editors, *Climate Since A.D. 1500*, pages 118–142. Routledge, London.

Pfister, C. and Lauterburg, A. (1992). Spatial variability of cliamtic change in Europe 1780-1960. In B. Frenzel, C. , and B. Gläser, editors, *European climate reconstructed from documentary data: methods and results*, volume 7 of *Palaeoclimate Research*, pages 177–192. Gustav Fischer, Stuttgart, Jena, Lübeck, Ulm.

Phillips, C. and Watson, A. (1994). Structural tree root research in New Zealand: A review. *Landcare Research science series*, **7**.

Phillips, J. D. (1999). *Earth surface systems*. Blackwell, Oxford.

Preston, N. (1996). *Spatial and temporal changes in terrain resistance to shallow translational regolith landsliding*. Master's thesis, School of Earth Sciences, Victoria University of Wellington.

Preston, N. (1999). Event–induced changes in landsurface condition — implications for subsequent slope stability. *Zeitschrift für Geomorphologie, N.F., Supplement Band*, **115**, 157–173.

Preston, N. (2001). *Geomorphic response to environmental change: the imprint of deforestation and agricultural land use on the contemporary landscape of the Pleiser Hügelland, Bonn, Germany*. Ph.D. thesis, Department of Geography, University of Bonn.

Preston, N., Schmidt, J., Dikau, R., *et al.* (rev). Modelling sediment fluxes at large spatial and temporal scales. In A. Lang, editor, *Modelling concepts for the Rhine–LUCIFS research framework*, Lecture notes in Earth sciences. Springer–Verlag. (in review).

Prinz, H. (1991). *Abriß der Ingenieurgeologie*. Enke, Stuttgart.

Rasemann, S. (1999). *Geomorphometrische Charakterisierung von Hängen durch Profilanalyse*. Master's thesis, Department of Geography, University of Bonn.

Richards, K. (1999). The magnitude–frequency concept in fluvial geomorphology: a component of a degenerating research programme? *Zeitschrift für Geomorphologie, N.F., Supplement Band*, **115**, 1–18.

Richwien, W. and Golücke, K. (1997). *Bodenmechanisches Praktikum*. Verlag Glückauf, Essen.

Roering, J. J., Kirchner, J. W., and Dietrich, W. E. (1999). Evidence for nonlinear, diffusive sediment transport on hillslopes and implications for landscape morphology. *Water Resources Research*, **35**(3), 853–870.

Roering, J. J., Kirchner, J. W., Sklar, L. S., *et al.* (2001). Hillslope evolution by nonlinear creep and landsliding: an experimental study. *Geology*, **29**(2), 143–146.

Rogozia, J. (2000). *Zweidimensionale, regionale Hangstabilitätsmodellierung der Dollendorfer Hardt bei Bonn.* Master's thesis, Department of Geography, University of Bonn.

Schegiewal, A. (1972). *Geologische und bodenkundliche Untersuchungen am Nordabfall des Siebengebierges bei Römlinghoven.* Master's thesis, Department of Geology, University of Bonn.

Schegiewal, A. (1976). *Die Böden am Nordabfall des Siebengebirges und deren physikalischen und chemischen Eigenschaften in Abhängigkeit vom Ausgangsgestein.* Ph.D. thesis, Department of Soil Sciences, University of Bonn.

Scheller, E. (1996). Geophysikalische Methoden. In B. Oddsson, editor, *Instabile Hänge und andere risikorelevante natürliche Prozesse*, pages 119–132. Birkhäuser, Basel Boston Berin.

Schmanke, V. (1999). Untersuchungen zur Hanggefährdung im Bonner Raum — Eine Bewertung mit Hilfe unterschiedlicher Modellansätze. *Mainzer Geographische Studien*, **44**. Ph.D. thesis, Department of Geography, University of Bonn.

Schmidt, J. (1996). *Untersuchungen zum Einfluß geomorphologischer Variabilität und Struktur auf den Niederschlag–Abfluß–Prozeß in kleinskaligen Einzugsgebieten.* Master's thesis, Department of Geography, University of Heidelberg.

Schmidt, J. and Dikau, R. (1999). Extracting geomorphometric attributes and objects from digital elevation models — Semantics, methods, future needs. In R. Dikau and H. Saurer, editors, *GIS for Earth Surface Systems — Analysis and Modelling of the Natural Environment*, pages 153–173. Schweizbart'sche Verlagsbuchhandlung, Berlin Stuttgart.

Schmidt, J. and Gärtner, H. (2000). Investigations of geomorphometric significance in hydrologic processes using Geo–Information–Technologies — results and implications for GIS needs in geomorphology. *Schriftenreihe des SFB 350*, **83**.

Schmidt, J., Merz, B., and Dikau, R. (1998). Morphological structure and hydrological process modelling. *Zeitschrift für Geomorphologie, N.F., Supplement Band*, **112**, 55–66.

Schmidt, J., Hennrich, K., and Dikau, R. (2000). Scales and similarities in runoff processes with respect to geomorphometry. *Hydrologic Processes*, **14**(11-12), 1963–1979.

Schrödter, H. (1985). *Verdunstung.* Springer–Verlag, Berlin Heidelberg New York.

Schüle, H. and Pfister, C. (1992). EURO–CLIMHIST — outlines of a multi proxy data base for investigating the climate of Europe over the last centuries. In B. Frenzel, C. , and B. Gläser, editors, *European climate reconstructed from documentary data: methods and results*, volume 7 of *Palaeoclimate Research*, pages 211–219. Gustav Fischer, Stuttgart, Jena, Lübeck, Ulm.

Schumm, S. (1979). Geomorphic thresholds: the concept and its application. *Transactions, Institute of British Geographers, New Series*, **4**, 485–515.

Schumm, S. and Lichty, R. (1965). Time, space and causality in geomorphology. *American Journal of Science*, **263**, 110–119.

Selby, M. (1993). *Hillslope Materials and Processes.* Oxford University Press.

Siegburg, W. (1987). Großmaßstäbige Hangneigungs– und Hangformenanalyse mittels statistischer Verfahren. Dargestellt am Beispiel der Dollendorfer Hardt (Siebengebirge). *Bonner Geographische Abhandlungen*, **75**.

Siehl, A. (1993). Interaktive geometrische Modellierung geologischer Flächen und Körper. *Die Geowissenschaften*, **11**(10–11), 342–346.

Skempton, A. (1964). Long–term stability of clay slopes. *Geotechnique*, **14**, 77–101.

Skempton, A. (1985). Residual strength of clays in landslides, folded strata and the laboratory. *Geotechnique*, **35**(1), 1–18.

Slaymaker, O. (1992). Ahnert's process–response models of denudation and the scale dependence of sediment yield models — an attempted reconcilation. *Catena Supplement*, **23**, 125–134.

Starkel, L. (1999). Space and time scales in geomorphology. *Zeitschrift für Geomorphologie, N.F., Supplement Band*, **115**, 19–33.

Sutton, B. (1993). *Solving problems in soil mechanics*. Longman.

Terlien, M., de Louw, P., van Asch, T., *et al.* (1996). The assessment and modelling of hydrologic failure conditions of landslides in the Puriscal region (Costa Rica) and the Manizales region (Colombia). In *Advances in Hillslope Processes*, volume 2, pages 837–855. John Wiley & Sons, Chichester.

Terzaghi, K. (1950). Mechanisms of landslides. *Engineering Geology (Berkey) Volume*, pages 83–123.

Thompson, W. I., Ruddiman, W. F., Steet-Perrott, F., *et al.* (1993). Climatic changes during the past 18000 years: regional synthesis, mechanims, and causes. In H. Wright, Jr., J. E. Kutzbach, W. F. Ruddiman, *et al.*, editors, *Global climates since the last glacial maximum*, pages 514–535. University of Minnesota Press.

van Asch, T., van Westen, C., Blijenberg, H., *et al.* (1992). Quantitative landslide hazard analysis in volcanic ashes of the Chinchina area, Colombia. In *Proceedings of the Primer Simposio Internacional sobre sensores reomtes y sistemas de informacion geografica para el estudio de riesgos naturales*, pages 433–443. Bogota, Colombia.

van Beek, L. and van Asch, T. (1999). A combined conceptual model for the effects of fissure–induced infiltration on slope stability. In S. Hergarten and H. Neugebauer, editors, *Process modelling and landform evolution*, volume 78 of *Lecture Notes in Earth Sciences*, pages 147–167. Springer–Verlag, Berlin Heidelberg New York.

van Beurden, S. (1997). Hydrology, soil mechanics and kinematics of slow mass movements in the Widenbach catchment, Switzerland. *Netherlands Geographical Studies*, **225**.

van Westen, C., Rengers, N., Terlien, M., *et al.* (1997). Prediction of the occurence of slope instability phenomena through GIS–absed hazard zonation. *Geologische Rundschau*, **86**, 404–414.

Varnes, D. (1978). Slope Movement. Types and Processes. In R. Schuster and R. Krizek, editors, *Landslides. Analysis and Control*, volume 176 of *Special Report*, pages 11–33. National Academy of Sciences.

Vickers, B. (1978). *Laboratory work in civil Engineering — Soil mechanics*, pages 58–110. Granada.

Voight, B. (1973). Correlation between Atterberg plasticity limits and residual shear strength of natural soils. *Geotechnique*, **23**, 265–267.

Wall, L. and Schwartz, R. (1991). *Programming Perl*. O'Reilly, Sebastopol (CA).

Weber, M. (1991). Welchen Beitrag kann die Luftbildinterpretation zur Erfassung und Datierung von Hangrutschungen leisten – Erste Ergebnisse aus dem Bonner Raum. *Arbeiten zur Rheinischen Landeskunde*, **60**, 19–30.

Weischet, W. (1991). *Einführung in die Klimatologie*. Teubner.

Werner, B. (1999). Complexity in natural landform patterns. *Science*, **284**, 102–104.

Wesseling, C., Karssenberg, D., Burrough, P., *et al.* (1996). Integrating dynamic environmental models in GIS: the development of a dynamic Modelling language. *Transactions in GIS*, **1**(1), 40–48.

Whyte, I. (1982). Soil plasticity and strength — a new approach using extrusion. *Ground Engineering*, **15**(1), 16–24.

Willgoose, G., Bras, R. L., and Rodriguez-Iturbe, I. (1991). Results from a new model of river basin evolution. *Earth Surface Processes and Landforms*, **16**, 237–254.

Yamada, S. (1999). The role of soil creep and slope failure in the landscape evolution of a head water basin: field measurements in a zero order basin of northern Japan. *Geomorphology*, **28**(3–4), 329–344.

Zhang, X., Drake, N. A., and Wainwright, J. (pres). Scaling Issues in Environmental Modelling. In J. Wainwright and M. Mulligan, editors, *Environmental Modelling: Finding Simplicity in Complexity*, pages 33–46. John Wiley & Sons, Chichester. (in press).

The role of mass movements for slope evolution

conceptual approaches and model applications in the Bonn area

Jochen Schmidt

— Appendix —

Bonn 2001

Appendix

A. Introductory Notes

This Appendix includes results of the lab and field data (Appendix B.1, B, C), references for the used techniques (Appendix F), and information about some specific data processing steps (Appendix F.2).

The lists and data displayed in the following chapters represent an overview of the of results of field and lab analyses, and should be useful to follow some of the interpretations of this thesis. Complete information can be queried from the database (Chapter 9), e.g. for a list of meta information on laboratory experiments the following SQL–code can be used.

```
SELECT l.id, e.name AS experiment, p.name AS project, l.date, l.persons, l.sample_id
FROM lab l,experiment e,project p
WHERE l.exp_id=e.id AND l.proj_id=p.id
ORDER BY e.name,p.name;
```

SQL–code similar to the following example can be used querying a specific lab result.

Listing: Query example for all determinations of moisture content from outcrop *dobo180400.1*, ordered by depth

```
SELECT l.lab_id,l.persons,l.date,
g.contno, g.tara,g.wet, g.dry, (wet−dry)/(dry−tara) AS watercont
FROM gravwatcont g, lab l, soilsample s
WHERE g.lab_id=l.id AND l.sample_id=s.id
AND s.sample_id like 'dobo180400.1%'
ORDER BY s.upperdepth;
```

For the technical interested reader, the SQL–codes which were used to produce the lists, are mostly included at the beginning of the lists and can be compared with the database structure described in Chapter 9.

The lists presented in Appendix F are also created automatically from the XML–database (Chapter 9) using extensible stylesheet language (XSL). For lack of space the rather longish XSL–scripts could not be provided.

Note. *Gauss–Krüger coordinates are used in the lists for georefenrence.*

B. Selected field data

B.1. Drilling results

Listing: SQL–code for querying drillings from database. (Shallow drillings (¡2m) are exluded)

```
SELECT f.field_id AS ID, f.date AS date, po.point AS coordinate, po.height AS "h_[m]", lowerdepth AS "d_[m]",
       l2.name AS location, p.name AS project
FROM field f, experiment e, location lo, location l2, points po, soilsample s, project p
WHERE f.exp_id=e.id AND f.georef_id=lo.id AND f.georef_id=po.loc_id AND lo.oloc_id=l2.id AND f.id=s.field_id
      AND (s.sampletype='Bohrkern' OR s.sampletype='Profil') AND (f.exp_id=26 OR f.exp_id=22
      OR f.exp_id=2 OR f.exp_id=4) AND f.proj_id=p.id
ORDER BY location,f.date,f.field_id;
```

Selected Drilling & outcrop results from database. Shallow drillings (¡2m) are exluded.
(h: height above sea level in m; d: depth of drilling in m)

id	date	coordinate	h [m]	d [m]	location	project
dobo190398.2	1998-03-19	(2584860,5618990)	141	4.5	Dollendorfer Hardt	subproject B13, SFB350
dobo110898.1	1998-08-11	(2584792,5619125)	181	8	Dollendorfer Hardt	subproject B13, SFB350
dobo110898.2	1998-08-11	(2584806,5619104)	175	4	Dollendorfer Hardt	subproject B13, SFB350
dobo130898.1	1998-08-13	(2584811,5619112)	177	6	Dollendorfer Hardt	subproject B13, SFB350
dobo200898.1	1998-08-20	(2584831,5619090)	169	7	Dollendorfer Hardt	subproject B13, SFB350
dobo250898.1	1998-08-25	(2584845,5619057)	158	7	Dollendorfer Hardt	subproject B13, SFB350
haldedolP1		(2584084,5619977)	105	6.8	Dollendorfer Hardt	consultancy report, landfill Dollendorfer Hardt
haldedolP2		(2584138,5619905)	118	6	Dollendorfer Hardt	consultancy report, landfill Dollendorfer Hardt
haldedolb1		(2584246,5619708)	141	1.5	Dollendorfer Hardt	consultancy report, landfill Dollendorfer Hardt
haldedolb1a		(2584247,5619692)	141	4	Dollendorfer Hardt	consultancy report, landfill Dollendorfer Hardt
haldedolb2		(2584235,5619749)	137	8	Dollendorfer Hardt	consultancy report, landfill Dollendorfer Hardt
haldedolb3		(2584202,5619780)	130	4	Dollendorfer Hardt	consultancy report, landfill Dollendorfer Hardt
haldedolb4		(2584151,5619835)	126	6	Dollendorfer Hardt	consultancy report, landfill Dollendorfer Hardt
haldedolb5		(2584130,5619892)	120	2.75	Dollendorfer Hardt	consultancy report, landfill Dollendorfer Hardt
haldedolb5a		(2584135,5619892)	120	4	Dollendorfer Hardt	consultancy report, landfill Dollendorfer Hardt
haldedolb6		(2584124,5619918)	111	4	Dollendorfer Hardt	consultancy report, landfill Dollendorfer Hardt
haldedolb7		(2584092,5619967)	107	2	Dollendorfer Hardt	consultancy report, landfill Dollendorfer Hardt
haldedolb8		(2584122,5619953)	106	3	Dollendorfer Hardt	consultancy report, landfill Dollendorfer Hardt
mebo010999.1	1999-09-01	(2576752,5619800)	122	8	Melbtal	masters thesis T. May
mebo060999.1	1999-09-06	(2576707,5619715)	125	9	Melbtal	masters thesis T. May
mebo070999.1	1999-09-07	(2576653,5619632)	129	8	Melbtal	masters thesis T. May
mebo051099.1	1999-10-05	(2576682,5619571)	123	7	Melbtal	field seminar (SS 1999)
mebo061099.1	1999-10-06	(2576770,5619644)	126	9	Melbtal	field seminar (SS 1999)
mebo071099.1	1999-10-07	(2576830,5620000)	107	7	Melbtal	field seminar (SS 1999)
mebo161299.1	1999-12-16	(2576938,5620023)	108	6	Melbtal	masters thesis T. May

continued on next page

continued from previous page

id	date	coordinate	h [m]	d [m]	location	project
mebo160600.1	2000-06-16	(2576876,5619830)	114	10	Melbtal	subproject B13, SFB350
mebo010800.1	2000-08-01	(2576840,5619822)	116	8	Melbtal	masters thesis T. May
mebo010800.2	2000-08-01	(2576832,5619794)	113	6	Melbtal	masters thesis T. May
mebo170800.1	2000-08-17	(2576770,5619670)	117	7	Melbtal	masters thesis T. May
mebo170800.2	2000-08-17	(2576810,5619700)	123	9	Melbtal	masters thesis T. May
heideme1b01	1995-03-10	(2576806,5619843)	106	6	landslide me1	masters thesis T. Heidemann
heideme1b02	1995-03-10	(2576792,5619848)	110	8	landslide me1	masters thesis T. Heidemann
heideme1b03	1995-03-10	(2576780,5619851)	111	7	landslide me1	masters thesis T. Heidemann
heideme1b04	1995-03-24	(2576769,5619855)	112	9	landslide me1	masters thesis T. Heidemann
heideme1b05	1995-03-24	(2576754,5619861)	116.5	8.7	landslide me1	masters thesis T. Heidemann
heideme5b02	1995-05-10	(2576684,5619571)	117.6	8.9	landslide me5	masters thesis T. Heidemann
heideme5b03	1995-05-10	(2576676,5619575)	121	10	landslide me5	masters thesis T. Heidemann
heideme5b04	1995-05-17	(2576672,5619579)	121	8	landslide me5	masters thesis T. Heidemann
heideme5b05	1995-05-18	(2576660,5619583)	123	7.9	landslide me5	masters thesis T. Heidemann
heideme5b06	1995-05-19	(2576649,5619588)	127	7	landslide me5	masters thesis T. Heidemann
heideme5b07	1995-05-22	(2576644,5619591)	128.6	9	landslide me5	masters thesis T. Heidemann
heideme5b08	1995-05-22	(2576634,5619596)	131	9	landslide me5	masters thesis T. Heidemann
heideme5b11	1995-06-06	(2576702,5619600)	115	8	landslide me5	masters thesis T. Heidemann
heideme5b12	1995-06-07	(2576683,5619596)	118	8	landslide me5	masters thesis T. Heidemann
heideme5b13	1995-06-07	(2576666,5619602)	125	6.9	landslide me5	masters thesis T. Heidemann
heideme5b14	1995-06-13	(2576649,5619609)	129.5	8.9	landslide me5	masters thesis T. Heidemann
heideme5b15	1995-06-13	(2576640,5619613)	132	9	landslide me5	masters thesis T. Heidemann
heideme5b16	1995-06-13	(2576672,5619645)	128	9	landslide me5	masters thesis T. Heidemann
heideme5b01	1995-07-05	(2576703,5619566)	118.6	7.5	landslide me5	masters thesis T. Heidemann
heideme5b09	1995-07-05	(2576619,5619603)	135.5	8	landslide me5	masters thesis T. Heidemann
heideme5b10	1995-07-05	(2576609,5619608)	140	5	landslide me5	masters thesis T. Heidemann
dobo190398.1	1998-03-19	(2584903,5618998)	132	4	landslide si7	subproject B13, SFB350
dobo050698.1	1998-06-05	(2584784,5619142)	186	3	landslide si7	subproject B13, SFB350
dobo050698.2	1998-06-05	(2584789,5619130)	183	4	landslide si7	subproject B13, SFB350
dobo180698.1	1998-06-18	(2584901,5618879)	110	7	landslide si7	subproject B13, SFB350
dobo190698.1	1998-06-19	(2584888,5618876)	109	3	landslide si7	subproject B13, SFB350
dobo230698.1	1998-06-23	(2584888,5618878)	110	7	landslide si7	subproject B13, SFB350
dobo120898.1	1998-08-12	(2584853,5619107)	164	5	landslide si7	subproject B13, SFB350
dobo270898.1	1998-08-27	(2584811,5619142)	174	6	landslide si7	subproject B13, SFB350
dobo270898.2	1998-08-27	(2584825,5619136)	173	8	landslide si7	subproject B13, SFB350
dobo030998.1	1998-09-03	(2584910,5618880)	109	7	landslide si7	subproject B13, SFB350
dobo040998.1	1998-09-04	(2584837,5619130)	170	5	landslide si7	subproject B13, SFB350
dobo110998.1	1998-09-11	(2584818,5619148)	176	10	landslide si7	subproject B13, SFB350
dobo201098.1	1998-10-20	(2584850,5619115)	163	5	landslide si7	subproject B13, SFB350
dobo201098.2	1998-10-20	(2584872,5619101)	158	4	landslide si7	subproject B13, SFB350
dobo221098.1	1998-10-22	(2584910,5618982)	128	6	landslide si7	subproject B13, SFB350
dobo050400.1	2000-04-05	(2584911,5618975)	127	4	landslide si7	subproject C1, SFB350
dobo180400.1	2000-04-18	(2584905,5618993)	131	5	landslide si7	subproject C1, SFB350
dobo190400.1	2000-04-19	(2584911,5618982)	128	5.8	landslide si7	subproject C1, SFB350

B.1.1. Drilling results, field site Dollendorfer Hardt

The following graphs display generalised borehole logs, lab results from samples taken from the drilling cores and the lithological interpretations of the borehole logs.

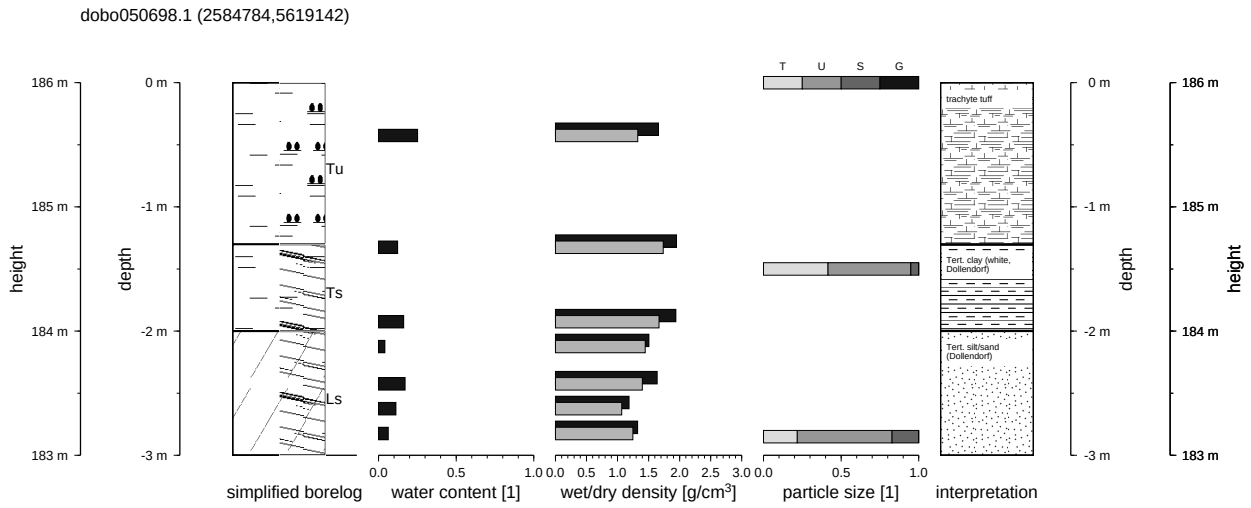

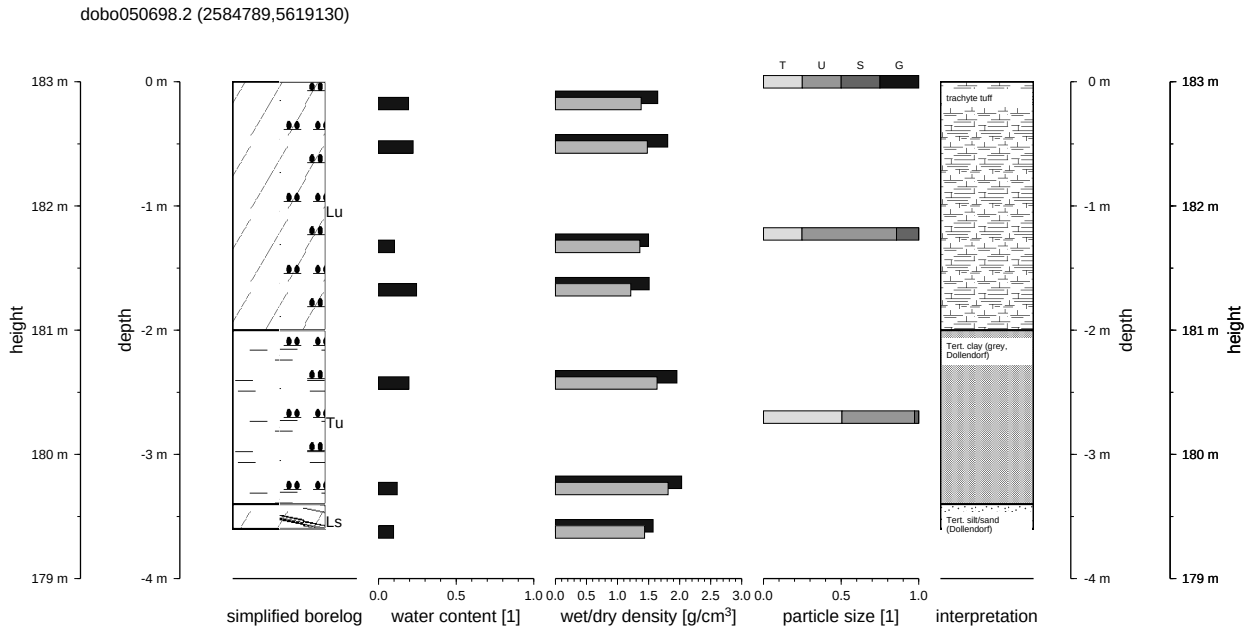

dobo110898.1 (2584792,5619125)

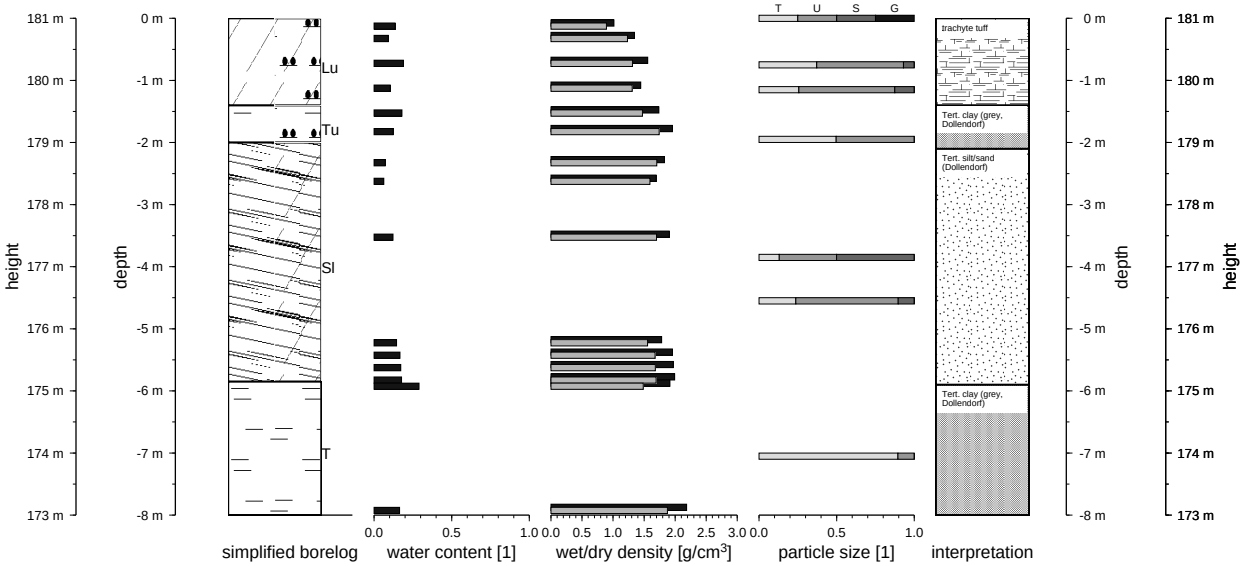

dobo110898.2 (2584806,5619104)

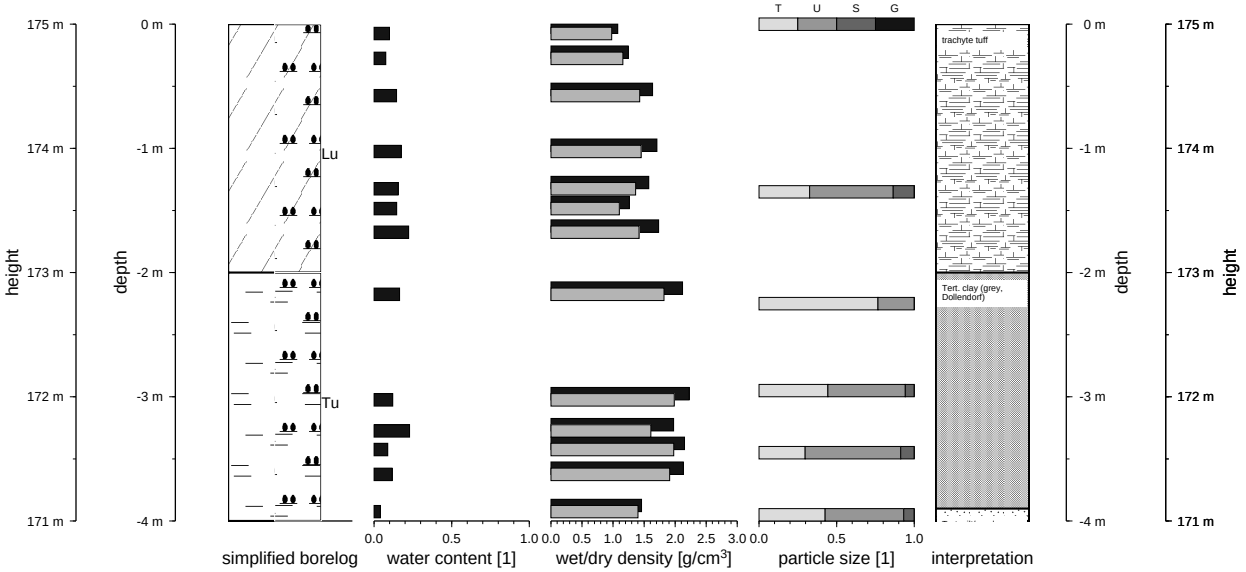

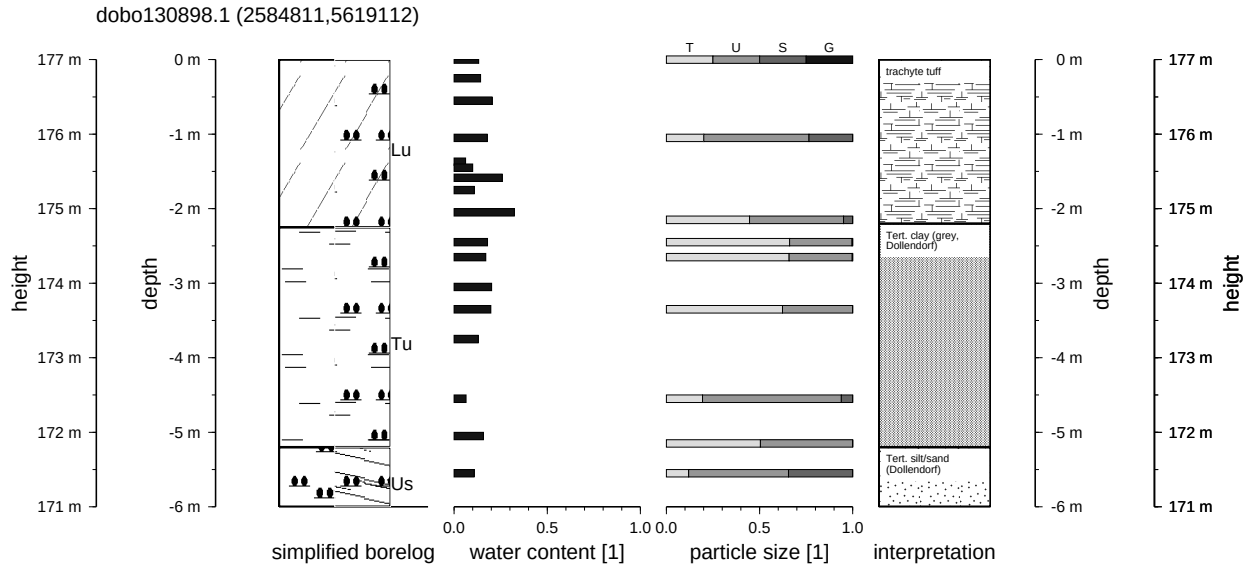
dobo130898.1 (2584811,5619112)
height
depth
Lu
Tu
Us
T U S G
trachyte tuff
Tert. clay (grey, Dollendorf)
Tert. silt/sand (Dollendorf)
0.0 0.5 1.0
simplified borelog
water content [1]
particle size [1]
interpretation

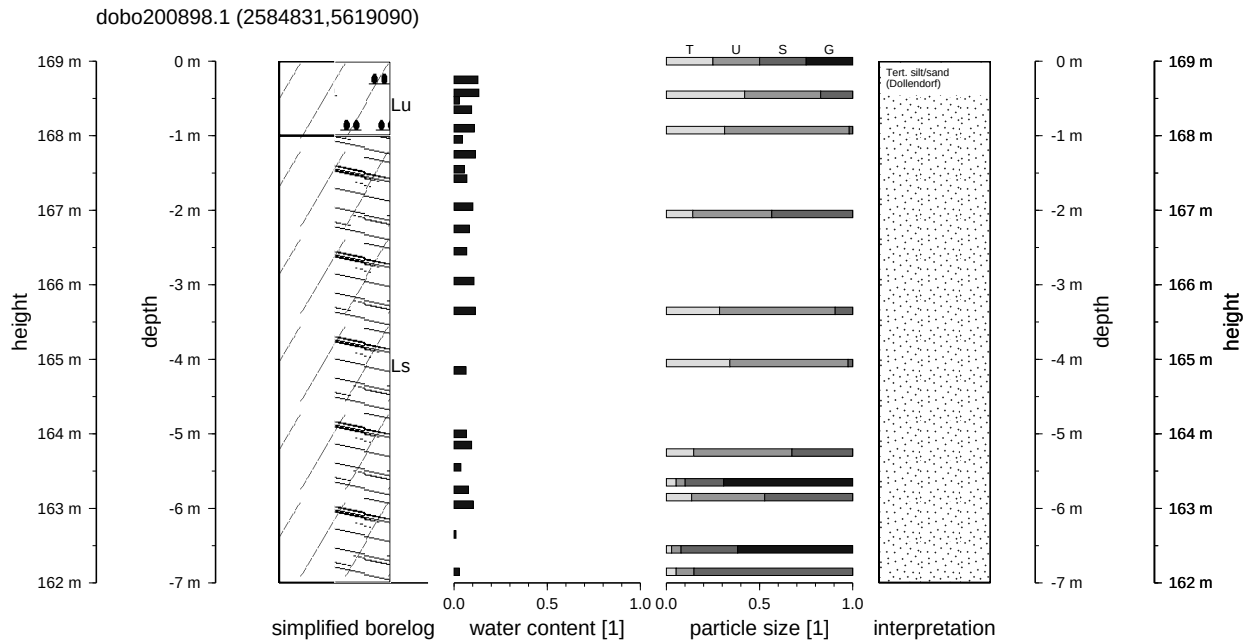
dobo200898.1 (2584831,5619090)
height
depth
Lu
Ls
T U S G
Tert. silt/sand (Dollendorf)
0.0 0.5 1.0
simplified borelog
water content [1]
particle size [1]
interpretation

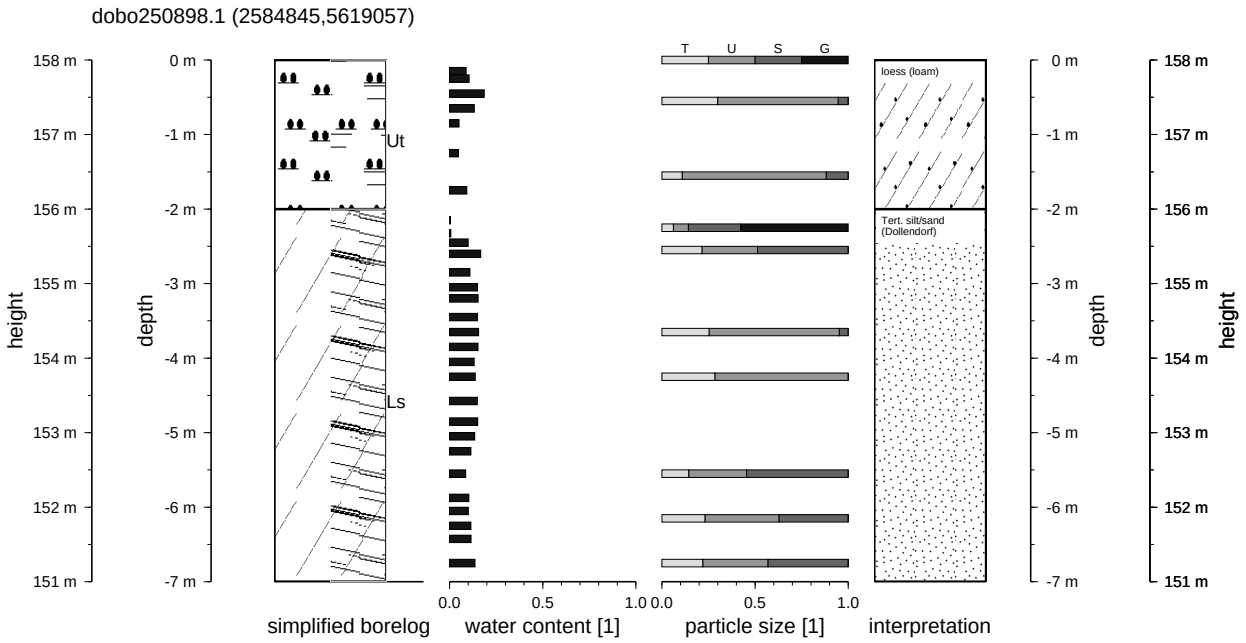
dobo250898.1 (2584845,5619057)
height
depth
Ut
Ls
T U S G
loess (loam)
Tert. silt/sand (Dollendorf)
simplified borelog
water content [1]
particle size [1]
interpretation

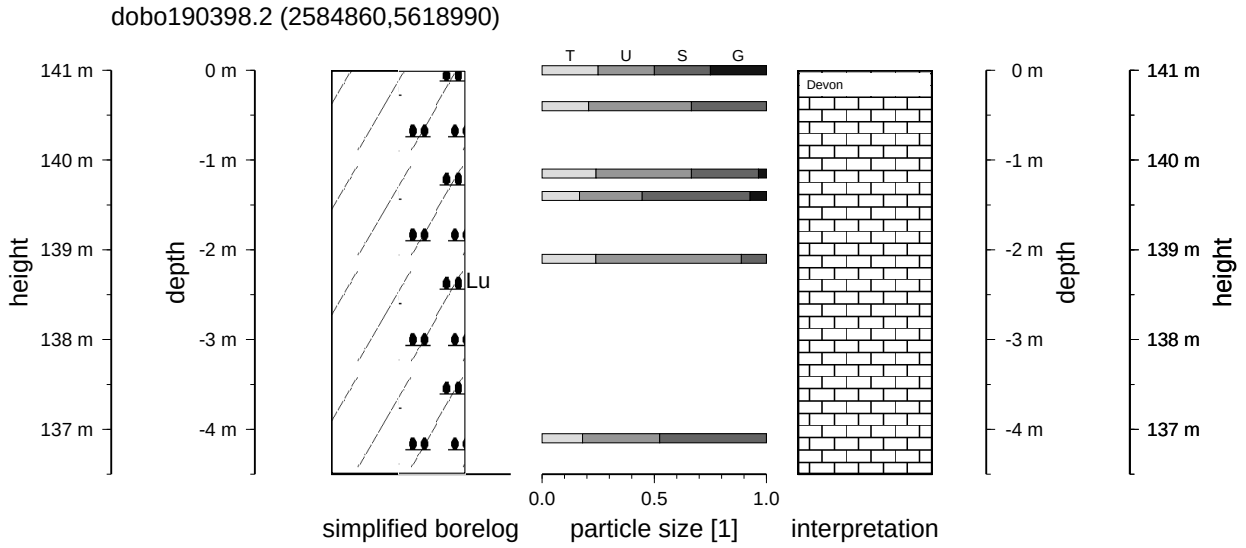
dobo190398.2 (2584860,5618990)
height
depth
Lu
T U S G
Devon
simplified borelog
particle size [1]
interpretation

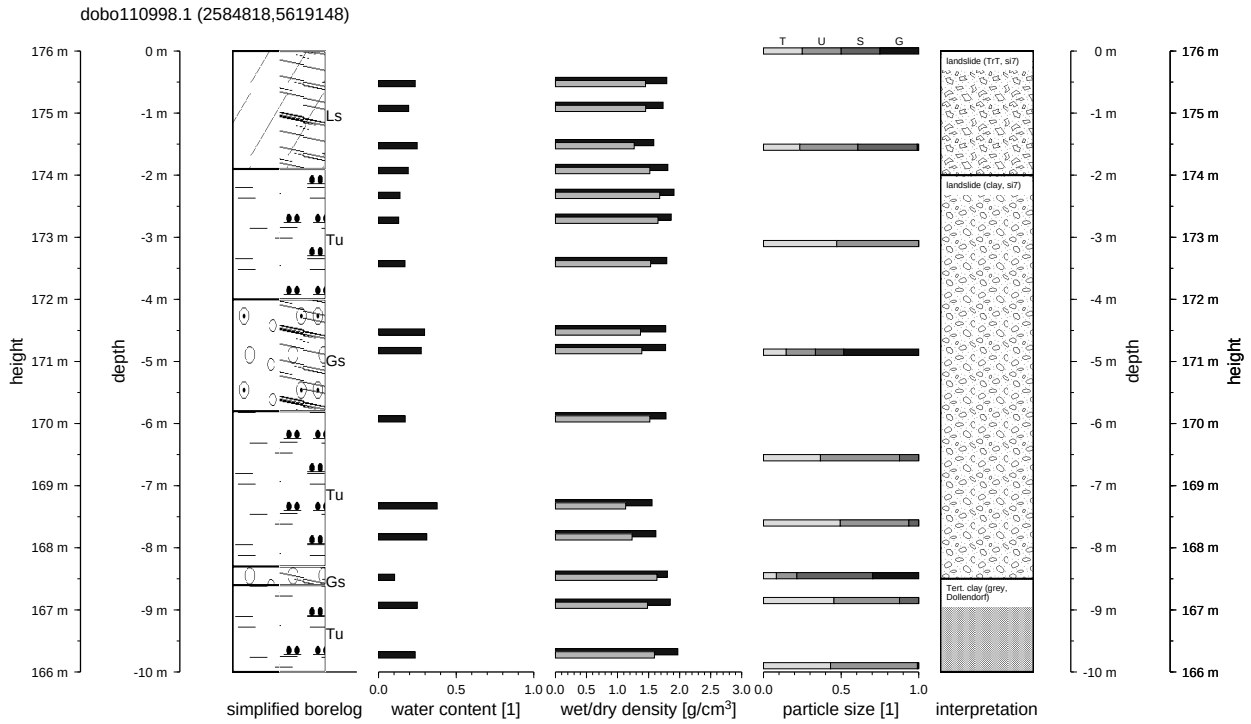
dobo110998.1 (2584818,5619148)
height
depth
Ls
Tu
Gs
Tu
Gs
Tu
T U S G
landslide (TrT, si7)
landslide (clay, si7)
Tert. clay (grey, Dollendorf)
simplified borelog
water content [1]
wet/dry density [g/cm³]
particle size [1]
interpretation

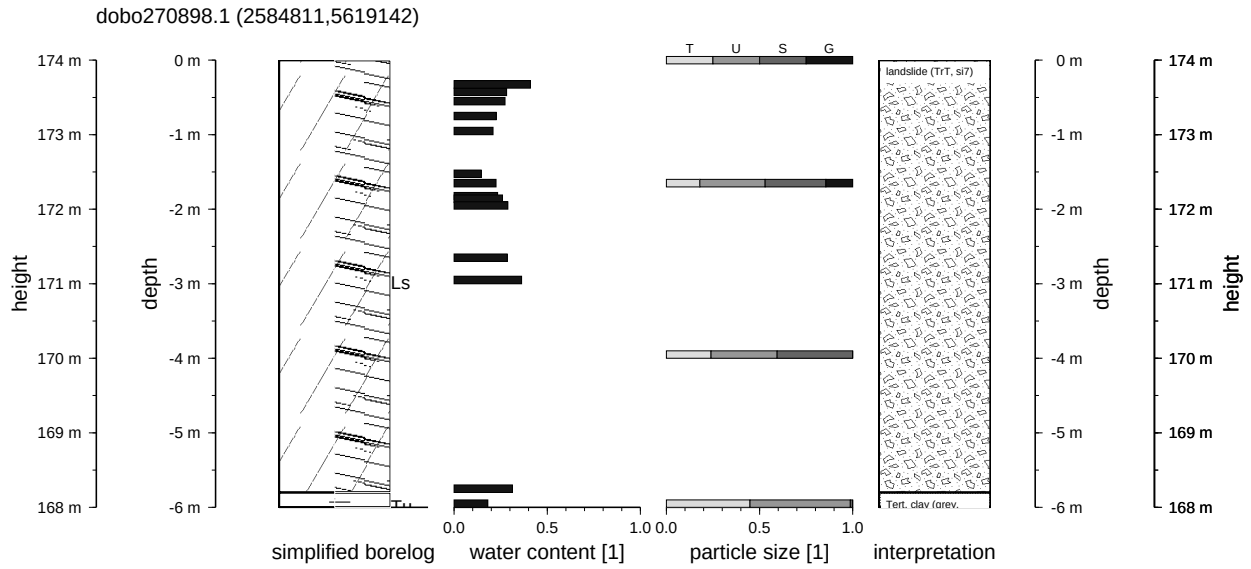
dobo270898.1 (2584811,5619142)
height
depth
Ls
T U S G
landslide (TrT, si7)
Tert. clay (grey,
simplified borelog
water content [1]
particle size [1]
interpretation

dobo270898.2 (2584825,5619136)

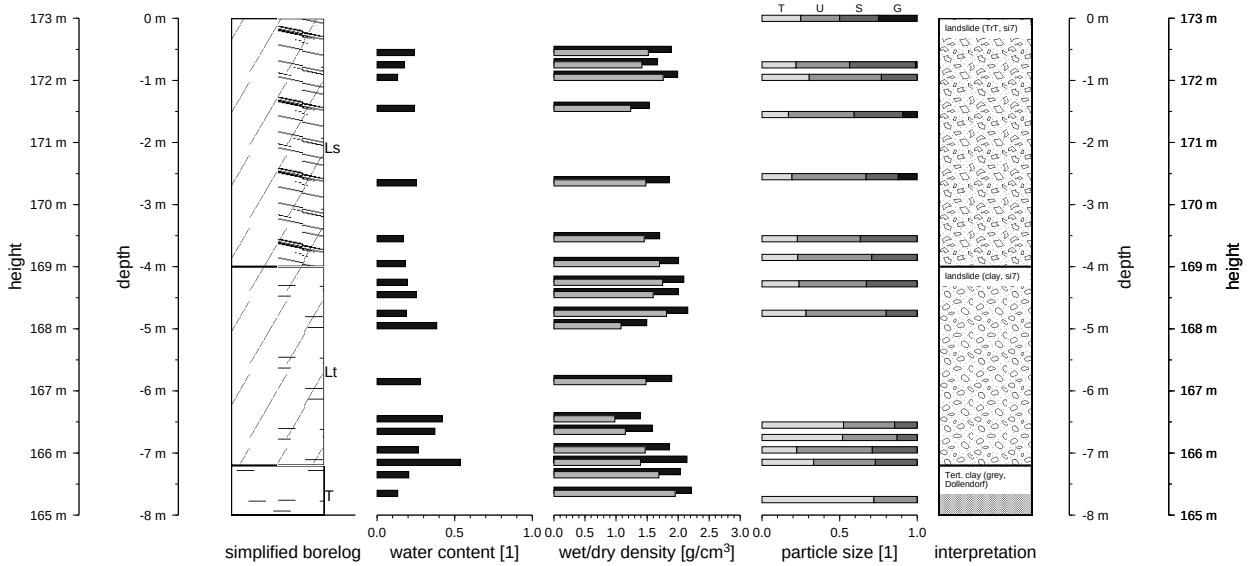

dobo040998.1 (2584837,5619130)

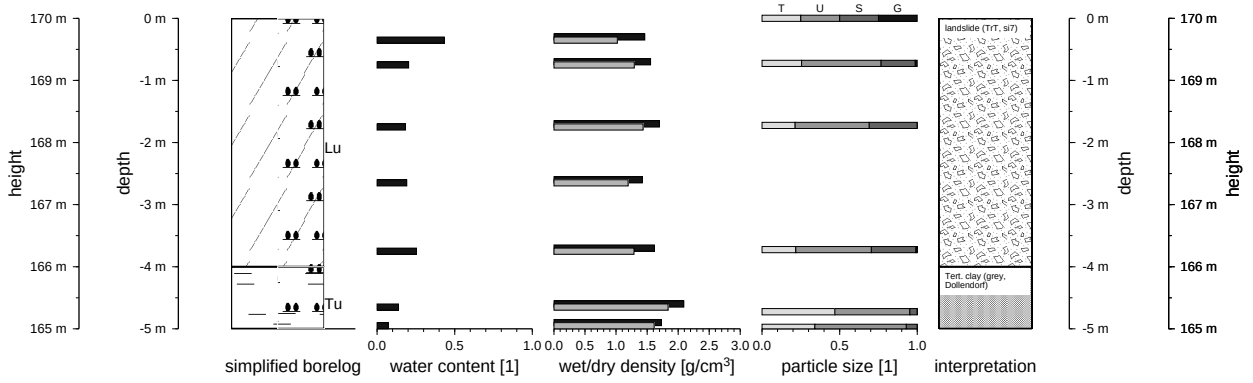

dobo201098.1 (2584850,5619115)

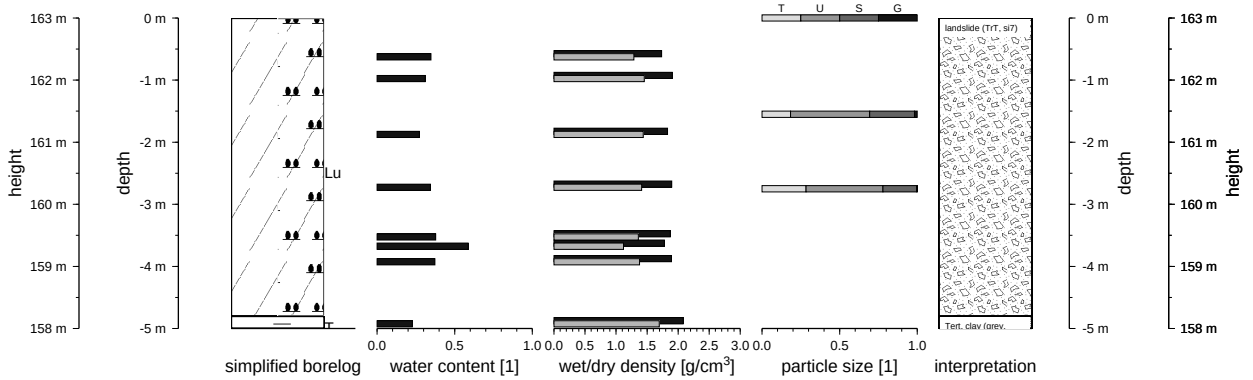

dobo120898.1 (2584853,5619107)

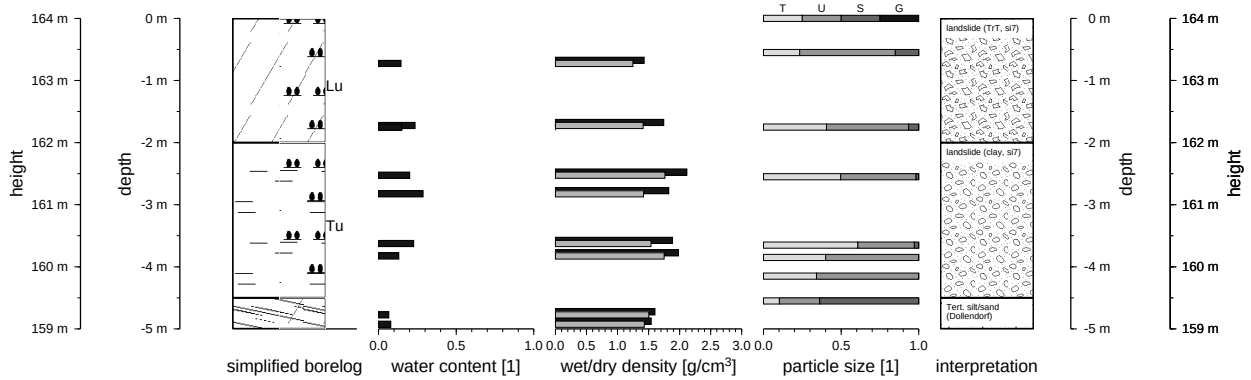

dobo201098.2 (2584872,5619101)

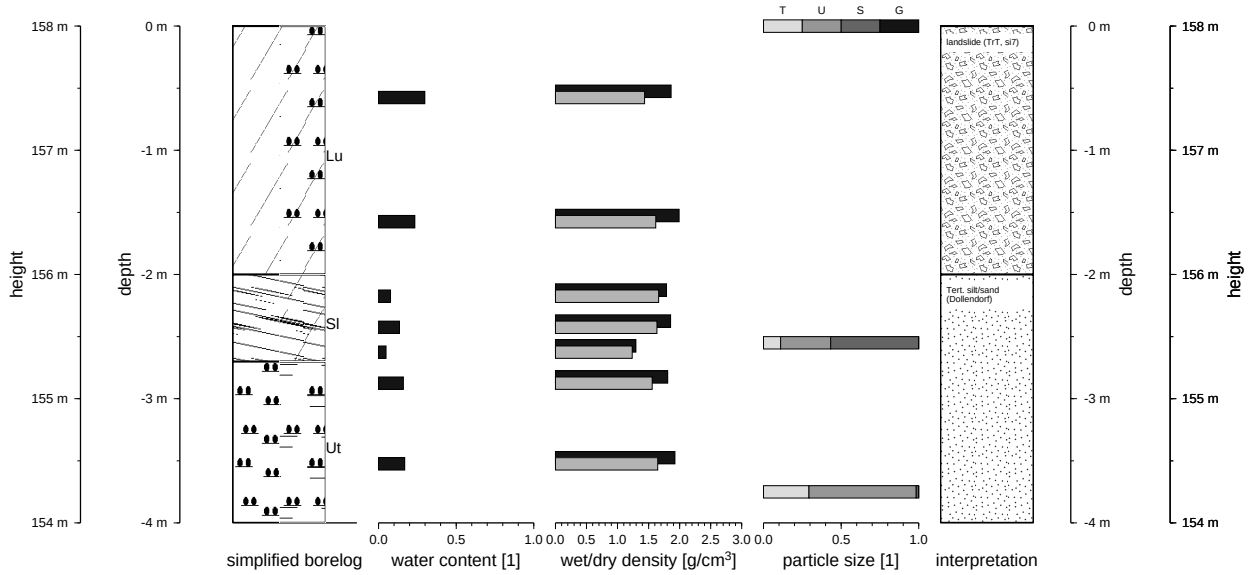

dobo190398.1 (2584903,5618998)

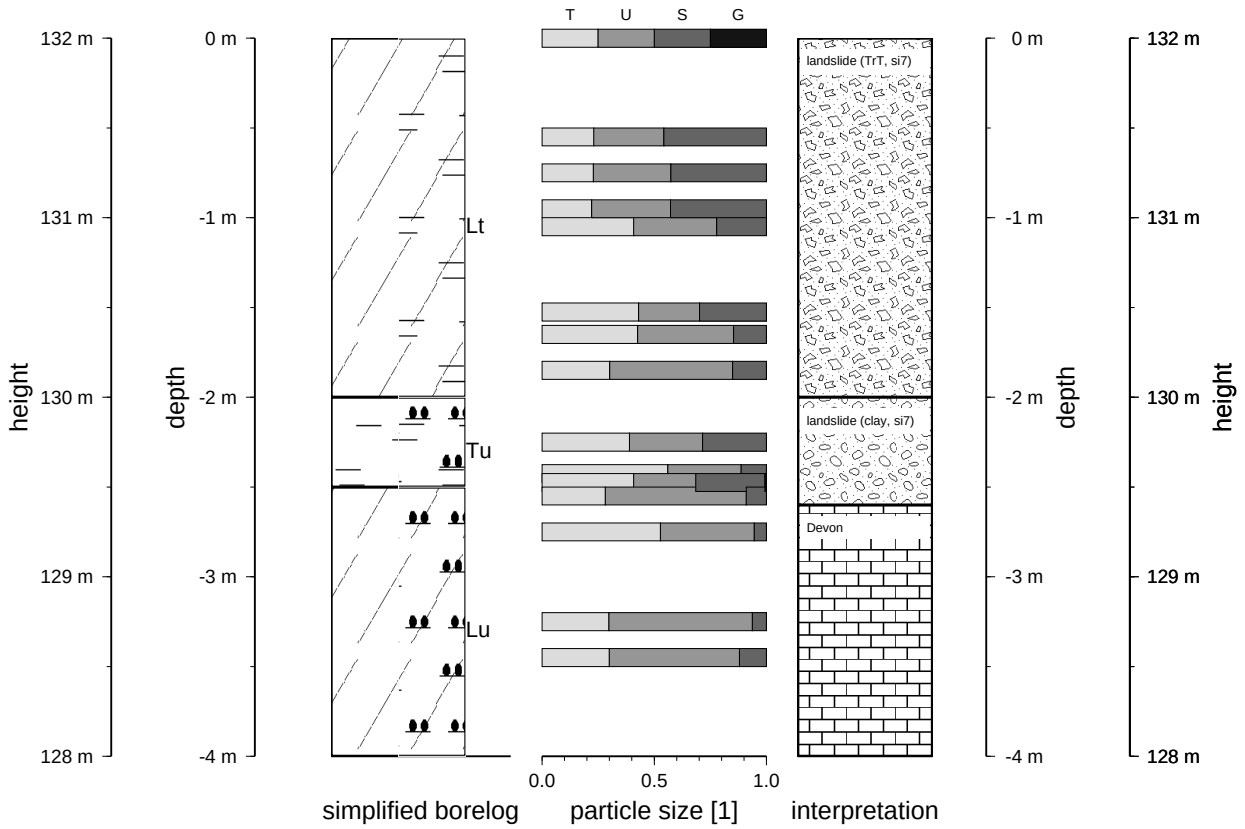

dobo180400.1 (2584905,5618993)

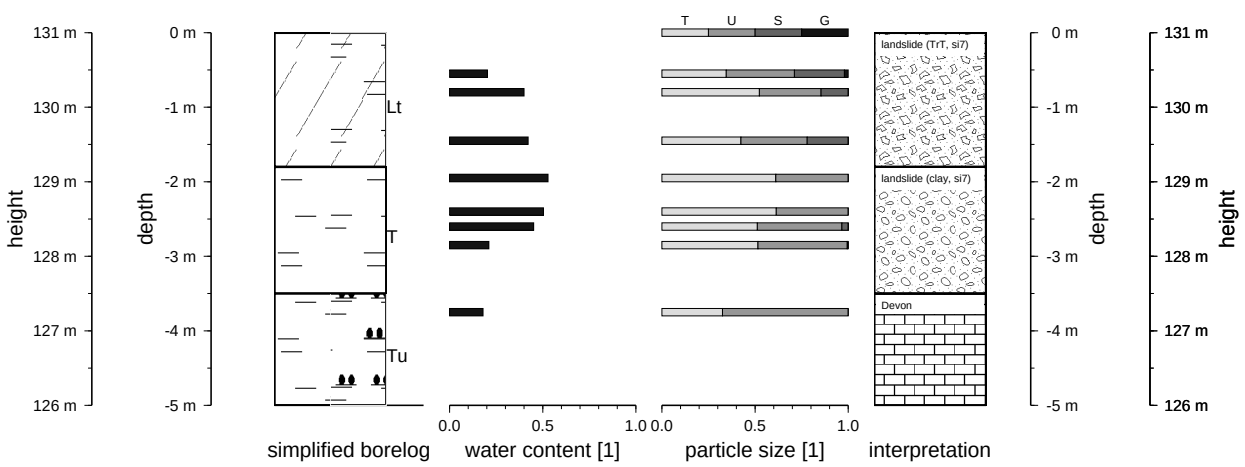

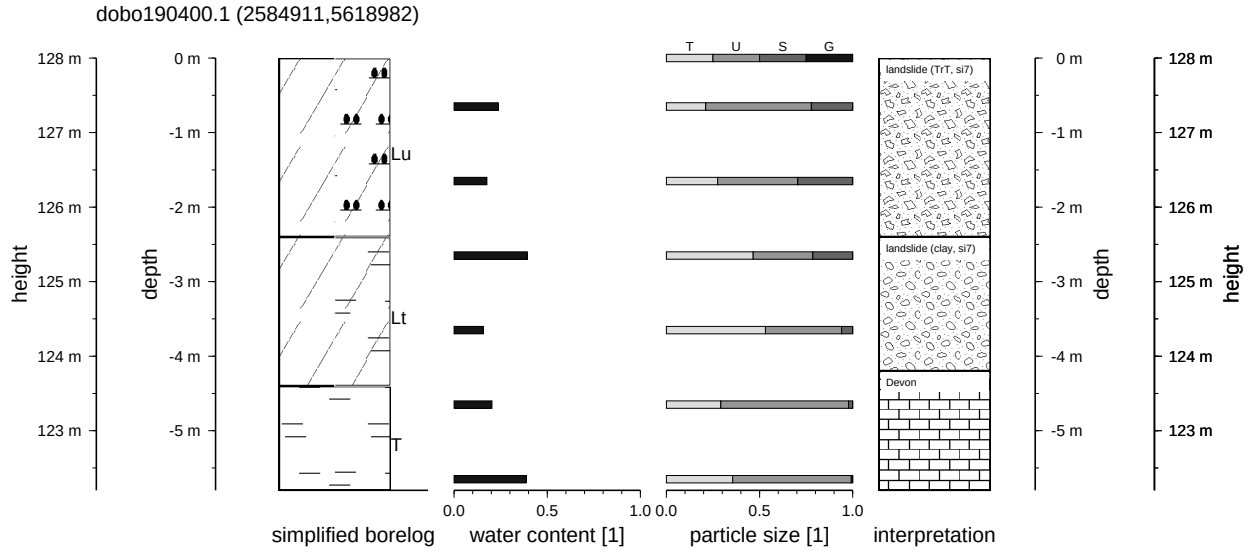
dobo190400.1 (2584911,5618982)
height
depth
Lu
Lt
T
T U S G
landslide (TrT, si7)
landslide (clay, si7)
Devon
simplified borelog
water content [1]
particle size [1]
interpretation

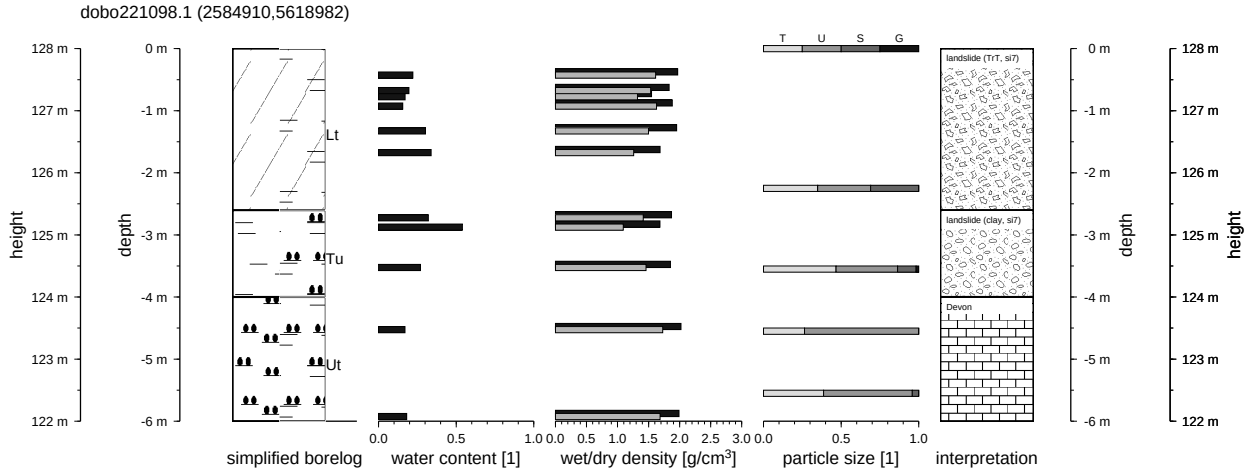
dobo221098.1 (2584910,5618982)
height
depth
Lt
Tu
Ut
T U S G
landslide (TrT, si7)
landslide (clay, si7)
Devon
simplified borelog
water content [1]
wet/dry density [g/cm3]
particle size [1]
interpretation

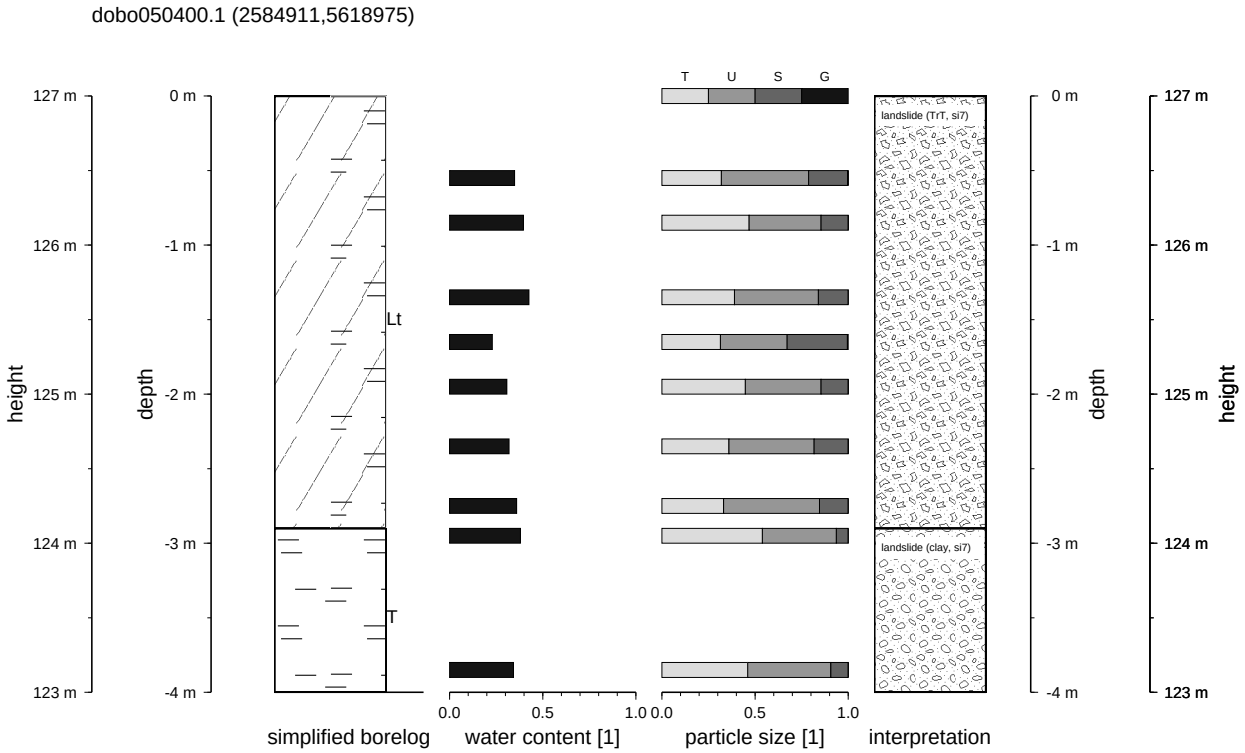
dobo050400.1 (2584911,5618975)
127 m
126 m
125 m
124 m
123 m
height
0 m
-1 m
-2 m
-3 m
-4 m
depth
Lt
T
simplified borelog
0.0
0.5
1.0
water content [1]
T
U
S
G
particle size [1]
landslide (TrT, si7)
landslide (clay, si7)
interpretation

B.1.2. Drilling results, field site Melbtal

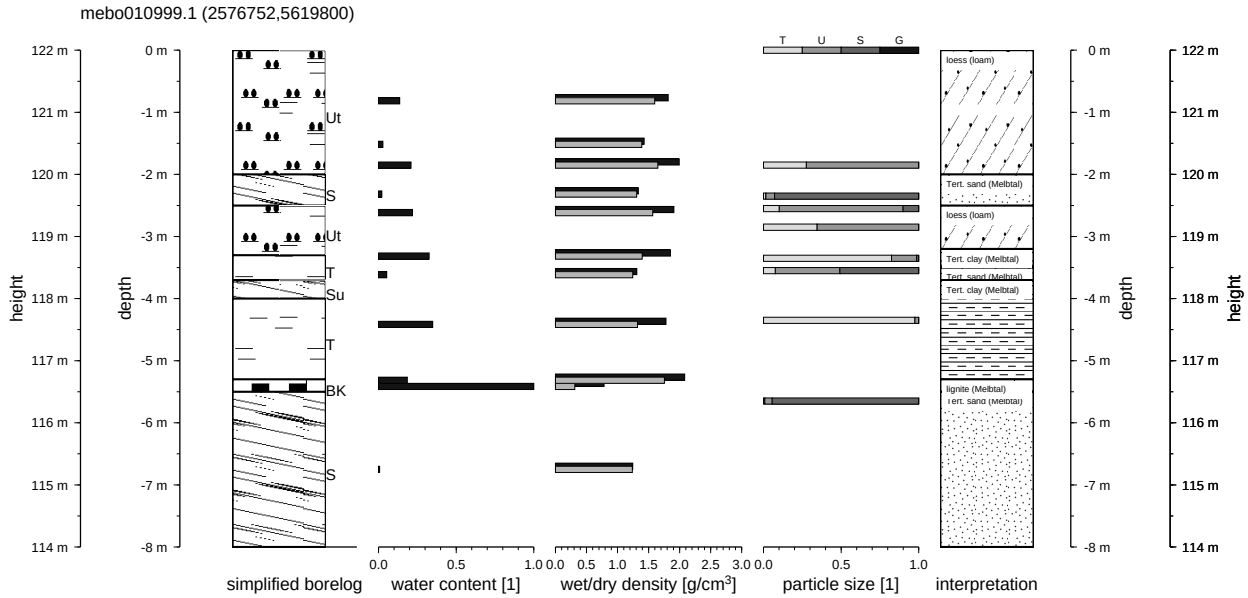

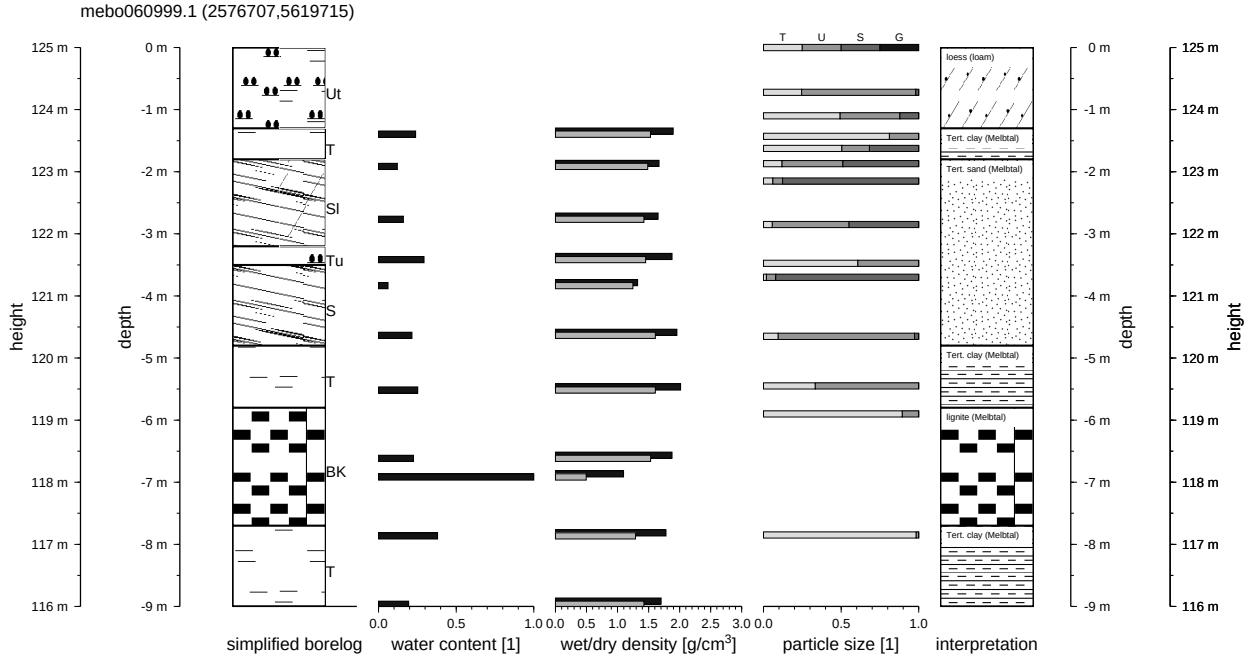

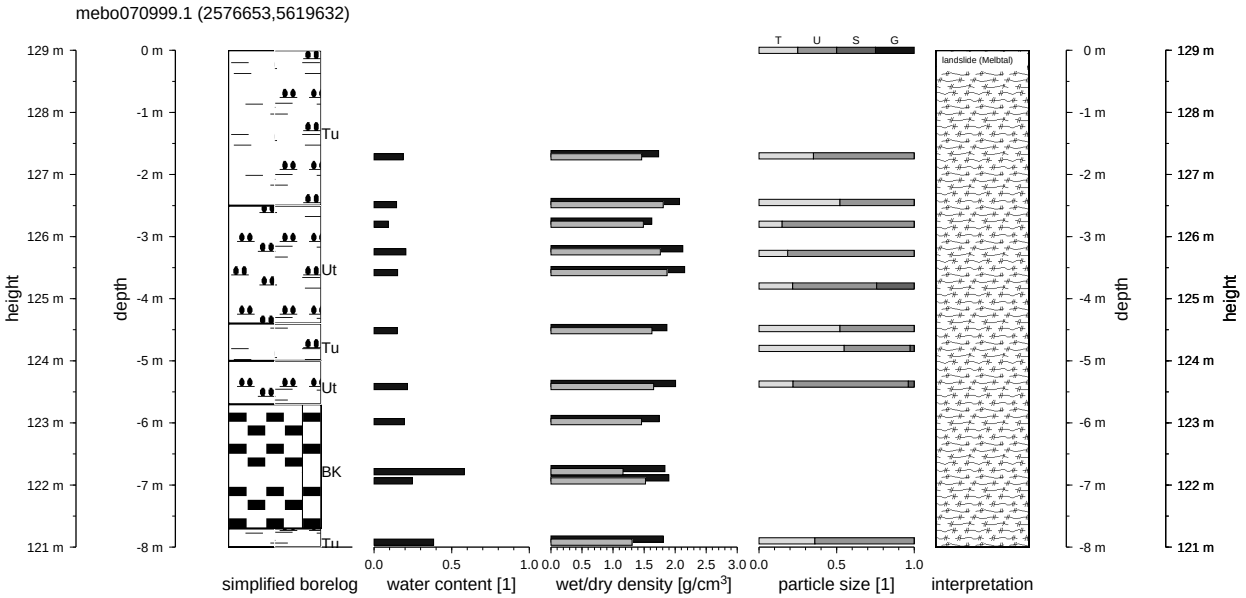
mebo070999.1 (2576653,5619632)
height
depth
Tu
Ut
Tu
Ut
BK
Tu
T U S G
landslide (Melbtal)
simplified borelog
water content [1]
wet/dry density [g/cm³]
particle size [1]
interpretation

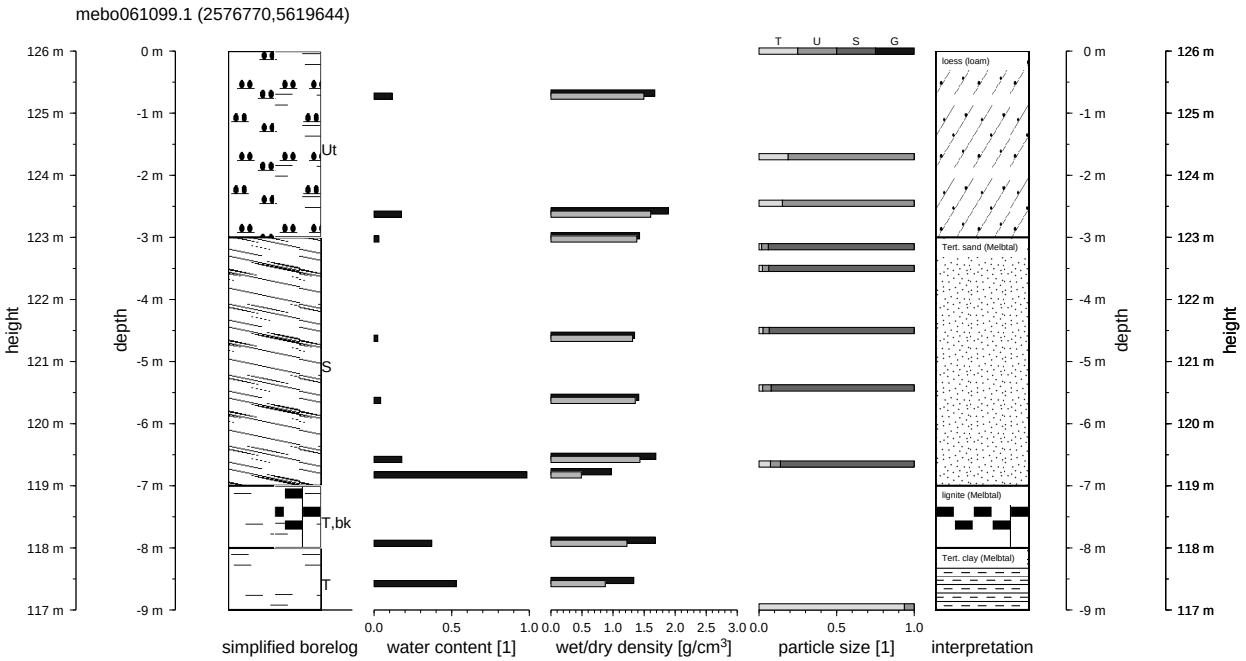
mebo061099.1 (2576770,5619644)
height
depth
Ut
S
T,bk
T
T U S G
loess (loam)
Tert. sand (Melbtal)
lignite (Melbtal)
Tert. clay (Melbtal)
simplified borelog
water content [1]
wet/dry density [g/cm³]
particle size [1]
interpretation

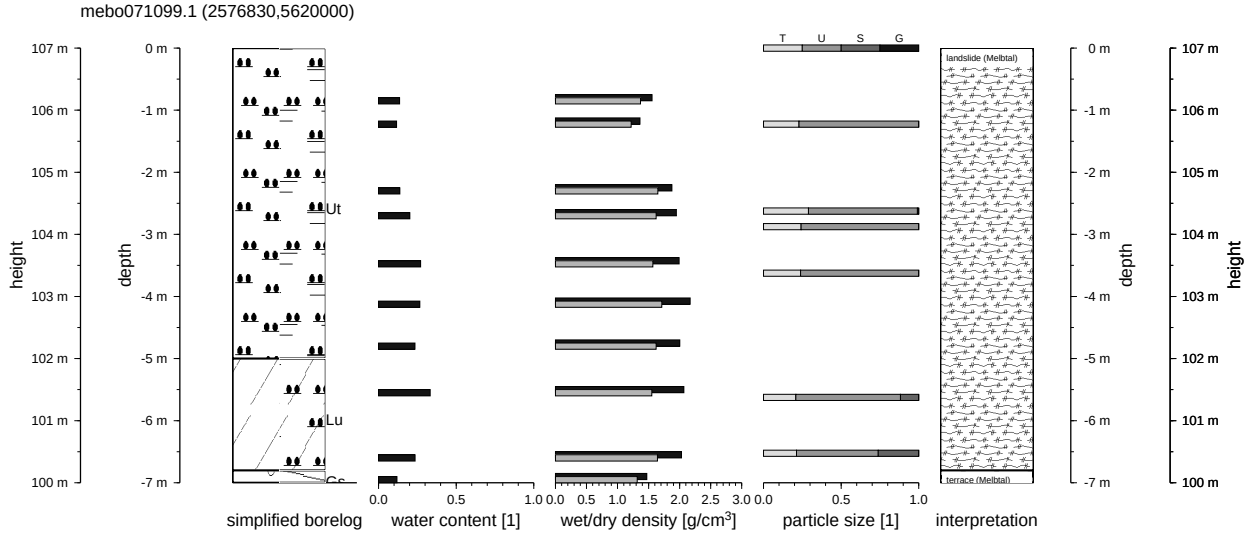
mebo071099.1 (2576830,5620000)
height
depth
Ut
Lu
Cc
T U S G
landslide (Melbtal)
terrace (Melbtal)
simplified borelog
water content [1]
wet/dry density [g/cm³]
particle size [1]
interpretation

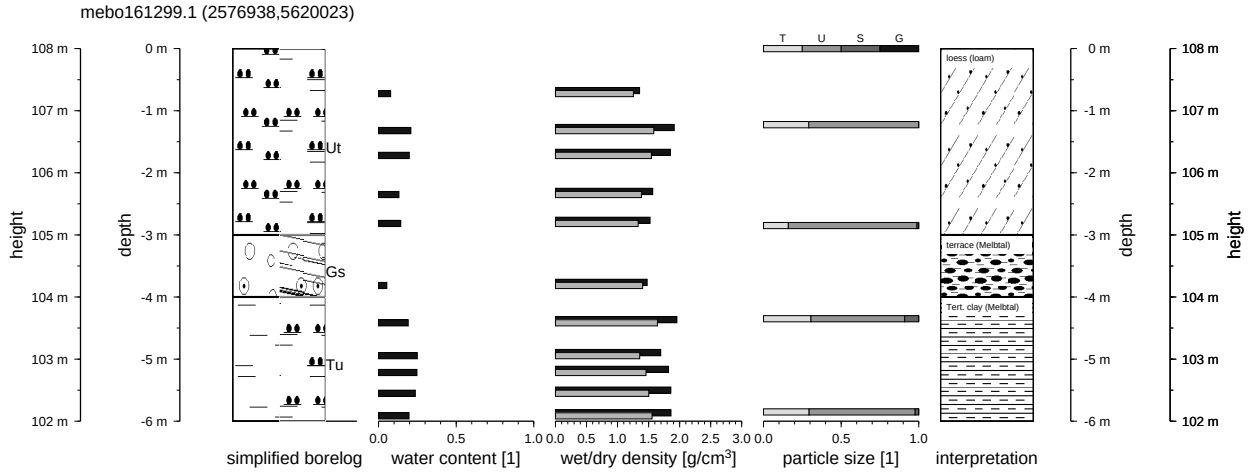
mebo161299.1 (2576938,5620023)
height
depth
Ut
Gs
Tu
T U S G
loess (loam)
terrace (Melbtal)
Tert. clay (Melbtal)
simplified borelog
water content [1]
wet/dry density [g/cm³]
particle size [1]
interpretation

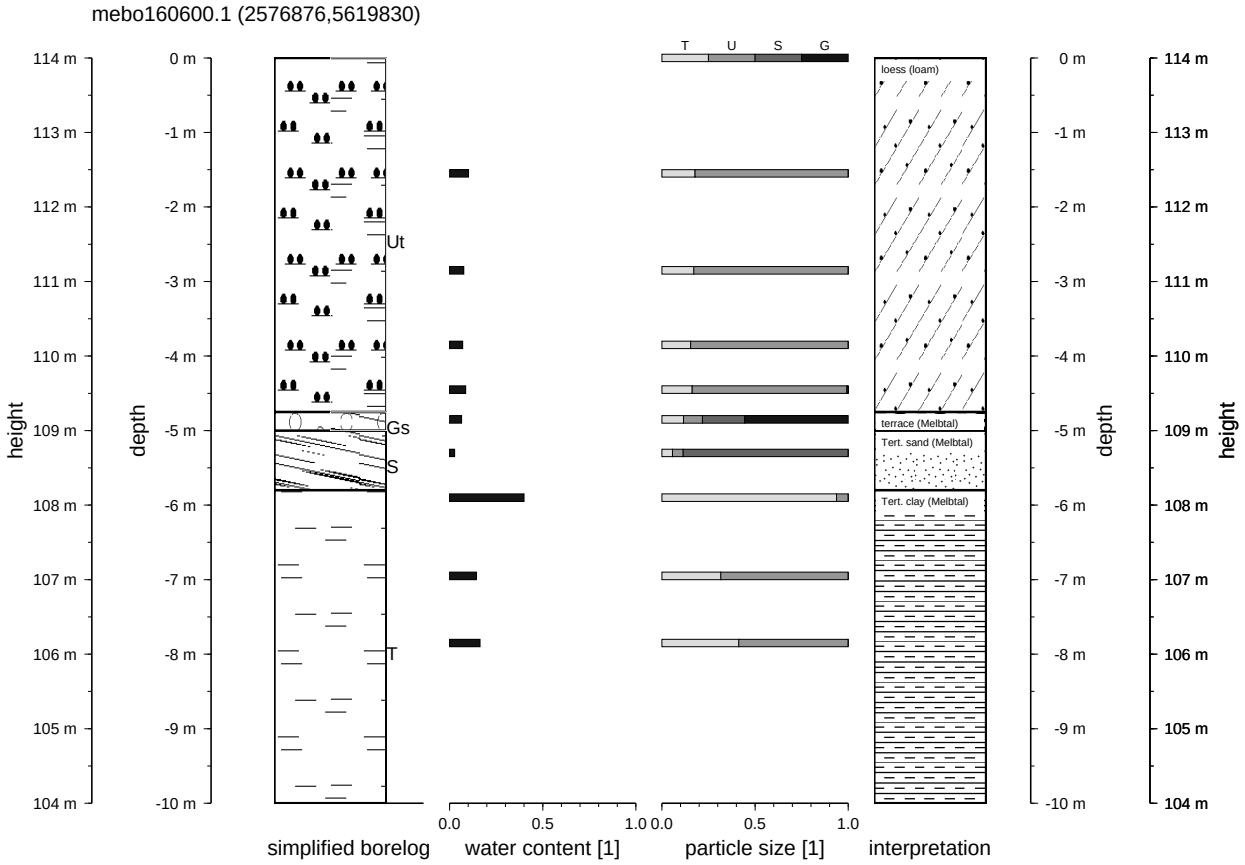
mebo160600.1 (2576876,5619830)
height
depth
Ut
Gs
S
T
T U S G
loess (loam)
terrace (Melbtal)
Tert. sand (Melbtal)
Tert. clay (Melbtal)
simplified borelog
water content [1]
particle size [1]
interpretation

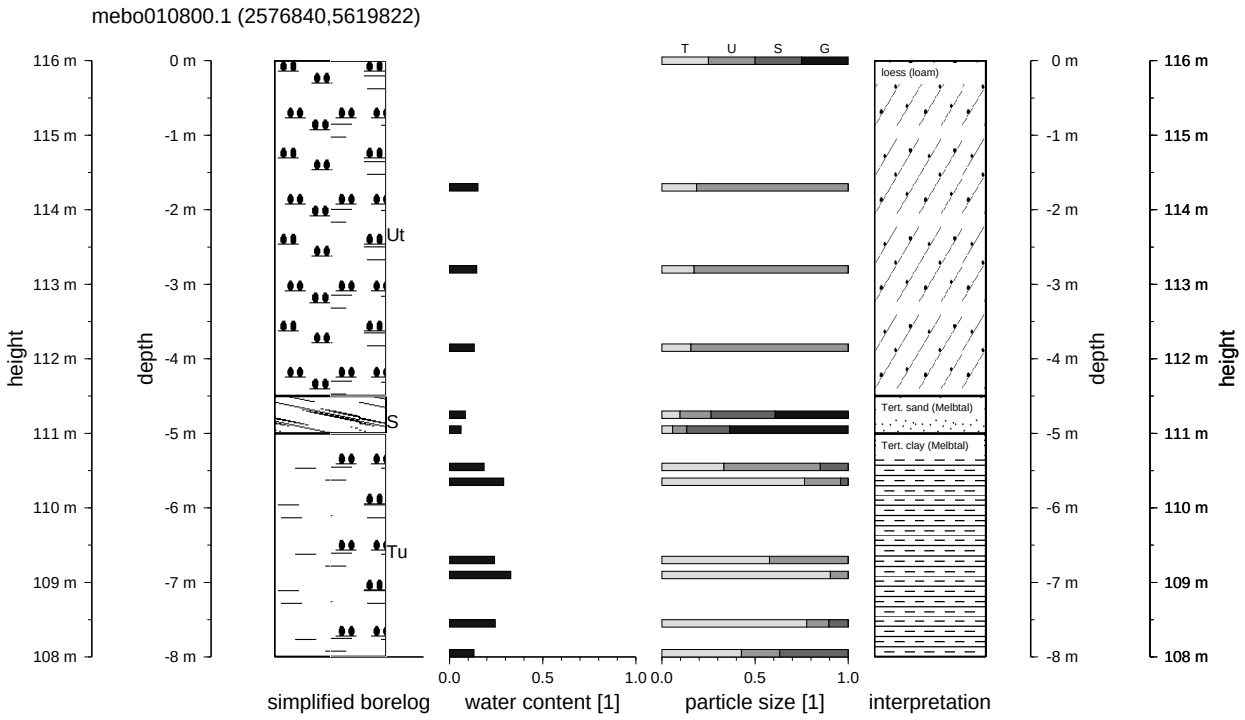
mebo010800.1 (2576840,5619822)
height
depth
Ut
S
Tu
T U S G
loess (loam)
Tert. sand (Melbtal)
Tert. clay (Melbtal)
simplified borelog
water content [1]
particle size [1]
interpretation

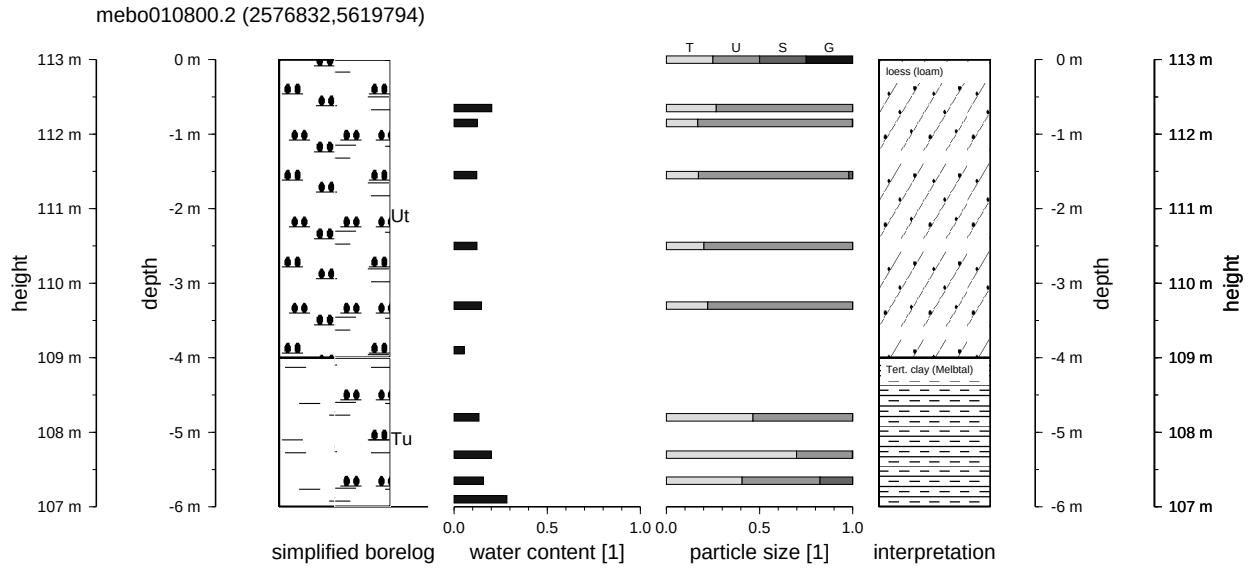
mebo010800.2 (2576832,5619794)
height
depth
Ut
Tu
T U S G
loess (loam)
Tert. clay (Melbtal)
simplified borelog
water content [1]
particle size [1]
interpretation

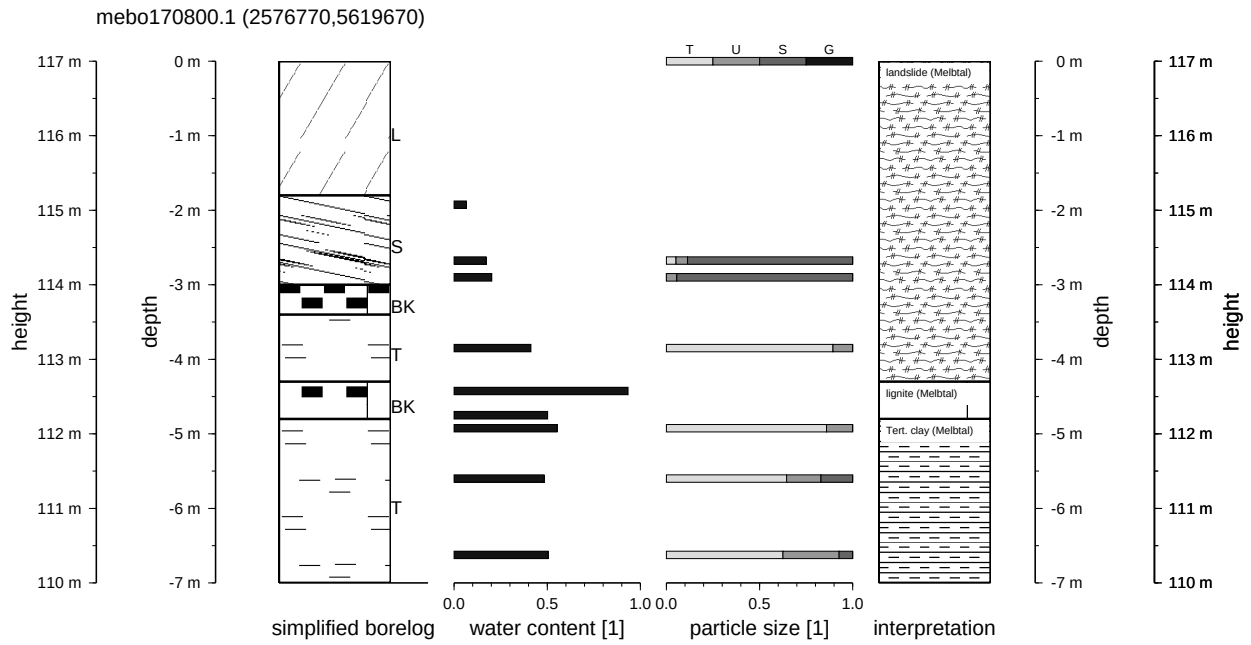
mebo170800.1 (2576770,5619670)
height
depth
L
S
BK
T
BK
T
T U S G
landslide (Melbtal)
lignite (Melbtal)
Tert. clay (Melbtal)
simplified borelog
water content [1]
particle size [1]
interpretation

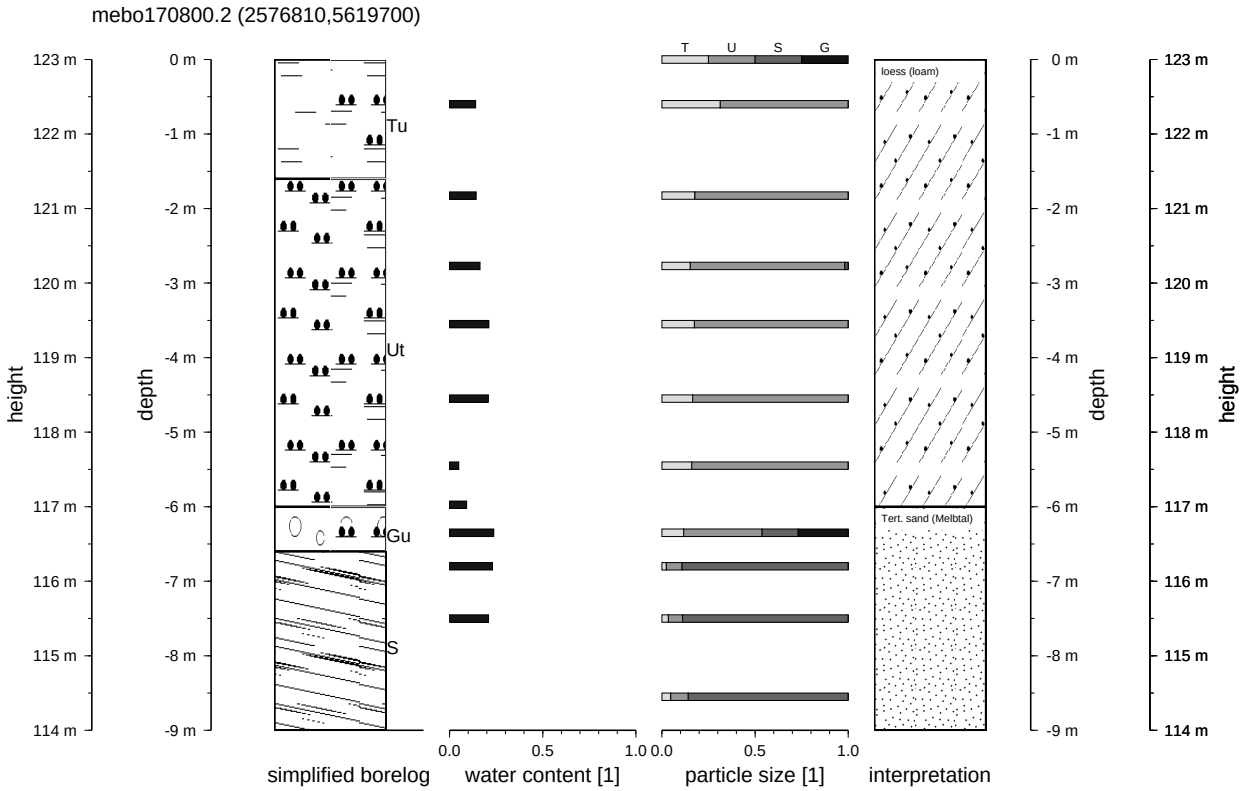
mebo170800.2 (2576810,5619700)
height
depth
Tu
Ut
Gu
S
T U S G
loess (loam)
Tert. sand (Melbtal)
simplified borelog
water content [1]
particle size [1]
interpretation

B.2. Field work & field installations

Listing: SQL–code for querying field work from database.

```
SELECT f.field_id AS id, f.date AS date, e.name AS experiment, p.name AS project, l2.name AS "field_site"
FROM field f,experiment e, location l, location l2 , project p
WHERE f.exp_id=e.id AND f.georef_id=l.id AND l.oloc_id=l2.id AND e.type like 'field'
  AND f.exp_id NOT IN (2,4,18,22,26,28,33,12) AND f.proj_id=p.id
ORDER BY p.proj_id,f.date,f.field_id;
```

List of field work on different field sites.

id	date	experiment	project	field site
mevane120298.1	1998-02-12	field vane test	subproject B13, SFB350	landslide me1
mevane120298.2	1998-02-12	field vane test	subproject B13, SFB350	landslide me1
doem090398.1	1998-03-09	electromagnetic survey	subproject B13, SFB350	Dollendorfer Hardt
doem090398.2	1998-03-09	electromagnetic survey	subproject B13, SFB350	Dollendorfer Hardt
doem090398.3	1998-03-09	electromagnetic survey	subproject B13, SFB350	Dollendorfer Hardt
doem090398.4	1998-03-09	electromagnetic survey	subproject B13, SFB350	Dollendorfer Hardt
doem100398.1	1998-03-10	electromagnetic survey	subproject B13, SFB350	Dollendorfer Hardt
doem100398.2	1998-03-10	electromagnetic survey	subproject B13, SFB350	Dollendorfer Hardt
doem100398.3	1998-03-10	electromagnetic survey	subproject B13, SFB350	Dollendorfer Hardt
doem100398.4	1998-03-10	electromagnetic survey	subproject B13, SFB350	Dollendorfer Hardt
dotach180598.1	1998-05-18	tachymetric measurement	subproject B13, SFB350	Dollendorfer Hardt
dotach220698.1	1998-06-22	tachymetric measurement	subproject B13, SFB350	Dollendorfer Hardt
dotach201098.1	1998-10-20	tachymetric measurement	subproject B13, SFB350	Dollendorfer Hardt
dotach211098.1	1998-10-21	tachymetric measurement	subproject B13, SFB350	Dollendorfer Hardt
dotach231098.1	1998-10-23	tachymetric measurement	subproject B13, SFB350	Dollendorfer Hardt
dotach261098.1	1998-10-26	tachymetric measurement	subproject B13, SFB350	Dollendorfer Hardt
dogpr101198.1	1998-11-10	GPR survey	subproject B13, SFB350	Dollendorfer Hardt
dogpr101198.2	1998-11-10	GPR survey	subproject B13, SFB350	Dollendorfer Hardt
dogpr241198.1	1998-11-24	GPR survey	subproject B13, SFB350	Dollendorfer Hardt
dogpr211298.1	1998-12-21	GPR survey	subproject B13, SFB350	Dollendorfer Hardt
dogpr211298.2	1998-12-21	GPR survey	subproject B13, SFB350	Dollendorfer Hardt
dogpr190199.1	1999-01-19	GPR survey	subproject B13, SFB350	Dollendorfer Hardt
dogpr190199.2	1999-01-19	GPR survey	subproject B13, SFB350	Dollendorfer Hardt
dogpr190199.3	1999-01-19	GPR survey	subproject B13, SFB350	Dollendorfer Hardt
dogpr210199.1	1999-01-21	GPR survey	subproject B13, SFB350	Dollendorfer Hardt
dogpr210199.2	1999-01-21	GPR survey	subproject B13, SFB350	Dollendorfer Hardt
dogpr240399.1	1999-03-24	GPR survey	subproject B13, SFB350	Dollendorfer Hardt
dogpr240399.2	1999-03-24	GPR survey	subproject B13, SFB350	Dollendorfer Hardt
dogpr240399.3	1999-03-24	GPR survey	subproject B13, SFB350	Dollendorfer Hardt
dogpr060599.1	1999-05-06	GPR survey	subproject B13, SFB350	Dollendorfer Hardt
doem020999.1	1999-09-02	electromagnetic survey	subproject B13, SFB350	Dollendorfer Hardt
doem020999.2	1999-09-02	electromagnetic survey	subproject B13, SFB350	Dollendorfer Hardt
doem020999.3	1999-09-02	electromagnetic survey	subproject B13, SFB350	Dollendorfer Hardt
doem020999.4	1999-09-02	electromagnetic survey	subproject B13, SFB350	Dollendorfer Hardt
dogpr020999.1	1999-09-02	GPR survey	subproject B13, SFB350	Dollendorfer Hardt
dogpr020999.2	1999-09-02	GPR survey	subproject B13, SFB350	Dollendorfer Hardt
megpr201099.1	1999-10-20	GPR survey	subproject B13, SFB350	Melbtal
megpr201099.2	1999-10-20	GPR survey	subproject B13, SFB350	Melbtal
megpr261099.1	1999-10-26	GPR survey	subproject B13, SFB350	Melbtal
megpr261099.1a	1999-10-26	GPR survey	subproject B13, SFB350	Melbtal
megpr261099.2	1999-10-26	GPR survey	subproject B13, SFB350	Melbtal
megpr261099.3	1999-10-26	GPR survey	subproject B13, SFB350	Melbtal
megpr261099.4	1999-10-26	GPR survey	subproject B13, SFB350	Melbtal
megpr261099.5	1999-10-26	GPR survey	subproject B13, SFB350	Melbtal
megpr091199.1	1999-11-09	GPR survey	subproject B13, SFB350	Melbtal
megpr091199.2	1999-11-09	GPR survey	subproject B13, SFB350	Melbtal

continued on next page

continued from previous page

id	date	experiment	project	field site
megpr091199.3	1999-11-09	GPR survey	subproject B13, SFB350	Melbtal
megpr091199.4	1999-11-09	GPR survey	subproject B13, SFB350	Melbtal
megpr091199.5	1999-11-09	GPR survey	subproject B13, SFB350	Melbtal
mera091199.1	1999-11-09	field penetration test	subproject B13, SFB350	Melbtal
mera091199.2	1999-11-09	field penetration test	subproject B13, SFB350	Melbtal
mevane250996.1	1996-09-25	field vane test	subproject B9, SFB350	landslide me5
meschlum051099.1	1999-10-05	geoelectric survey (Schlummberger)	field seminar (SS 99)	Melbtal
meseis051099.1	1999-10-05	seismic survey	field seminar (SS 99)	Melbtal
meseis051099.2	1999-10-05	seismic survey	field seminar (SS 99)	Melbtal
meseis061099.1	1999-10-06	seismic survey	field seminar (SS 99)	Melbtal
meseis061099.2	1999-10-06	seismic survey	field seminar (SS 99)	Melbtal
mevane061099.1	1999-10-06	field vane test	field seminar (SS 99)	Melbtal
meschlum071099.1	1999-10-07	geoelectric survey (Schlummberger)	field seminar (SS 99)	Melbtal
meschlum071099.2	1999-10-07	geoelectric survey (Schlummberger)	field seminar (SS 99)	Melbtal
meschlum081099.1	1999-10-08	geoelectric survey (Schlummberger)	field seminar (SS 99)	Melbtal
meseis081099.1	1999-10-08	seismic survey	field seminar (SS 99)	Melbtal
mera111199.1	1999-11-11	field penetration test	lab seminar (WS 99/00)	Melbtal
mera111199.2	1999-11-11	field penetration test	lab seminar (WS 99/00)	Melbtal

Listing: SQL–code for querying field installation from database.

```
SELECT l.loc_id AS station, l2.name AS location, f.date AS date,
       e.name AS installation, p.point AS coordinates, p.height AS "h[m]"
FROM field f,experiment e, points p, location l, location l2
WHERE f.exp_id=e.id AND f.georef_id=l.id AND f.georef_id=p.loc_id
  AND l.oloc_id=l2.id AND e.type='installation'
ORDER BY f.date;
```

List of field installations on different field sites. (h: height above sea level in m)

station	location	date	installation	coordinates	h[m]
dobo190398.2	Dollendorfer Hardt	1998-03-19	groundwater tube	(2584860,5618990)	141
dobo190398.1	landslide si7	1998-03-19	groundwater tube	(2584903,5618998)	132
dobo180698.1	landslide si7	1998-06-18	groundwater tube	(2584901,5618879)	110
dobo110898.1	Dollendorfer Hardt	1998-08-11	groundwater tube	(2584792,5619125)	181
dobo120898.1	landslide si7	1998-08-12	inclinometer tube	(2584853,5619107)	164
dobo130898.1	Dollendorfer Hardt	1998-08-13	groundwater tube	(2584811,5619112)	177
dobo200898.1	Dollendorfer Hardt	1998-08-20	groundwater tube	(2584831,5619090)	169
dobo250898.1	Dollendorfer Hardt	1998-08-25	groundwater tube	(2584845,5619057)	158
dobo270898.1	landslide si7	1998-08-27	groundwater tube	(2584811,5619142)	174
dobo270898.2	landslide si7	1998-08-27	groundwater tube	(2584825,5619136)	173
dobo030998.1	landslide si7	1998-09-03	inclinometer tube	(2584910,5618880)	109
dobo040998.1	landslide si7	1998-09-04	groundwater tube	(2584837,5619130)	170
dobo110998.1	landslide si7	1998-09-11	groundwater tube	(2584818,5619148)	176
dobo201098.1	landslide si7	1998-10-20	groundwater tube	(2584850,5619115)	163
dobo201098.2	landslide si7	1998-10-20	groundwater tube	(2584872,5619101)	158
dobo221098.1	landslide si7	1998-10-22	inclinometer tube	(2584910,5618982)	128
mebo010999.1	Melbtal	1999-09-01	groundwater tube	(2576752,5619800)	122
mebo060999.1	Melbtal	1999-09-06	groundwater tube	(2576707,5619715)	125
mebo070999.1	Melbtal	1999-09-07	groundwater tube	(2576653,5619632)	129
mebo051099.1	Melbtal	1999-10-05	inclinometer tube	(2576682,5619571)	123
mebo061099.1	Melbtal	1999-10-06	groundwater tube	(2576770,5619644)	126
mebo071099.1	Melbtal	1999-10-07	groundwater tube	(2576830,5620000)	107
mebo161299.1	Melbtal	1999-12-16	groundwater tube	(2576938,5620023)	108
dobo050400.1	landslide si7	2000-04-07	tiltmeter tube	(2584911,5618975)	127
dobo180400.1	landslide si7	2000-04-18	inclinometer tube	(2584905,5618993)	131
dobo180400.2	landslide si7	2000-04-18	groundwater tube	(2584913,5618976)	126
dobo190400.1	landslide si7	2000-04-19	inclinometer tube	(2584911,5618982)	128
dobo190400.2	landslide si7	2000-04-19	groundwater tube	(2584912,5618982)	128
mebo160600.1	Melbtal	2000-06-16	groundwater tube	(2576876,5619830)	114

B.3. Movement measurements

Listing: SQL–code for querying timeseries of movement monitoring from database.

```
SELECT max(l.loc_id) AS station, max(l2.name) AS location, max(e.name) AS method, min(f.date) AS "begin_(date)"
FROM field f, experiment e, points p, location l , location l2
WHERE f.exp_id=e.id AND f.georef_id=l.id AND f.georef_id=p.loc_id
      AND l.oloc_id=l2.id AND (f.exp_id=21 OR f.exp_id=49)
GROUP BY l.id
ORDER BY min(f.date);
```

List of timeseries of movement monitoring.

station	location	method	begin (date)
dobo030998.1	landslide si7	inclinometer measurements	1998-10-20
dobo120898.1	landslide si7	inclinometer measurements	1998-10-20
dobo221098.1	landslide si7	inclinometer measurements	1998-10-31
mebo051099.1	Melbtal	inclinometer measurements	1999-10-08
dobo050400.1	landslide si7	tiltmeter measurements	2000-05-01
dobo180400.1	landslide si7	inclinometer measurements	2000-05-24
dobo190400.1	landslide si7	inclinometer measurements	2000-05-24

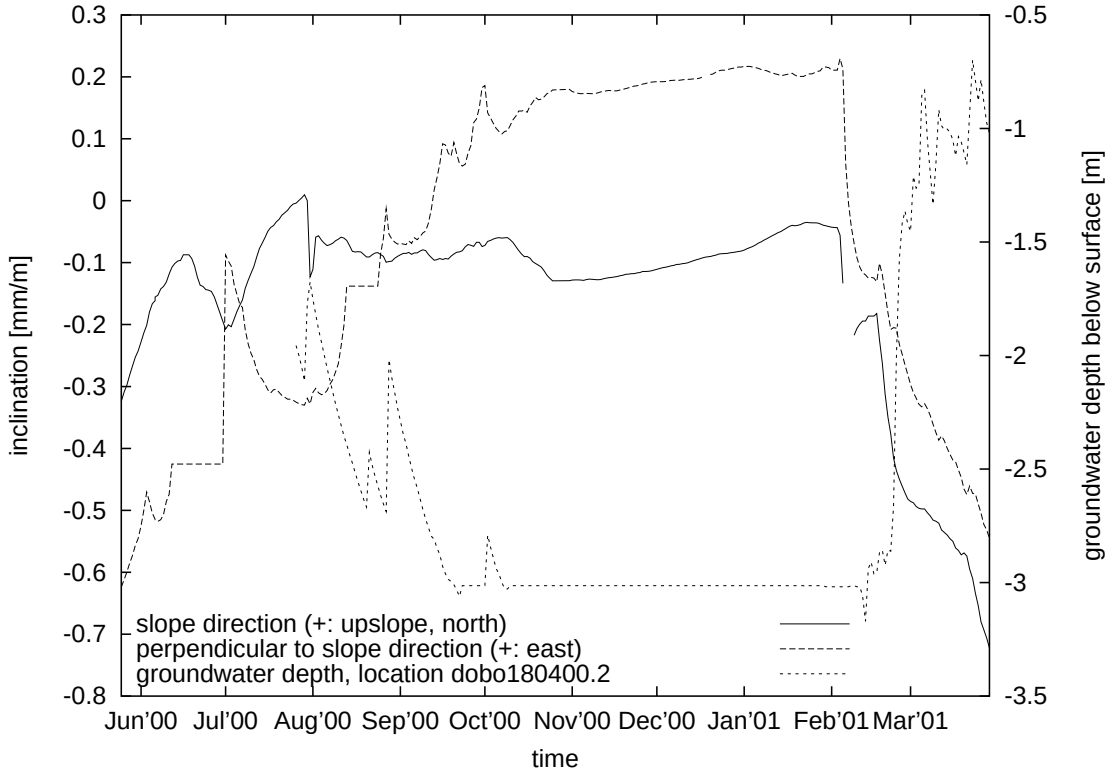

Tiltmeter measurements, location *dobo050400.1*. A tiltmeter station was set up after strong movements (see below) in the middle part of the landslide 'si7'. The signals show strong downslope movements, related to intensive rainfall events / groundwater rise in march/april 2001 (groundwater heights from location *'dobo180400.2'* are shown).

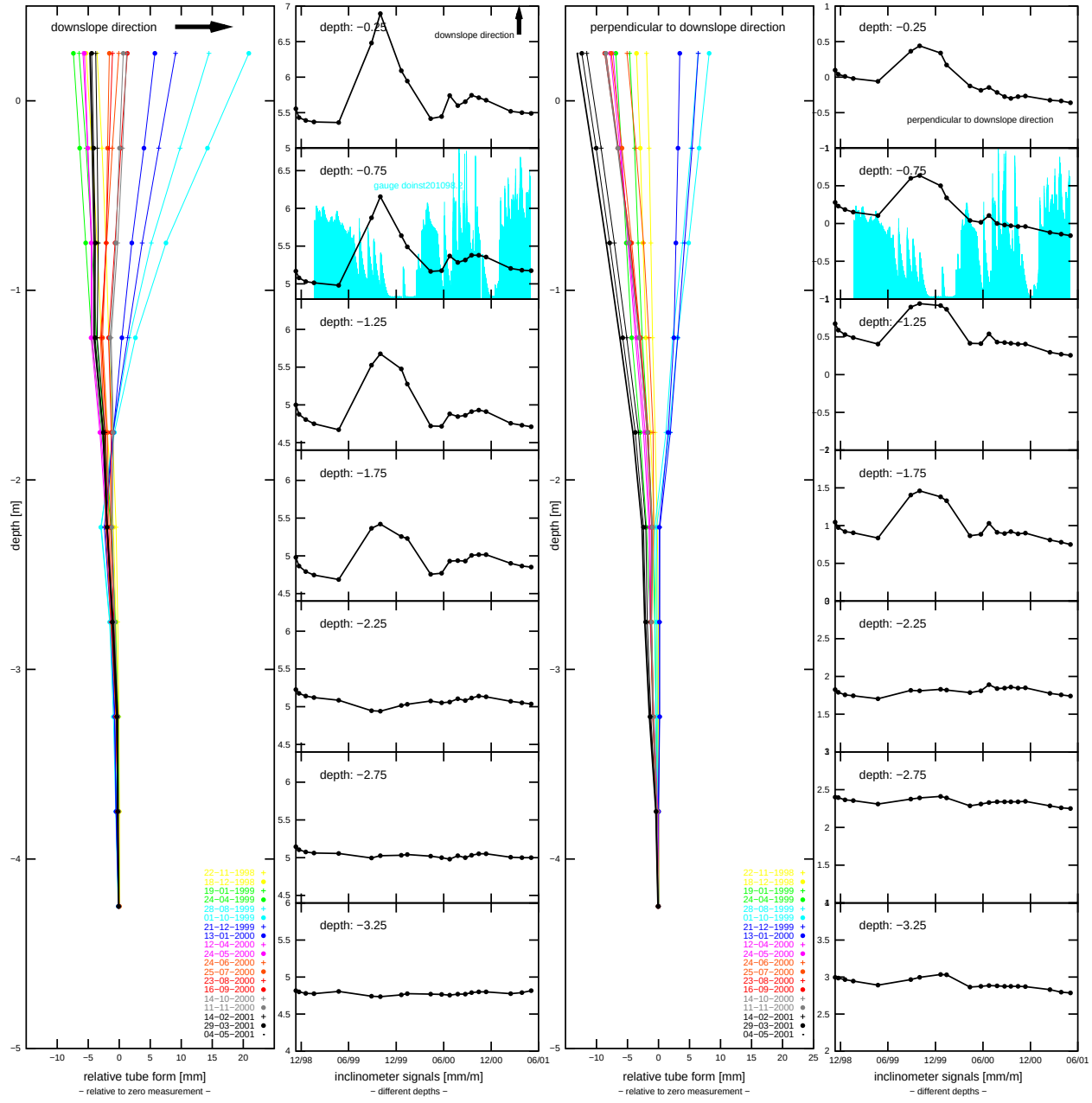

inclinometer tube: doinst120898.1 (coordinates (Gauss−−Krueger) 2584853,5619107; height 164m asl)

Inclinometer measurements, location *dobo120898.1*. Movement signals monitored by inclinometer techniques detected soil creep with a regular temporal pattern in the lowermost rotated landslide block direct above the landslide transport zone. Downslope movement occurred regularly in summer (related to intensive precipitation phases). However, these displacements tendency inverted in winter, indicating a elastic behaviour of the landslide block. Groundwater heights from location *'dobo201098.2'* are shown as blue impulses.

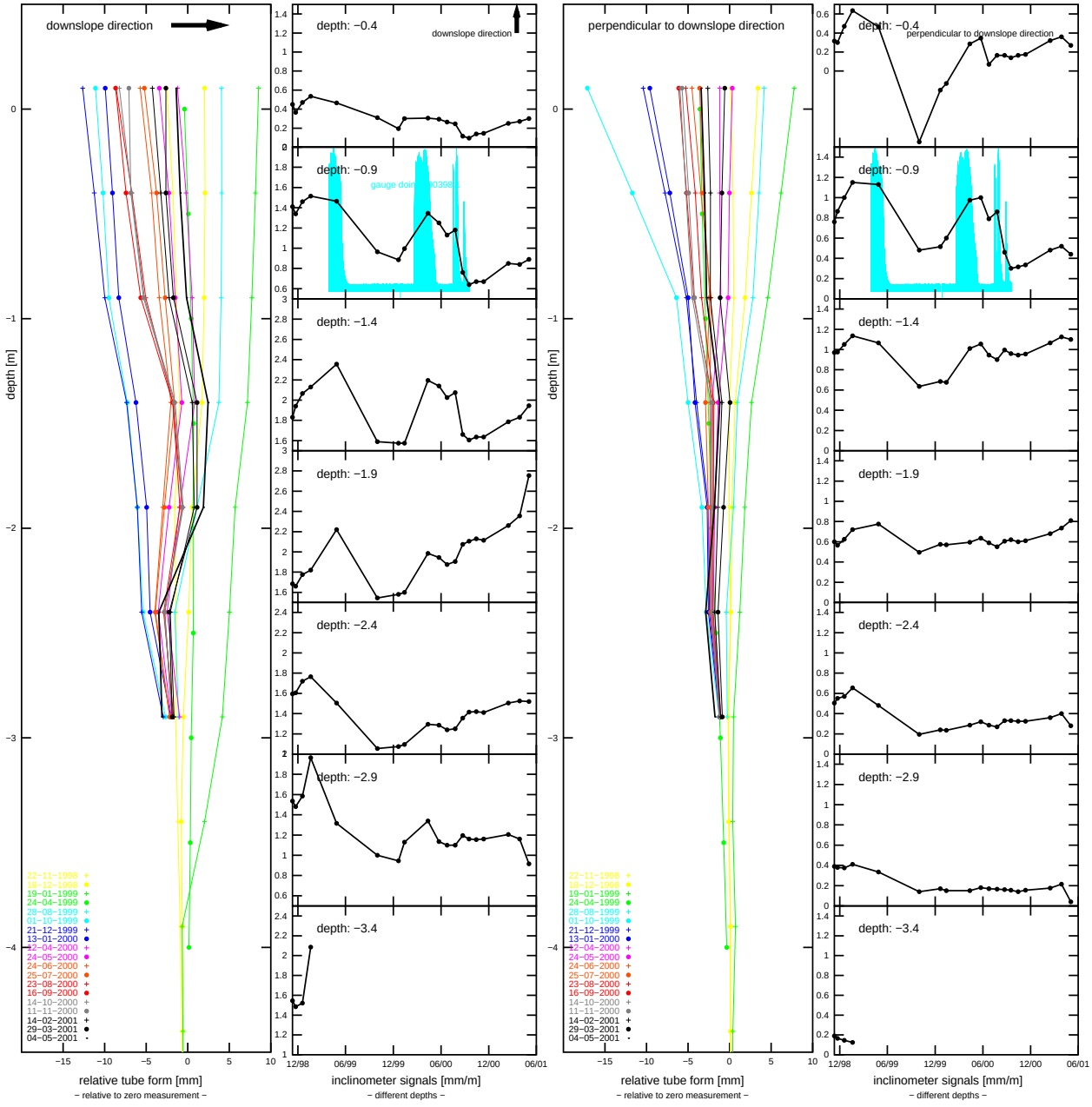

inclinometer tube: doinst221098.1 (coordinates (Gauss−−Krueger) 2584910,5618982; height 128m asl)

Inclinometer measurements, location *dobo221098.1*. Movement signals monitored by inclinometer techniques in a landslide block in the transport zone. Shearing of the tube occurred few month after installations (spring '99) at a depth of approx. 3 m. The continuing measurements indicated a continuous creep of the landslide mass in downslope direction. Groundwater heights from location *'dobo190398.1'* are shown as blue impulses.

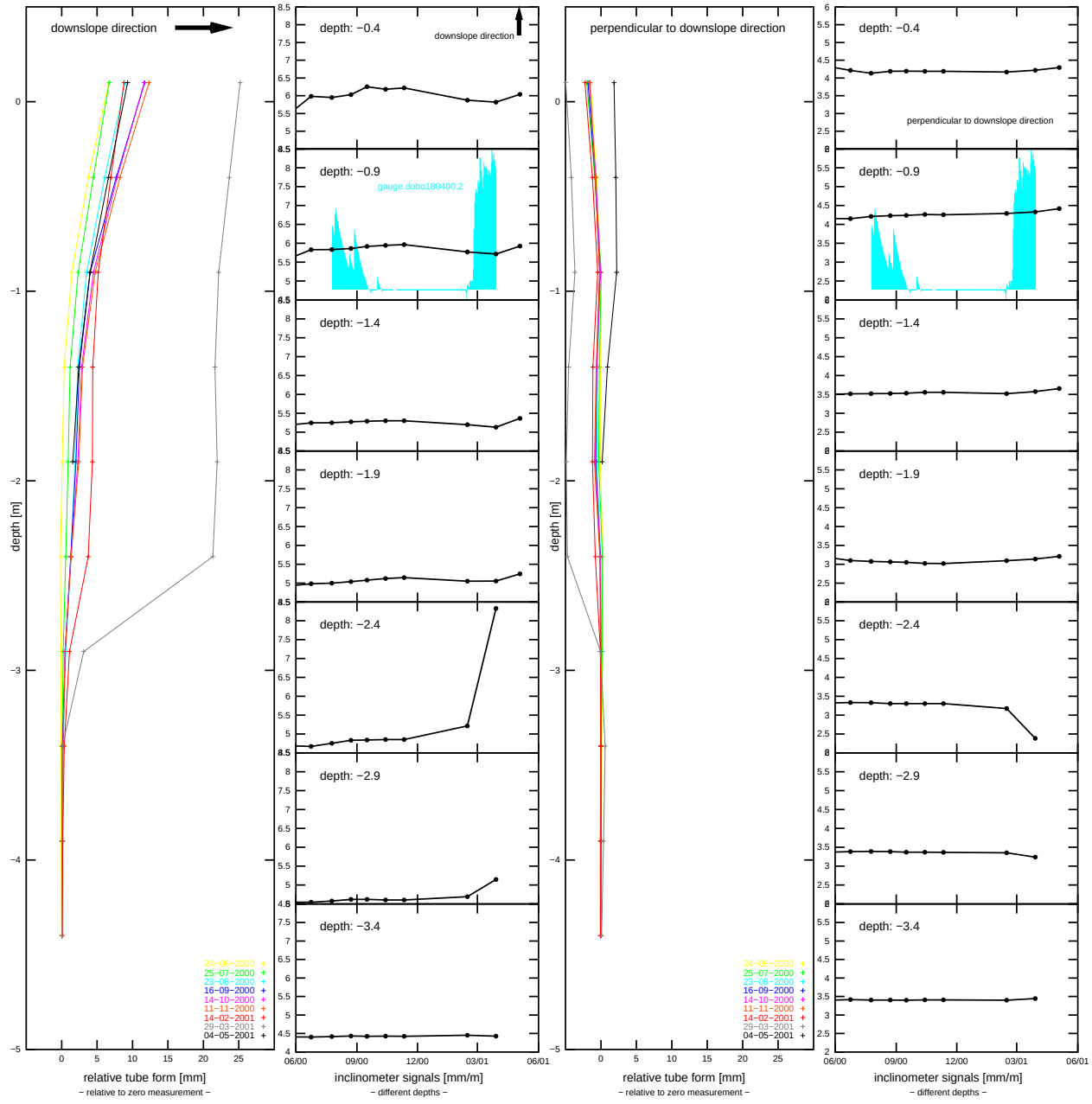

inclinometer tube: doinst180400.1 (coordinates (Gauss−−Krueger) 2584905,5618993; height 131m asl)

Inclinometer measurements, location *dobo180400.1*. Movement signals monitored by inclinometer techniques in a landslide block in the transport zone. The inclinometer tube sheared in April '01 (wet spring '01) at a depth of approx. 2.5 m to 3 m. Groundwater heights from location *'dobo180400.2'* are shown as blue impulses.

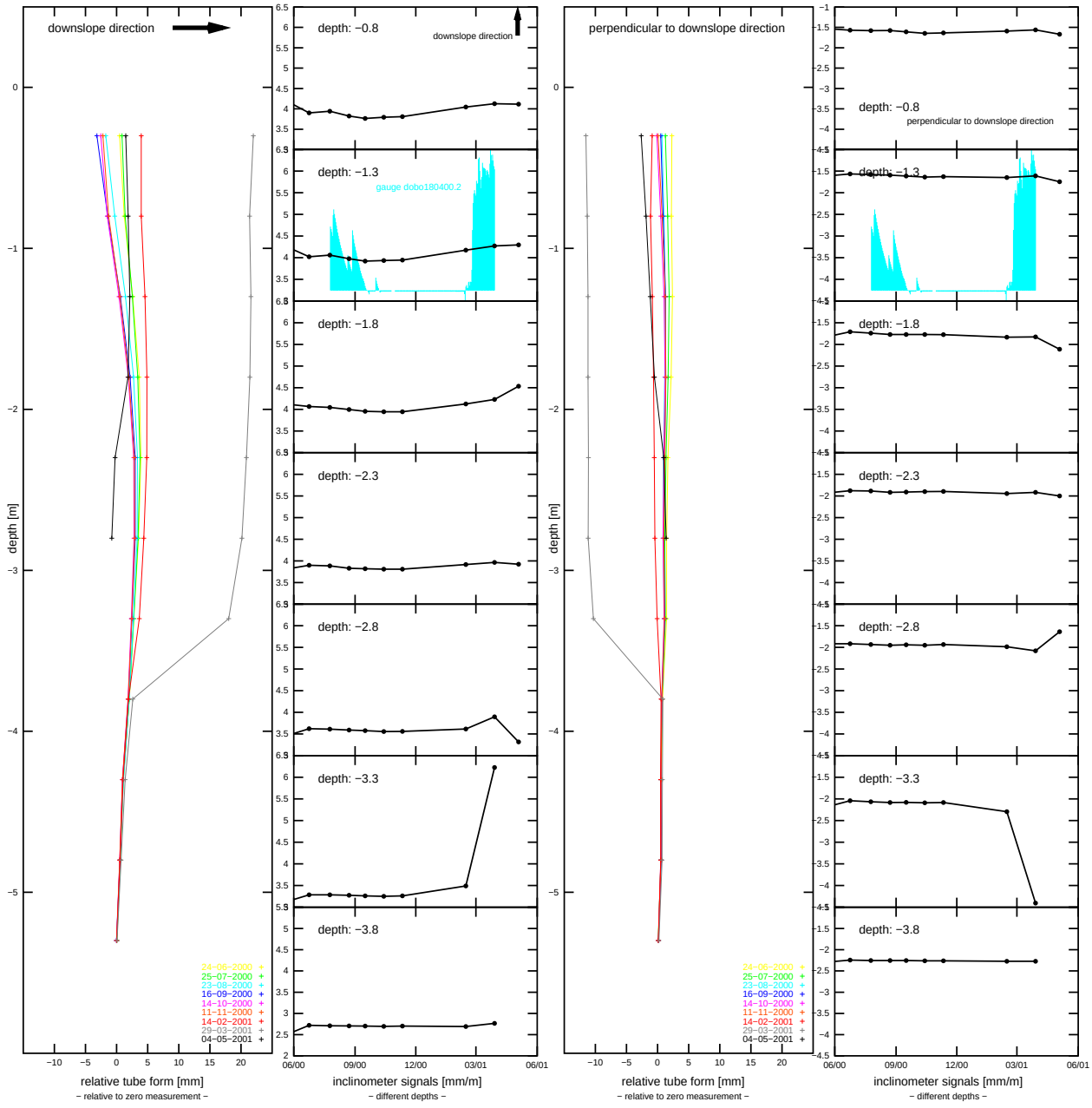

inclinometer tube: doinst190400.1 (coordinates (Gauss−−Krueger) 2584911,5618982; height 128m asl)

Inclinometer measurements, location *dobo190400.1*. Movement signals monitored by inclinometer techniques in a landslide block in the transport zone. The inclinometer tube sheared in April '01 (wet spring '01) at a depth of approx. 3 m. Groundwater heights from location *'dobo180400.2'* are shown as blue impulses.

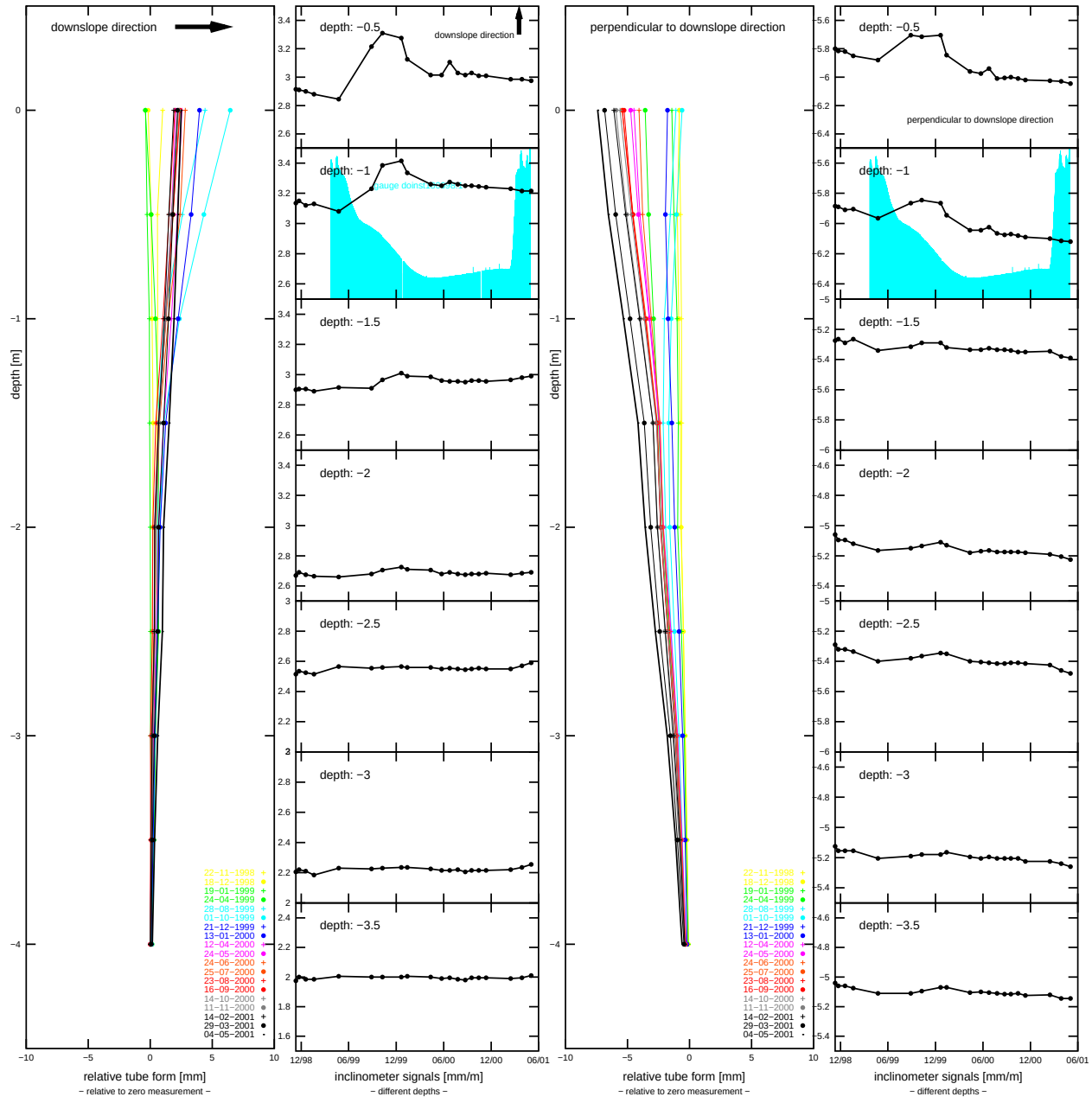

inclinometer tube: doinst030998.1 (coordinates (Gauss−−Krueger) 2584910,5618880; height 109m asl)

Inclinometer measurements, location *dobo030998.1*. Movement signals monitored by inclinometer techniques in the landslide tongue of the landslide 'si7'. Soil creep with low magnitudes (approx. 7 mm) occurred in autumn' 99 (groundwater heights from location *'dobo180698.1'* are shown as blue impulses). Again an elastic behaviour of the landslide mass was observed.

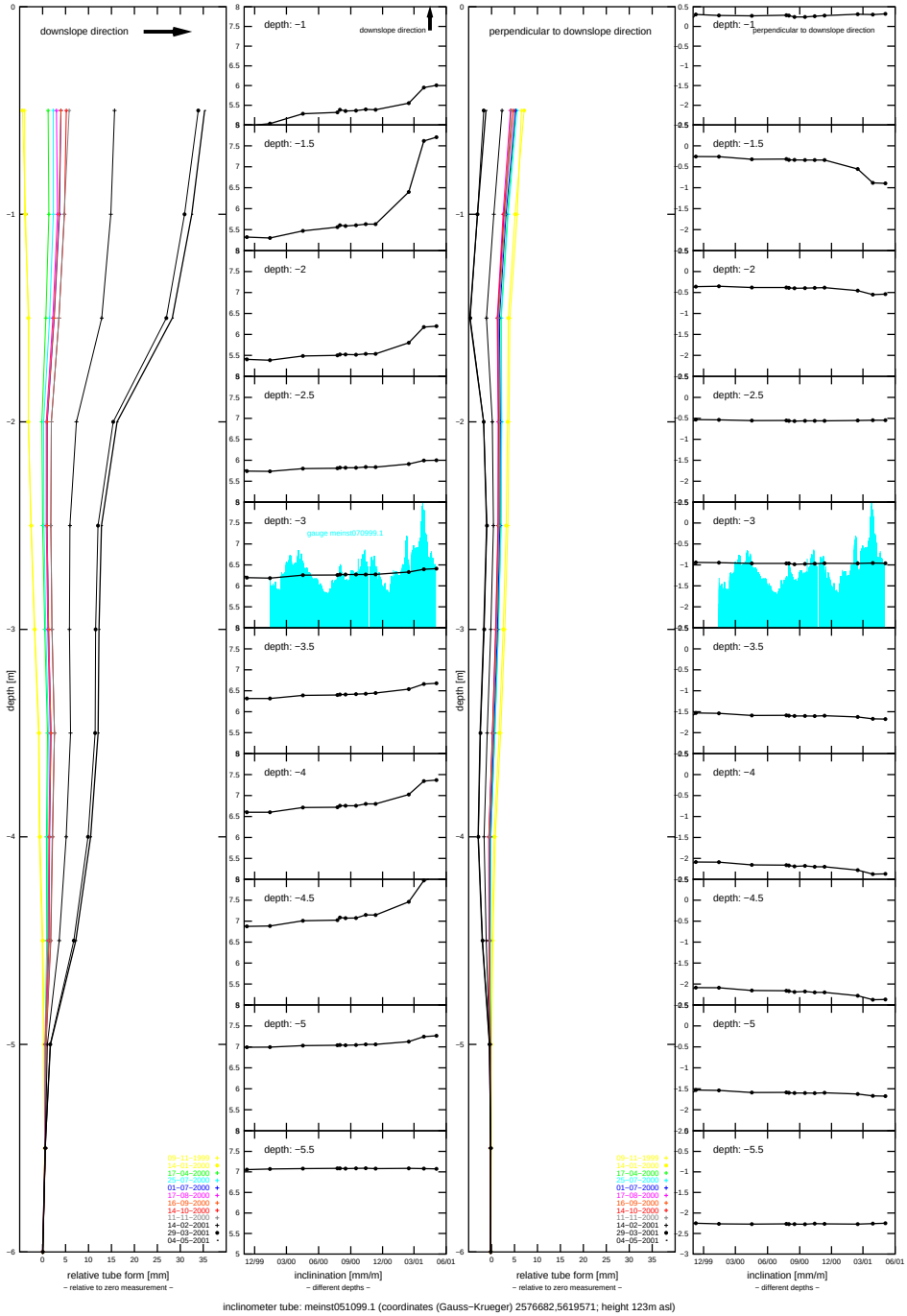

Inclinometer measurements, location *mebo051099.1*. After minor variations in 2000, a strong downslope movement were monitored in spring' 01 (groundwater heights from location *'mebo070999.1'* are shown as blue impulses). Moreover this signal indicates two different shear surfaces, one at between 1.5 m and 2 m (younger landslide mass, approx. 3 cm/m displacement), and one at approx 4.5 m (older landslide mass, approx. 1 cm/m displacement).

B.4. Groundwater measurements

Listing: SQL–code for querying groundwater time series from database.

```
SELECT max(l.loc_id) AS station, max(l2.name) AS location, max(e.name) AS method,
       min(tb.date) AS "begin_(date)", max(tb.date) AS "end_(date)"
FROM field f, experiment e, location l, location l2 , timeval tb
WHERE f.exp_id=e.id AND f.georef_id=l.id AND l.oloc_id=l2.id
        AND (f.exp_id=18 OR f.exp_id=19) AND tb.field_id=f.id
GROUP BY f.id
ORDER BY min(tb.date);
```

List groundwater time series. Timeseries captured with the D–DIVER have hourly resolution, the dipmeter was used irregularly only for initial checks. See Appendix B.2 for station details.

station	location	method	begin (date)	end (date)
dobo190398.1	landslide si7	dipmeter measurements	1998-04-02	1999-03-24
dobo190398.2	Dollendorfer Hardt	dipmeter measurements	1998-04-02	2000-07-25
dobo180698.1	landslide si7	dipmeter measurements	1998-06-19	1999-03-24
dobo270898.1	landslide si7	dipmeter measurements	1998-09-04	2000-08-23
dobo270898.2	landslide si7	dipmeter measurements	1998-09-04	2000-08-23
dobo110898.1	Dollendorfer Hardt	dipmeter measurements	1998-09-04	2000-02-16
dobo130898.1	Dollendorfer Hardt	dipmeter measurements	1998-09-04	2000-08-23
dobo200898.1	Dollendorfer Hardt	dipmeter measurements	1998-09-04	2000-08-23
dobo250898.1	Dollendorfer Hardt	dipmeter measurements	1998-09-04	2000-08-23
dobo040998.1	landslide si7	dipmeter measurements	1998-10-31	2000-08-23
dobo110998.1	landslide si7	dipmeter measurements	1998-10-31	1999-03-24
dobo201098.1	landslide si7	dipmeter measurements	1998-10-31	2000-08-23
dobo201098.2	landslide si7	dipmeter measurements	1998-10-31	1999-03-24
dobo040998.1	landslide si7	diver measurements	1999-01-21	1999-03-24
dobo110998.1	landslide si7	diver measurements	1999-01-21	2000-07-25
dobo270898.1	landslide si7	diver measurements	1999-01-21	2000-02-16
dobo270898.2	landslide si7	diver measurements	1999-01-21	2000-02-16
dobo201098.1	landslide si7	diver measurements	1999-01-21	2000-02-16
dobo201098.2	landslide si7	diver measurements	1999-01-21	2000-07-25
dobo180698.1	landslide si7	diver measurements	1999-03-24	2000-09-16
dobo190398.1	landslide si7	diver measurements	1999-03-31	2000-09-16
mebo010999.1	Melbtal	dipmeter measurements	1999-09-27	2000-08-17
mebo060999.1	Melbtal	dipmeter measurements	1999-09-27	2000-02-24
mebo070999.1	Melbtal	dipmeter measurements	1999-09-27	2000-02-05
mebo061099.1	Melbtal	dipmeter measurements	1999-10-08	2000-02-05
mebo071099.1	Melbtal	dipmeter measurements	1999-10-10	2000-02-24
mebo161299.1	Melbtal	dipmeter measurements	2000-01-14	2000-08-17
mebo061099.1	Melbtal	diver measurements	2000-01-14	2001-05-11
mebo070999.1	Melbtal	diver measurements	2000-01-14	2001-05-11
dobo110898.1	Dollendorfer Hardt	diver measurements	2000-02-16	2001-05-13
mebo060999.1	Melbtal	diver measurements	2000-02-24	2001-05-11
mebo071099.1	Melbtal	diver measurements	2000-02-24	2001-05-11
mebo160600.1	Melbtal	dipmeter measurements	2000-07-18	2000-08-17
dobo201098.2	landslide si7	diver measurements	2000-07-25	2001-05-13
dobo110998.1	landslide si7	diver measurements	2000-07-25	2001-05-13
dobo180698.1	landslide si7	diver measurements	2000-09-16	2001-05-04

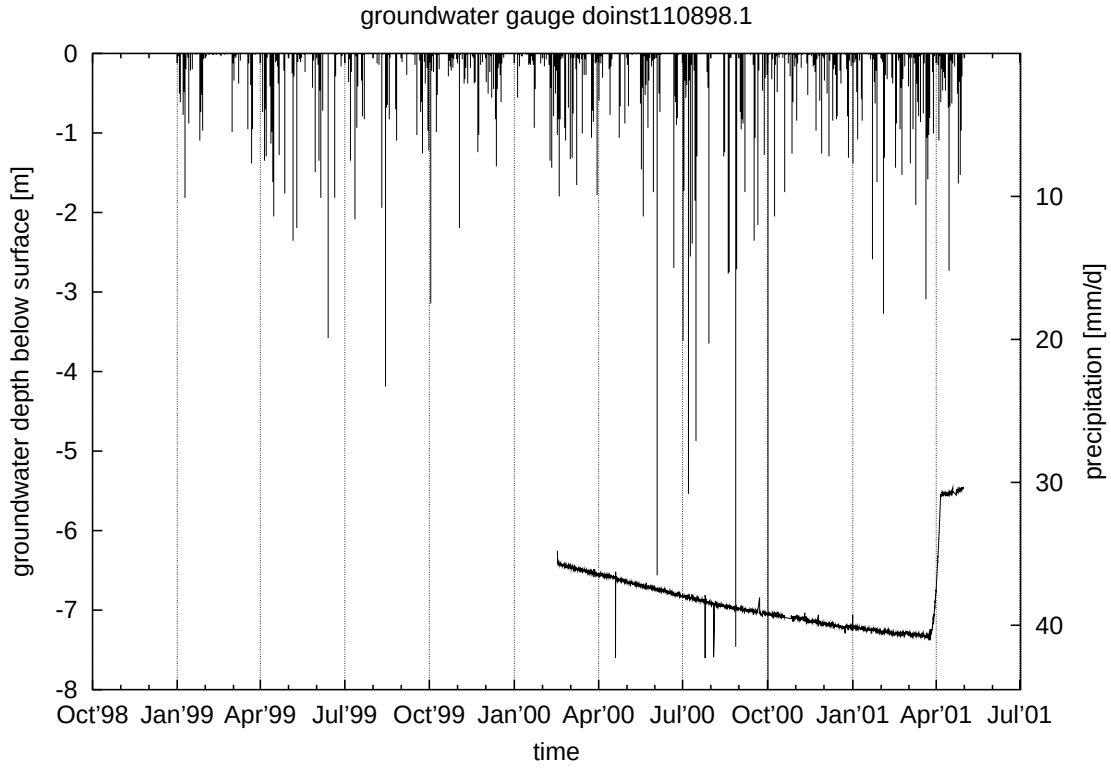
groundwater gauge doinst110898.1
groundwater depth below surface [m]
precipitation [mm/d]
0
-1
-2
-3
-4
-5
-6
-7
-8
10
20
30
40
Oct'98 Jan'99 Apr'99 Jul'99 Oct'99 Jan'00 Apr'00 Jul'00 Oct'00 Jan'01 Apr'01 Jul'01
time

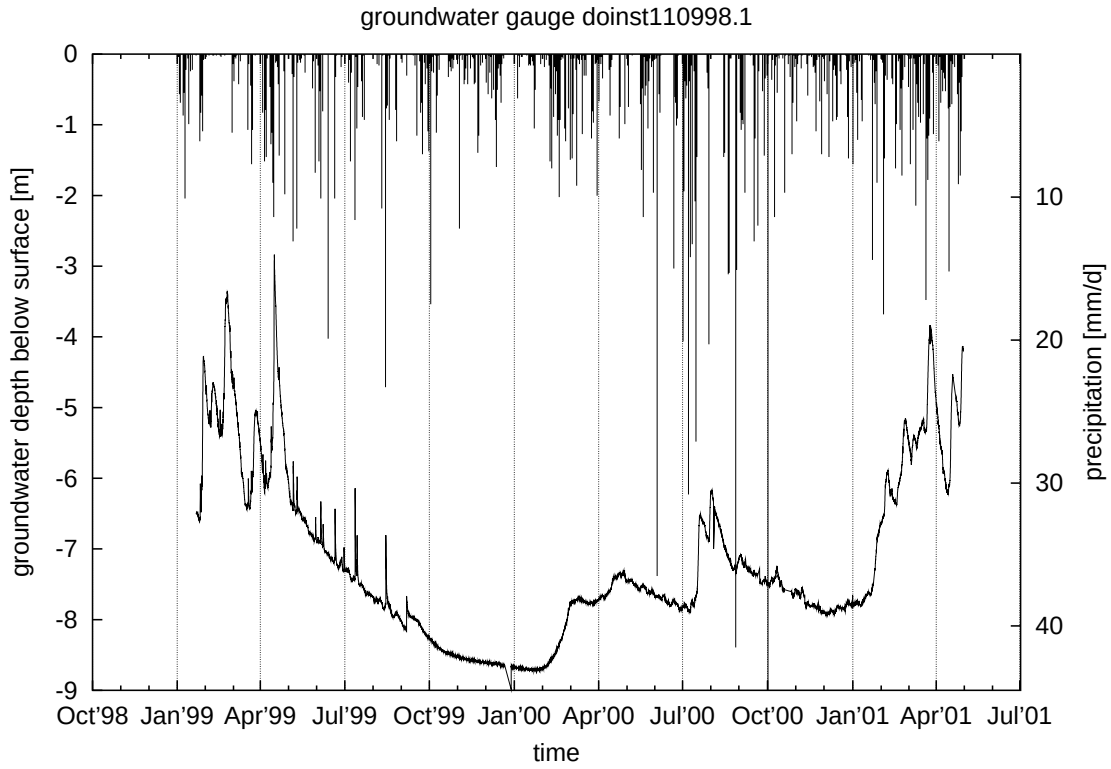
groundwater gauge doinst110998.1
groundwater depth below surface [m]
precipitation [mm/d]
0
-1
-2
-3
-4
-5
-6
-7
-8
-9
10
20
30
40
Oct'98 Jan'99 Apr'99 Jul'99 Oct'99 Jan'00 Apr'00 Jul'00 Oct'00 Jan'01 Apr'01 Jul'01
time

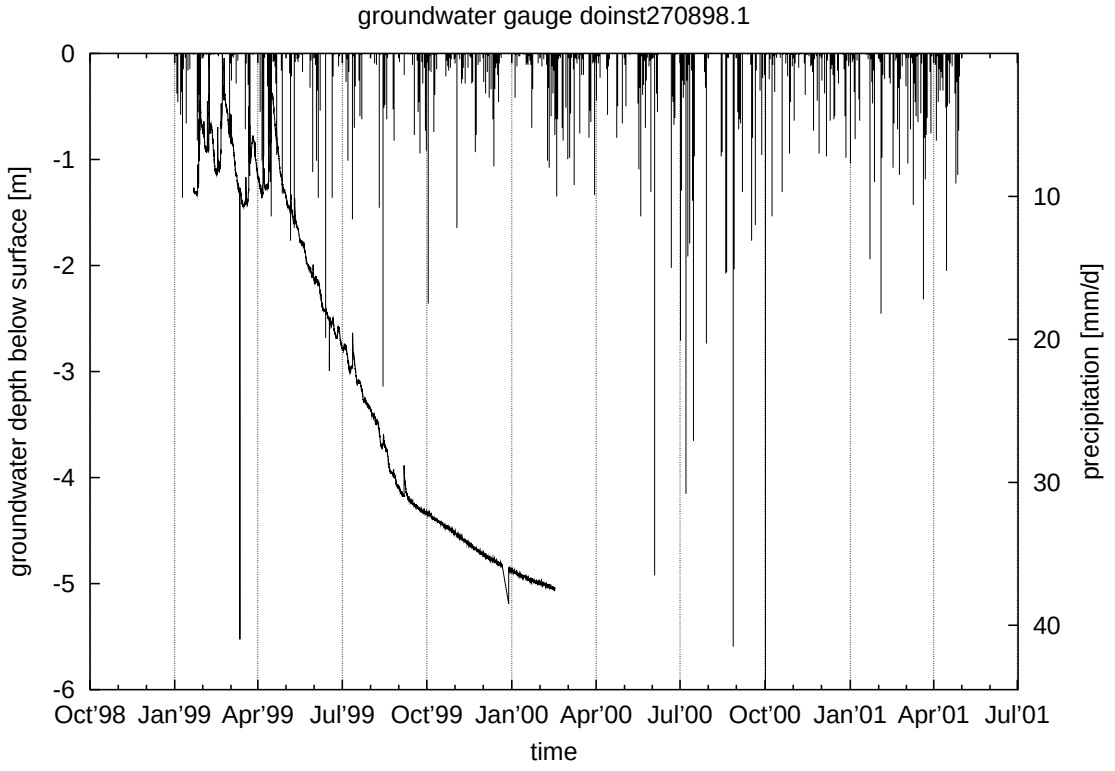
groundwater gauge doinst270898.1
groundwater depth below surface [m]
precipitation [mm/d]
0
-1
-2
-3
-4
-5
-6
10
20
30
40
Oct'98 Jan'99 Apr'99 Jul'99 Oct'99 Jan'00 Apr'00 Jul'00 Oct'00 Jan'01 Apr'01 Jul'01
time

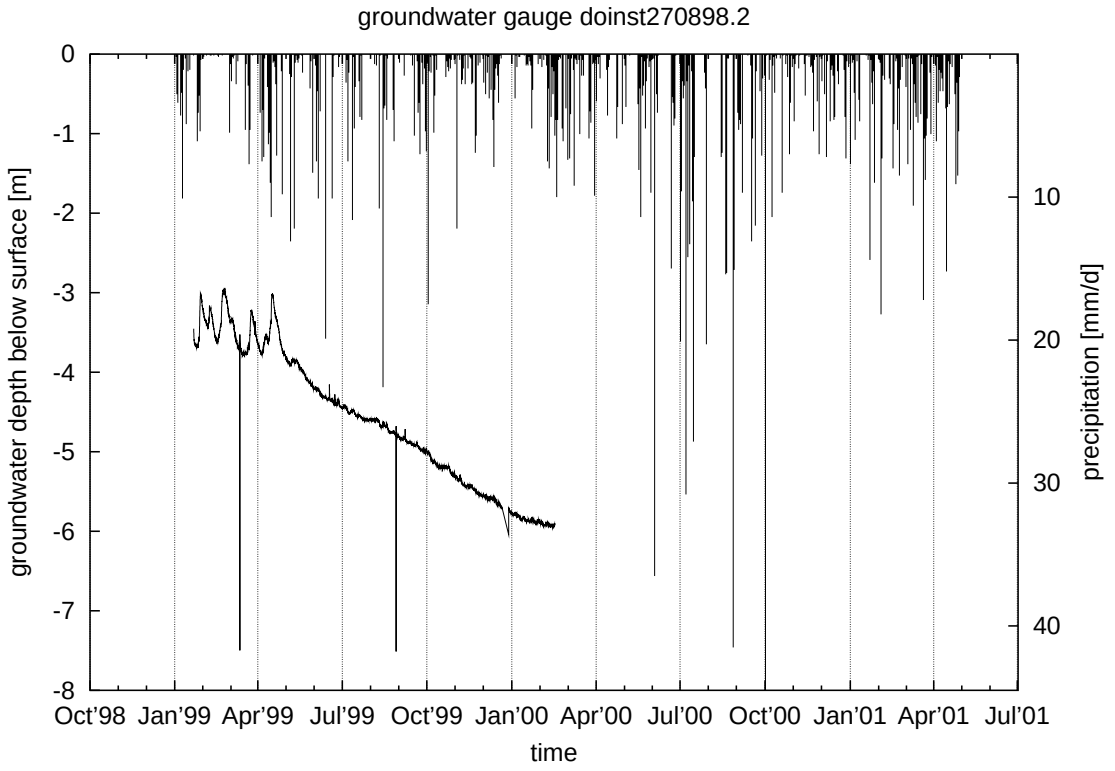
groundwater gauge doinst270898.2
groundwater depth below surface [m]
precipitation [mm/d]
0
-1
-2
-3
-4
-5
-6
-7
-8
10
20
30
40
Oct'98 Jan'99 Apr'99 Jul'99 Oct'99 Jan'00 Apr'00 Jul'00 Oct'00 Jan'01 Apr'01 Jul'01
time

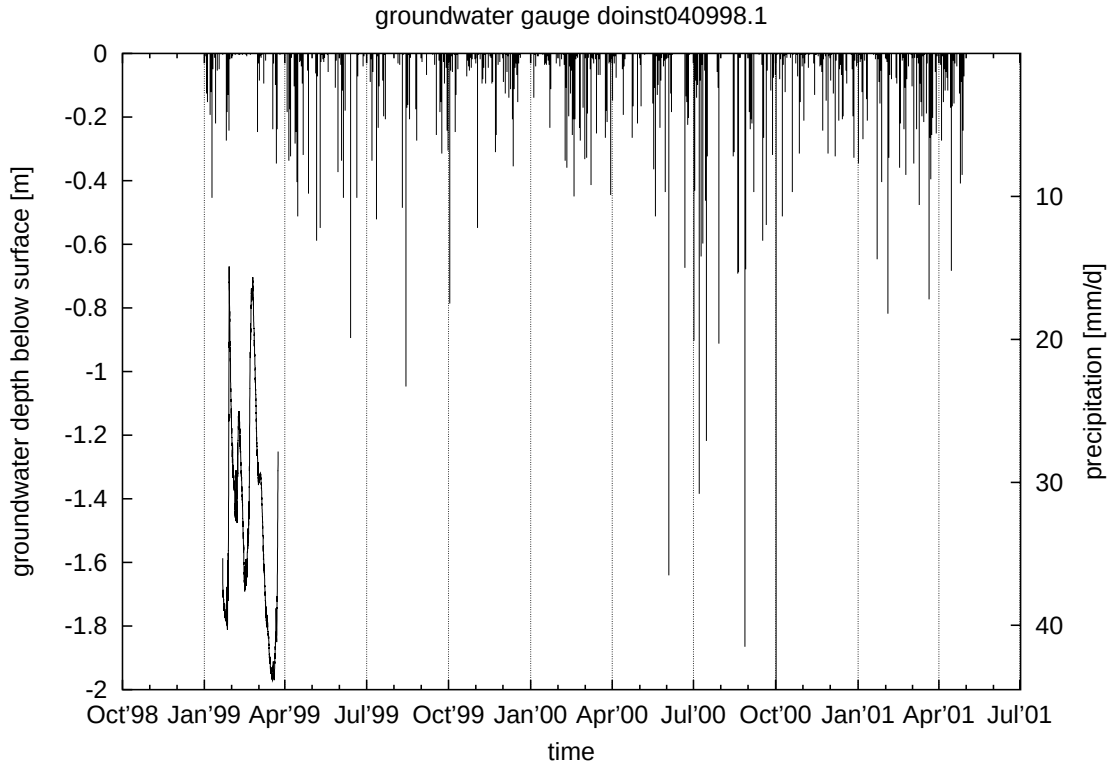
groundwater gauge doinst040998.1
groundwater depth below surface [m]
precipitation [mm/d]
0
-0.2
-0.4
-0.6
-0.8
-1
-1.2
-1.4
-1.6
-1.8
-2
10
20
30
40
Oct'98 Jan'99 Apr'99 Jul'99 Oct'99 Jan'00 Apr'00 Jul'00 Oct'00 Jan'01 Apr'01 Jul'01
time

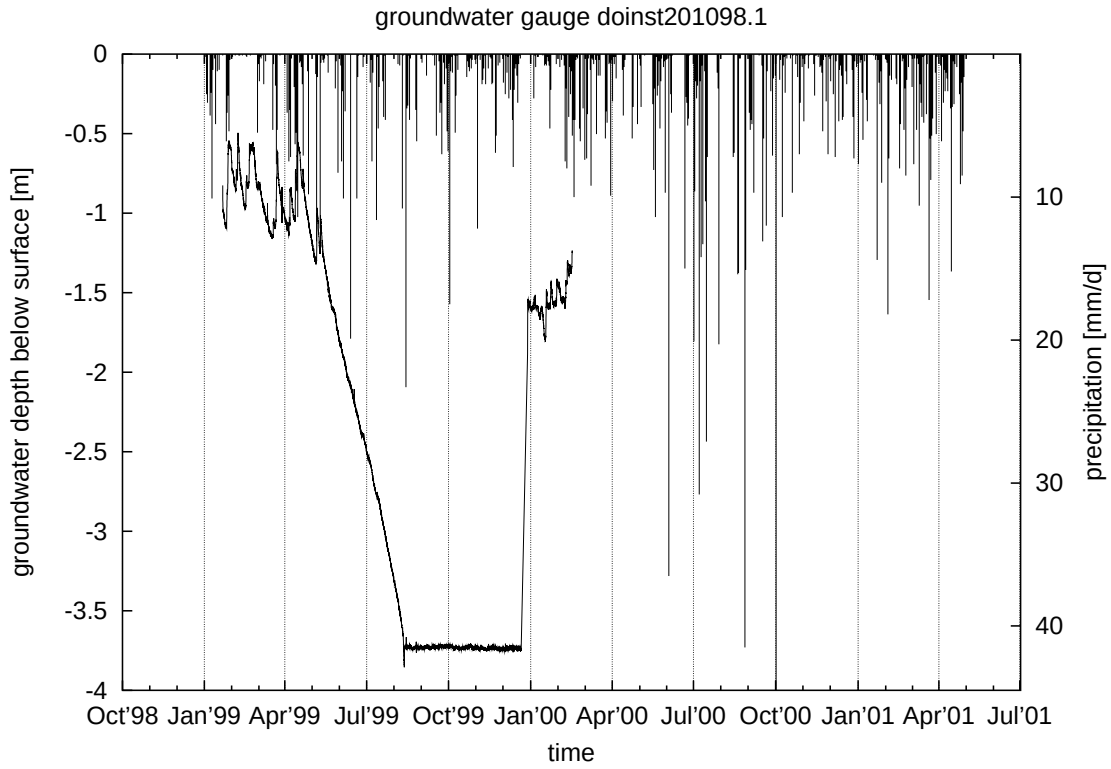
groundwater gauge doinst201098.1
groundwater depth below surface [m]
precipitation [mm/d]
0
-0.5
-1
-1.5
-2
-2.5
-3
-3.5
-4
10
20
30
40
Oct'98 Jan'99 Apr'99 Jul'99 Oct'99 Jan'00 Apr'00 Jul'00 Oct'00 Jan'01 Apr'01 Jul'01
time

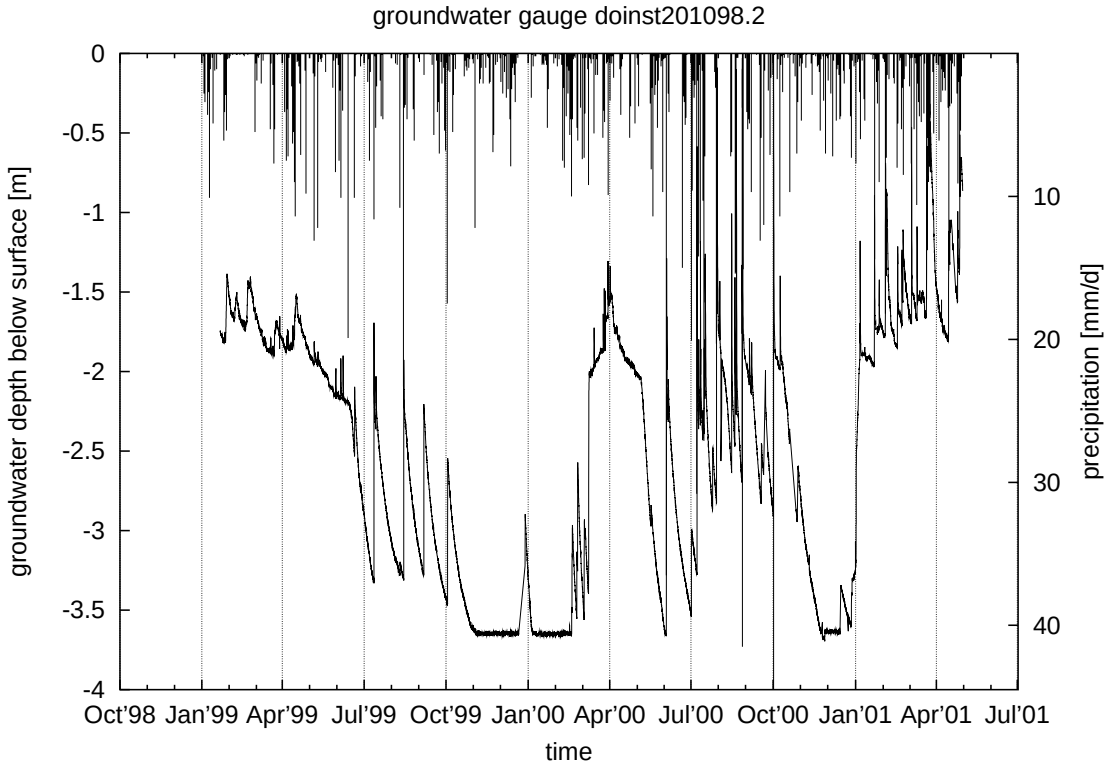
groundwater gauge doinst201098.2
groundwater depth below surface [m]
precipitation [mm/d]
0
-0.5
-1
-1.5
-2
-2.5
-3
-3.5
-4
10
20
30
40
Oct'98 Jan'99 Apr'99 Jul'99 Oct'99 Jan'00 Apr'00 Jul'00 Oct'00 Jan'01 Apr'01 Jul'01
time

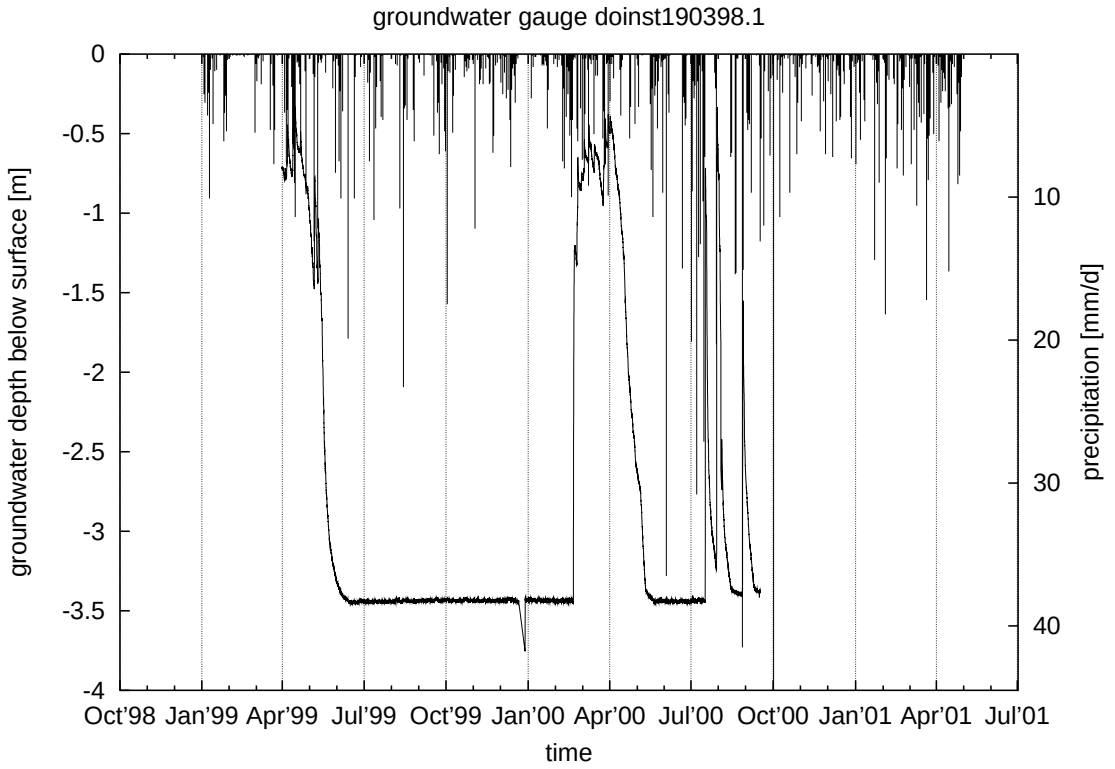
groundwater gauge doinst190398.1
groundwater depth below surface [m]
precipitation [mm/d]
0
-0.5
-1
-1.5
-2
-2.5
-3
-3.5
-4
10
20
30
40
Oct'98 Jan'99 Apr'99 Jul'99 Oct'99 Jan'00 Apr'00 Jul'00 Oct'00 Jan'01 Apr'01 Jul'01
time

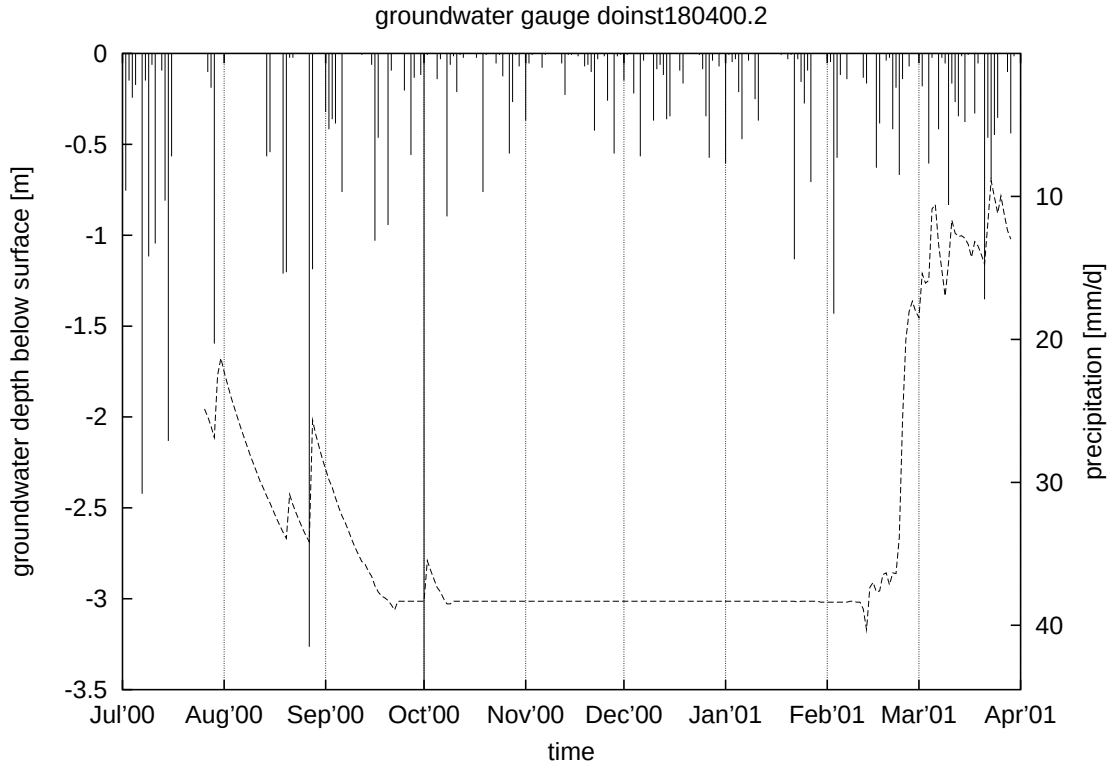
groundwater gauge doinst180400.2
groundwater depth below surface [m]
precipitation [mm/d]
0
-0.5
-1
-1.5
-2
-2.5
-3
-3.5
10
20
30
40
Jul'00
Aug'00
Sep'00
Oct'00
Nov'00
Dec'00
Jan'01
Feb'01
Mar'01
Apr'01
time

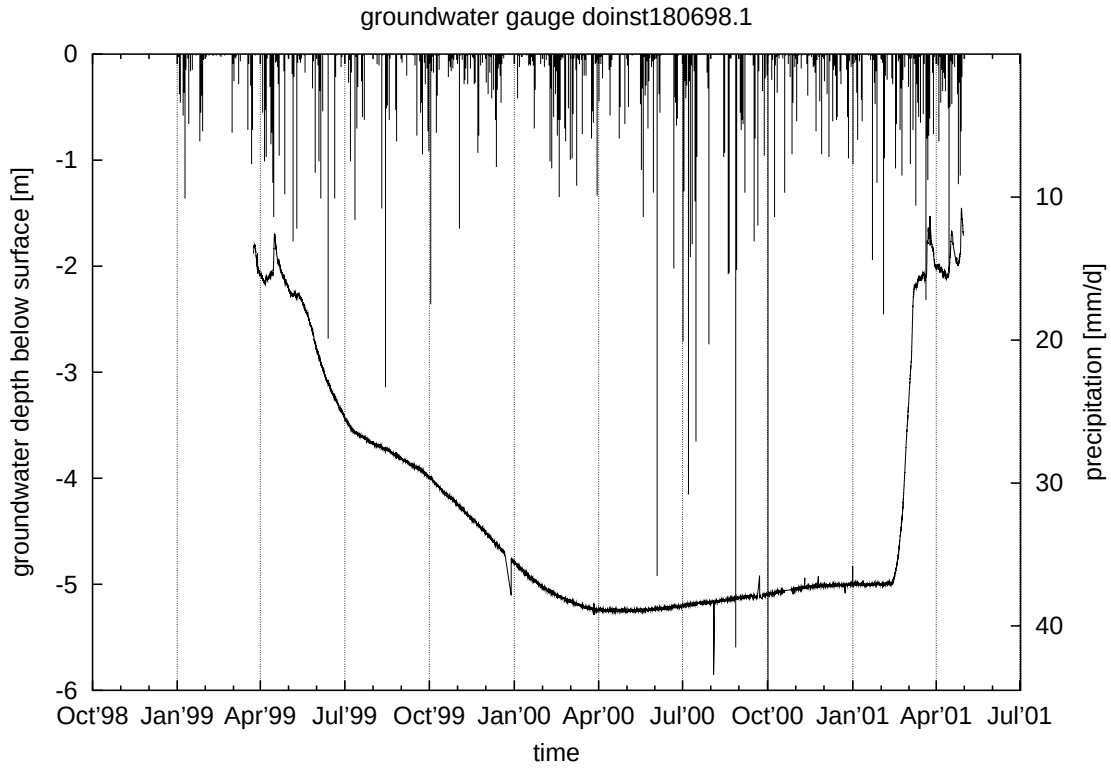
groundwater gauge doinst180698.1
groundwater depth below surface [m]
precipitation [mm/d]
0
-1
-2
-3
-4
-5
-6
10
20
30
40
Oct'98
Jan'99
Apr'99
Jul'99
Oct'99
Jan'00
Apr'00
Jul'00
Oct'00
Jan'01
Apr'01
Jul'01
time

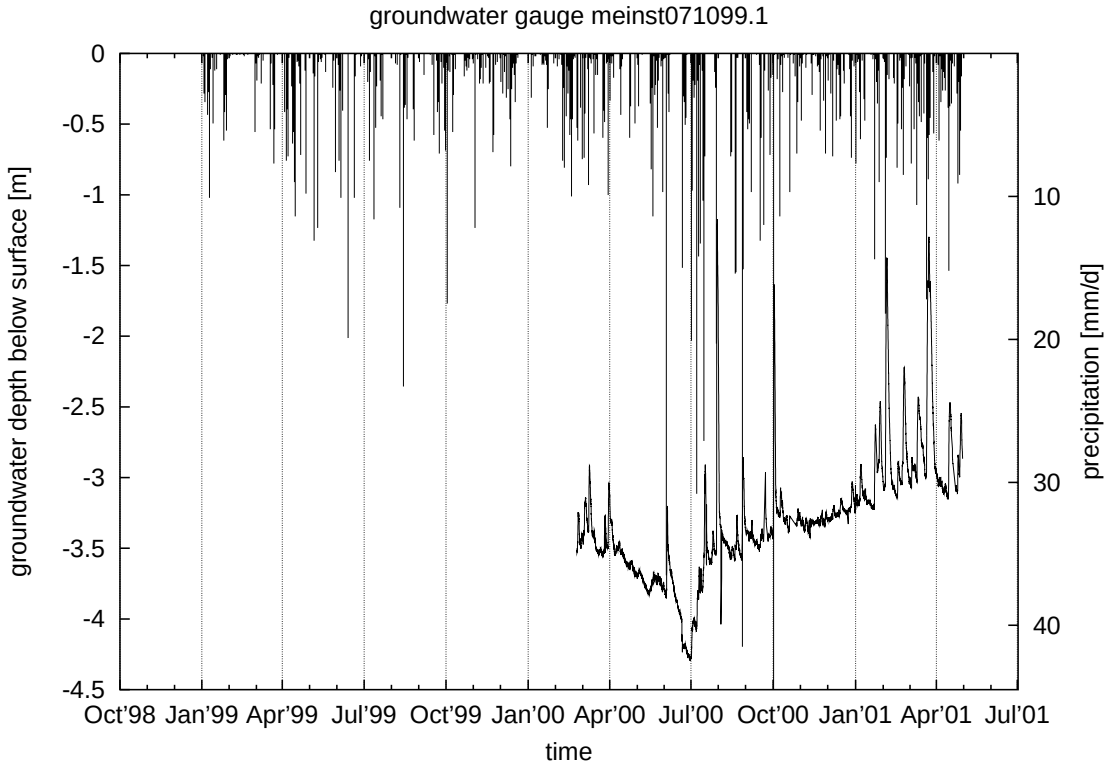
groundwater gauge meinst071099.1
groundwater depth below surface [m]
precipitation [mm/d]
0
-0.5
-1
-1.5
-2
-2.5
-3
-3.5
-4
-4.5
10
20
30
40
Oct'98 Jan'99 Apr'99 Jul'99 Oct'99 Jan'00 Apr'00 Jul'00 Oct'00 Jan'01 Apr'01 Jul'01
time

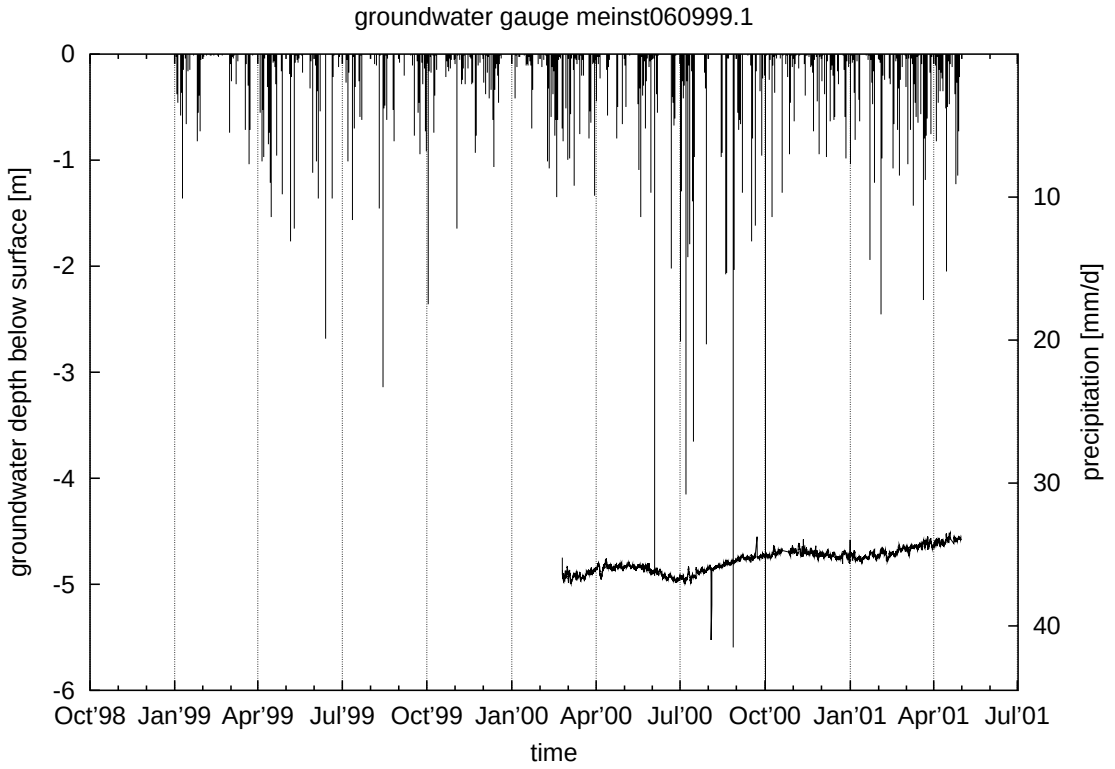
groundwater gauge meinst060999.1
groundwater depth below surface [m]
precipitation [mm/d]
0
-1
-2
-3
-4
-5
-6
10
20
30
40
Oct'98 Jan'99 Apr'99 Jul'99 Oct'99 Jan'00 Apr'00 Jul'00 Oct'00 Jan'01 Apr'01 Jul'01
time

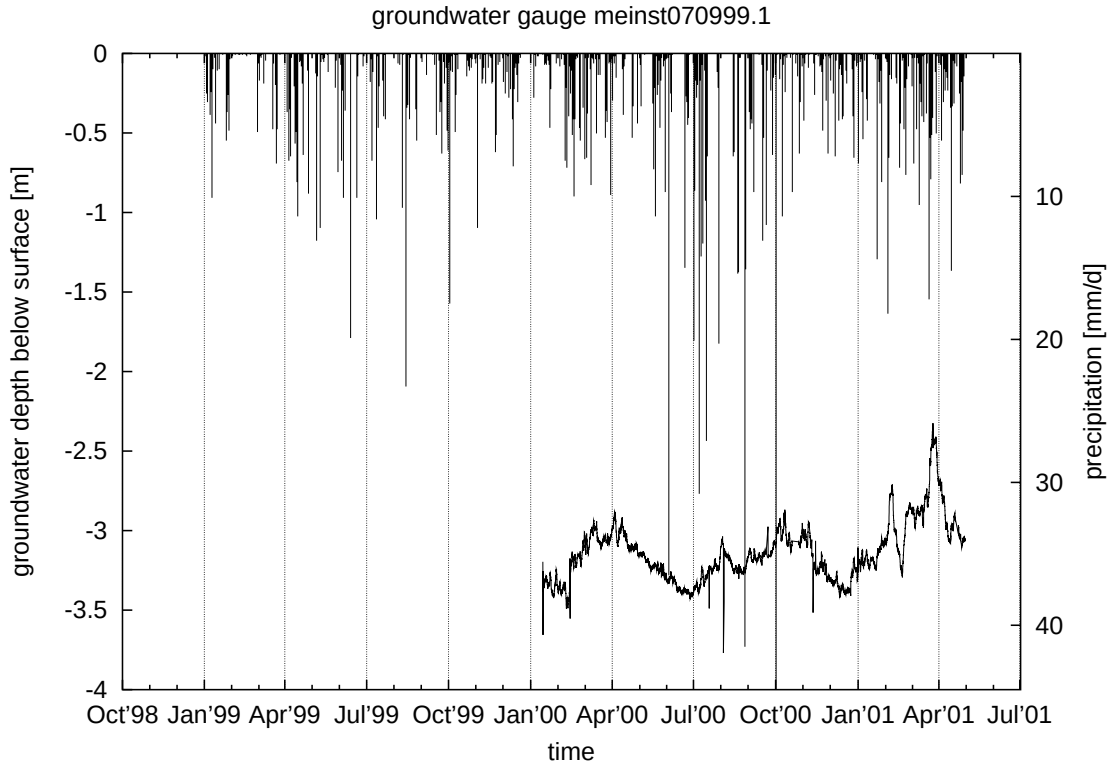
groundwater gauge meinst070999.1
groundwater depth below surface [m]
precipitation [mm/d]
0
-0.5
-1
-1.5
-2
-2.5
-3
-3.5
-4
10
20
30
40
Oct'98 Jan'99 Apr'99 Jul'99 Oct'99 Jan'00 Apr'00 Jul'00 Oct'00 Jan'01 Apr'01 Jul'01
time

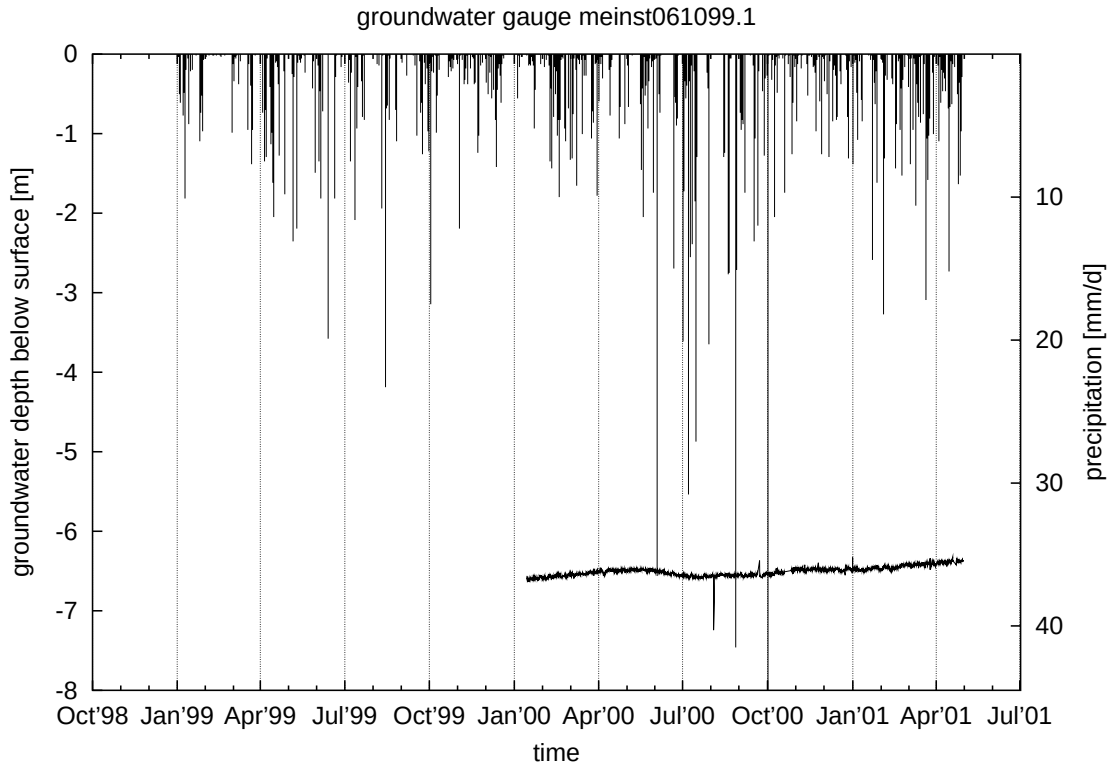
groundwater gauge meinst061099.1
groundwater depth below surface [m]
precipitation [mm/d]
0
-1
-2
-3
-4
-5
-6
-7
-8
10
20
30
40
Oct'98 Jan'99 Apr'99 Jul'99 Oct'99 Jan'00 Apr'00 Jul'00 Oct'00 Jan'01 Apr'01 Jul'01
time

C. Selected lab data

Listing: SQL–code for querying lab work from database. Shown is the query for number of experiments per experiment type and project.

```
SELECT max(e.name) AS "experiment_type", max(p.name) AS "project", count(l.id) AS "no_of_exps."
FROM lab l, experiment e, project p
WHERE l.exp_id=e.id AND l.proj_id=p.id
GROUP BY e.id, p.id
ORDER BY max(e.name);
```

List of lab work. Shown is the number of experiments per experiment type and project.

experiment type	project	no of exps.
bulk density	subproject B13, SFB350	332
bulk density	masters thesis R. Gerstenberger	2
bulk density	masters thesis T. May	11
bulk density	field seminar (SS 99)	19
bulk density	lab seminar (WS 97/98)	8
chalk content	subproject B13, SFB350	6
ignition loss	subproject B13, SFB350	51
lab vane test	subproject B13, SFB350	10
lab vane test	lab seminar (WS 97/98)	19
liquid limit	subproject B13, SFB350	256
liquid limit	masters thesis M. Gumpert	20
liquid limit	masters thesis H. Ingenpass	24
liquid limit	lab seminar (WS 97/98)	29
maximum water content (Enslin)	subproject B13, SFB350	27
maximum water content (Enslin)	masters thesis H. Ingenpass	15
moisture content	subproject B13, SFB350	291
moisture content	subproject B9, SFB350	35
moisture content	masters thesis M. Gumpert	4
moisture content	masters thesis H. Ingenpass	57
moisture content	masters thesis T. May	9
organic content (Lichterfeld)	subproject B13, SFB350	26
organic content (Lichterfeld)	masters thesis M. Gumpert	17
particle density (pycnometer)	subproject B13, SFB350	22
particle density (pycnometer)	masters thesis H. Ingenpass	89
particle density (pycnometer)	lab seminar (WS 97/98)	8
particle size (hydrometer method)	subproject B13, SFB350	17
particle sizes (pipette method)	subproject B13, SFB350	285
particle sizes (pipette method)	masters thesis M. Gumpert	32
particle sizes (pipette method)	masters thesis S. Holler	26
particle sizes (pipette method)	lab seminar (WS 97/98)	8
permeability (constant head)	subproject B13, SFB350	72
permeability (constant head)	masters thesis M. Gumpert	8

continued on next page

continued from previous page		
experiment type	project	no of exps.
permeability (falling head)	subproject B13, SFB350	41
plastic limit	subproject B13, SFB350	225
plastic limit	masters thesis M. Gumpert	12
plastic limit	masters thesis H. Ingenpass	12
plastic limit	lab seminar (WS 97/98)	29
pocket penetration test	subproject B13, SFB350	26
pocket vane test	subproject B13, SFB350	26
shear box test	subproject B13, SFB350	62
shear box test	masters thesis R. Gerstenberger	29
shear box test	masters thesis H. Ingenpass	57
shear box test	lab seminar (WS 97/98)	3
soil classification	subproject B13, SFB350	72
soil classification	subproject B9, SFB350	1
soil classification	masters thesis M. Gumpert	5
soil classification	masters thesis S. Holler	106
soil classification	masters thesis T. May	16
soil classification	field seminar (SS 99)	23
soil classification	Geologic mapping (Bichler 2001)	142
triaxial test	subproject B13, SFB350	22
unsaturated conductivity	subproject B13, SFB350	18

C.1. Particle size distribution

Pipette method

Listing: SQL–code querying grainsize results (pipette method) from database.

```
SELECT so.sample_id AS sample,f.field_id AS field,
%(100*COALESCE((so.upperdepth+so.lowerdepth)/2,so.upperdepth,so.lowerdepth)) AS "d_[cm]",
%(100*(coalesce(((vorabsieb-nachabsieb)/vorabsieb),0)+(coalesce((nachabsieb/vorabsieb),1)*(gbrutto-gtara)/
((coalesce(gbrutto,0)+gSbrutto+mSbrutto+fSbrutto-coalesce(gtara,0)-gStara-mStara-fStara)+
((gUbrutto-gUtara-(26.69*phosphat*pipsize/(schlaemmvol^2)))*schlaemmvol/pipsize)))))/100 AS "G",
%(100*(coalesce((nachabsieb/vorabsieb),1)*(gSbrutto-gStara)/((coalesce(gbrutto,0)+gSbrutto+mSbrutto+
fSbrutto-coalesce(gtara,0)-gStara-mStara-fStara)+((gUbrutto-gUtara-(26.69*phosphat*pipsize/(schlaemmvol^2)))
*schlaemmvol/pipsize))))/100 AS "gS",
%(100*(coalesce((nachabsieb/vorabsieb),1)*(mSbrutto-mStara)/((coalesce(gbrutto,0)+
gSbrutto+mSbrutto+fSbrutto-coalesce(gtara,0)-gStara-mStara-fStara)+((gUbrutto-gUtara-
(26.69*phosphat*pipsize/(schlaemmvol^2)))*schlaemmvol/pipsize))))/100 AS "mS",
%(100*(coalesce((nachabsieb/vorabsieb),1)*(fSbrutto-fStara)/
((coalesce(gbrutto,0)+gSbrutto+mSbrutto+fSbrutto-coalesce(gtara,0)-gStara-mStara-fStara)+
((gUbrutto-gUtara-(26.69*phosphat*pipsize/(schlaemmvol^2)))*schlaemmvol/pipsize))))/100 AS "fS",
%(100*coalesce((nachabsieb/vorabsieb),1)*((gUbrutto-gUtara-mUbrutto+mUtara)*schlaemmvol/pipsize)/
((coalesce(gbrutto,0)+gSbrutto+mSbrutto+fSbrutto-coalesce(gtara,0)-gStara-mStara-fStara)+
((gUbrutto-gUtara-(26.69*phosphat*pipsize/(schlaemmvol^2)))*schlaemmvol/pipsize)))/100 AS "gU",
%(100*(coalesce((nachabsieb/vorabsieb),1)*((mUbrutto-mUtara-fUbrutto+fUtara)*schlaemmvol/pipsize)/
((coalesce(gbrutto,0)+gSbrutto+mSbrutto+fSbrutto-coalesce(gtara,0)-gStara-mStara-fStara)+
((gUbrutto-gUtara-(26.69*phosphat*pipsize/(schlaemmvol^2)))*schlaemmvol/pipsize))))/100 AS "mU",
%(100*(coalesce((nachabsieb/vorabsieb),1)*((fUbrutto-fUtara-tbrutto+ttara)*
schlaemmvol/pipsize)/((coalesce(gbrutto,0)+gSbrutto+mSbrutto+fSbrutto-
coalesce(gtara,0)-gStara-mStara-fStara)+((gUbrutto-gUtara-(26.69*phosphat*pipsize/(schlaemmvol^2)))*
schlaemmvol/pipsize))))/100 AS "fU",
%(100*(coalesce((nachabsieb/vorabsieb),1)*((tbrutto-ttara-(26.69*phosphat*pipsize/(schlaemmvol^2)))
*schlaemmvol/pipsize)/((coalesce(gbrutto,0)+gSbrutto+mSbrutto+fSbrutto-coalesce(gtara,0)
-gStara-mStara-fStara)+((gUbrutto-gUtara-(26.69*phosphat*pipsize/(schlaemmvol^2)))
*schlaemmvol/pipsize))))/100 AS "T",
%(-100+100*((coalesce(gbrutto,0)+gSbrutto+mSbrutto+fSbrutto-coalesce(gtara,0)-gStara-mStara-fStara)+
((gUbrutto-gUtara-(26.69*phosphat*pipsize/(schlaemmvol^2)))*schlaemmvol/pipsize))/einwaage)/100.0 AS "error"
FROM sedgrainsize s,lab l ,soilsample so, field f
WHERE s.lab_id = l.id AND l.sample_id=so.id AND so.field_id=f.id
AND s.tbrutto<>"

UNION

SELECT f.field_id AS outcrop, so.sample_id AS sample,
%(100*COALESCE((so.upperdepth+so.lowerdepth)/2,so.upperdepth,so.lowerdepth)) AS "d_[cm]",
 %(100*g.value)/100.0 AS G,
 %(100*(gs.value))/100.0 AS gS,
 %(100*(ms.value))/100.0 AS mS,
 %(100*(fs.value))/100.0 AS fS,
 %(100*(gu.value))/100.0 AS gU,
 %(100*(mu.value))/100.0 AS mU,
 %(100*(fu.value))/100.0 AS fU,
 %(100*t.value)/100.0 AS T,
 " AS error
FROM labvalue g, labvalue gs, labvalue ms, labvalue fs, labvalue gu, labvalue mu, labvalue fu, labvalue t,
lab l, soilsample so, field f
WHERE g.lab_id=l.id AND gs.lab_id=l.id AND ms.lab_id=l.id AND fs.lab_id=l.id AND gu.lab_id=l.id
AND mu.lab_id=l.id AND fu.lab_id=l.id AND t.lab_id=l.id AND l.sample_id=so.id AND so.field_id=f.id
AND g.par_id=20 AND gs.par_id=26 AND ms.par_id=25 AND fs.par_id=24 AND gu.par_id=23
AND mu.par_id=22 AND fu.par_id=21 AND t.par_id=17

ORDER BY field,sample,"d_[cm]";
```

Results of laboratory experiments for particle size determination (pipette method). Calculated values per lab experiment. Particle size fractions and errors are shown relative to [1].

sample	field	d [cm]	G	gS	mS	fS	gU	mU	fU	T	error
doauf020498.1.020400.3	doauf020498.1	25	0	0	0.01	0	0.12	0.23	0.2	0.41	-0.02
doauf020498.1.1	doauf020498.1	25	0.01	0	0.01	0.04	0.11	0.2	0.18	0.4	-0
doauf020498.1.160900.1	doauf020498.1	25	0.02	0.01	0.01	0.04	0.1	0.19	0.19	0.39	-0.01
doauf020498.2.1	doauf020498.2	35	0	0.01	0.06	0.11	0.16	0.16	0.14	0.32	-0.02
doauf020498.2.160900.1	doauf020498.2	35	0.02	0.02	0.03	0.07	0.12	0.15	0.18	0.37	-0.01
doauf020498.3.1	doauf020498.3	55	0	0	0	0.01	0.09	0.29	0.11	0.46	-0
doauf180898.1.160300.1	doauf180898.1	35	0	0	0.11	0.45	0.11	0.04	0.02	0.22	-0.01
doauf180898.1.160300.1	doauf180898.1	35	0	0	0.12	0.45	0.1	0.04	0.03	0.23	-0.01
doauf180898.1.160300.1	doauf180898.1	35	0	0.01	0.19	0	0.22	0.08	0.05	0.41	-0.42
doauf180898.1.160900.1	doauf180898.1	35	0	0.02	0.02	0.26	0.14	0.06	0.05	0.41	-0.04
doauf240398.1.1g	doauf240398.1	50	0	0	0.01	0.01	0.1	0.26	0.07	0.52	-0.05
doauf240398.1.2g	doauf240398.1	50	0	0	0	0.01	0.07	0.23	0.15	0.51	-0.03
doauf240398.1.3g	doauf240398.1	50	0.01	0.01	0.02	0.02	0.05	0.17	0.12	0.57	-0.07
doauf240398.2.10	doauf240398.2	5	0	0.04	0.11	0.21	0.13	0.15	0.13	0.2	-0.1
doauf240398.2.160900.1	doauf240398.2	675	0.1	0.19	0.19	0.1	0.06	0.13	0.09	0.1	-0.06
doauf240398.2.1g	doauf240398.2	675	0.02	0.15	0.19	0.12	0.08	0.14	0.12	0.15	-0
doauf240398.2.2g	doauf240398.2	675	0.02	0.13	0.21	0.12	0.08	0.14	0.09	0.16	-0
doauf240398.2.3g	doauf240398.2	675	0.01	0.05	0.11	0.17	0.1	0.15	0.12	0.25	-0.02
doauf240398.2.4g	doauf240398.2	675	0.02	0.12	0.22	0.12	0.09	0.14	0.09	0.16	0
doauf240398.2.5g	doauf240398.2	675	0.01	0.05	0.1	0.17	0.11	0.15	0.11	0.25	-0.02
doauf240398.2.6g	doauf240398.2	675	0.01	0.06	0.18	0.15	0.08	0.14	0.07	0.27	-0.01
doauf020498.4.1	doauf240398.3	55	0	0	0	0.04	0.12	0.1	0.13	0.59	0.01
doauf240398.3.160900.1	doauf240398.3	55	0	0	0	0.06	0.1	0.11	0.11	0.6	-0.09
doauf240398.3.1g	doauf240398.3	55	0	0	0.01	0.06	0.1	0.11	0.11	0.58	-0.02
doauf240398.3.2g	doauf240398.3	55	0	0	0	0.06	0.15	0.18	0.13	0.46	-0.01
doauf290998.1.160900.1	doauf290998.1	35	0	0	0	0.21	0.22	0.16	0.08	0.29	-0.07
dobo030998.1.1	dobo030998.1	85	0	0.01	0.03	0.06	0.07	0.09	0.1	0.6	-0.01
dobo030998.1.1	dobo030998.1	85	0.02	0.02	0.03	0.04	0.09	0.13	0.12	0.52	-0.08
dobo030998.1.2	dobo030998.1	104	0	0.01	0.01	0.04	0.26	0.23	0.1	0.3	-0.05
dobo030998.1.3	dobo030998.1	184	0	0.01	0.03	0.05	0.12	0.13	0.11	0.52	-0.06
dobo030998.1.4	dobo030998.1	295	0.01	0.02	0.03	0.07	0.15	0.12	0.09	0.47	-0.03
dobo030998.1.5	dobo030998.1	375	0	0.03	0.05	0.06	0.1	0.11	0.09	0.52	-0.04
dobo040998.1.1	dobo040998.1	72	0.04	0.04	0.07	0.09	0.23	0.19	0.04	0.25	-0
dobo040998.1.2	dobo040998.1	172	0.01	0.09	0.11	0.12	0.14	0.14	0.14	0.21	-0.01
dobo040998.1.3	dobo040998.1	372	0.04	0.06	0.11	0.1	0.2	0.15	0.1	0.21	-0.06
dobo040998.1.4	dobo040998.1	472	0	0	0	0.06	0.14	0.16	0.13	0.46	-0
dobo040998.1.5	dobo040998.1	497	0	0	0.01	0.07	0.18	0.18	0.18	0.34	-0
dobo050400.1.1	dobo050400.1	55	0.03	0.03	0.06	0.1	0.12	0.16	0.13	0.31	-0.11
dobo050400.1.2	dobo050400.1	85	0	0.02	0.06	0.08	0.08	0.12	0.14	0.46	-0.06
dobo050400.1.3	dobo050400.1	134	0	0.05	0.06	0.08	0.11	0.16	0.13	0.39	-0.11
dobo050400.1.4	dobo050400.1	165	0.03	0.07	0.13	0.11	0.08	0.11	0.12	0.31	-0.07
dobo050400.1.5	dobo050400.1	195	0	0.02	0.05	0.09	0.1	0.13	0.13	0.44	-0.05
dobo050400.1.6	dobo050400.1	234	0	0.04	0.06	0.1	0.13	0.15	0.13	0.36	-0.13
dobo050400.1.7	dobo050400.1	275	0.01	0.02	0.06	0.08	0.13	0.17	0.16	0.33	-0.11
dobo050400.1.8	dobo050400.1	295	0	0.01	0.02	0.06	0.15	0.1	0.09	0.53	-0.07
dobo050400.1.9	dobo050400.1	384	0.01	0.01	0.02	0.07	0.17	0.13	0.09	0.46	-0.04
dobo050698.1.1	dobo050698.1	150	0	0	0	0.08	0.14	0.19	0.15	0.41	-0.03
dobo050698.1.2	dobo050698.1	284	0	0	0	0.19	0.33	0.17	0.05	0.21	-0.02
dobo050698.2.1	dobo050698.2	122	0	0.02	0.04	0.1	0.32	0.17	0.07	0.24	-0.04
dobo050698.2.2	dobo050698.2	270	0	0	0	0.06	0.18	0.17	0.07	0.5	-0.02
dobo110898.1.1	dobo110898.1	75	0.02	0	0.01	0.06	0.29	0.16	0.06	0.37	-0.01
dobo110898.1.2	dobo110898.1	115	0	0.01	0.03	0.1	0.34	0.16	0.07	0.25	0
dobo110898.1.3	dobo110898.1	195	0	0	0	0.02	0.16	0.2	0.11	0.48	0
dobo110898.1.3	dobo110898.1	195	0	0	0	0.03	0.16	0.19	0.1	0.5	-0.06
dobo110898.1.4	dobo110898.1	385	0	0	0	0.52	0.24	0.05	0.03	0.13	-0.01
dobo110898.1.5	dobo110898.1	455	0	0	0	0.12	0.4	0.16	0.05	0.23	-0.03
dobo110898.1.6	dobo110898.1	705	0	0	0	0	0.01	0.02	0.06	0.89	-0.12
dobo110898.2.1	dobo110898.2	134	0	0.01	0.03	0.08	0.22	0.18	0.09	0.36	-0.04
dobo110898.2.1	dobo110898.2	134	0	0.04	0.05	0.11	0.25	0.16	0.08	0.28	-0.12
dobo110898.2.2	dobo110898.2	225	0	0	0	0	0.01	0.03	0.05	0.88	0
dobo110898.2.2	dobo110898.2	225	0	0	0	0.03	0.06	0.13	0.12	0.64	-0.07

continued on next page

continued from previous page

sample	field	d [cm]	G	gS	mS	fS	gU	mU	fU	T	error
dobo110898.2.3	dobo110898.2	295	0	0	0	0.07	0.16	0.18	0.11	0.44	-0.01
dobo110898.2.4	dobo110898.2	345	0	0	0	0.07	0.18	0.24	0.16	0.31	-0
dobo110898.2.4	dobo110898.2	345	0	0	0.01	0.14	0.19	0.22	0.14	0.28	-0
dobo110898.2.5	dobo110898.2	395	0	0	0.08	0.01	0.16	0.18	0.11	0.42	-0.04
dobo110998.1.1	dobo110998.1	154	0.04	0.08	0.15	0.13	0.07	0.12	0.13	0.23	-0.05
dobo110998.1.2	dobo110998.1	309	0	0	0	0	0.04	0.13	0.25	0.55	-0
dobo110998.1.2	dobo110998.1	309	0	0	0	0.06	0.17	0.19	0.17	0.38	-0.09
dobo110998.1.3	dobo110998.1	485	0.5	0.05	0.06	0.06	0.06	0.05	0.05	0.14	-0.03
dobo110998.1.4	dobo110998.1	655	0	0	0.01	0.13	0.19	0.14	0.13	0.36	-0.02
dobo110998.1.5	dobo110998.1	760	0.02	0.01	0.02	0.03	0.05	0.18	0.17	0.49	-0.09
dobo110998.1.6	dobo110998.1	844	0.32	0.1	0.18	0.19	0.03	0.03	0.03	0.08	-0.05
dobo110998.1.7	dobo110998.1	885	0.02	0.02	0.03	0.06	0.09	0.14	0.14	0.45	-0.02
dobo110998.1.8	dobo110998.1	989	0	0	0	0.04	0.14	0.21	0.16	0.43	-0.05
dobo120898.1.1	dobo120898.1	55	0	0.04	0.04	0.09	0.33	0.15	0.08	0.23	-0.03
dobo120898.1.2	dobo120898.1	175	0	0.01	0.01	0.07	0.27	0.15	0.06	0.4	-0.02
dobo120898.1.3	dobo120898.1	254	0	0	0	0.03	0.13	0.17	0.14	0.49	-0.04
dobo120898.1.4	dobo120898.1	365	0	0.02	0	0.03	0.08	0.1	0.13	0.6	-0.03
dobo120898.1.5	dobo120898.1	384	0	0	0	0	0.13	0.22	0.23	0.4	0.01
dobo120898.1.6	dobo120898.1	414	0	0	0	0.01	0.18	0.27	0.17	0.34	-0
dobo120898.1.7	dobo120898.1	455	0	0	0.02	0.63	0.15	0.03	0.02	0.1	-0.03
dobo130898.1.1	dobo130898.1	104	0	0.05	0.05	0.13	0.28	0.18	0.08	0.2	-0.08
dobo130898.1.1	dobo130898.1	104	0	0.09	0.1	0.1	0.24	0.18	0.07	0.19	-0.04
dobo130898.1.2	dobo130898.1	215	0.01	0	0.02	0.04	0.08	0.24	0.13	0.44	-0.05
dobo130898.1.3	dobo130898.1	245	0	0	0	0.02	0.07	0.09	0.12	0.66	0
dobo130898.1.4	dobo130898.1	265	0	0	0	0.03	0.08	0.09	0.12	0.65	-0.01
dobo130898.1.5	dobo130898.1	334	0	0	0	0	0.05	0.15	0.1	0.68	0.01
dobo130898.1.5	dobo130898.1	334	0	0	0	0	0.06	0.21	0.15	0.55	-0.06
dobo130898.1.6	dobo130898.1	455	0	0	0	0.09	0.3	0.28	0.11	0.19	-0.05
dobo130898.1.7	dobo130898.1	514	0	0	0	0.03	0.08	0.16	0.2	0.5	-0.07
dobo130898.1.8	dobo130898.1	555	0	0.15	0.12	0.09	0.17	0.18	0.14	0.12	-0.04
dobo180400.1.1	dobo180400.1	55	0.05	0.04	0.09	0.12	0.1	0.11	0.11	0.34	-0.01
dobo180400.1.2	dobo180400.1	80	0.01	0.01	0.05	0.09	0.07	0.1	0.11	0.52	-0.05
dobo180400.1.3	dobo180400.1	145	0	0	0.08	0.16	0.1	0.09	0.11	0.42	-0.06
dobo180400.1.4	dobo180400.1	195	0.01	0	0	0	0.11	0.1	0.14	0.61	-0.07
dobo180400.1.5	dobo180400.1	240	0	0	0.01	0	0.12	0.1	0.12	0.61	-0.07
dobo180400.1.6	dobo180400.1	259	0.02	0.02	0.02	0	0.09	0.16	0.15	0.51	-0.13
dobo180400.1.7	dobo180400.1	284	0	0.01	0.01	0	0.16	0.14	0.12	0.51	0
dobo180400.1.8	dobo180400.1	375	0	0	0	0	0.14	0.29	0.21	0.32	-0.01
dobo180698.1.1	dobo180698.1	319	0	0.01	0.05	0.07	0.09	0.11	0.11	0.53	-0.03
dobo190398.1.10	dobo190398.1	247	0.04	0.04	0.12	0.13	0.06	0.09	0.08	0.4	-0.03
dobo190398.1.11	dobo190398.1	254	0.01	0.02	0.02	0.05	0.19	0.24	0.16	0.28	-0
dobo190398.1.12	dobo190398.1	275	0	0	0.01	0.06	0.1	0.14	0.13	0.52	-0.02
dobo190398.1.13	dobo190398.1	325	0	0.02	0.02	0.04	0.17	0.27	0.15	0.29	-0.02
dobo190398.1.14	dobo190398.1	345	0.02	0.04	0.03	0.03	0.1	0.26	0.17	0.29	0
dobo190398.1.1t	dobo190398.1	55	0.01	0.12	0.2	0.14	0.09	0.1	0.08	0.23	-0.01
dobo190398.1.2	dobo190398.1	75	0.01	0.09	0.19	0.16	0.07	0.11	0.11	0.22	-0.01
dobo190398.1.3	dobo190398.1	94	0.02	0.08	0.17	0.17	0.08	0.13	0.09	0.22	-0
dobo190398.1.4	dobo190398.1	104	0	0	0.05	0.19	0.09	0.12	0.11	0.4	-0.02
dobo190398.1.5	dobo190398.1	152	0	0.02	0.15	0.14	0.05	0.09	0.08	0.43	-0.02
dobo190398.1.6	dobo190398.1	165	0	0.02	0.06	0.09	0.1	0.15	0.12	0.42	-0.01
dobo190398.1.7	dobo190398.1	184	0	0.01	0.07	0.08	0.17	0.19	0.14	0.3	-0.01
dobo190398.1.8	dobo190398.1	225	0.01	0.06	0.12	0.11	0.07	0.09	0.12	0.38	-0.02
dobo190398.1.9	dobo190398.1	242	0	0.01	0.03	0.08	0.06	0.11	0.1	0.56	-0.03
dobo190398.2.1	dobo190398.2	40	0.02	0.03	0.04	0.25	0.2	0.12	0.1	0.2	-0.03
dobo190398.2.2	dobo190398.2	115	0.06	0.05	0.09	0.14	0.12	0.14	0.11	0.24	-0.04
dobo190398.2.3	dobo190398.2	139	0.1	0.12	0.2	0.14	0.07	0.09	0.08	0.16	0
dobo190398.2.4	dobo190398.2	209	0.01	0	0	0.11	0.25	0.21	0.14	0.23	0
dobo190398.2.5	dobo190398.2	409	0.01	0.03	0.12	0.34	0.11	0.09	0.09	0.18	0
dobo190400.1.1	dobo190400.1	64	0.03	0.04	0.06	0.11	0.33	0.12	0.07	0.21	-0.04
dobo190400.1.2	dobo190400.1	165	0	0.03	0.09	0.19	0.14	0.13	0.11	0.27	-0
dobo190400.1.3	dobo190400.1	265	0	0.04	0.1	0.09	0.06	0.1	0.11	0.46	-0.03
dobo190400.1.4	dobo190400.1	365	0	0	0	0.07	0.12	0.13	0.11	0.53	-0.01
dobo190400.1.5	dobo190400.1	464	0	0.01	0.01	0.02	0.16	0.28	0.19	0.29	0.01
dobo190400.1.6	dobo190400.1	564	0	0.01	0.01	0	0.11	0.26	0.22	0.35	-0.03
dobo200898.1.1	dobo200898.1	44	0	0	0	0.19	0.17	0.12	0.07	0.42	-0.02

continued on next page

continued from previous page

sample	field	d [cm]	G	gS	mS	fS	gU	mU	fU	T	error
dobo200898.1.10	dobo200898.1	685	0	0.03	0.65	0.19	0.02	0.01	0.01	0.05	-0
dobo200898.1.2	dobo200898.1	92	0	0	0	0.04	0.25	0.24	0.13	0.31	0.01
dobo200898.1.3	dobo200898.1	204	0.02	0.01	0.06	0.35	0.23	0.09	0.05	0.14	-0.01
dobo200898.1.4	dobo200898.1	334	0	0	0	0.11	0.29	0.17	0.11	0.28	0
dobo200898.1.5	dobo200898.1	405	0	0	0	0.05	0.26	0.22	0.11	0.34	-0.05
dobo200898.1.6	dobo200898.1	525	0	0	0.02	0.33	0.32	0.1	0.05	0.14	-0.02
dobo200898.1.7	dobo200898.1	564	0.7	0.06	0.04	0.08	0.01	0.01	0	0.05	-0
dobo200898.1.8	dobo200898.1	585	0	0.01	0.11	0.37	0.2	0.09	0.05	0.13	-0.02
dobo200898.1.9	dobo200898.1	655	0.62	0.11	0.1	0.08	0.02	0	0	0.02	-0
dobo201098.1.1	dobo201098.1	154	0.05	0.08	0.1	0.09	0.18	0.17	0.11	0.18	-0.06
dobo201098.1.2	dobo201098.1	275	0	0.04	0.06	0.1	0.24	0.15	0.08	0.3	-0.03
dobo201098.1.2	dobo201098.1	275	0.07	0.06	0.06	0.08	0.23	0.13	0.06	0.26	-0.07
dobo201098.2.2	dobo201098.2	254	0	0.18	0.08	0.32	0.18	0.06	0.03	0.11	-0.04
dobo201098.2.3	dobo201098.2	375	0	0	0	0.03	0.25	0.24	0.15	0.29	-0
dobo221098.1.1	dobo221098.1	225	0.01	0.09	0.13	0.09	0.08	0.13	0.12	0.3	-0.12
dobo221098.1.1	dobo221098.1	225	0.05	0.07	0.12	0.09	0.07	0.1	0.09	0.38	-0.05
dobo221098.1.2	dobo221098.1	354	0.02	0.02	0.03	0.07	0.13	0.13	0.1	0.47	-0.1
dobo221098.1.2	dobo221098.1	354	0.07	0.02	0.03	0.05	0.13	0.12	0.09	0.46	-0.02
dobo221098.1.3	dobo221098.1	455	0	0	0	0	0.3	0.25	0.15	0.26	-0.04
dobo221098.1.4	dobo221098.1	555	0.01	0	0.05	0	0.09	0.21	0.23	0.38	-0.04
dobo230698.1.1	dobo230698.1	555	0	0	0.03	0.06	0.1	0.1	0.09	0.58	-0.02
dobo230698.1.1	dobo230698.1	555	0	0.02	0.04	0.06	0.07	0.1	0.09	0.59	-0.08
dobo230698.1.2	dobo230698.1	697	0	0.01	0.08	0.17	0.17	0.13	0.08	0.33	-0.04
dobo250898.1.1	dobo250898.1	55	0	0	0	0.07	0.41	0.14	0.05	0.29	-0.01
dobo250898.1.2	dobo250898.1	154	0	0	0.01	0.13	0.54	0.15	0.03	0.1	-0.05
dobo250898.1.3	dobo250898.1	225	0.59	0.09	0.1	0.07	0.03	0.01	0	0.06	-0
dobo250898.1.4	dobo250898.1	254	0	0.01	0.13	0.36	0.07	0.1	0.07	0.21	-0.01
dobo250898.1.5	dobo250898.1	365	0	0	0.01	0.06	0.27	0.24	0.14	0.25	-0.05
dobo250898.1.6	dobo250898.1	425	0	0	0	0.02	0.2	0.27	0.2	0.28	0
dobo250898.1.7	dobo250898.1	555	0	0	0.21	0.35	0.08	0.1	0.08	0.14	-0.02
dobo250898.1.8	dobo250898.1	614	0.01	0.01	0.07	0.3	0.13	0.12	0.11	0.23	0.01
dobo250898.1.9	dobo250898.1	675	0	0	0.08	0.37	0.1	0.1	0.11	0.22	0.01
dobo270898.1.1	dobo270898.1	165	0.17	0.08	0.11	0.12	0.1	0.11	0.1	0.17	-0.03
dobo270898.1.2	dobo270898.1	395	0	0.22	0.11	0.09	0.12	0.12	0.06	0.23	-0.04
dobo270898.1.3	dobo270898.1	594	0	0.01	0.01	0.02	0.16	0.21	0.13	0.44	-0.02
dobo270898.2.1	dobo270898.2	75	0.04	0.1	0.16	0.15	0.09	0.09	0.11	0.22	-0.02
dobo270898.2.10	dobo270898.2	675	0	0.01	0.05	0.07	0.06	0.12	0.12	0.51	-0.08
dobo270898.2.11	dobo270898.2	694	0.03	0.07	0.1	0.11	0.19	0.15	0.09	0.22	-0.02
dobo270898.2.12	dobo270898.2	714	0	0.02	0.07	0.2	0.13	0.13	0.08	0.33	-0.03
dobo270898.2.13	dobo270898.2	775	0	0	0	0	0.01	0.01	0.03	0.93	-0
dobo270898.2.13	dobo270898.2	775	0	0	0	0.02	0.08	0.13	0.12	0.63	0
dobo270898.2.13	dobo270898.2	775	0	0	0	0.03	0.1	0.13	0.12	0.59	-0.06
dobo270898.2.2	dobo270898.2	94	0	0	0.02	0.24	0.22	0.13	0.06	0.3	-0.06
dobo270898.2.3	dobo270898.2	154	0.12	0.08	0.11	0.11	0.13	0.15	0.1	0.17	-0.03
dobo270898.2.4	dobo270898.2	254	0.15	0.04	0.07	0.09	0.21	0.14	0.08	0.19	-0.08
dobo270898.2.5	dobo270898.2	354	0	0.08	0.11	0.2	0.09	0.14	0.12	0.22	-0.03
dobo270898.2.6	dobo270898.2	384	0	0.02	0.09	0.21	0.16	0.14	0.12	0.23	-0.01
dobo270898.2.7	dobo270898.2	427	0	0.04	0.12	0.19	0.13	0.14	0.11	0.23	-0.01
dobo270898.2.8	dobo270898.2	475	0	0	0.01	0.21	0.24	0.15	0.08	0.28	-0.01
dobo270898.2.9	dobo270898.2	655	0	0.02	0.05	0.1	0.09	0.1	0.09	0.52	-0.07
hollersi7b1.1	hollersi7b1	2	0	0.01	0.09	0.02	0.25	0.27	0.08	0.26	
hollersi7b1.2	hollersi7b1	42	0	0	0	0.01	0.44	0.2	0.04	0.27	
hollersi7b1.3	hollersi7b1	95	0	0	0	0.02	0.54	0.21	0.04	0.16	
hollersi7b20.1	hollersi7b20	5	0	0	0	0.01	0.48	0.2	0.07	0.22	
hollersi7b20.2	hollersi7b20	35	0	0	0	0.01	0.51	-2.76	2.99	0.23	
hollersi7b20.3	hollersi7b20	129	0	0.01	0	0	0.58	0.19	0.02	0.15	
hollersi7b7.1	hollersi7b7	2	0.03	0.01	0.01	0.03	0.18	0.17	0.14	0.39	-0.24
hollersi7b7.2	hollersi7b7	42	0.02	0.02	0.04	0.07	0.19	0.13	0.09	0.4	-0.07
hollersi7b7.3	hollersi7b7	114	0.02	0.03	0.05	0.07	0.17	0.12	0.1	0.42	
hollersi9b23.1	hollersi9b23	5	0.01	0	0.02	0.03	0.12	0.26	0.23	0.29	
hollersi9b23.2	hollersi9b23	45	0.01	0.03	0.11	0.17	0.19	0.12	0.09	0.25	
hollersi9b23.3	hollersi9b23	95	0	0.02	0.03	0.04	0.25	0.15	0.07	0.42	
hollersi9b23.4	hollersi9b23	154	0	0	0	0	0.11	0.1	0.11	0.64	
hollersi9b29.2	hollersi9b29	35	0.03	0.03	0.11	0.14	0.15	0.13	0.18	0.18	
hollersi9b29.3	hollersi9b29	125	0.03	0.07	0.14	0.16	0.12	0.1	0.13	0.21	

continued on next page

continued from previous page

sample	field	d [cm]	G	gS	mS	fS	gU	mU	fU	T	error
hollersi9b29.4	hollersi9b29	195	0	0.01	0.03	0.05	0.21	0.13	0.07	0.46	
hollersi9b7.1	hollersi9b7	5	0.01	0.01	0.07	0.12	0.24	0.17	0.2	0.14	
hollersi9b7.2	hollersi9b7	50	0.05	0.03	0.04	0.15	0.21	0.15	0.13	0.2	
hollersi9b7.3	hollersi9b7	109	0	0.01	0.02	0.06	0.11	0.14	0.18	0.45	
hollersi9b7.4	hollersi9b7	145	0	0.02	0.02	0.07	0.14	0.17	0.19	0.35	
meauf270499.1	lp97parkner		0	0	0	0.08	0.29	0.24	0.08	0.28	0
lp97arns.1a	meauf270499.1		0	0	0	0	0.02	-0	0.05	0.9	-0.07
lp97arns.1b	meauf270499.1		0	0	0	0	0.02	-0	0.07	0.89	-0.02
lp97arns.3	meauf270499.1		0	0	0	0.03	0.32	0.24	0.09	0.29	-0.02
lp97mays.1	meauf270499.1		0	0	0	0.08	0.28	0.24	0.09	0.28	-0.02
lp97mays.2	meauf270499.1		0	0	0	0.03	0.33	0.25	0.08	0.28	-0.01
lp97mays.3	meauf270499.1		0	0	0	0	0.01	0	0.02	0.93	-0.03
lp97mays.5	meauf270499.1		0	0	0	0	0.02	0	0.01	0.93	-0.01
meauf270499.1.140201.1	meauf270499.1	170	0	0	0.04	0.1	0.46	0.09	0.04	0.24	-0
meauf270499.1.140201.2	meauf270499.1	304	0	0	0.01	0.03	0.46	0.28	0.09	0.1	-0.01
meauf270499.1.140201.3	meauf270499.1	490	0	0	0	0	0.04	0	0.09	0.85	0.02
meauf270499.1.140201.4	meauf270499.1	590	0	0	0	0.02	0.26	0.22	0.13	0.34	0.02
meauf270499.1.140201.5	meauf270499.1	644	0	0	0	0.03	0.31	0.24	0.08	0.32	-0
mebo010800.1.1	mebo010800.1	170	0	0	0	0.01	0.49	0.24	0.05	0.18	-0.05
mebo010800.1.10	mebo010800.1	755	0	0	0.1	0.01	0.01	0.02	0.04	0.77	0
mebo010800.1.11	mebo010800.1	794	0	0.02	0.36	0.04	0.05	0.03	0.05	0.42	0
mebo010800.1.2	mebo010800.1	279	0	0	0	0	0.48	0.27	0.06	0.17	-0.02
mebo010800.1.3	mebo010800.1	384	0	0	0	0	0.61	0.18	0.03	0.15	-0
mebo010800.1.4	mebo010800.1	475	0.41	0.05	0.18	0.1	0.1	0.03	0.01	0.09	-0.01
mebo010800.1.5	mebo010800.1	494	0.64	0.06	0.09	0.06	0.03	0.01	0.01	0.05	-0
mebo010800.1.6	mebo010800.1	544	0	0.01	0.04	0.12	0.24	0.16	0.07	0.33	-0.02
mebo010800.1.7	mebo010800.1	564	0	0	0.01	0.05	0.07	0.05	0.03	0.76	0
mebo010800.1.8	mebo010800.1	669	0	0	0	0.01	0.07	0.09	0.22	0.57	-0
mebo010800.1.9	mebo010800.1	689	0	0	0	0	0.01	0	0.07	0.9	0
mebo010800.2.1	mebo010800.2	64	0	0	0	0.02	0.43	0.21	0.05	0.26	-0.01
mebo010800.2.2	mebo010800.2	85	0	0	0	0.02	0.49	0.23	0.06	0.16	-0.04
mebo010800.2.3	mebo010800.2	154	0	0.02	0	0.02	0.48	0.23	0.05	0.17	-0.01
mebo010800.2.4	mebo010800.2	250	0	0	0	0.02	0.48	0.22	0.05	0.2	-0.01
mebo010800.2.5	mebo010800.2	329	0	0	0	0.01	0.48	0.21	0.05	0.22	-0.01
mebo010800.2.7	mebo010800.2	480	0	0	0	0.02	-0.02	0.37	0.15	0.46	-0.18
mebo010800.2.8	mebo010800.2	530	0	0	0	0.02	0.04	0.1	0.11	0.69	0
mebo010800.2.9	mebo010800.2	565	0	0.07	0.05	0.07	0.14	0.15	0.07	0.4	0
mebo010999.1.1	mebo010999.1	184	0	0	0	0	0.19	0.39	0.11	0.27	0.01
mebo010999.1.2	mebo010999.1	234	0	0	0.12	0.83	0.01	0	0	0.01	-0
mebo010999.1.3	mebo010999.1	254	0	0	0	0.13	0.27	0.41	0.07	0.1	-0.01
mebo010999.1.4	mebo010999.1	284	0	0	0	0	0.1	0.42	0.12	0.34	-0
mebo010999.1.5	mebo010999.1	334	0	0	0	0.04	0.09	0.01	0.02	0.82	-0.04
mebo010999.1.6	mebo010999.1	354	0	0	0	0.54	0.3	0.04	0.03	0.07	-0.01
mebo010999.1.7	mebo010999.1	435	0	0	0	0	0	0.01	0	0.97	-0.01
mebo010999.1.8	mebo010999.1	564	0	0	0.36	0.61	0	0	0	0	0
mebo051099.1.1	mebo051099.1	215	0	0	0.01	0.09	0.32	0.21	0.08	0.26	-0.01
mebo051099.1.2	mebo051099.1	254	0	0.01	0	0.03	0.39	0.21	0.07	0.25	-0
mebo051099.1.3	mebo051099.1	395	0	0	0	0.01	0.23	0.25	0.11	0.36	-0
mebo060999.1.1	mebo060999.1	72	0	0.01	0.01	0.02	0.35	0.25	0.09	0.24	-0
mebo060999.1.10	mebo060999.1	464	0	0	0	0.06	0.37	0.4	0.06	0.09	-0.02
mebo060999.1.11	mebo060999.1	544	0	0	0	0	0.08	0.46	0.11	0.33	0.01
mebo060999.1.12	mebo060999.1	589	0	0	0	0.01	0.05	0.01	0.02	0.89	-0.03
mebo060999.1.14	mebo060999.1	785	0	0	0	0	-0	0.01	0	0.98	-0.02
mebo060999.1.2	mebo060999.1	110	0	0.06	0.04	0.04	0.11	0.13	0.09	0.49	-0.02
mebo060999.1.3	mebo060999.1	143	0	0.01	0	0	0.01	0.02	0.13	0.81	-0.01
mebo060999.1.4	mebo060999.1	162	0	0	0.05	0.29	0.04	0.03	0.06	0.5	-0.03
mebo060999.1.5	mebo060999.1	187	0	0	0.02	0.5	0.28	0.04	0.03	0.12	-0.04
mebo060999.1.6	mebo060999.1	215	0	0	0.33	0.56	0.01	0	0.01	0.06	-0
mebo060999.1.7	mebo060999.1	284	0	0	0	0.47	0.38	0.04	0.02	0.05	-0.05
mebo060999.1.8	mebo060999.1	347	0	0	0	0.01	0.09	0.15	0.12	0.6	-0.03
mebo060999.1.9	mebo060999.1	370	0	0	0.14	0.81	0.02	0	0	0.01	-0
mebo061099.1.1	mebo061099.1	170	0	0	0	0.01	0.48	0.24	0.06	0.18	-0.01
mebo061099.1.2	mebo061099.1	245	0	0	0	0.01	0.49	0.21	0.12	0.15	-0
mebo061099.1.3	mebo061099.1	315	0	0	0.17	0.79	0	0	0	0.01	0
mebo061099.1.4	mebo061099.1	350	0	0.14	0.31	0.51	0	0	0	0.02	0

continued on next page

continued from previous page

sample	field	d [cm]	G	gS	mS	fS	gU	mU	fU	T	error
mebo061099.1.5	mebo061099.1	450	0	0	0.15	0.81	0	0	0	0.02	0
mebo061099.1.6	mebo061099.1	542	0	0	0.23	0.71	0	0	0	0.02	0
mebo061099.1.7	mebo061099.1	664	0	0	0.02	0.87	0.01	0	0.01	0.07	0
mebo061099.1.9	mebo061099.1	894	0	0	0	0	0	0	0.04	0.93	0.02
mebo070999.1.1	mebo070999.1	170	0	0	0	0.01	0.41	0.17	0.03	0.35	-0.02
mebo070999.1.2	mebo070999.1	245	0	0	0	0	0.06	0.21	0.19	0.52	-0
mebo070999.1.3	mebo070999.1	279	0	0.01	0	0.01	0.56	0.2	0.05	0.14	0
mebo070999.1.4	mebo070999.1	326	0	0	0	0.01	0.5	0.23	0.06	0.18	0
mebo070999.1.5	mebo070999.1	379	0	0.09	0.11	0.06	0.31	0.13	0.05	0.21	0
mebo070999.1.6	mebo070999.1	448	0	0	0	0.01	0.09	0.18	0.16	0.52	-0
mebo070999.1.7	mebo070999.1	480	0	0.03	0.01	0	0.06	0.13	0.18	0.54	0
mebo070999.1.8	mebo070999.1	537	0	0.03	0.01	0.02	0.43	0.2	0.06	0.21	-0
mebo070999.1.9	mebo070999.1	789	0	0	0.01	0	0.13	0.35	0.12	0.36	0
mebo071099.1.1	mebo071099.1	122	0	0	0	0.01	0.46	0.22	0.06	0.22	0
mebo071099.1.2	mebo071099.1	262	0	0.01	0.01	0.01	0.39	0.2	0.06	0.29	-0
mebo071099.1.3	mebo071099.1	287	0	0	0	0.01	0.45	0.22	0.05	0.24	-0
mebo071099.1.4	mebo071099.1	362	0	0	0	0.01	0.44	0.21	0.06	0.23	0
mebo071099.1.5	mebo071099.1	562	0	0	0.03	0.1	0.38	0.18	0.06	0.2	-0
mebo071099.1.6	mebo071099.1	652	0	0	0.06	0.22	0.31	0.12	0.05	0.21	0
mebo160600.1.1	mebo160600.1	154	0	0	0	0.02	0.52	0.21	0.05	0.17	0
mebo160600.1.2	mebo160600.1	284	0	0	0	0.01	0.47	0.28	0.05	0.17	-0.02
mebo160600.1.3	mebo160600.1	384	0	0	0	0	0.46	0.31	0.05	0.15	0
mebo160600.1.4	mebo160600.1	444	0	0	0	0.03	0.52	0.21	0.05	0.16	0
mebo160600.1.5	mebo160600.1	485	0.56	0.04	0.1	0.06	0.03	0.02	0.01	0.11	0
mebo160600.1.6	mebo160600.1	530	0	0	0.4	0.5	0.01	0	-0	0.05	0
mebo160600.1.7	mebo160600.1	589	0	0	0	0.01	0.01	0	0.01	0.93	0
mebo160600.1.8	mebo160600.1	694	0	0	0	0.02	0.3	0.25	0.1	0.31	-0
mebo160600.1.9	mebo160600.1	785	0	0	0	0	0.16	0.26	0.15	0.41	0.01
mebo161299.1.1	mebo161299.1	122	0	0	0	0.02	0.36	0.27	0.04	0.29	-0
mebo161299.1.2	mebo161299.1	284	0	0	0	0.04	0.55	0.18	0.05	0.16	0.07
mebo161299.1.3	mebo161299.1	435	0	0.02	0.02	0.07	0.17	0.23	0.16	0.3	0
mebo161299.1.4	mebo161299.1	585	0	0.01	0.01	0.03	0.16	0.27	0.2	0.29	0.01
mebo170800.1.2	mebo170800.1	267	0	0.05	0.55	0.3	0	0	0	0.05	-0
mebo170800.1.3	mebo170800.1	290	0	0.01	0.32	0.66	0	0	0	0	-0.1
mebo170800.1.4	mebo170800.1	384	0	0	0	0.01	0.01	0	0.06	0.89	-0
mebo170800.1.7	mebo170800.1	492	0	0	0	0	-0	0.01	0.11	0.85	0.01
mebo170800.1.8	mebo170800.1	559	0	0	0.06	0.13	0.05	0.02	0.05	0.64	-0
mebo170800.1.9	mebo170800.1	662	0	0	0.02	0.07	0.08	0.09	0.08	0.62	-0
mebo170800.2.1	mebo170800.2	60	0	0	0	0.01	0.19	0.41	0.05	0.31	-0.18
mebo170800.2.10	mebo170800.2	750	0	0	0.33	0.57	0.02	0.01	0	0.03	0
mebo170800.2.11	mebo170800.2	855	0	0	0.21	0.67	0.03	0.01	0	0.04	0
mebo170800.2.2	mebo170800.2	182	0	0	0	0.03	0.48	0.25	0.04	0.17	-0.01
mebo170800.2.3	mebo170800.2	276	0.02	0	0	0.01	0.57	0.18	0.03	0.15	-0.02
mebo170800.2.4	mebo170800.2	355	0	0	0	0.01	0.56	0.18	0.04	0.17	-0.02
mebo170800.2.5	mebo170800.2	455	0	0.01	0	0.01	0.49	0.24	0.06	0.16	-0.02
mebo170800.2.6	mebo170800.2	544	0	0	0	0.02	0.52	0.23	0.04	0.16	-0.01
mebo170800.2.8	mebo170800.2	634	0.29	0.07	0.05	0.05	0.25	0.11	0.02	0.11	-0.03
mebo170800.2.9	mebo170800.2	680	0.02	0.02	0.24	0.63	0.02	0.01	0	0.02	0

Hydrometer method

Listing: SQL–code querying grainsize results from database.

```
SELECT max(f.field_id) AS outcrop, max(so.sample_id) AS sample,
max(%(100*COALESCE((so.upperdepth+so.lowerdepth)/2,so.upperdepth,so.lowerdepth))) AS "depth_[cm]",
l.id AS labid,
%(100*(1-max((1/(a.brutto-a.tara))*(a.corndens/(a.corndens-1))*((u.hilfswert+a.cm)+
(1000*((1/(1+0.000001*(((2.31*a.t0-2)^2)-182)))-(1/(1+0.000001*(((2.31*u.temperature-2)^2)-182)))
-(25/1000000)*(u.temperature-a.t0)))))))/100.0 AS "S,G",
%(100*(max((1/(a.brutto-a.tara))*(a.corndens/(a.corndens-1))*((u.hilfswert+a.cm)+
(1000*((1/(1+0.000001*(((2.31*a.t0-2)^2)-182)))-(1/(1+0.000001*(((2.31*u.temperature-2)^2)-182)))-
(25/1000000)*(u.temperature-a.t0)))))-max((1/(a.brutto-a.tara))*(a.corndens/(a.corndens-1))*((t.hilfswert+a.cm)+
(1000*((1/(1+0.000001*(((2.31*a.t0-2)^2)-182)))-(1/(1+0.000001*(((2.31*t.temperature-2)^2)-182)))-
(25/1000000)*(t.temperature-a.t0)))))))/100.0 AS "U",
%(100*(max((1/(a.brutto-a.tara))*(a.corndens/(a.corndens-1))*((t.hilfswert+a.cm)+
(1000*((1/(1+0.000001*(((2.31*a.t0-2)^2)-182)))-(1/(1+0.000001*(((2.31*t.temperature-2)^2)-182)))-
(25/1000000)*(t.temperature-a.t0)))))))/100.0 AS "T"

FROM areo a, areo_ser t, areo_ser u, lab l, soilsample so, field f

WHERE l.id=a.lab_id AND a.lab_id=t.lab_id AND a.lab_id=u.lab_id
AND l.sample_id=so.id AND so.field_id=f.id
AND ((18.35*(0.00178/(1+0.0337*t.temperature+0.00022*t.temperature^2))*(((a.s*(rhomin-
(((t.hilfswert+a.cm)/1000)+1))/(rhomin-rhomax))+a.h0+0.5*(a.h-(a.va/a.az))))))/
((a.corndens-(1/(1+0.000001*(((2.31*t.temperature-2)^2)-182))))*t.time*60))^0.5 <0.002
AND ((18.35*(0.00178/(1+0.0337*u.temperature+0.00022*u.temperature^2))*(((a.s*(rhomin-
(((u.hilfswert+a.cm)/1000)+1))/(rhomin-rhomax))+a.h0+0.5*(a.h-(a.va/a.az))))))/
((a.corndens-(1/(1+0.000001*(((2.31*u.temperature-2)^2)-182))))*u.time*60))^0.5 <0.063
GROUP BY l.id
ORDER BY l.id
```

Results of laboratory experiments for particle size determination (hydrometer method). Calculated values per lab experiment. Particle size fractions are shown relative to 1.

outcrop	sample	depth [cm]	labid	S,G	U	T
meauf010299.1	meauf010299.1.1	395	1378	0.05	0.41	0.53
meauf010299.1	meauf010299.1.4	395	1385	0.05	0.66	0.28
meauf270499.1	meauf270499.1.221199.1	609	1400	0.14	0.59	0.26
meauf270499.1	meauf270499.1.221199.2	609	1407	0.14	0.53	0.31
meauf270499.1	meauf270499.1.031199.3	575	1410	0.07	0.6	0.31
meauf270499.1	meauf270499.1.061299.1	609	1415	0.13	0.59	0.26
meauf270499.1	meauf270499.1.061299.1	609	1420	0.16	0.56	0.26
meauf270499.1	meauf270499.1.091299.1	609	1427	0.12	0.58	0.28
doauf240398.3	doauf240398.3.8	55	2446	0.12	0.33	0.53
doauf240398.3	doauf240398.3.8	55	2447	0.09	0.34	0.55
doauf240398.3	doauf240398.3.8	55	2448	0.09	0.38	0.51
doauf240398.3	doauf240398.3.020400.2	55	2927	0.06	0.32	0.61
doauf180898.1	doauf180898.1.020400.1	35	2928	0.37	0.47	0.14
doauf290998.1	doauf290998.1.020400.1	35	2929	0.44	0.4	0.15
doauf240398.2	doauf240398.2.020400.2	675	2930	0.76	0.21	0.02
doauf240398.2	doauf240398.2.020400.1	675	2931	0.74	0.21	0.03
doauf020498.1	doauf020498.1.020400.2	25	2935	0.02	0.63	0.33

Particle size diagrams for different material types for the field site Dollendorfer Hardt

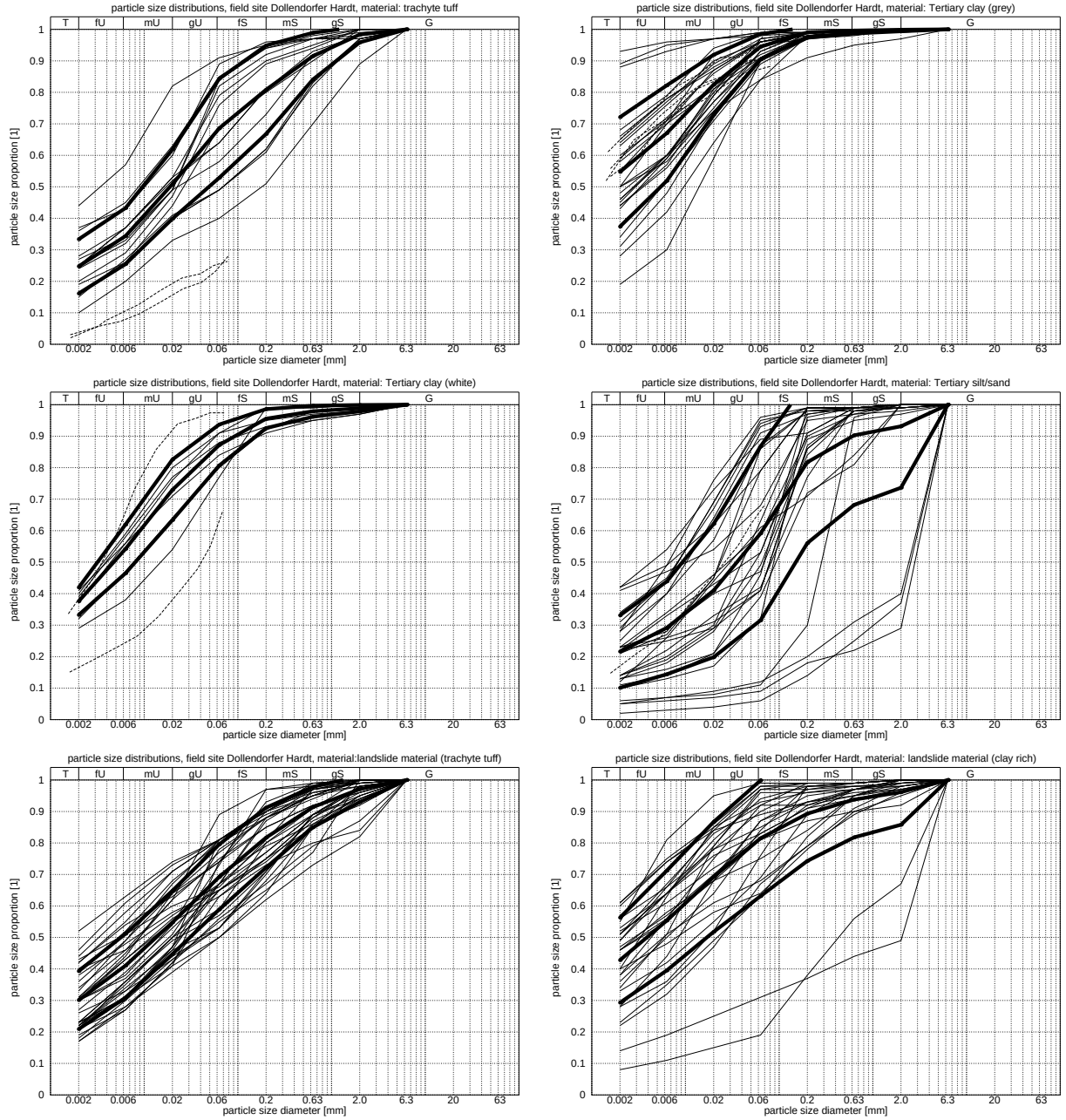

Results from particle size experiments for different material types for the field site Dollendorfer Hardt. Dashed lines indicate results from hydrometer method. Shown are results from individual experiments and average curves ($\mu \pm \sigma$).

Statistical properties of particle size proportions from lab results, landslide 'si7'. ($\mu \pm \sigma$)									
material	n	G	mS	gS	fS	gU	mU	fU	T
Devon	13	0.02±0.02	0.02±0.03	0.04±0.05	0.09±0.1	0.15±0.06	0.2±0.07	0.15±0.04	0.29±0.09
landslide (TrT, si7)	38	0.02±0.04	0.05±0.04	0.09±0.04	0.12±0.04	0.14±0.07	0.13±0.02	0.1±0.02	0.3±0.09
landslide (clay, si7)	30	0.03±0.1	0.02±0.02	0.04±0.04	0.07±0.06	0.12±0.05	0.13±0.04	0.12±0.04	0.42±0.13
trachyte tuff	16	0.01±0.02	0.06±0.05	0.1±0.07	0.12±0.04	0.17±0.09	0.16±0.02	0.09±0.02	0.24±0.08
Tert. clay (grey, Dollendorf)	27	0±0	0±0	0±0	0.04±0.03	0.12±0.06	0.15±0.06	0.12±0.03	0.54±0.17
Tert. clay (white, Dollendorf)	7	0.01±0.01	0±0	0.02±0.01	0.08±0.06	0.14±0.03	0.18±0.02	0.16±0.03	0.37±0.04
Tert. silt/sand (Dollendorf)	29	0.06±0.19	0.02±0.04	0.08±0.12	0.22±0.17	0.18±0.09	0.11±0.07	0.07±0.05	0.21±0.11
loess (loam)	2	0±0	0±0	0.01±0	0.1±0.02	0.47±0.06	0.15±0	0.04±0	0.2±0.09
basalt	3	0±0	0±0	0.01±0	0.01±0	0.08±0.02	0.22±0.03	0.11±0.03	0.53±0.02

Particle size diagrams for different material types for the field site Melbtal

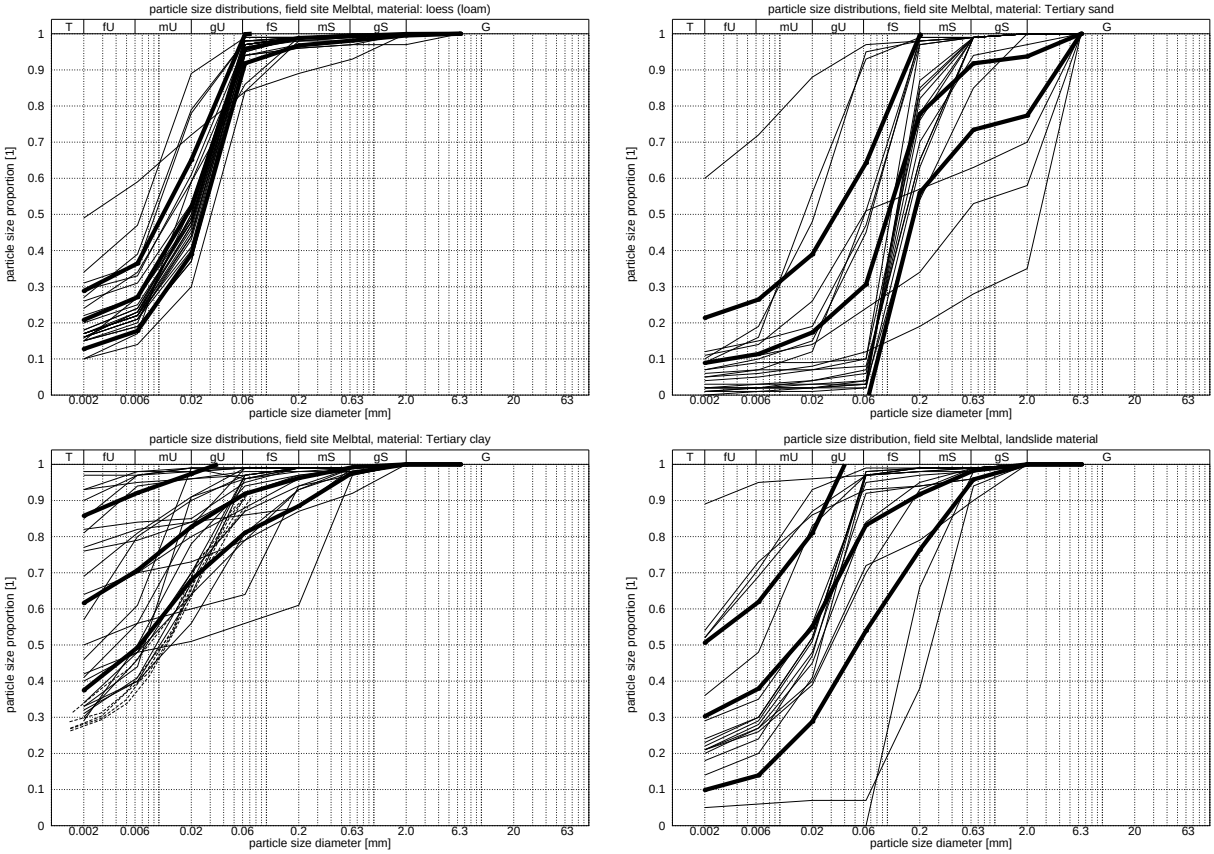

Results from particle size experiments for different material types for the field site Melbtal. Dashed lines indicate results from hydrometer method. Shown are results from individual experiments and average curves ($\mu \pm \sigma$).

Statistical properties of particle size proportions from lab results, Melbtal. ($\mu \pm \sigma$)									
material	n	G	gS	mS	fS	gU	mU	fU	T
Tert. sand (Melbtal)	22	0.06±0.16	0.01±0.03	0.14±0.12	0.47±0.29	0.13±0.16	0.05±0.1	0.02±0.03	0.08±0.12
Tert. clay (Melbtal)	27	0±0	0±0.01	0.03±0.07	0.04±0.06	0.09±0.09	0.11±0.12	0.09±0.05	0.61±0.24
lignite (Melbtal)	1	0±0	0±0	0±0	0.01±0	0.05±0	0.01±0	0.02±0	0.89±0
terrace (Melbtal)	1	0.56±0	0.04±0	0.1±0	0.06±0	0.03±0	0.02±0	0.01±0	0.11±0
loess (loam)	27	0±0	0±0.01	0±0	0.02±0.02	0.43±0.13	0.25±0.07	0.06±0.02	0.2±0.07
landslide (Melbtal)	18	0±0	0.01±0.02	0.06±0.13	0.08±0.16	0.28±0.19	0.16±0.08	0.07±0.05	0.3±0.2

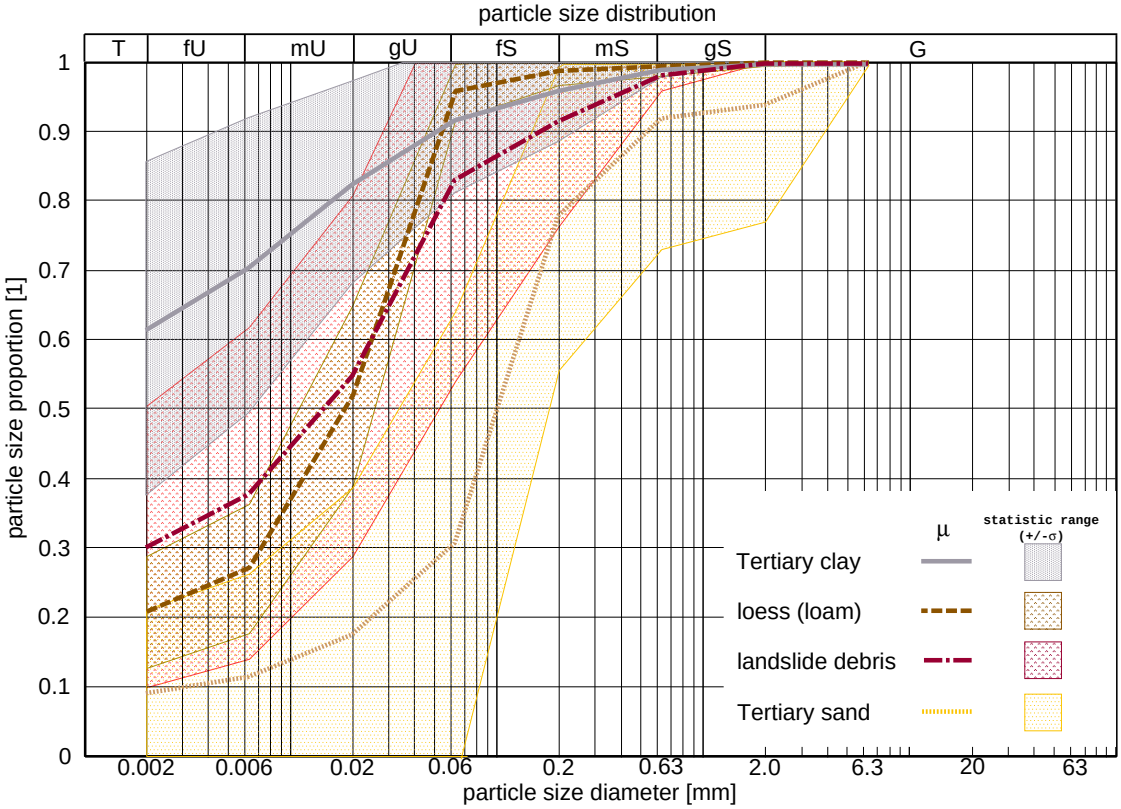

Particle size distributions for soils of the Melbtal. The diagram indicates typical value ranges from statistics of lab experiments

C.2. Density

Bulk density

Listing: SQL–code querying density measurement results from database.

```
SELECT f.field_id AS outcrop, so.sample_id AS sample,
%(100*COALESCE((so.upperdepth+so.lowerdepth)/2,so.upperdepth,so.lowerdepth)) AS "d_[cm]",
COALESCE(%(100*(wet-tara)/(COALESCE((cylheight*cyldiameter*cyldiameter*3.14152/4),cylvol)))/100,0)
AS "\density",
COALESCE(%(100*(dry-tara)/(COALESCE((cylheight*cyldiameter*cyldiameter*3.14152/4),cylvol)))/100,0)
AS "\drydensity",
COALESCE(%(100*(saturated-tara)/(COALESCE((cylheight*cyldiameter*cyldiameter*3.14152/4),cylvol)))/100,0)
AS "\satdensity"
FROM wetdrydens w,lab l,soilsample so, field f
WHERE w.lab_id=l.id AND l.sample_id=so.id AND so.field_id=f.id AND f.exp_id=28
UNION
SELECT f.field_id AS outcrop, so.sample_id AS sample,
%(100*COALESCE((so.upperdepth+so.lowerdepth)/2,so.upperdepth,so.lowerdepth)) AS "d_[cm]",
COALESCE(%(100*(w.bruttoin-w.ring)/(2*3.14152*3.5*3.5))/100,0) AS "\density",
0 AS "\drydensity",
0 AS "\satdensity"
FROM shear w, lab l, soilsample so, field f
WHERE w.lab_id=l.id AND l.sample_id=so.id AND so.field_id=f.id AND w.bruttoin<>"
ORDER BY sample;
```

Results of laboratory experiments for bulk density ρ_b, dry density ρ_d, and saturated density ρ_{sat}. Calculated values per lab experiment. Density units are g/cm^3, fractions are shown relative to 1. Density values derived from drilling cores are not included. ('0' indicates missing data)

outcrop	sample	d [cm]	ρ_b	ρ_d	ρ_{sat}
doauf020498.1	doauf020498.1.020400.3	25	1.88	0	0
doauf020498.1	doauf020498.1.020400.3	25	1.9	0	0
doauf020498.1	doauf020498.1.020400.3	25	3.04	0	0
doauf020498.1	doauf020498.1.2z	25	2.13	1.79	0
doauf020498.1	doauf020498.1.4z	35	1.97	0	0
doauf020498.1	doauf020498.1.4z	35	2.02	0	0
doauf020498.1	doauf020498.1.4z	35	2.06	0	0
doauf020498.2	doauf020498.2.2z	35	1.69	1.33	0
doauf020498.2	doauf020498.2.4z	25	1.93	0	0
doauf020498.2	doauf020498.2.4z	25	2.08	0	0
doauf020498.3	doauf020498.3.2z	55	1.53	1.05	0
doauf020498.3	doauf020498.3.3z	55	1.55	0.98	0
doauf020498.3	doauf020498.3.4z	55	1.46	0.93	0
doauf240398.3	doauf020498.4.2z	55	1.96	1.55	0
doauf050598.2	doauf050598.2.1	35	1.79	0	0
doauf050598.2	doauf050598.2.1	35	1.8	0	0
doauf050598.2	doauf050598.2.1	35	1.81	0	0
doauf050598.3	doauf050598.3.1	104	1.51	0	0
doauf050598.3	doauf050598.3.1	104	1.57	0	0
doauf050598.3	doauf050598.3.1	104	1.64	0	0
doauf180898.1	doauf180898.1.1	204	1.64	0	0
doauf180898.1	doauf180898.1.1	204	1.78	0	0
doauf180898.1	doauf180898.1.1	204	1.83	0	0
doauf180898.1	doauf180898.1.160200.kf1	35	1.6	1.34	1.81
doauf180898.1	doauf180898.1.160200.kf2	35	1.76	1.38	1.88
doauf180898.1	doauf180898.1.160200.kf3	35	1.41	1.1	1.66
doauf180898.1	doauf180898.1.160200.kf4	35	1.64	1.44	1.89
doauf180898.1	doauf180898.1.160200.kf5	35	1.71	1.5	1.92

continued on next page

continued from previous page

outcrop	sample	d [cm]	ρ_b	ρ_d	ρ_{sat}
doauf180898.1	doauf180898.1.160200.kf6	35	1.79	1.55	1.97
doauf180898.1	doauf180898.1.160200.kf7	35	1.79	1.57	2
doauf180898.1	doauf180898.1.160300.1	35	1.94	0	0
doauf180898.1	doauf180898.1.160300.1	35	1.95	0	0
doauf180898.1	doauf180898.1.160300.1	35	1.96	0	0
doauf180898.1	doauf180898.1.2	204	1.74	0	0
doauf180898.1	doauf180898.1.2	204	1.84	0	0
doauf180898.1	doauf180898.1.2	204	1.92	0	0
doauf180898.1	doauf180898.1.3	204	1.66	0	0
doauf180898.1	doauf180898.1.3	204	1.67	0	0
doauf180898.1	doauf180898.1.3	204	1.77	0	0
doauf180898.1	doauf180898.1.4	35	1.82	0	0
doauf180898.1	doauf180898.1.4	35	1.89	0	0
doauf180898.1	doauf180898.1.4	35	1.94	0	0
doauf240398.1	doauf240398.1.150899.3	50	0	1.05	2.03
doauf240398.1	doauf240398.1.2z	50	1.43	0	0
doauf240398.1	doauf240398.1.2z	50	1.46	0	0
doauf240398.1	doauf240398.1.2z	50	1.48	0	0
doauf240398.2	doauf240398.2.10	5	1.92	0	0
doauf240398.2	doauf240398.2.10	5	1.94	0	0
doauf240398.2	doauf240398.2.10	5	1.98	0	0
doauf240398.2	doauf240398.2.130100.kf1	675	0	1.3	0
doauf240398.2	doauf240398.2.130100.kf2	675	0	1.31	0
doauf240398.2	doauf240398.2.130100.kf3	675	0	1.43	0
doauf240398.2	doauf240398.2.130100.kf4	675	0	1.45	0
doauf240398.2	doauf240398.2.130100.kf5	675	0	1.36	0
doauf240398.2	doauf240398.2.130100.kf6	675	0	1.45	0
doauf240398.2	doauf240398.2.130100.kf7	675	0	1.41	0
doauf240398.2	doauf240398.2.130100.kf8	675	0	1.52	0
doauf240398.2	doauf240398.2.130100.ku1	675	2.04	1.72	0
doauf240398.2	doauf240398.2.130100.ku10	675	1.96	1.53	0
doauf240398.2	doauf240398.2.130100.ku2	675	1.97	1.59	0
doauf240398.2	doauf240398.2.130100.ku3	675	2.04	1.6	0
doauf240398.2	doauf240398.2.130100.ku4	675	1.95	1.5	0
doauf240398.2	doauf240398.2.130100.ku5	675	2.1	1.72	0
doauf240398.2	doauf240398.2.130100.ku6	675	2.11	1.7	0
doauf240398.2	doauf240398.2.130100.ku7	675	2.14	1.73	0
doauf240398.2	doauf240398.2.130100.ku8	675	2.05	1.68	0
doauf240398.2	doauf240398.2.130100.ku9	675	2.07	1.67	0
doauf240398.2	doauf240398.2.150899.1	675	0	1.55	2.35
doauf240398.2	doauf240398.2.150899.2	675	0	1.37	2.21
doauf240398.2	doauf240398.2.160200.1	675	1.85	0	0
doauf240398.2	doauf240398.2.160200.1	675	1.89	0	0
doauf240398.2	doauf240398.2.160200.1	675	1.9	0	0
doauf240398.2	doauf240398.2.160200.kf1	675	1.97	1.6	1.99
doauf240398.2	doauf240398.2.160200.kf2	675	2.03	1.75	2.12
doauf240398.2	doauf240398.2.160200.kf3	675	1.74	1.39	1.83
doauf240398.2	doauf240398.2.160200.kf4	675	1.81	1.46	1.91
doauf240398.2	doauf240398.2.160200.kf5	675	1.88	1.55	1.95
doauf240398.2	doauf240398.2.160200.kf6	675	1.82	1.5	1.92
doauf240398.2	doauf240398.2.160799.1	675	0	1.34	1.8
doauf240398.2	doauf240398.2.160799.2	675	0	1.46	1.92
doauf240398.2	doauf240398.2.2z	675	1.62	0	0
doauf240398.2	doauf240398.2.2z	675	1.67	0	0
doauf240398.2	doauf240398.2.2z	675	1.75	0	0

continued on next page

continued from previous page

outcrop	sample	d [cm]	ρ_b	ρ_d	ρ_{sat}
doauf240398.2	doauf240398.2.7	5	1.79	0	0
doauf240398.2	doauf240398.2.7	5	1.94	0	0
doauf240398.2	doauf240398.2.7	5	1.95	0	0
doauf240398.2	doauf240398.2.8	5	1.76	0	0
doauf240398.2	doauf240398.2.8	5	1.85	0	0
doauf240398.2	doauf240398.2.8	5	1.89	0	0
doauf240398.2	doauf240398.2.9	5	1.73	0	0
doauf240398.2	doauf240398.2.9	5	1.75	0	0
doauf240398.2	doauf240398.2.z44	675	0	1.17	1.98
doauf240398.3	doauf240398.3.1	45	1.98	0	0
doauf240398.3	doauf240398.3.1	45	1.99	0	0
doauf240398.3	doauf240398.3.130100.kf1	55	0	1.69	0
doauf240398.3	doauf240398.3.130100.kf2	55	0	1.71	0
doauf240398.3	doauf240398.3.130100.kf3	55	0	1.75	0
doauf240398.3	doauf240398.3.130100.kf4	55	0	1.68	0
doauf240398.3	doauf240398.3.130100.kf5	55	0	1.65	0
doauf240398.3	doauf240398.3.130100.kf6	55	0	1.77	0
doauf240398.3	doauf240398.3.130100.kf7	55	0	1.69	0
doauf240398.3	doauf240398.3.130100.kf8	55	0	1.69	0
doauf240398.3	doauf240398.3.160200.1	55	2.02	0	0
doauf240398.3	doauf240398.3.160200.2	55	1.96	0	0
doauf240398.3	doauf240398.3.160200.3	55	1.71	0	0
doauf240398.3	doauf240398.3.160200.3	55	1.72	0	0
doauf240398.3	doauf240398.3.160200.3	55	1.96	0	0
doauf240398.3	doauf240398.3.160200.kf1	55	1.94	1.55	1.97
doauf240398.3	doauf240398.3.160200.kf2	55	1.91	1.51	1.93
doauf240398.3	doauf240398.3.160200.kf3	55	2	1.6	2.01
doauf240398.3	doauf240398.3.160200.kf4	55	1.96	1.59	2.02
doauf240398.3	doauf240398.3.160200.kf5	55	2	1.64	2.07
doauf240398.3	doauf240398.3.160200.kf6	55	2.02	1.65	2.08
doauf240398.3	doauf240398.3.211299.ku1	55	2.02	1.71	2.06
doauf240398.3	doauf240398.3.211299.ku2	55	2.02	1.73	2.07
doauf240398.3	doauf240398.3.211299.ku3	55	2.07	1.8	2.1
doauf240398.3	doauf240398.3.211299.ku4	55	1.98	1.63	2
doauf240398.3	doauf240398.3.211299.ku5	55	2.03	1.73	2.06
doauf240398.3	doauf240398.3.211299.ku6	55	1.99	1.67	2.04
doauf240398.3	doauf240398.3.211299.ku7	55	1.98	1.66	2.01
doauf240398.3	doauf240398.3.211299.ku8	55	1.98	1.64	2
doauf240398.3	doauf240398.3.211299.ku9	55	2.01	1.71	2.06
doauf240398.3	doauf240398.3.4z	55	1.92	0	0
doauf240398.3	doauf240398.3.4z	55	1.96	0	0
doauf240398.3	doauf240398.3.4z	55	1.98	0	0
doauf240398.3	doauf240398.3.5	35	1.72	0	0
doauf240398.3	doauf240398.3.5	35	1.8	0	0
doauf240398.3	doauf240398.3.6	44	1.81	0	0
doauf240398.3	doauf240398.3.6	44	1.86	0	0
doauf240398.3	doauf240398.3.6	44	1.9	0	0
doauf240398.3	doauf240398.3.7	44	1.98	0	0
doauf240398.3	doauf240398.3.7	44	2.06	0	0
doauf240398.3	doauf240398.3.7	44	2.08	0	0
doauf290998.1	doauf290998.1.1	35	1.94	0	0
doauf290998.1	doauf290998.1.1	35	2.03	0	0
doauf290998.1	doauf290998.1.1	35	2.06	0	0
doauf290998.1	doauf290998.1.130100.kf1	35	0	1.64	0
doauf290998.1	doauf290998.1.130100.kf2	35	0	1.6	0

continued on next page

continued from previous page

outcrop	sample	d [cm]	ρ_b	ρ_d	ρ_{sat}
doauf290998.1	doauf290998.1.130100.kf3	35	0	1.57	0
doauf290998.1	doauf290998.1.130100.kf4	35	0	1.74	0
doauf290998.1	doauf290998.1.130100.kf5	35	0	1.63	0
doauf290998.1	doauf290998.1.130100.kf6	35	0	1.66	0
doauf290998.1	doauf290998.1.130100.kf7	35	0	1.44	0
doauf290998.1	doauf290998.1.130100.kf8	35	0	1.58	0
doauf290998.1	doauf290998.1.160200.kf1	35	2.09	1.76	2.12
doauf290998.1	doauf290998.1.160200.kf2	35	2.09	1.77	2.12
doauf290998.1	doauf290998.1.160200.kf3	35	2.14	1.82	2.17
doauf290998.1	doauf290998.1.160200.kf4	35	2.14	1.81	2.17
doauf290998.1	doauf290998.1.160200.kf5	35	2.09	1.77	2.13
doauf290998.1	doauf290998.1.160200.kf6	35	2.05	1.71	2.08
doauf290998.1	doauf290998.1.160300.1	35	2.1	0	0
doauf290998.1	doauf290998.1.2	35	1.98	0	0
doauf290998.1	doauf290998.1.2	35	2.01	0	0
doauf290998.1	doauf290998.1.2	35	2.02	0	0
doauf290998.1	doauf290998.1.3	35	1.91	0	0
doauf290998.1	doauf290998.1.3	35	1.95	0	0
doauf290998.1	doauf290998.1.3	35	1.99	0	0
doauf290998.1	doauf290998.1.3	35	2	0	0
doauf290998.1	doauf290998.1.z11	35	2.05	0	0
doauf290998.1	doauf290998.1.z11	35	2.06	0	0
doauf290998.1	doauf290998.1.z11	35	2.07	0	0
doauf290998.1	doauf290998.1.z20	35	2	0	0
doauf290998.1	doauf290998.1.z20	35	2.08	0	0
doauf290998.1	doauf290998.1.z20	35	2.1	0	0
doauf290998.1	doauf290998.1.z21	35	2	0	0
doauf290998.1	doauf290998.1.z21	35	2.09	0	0
doauf290998.1	doauf290998.1.z21.2	35	0	1.77	2.08
doauf290998.1	doauf290998.1.z24	35	1.9	0	0
doauf290998.1	doauf290998.1.z24	35	1.94	0	0
doauf290998.1	doauf290998.1.z24	35	2.01	0	0
doauf290998.1	doauf290998.1.zPV32	35	0	1.84	2.56
doauf290998.1	doauf290998.1.zPV6	35	1.99	0	0
dobo190400.1	dobo190400.1.6	564	1.76	0	0
dobo190400.1	dobo190400.1.6	564	1.77	0	0
dobo221098.1	dobo221098.1.5	655	1.98	0	0
meauf270499.1	lp97arns.1a		1.81	1.32	0
meauf270499.1	lp97arns.1b		1.69	1.2	0
meauf270499.1	lp97arns.3		2.14	1.81	0
meauf270499.1	lp97mays.1		1.8	1.19	0
meauf270499.1	lp97mays.2		1.68	1.07	0
meauf270499.1	lp97mays.3		1.76	1.19	0
meauf270499.1	lp97mays.4		1.81	1.22	0
meauf010299.1	meauf010299.1.1	395	2.13	0	0
meauf010299.1	meauf010299.1.2	395	2.02	0	0
meauf010299.1	meauf010299.1.2	395	2.06	0	0
meauf010299.1	meauf010299.1.2	395	2.15	0	0
meauf010299.1	meauf010299.1.3	395	2.09	0	0
meauf010299.1	meauf010299.1.4	395	2.15	0	0
meauf051099.1	meauf051099.1.240200.kf1	225	1.9	1.65	2.02
meauf051099.1	meauf051099.1.240200.kf10	64	1.52	1.45	1.97
meauf051099.1	meauf051099.1.240200.kf11	64	1.44	1.37	1.9
meauf051099.1	meauf051099.1.240200.kf12	64	1.47	1.4	1.92
meauf051099.1	meauf051099.1.240200.kf13	64	1.43	1.37	1.89

continued on next page

continued from previous page

outcrop	sample	d [cm]	ρ_b	ρ_d	ρ_{sat}
meauf051099.1	meauf051099.1.240200.kf14	64	1.32	1.25	1.76
meauf051099.1	meauf051099.1.240200.kf15	64	1.48	1.4	1.91
meauf051099.1	meauf051099.1.240200.kf16	64	1.36	1.29	1.82
meauf051099.1	meauf051099.1.240200.kf2	225	1.81	1.57	1.99
meauf051099.1	meauf051099.1.240200.kf3	225	1.91	1.63	2.02
meauf051099.1	meauf051099.1.240200.kf4	225	1.85	1.6	2.01
meauf051099.1	meauf051099.1.240200.kf5	225	1.82	1.61	2
meauf051099.1	meauf051099.1.240200.kf6	225	1.91	1.7	2.06
meauf051099.1	meauf051099.1.240200.kf7	225	1.88	1.64	2.02
meauf051099.1	meauf051099.1.240200.kf8	225	1.93	1.69	2.06
meauf051099.1	meauf051099.1.240200.kf9	64	1.38	1.31	1.84
meauf270499.1	meauf270499.1.031199.1	575	2.06	0	0
meauf270499.1	meauf270499.1.031199.1	575	2.1	0	0
meauf270499.1	meauf270499.1.031199.1	575	2.12	0	0
meauf270499.1	meauf270499.1.031199.2	575	1.58	0	0
meauf270499.1	meauf270499.1.031199.3	575	1.83	0	0
meauf270499.1	meauf270499.1.031199.3	575	1.84	0	0
meauf270499.1	meauf270499.1.031199.3	575	1.85	0	0
meauf270499.1	meauf270499.1.061299.1	609	2.1	0	0
meauf270499.1	meauf270499.1.061299.2	609	2.09	0	0
meauf270499.1	meauf270499.1.061299.3	609	1.83	0	0
meauf270499.1	meauf270499.1.061299.3	609	1.84	0	0
meauf270499.1	meauf270499.1.091299.1	609	2.14	0	0
meauf270499.1	meauf270499.1.091299.2	609	2.1	0	0
meauf270499.1	meauf270499.1.131299.1	609	2.07	0	0
meauf270499.1	meauf270499.1.131299.1	609	2.08	0	0
meauf270499.1	meauf270499.1.131299.1	609	2.11	0	0
meauf270499.1	meauf270499.1.140100.1	609	2.11	0	0
meauf270499.1	meauf270499.1.140100.2	609	2.04	0	0
meauf270499.1	meauf270499.1.161299.ku1	609	2.08	1.77	2.11
meauf270499.1	meauf270499.1.161299.ku2	609	2.09	1.78	2.07
meauf270499.1	meauf270499.1.161299.ku3	609	2.1	1.78	2.11
meauf270499.1	meauf270499.1.161299.ku4	609	2.12	1.8	2.12
meauf270499.1	meauf270499.1.161299.ku5	609	2.11	1.8	2.12
meauf270499.1	meauf270499.1.161299.ku6	609	2.09	1.78	2.11
meauf270499.1	meauf270499.1.161299.ku7	609	2.09	1.77	2.09
meauf270499.1	meauf270499.1.161299.ku8	609	2.09	1.77	2.09
meauf270499.1	meauf270499.1.161299.ku9	609	2.1	1.78	2.1
meauf270499.1	meauf270499.1.170400.1	609	2.09	0	0
meauf270499.1	meauf270499.1.210100.kf1	665	2.04	1.94	2.28
meauf270499.1	meauf270499.1.210100.kf10	509	1.23	0.82	1.55
meauf270499.1	meauf270499.1.210100.kf11	509	1.46	1.1	1.75
meauf270499.1	meauf270499.1.210100.kf12	509	1.23	0.76	1.51
meauf270499.1	meauf270499.1.210100.kf13	509	1.29	1.11	1.85
meauf270499.1	meauf270499.1.210100.kf14	509	1.22	0.82	1.56
meauf270499.1	meauf270499.1.210100.kf15	509	1.31	0.84	1.59
meauf270499.1	meauf270499.1.210100.kf16	509	1.2	0.73	1.5
meauf270499.1	meauf270499.1.210100.kf17	365	1.66	1.73	2.28
meauf270499.1	meauf270499.1.210100.kf18	365	1.59	1.81	2.38
meauf270499.1	meauf270499.1.210100.kf19	365	1.54	1.33	1.93
meauf270499.1	meauf270499.1.210100.kf2	665	2.09	2	2.35
meauf270499.1	meauf270499.1.210100.kf20	365	1.59	1.35	1.95
meauf270499.1	meauf270499.1.210100.kf21	365	1.65	1.43	2.01
meauf270499.1	meauf270499.1.210100.kf22	365	1.64	1.41	1.98
meauf270499.1	meauf270499.1.210100.kf23	365	1.57	1.48	2.04

continued on next page

continued from previous page					
outcrop	sample	d [cm]	ρ_b	ρ_d	ρ_{sat}
meauf270499.1	meauf270499.1.210100.kf3	665	2.08	2	2.33
meauf270499.1	meauf270499.1.210100.kf4	665	2.13	2.04	2.39
meauf270499.1	meauf270499.1.210100.kf5	665	2.08	2.27	2.62
meauf270499.1	meauf270499.1.210100.kf6	665	2.13	2.32	2.65
meauf270499.1	meauf270499.1.210100.kf7	665	2.07	1.95	1.94
meauf270499.1	meauf270499.1.210100.kf8	665	2.11	2.29	2.64
meauf270499.1	meauf270499.1.210100.kf9	509	1.57	1.27	1.92
meauf270499.1	meauf270499.1.221199.1	609	2.08	0	0
meauf270499.1	meauf270499.1.240200.1	609	2.13	0	0
meauf270499.1	meauf270499.1.240200.2	609	2.02	0	0

Particle density

Listing: SQL–code querying particle density measurement results from database.

```
SELECT f.field_id AS outcrop, so.sample_id AS sample,
%(100*COALESCE((so.upperdepth+so.lowerdepth)/2,so.upperdepth,so.lowerdepth)) AS "depth_[cm]", l.id AS labid,
%(100*(sample-tara)/(((water-tara)/((1/(1+0.000001*(((2.31*tempwater-2)^2)-182)))))-
((samplewater-sample)/((1/(1+0.000001*(((2.31*tempsampwater-2)^2)-182)))))))/100 AS "particle_density"
FROM pycn p, lab l, soilsample so, field f
WHERE p.lab_id=l.id AND l.sample_id=so.id AND so.field_id=f.id
AND %(100*(sample-tara)/(((water-tara)/((1/(1+0.000001*(((2.31*tempwater-2)^2)-182)))))-
((samplewater-sample)/((1/(1+0.000001*(((2.31*tempsampwater-2)^2)-182)))))))/100 > 1
ORDER BY so.sample_id, "particle_density";
```

Results of particle density (pycnometer–method). Calculated values particle densities per laboratory experiment. Units are g/cm^3.

outcrop	sample	depth [cm]	labid	particle density
doauf020498.1	doauf020498.1.1	25	1065	2.39
doauf020498.1	doauf020498.1.1	25	333	2.6
doauf020498.1	doauf020498.1.1	25	1066	2.66
doauf020498.1	doauf020498.1.1	25	1067	2.7
doauf020498.2	doauf020498.2.1	35	1068	2.52
doauf020498.2	doauf020498.2.1	35	1069	2.64
doauf020498.2	doauf020498.2.1	35	334	2.65
doauf020498.3	doauf020498.3.1	55	1071	2.52
doauf020498.3	doauf020498.3.1	55	1070	2.61
doauf020498.3	doauf020498.3.1	55	335	2.62
doauf240398.3	doauf020498.4.1	55	1073	2.49
doauf240398.3	doauf020498.4.1	55	1072	2.53
doauf240398.3	doauf020498.4.1	55	336	2.61
doauf180898.1	doauf180898.1.160300.1	35	2435	2.58
doauf180898.1	doauf180898.1.160300.1	35	2437	2.58
doauf180898.1	doauf180898.1.160300.1	35	2436	2.59
doauf180898.1	doauf180898.1.160300.1	35	2434	2.63
doauf240398.2	doauf240398.2.10	5	2378	2.47
doauf240398.2	doauf240398.2.10	5	2379	2.49
doauf240398.2	doauf240398.2.10	5	2377	2.6
doauf240398.3	doauf240398.3.190199.1	55	2422	2.67
doauf240398.3	doauf240398.3.190199.1	55	2423	2.69
doauf240398.3	doauf240398.3.190199.1	55	2424	2.69
doauf290998.1	doauf290998.1.4	35	2399	2.7
doauf290998.1	doauf290998.1.4	35	2398	2.72
doauf290998.1	doauf290998.1.4	35	2400	2.75
dobo040998.1	dobo040998.1.4	472	1088	2.52
dobo040998.1	dobo040998.1.4	472	728	2.55
dobo040998.1	dobo040998.1.4	472	1087	2.57
dobo050698.1	dobo050698.1.2	284	1098	2.62
dobo050698.1	dobo050698.1.2	284	734	2.65
dobo050698.1	dobo050698.1.2	284	1097	2.74
dobo050698.2	dobo050698.2.1	122	1099	2.64
dobo050698.2	dobo050698.2.1	122	736	2.67
dobo050698.2	dobo050698.2.1	122	1100	2.68
dobo050698.2	dobo050698.2.2	270	738	2.29
dobo050698.2	dobo050698.2.2	270	1101	2.78
dobo050698.2	dobo050698.2.2	270	1102	2.78

continued on next page

continued from previous page

outcrop	sample	depth [cm]	labid	particle density
dobo110898.1	dobo110898.1.3	195	739	2.16
dobo110898.1	dobo110898.1.3	195	1104	2.43
dobo110898.1	dobo110898.1.3	195	1103	2.45
dobo110898.1	dobo110898.1.5	455	740	2.46
dobo110898.1	dobo110898.1.5	455	1106	2.54
dobo110898.1	dobo110898.1.5	455	1105	2.64
dobo110898.1	dobo110898.1.6	705	1108	2.55
dobo110898.1	dobo110898.1.6	705	1107	2.59
dobo110898.1	dobo110898.1.6	705	742	2.6
dobo110898.2	dobo110898.2.1	134	1110	2.4
dobo110898.2	dobo110898.2.1	134	743	2.7
dobo110898.2	dobo110898.2.1	134	1109	3.06
dobo110998.1	dobo110998.1.2	309	1076	2.06
dobo110998.1	dobo110998.1.2	309	392	2.12
dobo110998.1	dobo110998.1.8	989	1075	2.19
dobo110998.1	dobo110998.1.8	989	1074	2.26
dobo110998.1	dobo110998.1.8	989	388	2.32
dobo120898.1	dobo120898.1.3	254	1081	1.92
dobo120898.1	dobo120898.1.3	254	722	2.01
dobo120898.1	dobo120898.1.4	365	724	2.22
dobo120898.1	dobo120898.1.4	365	1084	2.25
dobo120898.1	dobo120898.1.4	365	1083	2.34
dobo120898.1	dobo120898.1.6	414	1085	1.95
dobo120898.1	dobo120898.1.6	414	1086	2
dobo120898.1	dobo120898.1.6	414	726	2.33
dobo130898.1	dobo130898.1.1	104	1111	2.71
dobo130898.1	dobo130898.1.1	104	1112	2.94
dobo130898.1	dobo130898.1.1	104	745	4.18
dobo130898.1	dobo130898.1.5	334	1113	2.45
dobo130898.1	dobo130898.1.5	334	1114	2.53
dobo130898.1	dobo130898.1.5	334	747	2.55
dobo130898.1	dobo130898.1.6	455	1115	2.49
dobo130898.1	dobo130898.1.6	455	1116	2.52
dobo130898.1	dobo130898.1.6	455	749	2.53
dobo130898.1	dobo130898.1.7	514	1118	2.37
dobo130898.1	dobo130898.1.7	514	750	2.41
dobo130898.1	dobo130898.1.7	514	1117	2.42
dobo130898.1	dobo130898.1.8	555	1119	2.52
dobo130898.1	dobo130898.1.8	555	751	2.71
dobo200898.1	dobo200898.1.10	685	1123	2.52
dobo200898.1	dobo200898.1.10	685	753	2.56
dobo200898.1	dobo200898.1.10	685	1124	2.56
dobo200898.1	dobo200898.1.5	405	1121	2.36
dobo200898.1	dobo200898.1.5	405	1122	2.45
dobo200898.1	dobo200898.1.5	405	752	2.49
dobo201098.2	dobo201098.2.2	254	1078	2.28
dobo201098.2	dobo201098.2.2	254	1077	2.43
dobo201098.2	dobo201098.2.2	254	719	2.5
dobo201098.2	dobo201098.2.3	375	1080	2.57
dobo201098.2	dobo201098.2.3	375	1079	2.6
dobo201098.2	dobo201098.2.3	375	720	2.64

continued on next page

continued from previous page				
outcrop	sample	depth [cm]	labid	particle density
dobo250898.1	dobo250898.1.2	154	754	2.48
dobo250898.1	dobo250898.1.2	154	1125	2.57
dobo250898.1	dobo250898.1.2	154	1126	2.58
dobo250898.1	dobo250898.1.4	254	1127	2.4
dobo250898.1	dobo250898.1.4	254	755	2.43
dobo250898.1	dobo250898.1.4	254	1128	2.49
dobo250898.1	dobo250898.1.5	365	756	2.16
dobo250898.1	dobo250898.1.5	365	1129	2.3
dobo250898.1	dobo250898.1.5	365	1130	2.39
dobo270898.1	dobo270898.1.2	395	1094	2.12
dobo270898.1	dobo270898.1.2	395	732	2.29
dobo270898.1	dobo270898.1.2	395	1093	2.56
dobo270898.1	dobo270898.1.3	594	733	2.06
dobo270898.1	dobo270898.1.3	594	1096	2.24
dobo270898.1	dobo270898.1.3	594	1095	2.32
dobo270898.2	dobo270898.2.13	775	1091	2.53
dobo270898.2	dobo270898.2.13	775	731	2.58
dobo270898.2	dobo270898.2.13	775	1092	2.6
dobo270898.2	dobo270898.2.5	354	730	2.58
dobo270898.2	dobo270898.2.5	354	1090	2.58
meauf270499.1	lp97arns.1a		2522	2.91
meauf270499.1	lp97arns.1b		2523	2.6
meauf270499.1	lp97arns.3		2524	2.54
meauf270499.1	lp97mays.1		2469	2.64
meauf270499.1	lp97mays.2		2471	2.61
meauf270499.1	lp97mays.3		2472	2.67
meauf270499.1	lp97mays.5		2470	2.61

C.3. Consistency limits

Listing: protect SQL–code querying results for consistency limits from database.

```
SELECT max(f.field_id) AS outcrop, so.sample_id AS sample,
max(%(100*COALESCE((so.upperdepth+so.lowerdepth)/2,
so.upperdepth,so.lowerdepth))) AS "depth_[cm]",
%(100*(ln(25.0)*((sum(ln(float8(l.n))*((l.wet-l.dry)/(l.dry-l.tara)))*
count(l.n)-sum(ln(float8(l.n)))*sum((l.wet-l.dry)/(l.dry-l.tara)))/
(count(l.n)*sum(ln(float8(l.n))*ln(float8(l.n)))-sum(ln(float8(l.n)))*
sum(ln(float8(l.n)))))+(sum((l.wet-l.dry)/(l.dry-l.tara))/count(l.n))-
(((sum(ln(float8(l.n))*((l.wet-l.dry)/(l.dry-l.tara)))*count(l.n)-
sum(ln(float8(l.n)))*sum((l.wet-l.dry)/(l.dry-l.tara)))/(count(l.n)*
sum(ln(float8(l.n))*ln(float8(l.n)))-sum(ln(float8(l.n)))*
sum(ln(float8(l.n)))))*sum(ln(float8(l.n))))/count(l.n)))))/100 AS "liquid_limit",
%(100*avg((p.wet-p.dry)/(p.dry-p.tara)))/100 AS "plastic_limit"
FROM lab l1, lab l2, liqlimit l, plastlimit p, soilsample so, field f
WHERE l1.id=l.lab_id AND l2.id=p.lab_id
  AND l1.sample_id=so.id AND l2.sample_id=so.id
  AND so.field_id=f.id
GROUP BY so.sample_id
UNION
SELECT f.field_id AS outcrop, so.sample_id AS sample,
%(100*COALESCE((so.upperdepth+so.lowerdepth)/2,
so.upperdepth,so.lowerdepth)) AS "depth_[cm]",
%(100*l.value)/100 AS "liquid_limit", %(100*p.value)/100 AS "plastic_limit"
FROM labvalue l, labvalue p, lab l1, lab l2, soilsample so, field f
WHERE l.par_id=14 AND p.par_id=13 AND l.lab_id=l1.id AND p.lab_id=l2.id
  AND l1.sample_id=l2.sample_id AND l1.sample_id=so.id AND so.field_id=f.id
ORDER BY outcrop, sample
```

Results of Atterberg tests. Calculated parameters per sample. Consistency limits are shown as fractions relative to [1].

outcrop	sample	depth [cm]	liquid limit	plastic limit
doauf020498.1	doauf020498.1.020400.3	25	0.32	0.22
doauf020498.1	doauf020498.1.1	25	0.34	0.23
doauf020498.1	doauf020498.1.160900.1	25	0.34	0.21
doauf020498.2	doauf020498.2.1	35	0.35	0.2
doauf020498.2	doauf020498.2.160900.1	35	0.28	0.15
doauf020498.3	doauf020498.3.1	55	0.54	0.48
doauf020498.3	doauf020498.3.2	64	0.58	0.47
doauf180898.1	doauf180898.1.160300.1	35	0.22	0.15
doauf180898.1	doauf180898.1.160900.1	35	0.32	0.17
doauf240398.2	doauf240398.2.10	5	0.28	0.17
doauf240398.2	doauf240398.2.160200.1	675	0.31	0.16
doauf240398.2	doauf240398.2.160900.1	675	0.36	0.21
doauf240398.3	doauf020498.4.1	55	0.44	0.2
doauf240398.3	doauf240398.3.020400.2	55	0.53	0.17
doauf240398.3	doauf240398.3.160200.3	55	0.48	0.21
doauf240398.3	doauf240398.3.160900.1	55	0.46	0.2
doauf240398.3	doauf240398.3.8	55	0.44	0.16
doauf240398.3	doauf240398.3.9	55	0.4	0.16
doauf290998.1	doauf290998.1.020400.1	35	0.22	0.14
doauf290998.1	doauf290998.1.160900.1	35	0.29	0.18
doauf290998.1	doauf290998.1.4	35	0.3	0.18
dobo040998.1	dobo040998.1.4	472	0.34	0.18
dobo050698.1	dobo050698.1.1	150	0.37	0.19
dobo050698.1	dobo050698.1.2	284	0.25	0.18
dobo050698.2	dobo050698.2.1	122	0.31	0.2
dobo050698.2	dobo050698.2.2	270	0.44	0.18
dobo110898.1	dobo110898.1.3	195	0.39	0.2
dobo110898.1	dobo110898.1.5	455	0.22	0.14
dobo110898.1	dobo110898.1.6	705	0.78	0.34
dobo110898.2	dobo110898.2.1	134	0.43	0.27
dobo110898.2	dobo110898.2.2	225	0.42	0.22

continued on next page

continued from previous page

outcrop	sample	depth [cm]	liquid limit	plastic limit
dobo110998.1	dobo110998.1.2	309	0.44	0.24
dobo110998.1	dobo110998.1.8	989	0.31	0.16
dobo120898.1	dobo120898.1.3	254	0.37	0.18
dobo120898.1	dobo120898.1.4	365	0.47	0.22
dobo120898.1	dobo120898.1.6	414	0.22	0.14
dobo130898.1	dobo130898.1.1	104	0.32	0.25
dobo130898.1	dobo130898.1.5	334	0.48	0.22
dobo130898.1	dobo130898.1.6	455	0.18	0.12
dobo130898.1	dobo130898.1.7	514	0.34	0.16
dobo130898.1	dobo130898.1.8	555	0.15	0.14
dobo180400.1	dobo180400.1.3	145	0.52	0.31
dobo180400.1	dobo180400.1.4	195	0.58	0.38
dobo180400.1	dobo180400.1.7	284	0.4	0.21
dobo180400.1	dobo180400.1.8	375	0.38	0.24
dobo190400.1	dobo190400.1.2	165	0.25	0.15
dobo190400.1	dobo190400.1.3	265	0.51	0.25
dobo190400.1	dobo190400.1.4	365	0.39	0.18
dobo190400.1	dobo190400.1.6	564	0.38	0.24
dobo200898.1	dobo200898.1.5	405	0.25	0.15
dobo201098.2	dobo201098.2.3	375	0.35	0.22
dobo250898.1	dobo250898.1.2	154	0.24	0.22
dobo250898.1	dobo250898.1.4	254	0.23	0.18
dobo250898.1	dobo250898.1.5	365	0.36	0.25
dobo270898.1	dobo270898.1.2	395	0.39	0.22
dobo270898.1	dobo270898.1.3	594	0.38	0.16
dobo270898.2	dobo270898.2.13	775	0.43	0.21
dobo270898.2	dobo270898.2.5	354	0.3	0.19
meauf010299.1	meauf010299.1.1	395	0.48	0.24
meauf010299.1	meauf010299.1.3	395	0.48	0.26
meauf270499.1	lp97arns.1a		1.2	0.29
meauf270499.1	lp97arns.1b		0.67	0.17
meauf270499.1	lp97arns.3		0.31	0.16
meauf270499.1	lp97mays.1		0.27	0.15
meauf270499.1	lp97mays.2		0.28	0.14
meauf270499.1	lp97mays.3		0.71	0.37
meauf270499.1	lp97mays.5		0.68	0.39
meauf270499.1	lp97parkner		0.38	0.15
meauf270499.1	meauf270499.1.031199.1	575	0.31	0.15
meauf270499.1	meauf270499.1.061299.1	609	0.3	0.15
meauf270499.1	meauf270499.1.091299.1	609	0.34	0.16
meauf270499.1	meauf270499.1.221199.1	609	0.28	0.15
meauf270499.1	meauf270499.1.221199.2	609	0.38	0.18
meauf270499.1	meauf270499.1.lab991	304	0.31	0.25
meauf270499.1	meauf270499.1.lab992	490	0.82	0.41
meauf270499.1	meauf270499.1.lab993	590	1.1	0.61
meauf270499.1	meauf270499.1.lab994	644	0.25	0.17
tueg1	tueg1.12	125	0.73	0.42
tueg1	tueg1.13	134	0.72	0.37
tueg1	tueg1.14	145	0.73	0.35
tueg1	tueg1.15	154	0.59	0.35

C.4. Shear strength

Direct shear tests

Listing: SQL–code querying results for shear strength from shear box tests from database.

```
CREATE TEMP TABLE effshear AS
SELECT max(f.field_id) AS outcrop, max(so.sample_id) AS sample, sh.lab_id AS labid,
        CASE WHEN max(sampletreat)<>" THEN '+'ELSE '−'END AS treat,
        max((sh.cons∗10∗9.81)/(0.035∗0.035∗3.14152∗1000)) AS normstress,
        max(s.force/(0.035∗0.035∗3.14152)) AS peakstress,
        avg((bruttoin−ring)/(3.5∗3.5∗pi()∗2)) AS density
FROM shear sh, shear_shearser s, lab l, soilsample so , field f
WHERE sh.lab_id=s.lab_id AND l.id=sh.lab_id AND l.sample_id=so.id AND so.field_id=f.id
GROUP BY sh.lab_id
UNION
SELECT f.field_id AS outcrop, so.sample_id AS sample, s.lab_id AS labid,
        CASE WHEN sampletreat<>" THEN '+'ELSE '−'END AS treat,
        (s.cons∗10∗9.81)/(0.035∗0.035∗3.14152∗1000) AS normstress,
        s.maxforce/(0.035∗0.035∗3.14152) AS peakstress,
        (bruttoin−ring)/(3.5∗3.5∗pi()∗2) AS density
FROM shear s, lab l, soilsample so, field f
WHERE s.lab_id NOT IN (select lab_id from shear_shearser) AND l.id=s.lab_id
AND l.sample_id=so.id AND so.field_id=f.id;
CREATE TEMP TABLE resshear AS
SELECT sh.lab_id AS labid, s.force/(0.035∗0.035∗3.14152) AS resstress
FROM shear sh, shear_shearser s
WHERE sh.lab_id=s.lab_id AND s.id IN (select max(id) from shear_shearser group by lab_id)
UNION
SELECT s.lab_id AS labid, "AS resstress
FROM shear s
WHERE s.lab_id NOT IN (select lab_id from shear_shearser);
SELECT max(outcrop) AS outcrop, sample AS sample, max(treat) AS "sample_prep.",
%(avg(peakstress)−(((count(peakstress)∗sum(peakstress∗normstress)−sum(normstress)∗sum(peakstress))/(count(peakstress)∗
sum(normstress∗normstress)−sum(normstress)∗sum(normstress)))∗avg(normstress))) AS "\effcohesion",
%(degrees(atan((count(peakstress)∗sum(peakstress∗normstress)−sum(normstress)∗sum(peakstress))/(count(peakstress)∗
sum(normstress∗normstress)−sum(normstress)∗sum(normstress))))) AS "\effshearangle",
%(degrees(atan(sum(peakstress)/sum(normstress)))) AS "\effshearangle_(c=0)",
%(avg(resstress)−(((count( resstress )∗sum(resstress∗normstress)−sum(normstress)∗sum(resstress))/(count(resstress)∗
sum(normstress∗normstress)−sum(normstress)∗sum(normstress)))∗avg(normstress))) AS "\rescohesion",
%(degrees(atan((count(resstress)∗sum(resstress∗normstress)−sum(normstress)∗sum(resstress))/(count(resstress)∗
sum(normstress∗normstress)−sum(normstress)∗sum(normstress))))) AS "\resshearangle",
%(degrees(atan(sum(resstress)/sum(normstress)))) AS "\resshearangle_(c=0)",
%(10∗avg(density))/10 AS "\density"
FROM effshear p,resshear r WHERE p.labid=r.labid
GROUP BY sample
ORDER BY outcrop, "sample_prep.", sample;
```

Results of shear box tests. Calculated shear parameters per sample. 'Sample prep.' indicates prepared samples. Additionally, values for no cohesion (c =0) are calculated.

outcrop	sample	sample prep.	c'	ϕ'	ϕ' (c=0)	c_r	ϕ_r	ϕ_r (c=0)	ρ_b
doauf020498.1	doauf020498.1.020400.3	+	28	20	26	11	16	18	2.2
doauf020498.1	doauf020498.1.4z	-	39	24	33	38	14	24	2
doauf020498.2	doauf020498.2.4z	-	94	13	31	73	14	28	1.9
doauf050598.2	doauf050598.2.1	-	12	21	23	24	17	22	1.8
doauf050598.3	doauf050598.3.1	-	70	27	57	10	27	34	1.5
doauf180898.1	doauf180898.1.160300.1	+	39	22	29	31	18	25	1.9
doauf180898.1	doauf180898.1.1	-	110	14	34	71	7	22	1.7
doauf180898.1	doauf180898.1.2	-	12	37	39	21	31	35	1.8
doauf180898.1	doauf180898.1.3	-	54	23	32	58	20	31	1.7
doauf180898.1	doauf180898.1.4	-	70	23	35	49	20	29	1.8
doauf240398.1	doauf240398.1.2z	-	88	34	46	29	30	35	1.4

continued on next page

continued from previous page

outcrop	sample	sample prep.	c'	ϕ'	ϕ' (c=0)	c_r	ϕ_r	ϕ_r (c=0)	ρ_b
doauf240398.2	doauf240398.2.160200.1	+	52	27	36	44	24	32	1.8
doauf240398.2	doauf240398.2.10	-	73	24	43	54	26	40	1.9
doauf240398.2	doauf240398.2.2z	-	61	27	37	38	29	35	1.6
doauf240398.2	doauf240398.2.7	-	-8	33	32	19	26	29	1.8
doauf240398.2	doauf240398.2.8	-	12	30	33	16	27	31	1.8
doauf240398.2	doauf240398.2.9	-	7	27	30	5	26	28	1.7
doauf240398.3	doauf240398.3.160200.3	+	37	11	20	14	7	11	1.7
doauf240398.3	doauf240398.3.1	-	6	31	32	-135	38	14	1.9
doauf240398.3	doauf240398.3.4z	-	-4	21	20	12	13	15	1.9
doauf240398.3	doauf240398.3.5	-	6	16	18	-3	15	13	1.7
doauf240398.3	doauf240398.3.6	-	-16	25	22	22	12	16	1.8
doauf240398.3	doauf240398.3.7	-	225	-10	42	119	-5	25	2
doauf290998.1	doauf290998.1.1	-	39	20	28	-88	27	9	2
doauf290998.1	doauf290998.1.2	-	47	23	31	-121	35	13	2
doauf290998.1	doauf290998.1.3	-	-27	31	27	-7	22	21	1.9
doauf290998.1	doauf290998.1.z11	-	3	30	30	-0	29	29	2
doauf290998.1	doauf290998.1.z20	-	10	35	42	4	35	38	2
doauf290998.1	doauf290998.1.z21	-	-3	38	37	-13	35	30	2
doauf290998.1	doauf290998.1.z24	-	-20	35	28	-6	27	24	1.9
dobo190400.1	dobo190400.1.6	+	36	18	25	11	13	15	1.7
dobo221098.1	dobo221098.1.5	-	40	12	27	40	7	23	1.9
meauf010299.1	meauf010299.1.2	-	-10	34	30	-9	26	22	2
meauf270499.1	meauf270499.1.031199.3	+	29	21	27	11	21	24	1.8
meauf270499.1	meauf270499.1.061299.3	+	23	26	30	15	24	27	1.8
meauf270499.1	lp97parkner	-	56	13	24	74	1	17	
meauf270499.1	meauf270499.1.031199.1	-	48	19	39	36	19	35	2
meauf270499.1	meauf270499.1.131299.1	-	61	25	47	47	23	42	2

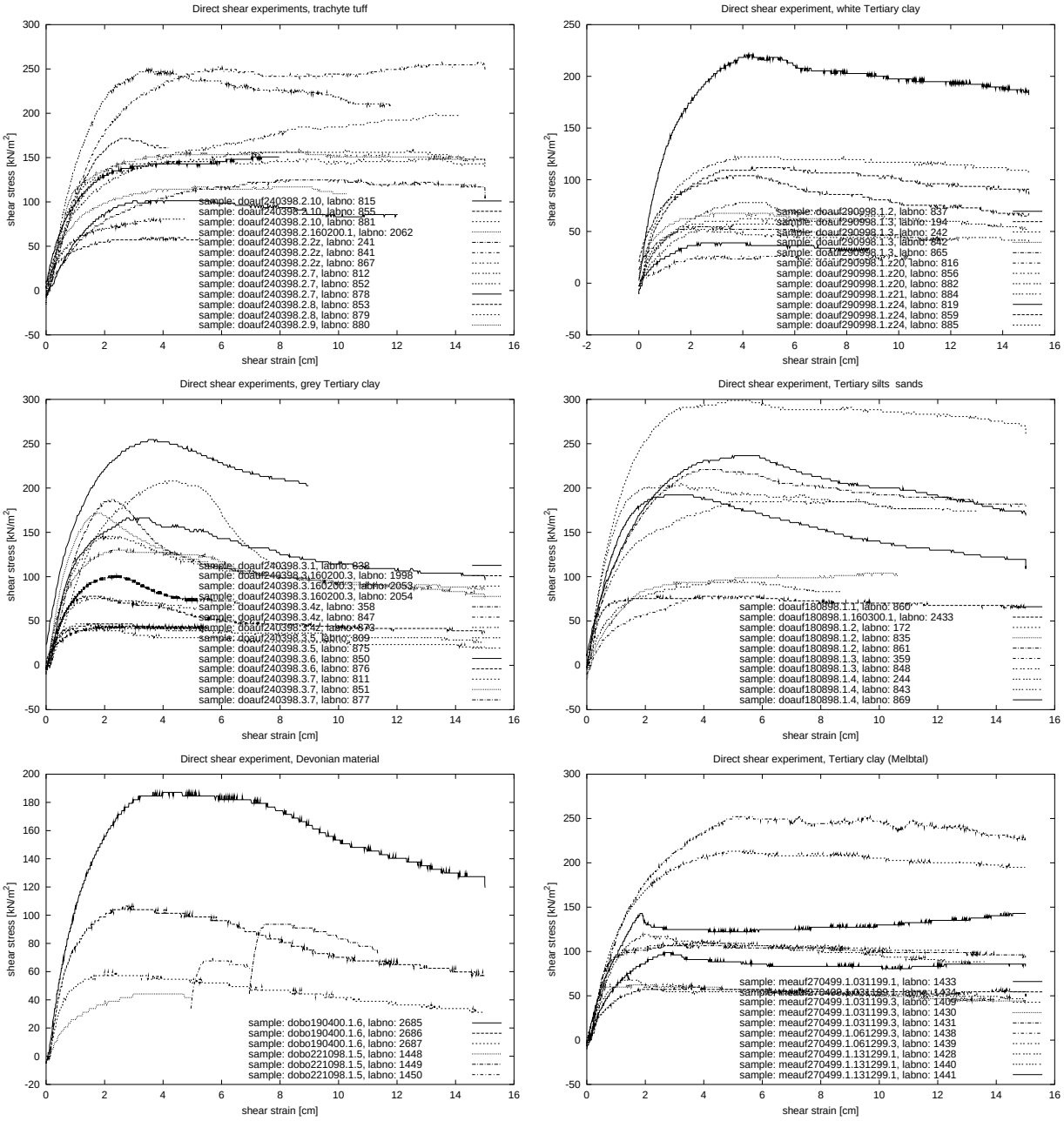

Stress–strain diagrams from shear tests for different material types, field sites Dollendorfer Hardt and Melbtal. The graphs indicate that distinct differences between peak and residual shear strength exist for Tertiary clays and Devonian sediments of the field site Dollendorfer Hardt.

Triaxial tests

Listing: SQL–code querying data from triaxial tests from database.

```
SELECT f.field_id AS outcrop, so.sample_id AS sample,
t.sheartype AS "exp._type", t.diain AS "d",
t.heightin AS "h",
100*(t.conscellpress -t.consbackpress) AS "consolidation",
100*(t.consbackpress) AS "back_pressure",
coalesce(100*(t. swellcellpress -t.swellbackpress),100*(t. conscellpress -t.consbackpress))
AS "consolidation_at_shear_begin"
FROM triax t, lab l, soilsample so, field f
WHERE t.lab_id=l.id AND l.sample_id=so.id AND so.field_id=f.id;
```

Results of triaxial tests. Meta data and stress conditions. (d: sample diameter [mm]; h: sample height [mm])

outcrop	sample	exp. type	d [mm]	h [mm]	consolidation	back pressure	consolidation at shear begin
doauf240398.3	doauf240398.3.160200.1	cu	50	120	400	700	400
doauf240398.3	doauf240398.3.160200.2	cu	50	120	300	700	300
doauf240398.3	doauf240398.3.160200.3	cu	50	120	300	700	300
doauf290998.1	doauf290998.1.z44.2	cu	96	85	100	400	100
doauf290998.1	doauf290998.1.zPV6		95	82	100	600	100
doauf290998.1	doauf290998.1.z44.1	cu	95	90	200	600	200
doauf290998.1	doauf290998.1.z6	cu	95	85	500	400	500
doauf290998.1	doauf290998.1.z29		90	87	100	500	100
doauf290998.1	doauf290998.1.160300.1	cu	95	120	300	700	300
doauf020498.1	doauf020498.1.050598.z15	cu	95	80	100	600	100
doauf020498.1	doauf020498.1.050598.z20	cd	95	94	400	0	400
meauf270499.1	meauf270499.1.221199.1	cu	50	81	300	700	300
meauf270499.1	meauf270499.1.221199.2	cu	50	91	300	700	300
meauf270499.1	meauf270499.1.061299.1	cu	50	92	300	700	300
meauf270499.1	meauf270499.1.091299.1	cu	50	120	300	900	200
meauf270499.1	meauf270499.1.140100.1	cu	50	120	400	700	400
meauf270499.1	meauf270499.1.140100.2	cu	50	120	300	900	100
meauf270499.1	meauf270499.1.240200.1	cu	95	121	300	700	200
meauf270499.1	meauf270499.1.240200.2	cu	95	119	300	700	100
meauf270499.1	meauf270499.1.170400.1	cu	95	120	300	700	300

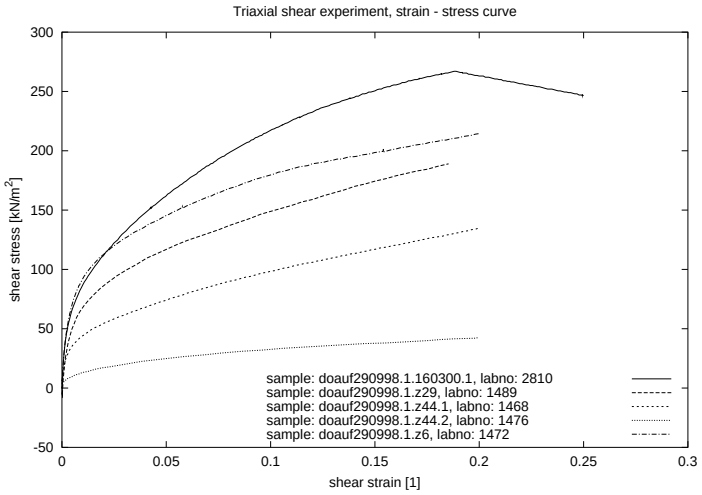

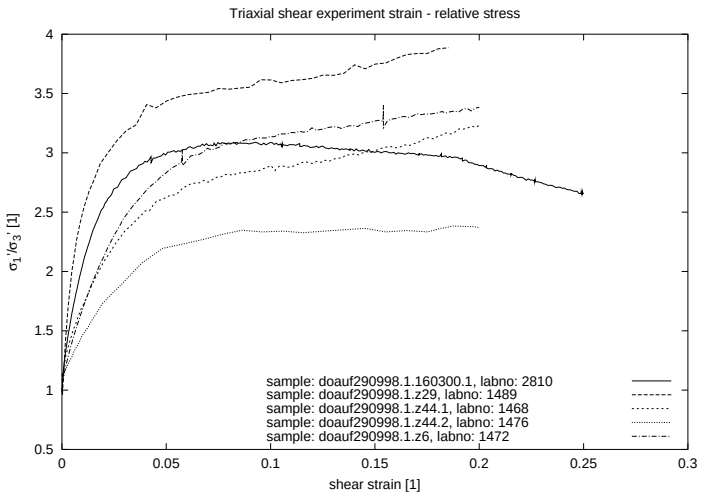

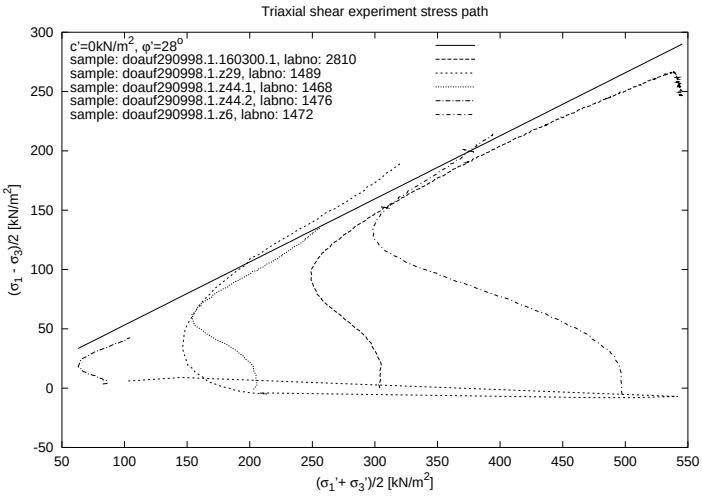

Triaxial tests on samples of white tertiary clay and sand, field site Dollendorfer Hardt.

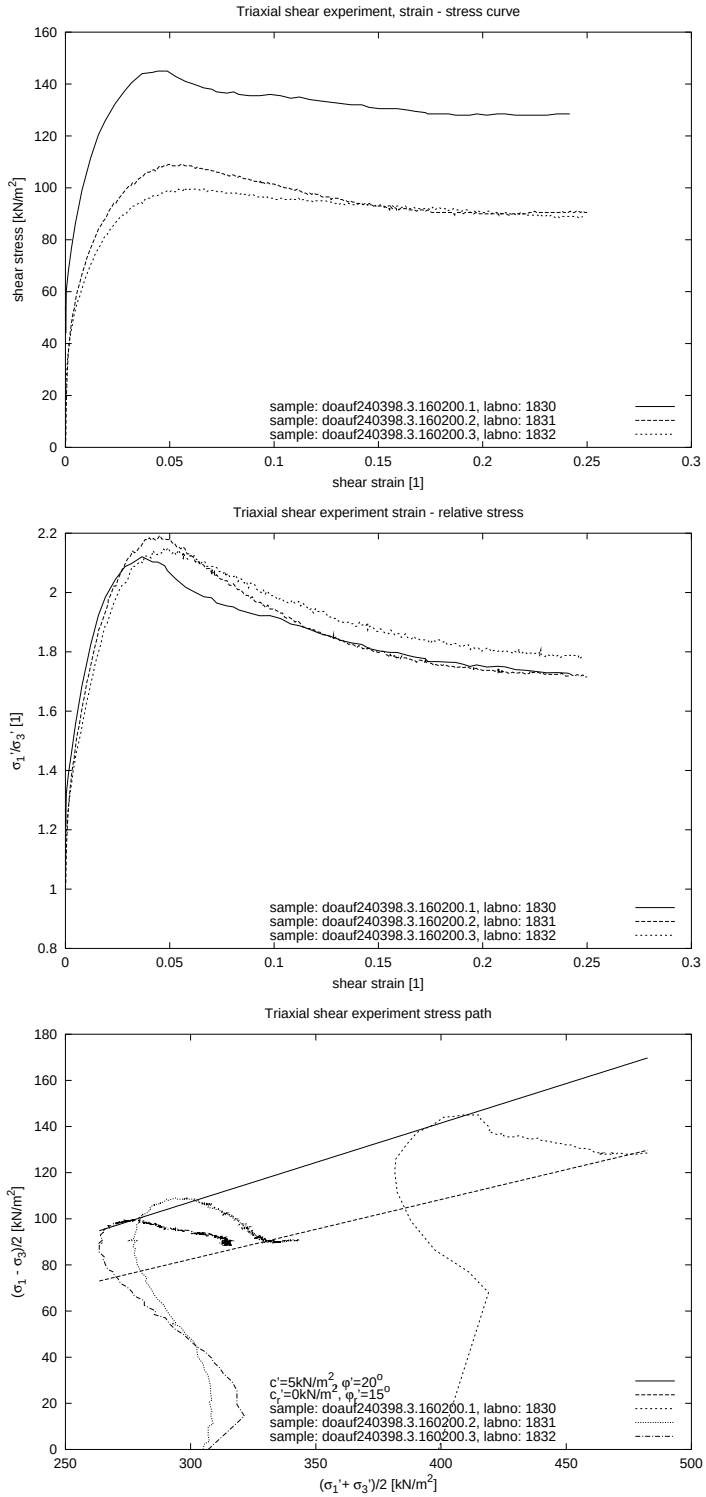

Triaxial tests on samples of grey tertiary clay, field site Dollendorfer Hardt. The test results also allowed the calculation of the residual strength.

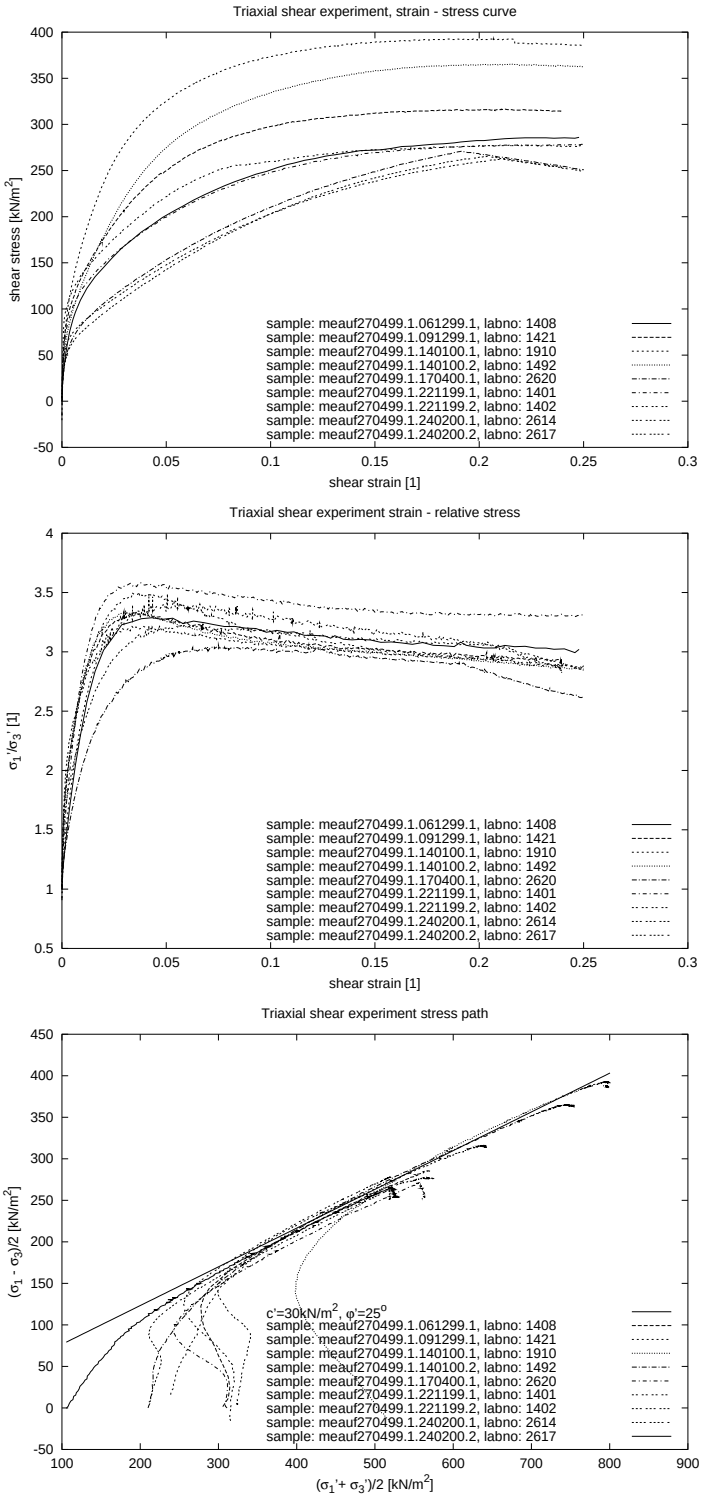

Triaxial tests on samples of tertiary clay, field site Melbtal.

C.5. Permeability

Listing: SQL–code querying results for saturated conductivity k_s from permeability tests from database.

```
SELECT /* constant head */
f. field_id  AS outcrop, s.sample_id AS sample,
l1.id  AS labid, e.name AS experiment,
to_char(-log((COALESCE(k.volume,(k.brutto-k.tara)/\
(1/(1+0.000001*(((2.31*k.temperature-2)^2)-182))))*w.cylheight)/\
(k.time*(w.cyldiameter*w.cyldiameter*3.14152/4)*(k.ho-k.hu)*100)),'99.99') AS kf
FROM kf k,wetdrydens w,lab l1, lab l2, soilsample s, field  f, experiment e
WHERE k.lab_id=l1.id
  AND w.lab_id=l2.id
  AND l1.sample_id=l2.sample_id
  AND l1.exp_id=e.id
  AND l1.exp_id=5
  AND l1.sample_id=s.id
  AND s.field_id=f.id
UNION
SELECT /* falling head */
f. field_id  AS outcrop, s.sample_id AS sample,
l1.id  AS labid, e.name AS experiment,
to_char(-log((k.f*w.cylheight)*(;(k.ho/k.hu))/\
(k.time*(w.cyldiameter*w.cyldiameter*3.14152/4)*100)),'9.99') AS kf
FROM kf k,wetdrydens w,lab l1, lab l2, soilsample s, field  f, experiment e
WHERE k.lab_id=l1.id
  AND w.lab_id=l2.id
  AND l1.sample_id=l2.sample_id
  AND l1.exp_id=e.id
  AND l1.exp_id=6
  AND l1.sample_id=s.id
  AND s.field_id=f.id
ORDER BY outcrop,sample;
```

Results of permeability tests. Conductivity shown as negative logarithm.

outcrop	sample	labid	experiment	kf
doauf180898.1	doauf180898.1.160200.kf1	2145	permeability (constant head)	4.97
doauf180898.1	doauf180898.1.160200.kf2	2146	permeability (constant head)	6.38
doauf180898.1	doauf180898.1.160200.kf3	2147	permeability (constant head)	4.49
doauf180898.1	doauf180898.1.160200.kf4	2148	permeability (constant head)	5.49
doauf180898.1	doauf180898.1.160200.kf5	2149	permeability (constant head)	4.68
doauf180898.1	doauf180898.1.160200.kf6	2150	permeability (constant head)	5.81
doauf180898.1	doauf180898.1.160200.kf7	2151	permeability (constant head)	5.58
doauf240398.1	doauf240398.1.150899.3	1649	permeability (constant head)	6.59
doauf240398.1	doauf240398.1.150899.3	1658	permeability (constant head)	6.71
doauf240398.1	doauf240398.1.150899.3	1667	permeability (constant head)	6.75
doauf240398.1	doauf240398.1.150899.3	1675	permeability (constant head)	6.76
doauf240398.1	doauf240398.1.150899.3	1676	permeability (constant head)	6.75
doauf240398.2	doauf240398.2.130100.kf1	1598	permeability (constant head)	5.86
doauf240398.2	doauf240398.2.130100.kf2	1599	permeability (constant head)	5.43
doauf240398.2	doauf240398.2.130100.kf3	1600	permeability (falling head)	7.49
doauf240398.2	doauf240398.2.130100.kf4	1601	permeability (constant head)	4.60
doauf240398.2	doauf240398.2.130100.kf5	1602	permeability (constant head)	5.31
doauf240398.2	doauf240398.2.130100.kf6	1603	permeability (constant head)	5.38
doauf240398.2	doauf240398.2.130100.kf7	1604	permeability (constant head)	6.62
doauf240398.2	doauf240398.2.130100.kf8	1605	permeability (constant head)	5.35
doauf240398.2	doauf240398.2.150899.1	1647	permeability (constant head)	8.48
doauf240398.2	doauf240398.2.150899.1	1656	permeability (constant head)	8.63
doauf240398.2	doauf240398.2.150899.1	1665	permeability (constant head)	8.53
doauf240398.2	doauf240398.2.150899.2	1648	permeability (constant head)	6.15
doauf240398.2	doauf240398.2.150899.2	1657	permeability (constant head)	6.13

continued on next page

continued from previous page

outcrop	sample	labid	experiment	kf
doauf240398.2	doauf240398.2.150899.2	1666	permeability (constant head)	6.11
doauf240398.2	doauf240398.2.150899.2	1677	permeability (constant head)	6.26
doauf240398.2	doauf240398.2.150899.2	1678	permeability (constant head)	6.22
doauf240398.2	doauf240398.2.150899.2	1679	permeability (constant head)	6.20
doauf240398.2	doauf240398.2.160799.1	1645	permeability (constant head)	6.41
doauf240398.2	doauf240398.2.160799.1	1650	permeability (constant head)	6.41
doauf240398.2	doauf240398.2.160799.1	1668	permeability (constant head)	6.53
doauf240398.2	doauf240398.2.160799.1	1680	permeability (constant head)	6.50
doauf240398.2	doauf240398.2.160799.1	1681	permeability (constant head)	6.54
doauf240398.2	doauf240398.2.160799.1	1682	permeability (constant head)	6.55
doauf240398.2	doauf240398.2.160799.2	1646	permeability (falling head)	7.31
doauf240398.2	doauf240398.2.160799.2	1655	permeability (falling head)	7.30
doauf240398.2	doauf240398.2.160799.2	1664	permeability (falling head)	6.32
doauf240398.2	doauf240398.2.160799.2	1683	permeability (falling head)	7.34
doauf240398.2	doauf240398.2.160799.2	1684	permeability (falling head)	7.31
doauf240398.2	doauf240398.2.160799.2	1685	permeability (falling head)	7.30
doauf240398.2	doauf240398.2.z44	1653	permeability (falling head)	2.99
doauf240398.2	doauf240398.2.z44	1654	permeability (falling head)	2.99
doauf240398.2	doauf240398.2.z44	1659	permeability (falling head)	2.99
doauf240398.2	doauf240398.2.z44	1662	permeability (falling head)	2.99
doauf240398.2	doauf240398.2.z44	1663	permeability (falling head)	2.99
doauf240398.2	doauf240398.2.z44	1671	permeability (falling head)	3.11
doauf240398.2	doauf240398.2.z44	1697	permeability (falling head)	3.11
doauf240398.3	doauf240398.3.130100.kf1	1606	permeability (falling head)	7.39
doauf240398.3	doauf240398.3.130100.kf2	1607	permeability (falling head)	8.17
doauf240398.3	doauf240398.3.130100.kf3	1608	permeability (falling head)	7.46
doauf240398.3	doauf240398.3.130100.kf4	1609	permeability (constant head)	5.11
doauf240398.3	doauf240398.3.130100.kf5	1610	permeability (falling head)	7.66
doauf240398.3	doauf240398.3.130100.kf6	1611	permeability (falling head)	7.40
doauf240398.3	doauf240398.3.130100.kf7	1612	permeability (falling head)	7.39
doauf240398.3	doauf240398.3.130100.kf8	1613	permeability (falling head)	7.38
doauf290998.1	doauf290998.1.130100.kf1	1614	permeability (falling head)	7.72
doauf290998.1	doauf290998.1.130100.kf2	1615	permeability (falling head)	7.36
doauf290998.1	doauf290998.1.130100.kf3	1616	permeability (falling head)	7.55
doauf290998.1	doauf290998.1.130100.kf4	1617	permeability (falling head)	7.89
doauf290998.1	doauf290998.1.130100.kf5	1618	permeability (falling head)	7.61
doauf290998.1	doauf290998.1.130100.kf6	1619	permeability (constant head)	5.02
doauf290998.1	doauf290998.1.130100.kf7	1620	permeability (falling head)	7.57
doauf290998.1	doauf290998.1.130100.kf8	1621	permeability (falling head)	7.46
doauf290998.1	doauf290998.1.z21.2	1652	permeability (falling head)	9.16
doauf290998.1	doauf290998.1.z21.2	1661	permeability (falling head)	9.30
doauf290998.1	doauf290998.1.z21.2	1670	permeability (falling head)	9.45
doauf290998.1	doauf290998.1.z21.2	1686	permeability (falling head)	9.59
doauf290998.1	doauf290998.1.z21.2	1687	permeability (falling head)	9.48
doauf290998.1	doauf290998.1.zPV32	1660	permeability (falling head)	9.20
doauf290998.1	doauf290998.1.zPV32	1669	permeability (falling head)	9.63
doauf290998.1	doauf290998.1.zPV32	1672	permeability (falling head)	9.39
doauf290998.1	doauf290998.1.zPV32	1673	permeability (falling head)	8.92
doauf290998.1	doauf290998.1.zPV32	1674	permeability (falling head)	9.18
meauf051099.1	meauf051099.1.240200.kf1	2152	permeability (constant head)	4.87
meauf051099.1	meauf051099.1.240200.kf10	2170	permeability (constant head)	6.04
meauf051099.1	meauf051099.1.240200.kf11	2172	permeability (constant head)	5.83
meauf051099.1	meauf051099.1.240200.kf12	2174	permeability (constant head)	6.22
meauf051099.1	meauf051099.1.240200.kf13	2176	permeability (constant head)	5.78
meauf051099.1	meauf051099.1.240200.kf14	2178	permeability (constant head)	5.09

continued on next page

continued from previous page

outcrop	sample	labid	experiment	kf
meauf051099.1	meauf051099.1.240200.kf15	2180	permeability (constant head)	5.76
meauf051099.1	meauf051099.1.240200.kf16	2182	permeability (constant head)	5.19
meauf051099.1	meauf051099.1.240200.kf2	2154	permeability (constant head)	3.14
meauf051099.1	meauf051099.1.240200.kf3	2156	permeability (constant head)	4.68
meauf051099.1	meauf051099.1.240200.kf4	2158	permeability (constant head)	3.60
meauf051099.1	meauf051099.1.240200.kf5	2160	permeability (constant head)	3.27
meauf051099.1	meauf051099.1.240200.kf6	2162	permeability (constant head)	3.75
meauf051099.1	meauf051099.1.240200.kf7	2164	permeability (constant head)	3.23
meauf051099.1	meauf051099.1.240200.kf8	2166	permeability (constant head)	4.30
meauf051099.1	meauf051099.1.240200.kf9	2168	permeability (constant head)	6.08
meauf270499.1	meauf270499.1.210100.kf1	1622	permeability (constant head)	6.78
meauf270499.1	meauf270499.1.210100.kf10	1631	permeability (constant head)	7.26
meauf270499.1	meauf270499.1.210100.kf11	1632	permeability (constant head)	6.89
meauf270499.1	meauf270499.1.210100.kf12	1633	permeability (falling head)	7.66
meauf270499.1	meauf270499.1.210100.kf13	1634	permeability (constant head)	6.70
meauf270499.1	meauf270499.1.210100.kf14	1635	permeability (constant head)	5.06
meauf270499.1	meauf270499.1.210100.kf15	1636	permeability (falling head)	7.72
meauf270499.1	meauf270499.1.210100.kf16	1637	permeability (constant head)	5.45
meauf270499.1	meauf270499.1.210100.kf17	1638	permeability (constant head)	5.49
meauf270499.1	meauf270499.1.210100.kf18	1639	permeability (constant head)	5.95
meauf270499.1	meauf270499.1.210100.kf19	1640	permeability (constant head)	6.13
meauf270499.1	meauf270499.1.210100.kf2	1623	permeability (constant head)	6.85
meauf270499.1	meauf270499.1.210100.kf20	1641	permeability (falling head)	7.43
meauf270499.1	meauf270499.1.210100.kf21	1642	permeability (constant head)	6.44
meauf270499.1	meauf270499.1.210100.kf22	1643	permeability (constant head)	6.64
meauf270499.1	meauf270499.1.210100.kf23	1644	permeability (constant head)	5.66
meauf270499.1	meauf270499.1.210100.kf3	1624	permeability (constant head)	6.06
meauf270499.1	meauf270499.1.210100.kf4	1625	permeability (constant head)	5.66
meauf270499.1	meauf270499.1.210100.kf5	1626	permeability (constant head)	6.04
meauf270499.1	meauf270499.1.210100.kf6	1627	permeability (constant head)	5.97
meauf270499.1	meauf270499.1.210100.kf7	1628	permeability (constant head)	5.83
meauf270499.1	meauf270499.1.210100.kf8	1629	permeability (constant head)	5.81
meauf270499.1	meauf270499.1.210100.kf9	1630	permeability (constant head)	7.18

C.6. Variability of soil parameters from lab results

The lab analysis presented in this work aimed at the estimation of representative soil parameters as described subsection 10.1.2. The following tables and graphs give some indication of the variability of the soil parameters within the different soil types.

Results of T–test, for lab analysis results, landslide 'si7' and Melbtal. Tested: clay content c_T, silt content c_U, sand contentc_S, dry density ρ_d, bulk density ρ_b, satuirated density ρ_{sat}, plastic limit w_p, liquid limit w_l, saturated conductivity k_s. Null hypothesis: equal means for the different soil types (95%–level). Shown are configurations, for which null hypothesis was accepted.

T–test, for lab analysis results, landslide 'si7'.

	Trt	clay (white)	clay (grey)	sand/silt	Devon
Trt		ρ_d,w_p	c_U,ρ_d,ρ_b,ρ_{sat},w_p	c_T	c_T,c_U,c_S
clay (white)			ρ_d,w_p,k_s		
clay (grey)					
sand/silt					c_T
Devon					

T–test, for lab analysis results, Melbtal.

	loess	terrace	clay	sand/silt	lignite
loess			c_S		k_s
terrace					
clay				c_U	k_s
sand					
lignite					

The following graphs give some indication about variability of a series of soil parameters, derived from laboratory experiments. The boxplots indicate median, lower and upper quartiles, data range, and eventually possible outliers.

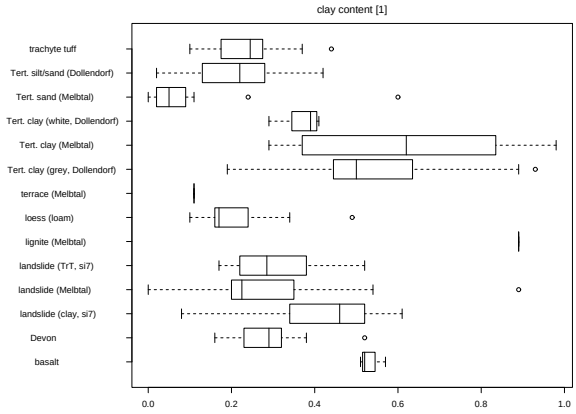

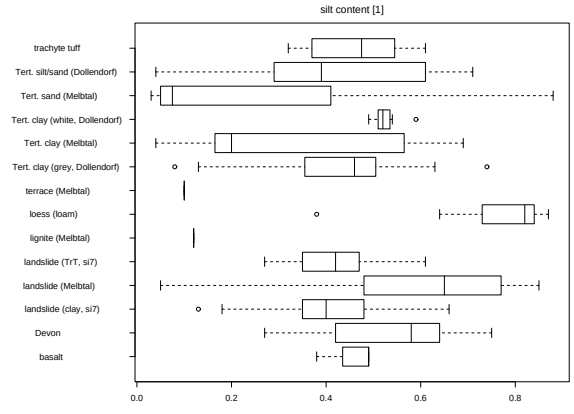

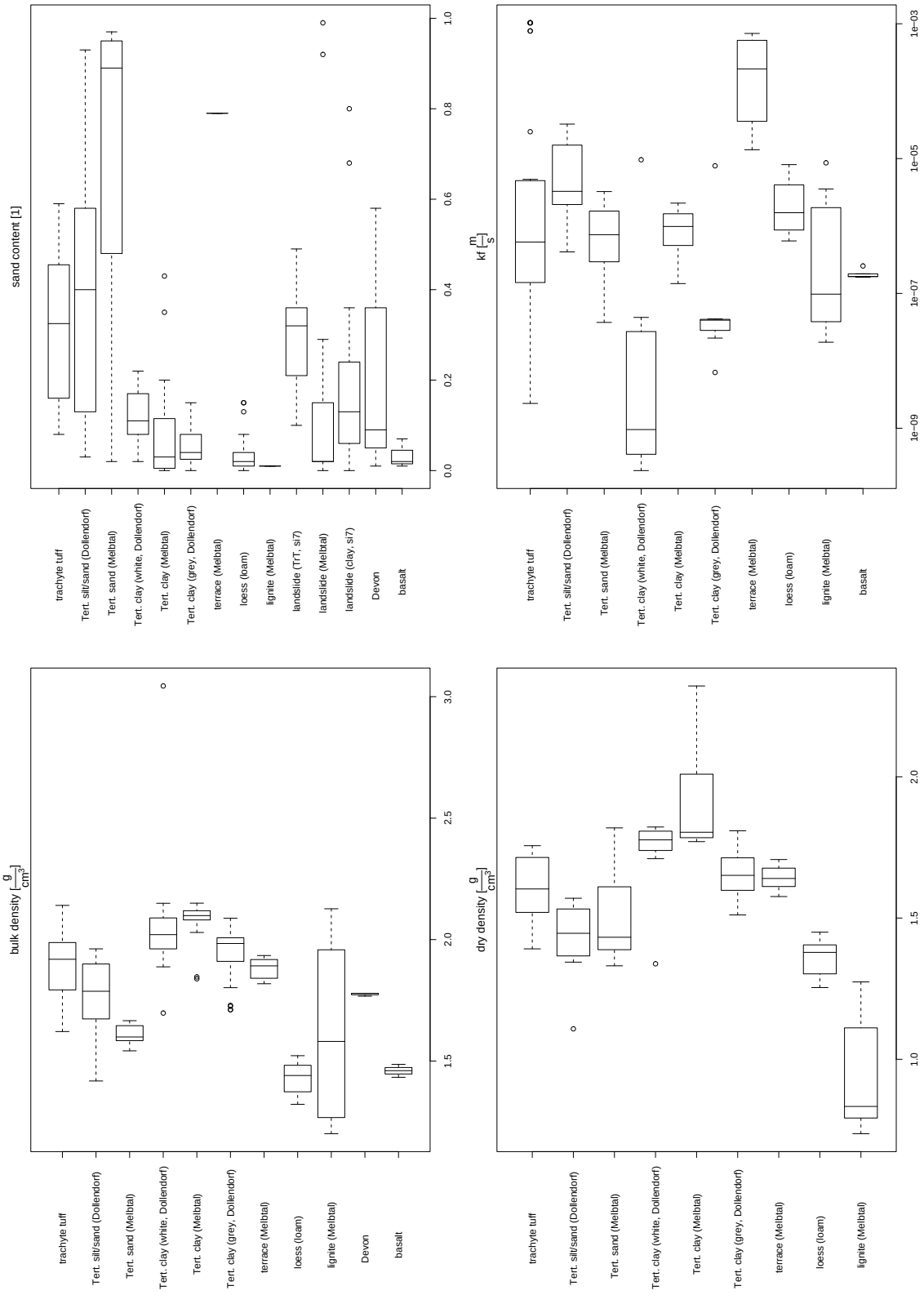
sand content [1]
kf [m/s]
bulk density [g/cm³]
dry density [g/cm³]
trachyte tuff
Tert. silt/sand (Dollendorf)
Tert. sand (Melbtal)
Tert. clay (white, Dollendorf)
Tert. clay (Melbtal)
Tert. clay (grey, Dollendorf)
terrace (Melbtal)
loess (loam)
lignite (Melbtal)
landslide (TrT, si7)
landslide (Melbtal)
landslide (clay, si7)
Devon
basalt

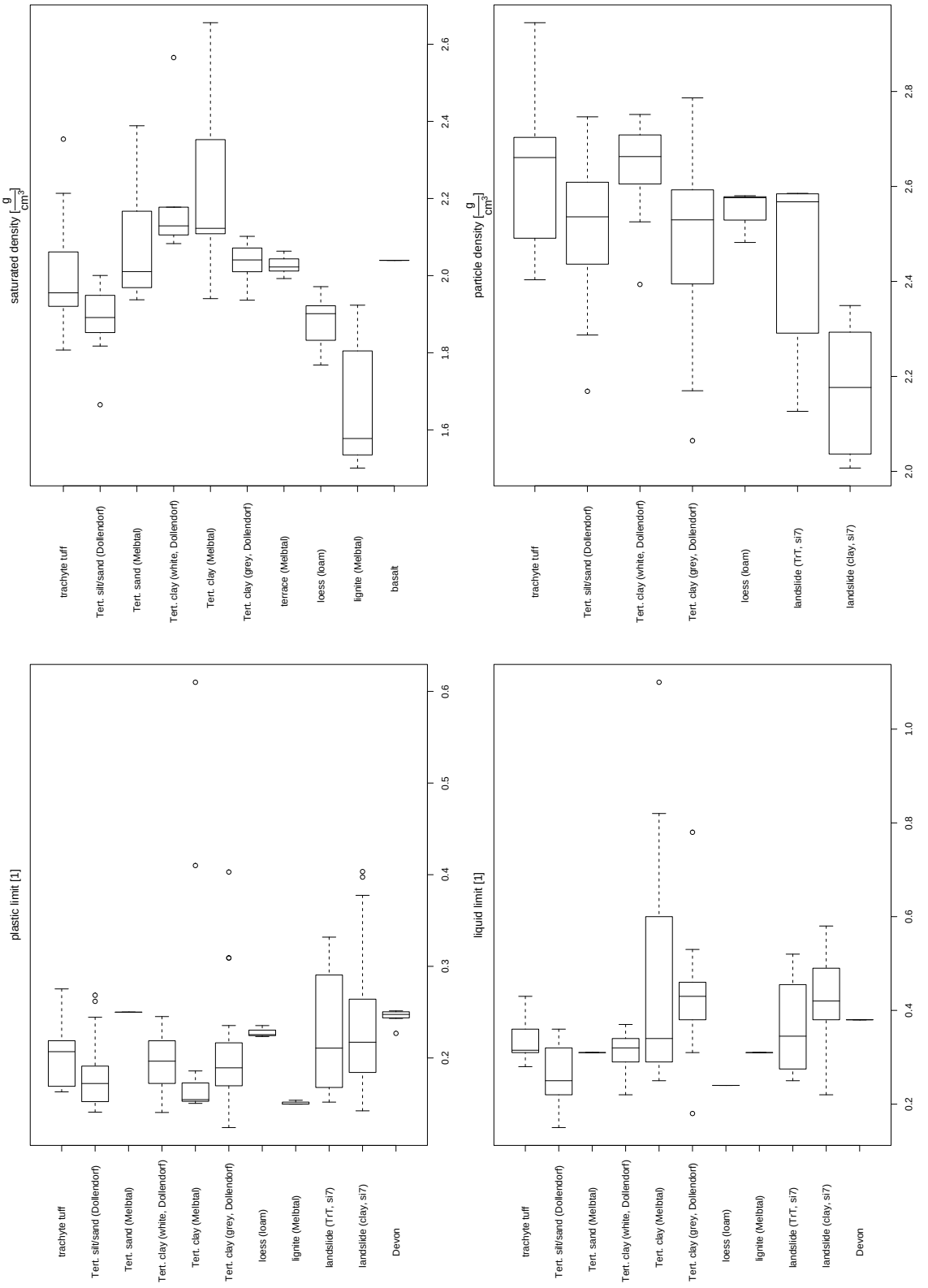
saturated density [g/cm³]
trachyte tuff
Tert. silt/sand (Dollendorf)
Tert. sand (Melbtal)
Tert. clay (white, Dollendorf)
Tert. clay (Melbtal)
Tert. clay (grey, Dollendorf)
terrace (Melbtal)
loess (loam)
lignite (Melbtal)
basalt
particle density [g/cm³]
trachyte tuff
Tert. silt/sand (Dollendorf)
Tert. clay (white, Dollendorf)
Tert. clay (grey, Dollendorf)
loess (loam)
landslide (TrTf, si7)
landslide (clay, si7)
plastic limit [1]
trachyte tuff
Tert. silt/sand (Dollendorf)
Tert. sand (Melbtal)
Tert. clay (white, Dollendorf)
Tert. clay (Melbtal)
Tert. clay (grey, Dollendorf)
loess (loam)
lignite (Melbtal)
landslide (TrTf, si7)
landslide (clay, si7)
Devon
liquid limit [1]
trachyte tuff
Tert. silt/sand (Dollendorf)
Tert. sand (Melbtal)
Tert. clay (white, Dollendorf)
Tert. clay (Melbtal)
Tert. clay (grey, Dollendorf)
loess (loam)
lignite (Melbtal)
landslide (TrTf, si7)
landslide (clay, si7)
Devon

D. Error assessment

technique	parameter(s)	error sources	type	estimated error
pipette method	particle size	weighing ($\Delta M \approx 0.0002$g)	statistical	1-5%
		limited applicability for clay–rich material	systematic	dep. on soil type
oven drying	moisture content	weighing ($\Delta M \approx 0.0002$g)	statistical	negligible
		definition of 'dry'	systematic	dep. on soil type
ignition loss	organic content	weighing ($\Delta M \approx 0.0002$g)	statistical	negligible
		definition of 'loss of organic content'	systematic	dep. on soil type
determination of bulk density	density & related properties	weighing ($\Delta M \approx 0.1$g)	statistical	¡1%
		volume determination	statistical	2–10%
pycnometer method	particle density	weighing ($\Delta M \approx 0.0002$g)	statistical	negligible
		determination of volume from mass (by temperature $\Delta T \approx 0.2$)	statistical	negligible
		sensitivity of experiment	statistical	? (high!)
Casagrande test	consistency limits	weighing ($\Delta M \approx 0.0002$g)	statistical	negligible
		subjectivity of lab person	systematic	?
shear tests	shear parameters	Lots of technical and conceptual problems lead to a variety of error sources. Systematic errors due to the concept itself and the heterogeneity of soil samples will dominate error and leading to a large variability in results (Appendix C.4).		
constant&falling head permeameter	saturated hydraulic conductivity	Systematic errors due to the concept itself and the heterogeneity of soil samples will dominate error and leading to a large variability in results (Appendix C.6). The derived values should only be used as an indication of the order of magnitude.		
pressure transducer (D–DIVER)	pressure, groundwater height	transducer resolution	statistical	10 cm
		postprocessing	statistical	Appendix F.2.3
		disturbance by dirt, freeze	systematic	?
inclinometer	tube inclination, displacement	transducer resolution, measurement uncertainty	statistical	1 mm/m
		connection to 'real movement'	systematic	?
terrestrial surveying (TCL 1800)	point (x,y,z)	measurement system, air temperature, etc	statistical	negligible
		measurement errors of target and height of station	statistical	$\Delta z \approx 1-5$cm, $\Delta x \approx 1-10$cm

E. Typical soil properties

Soil properties from various references, with specific emphasis on data for the Bonn area (after Rogozia 2000, extended)

reference	**soil type**	γ_b [kN/m^2]	γ_d [kN/m^2]	ρ_s [g/c^{3}m]	c' [kN/m^2]	ϕ' [°]	ϕ_r [°]	k_s [-log(m/s)]
Barnes (1995)	*S* and *G*	16–22						
	U	16–20						
	T (soft)	17–20						
	T (stiff)	19–23						
	weak rock (crushed, compacted)	18–21						
	hard rock (crushed, compacted)	19–22						
Chow *et al.* (1988)	*G*			0.25–0.4				1–2
	S			0.25–0.5			5–0	
	U			0.35–0.5			7–3	
	T			0.4–0.7			9–5	
Selby (1993)	*U*					27–34		
	Su					27–35		
	S (uniform)					28–34		
	S (rounded)					33–45		
	Gs					35–50		
	S (uniform, loose)	19	14			28–34		
	S (uniform, dense)	21	17			32–40		
	S (mixed, loose)	20	16			34–40		
	S (mixed, dense)	21	18			38–46		
	G (uniform)	22	20			34–37		
	Gs	19	17			48–45		
	basalt	22	17			40–50		
	sandstone	17	13			35–45		
	schist	20	16			30–35		
	tuff	13	6		10–20	7–13		
	T (soft,organic)	14	6		10–30	12–16		
	T (soft)	16	10		20–50	22–27		
	T (glacial,soft)	17	12		30–70	27–32		
	T (glacial,stiff)	20	17		70–150	30–32		
	till	23	20		150–250	32–35		
	vulcanic rocks	25–30			35000–55000	35–45		
DIN 1055 part 2	*S*,Su,Gs	19–21	17–19			30–35		
	Gu	19–21	17–19			32.5–37.5		
	S, Gs, *G*	20–22	18–20			30–35		
	S,Gs,*G*,Gu	20–24	18–22			30–35		
Prinz (1991)	*S*					30–35		
	S,*G*					35–40		
	G					35–45		
	T (high plasticity)				0–5	25–27.5		
	T (low plasticity)				10–25	15–20		
	T (organic)				0–5	5–15		
	quarzite, sandstone, Siebengebirge				0	¿40		
	schist, Siebengebirge				0	27–40		
	soil (*G*,*S*), *T*,*U* ¡ 5–8%				0–5	35–40		

continued on next page

continued from previous page

ref.	**soil type**	γ_b	γ_d	n	c'	ϕ'	ϕ_r	k_s
	soil , T,U ¡ 25%				0–10	32.5–37.5		
	soil, T,U ¡ 40%					30		
	soil T,U ¿ 40%				20–40	25–30		
	tuff				20	20–23		
Jäger (1991)	Devonian sediments, Dollendorf	19–20	14–17		10–30	18–27		
Nienhaus (1990)	loess, Dollendorf							5–6
	terrace, Dollendorf							5
	trachyte tuff, Dollendorf							6–11
Müller (1987)	trachyte tuff, Siebengebirge							6–10
	Tertiary sediments, Siebengebirge							5–10
	Devonian sediments, Siebengebirge							5–10

F. Reference lists & technical descriptions

F.1. Equipment

AGI-722A Borehole Tiltmeter
Applied Geomechanics Inc.
Santa Cruz
CA,USA

Direct shear box
Dieter Moser GmbH Systemtechnik
Reutackerweg 4
D-76706 Dettenheim–Liedolsheim
Germany

pressure transducer D–DIVER (van Essen)(D–DIVER).
Van Essen Instruments bv
Westlandseweg 7
2624 AN Delft
Netherlands

dipmeter
Abovo GmbH
Dorfbachstr. 19
D-655589 Hadamar
Germany

Tachymeter TCL1800 (Leica)(TCL 1800).
Leica Geosystems GmbH
Münsterstr. 306
D-40470 Düsseldorf
Germany

Triaxial apparatus
Dieter Moser GmbH Systemtechnik
Reutackerweg 4
D-76706 Dettenheim–Liedolsheim
Germany

F.2. Special data processing steps

F.2.1. Postprocessing of measurement data

Data transfer from TCL 1800 to ArcInfo
Data captured by terrestrial measurement using the TCL 1800 is stored in a specific file format (*Leica–GSI*). Basic post procedure steps were transferring the data to the GIS (ArcInfo), homog-

enizing data from different measurement campaigns (i.e. different base stations), data verification and georeferencing.

- The Perl–script gsi2arc.pl (section F.3) was used to transfer the *Leica–GSI*–format to an AML–script, which produces an ArcInfo point coverage containing the necessary meta–information to prove the data quality and relevant references (e.g. base station for each measured point). The data transfer key from the *Leica–GSI*–format in the ArcInfo point coverage is shown in the table below.

Codes and semantics of data in GSI–files by Tachymeter TCL1800 (Leica). The format of the actual data depends on the settings defined in the TCL 1800. Additionally shown are point coverage items created by the Perl–script gsi2arc.pl for transferring data from GSI–format to ArcInfo.

GSI-ID	semantics	items of coverage
1100xx	ID	leicaid
71	remark 1	remark1
87..16	reflector height	reflectorheight
21.323	horizontal angle	horizontalangle
22.323	vertical angle	verticalangle
31..06	height difference to reflektor	heightdiff
33..16	height of measured point (relative to base station)	heightpoint
81..06	x–coordinate of measured point	X
82..06	y–coordinate of measured point	Y
83..06	z–coordinate of measured point	Z
32..16	horizontal distance	horizontaldist
88..16	height of station	statheight
19....	date (format: monthdayhourminutes)	date

- The ArcInfo modules `Generate` and `Arc/Edit` were used to combine data from different base stations into one unique georeferenced system. Principles of this procedure are described below.

Postprocessing of survey data in the GIS ArcInfo

Data from terrestrial survey, which have been imported in the GIS (ArcInfo), require a series of postprocessing steps. First, if necessary, data from different measurement campaigns are combined and homogenised.

case 1. same base station, same reference direction.

Data from different survey campaigns, which used the same base station and (!) the same reference direction direction can be combined directly, because the data are captured in the same coordinate system. This can be done in ArcInfo using the tool `append`. The following example code shows the usage of ArcInfo command `append` to combine coverages.

```
Arc: append vermges point
Enter Coverages to be APPENDed (Type END or a blank line when done):

Enter the 1st coverage: verm1805
Enter the 2nd coverage: verm2206
Enter the 3rd coverage: verm2610
Enter the 4th coverage:
```

```
Done entering coverage names (Y/N)? y
Do you wish to use the above coverages (Y/N)? y
 Appending coverages...
Arc:
```

case 2. different base station or different reference direction.
Data from different survey campaigns, which used different base stations and/or different reference direction need to be transformed in a homogeneous coordinate system. Therefore, at least two points are required, which have been measured from both considered campaigns. The technical procedure in ArcInfo is to determine common TICs in two coverages using the module `ArcEdit`. Therefore the common points of the surveying campaigns are used. Once common TICs are defined, two point coverages can be easily brought into the same system using the ArcInfo command `transform` (compare subsection F.2.2). Moreover, to insure not only horizontal coincidence, but also vertical matching after combining two data sets, the height differences have to be adjusted. This is done by calulating the height difference of the base stations via the common TICs. The height difference can be then be used to correct the height values of the survey dates using `ArcEdit`. The following example code exemplifies height correction of point coverages in `ArcEdit`.

```
Arcedit: edit vermwork
Arcedit: ef points
Arcedit: sel all
Arcedit: sel station lk 'doll2'
321 element(s) now selected
Arcedit: calculate z = z - 20
Arcedit: sel station lk 'doll3'
294 element(s) now selected
Arcedit: calculate z = z - 33.7
```

Additionally, if requested, the height values can be corrected to "real world" values, if a matching point with known height is found, using similar code.

A second postprocessing step is to georeference the survey data to coordinates using some map projection. This procedure can be performed similarly like the combining steps above using the tool `transform` and is described in subsection F.2.2. Another possibility is provided by the `ArcEdit` tools `move` and `rotate`. Thereby, an interactive transversal and rotational transformation can be performed insuring an internal integrity of the survey data, which should deliver correct distances.

F.2.2. Georefencing in ArcInfo

Georeferencing is a basic and typical step in processing of digital spatial data. Normally, spatial information is captured in various formats and referene systems. Data converting and georeferencing are therefore necessary and error prone steps. The following notes indicate the basic procedures used in this work for georeferencing spatial data which have been obtained from various sources (e.g. field measurements, digital maps, or aerial photographs).

Georeferencing of ArcInfo coverages using `transform`
Problem. A coverage using any (unwished) coordinate system has to be transformed in new coordinates.

Note. *This step is not a geographic transformation to a new map projection like UTM or Gauss-Krüger!*

Prerequisite. Either (1) a coverage with target coordinates is available, which has at least two coincided points with the coverage to transform, or (2) at least two reference points can be determined (e.g. from maps).
Procedure.

1. A coverage *cover1* shall be transformed to the coordinate system of another coverage *cover2*. The following code shows the usage of the ArcInfo command `transform` to transform *cover1* to the coordinate system of *cover2*.

```
Arc: copy cover2 coverneu
Arc: transform cover1 coverneu
```

   Note. *transform destroys the contents of coverneu !*

2. A series of coverages shall be combined. The following code shows the how to combine coverages in ArcInfo using `transform` and `append`.

```
Arc: copy cover2 temp
Arc: transform cover1 temp
Arc: append coverneu points
Enter Coverages to be APPENDed (Type END or a blank line when done):


Enter the 1st  coverage: temp
Enter the 2nd coverage: cover2
Enter the 3rd coverage:
Done entering coverage names (Y/N)? y
Do you wish to use the above coverages (Y/N)? y

 Appending coverages...
Arc:
```

3. A coverage *cover1* shall be transformed to a new coordinate system using reference points. First, a reference coverage has to be created by digitizing the refernce points. After this step the procedure continues as in step 1.

Georefencing ArcInfo GRIDs using `shift` and `adjust`
SHIFT (Grid). This command shifts a GRID to a new coordinate position. As the GRID is shifted as a whole block, no internal distortion is created.
ADJUST (Grid). This command enables the definition of a series of transformation points, i.e. the pre–adjust and post–adjust coordinates have to be given. Then `adjust` interpolates (nearest neighbor, bilinear or cubic) a new GRID based of the information from the old GRID and the given point transformation rules. Thereby, the whole internal structure of the GRID can be changed. The transformation points can be provided as a *link–coverage* (using the `ArcEdit` command `editfeature link`) or as a *link–file* (using the ArcInfo command `controlpoints`).

F.2.3. Postprocessing of D–DIVER data

The pressure transducer pressure transducer D–DIVER (van Essen), which has been used in this study for groundwater logging, delivers pressure data of the surrounding media as height of water column [cm] (D–Diver Manual 1998), relative to an reference level of 950 cm ($\approx$ 930 mbar) of air pressure. Deriving of actual water heights therefore requires the recalculation of these data relative to an actual reference level, which is given by actual air pressure at the point of measurement. Normally, actual air pressure should be measured directly at the point, e.g. using a second pressure

transducer (D–Diver Manual 1998). In this study, the air pressure for the measurement points have been calculated from air pressure and air temperature logged at the meteorological station the the 'Meteorologisches Institut, Universität Bonn' (*Department of Meteorology, University of Bonn*) (compare section 8.4) using the convenient method of barometric height correction (e.g. Weischet 1991).

$$p_i = p_m e^{\frac{g(z_i - z_m)}{RT}}$$

p_i	*air pressure at measurement point i* [Pa]
p_m	*air pressure at meteorological station* [Pa]
z_i	*elevation of measurement point i* [m]
z_m	*elevation of meteorological station* [m]
R	*gas constant* [287 J/kgK]
T	*average temperature between stations* [°K]

The average air temperature can be estimated using an average temperature gradient of $\frac{-0.5\text{K}}{100\text{m}}$.

$$p_i = p_m e^{\frac{g(z_i - z_m)}{R(T_i - 0.0025\left[\frac{\text{K}}{\text{m}}\right](z_i - z_m))}}$$

T_i	*temperature at the Meteorological station* [K]

The maximum error produced by using this approximation can be assessed using an estimate of error in height difference $\Delta h = \Delta(z_i - z_m)$ and error in temperature ΔT (from error in temperature gradient) and the following error propagation.

For Δh, the relative error of the air pressure at measurement point $\frac{\Delta p_i}{p_i}$ is

$$\frac{\Delta p_i}{p_i} = \Delta h \frac{g}{RT},$$

i.e. an error of $\frac{\Delta p_i}{p_i} \approx 0.0125\%/\text{m}$ (for T =275 K) can be estimated.
For ΔT, the relative error of the air pressure at measurement point $\frac{\Delta p_i}{p_i}$ is

$$\frac{\Delta p_i}{p_i} = \Delta T \frac{gh}{RT^2},$$

i.e. an error of $\frac{\Delta p_i}{p_i} \approx 0.005\%/\text{K}$ (T =275 K, h=100 m) can be estimated. These estimations show the low sensitivity of this procedure due to errors in height measurement or temperature correction and therefore justify the application.

F.3. Software programs

Used software

ArcInfo (ArcInfo) — A commercial GIS (ESRI) with a huge set of analysis capabilities for various data types.
http://www.esri.com/software/arcinfo/index.html

Arc macro language (AML) — Scripting language for developing GIS–tools under Arc/Info.

Combined Hydrology and Stability Model (CHASM) — Integrated slope hydrology / slope stability software package that assists in the assessment of slope stability.
http://www.chasm-env.com/

document type definition (DTD) — Formal description in XML declaration Syntax of a particular type of XML document.

extensible markup language (XML) — The universal format for structured documents and data on the Web.
http://www.w3.org/XML/

extensible stylesheet language (XSL) — An XSL stylesheet specifies the presentation of a class of XML documents by describing how an instance of the class is transformed into an XML document that uses the formatting vocabulary.
http://www.w3.org/XSL/

GnuPlot (GnuPlot) — Command-line driven interactive function and data plotting utility for various platforms and output formats.
http://www.gnuplot.org

Slope profile analysis package (HAP) — Software package to delineate and analyse hillslope profiles (*Author(s):* Rasemann, S.).

MS–Access.
http://www.microsoft.com/office/access/

Open Landform Geo–Informationsystem (OreGIS) — Software package to represent a Digital Surface Model, its derivatives and some landform classifications on various generalisation levels (*Author(s):* Hannappel, M.).

PCRASTER — A Geographical Information System especially useful for dynamic modelling.
http://www.frw.ruu.nl/pcraster.html

PostgreSQL (PostgreSQL) — A object-relational DBMS, supporting almost all SQL constructs, including subselects, transactions, and user-defined types and functions.
http://www.postgresql.org

Practical Extraction and Report Language (Perl) — A high-level programming language with process, file, and text manipulation facilities make it particularly well-suited for tasks involving quick prototyping, system utilities, software tools, system management tasks, database access, graphical programming, networking, and world wide web programming.
http://www.perl.com

Richard's n-store Hillslope Dynamics Simulator (HDS) — A Model for evolution of hillslope profiles (*Author(s):* Richard Tran Mills).
http://stderr.org/ hds/

R statitics package (R) — A language and environment for statistical computing and graphics.
http://www.r-project.org/

Samba — A suite of programs allowing clients to access to a server's filespace and printers via the SMB (Server Message Block) protocol.

Slope2d — A DOS–software for slope stability analysis using the Bishop and the simplified Janbu methods (*Author(s):* Hennig, A.).

Standard query language (SQL).

The Generic Mapping Tools (GMT) — A Collection of UNIX tools to manipulate spatial data sets (including filtering, trend fitting, gridding, projecting, etc.) and to produce Encapsulated PostScript File (EPS) illustrations.
http://imina.soest.hawaii.edu/gmt/

Virtual Reality Markup Language (VRML) — Markup language to deliver interactive 3D objects and worlds across the internet.

Developed software programs

boregen.pl — Perl script for generating borelogs.

NAME

boregen.pl

Perl script for generating borelogs

SYNOPSIS

boregen.pl [options] (try -h)

DESCRIPTION

Perl script for generating borelogs. The user provides ID's of drillings, and the script queries the database for information concerning drilling log, interpretation and related lab data (densities, moisture content, particle size distribution). A graph (GMT–code) is generated, displaying this information as a combined log.

AUTHOR(S)

Schmidt, J.

fieldlabb13.

NAME

fieldlabb13

DESCRIPTION

MS–ACCESS client for interfacing with the database backend of the database deceloped in the project B13. A series of queries and forms allow data input and management as well as display and hardcopy of data sheets.

AUTHOR(S)

Schmidt, J.

GSI2ARC.PL — Perl–script transferring gsi output to an Arc/Info AML.

NAME

gsi2arc.pl

Perl–script transferring gsi output to an Arc/Info AML

SYNOPSIS

gsi2arc.pl ¡STDIN¿ ¡STDOUT¿

DESCRIPTION

The Perl–script 'gsi2arc' accepts as standard input GSI–files and generates an Arc/Info AML. Multiple input files can be handled at once (e.g. cat file1.gsi file2.gsi ...). The AML can be executed in Arc/Info. An Arc/Info point coverage will be created and additional information from the .gsi–file will be appended to the *.pat–file* of the point coverage (e.g. height values, date, reference station). The Perl–script 'gsi2arc' scans the input GSI–files and detects the data types by means of the unique ID provided by the GSI–format. The data will be transferred in items of the point coverage. A specific procedure is required to ensure that the base station can be reconstructed for each measurement. A data row with the ID '0' in a GSI–file will be interpreted as base station data (This data row can be appended manually). The column "remark1" (71....) of this data row will be saved and appended to each following measurement data as item 'station'.

AUTHOR(S)

Schmidt, J.

MAPGEN.PL — Perl script for generating Arc/Info AMLs for map production.

NAME

mapgen.pl

Perl script for generating Arc/Info AMLs for map production

SYNOPSIS

mapgen.pl [options] (try -h)

DESCRIPTION

Perl script for generating Arc/Info AMLs for map production. The user has to sepcify the region of interest (series of regions available as default), and a series of map layers for displaying. The AML output can be postprocessed to match for specific needs.

AUTHOR(S)

Schmidt, J.

PROFGEN.PL — Perl–client for generating 2D/3D views.

NAME

profgen.pl

Perl–client for generating 2D/3D views

SYNOPSIS

profgen.pl [options] (try -h)

DESCRIPTION

Perl–client for generating 2D/3D views of surfaces and borelogs for drilling data stored in the database management system developed in the project B13. The output can be GMT–code, which can be postprocess and used to produce .eps–files, or VRML–code, for World Wide Web presentations.

AUTHOR(S)

Schmidt, J.

SQL2GNUPLOT–TOOLBOX.

NAME

sql2gnuplot–toolbox

SYNOPSIS

sql2gnuplot.pl [options] (try -h)

sql2incl.pl [options] (try -h)

sql2shear.pl [options] (try -h)

sql2cons.pl [options] (try -h) (some more)

DESCRIPTION

Series of Perl–clients for generating diagrams and analysing field and lab data for data stored in the database management system developed in the project B13. The user provides ID's of drillings, installations, samples and/or lab experiment types. The scripts query the database, extract relevant data matching the request, and writes GnuPlot code for displaying the data in suitable formats (e.g. particle size diagrams, stress–strain curves, etc).

AUTHOR(S)

Schmidt, J.

F.4. Analog Maps

'Geologische Kartierung des Siebengebirges' (*Geological mapping of the Siebengebirge, scale 1:10000*) (GK Bichler). Bichler, B. 2001.
(*source:* Bichler, B. **Diplomkartierung im nördlichen Siebengebirge vom Ennert bis zur Dollendorfer Hardt** *, 2001 (Department of Geology, University of Bonn).)*

'Bodenkarte des Staatsforstes Kottenforst 1:10000' (*soil map of the Kottenforst (Bonn, Germany), scale 1:10000*) (BK Kottenforst). 4 map sheets, 2 legends with comments. 1977.
(*source: 'Geologischer Dienst NRW' (Geological Survey, NRW))*

'Bodenkarte von NRW 1:50000, Blatt Bonn' (*Soil map of Nordrhein–Westfalen, scale 1:50000, map sheet Bonn*) (BK 5308). 1983.
(*source: 'Geologischer Dienst NRW' (Geological Survey, NRW))*

'Bodenkarte des Naturparks Siebengebirge 1:25000' (*soil map 'Siebengebirge', scale 1:25000*) (BK Burghardt). Burghardt, O. 1979.
(*source:* Burghardt, O. **Siebengebirge — Landschaft im Wandel** *, 1979.)*

'Geologische Karte der Umgebung von Römlinghoven' (*Geological map of the area of Römlinghoven (Bonn, Germany)*) (GK Schegiewal). Schegiewal, A. 1972.
(*source:* Schegiewal, A. **Geologische und bodenkundliche Untersuchungen am Nordabfall des Siebengebierges bei Römlinghoven** *, 1972.)*

'Geologische Karte von Preussen und benachbarten Bundesländern' (*Geological map of Nordrhein–Westfalen, scale 1:25000, map sheet Bonn*) (GK 5208). with explanations. 1923.
(*source: 'Geologischer Dienst NRW' (Geological Survey, NRW))*

'Geologische Karte von NRW 1:25000, Blatt Siegburg GK 5209' (*Geological map of Nordrhein–Westfalen 1:25000, map sheet Siegburg*) (GK 5209). with explanations. 1977.
(*source: 'Geologischer Dienst NRW' (Geological Survey, NRW))*

'Geologische Karte von NRW 1:25000, Blatt Bonn–Bad Godesberg GK 5308' (*Geological map of Nordrhein–Westfalen, scale 1:25000, map sheet Bonn–Bad Godesberg*) (GK 5308). with explanations. 1980.
(*source: 'Geologischer Dienst NRW' (Geological Survey, NRW))*

'Geologische Karte von NRW 1:25000, Blatt Königswinter, GK 5309' (*Geological map of Nordrhein–Westfalen, scale 1:25000, map sheet Königswinter*) (GK 5309). with explanations. 1995.
(*source: 'Geologischer Dienst NRW' (Geological Survey, NRW))*

'Bodenkarte 1:2500, Dollendorfer Hardt' (*soil map 1:2500, 'Dollendorfer Hardt'*) (BK Holler). Holler, S. 1998.
(*source:* Holler, S. **Bodentypenverbreitung in Beziehung zu gravitativen Prozessen im Bonner Raum** *, 1998.)*

'Hydrologische Karte von Nordrhein–Westfalen, Grundrisskarte, 5209 Siegburg' (*Hydrologic map of Nordrhein–Westfalen, plan map, 5209 Siegburg*) (HKG 5209). 1988.
(*source: Landesamt für Wasser und Abfall Nordrhein–Westfalen)*

'Hydrologische Karte von Nordrhein–Westfalen, Grundrisskarte, 5208 Bonn' (*Hydrologic map of Nordrhein–Westfalen, plan map, 5208 Bonn*) (HKG 5208). 1991.
(*source: Landesamt für Wasser und Abfall Nordrhein–Westfalen)*

'Bodenkundliche Karte der Umgebung von Römlinghoven' (*Soil map of the area of Römlinghoven (Bonn, Germany)*) (BK Schegiewal). Schegiewal, A. 1976.
(*source:* Schegiewal, A. **Die Böden am Nordabfall des Siebengebirges und deren physikalischen und chemischen Eigenschaften in Abhängigkeit vom Ausgangsgestein** *, 1976.)*

Additionally, a series of topographic map sheets were available for the research area at 1:5000 and 1:25000 map scales.

F.5. Digital Maps

Digital elevation model for Bonn area, resolution 1m (DEM 1) [Arc/Info Grid]. courtesy of Kataster- und Vermessungsamt, Stadt Bonn.
(*data basis: Laserscanning flights).*
(*source: Kataster- und Vermessungsamt, Stadt Bonn).*

Digital elevation model for Bonn area, resolution 10m (DEM 10) [Arc/Info Grid]. courtesy of Landesvermessungsamt Nordrhein–Westfalen, Contracts no. S 1244/98, no. S 1004/97, no. S 1084/97, no. S 744/98.
(*data basis: digitized from contours of the German Basemab 1:5000).*
(*source: 'Landesvermessungsamt Nordrhein–Westfalen' (Land Survey Department Nordrhein–Westfalen)).*

Digital elevation model for the Lower Rheinisch Bay area, resolution 50m (DEM 50) [Arc/Info Grid]. Courtesy of SFB 350, University of Bonn.
(*source: 'SFB 350, Universität Bonn' (Collaborative Research Centre 350, University of Bonn) — 'Wechselwirkungen kontinentaler Stoffsysteme und ihre Modellierung' (Interactions between and Modeling of Continental Geo-Systems)).*
http://www.sfb350.uni-bonn.de/Wob/de/view_frameset/class57_id2.html

Deutsche Grundkarte 1:5000 (DGK5) [Arc/Info image catalog]. courtesy of Kataster- und Vermessungsamt der Stadt Bonn and Rhein–Sieg–Kreis.
(*data basis: German Basemap 1:5000).*
(*source: Kataster- und Vermessungsamt der Stadt Bonn, Rhein–Sieg–Kreis)*

Geology, Bonn area [Arc/Info Polygon Coverage]. Geology of the Bonn area, digitized from geologic maps 1:25000.
(*author(s): Schmanke, V., Hardenbicker, U. & Kirschhausen, D.).*
(*data basis: Geologic map 1:25000 (GK5208, GK5209, GK5308, GK5309)).*

Geological map of the area of Römlinghoven (Bonn, Germany) [Arc/Info Polygon Coverage]. only geological units of the Dollendorfer Hardt digitized.
(*author(s): Schegiewal, A.).*
(*data basis: Geological map of the area of Römlinghoven (Bonn, Germany)).*
(*source:* Schegiewal, A. **Geologische und bodenkundliche Untersuchungen am Nordabfall des Siebengebierges bei Römlinghoven** *, 1972.).*

Active landslides, Bonn area [Arc/Info Polygon Coverage].
(*author(s): Schmanke, V., Hardenbicker, U. & Kirschhausen, D.).*
(*data basis: field mappings).*

inactive landslides, Bonn area [Arc/Info Polygon Coverage].
(*author(s): Schmanke, V., Hardenbicker, U. & Kirschhausen, D.).*
(*data basis: field mappings).*

Map of linear features, landslide SI7 [Arc/Info Line Coverage]. Linear features of the landslide SI7 (thalwegs, etc.).
(*author(s): Schmidt, J.).*
(*data basis: terrestrial measurement).*

Map of areal features, landslide si7 [Arc/Info Polygon Coverage]. Areal features of the landslide si7 (blocks, levees, etc.).

(*author(s): Schmidt, J.).*
(*data basis: terrestrial measurement).*

Digital elevation model, landslide si7 (DEM SI7) [Arc/Info Grid]. Resolution: 0.5m.
(*author(s): Schmidt, J.).*
(*data basis: terrestrial measurement).*

'Bodenkarte zur forstlichen Standorterkundung, 1:5000' (*Forest soil map 1:5000, Siebengebirge*) [Arc/Info Polygon Coverage]. Soil units of Dollendorfer Hardt (Bonn, Germany), digitized from soil maps.
(*data basis: Bodenkarte zur forstlichen Standorterkundung, 1:5000 (forest soil map, 1:5000)).*

'Bodenkarte des Staatsforstes Kottenforst 1:10000' (*soil map of the Kottenforst (Bonn, Germany), scale 1:10000*) [Arc/Info Polygon Coverage]. 4 map sheets, 2 legends with comments.
(*data basis: Soil map of the Kottenforst 1:10000).*
(*source: Geologisches Landesamt Nordrhein–Westfalen)*

'Bodenkundliche Karte der Umgebung von Römlinghoven' (*Soil map of the area of Römlinghoven (Bonn, Germany)*) [Arc/Info Polygon Coverage]. Only soil units of the Dollendorfer Hardt digitised.
(*author(s): Schegiewal, A.).*
(*data basis: Bodenkundliche Karte der Umgebung von Römlinghoven (Schegiewal, 1976)).*
(*source:* Schegiewal, A. **Die Böden am Nordabfall des Siebengebirges und deren physikalischen und chemischen Eigenschaften in Abhängigkeit vom Ausgangsgestein** *, 1976.).*

'Topographische Karte 1:25000, Bonner Gebiet' (*Topographic map 1:25000, Bonn area*) [Arc/Info image catalog]. courtesy of Landesvermessungsamt Nordrhein–Westfalen, contract no. S 938/99.
(*data basis: Topographic map 1:25000).*
(*source: 'Landesvermessungsamt Nordrhein–Westfalen' (Land Survey Department Nordrhein–Westfalen)).*

F.6. Institutions & projects

Institutions

'Angewandte Geophysik, Geologisches Institut, Universität Bonn' (*Geophysics, Department of Geology, University of Bonn*)
Nußallee 8
D-53115 Bonn
Germany
http://www.geo.uni-bonn.de

'Arbeitsgruppe Geomorphologie und Umweltforschung, Bonn' (*Geomorphological and Environmental Research Group, Bonn*)
Meckeneheimer Allee 166
D-53115 Bonn
Germany
http://slide.giub.uni-bonn.de

'Deutsche Forschungsgemeinschaft' (*German Research Foundation*)
Bonn
Germany
http://www.dfg.de/

Dieter Moser GmbH Systemtechnik
Reutackerweg 4
D-76706 Dettenheim–Liedolsheim

Germany
http://www.ilsystem.de

'Geodynamik, Geologisches Institut, Universität Bonn' (*Geodynamics, Department of Geology, University of Bonn*)
Nußallee 8
D-53115 Bonn
Germany
http://www.geo.uni-bonn.de

'Geographisches Institut, Universität Bonn' (*Department of Geography, University of Bonn*)
Meckenheimer Allee 166
D-53115 Bonn
Germany
http://www.giub.uni-bonn.de

'Geologischer Dienst NRW' (*Geological Survey, NRW*)
De-Greiff-Straße 195
D-47707 Krefeld
Germany
http://www.gd.nrw.de/

'Geologisches Institut, Universität Bonn' (*Department of Geology, University of Bonn*)
Nußallee 8
D-53115 Bonn
Germany
http://www.geologie.uni-bonn.de

'Geotechnisches Labor, Fachhochschule Wiesbaden, Fachbereich Bauingenieurwesen' (*Geotechnical Laboratory, Fachhochschule Wiesbaden, Fachbereich Bauingenieurwesen*)
Kurt-Schumacher-Ring 18
65197 Wiesbaden
Germany

'Insitut für Bodenkunde, Universität Bonn' (*Department of Soil Sciences, University of Bonn*)
Nußallee 13
D-53115 Bonn
Germany
http://www.boden.uni-bonn.de

Kataster- und Vermessungsamt, Stadt Bonn
Berliner Platz 2
D-53103 Bonn
Germany

'Landesvermessungsamt Nordrhein–Westfalen' (*Land Survey Department Nordrhein–Westfalen*)
Postfach 205007
D-53170 Bonn
Germany
http://www.lverma.nrw.de/

'Landesvermessungsamt Rheinland–Pfalz' (*Land Survey Department Nordrhein–Westfalen*)
Ferdinand-Sauerbruch-Str.15
56073 Koblenz
Germany
http://www.lverma.rlp.de/

'Meteorologisches Institut, Universität Bonn' (*Department of Meteorology, University of Bonn*)
Auf dem Hügel 20
D-53117 Bonn
Germany
http://www.meteo.uni-bonn.de

'Universität Bonn' (*University of Bonn*)
http://www.uni-bonn.de/

Research projects

'Teilprojekt B13 im SFB 350' (*Subprojekt B13 (SFB 350)*) — 'Kinematik und Dynamik gravitativer Prozesse und ihr Beitrag zur Reliefentwicklung' (*Kinematics and dynamics of gravitational processes and their contribution to landform evolution*) (B13).
'Geographisches Institut, Universität Bonn' (*Department of Geography, University of Bonn*)
Meckenheimer Allee 166
D-53115 Bonn
Germany
http://www.sfb350.uni-bonn.de/Wob/de/view/class58_id8.html

'Teilprojekt B15 im SFB 350' (*Subprojekt B15 (SFB 350)*) — 'Jungholozäne Reliefentwicklung in lössbedeckten Wassereinzugsgebieten und ihre Modellierung' (*Modelling of Late Holocene Relief Development in Loess-covered Catchments*) (B15).
'Geographisches Institut, Universität Bonn' (*Department of Geography, University of Bonn*)
Meckenheimer Allee 166
D-53115 Bonn
Germany
http://www.sfb350.uni-bonn.de/Wob/de/view/class58_id52.html

'Teilprojekt B9 im SFB 350' (*Subprojekt B9 (SFB 350)*) — Bodenabtrag in einem kleinen Wassereinzugsgebiet der Sieg: Erosionsstatus, aktuelle Prozesse und Anwendung von Prognosemodellen (B9).
'Geographisches Institut, Universität Bonn' (*Department of Geography, University of Bonn*)
Meckenheimer Allee 166
D-53115 Bonn
Germany
http://www.sfb350.uni-bonn.de/Wob/de/view/class58_id5.html

'Teilprojekt C1 im SFB 350' (*Subprojekt C1 (SFB 350)*) — Erfassung und Interpretation lokaler Krustendynamik im Zusammenhang mit Fluidbewegungen und rezenter Tektonik (C1).
'Geologisches Institut, Universität Bonn' (*Department of Geology, University of Bonn*)
Nußallee 8
D-53115 Bonn
Germany
http://www.sfb350.uni-bonn.de/Wob/de/view/class58_id9.html

'Graduiertenkolleg 437' (*Postgraduate School 437*) — 'Das Relief — eine strukturierte und veränderliche Grenzfläche' (*Landform — a structured and variable boundary surface*) (GRK 437).
'Geographisches Institut, Universität Bonn' (*Department of Geography, University of Bonn*)
Meckenheimer Allee 166
D-53115 Bonn
Germany
http://slide.giub.uni-bonn.de/Kolleg/

'Historische Klimadatenbank Deutschland' (*Historical climate database Germany*) — 'Historische Klimadatenbank Deutschland' (*Historical climate database Germany*) (HISKLID).
http://www.uni-wuerzburg.de/geographie/fachi/hisklid.htm

'Massenbewegungen in Süd- und Westdeutschland' (*mass movements in southwest Germany*) (MABIS).
'Geographisches Institut, Universität Bonn' (*Department of Geography, University of Bonn*)
Meckenheimer Allee 166
D-53115 Bonn
Germany
http://slide.giub.uni-bonn.de/ ruth/d_mabis.htm

'Offene Paläoökologische Informationsysteme' (*Open Paleoecological Information Systems*) — 'Offene Paläoökologische Informationsysteme' (*Open Paleoecological Information Systems*) (OPALIS).
http://slide.giub.uni-bonn.de/ holger/opalis1.html

'SFB 350, Universität Bonn' (*Collaborative Research Centre 350, University of Bonn*) — 'Wechselwirkungen kontinentaler Stoffsysteme und ihre Modellierung' (*Interactions between and Modeling of Continental Geo-Systems*) (SFB 350).
'Universität Bonn' (*University of Bonn*)
http://www.sfb350.uni-bonn.de

Curriculum Vitae

Jochen Schmidt

Date of Birth October 27, 1968
Nationality German
Present address Goethestr. 6
D–53113 Bonn (Germany)

Education

	institution	*degree*
1987		Abitur (*university entrance qualification)*
1987–1988	*Physics,Mathematics,Chemistry*, University of Karlsruhe (Germany)	
1988–1989	*Physics,Mathematics,Chemistry*, University of Kaiserslautern (Germany)	Vordiplom in Physics
1989–1991	*Geography,Physics,Mathematics,Education*, University of Heidelberg (Germany)	Vordiplom in Geography
1991–1996	*Geography,Physics,Mathematics,Education*, University of Heidelberg (Germany)	Diploma in Geography
Masters thesis: Untersuchungen zum Einfluß geomorphologischer Variabilität und Struktur auf den Niederschlag–Abfluß–Prozeß in kleinskaligen Einzugsgebieten *(Research on the influence of geomorphic variability and structure on the rainfall-runoff-process in small scale catchments)*. Department of Geography, University of Heidelberg, 1996.		
1997–2001	*Geography*, University of Bonn (Germany)	

Employment

January 1994 — June 1996	Student research assistant, Department of Geography, University of Heidelberg, within *Regionalization in Hydrology* research programme.
August 1996 — December 1996	Research assistant, Department of Geography, University of Bonn. Responsibility for setting up soil mechanics laboratory, teaching, financial management
January 1997 — June 2001	Research assistant, Department of Geography, University of Bonn, within *Collaborative Research Centre 350* research programme.

Publications

Brinkmann, J., Schmidt, J., and Dikau, R. (2001). Terrain modelling and soil distribution: possibilities, problems and future issues. *Transactions in GIS*. in press.

Dikau, R. and Schmidt, J. (1999). Georeliefklassifikation. In R. Schneider-Sliwa, D. Schaub, and G. Gerold, editors, *Angewandte Landschaftsökologie*, pages 217–244. Springer–Verlag, Berlin Heidelberg New York.

Dikau, R., Hennrich, K., and Schmidt, J. (1999). Untersuchungen zur computergestützten Regionalisierung von geomorphometrischen Reliefmerkmalen und ihre Parametrisierung in Niederschlags–Abflußmodellen in Einzugsgebieten unterschiedlicher Größenordnung. In H.-B. Kleeberg, W. Mauser, G. Peschke, *et al.*, editors, *Hydrologie uns Regionalisierung. Ergebnisse eines Schwerpunktprogramms (1992 bis 1998)*, pages 175–189. Wiley–VCH, Weinheim.

Gärtner, H., Bergmann, A., and Schmidt, J. (2001). Object–Oriented modeling of data sources as a tool for the integration of heterogeneous geoscientific information. *Computers and Geosciences*, **27**(8), 975–985.

Gimel'farb, G., Schmidt, J., and Braunmandl, A. (1999). Gibbs fields with multiple pairwise interactions as a tool for modeling grid–based data. In S. Hergarten and H. Neugebauer, editors, *Process Modelling and Landform Evolution*, pages 47–73. Springer–Verlag, Berlin Heidelberg New York.

Hennrich, K., Schmidt, J., and Dikau, R. (1999). Regionalization of geomorphometric parameters in hydrologic modelling using GIS. *IAHS–Publications*, **254**, 181–191. Proc. Conf. on Regionalization in Hydrology, Braunschweig, March 1997.

Schmidt, J. and Dikau, R. (1999). Extracting geomorphometric attributes and objects from digital elevation models — Semantics, methods, future needs. In R. Dikau and H. Saurer, editors, *GIS for Earth Surface Systems — Analysis and Modelling of the Natural Environment*, pages 153–173. Schweizbart'sche Verlagsbuchhandlung, Berlin Stuttgart.

Schmidt, J. and Dikau, R. (2000). Slope evolution and landslides — a multiscale research approach. *Schriftenreihe des SFB 350*, **88**.

Schmidt, J. and Gärtner, H. (2000). Investigations of geomorphometric significance in hydrologic processes using Geo–Information–Technologies — results and implications for GIS needs in geomorphology. *Schriftenreihe des SFB 350*, **83**.

Schmidt, J., Merz, B., and Dikau, R. (1998). Morphological structure and hydrological process modelling. *Zeitschrift für Geomorphologie, N.F., Supplement Band*, **112**, 55–66.

Schmidt, J., Gärtner, H., and Dikau, R. (2000a). Investigations in slope development through landslide activity — concepts, methods and implications for interdisciplinary and interoperable data management. *Schriftenreihe des SFB 350*, **84**.

Schmidt, J., Hennrich, K., and Dikau, R. (2000b). Scales and similarities in runoff processes with respect to geomorphometry. *Hydrologic Processes*, **14**(11-12), 1963–1979.